200009200057

AGARD-LS-136

AGARD

ADVISORY GROUP FOR AEROSPACE RESEARCH & DEVELOPMENT

7 RUE ANCELLE 92200 NEUILLY SUR SEINE FRANCE

AD-A154 081

AGARD LECTURE SERIES No.136
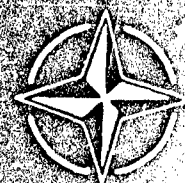
Ramjet and Ramrocket Propulsion Systems for Missiles

DTIC
ELECTE
JAN 1 8 1985
S
A

NORTH ATLANTIC TREATY ORGANIZATION

AGARD-LS-136

NORTH ATLANTIC TREATY ORGANIZATION

ADVISORY GROUP FOR AEROSPACE RESEARCH AND DEVELOPMENT

(ORGANISATION DU TRAITE DE L'ATLANTIQUE NORD)

AGARD Lecture Series No.136

RAMJET AND RAMROCKET PROPULSION

SYSTEMS FOR MISSILES

THE MISSION OF AGARD

The mission of AGARD is to bring together the leading personalities of the NATO nations in the fields of science and technology relating to aerospace for the following purposes:

— Exchanging of scientific and technical information;

— Continuously stimulating advances in the aerospace sciences relevant to strengthening the common defence posture;

— Improving the co-operation among member nations in aerospace research and development;

— Providing scientific and technical advice and assistance to the North Atlantic Military Committee in the field of aerospace research and development;

— Rendering scientific and technical assistance, as requested, to other NATO bodies and to member nations in connection with research and development problems in the aerospace field;

— Providing assistance to member nations for the purpose of increasing their scientific and technical potential;

— Recommending effective ways for the member nations to use their research and development capabilities for the common benefit of the NATO community.

The highest authority within AGARD is the National Delegates Board consisting of officially appointed senior representatives from each member nation. The mission of AGARD is carried out through the Panels which are composed of experts appointed by the National Delegates, the Consultant and Exchange Programme and the Aerospace Applications Studies Programme. The results of AGARD work are reported to the member nations and the NATO Authorities through the AGARD series of publications of which this is one.

Participation in AGARD activities is by invitation only and is normally limited to citizens of the NATO nations.

SPS

PREFACE

This Lecture Series provided an introduction to modern ramjet technology and applications to missiles were especially emphasized. The survey and characterization of various types of ramjets were followed by the discussion of ramjet components. Three of the lectures given on the second day dealt with the main types of subsonic combustion ramjets. These was one lecture devoted to supersonic combustion ramjets. The experience gained from the research and development of existing systems and components was covered in detail in all the lectures.

This AGARD Lecture Series was sponsored by the AGARD Propulsion and Energetics Panel and implemented by the Consultant and Exchange Programme.

LIST OF SPEAKERS

Lecture Series Director: Mr B.Crispin
Messerschmitt-Bölkow-Blohm GmbH
Unternehmensbereich Raumfahrt
Abt. RT 31
Postfach 80 11 69
D-8000 Munich 80
Germany

SPEAKERS

Mr J.G.Bendot
The Marquardt Company
16555 Saticoy Street
Van Nuys, California 91409
USA

Mr P.Cazin
O.N.E.R.A.
29, Avenue de la Division Leclerc
92320 Châtillon-sous-Bagneux
France

Professor F.S.Billig
The Johns Hopkins University
Applied Physics Laboratory
Johns Hopkins Road
Laurel, Maryland 20707
USA

Mr E.L.Goldsmith
Royal Aircraft Establishment
Aerodynamics Department
Clapham
Bedfordshire MK41 6AE
UK

Mr T.D.Myers
United Technologies
Chemical Systems Division
P.O. Box 50015
San Jose, California 95150-0015
USA

CONTENTS

INTRODUCTION AND OVERVIEW

by

B. Crispin
MESSERSCHMITT-BÖLKOW-BLOHM GMBH
Unternehmensbereich Apparate

Postfach 801149
8000 München 80

SUMMARY

Ramjet propulsion has gained importance as sustainer of missiles which have to combine long range and high speed. Its high specific impulse makes it favourable for this application. Moreover, military demands are satisfied by its simple design. The lecture describes the different types of ramjet propulsion and characterizes them by explaining their main features.

After a survey of the development of the design principles, the fields of application are mentioned and comparisons with other types of missile propulsion are made. The performance characteristics and the qualification of ramjet propulsion for different missions are discussed.

The lecture concludes with remarks on the present state of development and on the points of emphasis of further development.

1. INTRODUCTION

Modern concepts of guided missiles impose increased requirements for speed and range in order to improve the stand-off conditions of the carrier and the penetration capability of the missile.

In many cases the requirements for engine economy are so high that they cannot be fulfilled by rocket engines. Therefore, it becomes necessary to use airbreathing engines which offer a gain in specific impulse by about the factor of five. Among these airbreathing engines, the ram-type engine is particularly well suited as a missile sustainer because of its simple and rigid design. Compared with the turbojet engine, the ram-type engine exhibits nearly no disadvantage in fuel consumption if the Mach number is high enough. This will be demonstrated later.

The ram-type engine has two prominent characteristics, one being positive and the other being negative:
the positive feature is its extreme simplicity,
the negative characteristic is the lack of zero velocity start capability. Both characteristics have fascinate engineers since the first work of Lorin and various ramtype engines with different propellants have been designed. In order to compensate for the lack of zero velocity start capability the combination with various other engine types has been tried.

The multitude of systems shall not be discussed here, because this meeting will be confined to the aspects of military applications. For practical application in military systems, mainly three propulsion systems are of interest (Fig. 1):
- the conventional liquid fuel ramjet (using Kerosene or a liquid high density fuel)
- the solid fuel ramjet (with the solid fuel located in the ram-combustor)
- the solid propellant ramrocket (using a solid propellant for energy generation).

In the future, another type of ramengine will gain significance:
- the supersonic combustion ramjet.

Figure 2 illustrates the performance and adequate range of application of turbojet, ram-type and rocket engines. This figure shows the specific impulse of the particular engine type as a function of the flight Mach number. The propellant may change from type to type, the common feature being the storability. It has to be underlined that only mean values of performance can be given by this kind of representation. Considerable deviations will occur depending on the special design and the particular flight condition.

Pure hydrocarbons are assumed as fuel for turbojet and ramjet engines. Both engine types are almost equally efficient above Mach number three. Below this Mach number, the performance levels of both engine types diverge in the well-known manner. At zero speed, the specific impulse of the ramjet is of negative value while the turbojet reaches the maximum value. In the case of the ramrocket, a high energy propellant containing about 50 percent boron is assumed. The performance curves of ramrocket and ramjet do not differ substantially. The ramrocket, too, offers nearly no thrust at zero speed. Exceeding Mach number six approximately, performance advantages will be gained by using the method of supersonic combustion.

This presentation demonstrates the performance superiority of the ramtype engine to the rocket engine. But this superiority only exists in the middle of the Mach number range being considered and disappears at very low and very high Mach numbers.

2. INTEGRATION

generations. In the first generation, the ramjet engine was positioned within a nacelle outside the missile dart. In the following generation, the engine already was integrated in the dart. The inlet diffuser took an optimum position at the tip of the missile. But a considerable part of the dart volume was occupied by the long air duct between inlet and combustion chamber. The third generation, which represents the integration method of today, eliminates these disadvantages. The inlet system consisting of one or more inlet diffusers is laterally installed at the dart, avoiding any loss of volume due to an air duct. In addition, the free volume of the ram-combustor is used for installing the booster or a part of it. Thus an optimum of volume economy has been achieved.

The sequence of generations is demonstrated once more by fig. 4 which deals with systems being or having been in service. The first generation is formed by the systems Bomarc and Bloodhound, the second one is represented by the systems Talos, Sea Dart and Ganef.

By now, only one system of the third generation is in service:
        Gainful (SA 6).
In the near future, a new missile system using a ramjet of the third generation will have to be added:
        the French Air Surface missile ASMP
which will be the first ram-type engined system in service not belonging to the family of the surface-to-air missiles (leaving out the drones).

3. PROPELLANTS

The most important criteria for the selection of the propellant are

        the energy content
        the density and
        the storability.

Since the residence time of the combustion products within the ram-combustor is very short (5 msec or less), the requirement for good combustibility has to be added. For several applications, the aspect of smoke generation may become important. In the case of hypersonic propulsion the heat-sink capacity of the propellant has to be considered, too. The number of elements from which useful propellants may be composed is rather small. This fact becomes obvious by a diagram correlating the heat contents and the atomic numbers of the elements (a way of presentation used by several authors).

Fig. 5 shows the gravimetric as well as the volumetric heating values of the elements, since both are relevant to missile propulsion. The statement of the graph is clear:

The elements with both high gravimetric and volumetric heating values are situated in the region of small atomic numbers. It is evident, too, that only some light metals like aluminum, beryllium, - particularly boron - and besides them carbon, can compete with the usual hydrocarbons. One remark should be added. The noted heating values of the metals are valid only if their oxide produced during combustion is condensed. Actually, this assumption may be not at all or only partly realistic. At hypersonic flight conditions for example, the very high combustion temperatures may prevent the condensation of the metal oxides.

4. PERFORMANCE

One of the preceding graphs showed the relationship of specific impulse and Mach number being a characteristic of ramjet propulsion:

There is a steep increase of specific impulse in the low Mach number range, the maximum being situated at a moderately high Mach number and a decrease in the high Mach number range. This characteristic shape of the specific impulse curve derives from the ideal ramjet working cycle illustrated by fig. 6.

The ideal working cycle being identical with the "Brayton Circle" consists of

● isentropic compression of the ram air
● heat addition at constant pressure and
● isentropic expansion to the outside pressure.

Assuming ideal gas having constant specific heat, a simple formulation of the relationship between ideal specific impulse and Mach number can be found. In the particular cases of the Mach number approaching zero or infinite values, further simplifications are possible. Finally one can formulate:

● at low Mach numbers, the specific impulse is directly proportional
  to the flight Mach number and
● at very high Mach numbers the specific impulse is inversely proportional
  to the flight Mach number.

Though in reality, there are significant deviations from the conditions of the Brayton circle, the discussed tendencies remain:

● at very low and at very high Mach numbers, the specific impulse of
  the ram-type engine approaches zero.

This fact is illustrated by fig. 7 for the case of a kerosene-fueled ramjet.

a certain change of the relationship between performance and equivalence ratio discussed above. In addition, the range where equivalence ratio can be varied is confined by thrust requirements.

In the lower Mach number range, the increase of specific impulse with increasing Mach number exceeds the increase of thrust demand. For this reason, a Mach number exists where fuel consumption of the ramjet per unit range becomes a minimum. By this way and taking into account additional Mach number dependent effects to every mission, a flight Mach number can be attributed where the weight of the propulsion system or - what is finally interesting - the weight of the missile system is minimized.

This fact is demonstrated by fig. 8 for missiles flying at very low altitude. The dependence of missile weight is plotted as a function of the sustain Mach number for two different values of range without taking into account the weight of the booster. There is a flat minimum near the Mach number of 2.5.

The consideration is completed by taking into account the change of booster weight. The results of calculations are shown in fig. 9. Again the low altitude flight mission is taken as an example.

Parameters of this diagram are two different ranges and two different launch Mach numbers. Again, there is a flat minimum now near Mach number 2.

The position of the minimum is influenced to a certain amount by several other parameters as for example by the flight altitude. But these influences are of second order. Generally, it can be stated that the weight optimal Mach number lies between 2 and 2.5.

5. OPERATION

The off-design operational characteristics of the ramjet or ramrocket are primarily governed by the interactio of the inlet system and the sonic throat of the thrust nozzle. In the case of the engine with constant geometr the operation is influenced by the variable flight conditions (Mach number, altitude, angle of attack or sideslip) and the rate of heat addition in the combustor.

The matching of inlet and thrust nozzle is illustrated by fig. 10. Some simplifications have been made in order to concentrate on the determining factors: the changes of combustion chamber pressure loss and of mass flow due to fuel addition have been neglected.

It is assumed that the relation between total pressure at the end of the diffuser and air mass flow can be described by the well-known rectangular graph. A two shock inlet with external compression and stable subcritical operation will have a characteristic similar to this.

The critical or supercritical air mass flow of the diffuser is linear proportional to the flight Mach number during operation above the "shock-on-lip" Mach number. The dependence is of higher order below "shock-on-lip" conditions. (The flight altitude is always assumed to be constant.)

The total pressure at the entrance of the thrust nozzle is defined by the values of air mass flow, cross-sectional area of the sonic throat and combustion temperature. The dependence from mass flow is nearly linear if the combustion temperature is constant. In the case of constant heat addition (constant fuel flow, the dependence from mass flow can be approximately a square root function.

The synopsis shows a set of similar diffuser characteristics with the flight Mach number being the curve parameter. The critical total pressure of the diffuser strongly increases with the mass flow. The total pressure, necessary for swallowing the air mass flow has a less steep ascent with the increase of mass flow.

At the point of intersection, the engine is operating at critical diffuser conditions. Going to higher Mach numbers, the diffuser will become progressively supercritical. In the opposite direction, the engine works with subcritical diffuser, the pressure level being defined by the maximum pressure recovery of the inlet diffuser. (In most cases only part of the subcritical region can be used determined by the limits of stable operation of the diffuser.)

After these statements introducing to the matching problem of inlet and nozzle, the thrust characteristics of the ram-type engine shall be explained.

The equations describing thrust and thrust coefficient are formulated in fig. 11 in a notation which facilitates further transformation. The simplifications introduced before, for the reason of clearness shall be maintained. As an additional simplification, only operation above the "shock-on-lip" Mach number will be considered.

At first, critical operation shall be discussed (fig. 12). The relationship between critical total pressure of the diffuser and flight Mach number can be described by an exponential function of the Mach number. The exponent is between 2.5 and 3.5. According to the simplifications made above, this total pressure is identical to the total pressure within the thrust nozzle. Since the static pressure at the nozzle exit is discriminated from the total pressure only by a constant factor, the above mentioned exponential function finally is appropriate to describe the dependence of nozzle exit pressure, too.

By choosing a medium value of three as exponent, the simple relationship given by fig. 12 can be established. Mainly there is a linear proportionality at critical operation between the increase of flight Mach number and thrust coefficient.

In the supercritical regime, the relationship between thrust coefficient and flight Mach number at constant

flow. With this simplification at first the statement is established that for constant heat addition the nozzle exit pressure is proportional to the square root of the air mass flow. Because of the assumption to operate above the "shock-on-lip" Mach number, the air mass flow is directly proportional to the Mach number. Finally, the expression of fig. 13 follows, relating the thrust nozzle exit pressure to the square root of the Mach number. By using this result one gets the simple approximation of the supercritical thrust coefficient at constant fuel addition given by fig. 13.

The results of exact calculation of the thrust coefficients of a ramrocket are presented by fig. 14 a.

The thrust coefficient at critical operation rises steeply with increasing Mach number. The curves of the thrust coefficient at supercritical operation with constant fuel addition are mildly bent and decline in the direction of higher Mach numbers. As long as the inlet diffuser is stable, the subcritical region can be principally used. The calculated values of the thrust coefficient are indicated by the dotted lines.

In fact as shown by fig. 14, the pre-entry-drag of the diffuser strongly increases because of the normal shock spillage in the subcritical regime. As a result of this, only a marginal gain in the net value of thrust coefficient is attained. Besides, fig. 14 b gives information about the minimum operational Mach number of a ramjet. For that reason the drag coefficient of the missile (represented in the same manner as the thrust coefficient) is presented, too. If subcritical operation has to be excluded because of insufficient diffuser stability, the intersection point of the lines of critical thrust coefficient and of drag coefficient designates the minimum operational Mach number. But even if subcritical operation can be allowed, no remarkable change follows. This minimum operational Mach number is only a theoretical figure and the transition Mach number has to be well above this value if the flight mission requires maneuvering or climbing in the early sustain phase.

An impression of the dependence of the acceleration capability on the margin between transition Mach number and minimum operational Mach number is given by fig. 15.

This graph referring to a long range missile shows the acceleration (as multiples of the acceleration due to gravity) as a function of the time after transition. For this calculation, the assumption has been made that the transition Mach number exceeds the minimum operational Mach number by a value of 0.05. It is obvious that a certain value (being not too small) of this margin has to be provided because of the dynamic characteristics of the missile.

6. COMPARISON OF RAMJET PROPULSION WITH OTHER TYPES OF MISSILE PROPULSION

6.1 Comparison with Rocket Propulsion

Ramjet propulsion offers the advantage of low fuel consumption compared with rocket propulsion, but the disadvantage of additional structure weight has to be accepted. Therefore, the range of the missile has to exceed a minimum value in order to justify ramjet application. The minimum range where the propulsion system weight of a ramjet engine corresponds to a rocket engine, essentially depends on ambient pressure (flight altitude) and Mach number. Since the minimum range is approximately reciprocal to ambient pressure, the simple manner of representation of fig. 16 becomes possible.

This figure shows the product of minimum range and ambient pressure as a function of the flight Mach number. Basis of comparison is:

- a solid propellant rocket having a specific impulse of about 240 sec
  and
- a hydrocarbon-fueled ramjet or a ramrocket using a high energy propellant.

Since the dimension of ambient pressure is "bar", this graph directly informs about the minimum range of ramjet application for low altitude missions.

Of course, the statement of fig. 16 is only of theoretical nature. In practice, the range has to exceed these theoretical values considerably in order to justify the change from rocket propulsion to the more complicated ramjet propulsion.

An impression of the margin of propulsion weight which can be saved by using ram-type engines is given by fig. 17.

Fig. 17 indicates the propulsion weight per unit of range as a function of range at sea level conditions. A solid propellant rocket and ramrocket using a high energetic boron containing propellant are compared. Similar results will be attained if the ramrocket is replaced by a hydrocarbon-fueled ramjet. The calculated values apply to a missile of 0.1 m² cross-sectional area flying at sea level conditions with Mach number 2.

The advantage of using ram-type propulsion for medium or long range missions is clearly indicated by the graph. It must be added that only the weight of the sustainer propulsion module has been considered. If boost propulsion is taken into consideration, the gap between the weight characteristics of both propulsion types will increase further.

The influence of the Mach number on this comparison is illustrated by fig. 18, now referring to the aspect of volume requirement of the propulsion system.

In this graph, the length of the propellant section needed per unit of range, is shown as a function

The statement is: The application of ram propulsion is the appropriate way to reduce missile length at supersonic flight missions.

6.2 Comparison with Turbojet Propulsion

In the subsonic and transsonic region, there is a clear superiority of turbojet propulsion with regard to both fuel consumption and thrust coefficient. As far as fuel consumption is concerned, this superiority lasts up to a Mach number of about 3.5. But in the case of missile application the required thrust coefficients generally exceed by far the values which can be provided by a pure turbojet. The extreme thrust requirements only can be fulfilled by a turbojet if it is equipped with an afterburner. In this case the afore-mentioned superiority with respect to fuel economy diminishes at a Mach number of about 2. On the other hand, a lot of penalties (weight, complexity, problems concerning the accommodation of an integral boost motor and so on) arise for the application of the turbojet engine.

Situations may exist where advantages can be drawn from the self-acceleration characteristics of the turbojet. But in general, an additional boost motor is needed providing a sufficient thrust level to accelerate the missile as fast as possible to its sustain speed, thus minimizing the minimum operating range.

Keeping in mind these considerations in the case of missile applciation nearly no argument remains for using a turbojet instead of the much simplier ramjet if the flight Macn number exceeds a value of about 1.8 (even a lower value can be assumed).

7. FINAL REMARKS

At this time, development work or at least technology work in the field of ramjet or ramrocket propulsion is going on in several countries of the NATO community. But still there exist some reservations against the application of ramjet propulsion in the mind of the system engineers. This may be due to the following reasons:

● The development period is long (a period of five years has to be anticipated nowadays)
● Development and production costs are high. (Some components and the equipment are expensive in manufacturing. Compared with rocket propulsion ramjet testing is very expensive.)
● Some additional restrictions have to be accepted by the designer of the missile. (The restrictions concerning usable Mach number range, altitude range, margin of angle of attack or sideslip, and minimum launch Mach number are more severe as in the case of rocket propulsion.)

Some of the just mentioned facts are inevitably inherent in airbreathing propulsion and have to be accepted in return of a higher efficiency. But the remaining problems could be overcome by a better knowledge of the component technology leading from the variety observed now to more standardized solutions of component design and construction.

With respect to this, an improved cooperation between the different developing companies and institutions within the NATO community could be very helpful. Additional efforts have to be made in the following fields in order to improve the prospects of application of ram-type propulsion:

- inlet stability
- sensibility concerning angle of attack and sideslip
- combustion stability
- durability of heat protection
- high density fuel management
- particle combustion efficiency
- throttling mechanism for solid propellants
- consumable port covers and booster nozzles
- supersonic combustion of storable propellants

This list does not claim to be complete, but some of the topics are appropriate to be subject of a common technology work of the NATO countries.

Nomenclature

A	Cross-sectional area	$\dot{m}$	Mass flow
C_D	Drag coefficient	p	Pressure
C_F	Thrust coefficient	q	Dynamic Pressure
F	Thrust	R	Range
H	Altitude	S	Entropy
i	Enthalpy	T	Temperature
isp	Specific impulse	t	Time
M	Mach number	φ	Equivalence ratio

Subcripts: Supercripts:

0   Free stream cond: 0   Total
D   Design
f   Fuel

REFERENCES

General references are listed in the bibliography prepared by the AGARD TIP (Supplement of LS 136).

Pohl, W.D.   Flugleistungsaspekte bei Stauantrieben
                  MBB-Bericht UR-699/84, 1984

Crispin, B.   Betrachtungen zum Gesamtsystem eines Staustrahl- und eines Kombinationstriebwerks
                  MBB-Bericht UR-226-74, 1974

Voss, N.   Verbrauchsoptimale Marschflugmachzahl
                  MBB-TN RC1-32/73, 1974

Weinreich, H.L.   Overview of propulsion systems and related fluid-dynamic aspects
                  AGARD-VKI LS No. 98, Supplement, 1979

Besser, H.L.   Investigation of boron solid propellant combustion on ducted rockets
                  AGARD Symposium on Ramjets and Ramrockets for Military Applications,
                  26-29 Oct., 1981

Sarner, S.F.   Propellant Chemistry
                  Reinhold Publishing Corporation, N.Y., 1966
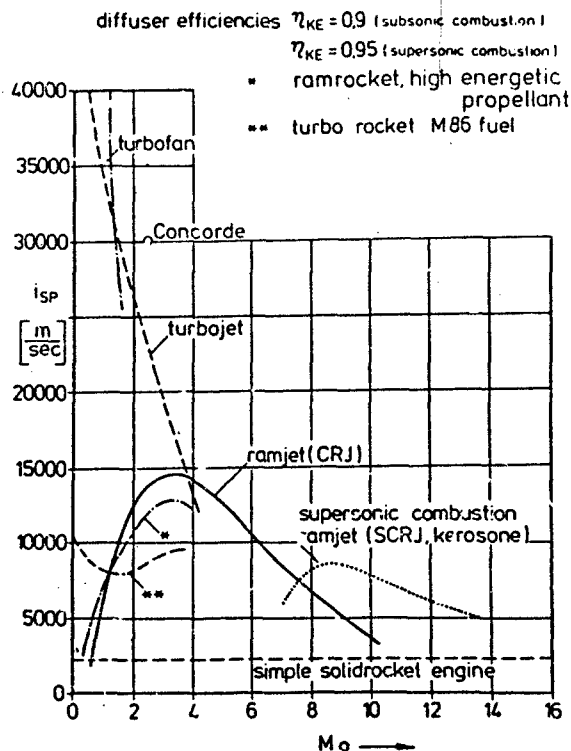
(liquid   fuel ramjet)
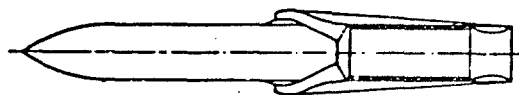
(solid fuel ramjet)

(solid propellant ramrocket)

Fig. 1 - Types of Ram Propulsion

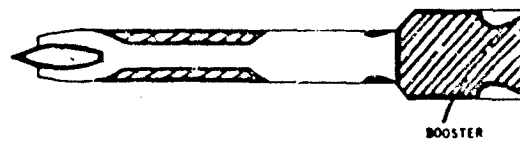**Specific Impulse of various propulsion types**

diffuser efficiencies $\eta_{KE} = 0.9$ (subsonic combustion)
$\eta_{KE} = 0.95$ (supersonic combustion)
* ramrocket, high energetic propellant
** turbo rocket M 86 fuel

1. GENERATION

Fig. 3
Engine Integration and
Booster Installation

BOOSTER

2. GENERATION

BOOSTER

3. GENERATION

BOOSTER

Fig. 4
Ramjet History

BOMARC 7250 KG				14 METER
				—12
		TALOS 3175 KG	GANEF SA 4 1800 KG	—10
	BLOODHOUND Mk 2 2000 KG			
			GAINFUL SA 6 550 KG	—8
		SEA DART 500 KG		—6
				—4
				—2
1. GENERATION		2. GENERATION		3. GENERATION

Gravimetric Heating Value
$[J/g]$
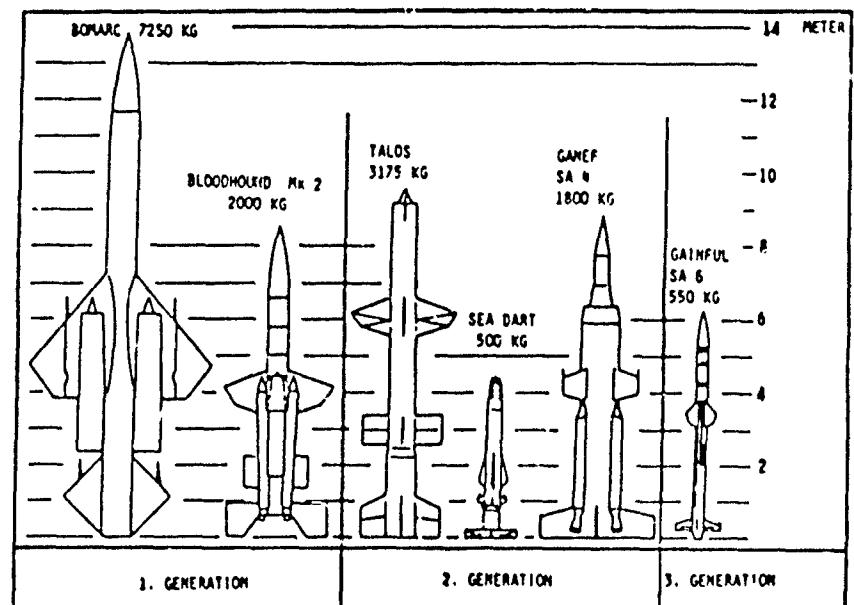
Fig. 5
Heating Value of
Elements

$[J/cm^3]$
Volumetric Heating Value

Specific impulse:

$$i_{sp} \propto w_0 \; (\frac{w_5}{w_0} - 1)$$

Fig. 6
Ideal Ramjet Working Cycle

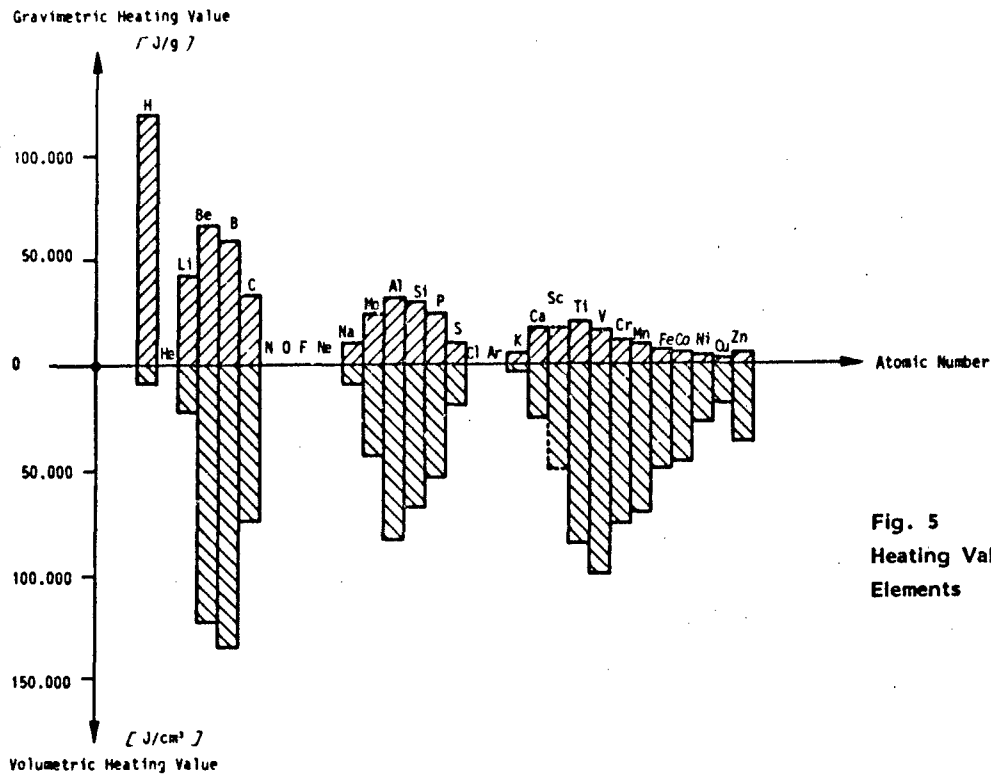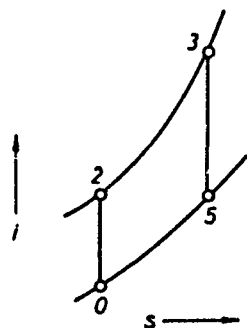$$\frac{w_5}{w_0} = \sqrt{\frac{T_3 - T_5}{T_2 - T_0}} = \sqrt{\frac{T_3}{T_2} \cdot \frac{1 - T_5/T_3}{1 - T_0/T_2}} = \sqrt{\frac{T_3}{T_2}}$$

$$T_3 = T_2 + \Delta T$$

$$T_2 = T_0 (1 - \frac{\varkappa - 1}{2} M_0^2)$$

$$w_0 \propto M_0$$

(1) $\quad I_{sp} \propto M_0 \cdot (\sqrt{1 + \frac{\Delta T}{T_0} \cdot \frac{1}{(1 + \frac{\varkappa - 1}{2} M_0^2)}} - 1)$

(2) $\quad M_0 \longrightarrow 0 : \quad I_{sp} \propto M_0 \; (\sqrt{1 + \frac{\Delta T}{T_0}} - 1) \propto M_0$

(3) $\quad M_0 \longrightarrow \infty : \quad I_{sp} \propto M_0 \; \frac{\Delta T}{T_1} \cdot \frac{1}{\varkappa - 1} \cdot \frac{1}{M_0^2} \propto \frac{1}{M_0}$
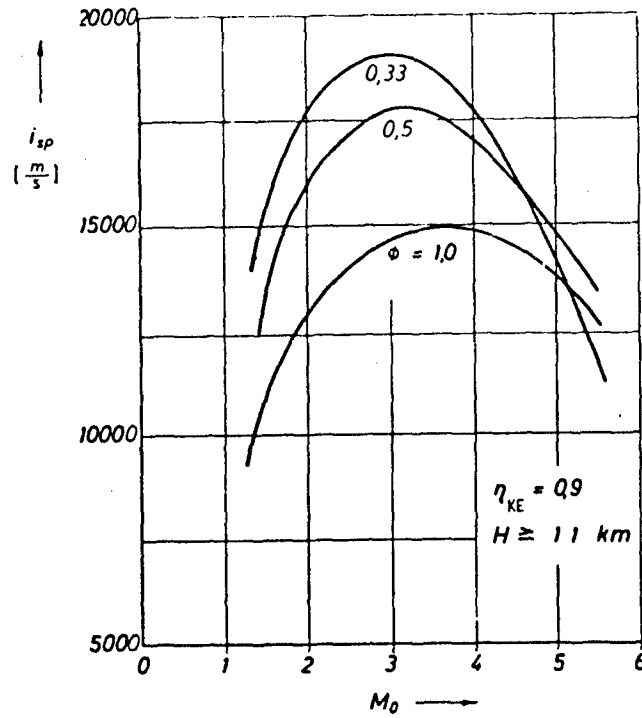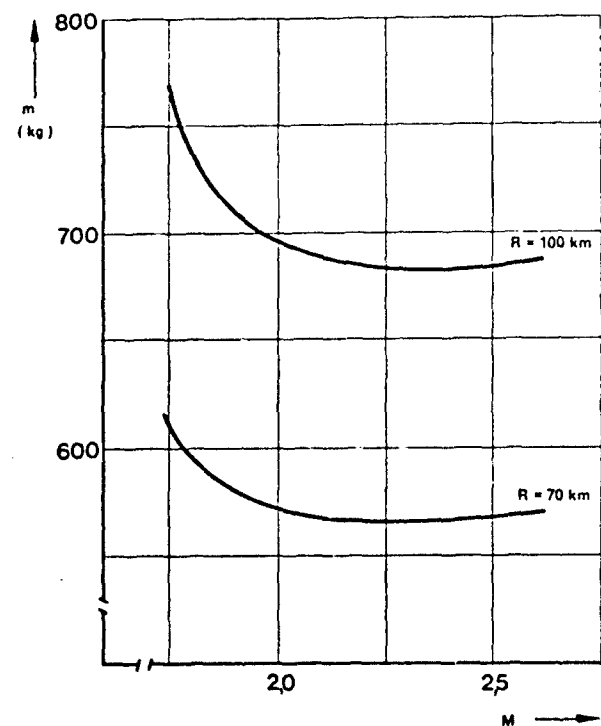
Fig. 7
Specific Impulse of a
Hydrocarbon-Fueled
Ramjet

Fig. 8
Weight of a Ramjet Powered
Missile as Function of
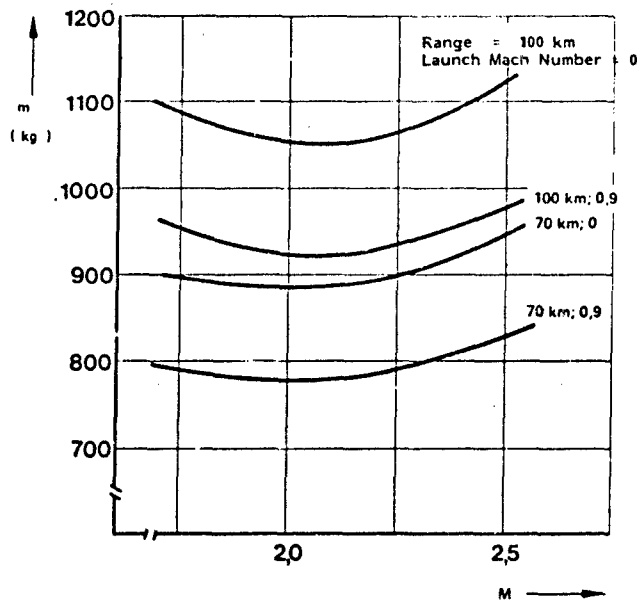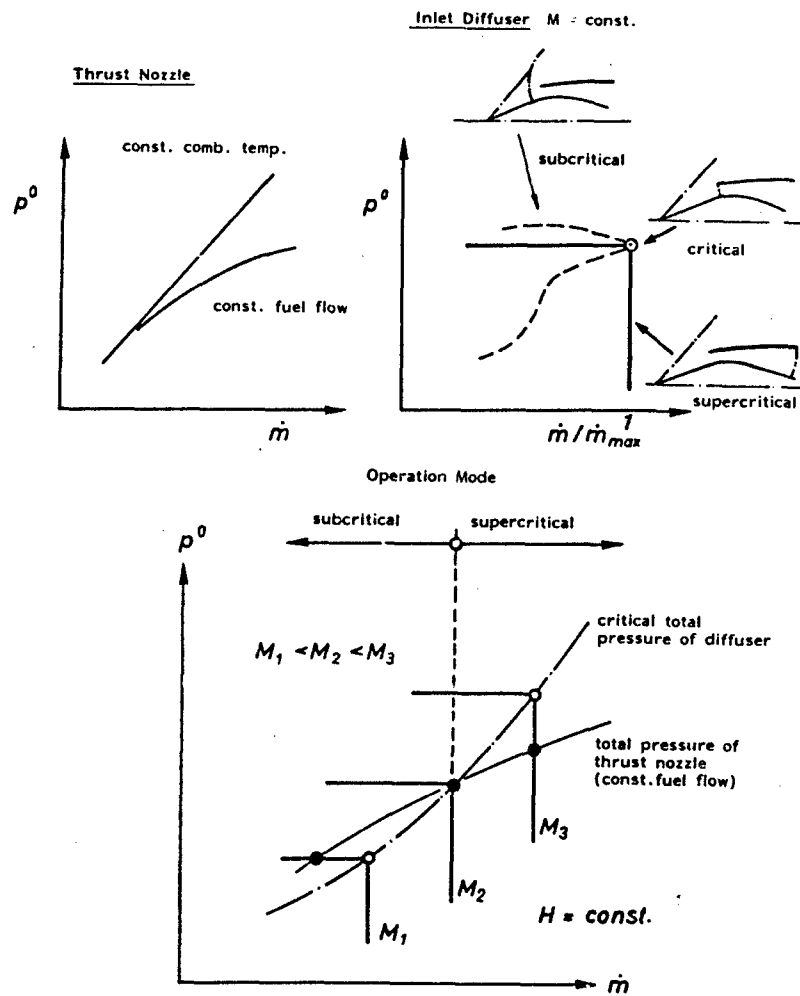Sustain Mach Number
(Booster Weight Excluded)

Fig. 9
Launch Weight of a Ramjet Powered
Missile as Function of Sustain Mach
Number, H = 0 km
(Booster Weight Included)
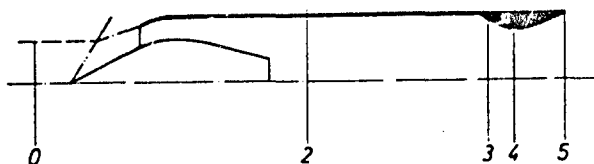
Fig. 10
Matching of Inlet and
Thrust Nozzle

Fig. 11

Thrust:

$$F = p_5 \cdot A_5(1 + \chi_5 M_5^2) - p_0 \cdot A_0 \chi M_0^2 - p_0 \cdot A_5$$

$$C_F = \frac{F}{A_5 \cdot q_0}$$

$$q_0 = \frac{\chi}{2} M_0^2$$

Thrust Coefficient:

$$C_F = 2 \left(\frac{p_5}{p_0} \cdot \frac{1 + \chi_5 M_5^2}{\chi M_0^2} - \frac{A_0}{A_5} - \frac{1}{\chi M_0^2} \right)$$

Specialization:

o Const. Geometry $\longrightarrow$ M_5 = const.

o $M_0 > M_D$ $\longrightarrow$ A_0 = const. at supercritical cond.

Simplification:

$$p_5^o \approx p_2^o$$

Critical Operation

Assumed dependence of inlet total pressure from flight Mach number at const. altitude:

$$p_2 \sim M_0^n \qquad n = 2.5 \text{ to } 3.5$$

$$p_5^o \approx p_0^o \qquad \text{(simplification)}$$

$$\frac{p_5}{p_5^o} = \text{const. (const. geom.)}$$

$$\frac{p_5}{p_0} \sim M_0^n$$

Using n = 3

$$\boxed{C_F = \text{const.}_1 \cdot M_0 - \text{const.}_2 - \frac{2}{\chi M_0^2}}$$
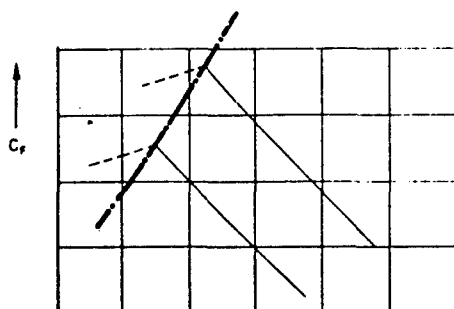
Supercritical Operation

Specialization: const. fuel flow
const. flight altitude

$$p_3^o \approx \dot{m}_5 \cdot \sqrt{T_5^o}$$

$$\dot{m}_5 \propto M_0 \qquad (M_0 \cdot M_D) \\ (H = \text{const.})$$

$$T_5 \approx \frac{f}{\dot{m}_5} \qquad \text{(simplification)}$$

$$p_5^o \propto \sqrt{M_0}$$

$$\frac{p_5}{p_5^o} = \text{const.} \quad \text{(const. geom.)}$$

$$\frac{p_5}{p_0} \approx \sqrt{M_0}$$

$$\boxed{C_F = \frac{\text{const.}_3}{M_0^{3/2}} - \text{const.}_2 - \frac{2}{\chi M_0^2}}$$
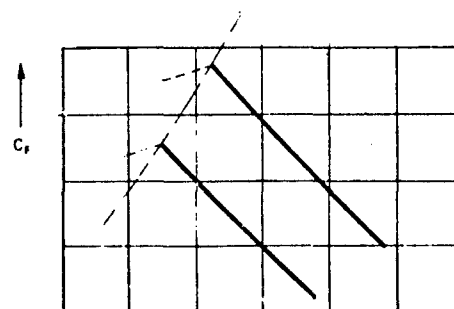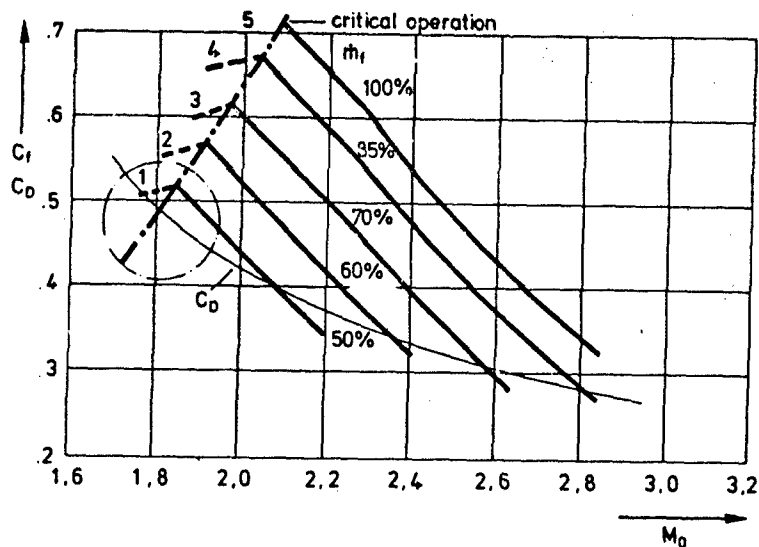
Fig. 14 a
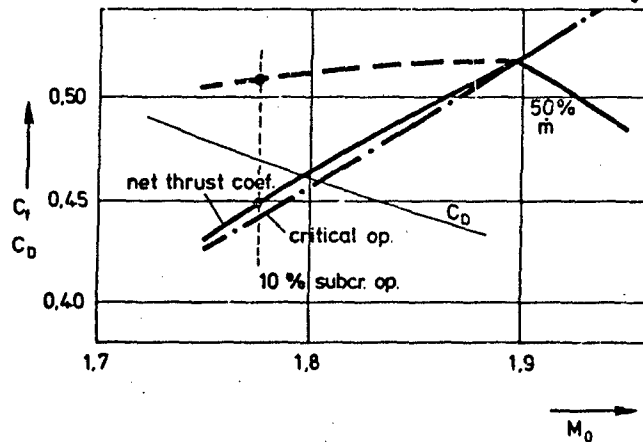
Fig. 14 b
Thrust Coefficient as
Function of Mach Number.
High Energy Ramrocket,
H = 0 km

Fig. 15
Acceleration of a Long Range
Missile (Multiples of Gravitational
Acceleration) as Function of Time.
Supercritical Margin of Inlet:
3 %, H = 0 km
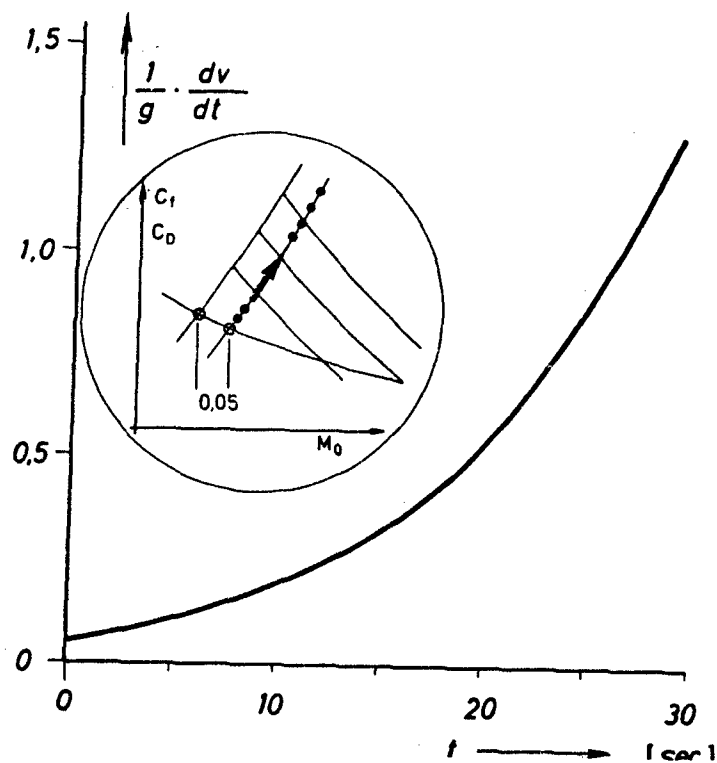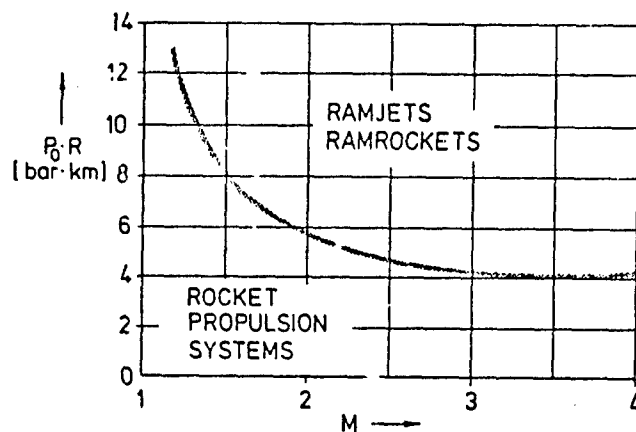
Fig. 16
Regions of Application of Ram-
rockets, Ramjets, and Rocket
Propulsion Systems
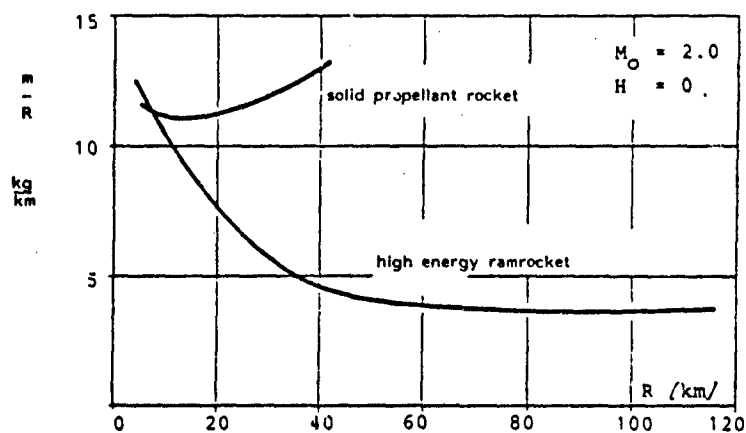
Fig. 17
Propulsion Weight per
Unit of Range
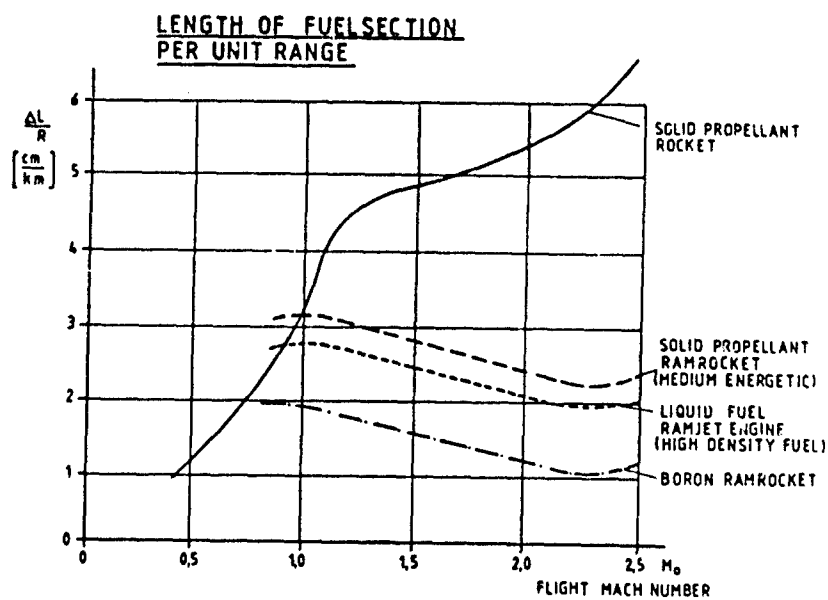
Fig. 18

RAMJET AIR INDUCTION SYSTEM DESIGN FOR TACTICAL MISSILE APPLICATION

J. G. Bendot
A. E. Heins, Jr.
T. G. Piercy

THE MARQUARDT COMPANY
16555 Saticoy Street
Van Nuys, California, 91409, U. S. A.

INTRODUCTION/SUMMARY

Active development of the liquid ramjet engine was undertaken by the United States in the early 1950's. Successful development of the BOMARC and Talos long range surface-to-air interceptor missiles was accomplished in this time period with initial operational deployment taking place in 1957 and 1959, respectively (Figure 1). Shortly thereafter, similar surface-to-air systems were developed and operationally deployed by the United Kingdom and the Soviet Union. The United Kingdom developed the Bloodhound MK1 and Bloodhound MK2 missile systems (Figure 2). Later it developed the Sea Dart shipboard based surface-to-air missile (Figure 2). During the same time frame, the Soviet Union developed the SA-4 GANEF mobile surface-to-air missile (Figure 3).

From the inlet designer's viewpoint, it is instructive to note that all of these missile systems incorporated an axisymmetric air induction system into the nose of the vehicle or the nose of externally mounted nacelle or pod mounted engines. By today's standards, the design of such inlets is quite straight forward, well documented and development undertaken with little risk.

In the 1960/1970 time period the Integral Rocket-Ramjet (IRR) type of engine was successfully developed. The operating principal of the IRR engine is described in Figure 4. Flight demonstrations were successfully accomplished in the following programs:

PROJECT CROW	1961
LOW ALTITUDE SUPERSONIC RAMJET MISSILE (LASRM)	1965/1966
ADVANCED LOW VOLUME RAMJET (ALVRJ)	1974/1976
SUPERSONIC TACTICAL MISSILE (STM)	1979

It is noted that each of the flight tested IRR systems (with the exception of the CROW test vehicle) utilized a multiple aft mounted inlet system (see Figure 5). Furthermore, the Soviet Union developed SA-6 GAINFUL surface-to-air missile system also utilizes a multiple aft mounted inlet system.

In recent years, we have seen a growing interest in the development of advanced tactical missile systems. Specifically, long range air-to-surface, air-to-air and surface-to-air systems are of interest. The generalized missile/propulsion system requirements for these missile systems are:

- Long Range
- High Speed
- Demanding Launch Aircraft Compatibility Requirements
- High Packaging Density (Missiles are typically volume limited)
- Low Cost

These design requirements are best satisfied with use of ramjet propulsion. Both liquid and solid fuel engines are of interest.

Four significant design/mission characteristics of these proposed new missile systems are of major interest to the ramjet inlet designer:

1. The vehicle forebody will house the missile guidance system, autopilot and payload. A nose inlet vehicle is no longer a viable design solution. (Missile systems specifically designed for storage/firing from a shipboard based box launcher may be an exception to this statement).

2. The ramjet air induction system must be highly integrated with the vehicle to result in an aerodynamically efficient, minimum weight design.

3. Integral rocket-ramjet engines are emphasized.

4. The vehicle flight profiles are typically highly transient in terms of flight Mach number, altitude and angle of attack. Particularly in the air-to-air application, vehicle maneuver requirements dictate high angle of attack operation (see Figure 6).

The above described design/mission requirements were initially viewed with concern by experienced inlet designers. They reasoned the following consequences of these requirements:

1. Installed inlet performance would be degraded as compared to nose inlet systems.

2. Successful development of these inlet systems would be more difficult and therefore require a longer, more expensive inlet development program.

The United States has conducted inlet design/performance studies for a number of candidate advanced ramjet powered missiles. By utilizing favorable interference design concepts (vehicle forebody and/or wing flow field effects, precompression shrouds) and compromises in inlet design parameters (design Mach number, contraction ratio, bleed flow) excellent installed inlet performance has resulted. In fact, installed inlet performance is often significantly improved when compared to nose inlet systems, especially at high angle of attack flight conditions. The inlet design concepts/trade-off parameters considered in these programs will be discussed in this lecture.

DESIGN/PERFORMANCE TRADE-OFF PARAMETERS

The inlet designer must properly consider/evaluate (analytically and/or experimentally) a number of design trade-off parameters to configure the air induction system which best meets specific vehicle/ system requirements. These inlet design parameters are discussed in the paragraphs which follow. To facilitate these discussions, the air induction system (inlet) station notation and nomenclature used throughout this paper is presented in Figure 7. In addition Figure 8 presents representative inlet performance curves. The classical P_{T2}/P_{T_∞} versus A_∞/A_C inlet performance curve is often referred to as a "candy cane" curve because of its characteristic shape. Figure 8 is representative of an inlet which employs boundary layer bleed. With such an inlet the inlet airflow definitions $(A_\infty/A_C)_{Total}$ and $(A_\infty/A_C)_{Plenum}$ are required.

Inlet Type

Typically, three inlet types are evaluated for application to advanced ramjet powered tactical missile systems. These inlet types are as follows:

    Axisymmetric
    Two-dimensional (2-D)
    Chin

Representative performance for these three inlet types is presented in Figure 9. As shown in this figure, axisymmetric inlet performance deteriorates rapidly with increasing angle of attack. In contrast to the axisymmetric inlet, the two-dimensional and chin inlet designs exhibit increasing inlet performance (total pressure recovery and engine airflow) with increasing angle of attack. These performance characteristics are well matched to advanced tactical missile system requirements.

Can the angle of attack performance of the axisymmetric inlet be improved? Yes by locating the inlet in the favorable flow field generated by the vehicle wing. Using this design technique, axisymmetric inlet performance closely approximates 2-D inlet performance (Figure 10). However, it must be recognized that this design approach has a serious limitation. The vehicle wing/inlet geometry established by wind tunnel testing must be maintained. This significantly increases the problem of meeting vehicle stability and control requirements. These requirements are significantly easier to satisfy if the wing and inlet locations can be treated as independent variables.

If a 2-D inlet is located in the wing flow field, is its performance improved? The test data trends of Figure 11 answer this question. Mid-wing performance is approximately equal to the no-wing data. However, a bottom mounted wing improves inlet performance. Location of the inlet between cruciform wings further improves 2-D inlet performance. While this increased performance is highly desirable, the fixed wing/inlet location problem discussed above presents the vehicle designer with serious stability and control design problems.

Is there another way to improve 2-D inlet performance with increasing angle of attack? Yes use of a precompression shroud can significantly increase 2-D inlet performance at angle of attack operating conditions (see Figure 12). The test data trends shown in Figure 12 are for a precompression shroud design which emphasized ramjet takeover thrust/drag margin and high Mach number/high altitude cruise conditions.

Can the precompression shroud design concept be applied to the axisymmetric inlet? Experimental studies conducted by NACA (National Advisory Committee for Aeronautics) and NWC (U.S. Navy - Naval Weapon Center) were disappointing.

For the reasons discussed above, modern high performance ramjet powered tactical missile designs typically incorporate a chin (see Figure 13) or two-dimensional inlet system. Use of a highly integrated two dimensional inlet is presented in Figure 14. Shown is an inboard profile drawing of a candidate ramjet powered long range air-to-air missile design. Axisymmetric inlets are specified where low development risk, low weight and low manufacturing cost are major vehicle design drivers.

Ramjet powered missile systems specifically designed for storage/firing from a shipboard based box launcher or a submarine torpedo tube may be special cases. The Johns Hopkins University/Applied Physics Laboratory conducted a design study for a SCRAMJET powered shipboard launched interceptor missile (reported in AGARD publication AGARD-CPP-307). Rectangular and round launchers were studied. The study considered the following inlet options: (1) an axisymmetric nose inlet; (2) a chin inlet; and (3) a single bottom mounted aft inlet. Missile storage constraints coupled with performance

requirements resulted in selection of a nose inlet system. Inlet cowl area limitations were a major factor in this conclusion. In contrast, several studies have shown the chin inlet to be compatible with ramjet powered missiles designed for firing from a submarine torpedo tube. The inevitable conclusion drawn from these studies is that the design of ramjet powered vehicles which are stored and/or fired from severely constrained launchers must be carefully structured to insure compliance with system performance requirements. Radar dish size and bank-to-turn versus skid-to-turn flight control must be considered.

Number of Inlets/Inlet Location

Multiple (four) aft-mounted inlet systems have been successfully employed in three ramjet propulsion flight research test vehicles and one operational surface-to-air missile (see Figure 5). This type of air induction system functions well when vehicle angle of attack/angle of yaw requirements are minimal. These are typical operating requirements for supersonic/low altitude missile systems. However, as discussed earlier in this paper and illustrated in Figure 6, today's advanced ramjet powered tactical missile systems (particularly air-to-air missiles) emphasize high angle of attack operation during guidance handover and terminal engagement maneuvers. Under these operating conditions, the performance of a multiple (four) aft mounted inlet system is poor as illustrated in Figure 15. Consequently, advanced high performance tactical missile designs typically employ one or two inlets. Furthermore, if a single inlet is used, it is usually bottom mounted. High inlet performance has been demonstrated with forward (chin) and aft bottom mounted single inlets. If two inlets are used, they are mounted approximately 45° from the horizontal centerline. The arguments for these inlet locations is the test data trends presented in Figures 16 and 17. Photographs of a high performance chin, aft bottom mounted single and aft mounted dual inlet wind tunnel test model are presented in Figures 18, 19 and 20 respectfully.

Design Mach Number

The inlet design Mach number not only strongly influences design point performance but also off-design performance. Figure 21 presents the classical maximum total pressure recovery versus design Mach number plot. Although the total pressure losses of external compression inlets decrease as the number of oblique shocks is increased, it has been found in practice that the use of discrete oblique shocks in excess of two offers greater flow complication and less satisfactory results than "isentropic" type inlets.

Normally, ramjet inlets are fixed geometry and designed for a single Mach number. Therefore, these inlets must accept the performance penalties associated with flying above and below design Mach number. What is the effect of design Mach number on off-design performance? This effect, at zero degrees angle of attack, is presented in Figure 22.

Low design Mach number inlets have higher capture area ratio (engine airflow) below the design Mach number and lower pressure recovery above the design Mach number when compared to high design Mach number inlets. The experimental axisymmetric inlet data presented in Figure 23 confirms these trends. Low design Mach number inlets emphasize ramjet takeover performance while high Mach number inlets emphasize high vehicle flight speed. However, it is important to recognize these performance trends can be significantly altered at moderate to high angle of attack flight conditions. Typical performance trends for isolated two-dimensional, mixed compression (internal and external) inlets at a moderate angle of attack are presented in Figure 24. The trends are for inlets designed to be near the maximum amount of external and internal compression at the design Mach number. In the middle Mach number range, the low design Mach number inlet can have both higher pressure recovery and capture area ratio. This is because the higher design Mach number inlet, at angle of attack, operates unstarted and with or without detached external shock waves over a large portion of the Mach number range. Therefore, selection of the inlet design Mach number must carefully consider all pertinent inlet design requirements and is a significant step in the definition of a new inlet design.

Contraction Ratio

Increasing the amount of external contraction increases the overall pressure recovery. This is accomplished by increasing the inlet initial cone or wedge angle and/or the amount of isentropic compression. Ultimately a "compression limit" is reached which precludes compression (externally) to a pressure higher than can be achieved behind a strong shock. The reason for this is shown in Figure 25. Static pressures must be balanced across the vortex sheet. This limits the degree of external compression to the values shown in the figure. Generally speaking the consequences of designing an inlet which exceeds the compression limit is to spill air (decreased thrust and increased drag) at high flight Mach numbers (Figure 25). Highly compressed inlets result in large flow angles at the cowl lip. If the cowl lip is flow aligned or positioned at some fixed angle relative to the approaching flow, then cowl drag increases with contraction ratio (cowl lip drag can be decreased by misaligning the cowl but this usually requires inlet bleed with associated bleed drag). The optimum amount of external contraction at a given Mach number can be found by computing net engine thrust (trading pressure recovery against cowl drag). The elements of this optimization analysis are presented in Figure 26. Such a design optimization is often accomplished for the ramjet takeover flight condition.

High performance aircraft typically employ variable geometry mixed compression inlets. Mixed compression inlets employ external and internal contraction. At first examination the use of a large amount of internal contraction would appear to benefit ramjet inlet performance. However, such is not the case for two reasons:

    1)   Variable geometry inlets are heavy and complex. Numerous ramjet design studies which examined the use of variable geometry inlets showed little or no payoff, primarily due to their added weight. However, hypersonic ramjet/SCRAMJET engines designed to operate over a

2)   Ramjet engines are typically designed to operate over a large range of flight Mach numbers and angle of attack. With a fixed geometry inlet and these demanding flight operating conditions, only a small amount of internal compression can be utilized (~10% contraction). Therefore, the maximum total pressure recovery performance presented in Figure 21, which strictly speaking applies to external compression inlets, also generally applies to fixed geometry ramjet mixed compression inlets.

Figure 27 illustrates the effect of inlet contraction on an installed bottom mounted, two-dimensional inlet at angle of attack. It should be noted at high angles of attack, the low contraction ratio inlet can be better in both pressure recovery and capture area ratio. The importance of establishing realistic inlet design requirements early in the missile development program is apparent.

Bleed Airflow Rate

Typically, inlet bleed flow can improve the total pressure recovery of an inlet but at the expense of drag. Therefore, in most cases, there is a bleed flow rate (and/or configuration) that produces maximum net engine thrust. Such a bleed flow rate/configuration optimization is usually accomplished experimentally for the critical ramjet takeover flight condition. The performance trends shown in Figure 28 are from experimental data for a bleed system with high bleed momentum recovery.

Use of an Aerodynamic Grid

During the flight test development of the BOMARC liquid fuel ramjet engine serious subsonic diffuser flow separation problems were experienced, especially at large angles of attack. These flow separations resulted in poor diffuser exit airflow and, therefore, combustor entrance fuel-air ratio profiles. The result was poor combustor performance and often combustor blow out. A device known as the aerodynamic grid solved this problem.

The aerodynamic grid is designed to choke as the ramjet engine is throttled to lean fuel air ratios. This limits the downstream travel of the normal shock system into the subsonic diffuser - the cause of diffuser flow separation. The choked grid also redistributes the diffuser airflow much as a screen. However, because of its carefully contoured shape, the effect on critical inlet recovery is small $(\Delta P_{T2}/P_{T2} \sim .02)$.

Figure 29 describes several types of aerodynamic grids tested in development ramjet engines. The round hole grid and the annular grid have found the most use.

Subsonic diffuser exit flow profile test data, with and without the use of an aerodynamic drag, are presented in Figure 30. These test results speak for themselves.

The aerodynamic grid has been used in a number of operational and flight test ramjet engines. Examples are BOMARC, Talos, Typhoon, Bloodhound, and ASALM. A grid will not be required if the design can tolerate shock induced separation in the subsonic diffuser without adverse effects on the structure (back burning) or on combustion efficiency.

Subsonic Diffuser Design

The design of a high performance subsonic diffuser is strongly influenced by flight vehicle geometric constraints such as available length and combustor offset. "S" shaped diffusers are often employed in ramjet powered flight vehicles and are particularly troublesome. Good performing diffusers (straight and "S" shaped) have been developed using an effective conical flow expansion angle of 3 to 5 degrees. Rapid inflections in diffuser wall contours should be avoided. If subsonic diffuser flow separation is experienced the use of an aerodynamic grid will often greatly improve diffuser performance.

Inlet Drag

Inlet drag plays a strong role in the design and development of a high performance ramjet inlet/diffuser. Mr. E. L. Goldsmith of the Royal Aircraft Establishment will address this important subject in his lecture.

Subcritical Stability

Figure 31 presents total pressure recovery/capture area ratio characteristics for a high performance and a low performance inlet design. Both inlets have the same supercritical A_ω/A_C. As is often true in practice, the low performance inlet $(P_{T2}/P_{T\infty})$ has subcritical margin while the high performance inlet does not. The constant slope lines $(P_{T2}/P_{T\infty} /A_\infty /A_C)$ represent lines of constant ramjet combustor heat release or fuel-air ratio. Since it is undesirable to permit the inlet to buzz, a high performance inlet is usually required to operate at some margin (5% to 10% in pressure recovery). This requirement is due to accuracy or repeatability in test data or changes in atmospheric conditions. This requires a pressure recovery limiter control. However, as can be seen in the figure, a lower performance inlet with sufficient subcritical stability can provide the same margin (or more), thus eliminating the need for a pressure recovery limiter control. This subject will be further discussed in the second portion of this lecture.

Vehicle Forebody Effects

For a given inlet geometry and location, the shape of the vehicle forebody can have a significant effect on inlet performance. Whether this effect is large or small depends on inlet size, inlet type and axial, radial and circumferential location. For completeness, it is pointed out that selection of the vehicle forebody shape is usually dictated by airframe packaging or radome slope error considerations.

Typical vehicle forebody shape effects on inlet performance are presented in Figure 32.

An important aspect of vehicle forebody effects is the definition of the local flow field delivered to the inlet. Rapid advances are being made in the modeling and computation of these flow fields. This important subject will also be discussed by Mr. Goldsmith.

Comparison of Wind Tunnel and Flight Test Inlet Data

The primary tool used to develop a high performance ramjet inlet is the high pressure (high Reynolds number) blow down type of wind tunnel. A question often asked is "How well do wind tunnel and flight test inlet data compare?" The test data typically compare quite favorably as demonstrated in Figure 33.

Additional Inlet Design Considerations

In addition to the major inlet design parameters discussed above, several other factors may significantly influence the air induction system design process. These additional considerations are listed below:

- Vehicle/Engine Radar Cross Section
- Air Induction System Impact on Vehicle Aerodynamics
- Inlet Pressure Margin
- Combustor Entrance Profiles
- Combustor Pressure Oscillations
- Inlet Fabrication Cost
- Inlet Weight

RECOMMENDED INLET DEVELOPMENT PLAN

The Marquardt Company has conducted inlet design/performance studies (including inlet model wind tunnel testing) for several advanced ramjet powered missiles. In the conduct of these design/development studies, a preferred or recommended inlet development plan has emerged.

The basic elements of this plan are presented below:

1. Establish inlet performance/design requirements.
2. Perform computer-aided inlet analysis and design studies.
3. Conduct inlet/vehicle system performance trade-off studies.
4. Conduct inlet wind tunnel test program:
    - Installed Tests
    - Isolated Tests
    - Flow Field Tests
5. Conduct vehicle force and moment wind tunnel test.
6. Estimate engine/vehicle system performance.

INLET SUBCRITICAL STABILITY/BUZZ

BACKGROUND

Virtually every inlet designer has experienced the phenomenon of inlet instability, commonly referred to as buzz, in the development of a high performance supersonic inlet. D. D. Wyatt in his excellent paper titled "A Review of Supersonic Air Intake Problems" (Reference 1) described inlet instability as follows:

> "Generally the supercritical flow regime of supersonic intake systems ischaracterized by a steady flow discharge rate. In some cases there are nonstationary oscillations but these are generally of such a low order of amplitude that serious structural or engine operation problems are unlikely. It is probable that these low-order oscillations arise from unsteady boundary-layer separation in the subsonic diffuser. In many intake designs, however, the steady flow breaks down in the subcritical regime. The terminal shock wave undergoes violent excursions in position from well ahead of the cowl to far down in the subsonic diffuser. This phenomenon is accompanied by severe fluctuations in mass flow and pressure recovery."

We believe this description is too good to be improved upon. During recent development of a high performance, dual aft mounted, two dimensional inlet, we installed a small, flush mounted, high frequency response, piezo electric static pressure transducer in the diffuser. A representative pressure trace from this test series is presented in Figure 34. In this test subsonic diffuser back pressure was increased (throttle plug movement) until buzz was experienced. Figure 1 clearly shows the noise output of the inlet normal shock system during "steady state" operation and the large amplitude pressure oscillations associated with classical "buzz". Thus Figure 34 clearly supports Wyatt's buzz description.

inlet instability with relatively little success. In reviewing the inlet literature there are data for a few inlet configurations which indicate some degree of stable subcritical operation, particularly at the lower Mach numbers ($M_0 \leq 2$). By and large, through, the approach taken has been to design a high performance inlet (which generally has little or no stable subcritical operation) and to avoid subcritical operation by providing an inlet supercritical operating mode insured by a shock position control. This control either limits fuel flow to the engine or opens up a bypass door downstream of the inlet minimum flow (throat) section. Such approaches are common in supersonic liquid-fueled ramjet and turbojet applications, respectively.

Recent impetus to provide a margin of stable subcritical inlet operation has come from the following sources: (1) In liquid-fueled systems, cost reductions could be achieved if the shock positioner control could be eliminated. (2) The development of the solid fueled ducted rocket (ramrocket) for tactical operations has indicated a possible need for some margin of subcritical operation. There is current interest in a throttleable solid fuel gas generator, however, the propellant flow rate will not be controllable to the same extent nor for the same reasons as the liquid system and, in addition, the flow rate is subject to large variations as a function of the gas generator soak temperature (π_K effects).

A third reason for reviewing the possibility of subcritical operation is shown in Figure 35. The dotted line represents a typical pressure recovery-airflow characteristic of a high performance inlet. The critical pressure recovery is point A; however, due to the lack of subcritical stability, an inlet margin is provided such that the inlet operates at point B. Now, if an inlet providing subcritical stability could be provided with a critical pressure recovery equal to the derated recovery of the high performance inlet (as shown by the solid lines in Figure 35), comparable internal performance and thrust would be generated. A brief look at the trade-offs between high performance and alternate inlet approaches suggest that, in order to be attractive, the alternate inlet should provide a critical pressure recovery within 10% of that of the conventional inlet. The amount of stable subcritical stability required is not well defined but probably should be in the range of 10%-20% in terms of capture airflow at the design Mach number. Due to the airflow matching characteristics of typical ramjet engines, subcritical stability is required mostly at the lower Mach numbers of the flight envelope. At the higher flight speeds the inlet generally operates with increasing amounts of supercritical operation unless a variable geometry exit nozzle is employed. Can inlets with a large measure of subcritical stability be developed? The answer is not clear as discussed below.

SOURCES OF INSTABILITY

The sources of instability are generally well known and are discussed in the literature. Ferri and Nucci in Reference 3, for example, explained a mechanism for buzz by the presence of a vortex sheet entering the inlet. Daily (Reference 4) attributed instability to choking on one side of the vortex sheet in the throat or minimum flow area of the inlet. Trommsdorff in Reference 5 noted that a strong expelled shock, during subcritical operation, could cause boundary layer separation which could alternately choke and unchoke the inlet throat. Ferri and Nucci also discussed the possibility of boundary layer separation from the inner cowl rather than the centerbody. Orlin and Dunsworth, in Reference 6, present two inlet stability criteria. They argue that if either of these criteria are exceeded, inlet buzz will occur. However, in order to make predictions as to when instability will occur, a knowledge of the flow field downstream of the expelled shock and on each side of the vortex sheet is required. Orlin and Dunsworth's stability criteria will be presented later in this paper (lecture).

INLET LITERATURE SURVEY

The following paragraphs of this paper (lecture) present a brief and highly selective survey of material that appears in the literature pertaining to the achievement of subcritical stability in supersonic inlets, including comments given either to explain the cause of the instability or means of alleviating it.

Boundary Layer Separation

Many researchers report that boundary layer separation on the centerbody (compression surface) reduces the subcritical stability margin and/or initiates buzz. The NACA, in 1953, designed and tested side inlets suitable for application to high performance aircraft. These inlets were designed for Mach 1.88 and 2.93 and were tested with various types of boundary layer removal systems. The inlets were half of an axisymmetric design mounted on a flat plate to generate a boundary layer approaching the inlets to simulate that generated on the fuselage. The cone half-angles were 25 and 30 degrees for the Mach 1.88 and 2.93 designs, respectively. Figure 36 presents a sketch of the cowl-lip scoop boundary layer removal system. It will be noted that the inlet centerbody was mounted flush to the flat plate. The data in Reference 7 indicates significant improvement in critical pressure recovery, peak pressure recovery, and subcritical stability when the height of the boundary layer scoop shown in Figure 36 was increased above the boundary layer thickness generated on the approach flat plate. These test results are reproduced in Figure 37. At the highest scoop heights tested the Mach 2.93 design achieved about 8.4 percent stable subcritical margin whereas the Mach 1.88 design achieved about 25 percent margin. With the conical compression surface mounted on a flat plate, the circumferential pressure gradient tends to direct the boundary layer off the cone toward the flat plate and the cowl lip scoop thus providing an effective boundary layer removal system. The test data of Reference 7 illustrates that effective boundary layer control upstream of the inlet throat delays the onset of instability related to boundary layer separation.

Project Rigel Inlet Development Experience

In the early 1950's a series of axisymmetric inlet development tests were conducted in support of the Rigel program. This ramjet powered test vehicle was designed for cruise at Mach 2.0. In this development program inlets were designed and tested with design Mach numbers of 2.0, 2.3, and 3.85. The salient design characteristics and subcritical stability performance of these inlets is summarized in Figure 38.

Inlet subcritical stability test data often follow the trend shown in Figure 39; inlet subcritical stability is minimum or nonexistent at the inlet design Mach number but increases significantly when the inlet is operated at less than design Mach number. The Rigel test data presented in Figure 38 generally follow this data trend. This subcritical stability data trend is one reason why inlets are often designed for a higher Mach number than the ramjet takeover Mach number.

Figure 40 is presented to show the effect of boundary layer bleed on the cone surface ahead of the cowl. These data are for the Mach number 3.85 inlet when tested at Mach 1.92. It is clear that boundary layer bleed significantly improved both critical pressure recovery and subcritical stability.

It is noted that all of the Rigel inlets were of the mixed compression type. Therefore, at the Mach 1.66 test condition, these inlets operated unstarted (choked inlet). We believe this contributed to their large subcritical stability margins but reduced total pressure recovery at this test condition.

University of Minnesota/R. Hermann's Supersonic Inlet Research

Rudolph Hermann, in his inlet textbook (Reference 11), reported the test results of an axisymmetric mixed compression inlet designed for Mach 3.0. The inlet had a half-cone angle of 30 degrees with a 9.2 percent internal contraction and an internal cowl angle of 21.7 degrees (flow aligned). The pressure recovery-capture area data for test Mach numbers of 2.0 and 3.0 are shown in Figure 41. When tested at the design condition, $M_0 = M_D = 3.0$, the inlet had zero subcritical margin. However, when tested at Mach 2.0, the inlet was unstarted (choked throat), and a 17 percent stable subcritical margin resulted. This represented only the last data point tested and thus the margin may have been greater than 17 percent. Hermann observed, that for an inlet operating unstarted, if the expelled shock wave becomes unstable it can only oscillate between an upstream position and the supercritical expelled position. This is because as the shock moves downstream a position is reached where the inlet throat becomes choked. This prevents further motion of the shock such that it cannot enter the cowl therefore the magnitude of the pressure variation is small.

It is noted that, for the inlet tested by Hermann, the triple point (origin of the vortex sheet) is outside the cowl lip at $M_0 = 2.0$ for supercritical and critical operation. As the inlet is throttled, the vortex sheet may cross the cowl lip but this will occur at large values of subcritical operation.

At $M_0 = M_D = 3.0$, the inlet operates in a mixed compression mode and the triple point crosses the cowl lip as the inlet is throttled. The vortex angle at the triple point is computed to be 4.5 degrees compared to the cowl lip internal angle of 21.7 degrees. This misalignment (16.2 degrees) is thought to contribute to the lack of subcritical stability observed at Mach 3.0.

COMPRESSION RATIO LIMITS ANALYSIS

Orlin and Dunsworth in 1951 published a report on criterion for flow instability in supersonic diffuser inlets (Reference 6). Stated briefly one of their conclusions was "The parameter determining the flow stability through a supersonic diffuser is the rate of change of inlet static pressure (at the cowl station) with mass flow. Stable subcritical flow occurs in the region of operation for which dP_1/dA_0 has negative values and the stability limit is reached when dP_1/dA_0 becomes equal to zero."

Two separate conditions lead to $dP_1/dA_0 = 0$ and hence to instability. As the inlet mass flow is reduced, the slope of the inlet total pressure curve with airflow may be negative, zero, or positive depending upon Mach number and inlet geometry. Continuity relations between the freestream and cowl station may be written to show that if the slope of the pressure recovery curve is negative or zero, the slope of the static pressure will be negative. If the slope of the pressure recovery curve is positive by a given amount, the slope of the static pressure curve will go to zero. Figure 42 presents an example of zero slope instability.

The second condition leading to instability is the reaching of a compression limit.* The following sketch is taken out of Reference 6 to illustrate this point. It was assumed that the static pressure across the cowl station CLB was
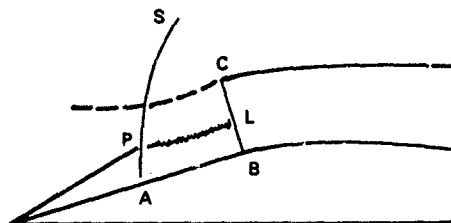
uniform. Through segment CL the total pressure P_{TO}' is essentially that associated with a normal shock at the local freestream Mach number M_0. The pressure recovery through segment LB in the sketch is somewhat higher than P_{TO}', having passed through an oblique shock and a strong shock at a Mach number less than M_0. In this sketch if the static pressure at the cowl station should equal or exceed the total pressure P_{TO}' the flow across CL will stagnate and require flow reversal (hence instability). Figures 43 and 44 present examples of compression limit instability. In these figures the term control pressure is equal to $P_{TO}'/\Gamma_{T_\infty}$.

Figures 43, 44 and 45 demonstrate that Orlin and Dunsworth instability criteria has merit. However, its value is limited unless an analytical technique is available to calculate the variation of total pressure recovery and cowl pressure as a function of airflow.

Marquardt has used a simplified procedure using the equations of continuity combined with assumptions of the expelled shock shape, to compute cowl pressure with variations in inlet airflow (A_0). This technique is tedious and approximate at best. With the rapid advances being made in computational aerodynamics, perhaps a good analytical model can be developed.

RECENT MARQUARDT TESTS

In 1974 Marquardt tested an axisymmetric inlet which operated in the unstarted mode at its design Mach number of approximately 2.0. Ferri suggested this design approach in 1958 (see Figure 45 and Reference 1). The subcritical stability of this inlet was excellent; however, its total pressure recovery was reduced when compared to high performance inlet designs.

Using the design philosophy of this inlet, its design Mach was increased to 3.0. The subcritical stability of this inlet, at its design point, was zero. Study of the test data and shadowgraphs, supported by analysis led to the following conclusions.

   1.   The achievement of stable subcritical operation becomes more difficult as the design Mach number is increased. The reasons for this increased difficulty are two-fold, namely, (1) the increased tendency for shock-induced boundary layer separation on the compression surfaces, see Figure 46, and (2) the inlet compression limits are more easily broached as the design Mach number is increased.

   2.   There is evidence that the entrance of a vortex sheet into the inlet is not of itself sufficient to cause inlet instability. There is evidence, however, that a highly negative angled vortex at the lip may cause boundary layer separation from the internal cowl lip. This situation can occur only at Mach numbers equal to the inlet design Mach number when the triple point is at or near the lip. At Mach numbers above the design Mach number the triple point is below and away from the inlet lip. At Mach numbers below the design Mach number the inlet must spill considerable airflow before the vortex sheet crosses the inlet lip. As the expelled shock moves forward, shadowgraph and schlieren photographs indicate that the vortex sheet angle rapidly departs from the two-dimensional value which must exist at the triple point. In the case of axially symmetric flow the vortex sheet angle appears to approach that of an axially symmetric flow field streamline. Thus, downstream of the triple point the vortex sheet angle is positive. It is thought that the angle of the vortex sheet relative to the internal cowl angle is important, with small displacements in these angles having less tendency for creating separation from the cowl lip. This observation leads to the conclusion that the internal cowl should not be flow aligned at the design Mach number as is done in many conventional inlet designs. Rather, the cowl should be aligned to produce a slight positive angle of attack with respect to the vortex sheet that results when the inlet goes subcritical at its design Mach number. In addition, it may be found that cowl bleed could enhance subcritical stability for those cases where internal cowl boundary layer separation is a factor.

   3.   The Orlin and Dunsworth inlet stability criteria were applicable to the Mach 2.0 and 3.0 designs. This provided valuable insight into the design modifications required to improve inlet stability at Mach 3.0.

Modified Mach 3.0 inlet designs were tested with success. Inlet stability was achieved at the design Mach number, without the use of boundary layer bleed. However, the use of bleed improved subcritical stability and total pressure recovery. As expected, however, inlet total pressure recovery was reduced when compared to high performance inlet designs. Specific missile system performance trade-off studies are required to properly evaluate the merit of this type of inlet.

EARLY MARQUARDT EFFORTS AT BUZZ SUPPRESSION

As an outcome of an extensive review of available information in the field, Marquardt, in 1955, designed a buzz suppression device which could be applied to any axisymmetric supersonic inlet and which would leave supercritical operation unaffected. The device consists of two parts (see Figure 47).

   1.   An annular slot, flush with the inlet center cone, located ahead of the cowl lip.

   2.   A chamber formed by the hollow inner body of the inlet cone, which communicates with the slot and is otherwise closed.

The mode of operation of the device is that the chamber acts as a pressure reservoir which absorbs or counteracts the pressure and shock wave fluctuations characteristic of the onset of diffuser instability. The stabilizing effect on the expelled shock wave is illustrated in the schlieren photograph (Figure 48).

Aerodynamic models of two different inlets, a 50 degree cone and an isentropic spike, were tested over a range of conditions with and without the suppressor and the results were encouraging. Figure 49 shows the improvement achieved through the use of the device in early tests. Of particular interest was the relatively greater improvement at Mach numbers near design. Here, stability fell to very low values without the suppressor, but with the suppressor attached, stability increased.

The buzz suppressor was also tested in 1956 on a ramjet engine at Mach 2.2/7 degrees angle of attack test conditions. Since percent spillage could not be measured accurately in the particular installation employed, the indications are qualitative. However, the baseline engine, which could be made to buzz and blow out at .072 fuel-air ratio, remained buzz-free at .074 fuel-air ratio when the suppressor was attached.

A buzz suppressor patent (No. 3,046,733) was granted to The Marquardt Company in 1962. Figure 50 from this patent, indicates that the surge chamber volume was divided up into four separate sections "so that each space operates independently of the other at angle of attack."

Although the buzz suppression research briefly described above was highly encouraging, ramjet engine packaging requirements precluded its use. The ramjet air turbine driven fuel pump and fuel control were packaged into the centerbody of the early ramjet engines such as BOMARC. The use of a buzz suppressor has not been considered in recent years.

CONCLUDING REMARKS

The arguments for a supersonic inlet which possesses a large amount of subcritical stability are impressive. However, survey of the extensive experience in this research field leads to two important conclusions:

1. Inlet designs which feature subcritical stability, almost without exception, operate at critical total pressure recoveries significantly less than can be achieved with high performance/no stability designs.

2. Currently there is no analytical technique that can be used to design high stability inlets. The inlet designers' experience and the wind tunnel are the tools used to develop such inlets. This is an expensive and sometimes dangerous path to follow. The development of a new ramjet engine/flight vehicle is initiated assuming specific engine component efficiencies and operating characteristics. If it is initially assumed that a high stability inlet can be developed and later test results say stability cannot be achieved, program cancellation is a real consideration. Most engine/inlet designers, faced with this possible situation, usually specify high performance inlet designs that do not require subcritical operation to meet engine/flight vehicle performance requirements. If a high stability inlet is truly required, its performance must be convincingly demonstrated before initiation of the engine development program.

MULTIPLE AFT INLET PERFORMANCE

Multiple (four) aft-mounted inlet systems have been successfully used in several ramjet flight test vehicles and one operational missile system (see Figure 5). We believe the reasons for selection of this type of inlet system were as follows:

1. Vehicle packaging constraints did not permit use of a nose inlet system.

2. With a liquid fuel ramjet the increased shear contact area provided by four inlets dumping into a common combustor results in high combustion efficiency with a short length combustor.

3. It is logical to assume that the performance of a ducted rocket ejector is maximized through use of a large number of air inlets located uniformly around the periphery of a centrally located gas generator (this subject is discussed later in this lecture).

4. The flight vehicles were designed for operation at low altitude, therefore, angle of attack and/or yaw requirements were quite small.

As flight vehicle attitude and maneuver operating requirements increase, the demand for inlet operation at high angle of attack becomes a demanding requirement. What are the performance characteristics of a multiple aft inlet system at large angles of attack? Figure 15 presents the performance trends for an aft mounted inlet system. The performance of such a system, at angle of attack, is poor. The test data also indicate that a "+" inlet configuration is preferred to an "X" configuration.

Are these inlet performance trends supported by other test programs? Yes - Krohn and Triesch of DFVLR (West Germany) reported similar results. Their test data for an "X" and a "+" aft-mounted inlet system (half axisymmetric inlets) is presented in Figures 51 and 52. Study of these data lead to the same conclusions as discussed above. Krohn and Triesch data also shows extensive regions of reversed inlet flow.

The reasons for the poor angle of attack performance of an aft-mounted inlet system is well understood. With a vehicle operating at large angle of attack, the four inlets "see" significantly different flow fields. These flow field characteristics are summarized as follows:

1. The local Mach number and flow angle delivered to the bottom inlet are reduced when compared to free stream Mach number and angle of attack. These characteristics result in high inlet performance.

2. The airflow is accelerated around the vehicle forebody such that the local flow angle and Mach number delivered to the side mounted inlet is often larger than the flight vehicle angle of attack. With most inlets this flow field results in degraded inlet performance.

3. The local flow delivered to the top inlet is the real problem. An inlet located on the lee side of the vehicle forebody typically sees regions of flow separation, reduced total pressure and vortices. The twin vortices are particularly troublesome. The flow field characteristics on the lee side of an ogive forebody were experimentally mapped by Triesch. The results of this test program are presented in Figure 53. The presence of the forebody twin vortices are beautifully illustrated.

Aft-mounted inlet systems typically employ a single combustion chamber. Therefore, as engine back pressure is increased, the inlet operating at the lowest total pressure recovery (usually the lee side inlet) is driven critical and then subcritical/buzz. Under these conditions the inlet system spills air with a major loss in engine thrust and in severe cases, experiences inlet flow reversal. Flight operation under these conditions is not practical. What can be done to improve the situation?

Strakes have been used with some success in high performance aircraft. However, as discussed earlier in this paper (lecture), we believe that high performance ramjet powered vehicles, which typically require high angle of attack operation, should employ one or two inlets. If a single inlet is used, it is usually bottom mounted. High inlet performance has been demonstrated with chin (forward) and aft bottom mounted inlets. If two inlets are used, they are mounted approximately 45 degrees from the horizontal centerline.

It has been implied throughout this discussion that a bank-to-turn flight vehicle guidance/control system will be used in advanced ramjet powered missiles. With a bank-to-turn flight control system the inlet(s) typically experience only small angles of yaw/sideslip. Obviously, this results in high inlet performance. The use of a bank-to-turn flight vehicle guidance/control system has been demonstrated in several ramjet powered flight test/operational vehicles: (1) BOMARC A and ~; (2) Bloodhound MK1 and MK2; and ASALM-PTV.

The use of a bank-to-turn versus skid-to-turn flight control system in advanced ramjet powered missiles is currently controversial. Rocket powered missiles, almost without exception, employ a skid-to-turn control system. What are the factors that must be considered in the design of a bank-to-turn guidance system?

1. What flight control algorithms need to be developed?

2. Can these algorithms be packaged into small flight vehicles?

3. Will the flight vehicle aerodynamic time constants permit use of a bank-to-turn system at high altitude flight conditions?

4. What is the effect of radome slope error (aberration) on missile miss distance?

We believe the radome slope error argument is the key issue. High performance air-to-air missiles, with a small warhead, designed to attack a maneuvering airborne target are most vulnerable to this argument. However, it is again pointed out that the ramjet powered BOMARC and Bloodhound surface-to-air interceptor missiles employed bank-to-turn steering logic, were equipped with semi-active radar terminal guidance and were operationally deployed for many years. In fact Bloodhound MK2, after twenty years, remains in operational status with the Royal Air Force, the Swiss government and the Singapore Air Defense Command. BOMARC also continues in use as a high speed target vehicle for the U.S. Air Force.

The bank-to-turn versus skid-to-turn controversy continues and is sufficiently important that a major technical meeting, dealing only with this subject, will be held in September (1984 at The Johns Hopkins University/Applied Physics Laboratory. The meeting is being sponsored by the Guidance and Control Information Analysis Center/ITT Research Institute.

Ramjet inlet performance is usually documented at 5 degrees, and in some cases 10 degrees angle of yaw/sideslip. However, virtually no research in the United States has been directed to the development of high performance ramjet inlets which tolerate operation at large yaw/sideslip angles.

COMBUSTION DRIVEN PRESSURE OSCILLATIONS/INLET INTERACTIONS

Combustion driven pressure oscillations have been experienced in several small diameter liquid fuel and solid ducted rocket engines (ramrocket). These pressure oscillations have generally been experienced in two frequency regions. Low frequency oscillations typically occur in the 100 to 500 Hz range and high frequency oscillations in the 1000 to 3000 Hz range. A Power Spectral Density (PSD) analysis of a representative combustion induced pressure oscillation signal measured with a high frequency response piezoelectric pressure transducer is shown in Figure 54.

The high frequency oscillations, commonly referred to as screech, are typically the first and/or the second combustor tangential modes. This oscillation mode(s) generally increases combustion efficiency

Can the low frequency oscillation, generally the first or fundamental combustor longitudinal mode, occur at a frequency sufficiently low to "drive" the normal shock system of the ramjet inlet/diffuser? The NACA, in 1950, demonstrated that a supersonic inlet could be driven critical and into buzz by both combustion and mechanically produced pressure oscillations. In these tests it was observed that pressure oscillations reduced the diffuser exit static pressure, at critical operation, by one half the total amplitude of the oscillation (see Figure 55). In addition, it was noted that critical inlet operation, with pressure oscillations, occurred when the maximum instantaneous diffuser exit static pressure equaled the steady state (no pressure oscillation) critical operation diffuser exit static pressure. Liquid fuel ramjet freejet engine tests conducted in support of the Naval Weapon Center GORJE Program, in 1977, again convincingly demonstrated that large amplitude/low frequency pressure oscillations can drive the normal shock system of a supersonic inlet into buzz. Figure 56 presents an inboard profile of the GORJE test vehicle and Figure 57 shows the pressure oscillation/inlet buzz test data. Notice that steady state instrumentation indicates a pressure margin of 10% yet the inlet was driven into buzz by combustion induced pressure oscillations. The basic conclusion drawn from the NACA and GORJE engine tests (and more recent test programs) is that the inlet/engine designer must provide for an increased inlet pressure margin when combustion induced pressure oscillations are experienced during the development cycle of a new engine. This increased pressure margin requirement is especially critical at ramjet takeover conditions where ramjet inlet margins are typically small. Representative ramjet inlet pressure margins during a mid to high altitude flight trajectory is presented in Figure 58. To compound this increased inlet pressure margin requirement, the correlation of pressure oscillation data shows rapidly increasing amplitude as free stream total temperature (flight Mach number) is reduced (see Figure 59). In other words, the amplitude of the low frequency combustor induced pressure oscillations are maximum at ramjet takeover conditions.

The combustion induced pressure oscillation problem is being actively researched by a number of skilled investigators. The purpose of this paper is not be present a treatise on the subject but rather to relate the importance of this combustion phenomena to the inlet designer.

It is also of interest to the inlet designer that limited ramjet engine freejet test data strongly suggests that the boundary layer bleed system of a supersonic inlet sharply attenuates the combustor pressure oscillations that reach the inlet throat/normal shock system (see Figure 60). Obviously, this acoustic attenuation process reduces inlet pressure margin requirements. This attenuation effect is not well understood and should be further studied.

DUCTED ROCKET EJECTOR PERFORMANCE WITH SINGLE, TWIN AND FOUR INLET SYSTEMS

BACKGROUND

The combined cycle engine combines the best features of the rocket and ramjet engines into a lightweight, efficient power plant. This type of propulsion system is particularly well suited to acceleration type missions. Three prime candidate missions for this type of engine are (1) surface-to-air missiles, (2) air-to-air missiles, and (3) air-to-surface missiles.

Today, there is strong interest in the ducted rocket type of combined cycle engine. This engine employs a solid fuel gas generator whose flow rate is fixed, or in more advanced designs, variable. This type of propulsion system is also commonly referred to as a ramrocket or a rocket-ramjet engine.

With prior ramjet and solid fuel rocket/gas generator development experience, the key technology areas in developing a ducted rocket engine are the ejector subsystem and the ramburner (afterburner). The ejector performance parameters of primary interest are the jet pumping ratio and the mixer length required to achieve full mixing of the secondary and primary flows. Jet pumping ratio is defined as the ratio of the flow total pressure at the mixer exit/combustor entrance to the air total pressure at the diffuser exit/ejector entrance. With ejector systems designed for application to ducted rocket engines, this pressure ratio can be quite high and can exceed one, thus, explaining the use of the term "jet pumping ratio".

It is logical to assume that the performance of a ducted rocket ejector system (total pressure ratio and required mixing length) is maximized through use of a large number of secondary air inlets located uniformly around the periphery of a centrally located gas generator. In recent years much interest has centered on use of a symmetric four aft inlet system. This geometric arrangement offers high ejector performance; however, there are airborne missile applications which will not permit the use of this design approach (see Figure 61). Shown in this figure are pylon and body mounted external carriage launch aircraft/missile installations and a semi-submerged launch aircraft installation. These launch aircraft/missile installations obviously lend themselves to twin and single inlet configurations.

Inlet performance also dictates consideration of single and twin inlet/air induction systems. The four aft mounted inlet system has been successfully employed in several flight research and operational missile systems. This system functions well when vehicle angle of attack and yaw requirements are small. However, advanced ramjet powered tactical missile systems under study today (particularly Air-To-Air Missiles) emphasize high angle of attack operation (see Figure 6). Under these operating conditions, the performance of the multiple (four) inlet system is poor (see Figure 62). In marked contrast, single and two inlet systems, when located on the lower surface of the vehicle forebody, feature significantly increased inlet total pressure recovery and capture area ratio with increasing angle of attack. These performance characteristics are well matched to advanced tactical missile system requirements. As a consequence of the launch aircraft/missile installation and inlet performance arguments presented above the basic objective of the experimental program described in this paper was to compare ejector/mixer performance of twin and single inlet systems as compared to a symmetrical four aft

EJECTOR TEST PROGRAM

Previous Marquardt testing with the liquid fueled Ejector Ramjet Engine (also a combined cycle engine) showed that subscale aerodynamic tests (no combustion) produced ejector design criteria/performance which were largely corroborated by later combustion tests. This type of testing is low cost and lends itself to a highly flexible test program. Therefore, in this exploratory multiple inlet ducted rocket ejector test program, a model aerodynamic test program was conducted.

The ejector test set-up used in this program is shown schematically in Figure 64 and Figure 65 is a photograph of the test set-up. Two ejector test items were fabricated. One test item simulated a four aft mounted inlet configuration while the second test item simulated either a twin or single inlet configuration. Both ejector test items were designed to accept removable ejector heads. This feature permitted variations in ejector nozzle geometry including evaluation of single and multiple ejector nozzles. Only sonic ejector nozzles were evaluated.

For this aerodynamic test program the ability of several inert gases to simulate the solid fuel gas generator efflux were compared. These gases were nitrogen, carbon dioxide, helium, ambient temperature air and heated air. No single gas met all simulation criteria. Heated air was selected as the best compromise. A SUE® burner was used to heat the primary air; the burner fuel was gaseous hydrogen. Ambient temperature air was used as the secondary test fluid.

A simulated ramburner or mixer/combustor was located downstream of the ejector test item. The length of this simulated combustor could be changed by insertion or removal of cylindrical spool sections. A large number of static pressure taps were located in the mixer/simulated combustor test hardware. In addition, two total pressure rakes were located downstream of the ejector test item. Initial tests employed a fixed ramburner exit nozzle; however later testing employed a variable area exit nozzle (moving plug) to more properly simulate engine back-pressure effects. Representative ejector total pressure ratio data measured with use of the variable area exit nozzle are presented in Figure 66.

It has been substantiated by other test programs that, when jet mixing takes place in a constant area duct between fluids initially at very different pressure and velocity (or momentum ratio), the degree to which mixing approaches completion is indicated by the axial wall static pressure gradient. Where the gradient passes from positive to negative, mixing is essentially complete and the losses due to wall friction again dominate. Measured diffuser/mixer static pressure distributions for the four inlet configuration tested are shown in Figure 67. It is clear from the static pressure data that mixing is essentially complete two to three diameters downstream of the ejector. Additional test data showed that the required mixing lengths for the twin and single inlet configurations were slightly longer (see Figure 68).

Fifteen ejector nozzle/inlet configurations were evaluated in this test program. Testing emphasized the twin and single inlet configurations because data showed these configurations to be sensitive to ejector nozzle geometry. This was particularly true for the single inlet configurations. Representative twin and single inlet test data are presented in Figure 69. Ejector/mixer performance sensitivity to changes in ejector nozzle geometry is clearly evident. The ejector/mixer total pressure ratio performance measured in this test program is summarized in Figure 70. Data are shown for the four, twin and single inlet configurations with secondary to primary flow ratio as the primary test variable. Test data for the best performing ejector heads were used to construct this figure.

CONCLUSIONS

The major conclusion drawn from study of the experimental data and supporting analysis developed in this program is that a high performance, ducted rocket ejector/mixer subsystem can be developed using any number of well developed/well integrated inlets. However, it is noted that ejector mixer performance with twin, and in particular, single inlet configurations, is more sensitive to ejector nozzle geometry. Although not the subject of this paper, it is pointed out that the basic findings developed in this exploratory development program were largely corroborated in later ducted rocket combustion tests.

REFERENCES

1. Fabri, J. (Editor), "Air Intake Problems in Supersonic Propulsion", Published by Pergamon Press, London-New York-Paris - Los Angeles, 1958.

2. Oswatitsch, K. L. (Translation), National Advisory Committee For Aeronautics, "Pressure Recovery for Missiles With Reaction Propulsion at High Supersonic Speeds (The Efficiency of Shock Diffusers)", June 1947, NACA TM 1140.

3. Ferri, A and Nucci, L., National Advisory Committee for the Aeronautics, "The Origin of Aerodynamic Instability of Supersonic Inlets at Subcritical Conditions", 1951, NACA RM L50K30.

4. Daily, C. L., "Supersonic Diffuser Instability", Journal of Aeronautical Sciences, Volume 22, No. 11, 1955, pp. 733-749.

5. Trommsdorff, W., Durchgefuhrt in der Abteilung "Triebwerksaerodynamik" des Institutes fur Angewandte Gasdynamik der Deutschen Versuchsanstalt fur Luft- und Raumfahrt e.V, "Untersuchung an Triebwerkseinlaufgen", August 1964.

7. Piercy, T. G. and Johnson, H. W., National Advisory Committee for Aeronautics, "A Comparison of Several Systems of Boundary Layer Removal Ahead of a Typical Conical External - Compression Side Inlet at Mach Numbers of 1.88 and 2.93", 1953. NACA RM E53F16.

8. Orlin, W. J. and Bajek, J. J., The Marquardt Company, "Results of Series I Tests of a One-Quarter Scale Diffuser Model of the Marquardt Model C28-2.0 C1 Ramjet for the X55M-N6 Project Rigel Configuration 7 Missile at OAL During the Period 11 to 15 December, 1950", March 1951. Marquardt Report 5093.

9. Humenick, W., The Marquardt Company, "Results of Tests of a One-Quarter Scale Diffuser for the Marquardt Model C28-2.3A Ramjet at OAL, Daingerfield During the Period 19 to 23 March, 1951", June 1951. Marquardt Report 5150.

10. Humenick, W. and Doyle, A. F., The Marquardt Company, "Results of Tests of the Marquardt Model AM-17 Aerodynamic Model for the X55M-N6 Project Rigel Configuration 4 Ramjet at OAL During the Period 25 June to 6 July, 1951", October 1951. Marquardt Report 5159

11. Hermann, R., "Supersonic Inlet Diffusers and Introduction to Internal Aerodynamics", Published by Minneapolis-Honeywell Regulator Company, Minneapolis, Minnesota, USA, 1956.

12. Connors, J. F. and Meyer, R. C. National Advisory Committee for Aeronautics, "Design Criteria for Axisymmetric and Two Dimensional Supersonic Inlets and Exits", January 1962. NACA TN 3589.

13. Kuehn, D. M., National Aeronautics and Space Administration, "Experimental Investigation of the Pressure Rise Required for the Incipient Separation of Turbulent Boundary Layers in Two-Dimensional Flow", February 1959, NASA Memo 1-21-59A.
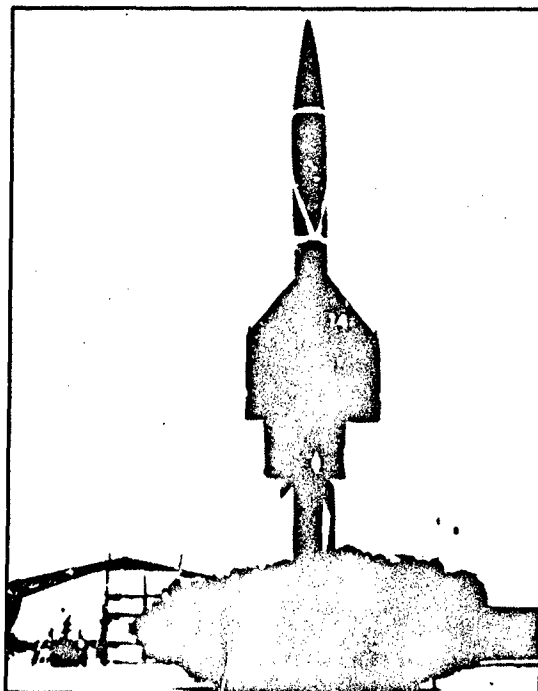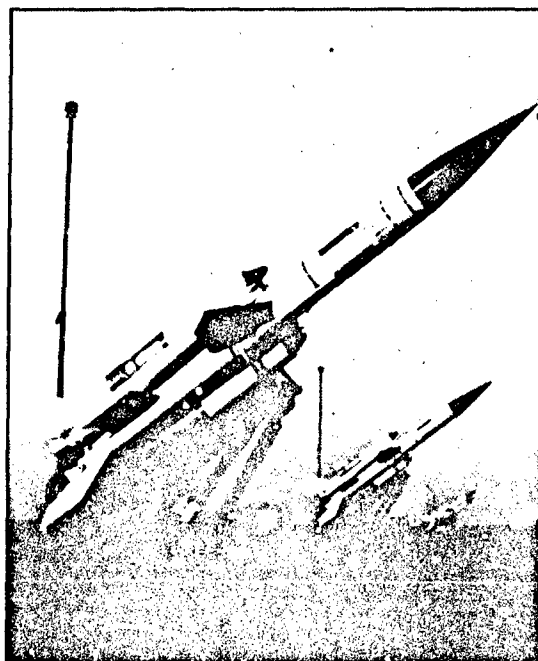
BOMARC
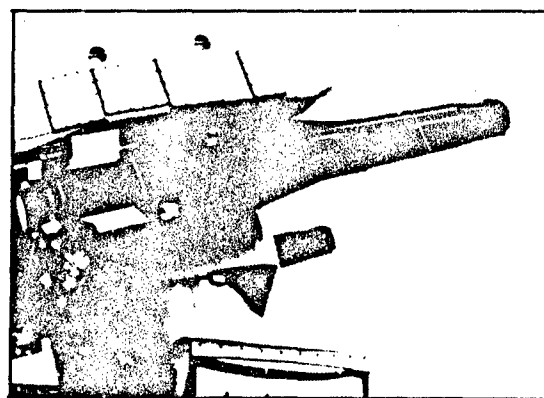SURFACE-TO-AIR INTERCEPTOR MISSILE
OPERATIONAL IN 1957
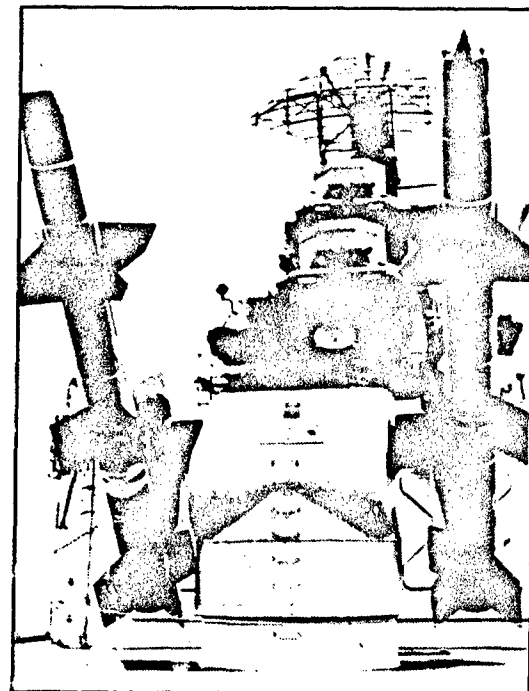
TALOS
SHIP LAUNCHED INTERCEPTOR MISSILE
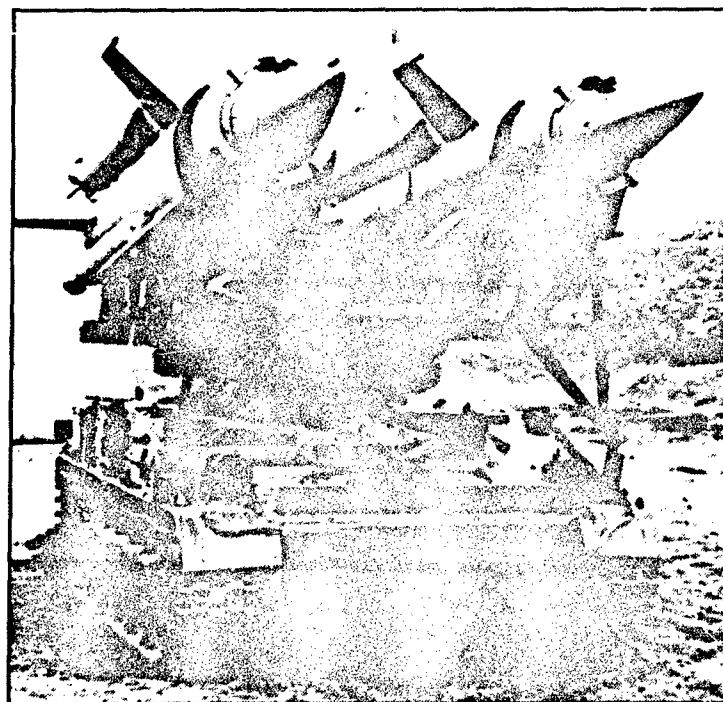OPERATIONAL IN 1959

FIGURE 1. OPERATIONAL U.S. RAMJET POWERED MISSILE SYSTEMS

BLOODHOUND MK1 & MK2
SURFACE-TO-AIR INTERCEPTOR MISSILE
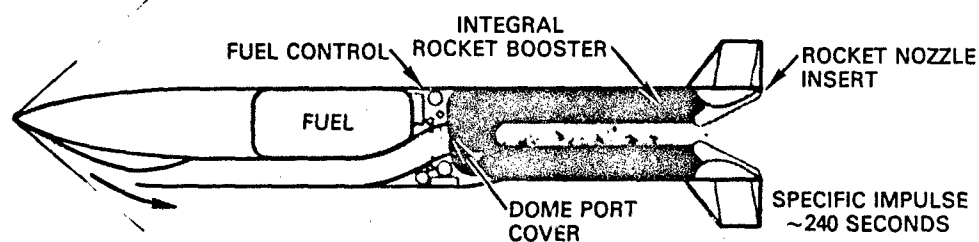OPERATIONAL 1959/1964

SEADART
SHIP LAUNCHED INTERCEPTOR MISSILE
OPERATIONAL IN 1975

2-15

SA-4 'GANEF
MOBILE SURFACE-TO-AIR INTERCEPTOR MISSILE
OPERATIONAL IN 1964 (JANE'S WEAPON SYSTEM)

FIGURE 3. OPERATIONAL USSR RAMJET POWERED MISSILE SYSTEMS

BOOST PHASE - The Integral Rocket-Ramjet is accelerated to ramjet takeover velocity by rocket propellant contained in the ramjet chamber.
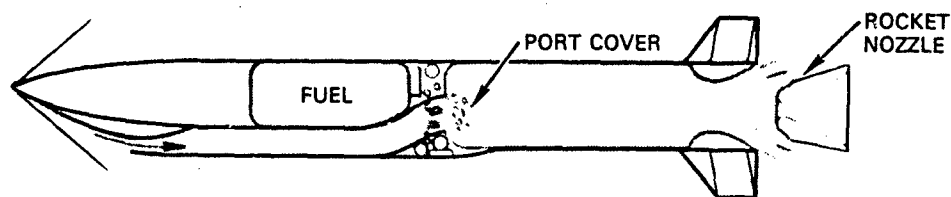
TRANSITION PHASE - Ejection of the rocket nozzle and port cover allows air to enter the combustor where the ramjet fuel is introduced and burned.
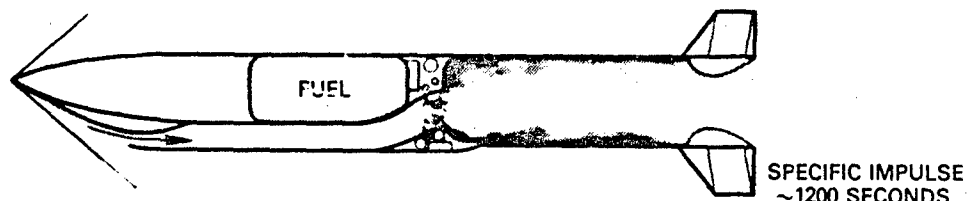
ACCELERATION AND CRUISE PHASE - On very efficient ramjet power, the missile can accelerate and cruise to its target
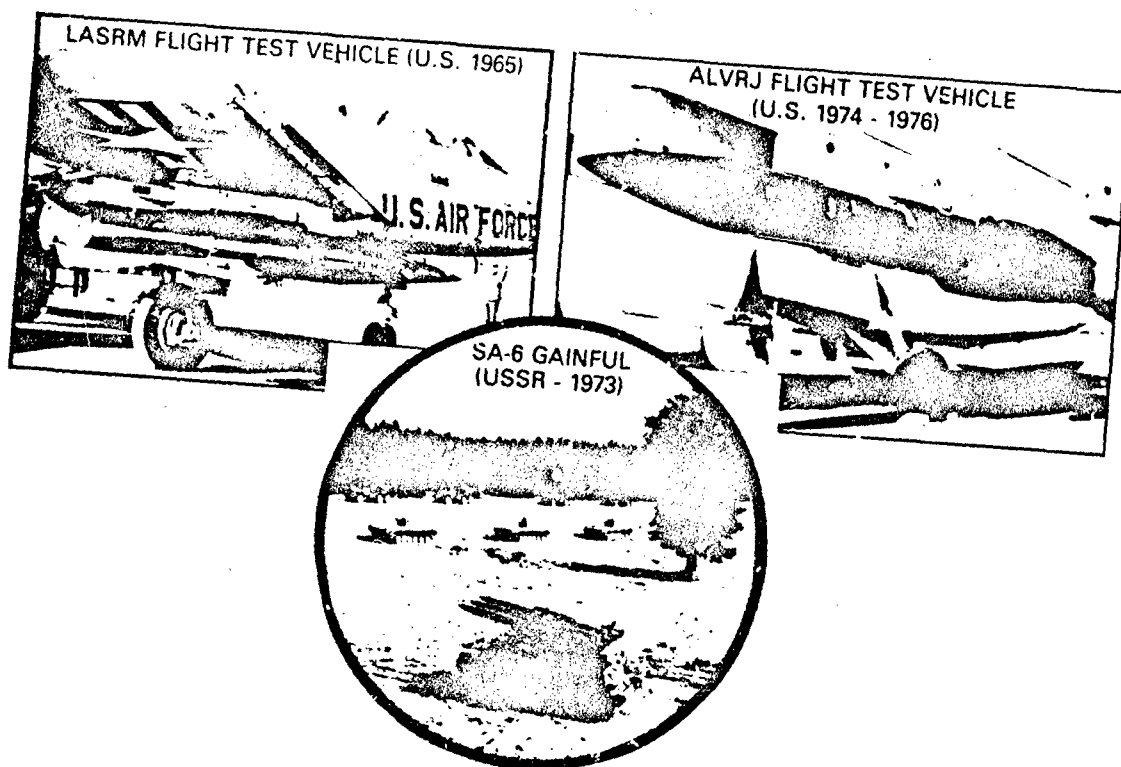
FIGURE 5. MULTIPLE AFT MOUNTED INLET/RAMJET PROPULSION SYTEMS

PT - TOTAL PRESSURE
M - MACH NUMBER
α - ANGLE OF ATTACK
A - INLET CAPTURE AREA
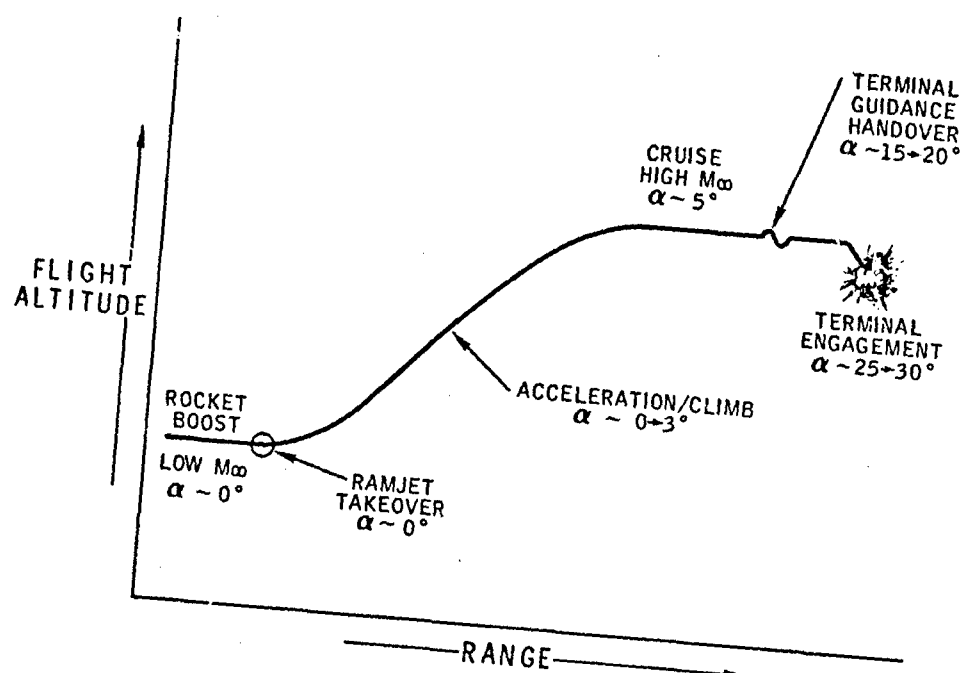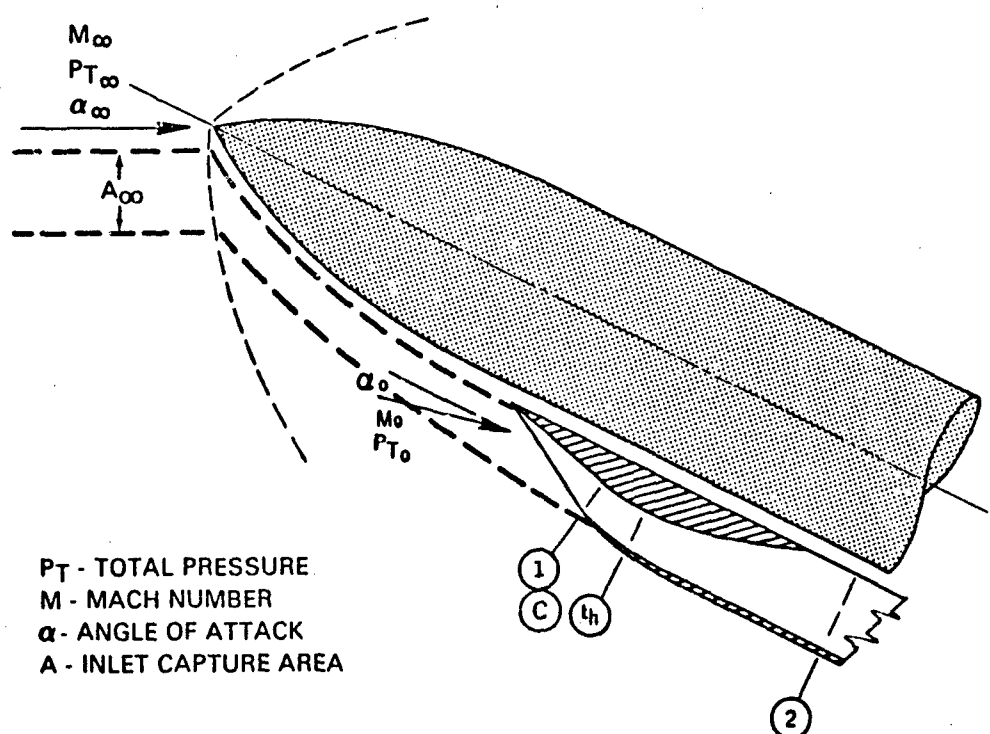
FIGURE 7. AIR INDUCTION SYSTEM STATION NOTATION/PERFORMANCE NOMENCLATURE
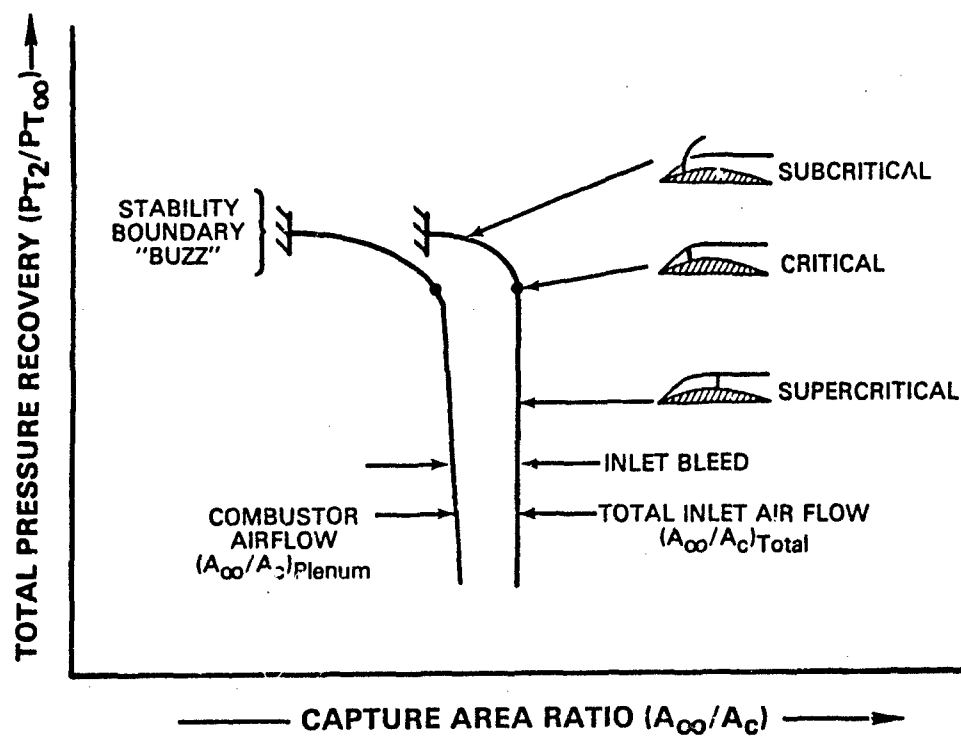
FIGURE 8. REPRESENTATIVE INLET PERFORMANCE CHARACTERISTICS
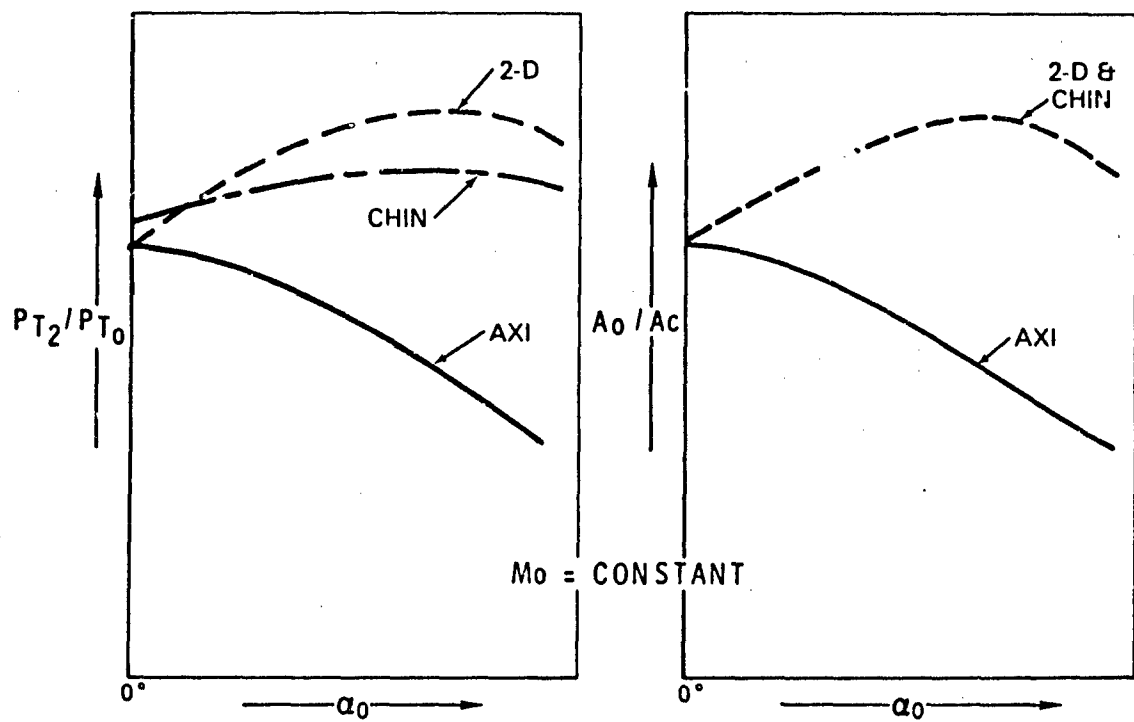
FIGURE 9. AXISYMMETRIC, TWO-DIMENSIONAL AND CHIN INLET PERFORMANCE (ISOLATED)
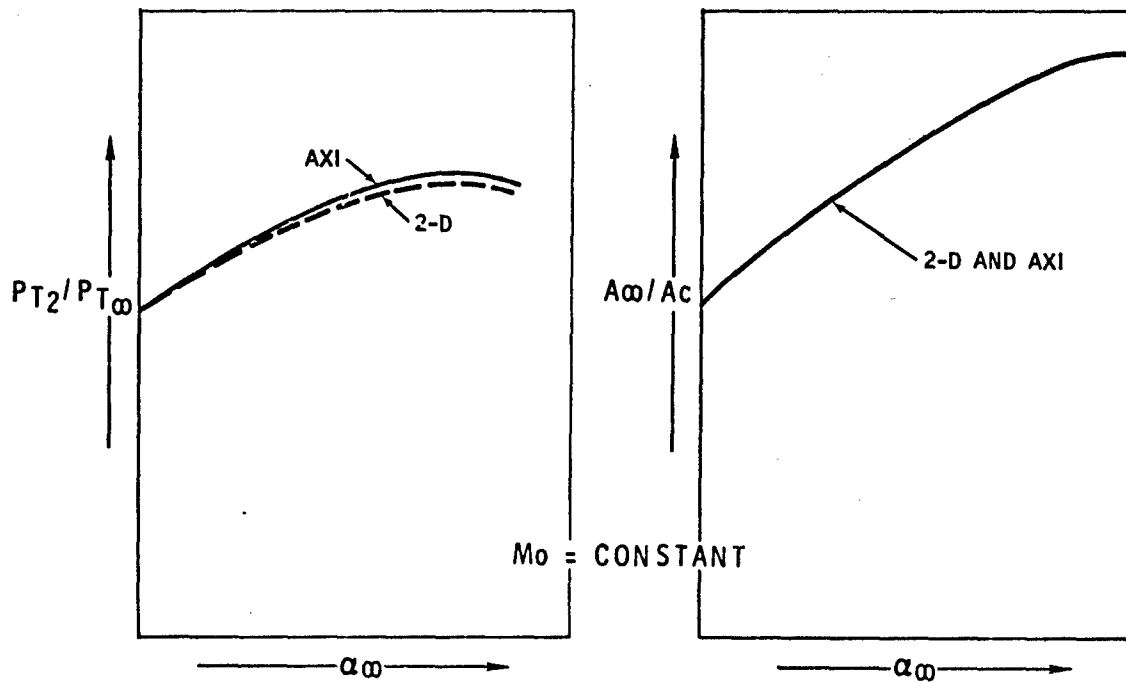
FIGURE 10. AXISYMMETRIC INLET PERFORMANCE - WING FLOW FIELD
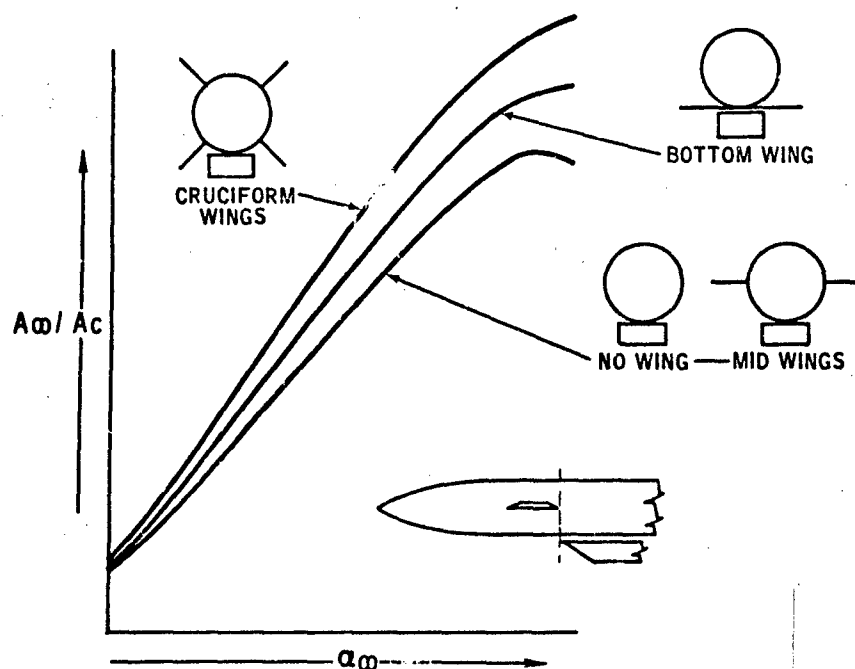
FIGURE 11. EFFECT OF WING ON INSTALLED CAPTURE AREA RATIO

ISOLATED TWO-DIMENSIONAL INLET
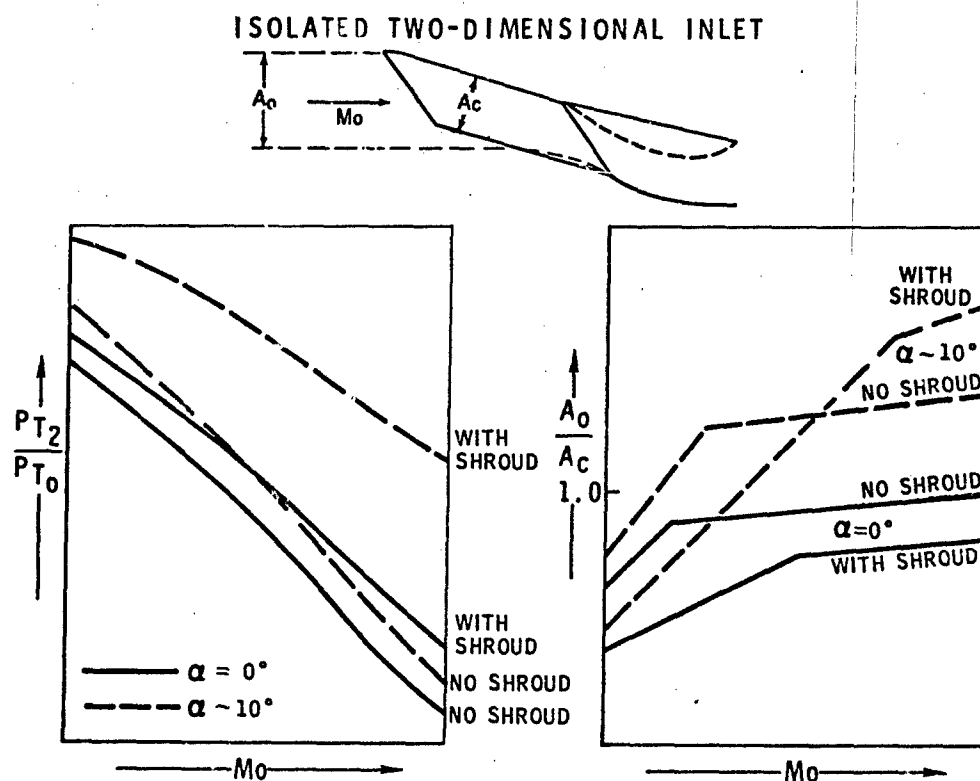
FIGURE 12. EFFECT OF PRECOMPRESSION SHROUD
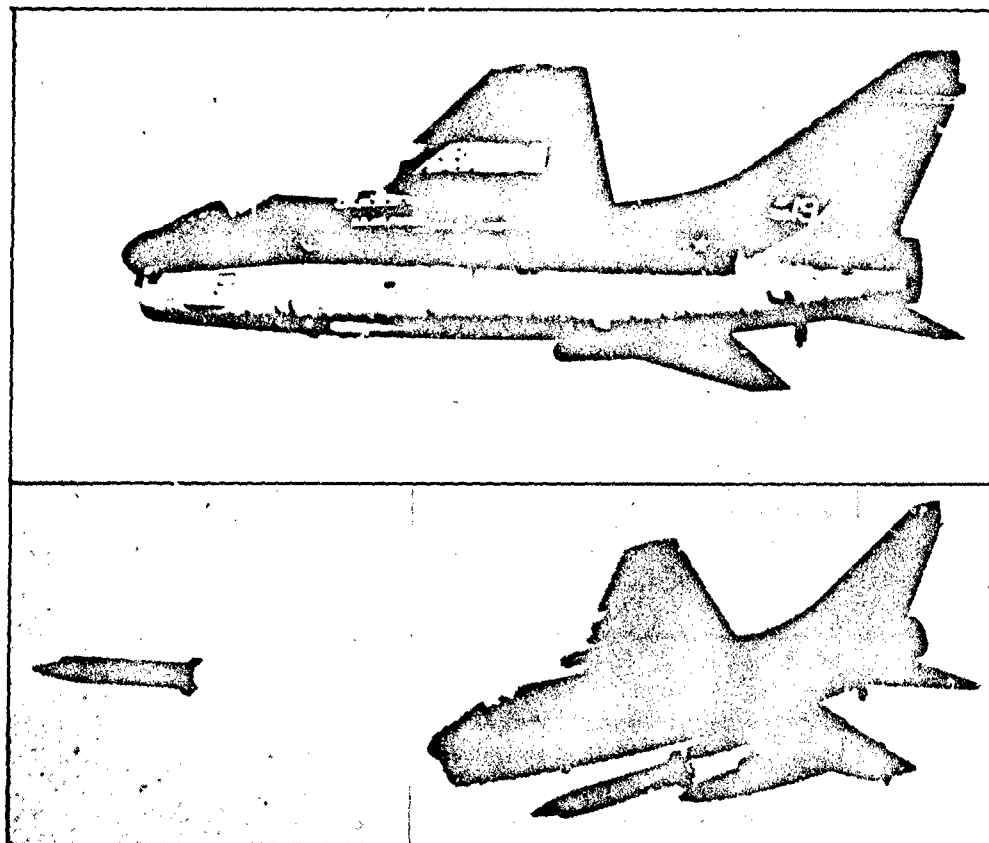
FIGURE 13. RAMJET POWERED FLIGHT TEST VEHICLE

GUIDANCE/FLIGHT CONTROL ELECTRONICS   PAYLOAD   RAMJET FUEL

RADOME

SEEKER

AIR INDUCTION SYSTEM

ROCKET BOOSTER/RAMJET COMBUSTOR
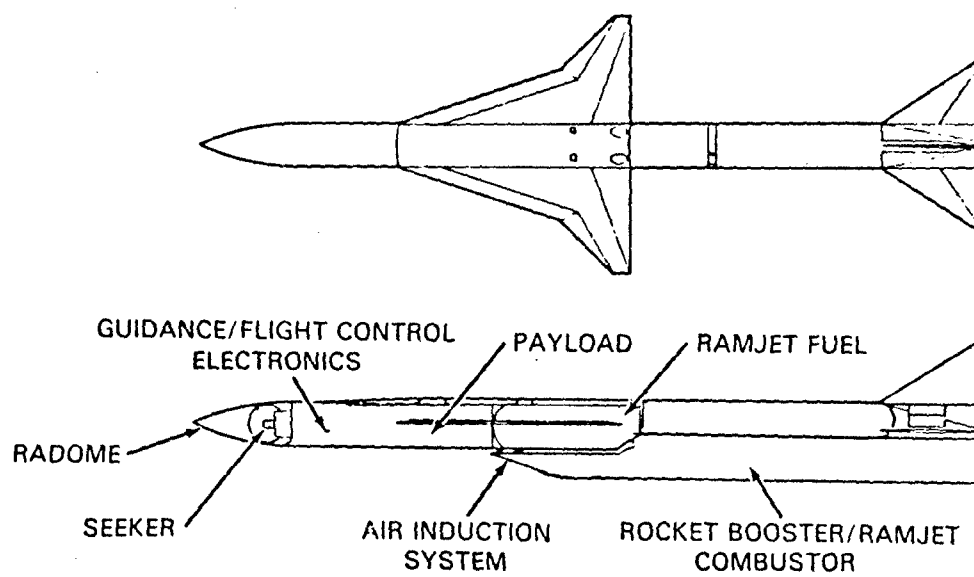
FIGURE 14. ADVANCED AIR-TO-AIR MISSLE DESIGN
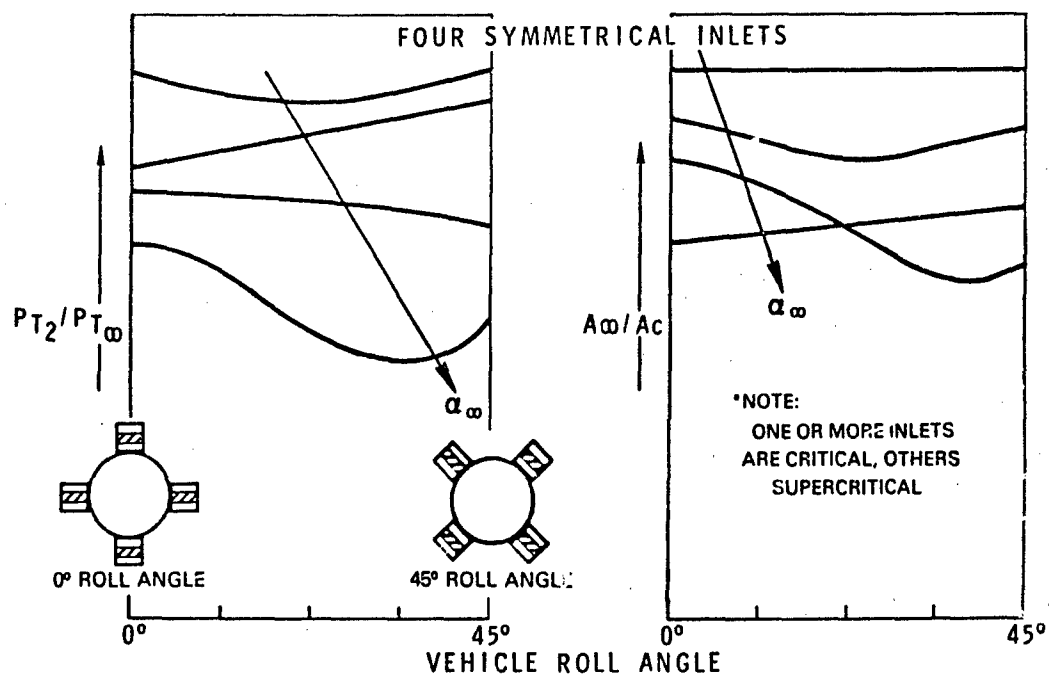
FIGURE 15. MULTIPLE AFT MOUNTED INLET SYSTEM PERFORMANCE
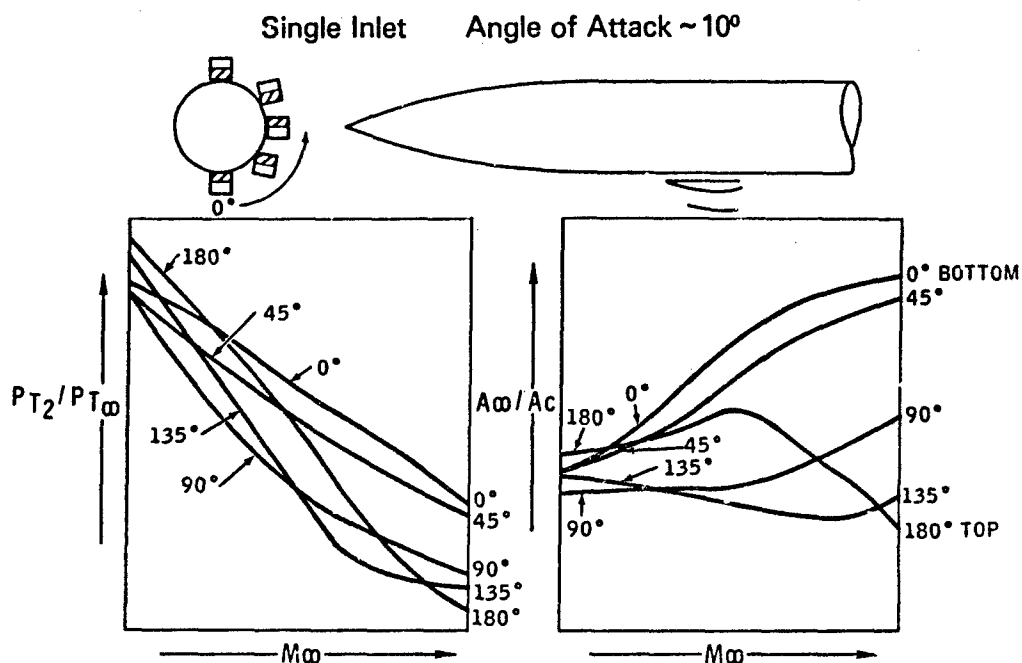
FIGURE 16. EFFECT ON INLET CIRCUMFERENTIAL POSITION
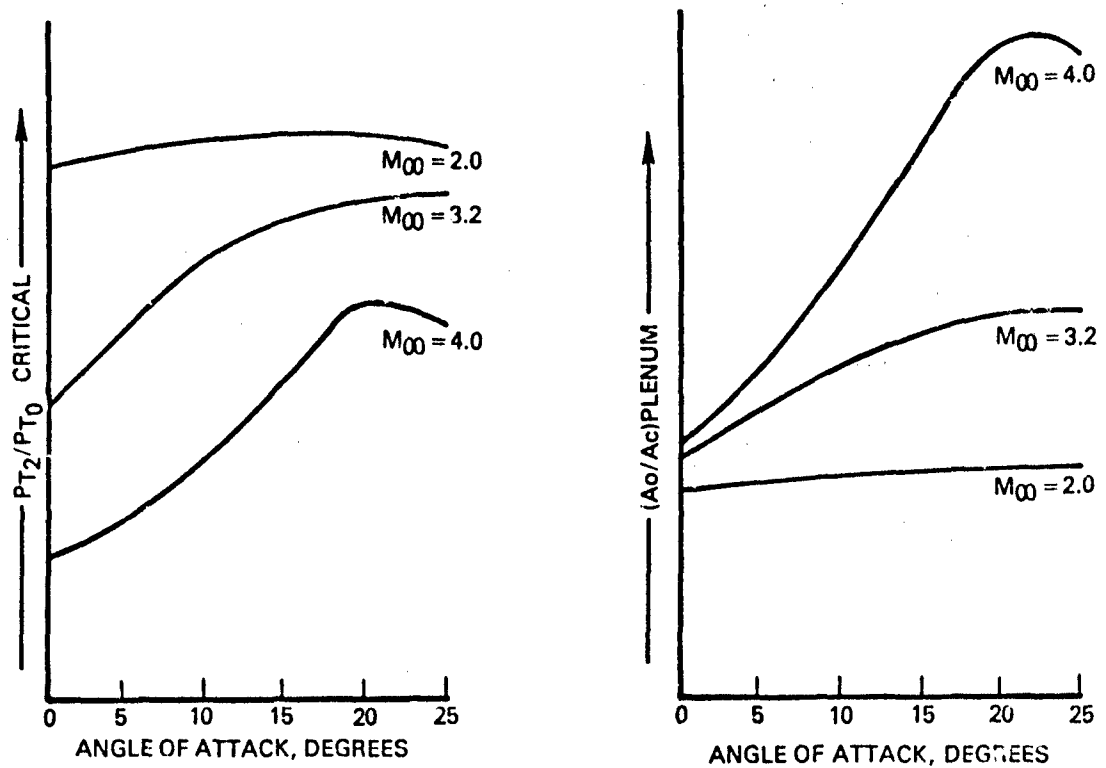
FIGURE 17. BOTTOM MOUNTED TWO-DIMENSIONAL INLET PERFORMANCE
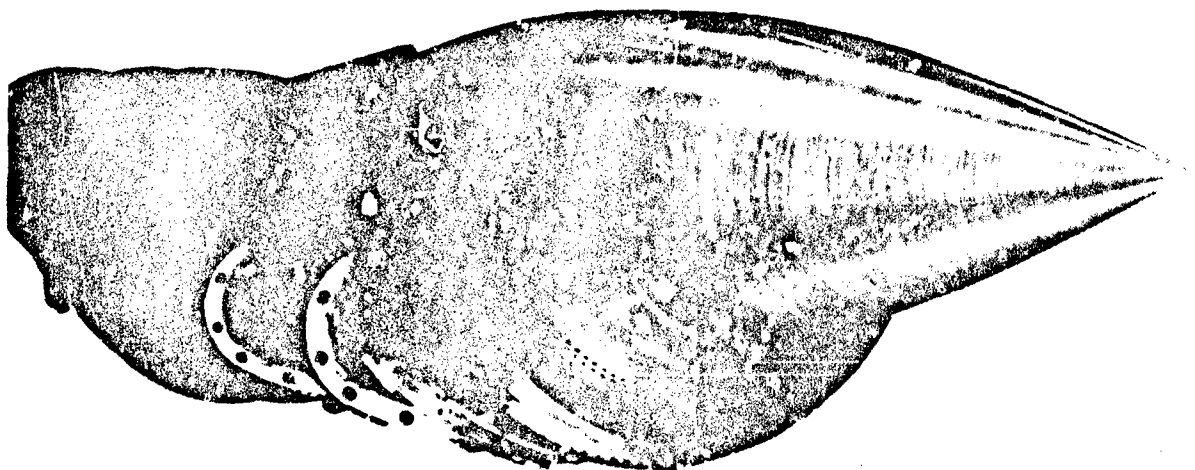
FIGURE 18. CHIN INLET WIND TUNNEL TEST MODEL
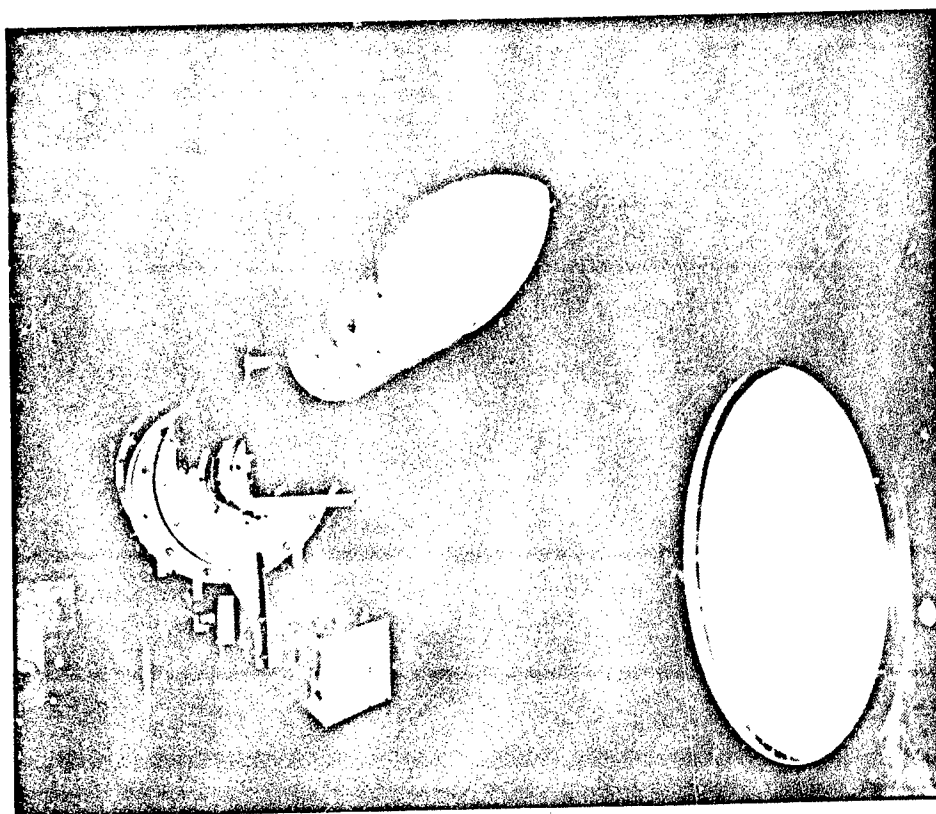
FIGURE 19. AFT SINGLE BOTTOM MOUNTED INLET TEST MODEL
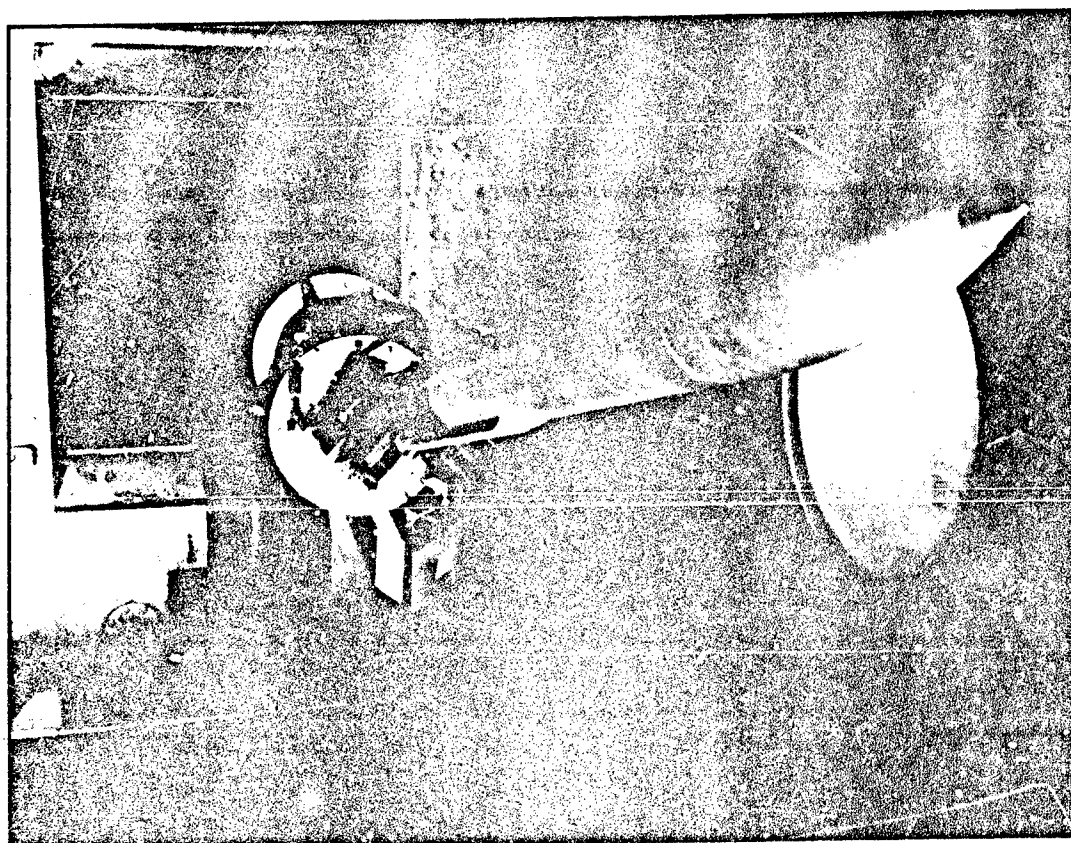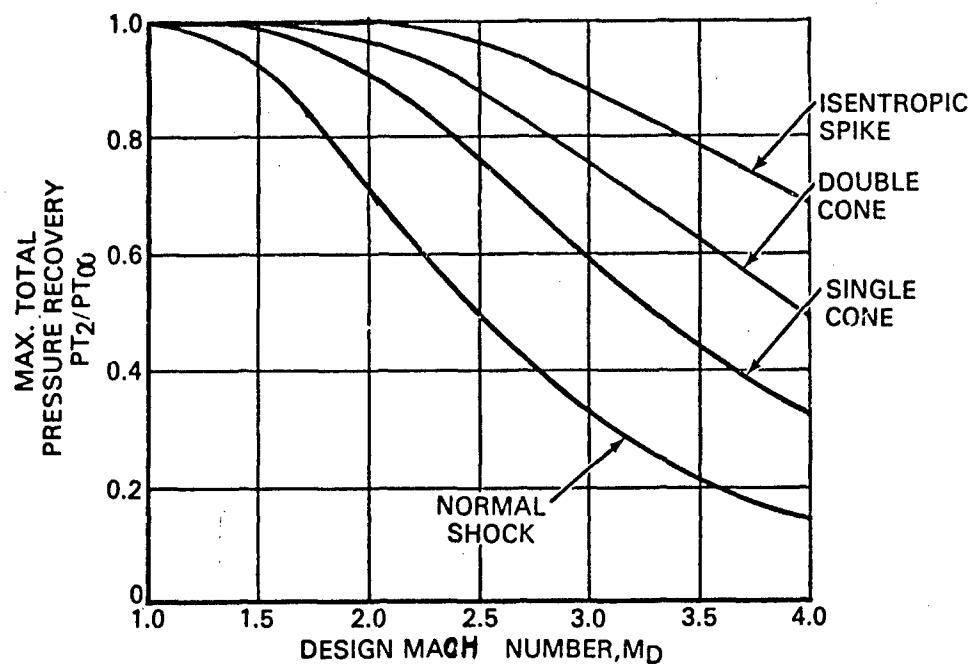
FIGURE 21. MAXIMUM TOTAL PRESSURE RECOVERY VERSUS DESIGN MACH NUMBER
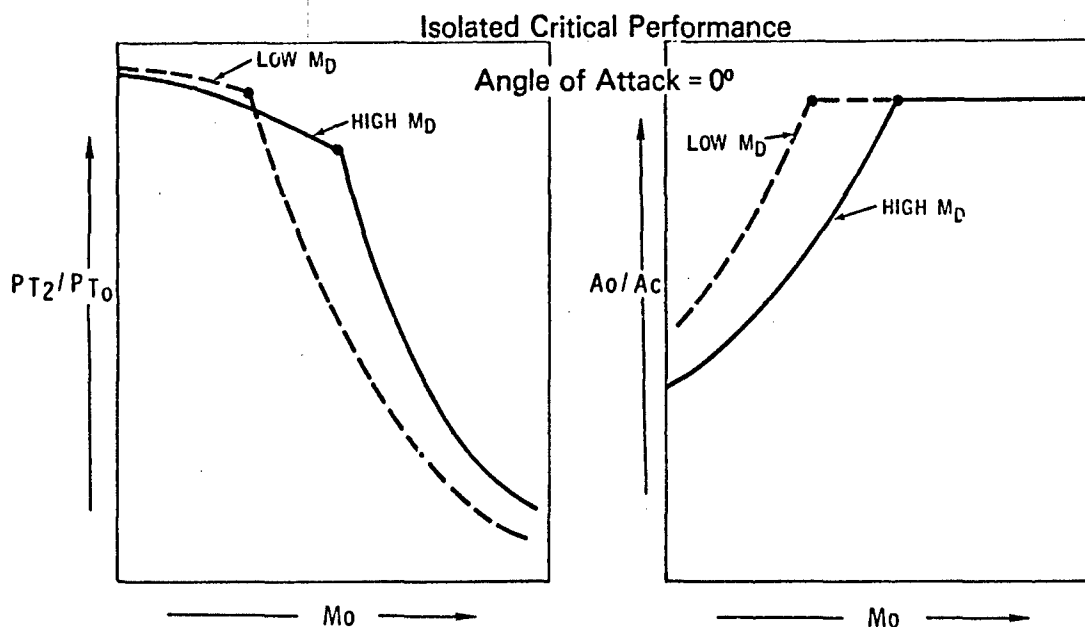
FIGURE 22. EFFECT OF DESIGN MACH NUMBER/ANGLE OF ATTACK = 0°

$$\alpha = 0°$$
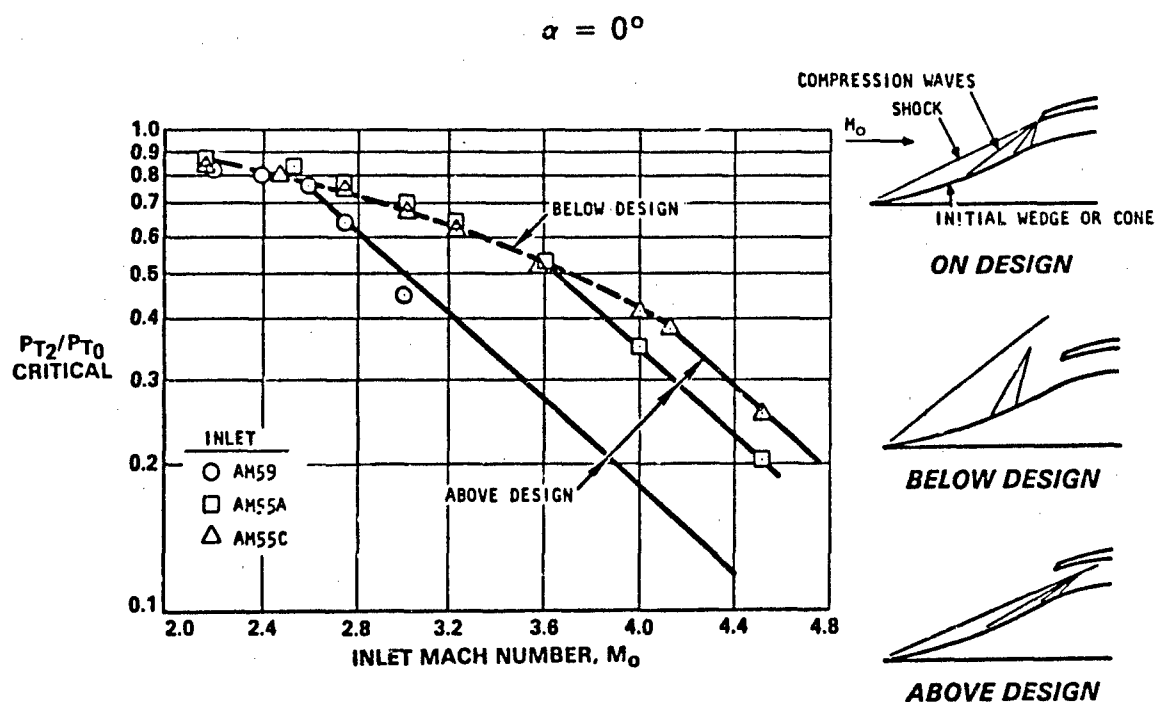
FIGURE 23. OFF-DESIGN INLET PERFORMANCE

Isolated Critical Performance

Two Dimensional Inlet   Mixed Compression   Angle of Attack ~10°
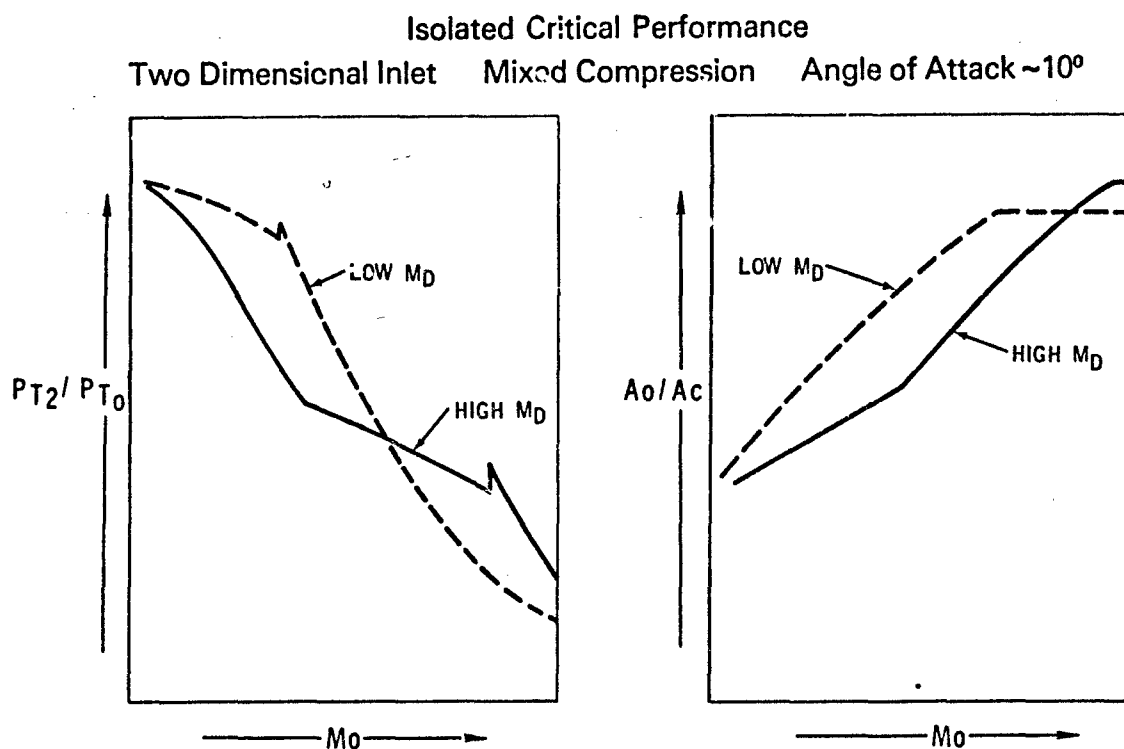
FIGURE 24. EFFECT OF DESIGN MACH NUMBER/ANGLE OF ATTACK = 10°
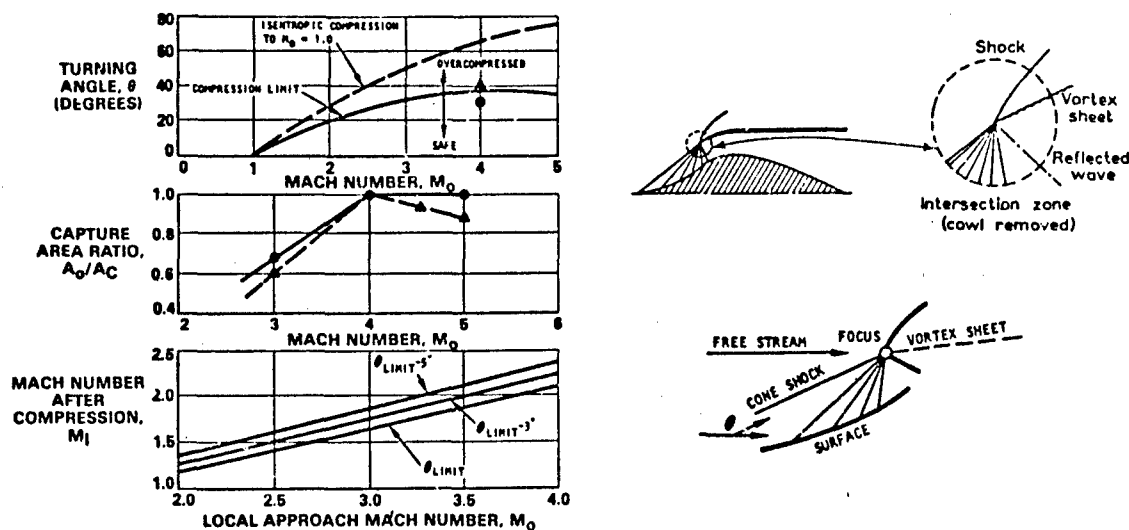
FIGURE 25. INLET EXTERNAL COMPRESSION LIMIT

EXTERNAL COMPRESSION
M_∞ = CONSTANT, α_∞ = 0°
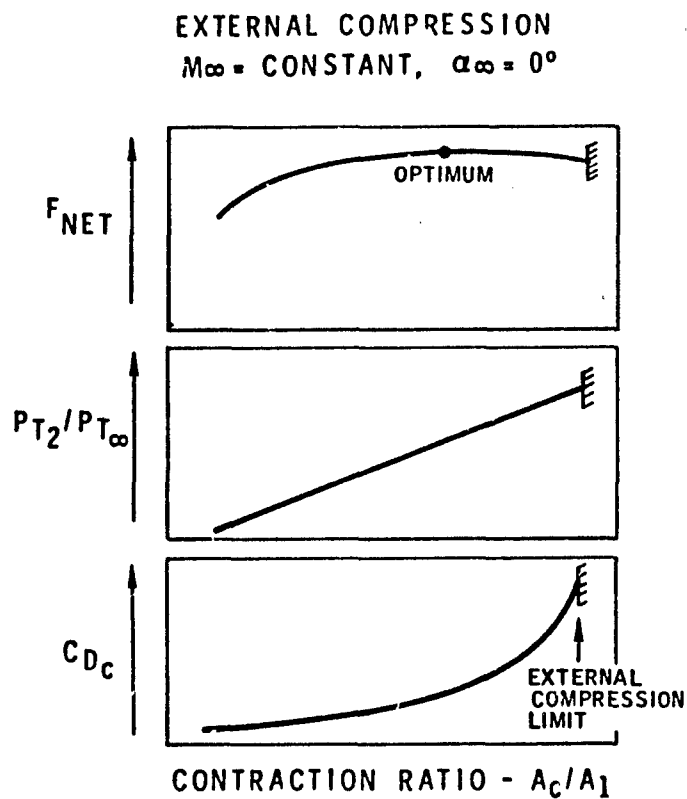
FIGURE 26. EFFECT OF INLET CONTRACTION RATIO/ANGLE OF ATTACK = 0°

Installed Critical Performance
Two Dimensional Inlet M_∞ = Constant
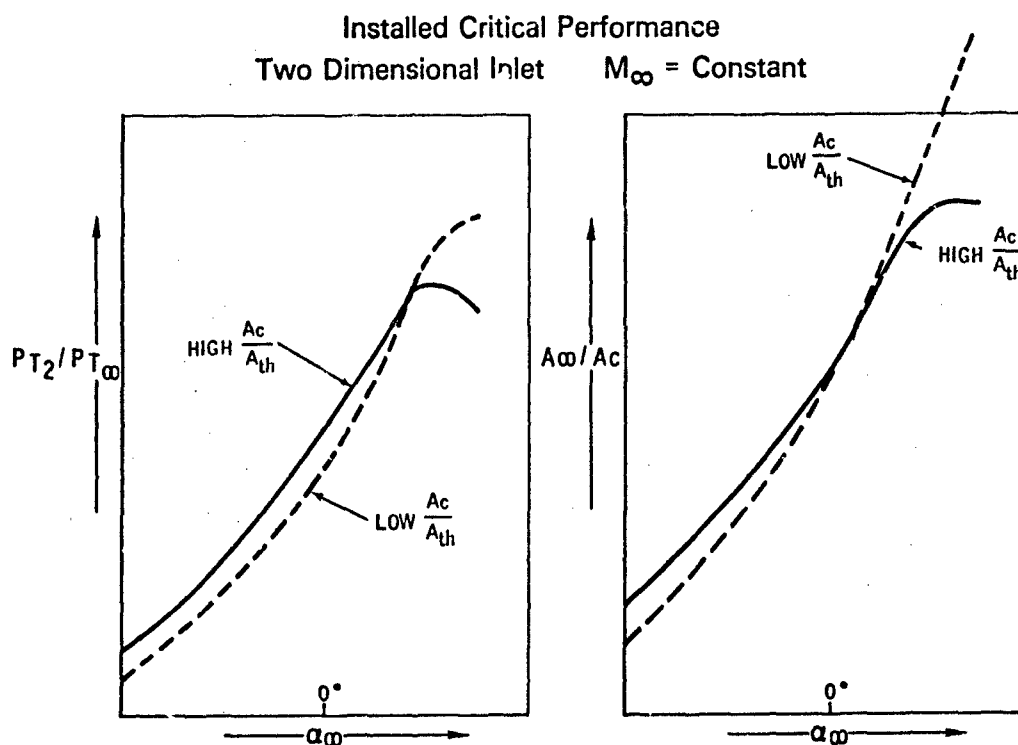
FIGURE 27. EFFECT OF INLET CONTRACTION RATIO/VARYING ANGLE OF ATTACK

Mixed Compression
Angle of Attack = 0° M_∞ = Constant
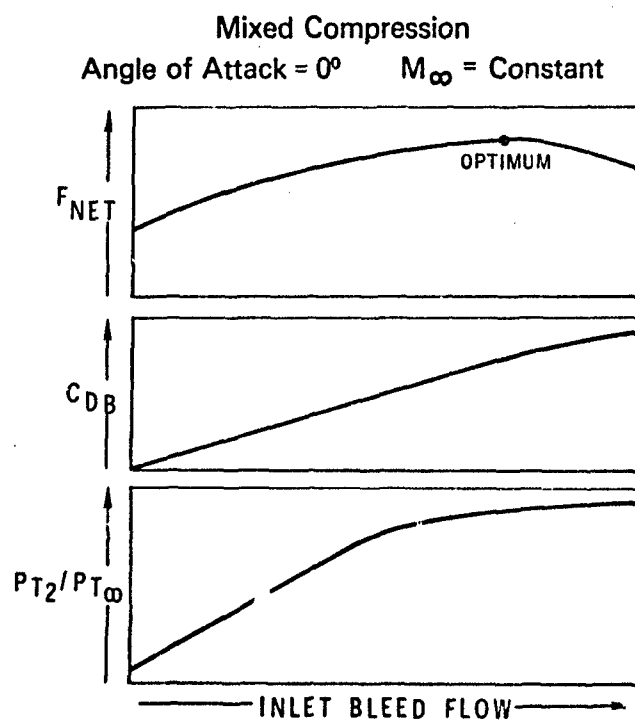
FIGURE 28. EFFECT OF INLET BLEED FLOW RATE
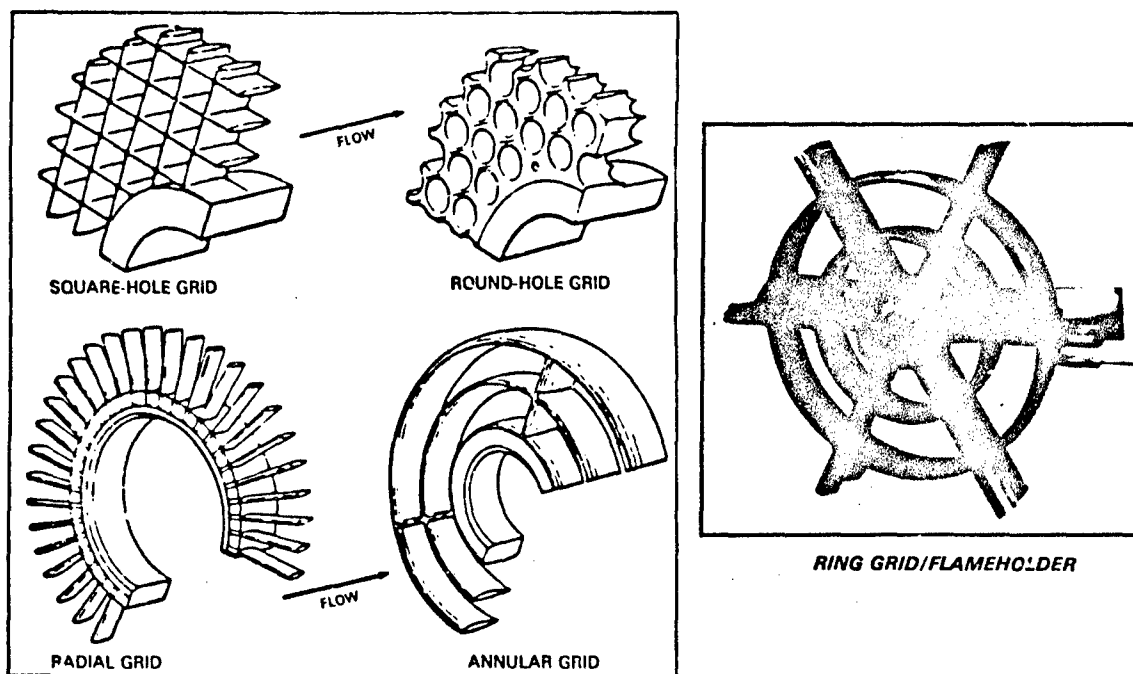
GRID CONFIGURATIONS

FIGURE 29. AERODYNAMIC GRID CONFIGURATIONS
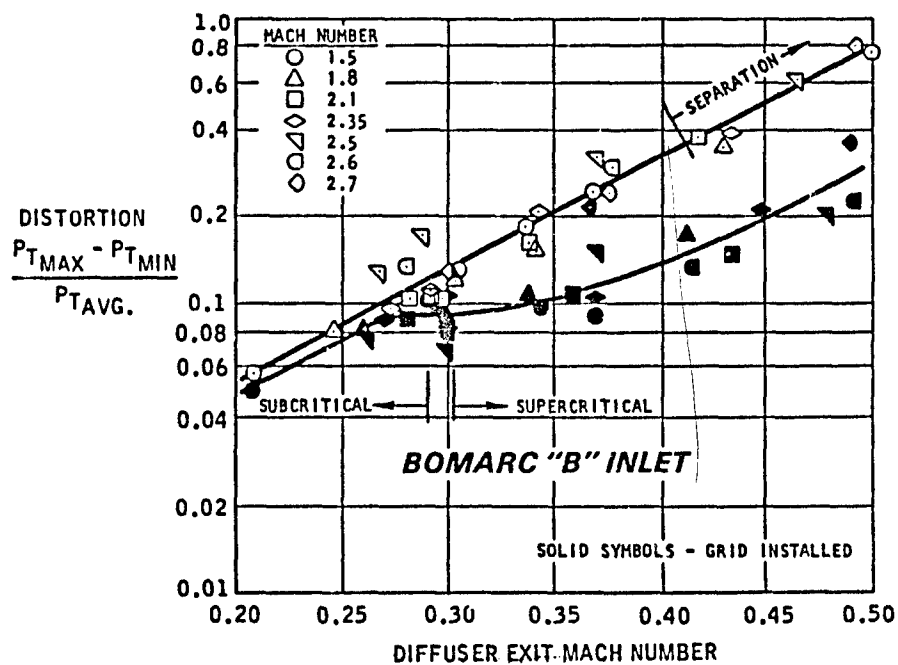
FIGURE 30. AIRFLOW PROFILE CONTROL WITH AN AERODYNAMIC GRID
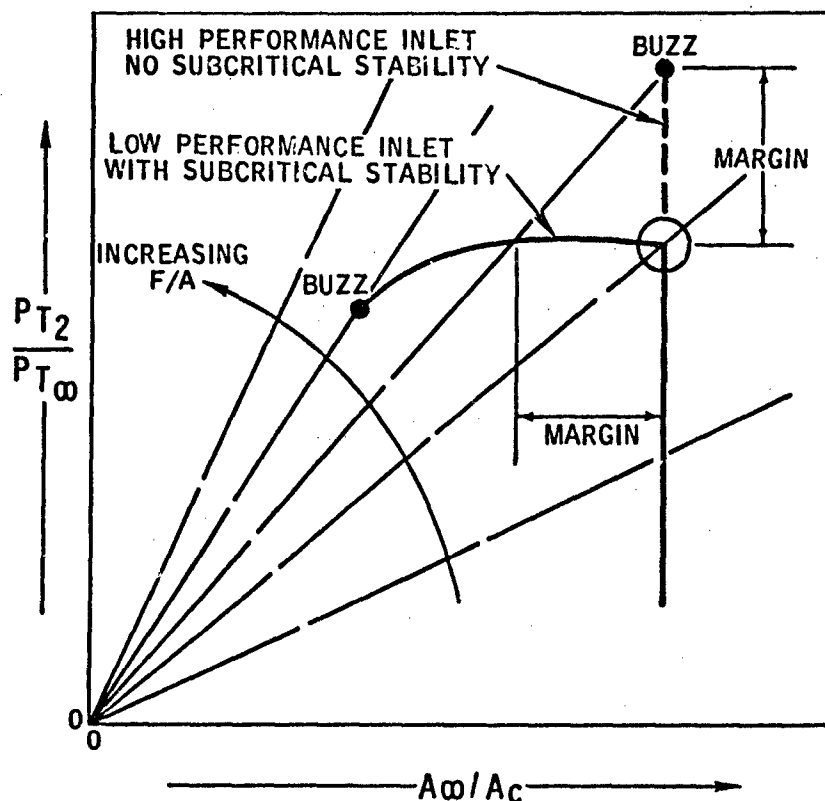
FIGURE 31. INLET SUBCRITICAL STABILITY PERFORMANCE COMPARISON
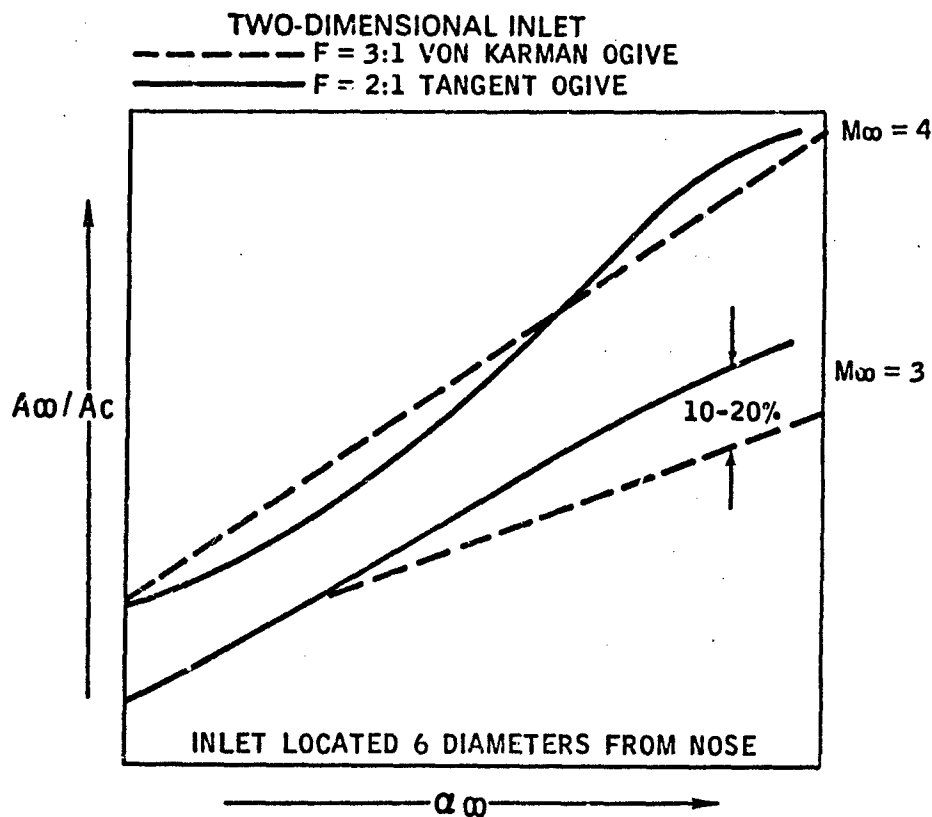
FIGURE 32. EFFECT OF FOREBODY SHAPE ON INLET PERFORMANCE
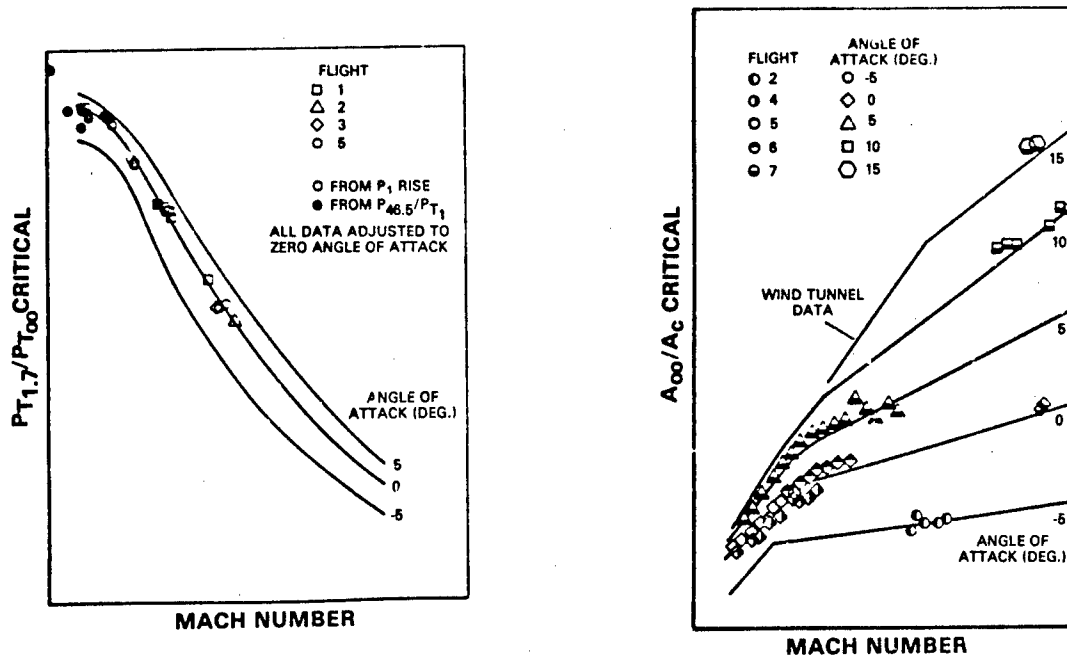
FIGURE 33. COMPARISON OF FLIGHT TEST AND WIND TUNNEL INLET TEST DATA
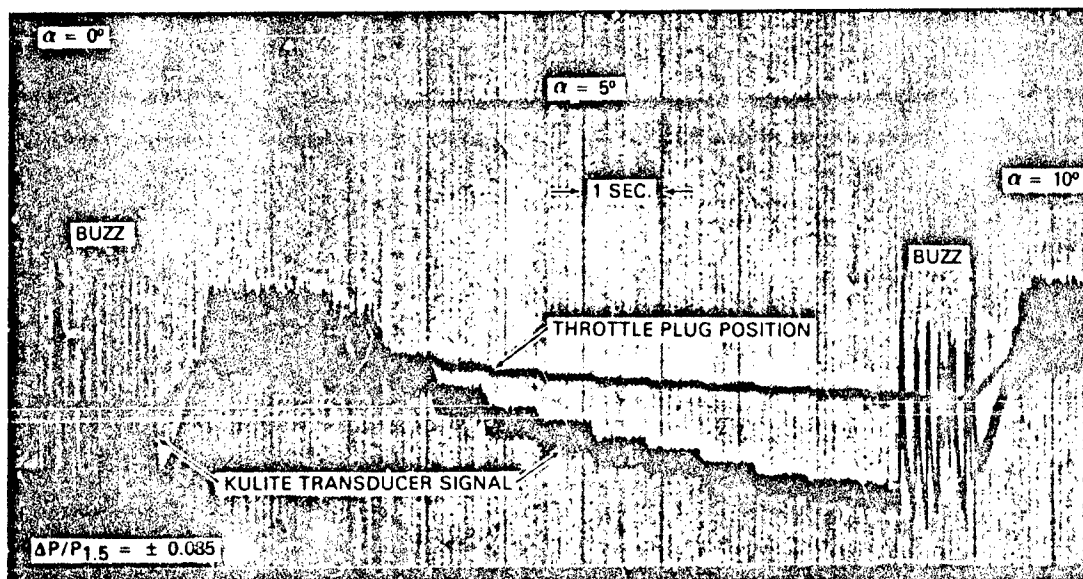
FIGURE 34. SUPERSONIC INLET DYNAMIC CHARACTERISTICS
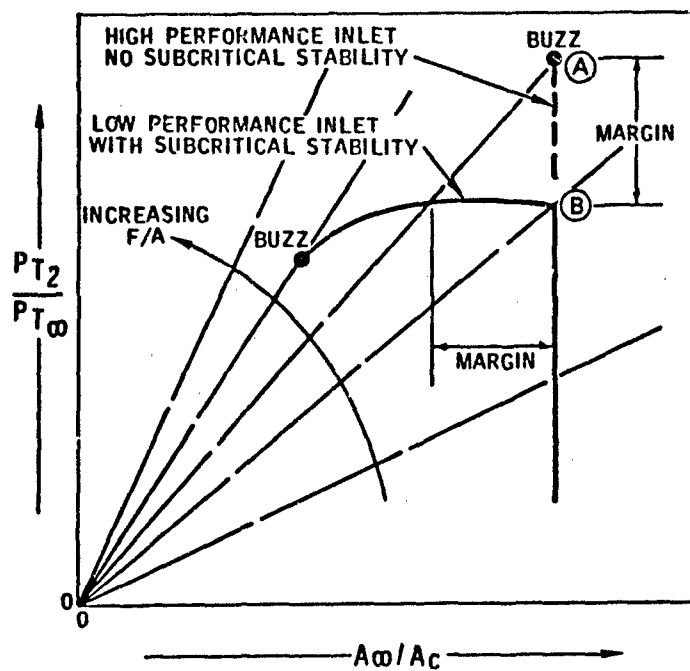
FIGURE 35. INLET PERFORMANCE COMPARISON

FIGURE 36. CONICAL EXTERNAL COMPRESSION SIDE INLET

DESIGN MACH No. = 1.88

BOUNDRY-LAYER
SCOOP HEIGHT
PARAMETER
h/δ
○ 1.361
□ 1.0

INLET TOTAL-PRESSURE RECOVERY, $P_{2,D}/P_{1,D}$

INLET MASS-FLOW RATIO, $m_D/m_{1,D}$

DESIGN MACH No. = 2.93

BOUNDRY-LAYER
SCOOP HEIGHT
PARAMETER
h/δ
○ 0.313
□ .603
△ .925
◇ 1.254

INLET TOTAL-PRESSURE RECOVERY, $P_{2,D}/P_{1,D}$

INLET MASS-FLOW RATIO, $m_D/m_{1,D}$
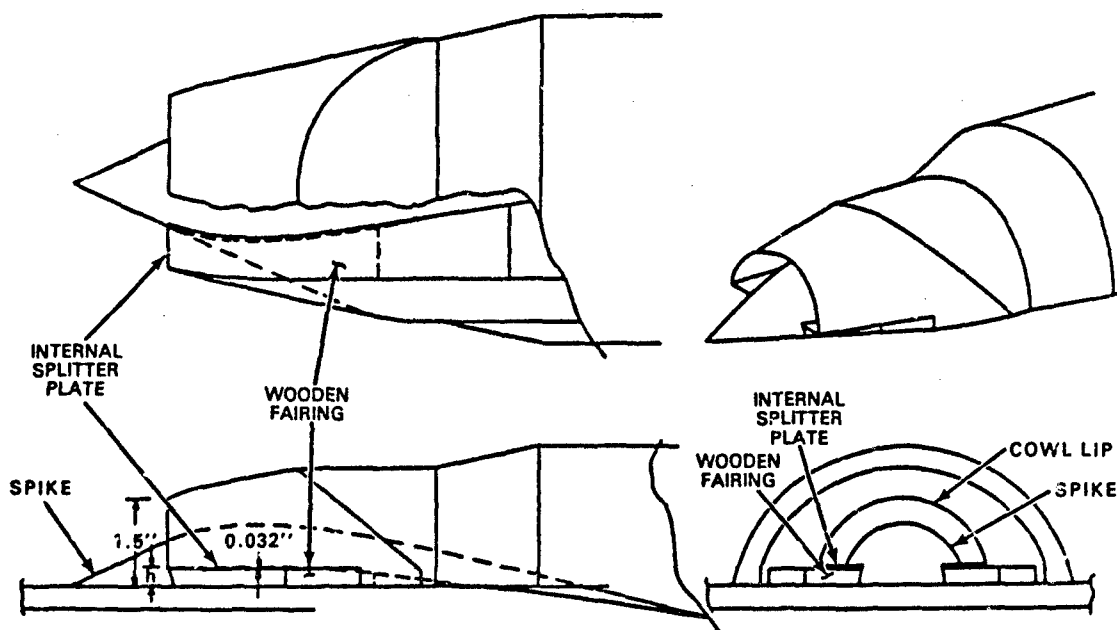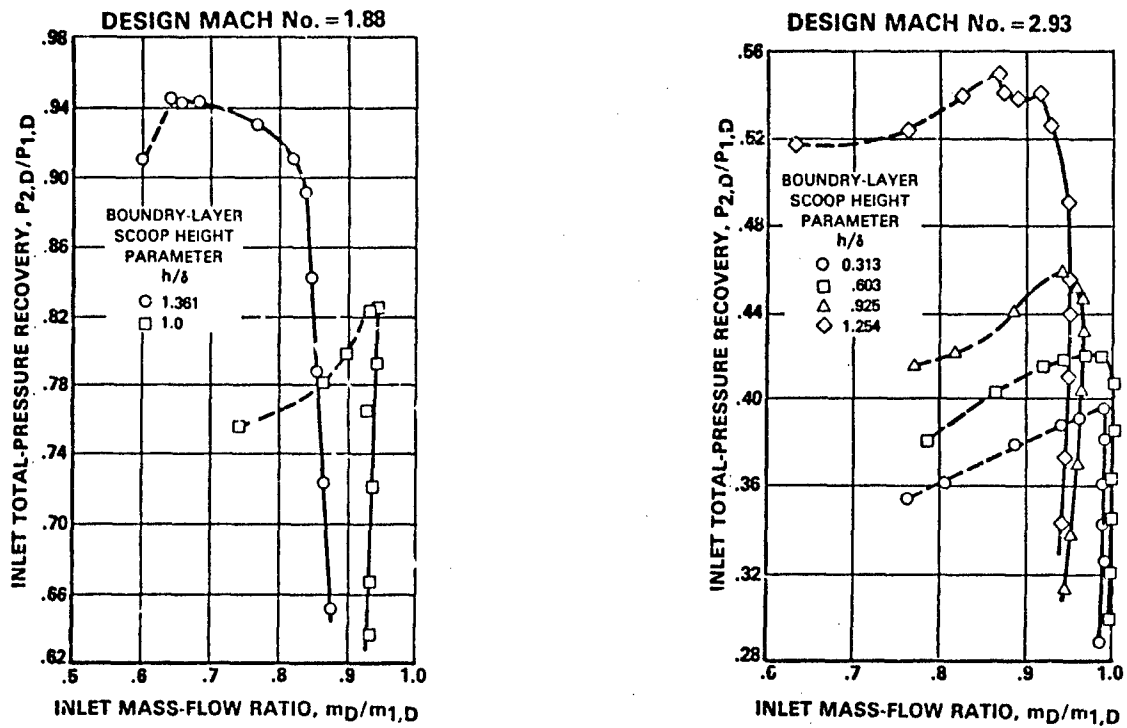
FIGURE 37. INLET CHARACTERISTICS WITH INCREASING BOUNDRY LAYER REMOVAL

AXISYMMETRIC NOSE INLET DESIGNS

INLET MODEL NO.	DESIGN MACH NO.	CONE ANGLE (DEG.)	BOUNDARY LAYER BLEED	SUBCRITICAL STABILITY* $M_o = 1.66$	$M_o = 1.92$
1	2.0	25°	NO	18%	6%
2	2.3	25°	NO	44%	11%
3	3.85	20°	NO	NOT TESTED	7%
			YES	16%	13.5%

*ANGLE OF ATTACK = 0°

FIGURE 38. PROJECT RIGEL INLET DEVELOPMENT EXPERIENCE

ANGLE OF ATTACK = 0°

SUBCRITICAL MARGIN (PERCENT)

INLET DESIGN MACH NUMBER

FLIGHT MACH NUMBER

$M_O = 1.92/\alpha_O = 0°$
INLET DESIGN MACH NO. = 3.85

∇ WITH BOUNDARY LAYER BLEED
$\square$ NO BOUNDARY LAYER BLEED

SOLID SYMBOLS INDICATE BUZZ
FLAGGED SYMBOLS INDICATE SLIGHT OSCILLATION (VISUAL)

TOTAL PRESSURE RECOVERY (P_{T_2}/P_{T_O})

FREESTREAM CAPTURE AREA RATIO (A_O/A_3)
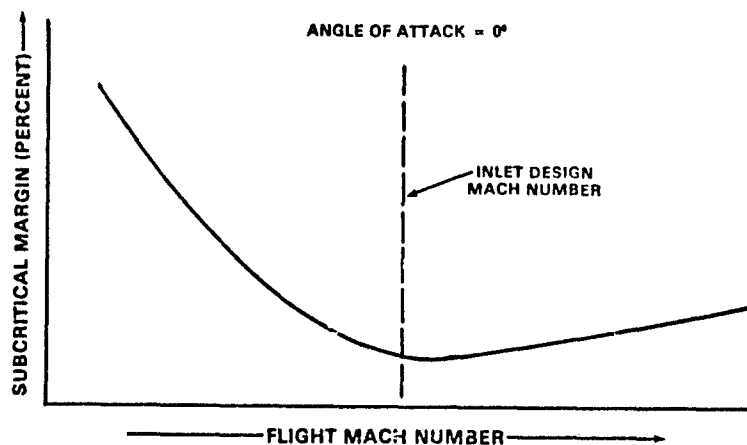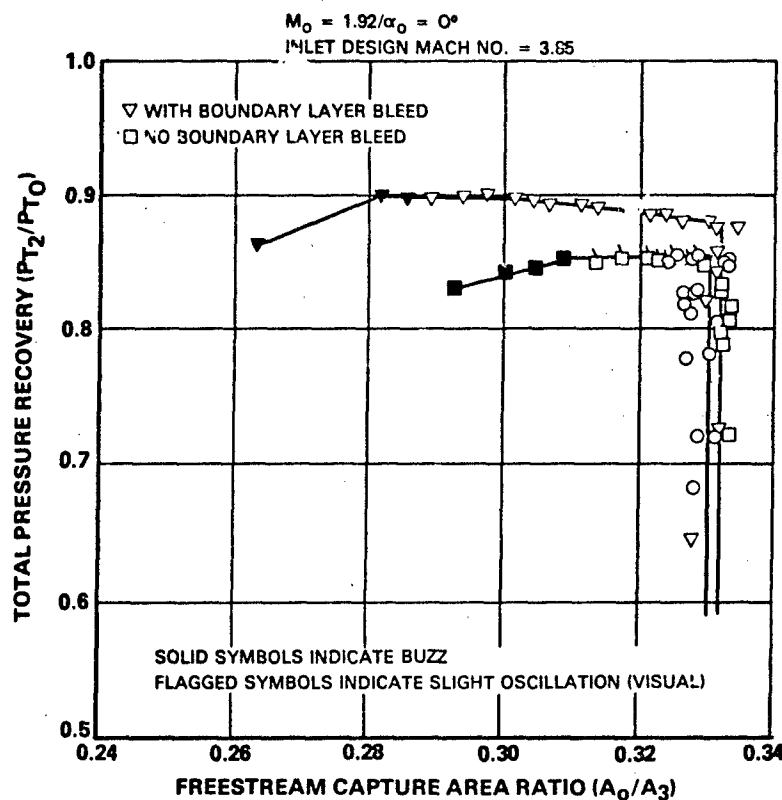
FIGURE 40. PROJECT RIGEL INLET TEST DATA

NO BUZZ
SUBCRITICAL

$M_O = 2.0$

BUZZ
SUBCRITICAL

$M_O = 3.0$

$\blacktriangle$ = BUZZ

$\theta_{Cone} = 30°$, CONTRACTION RATIO = 1.094
$\theta_{Lip\ (Int)} = 21.7°$

SEE REFERENCE 11

DIFFUSER TOTAL PRESSURE RECOVERY (P_{T_2}/P_{T_O})

INLET CAPTURE AREA RATIO (A_{OO}/A_c)
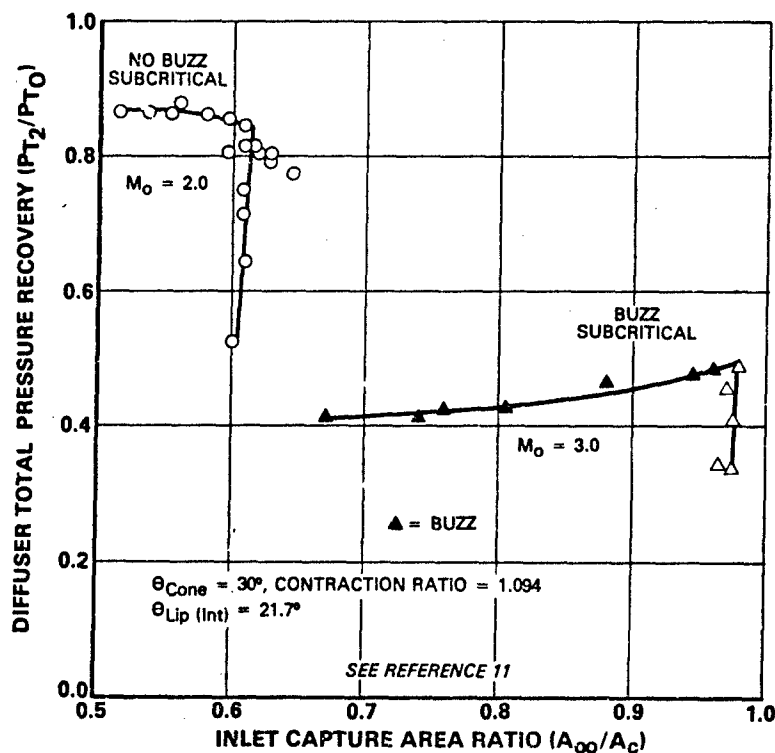
FIGURE 41. B. HERMANN DESIGNED MACH 2.0 INLET TEST RESULTS

SINGLE CONE INLET (25°)
DESIGN MACH NO. = 2.3
TEST MACH NO. = 1.66
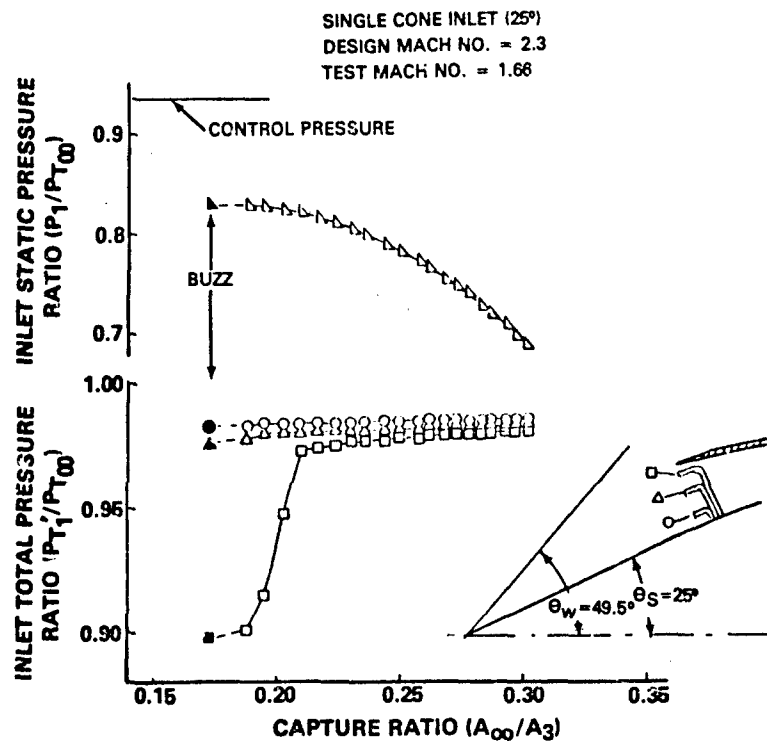
FIGURE 42. ZERO SLOPE INSTABILITY - BELOW THE CONTROL PRESSURE

SINGLE CONE INLET (50°)
DESIGN MACH NO. = 2.0
TEST MACH NO. = 1.92
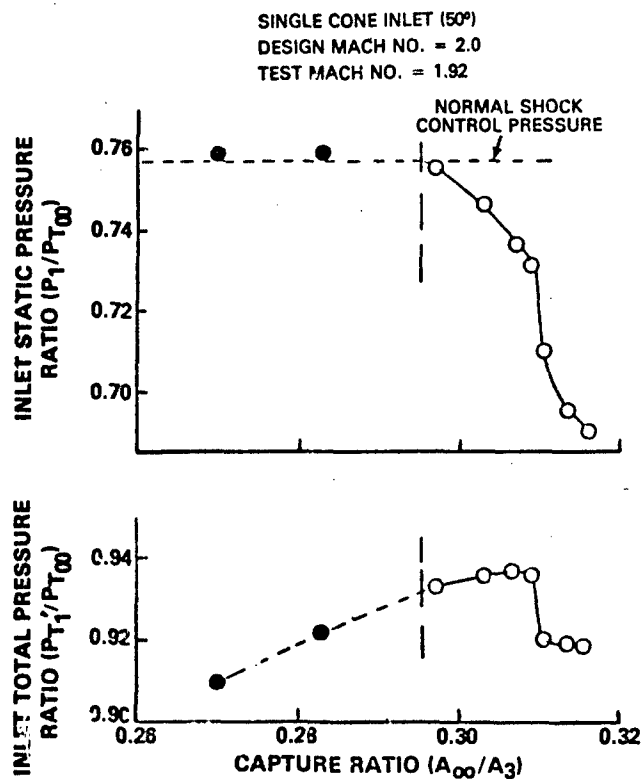
FIGURE 44. NORMAL SHOCK CONTROL PRESSURE INSTABILITY - DOUBLE CONE INLET
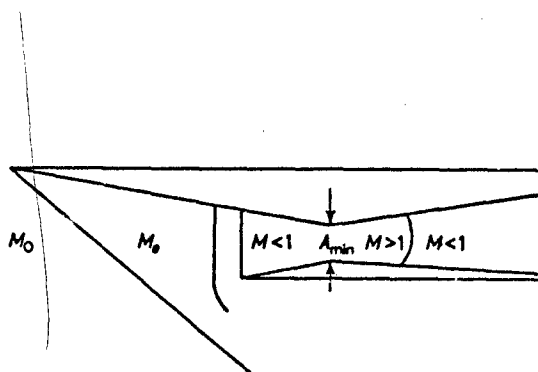
FIGURE 45. CHOKED INLET CONCEPT PROPOSED BY A. FERRI (REF. 1)
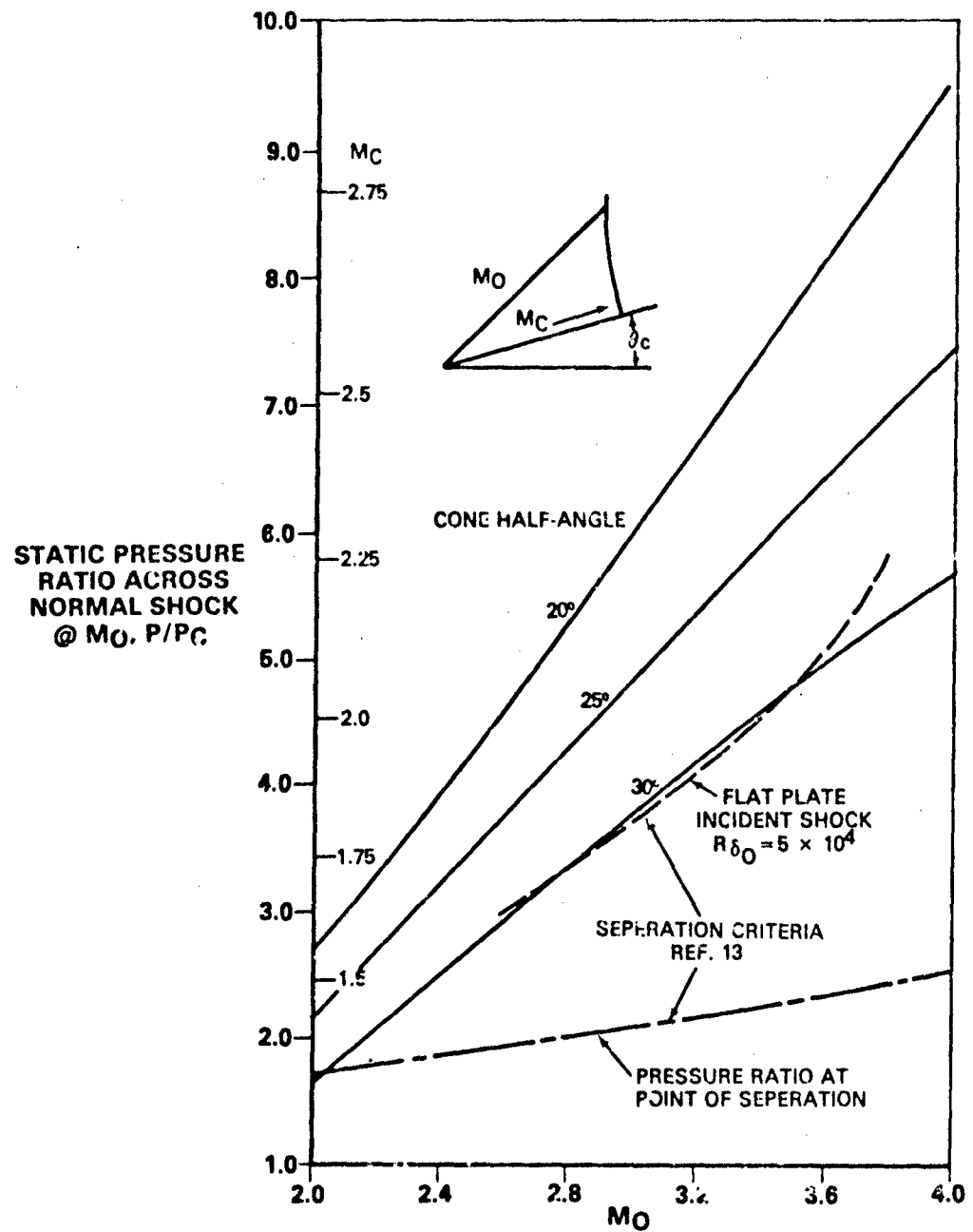
FIGURE 46. CONE STATIC PRESSURE RATIO AND SEPERATION CRITERIA

INLET WITHOUT
SLOT AND SURGE
CHAMBER

0.090 OR 0.180 FLUSH
SLOT IN SPIKE
TO SURGE CHAMBER

CENTRAL BODY
VOLUME(EMPTY
AND SEALED)ACTS
AS SURGE CHAMBER
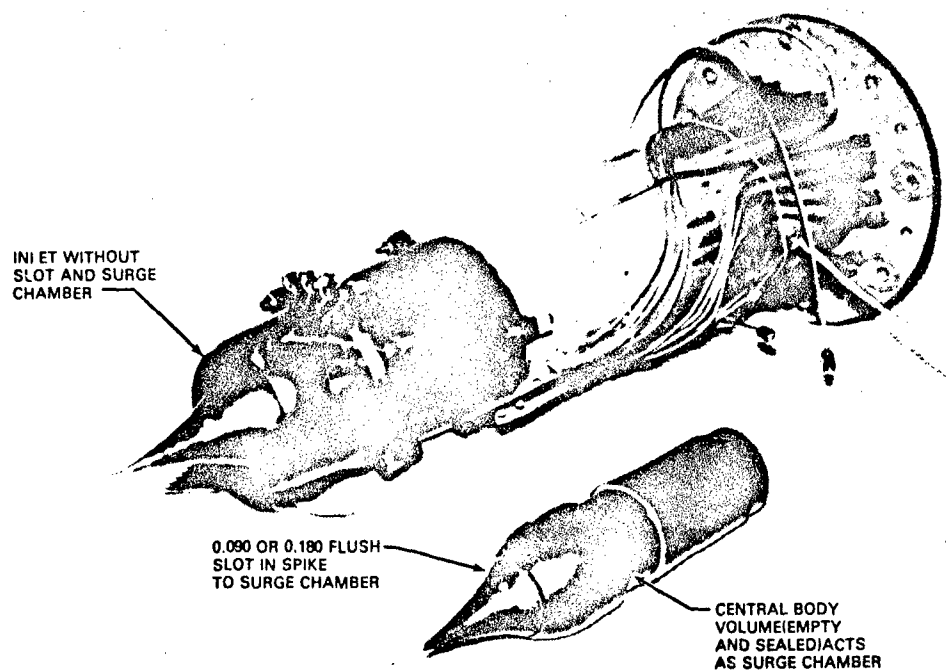
FIGURE 47. BUZZ SUPRESSOR INLET TEST MODEL

$M_0 = 2.35$ $a = 0°$

ISENTROPIC INLET
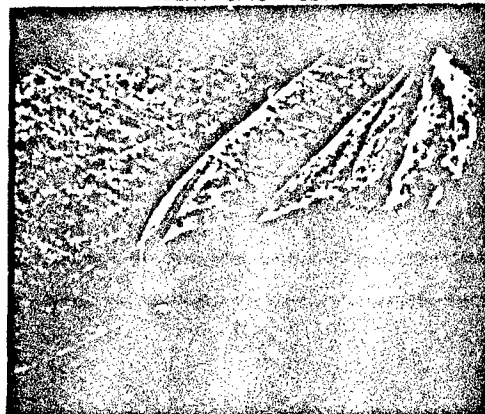
LAST STABLE POINT WITHOUT SURGE CHAMBER

OUTLINE OF
COWL LIP
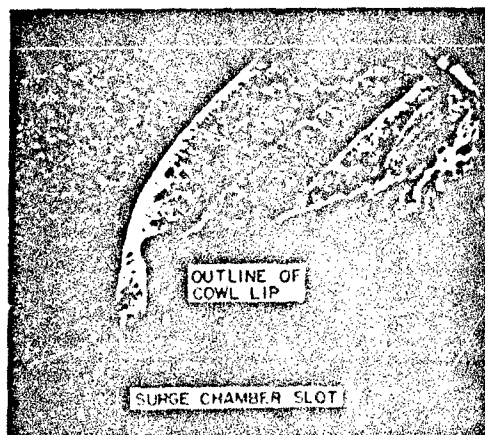
SURGE CHAMBER SLOT

LAST STABLE POINT WITH SURGE CHAMBER

ISENTROPIC SPIKE INLET — DESIGN MACH NO. 2.80

● WITH SUPPRESSOR
○ WITHOUT SUPPRESSOR

80° CONE INLET — DESIGN MACH NO. 2.57
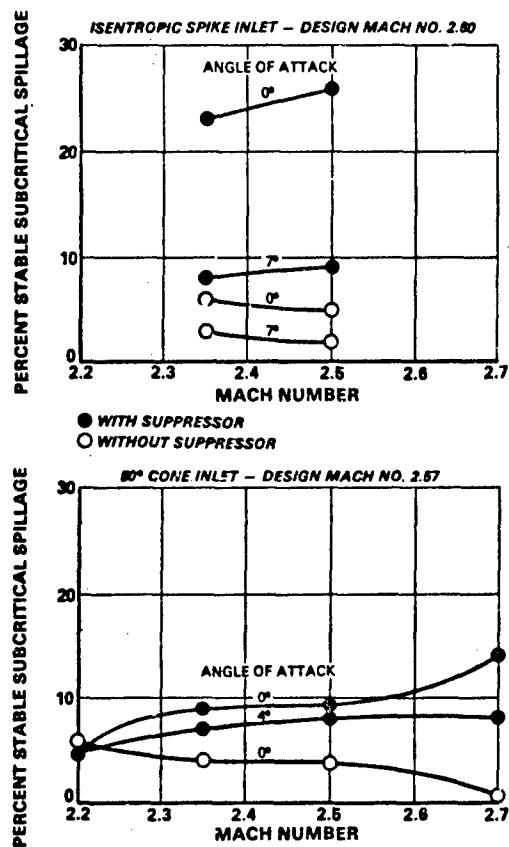
FIGURE 49. INLET MODEL TEST RESULTS WITH BUZZ SUPRESSOR

FIG. 1

FIG. 4

FIG. 2

FIG. 5

FIG. 3

ACOUSTIC BUZZ SUPPRESSOR
FILED MAY 29, 1959
INVENTORS
EDWARD P. FRENCH
STANLEY J. MINTON
by
R. S. _____
ATTORNEY
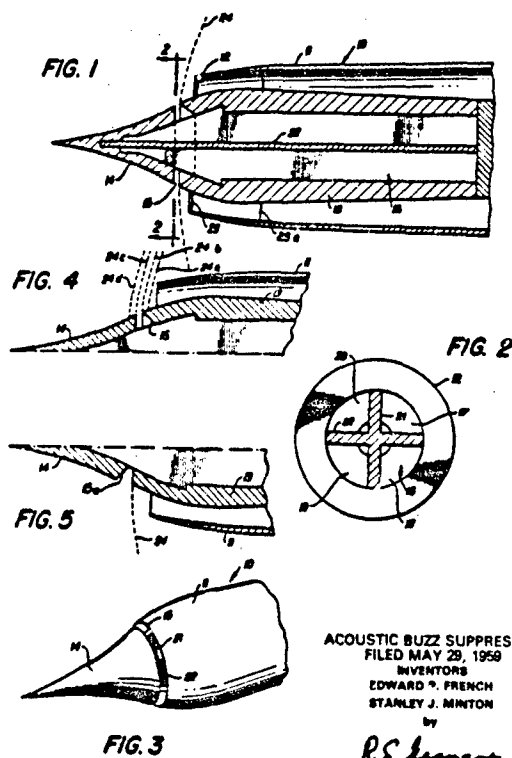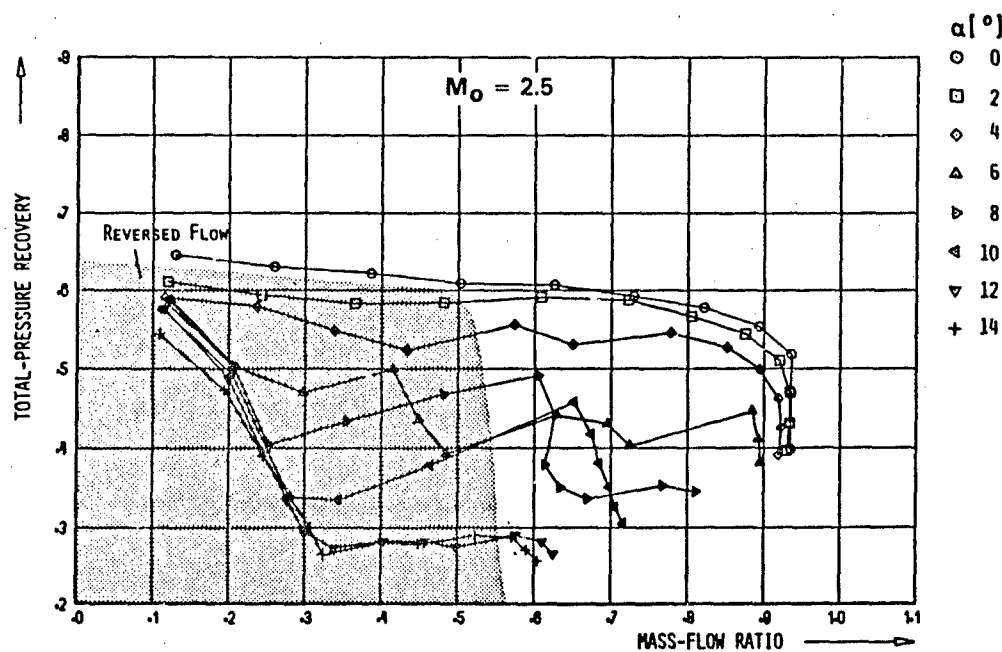
FIGURE 51. DFVLR MULTIPLE (4) AFT MOUNTED INLET TEST DATA - "X" CONFIGURATION
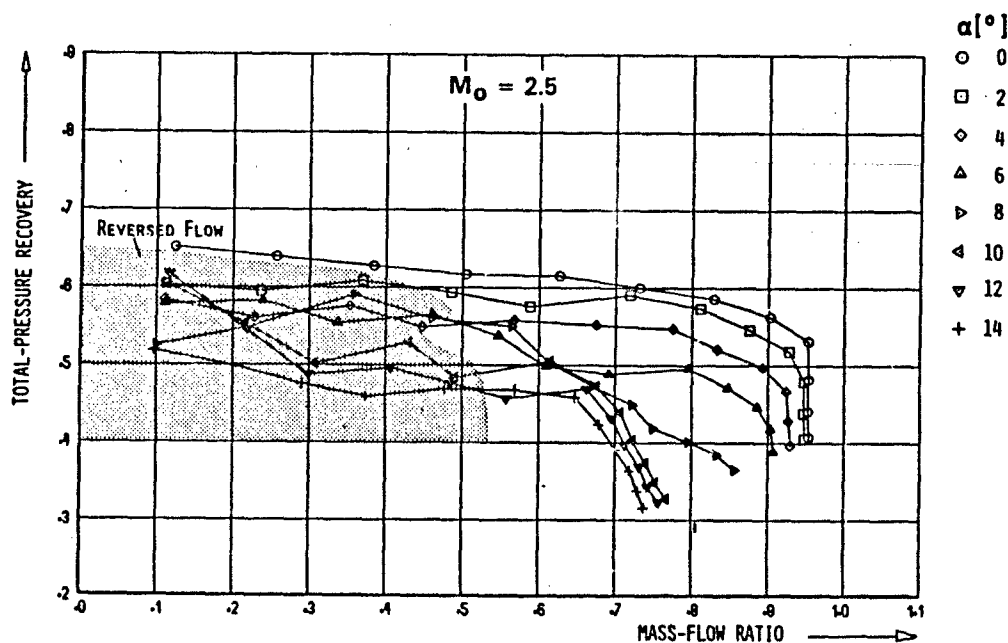
FIGURE 52. DFVLR MULTIPLE (4) AFT MOUNTED INLET TEST DATA - "+" CONFIGURATION

$\alpha = 5°$ $\alpha = 10°$ $\alpha = 15°$

x/d = 4

$M_O = 2.0$
REYNOLDS No. $= 3 \cdot 10^6$ (m^{-1})

PT_O'/PT_∞

.7   .8   .9

x/d = 8

x/d = 12
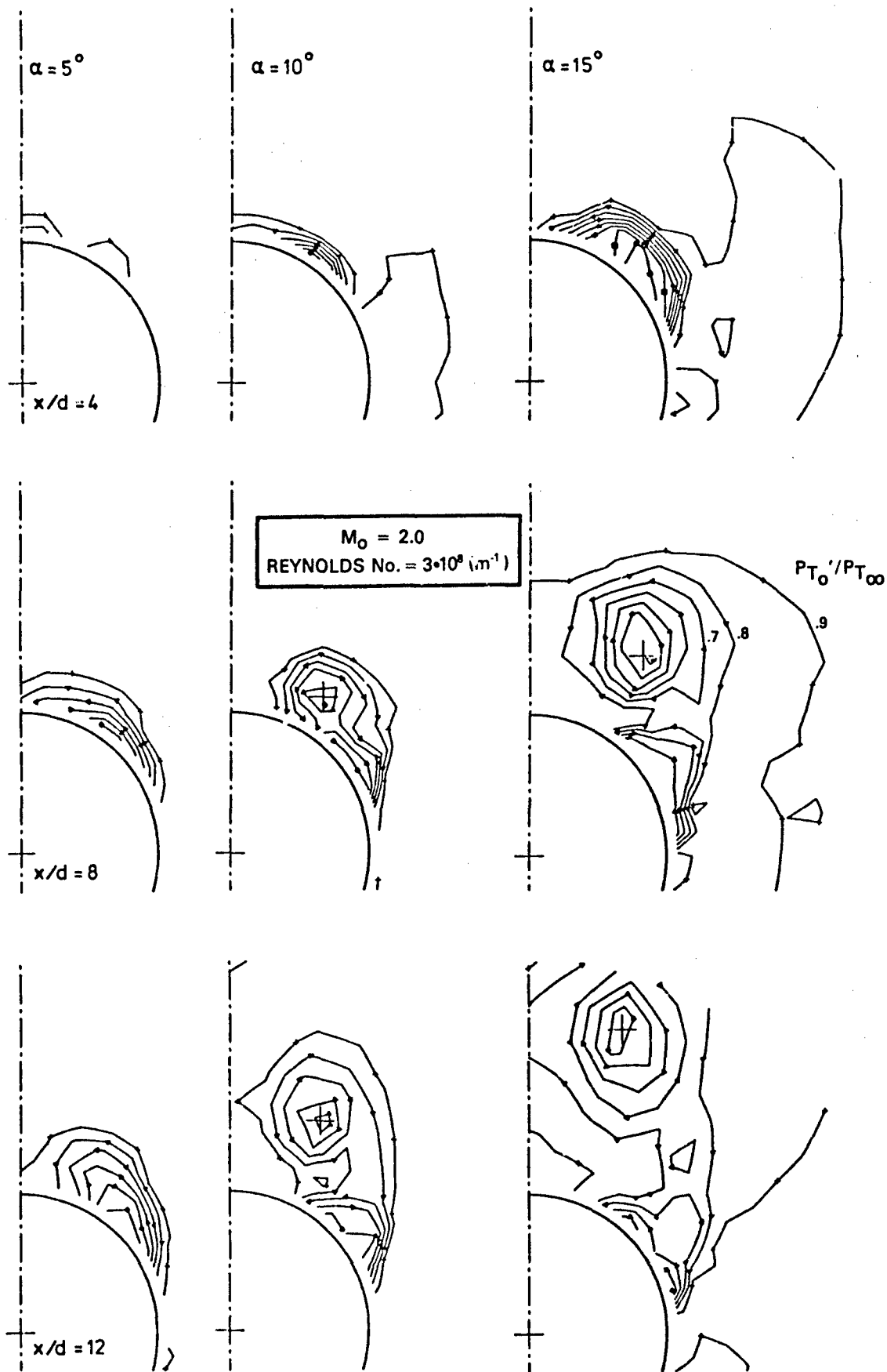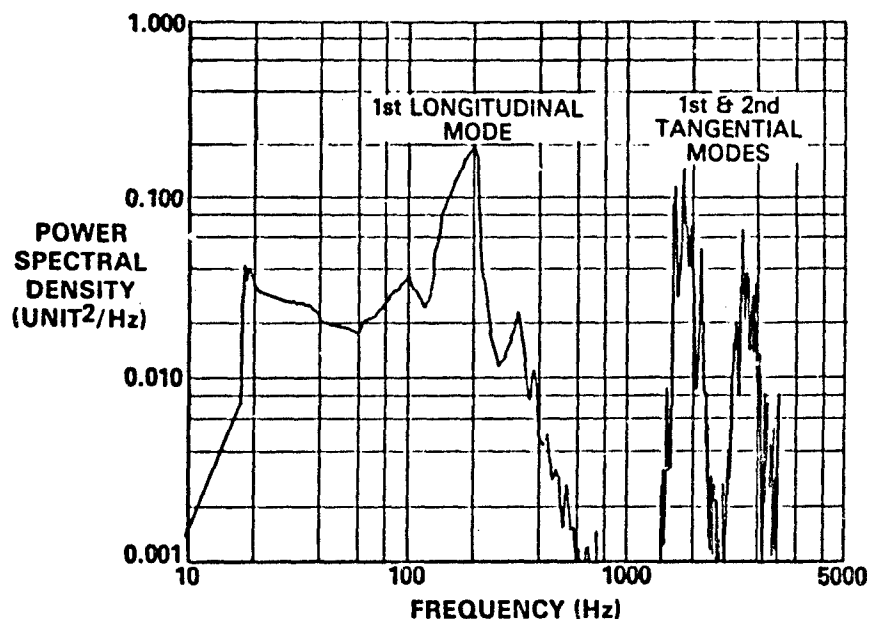
FIGURE 54. REPRESENTATIVE RAMJET PRESSURE OSCILLATION POWER SPECTRAL DENSITY TEST DATA

CONFIGURATION	MACH NUMBER	PRESSURE ALTITUDE (FEET)
O ANNULAR REGENERATIVE BURNER	1.87	45,000
□ LIQUID FUEL-INJECTION BURNER	1.87	45,000
△ ROTATING-DISK OSCILLATOR	1.87	45,000
◇ ROTATING-DISK OSCILLATOR	1.87	55,000
◁ 3.6 INCH RAMJET	1.92	47,000

REFERENCE: NACA RM E50H22

RATIO OF TOTAL AMPLITUDE(PEAK TO PEAK)OF PULSATION TO FREE-STREAM TOTAL PRESSURE

FOUR AXISYMMETRIC INLETS
NO BOUNDARY LAYER BLEED

COMBUSTOR

HYDRAULIC
CONTROL
GROUP

COMMAND
DESTRUCT

TELEMETRY
SECTION

AUTOPILOT

BALLAST

FUEL
TANK

FUEL
CONTROLLER

BLAST TUBE

BOOSTER
MOTOR

FMS
PRESSURE
TAP

RELIEF
VALVE

GAS
GENERATOR

LAUNCH

BOOSTER
BURN-OUT

IGNITER

RAMJET
BURN-OUT

BLADDER

SCREW
JOINT

FUEL
MANIFOLD

FUEL
INJECTOR
RING

FIGURE 56. GORJE PROPULSION TEST VEHICLE

*INLET WIND TUNNEL
TEST DATA

CRITICAL*
PRESSURE

BUZZ

DIFUSER STATIC PRESSURE
PSIA

10%
MARGIN

ΔP FROM PSD

ΔP FROM 0-GRAPH

STEADY STATE DATA

ΔP = ZERO-TO-PEAK AMPLITUDE

EQUIVALENCE RATIO φ

2ΔP
MIN

2ΔP
MAX

TYPICAL 0-GRAPH TRACE
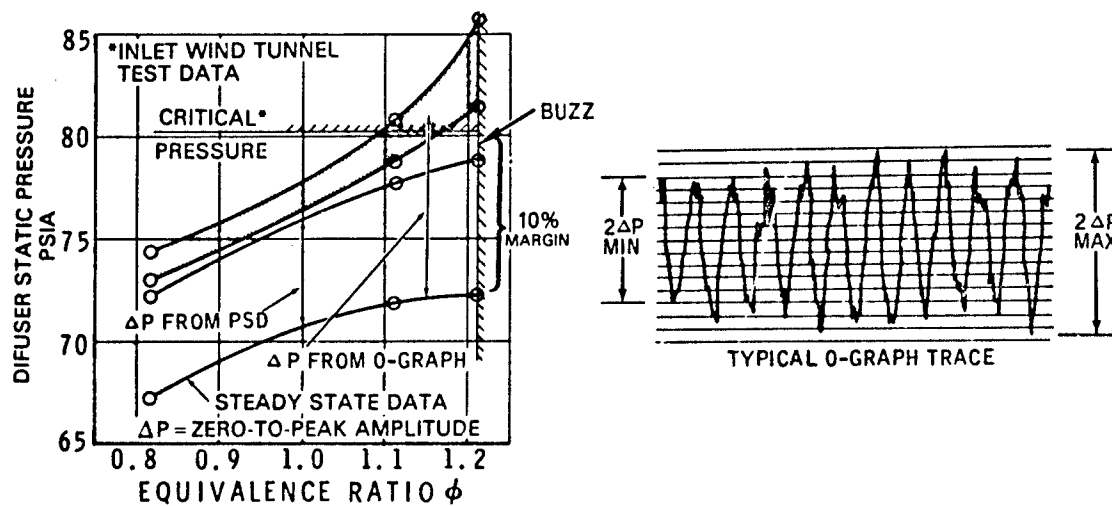
FIGURE 57. EFFECT OF PRESSURE OSCILLATIONS ON INLET MARGIN
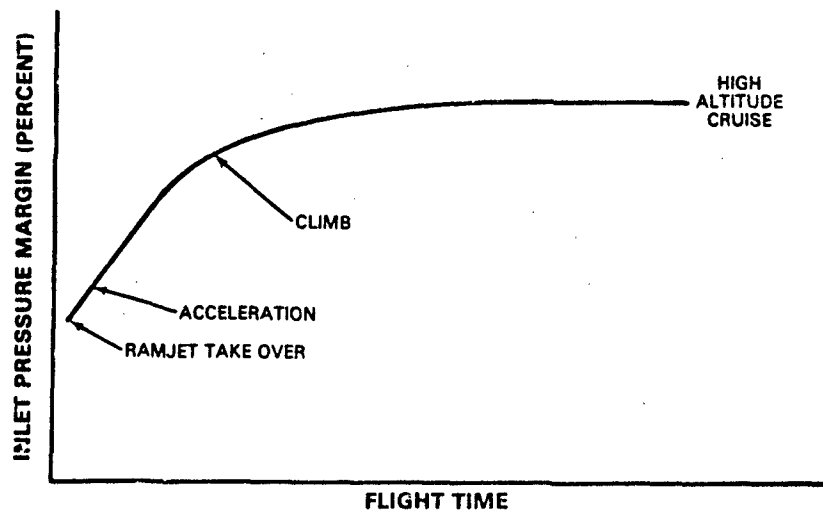
FIGURE 58. REPRESENTATIVE RAMJET INLET PRESSURE MARGIN HISTORY
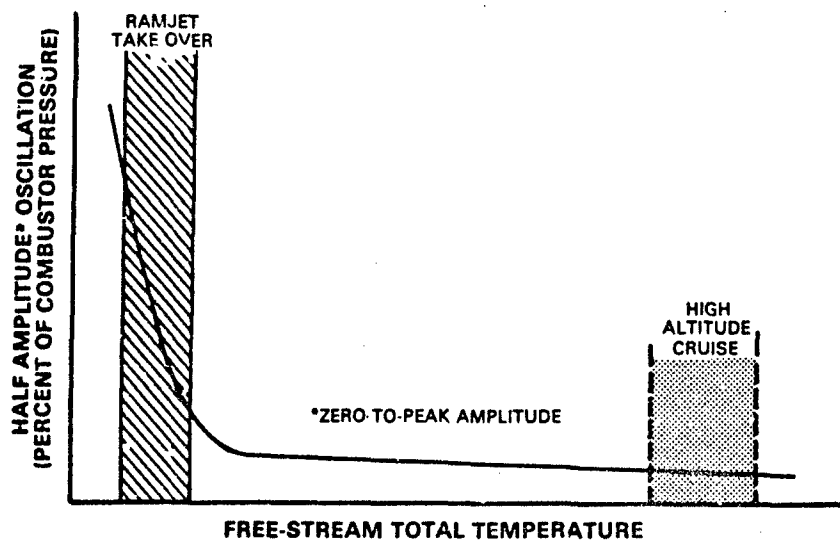
FIGURE 59. COMBUSTOR INDUCED PRESSURE OSCILLATION TEST DATA CORRELATION
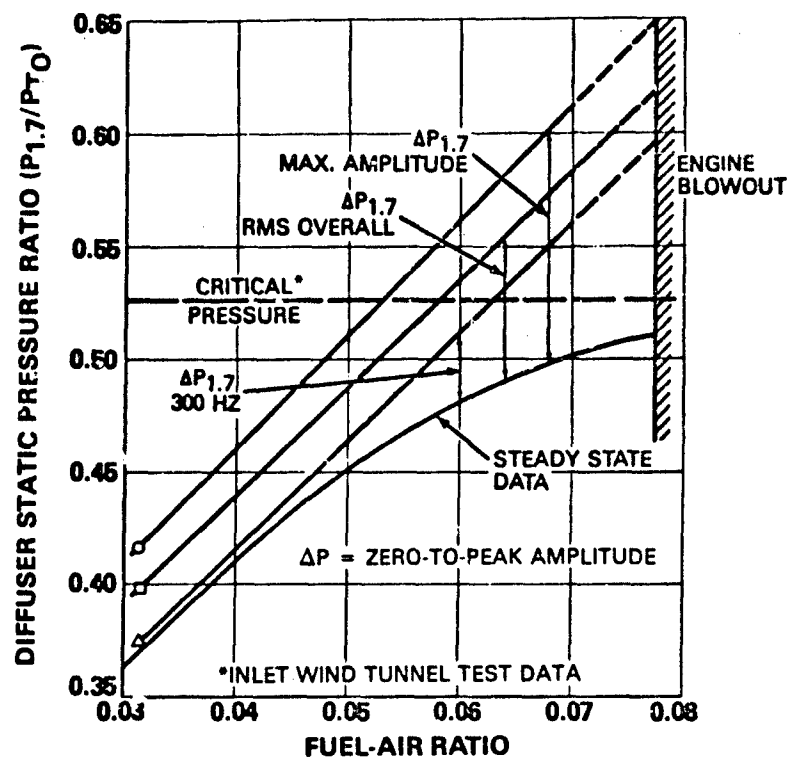
FIGURE 60. EFFECT OF PRESSURE OSCILLATIONS ON INLET MARGIN - TWO DIMENSIONAL
INLET WITH BOUNDARY LAYER BLEED
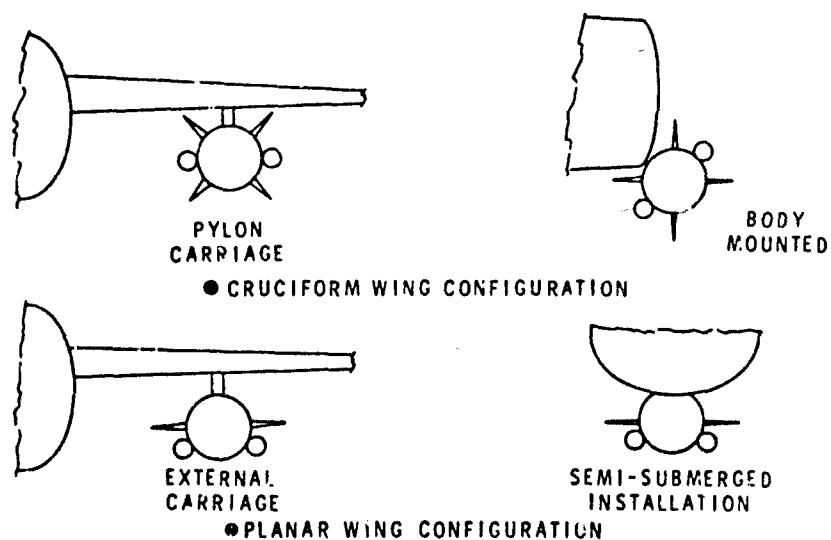
FIGURE 61. AIR LAUNCHED DUCTED ROCKET POWERED MISSLE APPLICATIONS
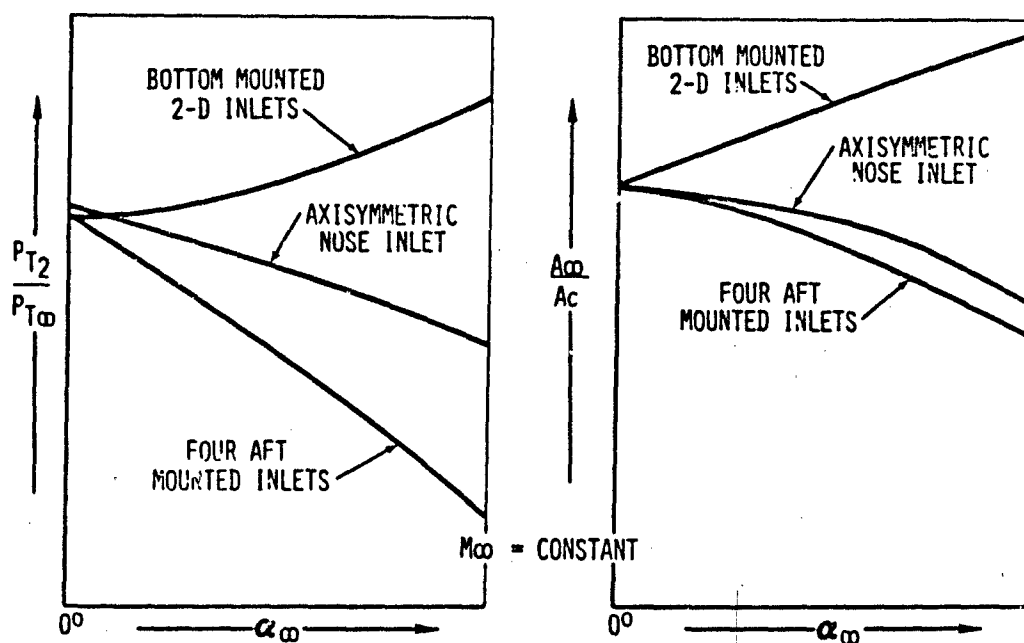
FIGURE 62. INSTALLED INLET PERFORMANCE COMPARISON
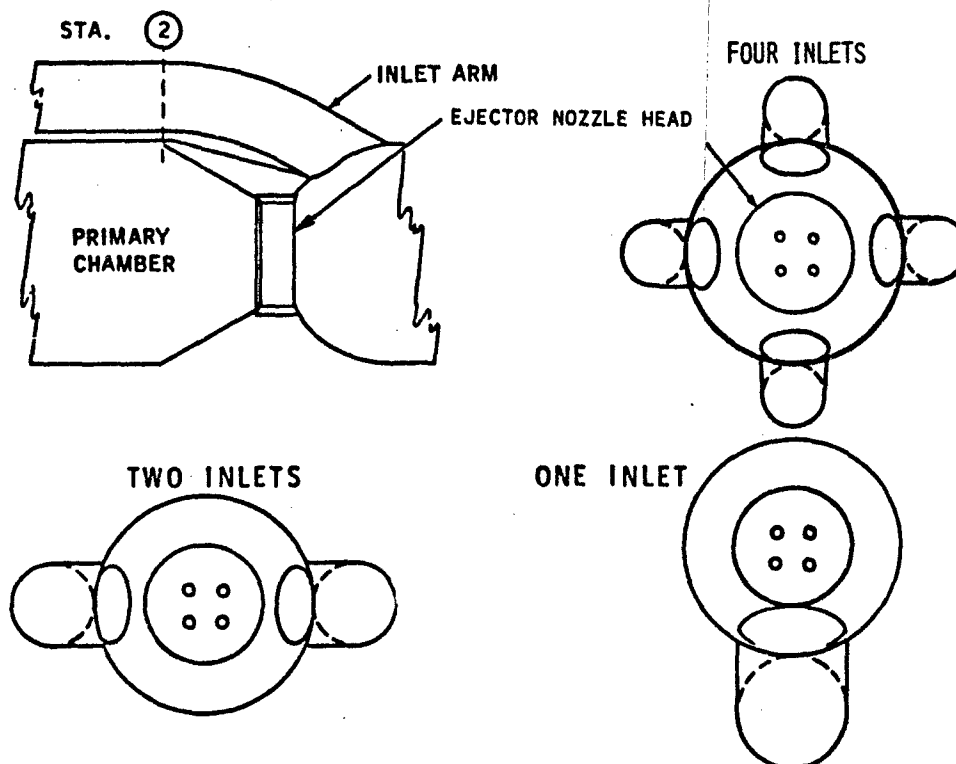
FIGURE 63. INLET/EJECTOR TEST CONFIGURATIONS
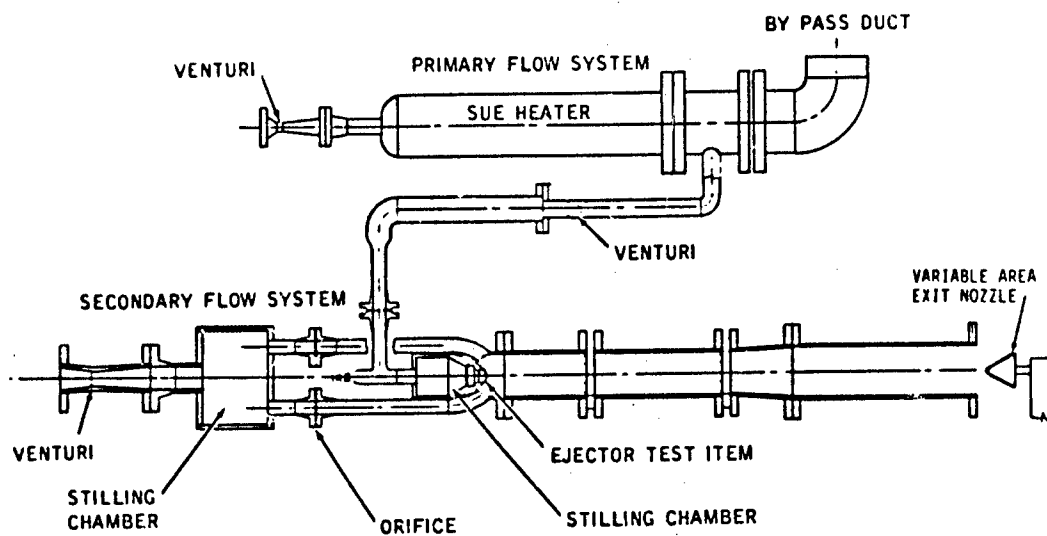
FIGURE 64. EJECTOR/MIXER TEST SETUP
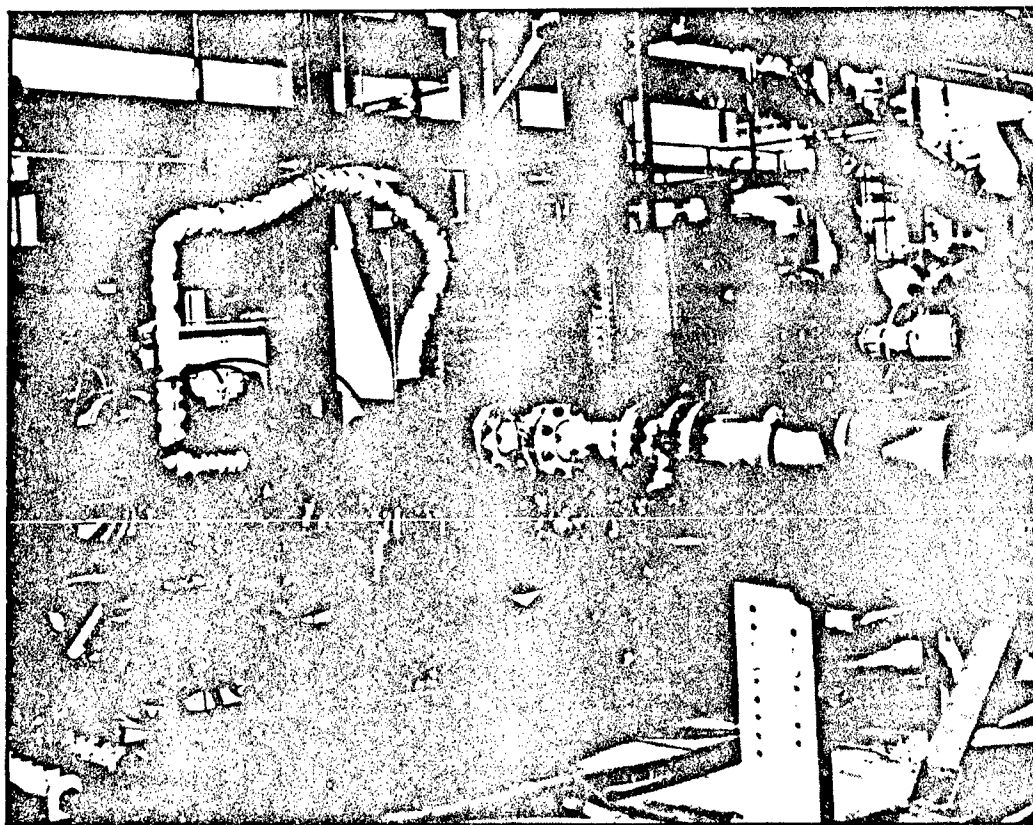
FIGURE 65. TEST SETUP - ¾ REAR VIEW
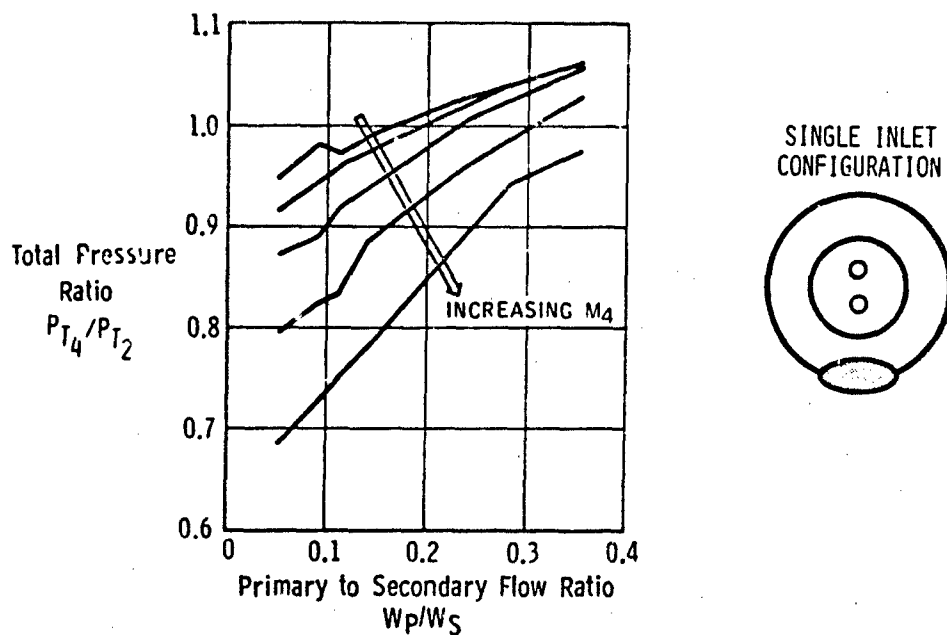
FIGURE 66. TYPICAL EJECTOR/MIXER PERFORMANCE TRENDS WITH FLOW RATIO AND MIXER EXIT MACH NUMBER
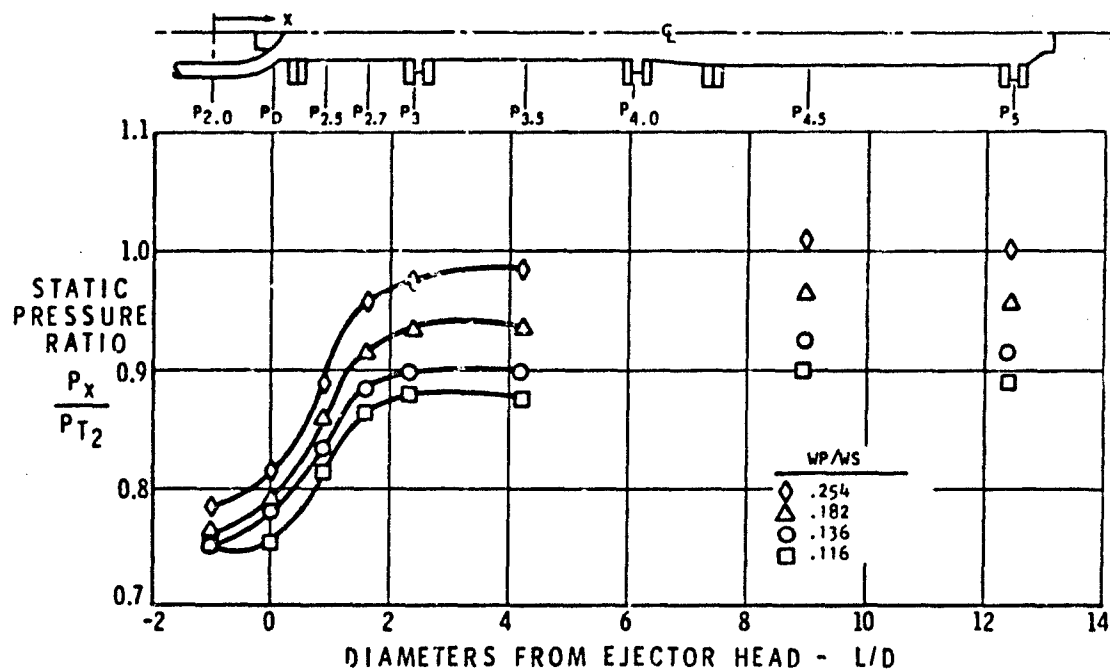
FIGURE 67. FOUR INLET DIFFUSER/MIXER STATIC PRESSURE DISTRIBUTIONS
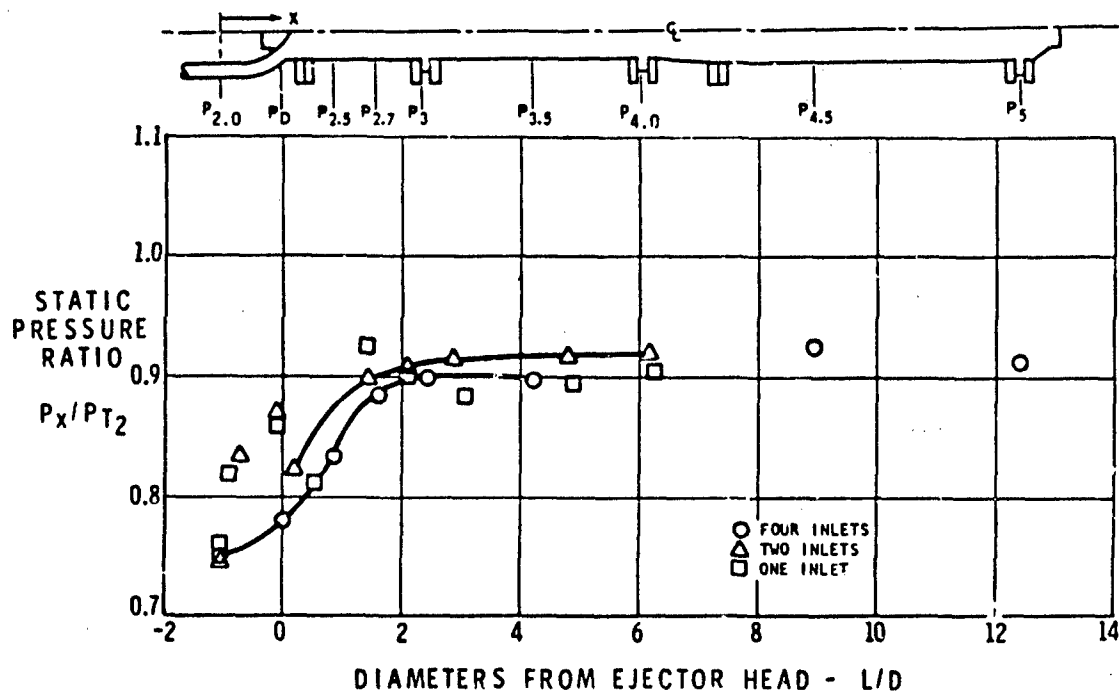
FIGURE 68. FOUR, TWO AND ONE INLET STATIC PRESSURE DISTRIBUTIONS

MIXER EXIT MACH NUMBER (M_4) = 0.25

EJECTOR CONFIGURATION	EJECTOR/MIXER TOTAL PRESSURE RECOVERY P_{T_4}/P_{T_2}	
● TWO INLET CONFIGURATIONS	W_P/W_S = 0.141	W_P/W_S = 0.350
	0.943	1.075
	0.941	1.089
	0.942	1.075
● SINGLE INLET CONFIGURATIONS		
	0.913	1.035
	0.917	1.044
	0.923	1.052

FIGURE 69. REPRESENTATIVE EJECTOR/MIXER PERFORMANCE

MIXER EXIT MACH NUMBER (M_4)$\cong$0.25
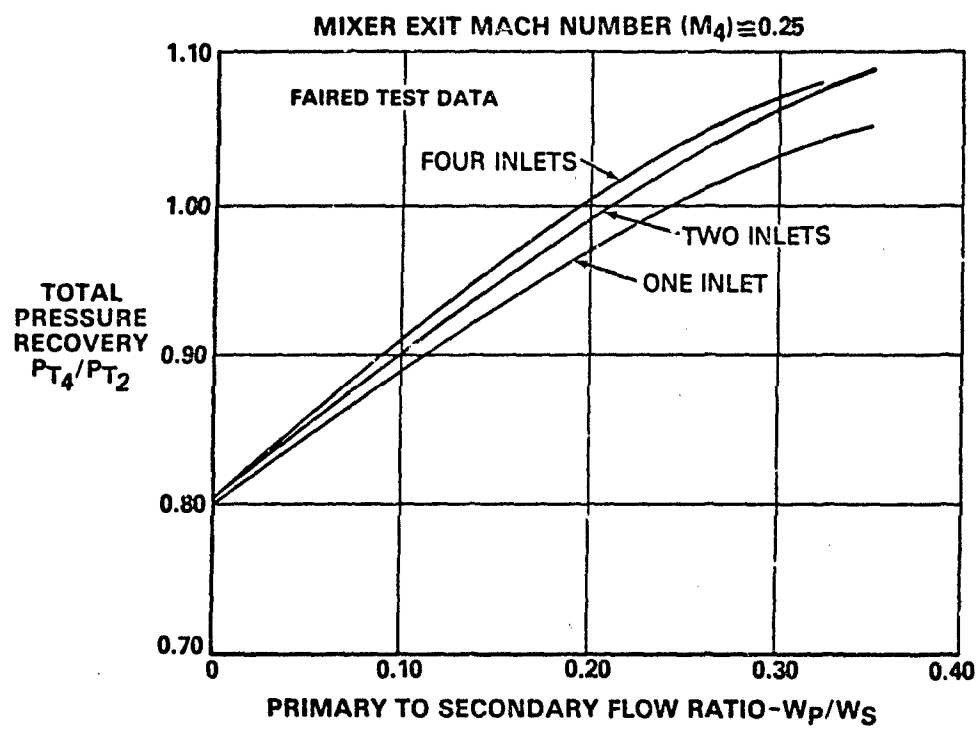
FIGURE 70. EJECTOR/MIXER PERFORMANCE COMPARISON

SOME ASPECTS OF ENGINE AND AIRFRAME INTEGRATION FOR RAMJET AND RAMROCKET POWERED MISSILES

by

E.L.Goldsmith

Royal Aircraft Establishment, Aerodynamics Department
Bedford MK41 6AE UK

SUMMARY

Ideally the subject of integration of a ramjet or ramrocket engine with an airframe covers all aspects of the differences between the performance of a complete configuration of a missile with air breathing propulsion installed and the test bed performance of an engine added to the external aerodynamic characteristics of a body, wings and controls but without nacelles.

The particular aspects that are covered herein concern the nature of the flow around a long circular body and the internal performance of single and multiple intakes in this flow. To understand this performance, the performance of isolated intakes at incidence and yaw conditions has been reviewed, together with ways that have been suggested for improving performance by use of variable geometry. The second half of the paper is concerned with external or airframe aspects of integration ie the measurement of forces and moments on missiles with and without nacelles and the estimation of drag components associated with nacelles.

NOMENCLATURE

A	area	Re	Reynolds number
a	speed of sound	$r,\dot{R}$	radius
b	wing span	x,y,z	spatial coordinates
C_D	drag coefficient (based on A_c or A_m)	α	angle of incidence
		γ	ratio of specific heats
C_N	normal force coefficient (based on A_b)	$\delta_{(\ )}$	surface slope
d	diameter	δ	boundary layer thickness
D	drag	ϕ	roll angle/circumferential position measured from windward bottom generator
L	length		
M	Mach number	θ	nose angle
P	total pressure	η, PR	pressure recovery $\dfrac{\bar{P}}{P_\infty}$
p	static pressure		
R	gas constant	ρ	density

SUFFICES

b	body	OP	operating condition
c	cone/capture plane	crit	critical flow condition
d	duct	t	total or stagnation
f	at the end of the subsonic diffuser or in the combustion chamber, skin friction	w,p	wave
		W	diverter
		L	local
CP	centre of pressure		
		S	survey station
l	lip position		
		∞	free stream

1   INTRODUCTION

The topics of airframe engine interaction and the closely allied, but not synono-
mous, one of airframe engine integration, have been subjects of international and of
national conference papers since the advent of jet propulsion[1,2,3,4]. In early designs of
jet propelled aircraft this interaction was often of a loosely coupled nature. With the
air intake in the nose of the aeroplane (as on the Gloster Whittle jet, the F86 and the
F100 etc aircraft) the interaction was more a problem of design than of aerodynamic per-
formance. The designer's problem was the location of fuel, armament, radar (and not least
the pilot) when the fuselage was largely occupied by duct and jet engine. When two
engines were needed the problem was more difficult, as witnessed by the convolutions of
the ducts of the British Aerospace Lightning aircraft, and engines were often placed in
separate nacelles on the wings as on the Messerschmitt 262, Gloster Meteor and more
recently SR71 aircraft. Here again, the interaction was more on overall aircraft design,
wing mounted nacelles affecting rolling moments of inertia, engine out yawing moments etc.

Many factors have been responsible for a closer integration of engine and airframe
for military aircraft, so that engine or engines remain in the body but the duct does not
completely obstruct the main carrying capacity of the fuselage. All current military
aircraft other than the large long range aircraft such as B52 and B1 adhere to this
formula.

The history of missiles with air breathing propulsion has followed a similar evolu-
tion. Early liquid fuel ramjet designs of the 1950s were a mixture of pod mounted
(Bomarc and Bloodhound Figs 1 and 2) and nose intake designs (Talos Fig 3) and even in
the 1960s, Sea Dart (Fig 4) continued this approach. With the need for more volume for
stowage of fuel and warhead in the body and the particular needs of the guidance and
homing radar to occupy an unobstructed position in the nose, more recent missile designs
have almost exclusively followed the aircraft trend. Intakes have been placed on the body
sides, top or bottom or in all four positions and usually located half way or even further
back along the body length, as in the ALVRJ (Fig 5). From the point of view of intake and
engine efficiency, undoubtedly the best place for an intake is under the body and close to
the nose as in ASALM (Fig 6). The missile must then be controlled as an aircraft by
banking to turn (twist and steer) so that whatever manoeuvre is pursued the intake always
remains on the underside of the body at positive incidence. Arguments between the merits
and elements of twist and steer versus Cartesian control for air-breathing weapons will
probably continue indefinitely.

With engines in the body and intakes on the side and/or top and bottom of the body
interaction between body and intake aerodynamics is closely coupled. At small angles of
incidence and in the absence of an adequate bleed or diverter, intake internal performance
is largely determined by the severity of the interaction of the intake shock system with
the body boundary layer. At larger angles of incidence the body flow field has a domi-
nating influence on intake internal performance and on the quality of the flow delivered
to the engine. Drag, lift and pitching moment increments due to the addition of nacelles
can be comparable to those due to wings and bodies. Other more subtle influences are felt
for instance in the design of the S-shaped ducts that are required to turn the air into
the body. If this portion of the duct can be kept short then less useful volume in the
body is consumed.

The object of successful engine-airframe integration is to make these closely
coupled configurations at least workable and possibly even competitive with nose mounted
intake or single intake bank-to-turn configurations. The object of this paper is to
summarise and correlate, where possible, some of the published (and unpublished) material
that is relevant to this aim.

2   BODY FLOW FIELDS

2.1   FLOW AROUND SLENDER CIRCULAR SECTION BODIES AT INCIDENCES FROM 0° TO 20°

For ogive nosed axi-symmetric bodies, flow changes in typical intake locations
compared to freestream conditions are fairly minor in the incidence range 0°-4° or 5° in
relation to the very considerable changes that take place between 6° and 20°.
Nevertheless, if an intake is placed in the nose flowfield effects are not insignificant
and indeed with the right choice of nose shape can be favourable to intake performance.
Fig 7 shows the variation in Mach number on the body surface with change in body shape at
M_∞ 2.0 and α 0°. The tangent ogive shape has advantages over only the first half of the
nose length. Fig 8 shows how the effect of the nose flow changes with distance away from
the body surface and position downstream from the nose. Radial changes near to the
tangent point of the nose profile are significant but are not so further downstream. At
small angles of incidence differences in local Mach number and flow angle start to appear
between top (leeward) side and bottom (windward) of the body which again vary with radial
and longitudinal position. The magnitude of these changes are illustrated in Fig 9. As
incidence increases the boundary layer thickens considerably on the lee side of the body
(Fig 10) and at incidences typically in the range 6°-10° (depending primarily on body nose
angle), boundary layer accumulation on the lee side forms into two discrete vertices
(Fig 11). When this happens, the flow around the upper half of the body becomes complex
and only windward and side positions can be expected to have reasonably uniform local

A complete flow field is shown in Fig 14. Intake centrelines are usually in the region $r-r_b/r_b$ of 0.3-0.5. On top and bottom generators local values of incidence are half to two thirds the freestream value. On the body side local incidence is 50-60% greater than freestream incidence. In the upper quadrant, local incidence is of the same order but the flow is now very non-uniform with local cross flows that may be supersonic and accompanied by embedded shocks. Even away from the core of the vortex where the intake might be expected to avoid ingesting very low total pressure air, the combined effect of high sidewash and upwash will be deleterious to any type or orientation of intake.

Experimental evidence on longitudinal location of vortex separation (Fig 15), together with vertical and lateral location of the vortex cores (Figs 16 and 17), is highly variable. This is probably due to the influences of Reynolds number, position and size of boundary layer trip and Mach number as well as the main geometric influence of nose fineness ratio. Most experimental observations however agree that vortex cores are located circumferentially between 20° and 40° from the top generator position (Fig 18) and this vitally affects intake performance in this region. Although the exact position of the twin symmetrical vortex cores is difficult to predict there is even more variability when at a higher angle of incidence the vortex cores become asymmetric and can vary in position with time. Fortunately, as shown in Fig 19, the combination of nose fineness ratio and incidence that leads to the production of asymmetric vortices is generally outside the region of interest to missiles with air-breathing engines (L_n/d_b 2 to 4 and α up to 20°).

2.2   THE INFLUENCE OF BODY MOUNTED STRAKES

When a body-mounted intake is rolled from the top position it must inevitably pass through or close to the vortex cores that are shed by the body at incidence (Fig 20). However, if sharp edged strakes are placed along the length of the body parallel to the centreline then these strakes will fix cross flow separation at a specific circumferential position. This position then moves round as roll angle is varied instead of remaining fixed in space as in the case with the unstraked body (Fig 20). Measurements have been made from vapour screen photographs taken with a camera mounted on the sting and downstream of a straked body. Data for α 10° at M_∞ 1.8 is shown in Fig 21. Vortex positions are shown relative to the viewpoint of an observer on the top strake looking upstream as the body is rolled from the top position to the side position (ϕ 180° to 90°). The particular orientation of the strake shown is for ϕ 165° but the envelope of the positions applies for all values of roll angle. It should be emphasised that these are not the absolute positions in space of the vortices but are the positions relative to the body as roll angle is changed. An indication of the size of the vortex cores as judged from the photographs is given by the width of the envelopes enclosing the vortex centre positions. It is clear that a location midway between the strakes is not a good position for an intake at this incidence of 10° as it will be affected by the vortices shed by the strakes on either side of it at the appropriate positive or negative roll angles. However there is a small region directly over the top of the strakes which is free (or nearly so) of vorticity at all positive and negative roll angles. This would be the best location for an intake (Fig 20). A similar situation would be obtained by the use of a square-section body, where the best position for an intake would be at the corners of the body (Fig 20).

Variation of pitot pressure for a radial position corresponding to the centre of a typical intake at L/d_b 7.5 is shown in Fig 22 as roll angle is varied at incidences of 10° and 14° both with and without strakes. Without strakes a large trough of low total pressure at about ϕ 150° appears as the pitot tube passes close to the vortex centre. With strakes this trough almost disappears at the lower incidence and is much reduced in extent at 14° incidence.

3   INTAKE AND ENGINE MATCHING AND DEFINITIONS OF INTAKE PRESSURE RECOVERY

Before considering intake performance, some digression is needed on the bases of comparison of pressure recovery. The intake flow states of supercritical, critical and subcritical are too well known to require explanation. Pressure recovery at the critical flow condition η_{crit} has been a convenient performance parameter for use in aircraft where variable geometry intakes and only small excursions from cruise incidence at supersonic speeds has also made this condition close to the matched intake and engine flow state. This is often not so however for highly manoeuvring missiles with fixed geometry intakes.

Matching of intake and engine flows for liquid fuelled ramjets is a relatively simple procedure.

Weight flow through a streamtube of cross sectional area A is:

$$W = \rho VA = \rho aMA = \sqrt{\frac{\gamma g}{RT}}\, pMA$$

$$\frac{A^*}{A} = \frac{M\left[1 + \frac{\gamma-1}{2}M^2\right]^{-\frac{\gamma+1}{2(\gamma-1)}}}{\left[\frac{\gamma+1}{2}\right]^{-\frac{\gamma+1}{2(\gamma-1)}}}$$

$$W = \sqrt{\frac{\gamma g}{RT_t}}\ AP\ \frac{A^*}{A}\left[\frac{\gamma+1}{2}\right]^{-\frac{\gamma+1}{2(\gamma-1)}} \tag{1}$$

At supersonic speeds when the nozzle at the end of the combustion chamber is choked:

$$W_n = \left[\frac{\gamma_n+1}{2}\right]^{-\frac{\gamma_n+1}{2(\gamma_n-1)}} \sqrt{\frac{\gamma_n g}{R_n}}\ \frac{A_n P_n}{\sqrt{T_{t_n}}} \quad \text{as } \frac{A^*}{A} = 1 \tag{2}$$

At entry to the combustion chamber:

$$W_f = \left[\frac{\gamma_f+1}{2}\right]^{-\frac{\gamma_f+1}{2(\gamma_f-1)}} \sqrt{\frac{\gamma_f g}{R_f}}\ \frac{A_f P_f}{\sqrt{T_{t_f}}}\ \left(\frac{A^*}{A}\right)_f \tag{3}$$

If the added fuel weight and the difference in γ and R between the incoming air and the exit gas stream after combustion are ignored then:

$$W_f = W_n \quad \text{and therefore} \quad \frac{A_n P_n}{\sqrt{T_{t_n}}} = \frac{A_f P_f}{\sqrt{T_{t_f}}}\left(\frac{A^*}{A}\right)_f$$

and if nozzle exit area A_n is constant

$$\frac{A_n}{A_f} = \text{constant} = \frac{\sqrt{T_{t_n}}}{\sqrt{T_{t_f}}}\ \frac{P_f}{P_n}\left(\frac{A^*}{A}\right)_f \tag{4}$$

Similarly the incoming free stream tube flow $W_\infty = W_f$ so that

$$\frac{A_\infty P_\infty}{\sqrt{T_{t_\infty}}}\left(\frac{A^*}{A}\right)_\infty = \frac{A_f P_f}{\sqrt{T_{t_f}}}\left(\frac{A^*}{A}\right)_f$$

and hence

$$\left(\frac{A^*}{A}\right)_f = \frac{A_\infty}{A_f}\ \frac{1}{P_f/P_\infty}\left(\frac{A^*}{A}\right)_\infty \quad \text{because } T_{t_\infty} = T_{t_f}$$

thus

$$\frac{A_n}{A_c} = \text{constant} = \frac{\sqrt{T_{t_n}}}{\sqrt{T_{t_f}}}\left(\frac{A^*}{A}\right)_\infty\ \frac{\frac{A_\infty}{A_c}}{P_f/P_\infty} \tag{5}$$

as $P_n/P_f = 1.0$

Engine operating curves for different values of heat addition T_{t_n}/T_{t_f} on the intake characteristic of A_∞/A_c versus P_f/P_∞ are thus straight lines through the origin with differing slopes.

In particular from equations (4) and (5) it follows that:

TABLE I

Variable	T_{t_n}	T_{t_f}	M_f	$\dfrac{A_\infty/A_c}{P_f/P_\infty}$	Intake operating point
If more fuel is added	increases	constant	decreases	decreases	)A_∞/A_c decreases at)constant P_f/P_∞ or)P_f/P_∞ increases at
If altitude is increased from sea level towards the tropopause	constant	decreases	decreases	decreases	)constant A_∞/A_c. Intake)moves from super-)critical to subcriti-)cal or from critical)to subcritical)conditions
If flight velocity increases at constant altitude	constant	increases	increases	increases	)A_∞/A_c increases at)constant P_f/P_∞ or P_f/P_∞)decreases at)constant A_∞/A_c.)Intake moves from)subcritical towards
If less fuel is added	decreases	constant	increases	increases	)supercritical)conditions

From this it can be seen that (a) it may be possible to keep the intake at approximately the same condition as the ramjet engine accelerates and climbs from a ground launch (b) for a given temperature rise there is a tendency for acceleration to be limited as intake recovery falls in the supercritical regime and thrust decreases.

The ramjet engine is opposite to the turbojet in its reaction to ambient and to engine conditions eg reduction of turbojet rpm on closing the throttle is associated with reduction in fuel flow and results in the intake moving towards the subcritical regime whereas closing the throttle and reducing fuel flow in the ramjet results in moving the intake towards the supercritical flow condition.

If the ramrocket and solid fuel ramjet are viewed as devices that increase the total temperature in the combustion chamber the same matching precepts apply. For the ramrocket the matching process could be complicated by the fuel rich under-expanded gas from a central nozzle restricting the passage of incoming air from the intake duct. In that case, part of the matching process could be similar to that encountered between secondary and primary streams of a supersonic ejector nozzle.

Fig 23 shows match points at the intersection of intake characteristics and the straight line constant M_f (constant temperature ratio) curves of an engine characteristic as angle of incidence changes at constant freestream Mach number. The parameters n_{crit}, the constant engine demand $n_{limiting\ \alpha}$ and $n_{operating}$ are made clear by the matching symbols used. $n_{operating}$ or n_{OP} is a more sophisticated version of $n_{limiting\ \alpha}$ in that it follows a constant engine demand line up to a limiting incidence α such as α_2 and then by decrease in fuel flow the operating point is made to move across engine demand lines to stay within the stable flow limit of an intake. $n_{utilisable}$ as the suffix suggests is French in origin. It is the pressure recovery at zero incidence imposed by the need for keeping constant engine demand lines at incidence within intake stable flow limits. When its value is lower than the zero incidence value the decrement is the penalty in pressure recovery incurred at zero incidence for operating the intake in a stable condition at incidence.

In this paper n_{crit} and n_{OP} are used. The former because it is widely available in the literature and the latter as it is a more realistic matching condition but nevertheless exploits the advantages of a ramjet than can be throttled.

4   EFFECT OF FLOW ANGLE VARIATION AND OF BODY FLOWFIELD ON INTAKE PERFORMANCE

4.1   EFFECT OF FLOW ANGLE VARIATION ON PERFORMANCE OF ISOLATED SUPERSONIC INTAKES

It is important to know the effect of flow angle variation on isolated intake performance before studying effects of the body flowfield.

For supersonic intakes with wedge compression surfaces that are normal to the plane of incidence, probably the most important influence on pressure recovery is the variation of shock loss with change in attitude of the compression surfaces. Fig 24 shows the

indicates that extra-to-shock losses are controlled so that pressure recovery change with incidence closely parallels the variation of shock recovery. If the wedge compression surface is parallel to the plane of incidence variation of shock recovery is not easily calculable. Flow over the yawed wedge compression surfaces is largely influenced by the presence or absence of swept endwalls that enclose the compression wedges. Flow expanding round the windward endwall may increase local Mach number in this region and the wedge shock will approach or enter the cowl lip. On the leeward endwall the opposite will occur. Reduced pressure recovery will result from coalescence of wedge shocks within the cowl lip and possibly from separation and vortex formation along the inside of the swept windward endwall. Removal of both and in particular the windward swept endwall reduces the fall off of pressure recovery with increase in angle of incidence (Fig 25). However, this increases drag and reduces pressure recovery at zero incidence due to supersonic spillage at the ends of the compression surfaces.

The flow pattern for an axisymmetric centrebody intake is generally more complex. The initial cone shock wave angle changes by much less than the change of centrebody centreline angle so that the windward lip moves towards the cone shock and the leeward lip away from it. Thus the variation of pressure recovery is largely affected by the shock wave angle θ_w relative to the lip position angle θ_l at zero incidence. If $\theta_w = \theta_l$ then intersection of cone and normal shock occurs within the windward cowl lip as incidence is increased, with a consequent loss in pressure recovery. The effect is clearly shown for single and two cone centrebody intakes in Fig 26(a). As freestream Mach number is reduced from the shock-on-lip Mach number (M_{SOL}) there is a reduction in both

terminal normal shock Mach number and a movement of the conical shocks away from the cowl lip which lessens the fall in recovery with incidence (Fig 27(a)). Decrease in θ_l (increase in M_{SOL}) to remove the cone shock from the cowl lip however results in a longer compression surface. This gives an increasing thickness of boundary layer which tends to accummulate on the leeside of the centrebody and results in lower recovery and increased engine face flow distortion (Fig 28). The corresponding changes to maximum flow ratio are shown in Figs 26(b) and 27(b).

4.2   REDUCING THE SENSITIVITY OF ISOLATED INTAKES TC CHANGE IN FLOW ANGLE

It is not difficult to devise ways of decreasing the rate of fall of pressure recovery as incidence increases in one direction. Intakes for highly manoeuvrable aircraft or missiles can be placed under the body or wing, so that local flow angle at intake entry plane is practically invariant with change of angle of incidence[23]. At supersonic speeds, increase in angle of incidence also decreases entry Mach number, usually with little decrease in local total pressure. The same result can be achieved by the addition of a plane surface above and in front of an intake. This is the principle used in the staggered or raked side intake proposed for highly manoeuvrable strike-fighter aircraft[24]. A rather larger pre-compression shroud has been shown to increase pressure recovery and capture flow for a rectangular intake at supersonic speeds in Ref 25 (Fig 29). The use of swept or unswept fisher plates for half axisymmetric intakes and a visor with axisymmetric intakes have been suggested (Ref 26, 27). At positive incidences above about 6° the half axisymmetric intake is generally superior (Fig 30) to the axisymmetric intake with or without a visor.

A slightly increased recovery is obtained at high incidence by pivoting the centrebody of an axisymmetric intake so that it is aligned with the incident flow. This is further enhanced by raking the entry plane so that the lower lip is clear of the conical shock (Fig 31). If the intake has to be equally efficient at both positive and negative incidences then the further complexity of pivoting both the centrebody and cowl is needed. Fig 31 shows this combination to be very efficient up to the highest angle of incidence tested (14°). Another variable geometry arrangement is the asymmetric compression surface housed within a circular section nacelle[29]. The only tests of this arrangement showed inferior performance at a 0° to the equivalent axisymmetric intake but better performance at incidence (Fig 32). Addition of boundary layer control on the compression surface and a more refined design method could probably enhance the performance of this intake which in concept should roll so that the compression surface is always in a favourable position with respect to the incident flow angle.

4.3   EFFECT OF BODY FLOWFIELD ON SINGLE INTAKE PRESSURE RECOVERY

Single intake pressure recovery is a function of angles of incidence and roll, of the longitudinal position of the intake on the body and of the boundary layer bleed or diverter height. At incidences up to about 6° before twin body vortices are formed (particularly if the intake is not far downstream of the body nose tangent point) the accummulation of boundary layer air on the leeside ensures that minimum recovery occurs at the ϕ 180° position (Figs 33 and 34). At a 10° the ingestion of a body vortex into the intake results in a minimum recovery at the ϕ 130°-150° position in accordance with body flowfield data (Fig 34).

The underbody intake (ϕ 0°) has an innate superiority at all incidences over all other positions (Figs 33 and 34), including the nose intake (Fig 26). However, despite the decrease in boundary layer thickness with increase in incidence on the windward side of the body (Fig 10), the effect of body cross flow leads to rapid deterioration of recovery as roll angle increases from 0° to 45° at a 10° (Figs 33 and 34).

Wedge intakes follow the same trends as half axisymmetric intakes (Fig 35). The beneficial effect of throat bleed and the deleterious effect of placing the intake on a flat face on the body should be noted (Fig 36). An inverted two wedge intake follows the same pattern with respect to variation of recovery with roll angle as the other intake types (Fig 37). The graph summarising recovery variation with roll angle at α 10° (Fig 38) is notable for showing the similarities rather than disparities in performance as intake type and freestream Mach number are varied which confirms the universality of the influence of ingestion of a body vortex. The graph summarising side intake performance (Fig 39) in contrast shows the wide variation in recovery obtained with different intake types in cross flow. This assumes great importance in the performance of multiple intakes as will be shown in the following section.

4.4   MULTIPLE INTAKE PERFORMANCE

The performance of multiple intakes is inferior to that of single intakes for the same incidence and roll angles for two reasons. The first is associated with the extra loss due to mixing (and in some cases due to 'dumping' ie a sudden enlargement loss) of the flow from the separate ducts at the entry to the combustion chamber. The second, with the matching that is imposed on individual duct flows by compatability conditions at the mixing plane which results in each intake operating at a different point on its individual characteristic of recovery versus flow.

Some indication of the relation between losses due to mixing and the angle at which the duct flows merge is given in Fig 40[35]. Overall loss for multiple intakes at 0°/180° roll angle as incidence is varied appears to collapse reasonably in to bands dependent on intake type by plotting the ratio of kinetic energy efficiency to that at zero incidence (at critical point conditions), Fig 41. Kinetic energy efficiency is defined as the ratio of the kinetic energy of the diffused stream after isentropic expansion back to freestream to that in the freestream. Its relationship to pressure recovery is shown in Fig 42. Variation of critical flow ratio with incidence is as important as the variation of pressure recovery and this is shown for ϕ 0° or 180° in Fig 43.

The influence of body vortices at angles of incidence above 6°-8° and roll angles of 20°-35° from the top position is as large as it is for single intakes. Fig 44 shows values for recovery variation with roll angle at α 8° for four axisymmetric intakes at two different diverter heights and with strakes placed between the intakes. At this incidence the affect of strakes is to anchor the body vortices in such a position that places them below the intake. At α 12° however (Fig 44) the stronger vortices shed by the strakes now impinge on the intakes and performance suffers accordingly. As with single intakes, the influence of increased diverter height is much smaller at this incidence than at lower angles.

Figs 45 and 46 show contours of constant η_{op} over a range of both incidence and roll angle for rectangular intakes mounted conventionally and inverted. Mismatching between intakes leading to unstable operation does not allow measurements to be made at some combinations of roll and incidence angles, particularly for the intakes mounted conventionally. The matching of individual intake flows has a large influence on the performance of multi-duct arrangements. Fig 47 shows that for two intakes at the top and bottom positions pressure recovery is almost invariant with change of incidence up to 16°. If four intakes are combined however the mean recovery of the top and bottom intakes falls with increased incidence at almost the same rate as the mean of the two side intakes.

The matching condition of equal static pressure where the four intake flows coincide results in the high performance at the top and bottom positions being reduced to the performance of the side intakes by forcing the top and bottom intakes to operate in a supercritical condition (Fig 48). Similarly when the body is rotated so that the two leeside intakes are ingesting the body vortices then these intakes are forcing the supercritical operation of the two windward intakes. The total extent of supercritical operation imposed upon one intake when operating in the presence of the other three as roll angle is varied is shown in Fig 49.

If the vortices can be prevented from being ingested, multiple intake performance will be raised at the ϕ 140°-160° position. However the poor performance of the side intakes at the $\phi = 90°$ position will still result in a minimal performance at this condition.

5   MEASUREMENT OF FORCES AND MOMENTS ON MISSILES WITH NACELLES

5.1   TECHNIQUES OF MEASUREMENT AND EXPERIMENTAL PROGRAMMES

Considerable experience has been obtained in the measurement of forces and moments on aircraft models that have nacelles with free flow ducts. Attempts to increase accuracy of measurement of external forces by mounting nacelles only on a balance have not been successful for a variety of practical reasons. Apart from these reasons measurement of forces on part of a complete configuration is not to be recommended because interference forces can be carried on parts of a model that are non-metric as well as on parts that are metric. It is better to measure forces and moments on a complete configuration and build up incremental values by the addition of components such as nacelles, wings, controls etc step by step. Models are almost invariably held by a rear sting with the ducted flow returning to the freestream around the central sting. Exit area that is continuously

can be attached to either the metric or the non-metric part of the model and cannot be
varied whilst the tunnel is operating. To provide sufficient exit area to ensure
supercritical operation of the intakes, the boattail region of the nacelles and body may
have to be modified or truncated. Incremental forces (particularly those associated with
correct geometric representation of the boattail and base regions and the effect of
underexpansion of the jet issuing from the real circular nozzles (as opposed to the free
flow annular nozzle of the model) have to be measured on a separate model with augmented
jet total pressure.

Similar programmes of measurement of forces and moments on bodies plus successive
additions of wings, controls and nacelles have been made at NASA, ONERA and RAE. The
models are all mounted on five or six component strain gauge balances that are shielded
from the duct flow, and measurements of base pressure and internal forces are made to
correct balance measurements and obtain external forces and moments. The extensive tests
reported in Refs 36-38 were conducted with single and twin intake configurations with and
without a wing and tail controls. The intakes were both rectangular and axisymmetric and
were tested with one value only of exit area (Fig 50). Tests in tunnel S2 Modane by ONERA
and in the 8ft x 8ft Tunnel at RAE (Bedford) have been done on models with about twice the
body diameter of the NASA model. The ONERA model (Fig 51) has a fixed choked exit with
exit contraction attached to the metric part of the model. Momentum at the choked exit is
estimated from static or total pressure measurements upstream of the exit. In the RAE
model (Fig 52) the exit momentum station is upstream of the non-metric variable exit area.
Skin friction forces are estimated on the small portion of the outer wall of the annular
duct that is downstream of the rake and added to the momentum change evaluated from
freestream to the rake station. The total pressure rakes have large clearances from both
outer and inner duct walls so that metric parts of the model are not contacted when the
model deflects under normal force loads at high incidence. A calibration using a static
flow   rig such as the Aircraft Research Association Mach Simulation Tank (MST) is
necessary for the accurate evaluation of internal momentum and mass flow from the rake
pitot and static pressure measurements. The current range of model geometries and test
conditions is shown in Fig 53.

5.2   NORMAL FORCE AND CENTRE OF PRESSURE CHANGES DUE TO ADDITION OF NACELLES

Although nacelles are separate entities that are added to the basic body, results
of Refs 36-38 (unlike ONERA and RAE measurements) do not include body alone data. Normal
force and centre of pressure estimates for a cylindrical body with a tangent ogive nose by
the semi-empirical British Aerospace ABACUS method have been shown to be accurate.
Estimates using ABACUS and incremental forces measured due to the addition of tails on the
single intake configuration have enabled incremental normal forces to be derived for both
single and twin intake configurations (Fig 54,55). Rectangular nacelles act as more effi-
cient wings than circular nacelles over the whole incidence range and, as would be
expected, the addition of nacelles and tails shifts the centre of pressure (measured from
the body apex) rearwards from the body alone position. Normal force increments measured
at ONERA on single and twin intakes at incidences from 0° to 7° agree very well with NASA
measurements. The addition of a single underbody intake results in a small deterioration
to the lifting efficiency of the body. Increase in freestream Mach number from 2.5 to
3.95 leads to reduced normal force slope from 0° to 10° incidence but thereafter the slope
is little changed (Fig 56).

RAE and ONERA measurements have mainly been made on four-intake arrangements.
Variations with incidence of incremental normal force and of centre of pressure position
are shown in Fig 57 and exhibit the same trends as those observed for the two intake
configurations. Variation of normal force increment with roll angle for four rectangular
intakes is quite small (Fig 58).

Fig 59 summarises the changes in nacelle normal force increment in comparison with
wing normal force increments with net span which is relevant to launcher dimensional
constraints and with net planform area. On a planform basis obviously the nacelles are
inefficient with respect to wings but on a span basis this is not so evident.

6   DRAG OF MISSILES WITH AIR BREATHING PROPULSION

6.1   COMPONENTS OF DRAG AND THEIR MAGNITUDE

Total missile drag is made up of wave and skin friction drag of the four main
components, body, wings, controls and engine installation together with interference
between these components and the drag of miscellaneous items such as aerials, leaks,
surface roughness and excrescences such as cable ducts etc. Engine installation drag
components are cowl, pre-entry (or additive as it is known in the USA) intake spillage,
body boundary layer bleed or diverter, compression surface bleed and afterbody.

These are illustrated diagrammatically in Fig 60 and all except afterbody drag will
be considered in more detail. The concept of pre-entry or additive drag is well known and
follows from the conventional definition of engine thrust as being the change of pressure
and momentum forces for the flow in the ingested streamtube from freestream to nozzle
exit. If engine and intake matching ensures that the intake is always operating in a
critical or supercritical condition then, depending on shock-on-lip Mach number M_{SOL},
the intake is operating at datum flow (Fig 60(a)) or at maximum (or full) flow with

confined to cowl wave drag D_{cowl_0} and skin friction drag. If at maximum flow, compression surface shocks are ahead of the cowl lip and there is a wave drag due to pre-entry or supersonic fore-spillage, D_{pre_0}, to be added to cowl wave drag (Fig 60(b)) so that:

$$D_{ext_0} = D_{pre_0} + D_{cowl_0}$$

If the intake is operating in the subcritical regime with the cowl lip shock detached (Fig 60(c)) then:

$$D_{ext} = D_{pre} + D_{cowl} = D_{pre_0} + D_{cowl_0} + D_{spill}$$

or

$$D_{spill} = D_{pre} - D_{pre_0} + D_{cowl} - D_{cowl_0}$$

The change in cowl wave drag ΔD_{cowl} ($= D_{cowl} - D_{cowl_0}$) is usually a small negative quantity that slightly offsets the large increase in pre-entry drag ($D_{pre} - D_{pre_0}$) that occurs when all or part of the fore-spillage is subsonic. Designers of missiles with ramjet engines generally try to avoid operating intakes subcritically. However, if the intake has excessive (ie non-self starting) internal contraction then the critical and supercritical flow regime is identical to a subcritical flow regime as regards external drag.

An illustration of the wide range of values for drag components for two designs (nose mounted intake and side mounted intakes) is shown in Table II.

TABLE II

Component	Nose mounted intake		Body side mounted intakes	
	Wave %	Skin friction %	Wave%	Skin friction %
Cowl	35		2)	
Diverter	-		12)	11
Afterbody	15		2)	
Wings and controls	15	7	21	
Body		14	) 52	
Miscellaneous	14		)	

A more detailed breakdown of intake drag for body mounted nacelles has been given in Ref 39 and is shown in Table III.

TABLE III

Intake type	Rectangular %	Half axisymmetric %	Axisymmetric %
Component			
Cowl and endwalls	6.0	6.5	6.0
Pre-entry	1.5	2.0	1.7
Diverter or bleed h/d $\quad$ 0.033	2.5		
0.053			2.0
0.066	6.5		
0.1	8		
Compression surface bleed	5		

Some of the large differences in component drag are due to different standards of

6.2 ESTIMATION OF DRAG

6.2.1 AXISYMMETRIC AND HALF AXISYMMETRIC COWLS

Historically some of the first predictions of wave drag for circular pitot intakes were obtained using linear or first order theory. Using the linearised equation:

$$\frac{\partial^2 \phi}{\partial r^2} - \beta^2 \frac{\partial^2 \phi}{\partial x^2} + \frac{1}{r}\frac{\partial \phi}{\partial r} = 0$$

where ϕ is a perturbation potential defined by

$$u_p = \frac{\partial \phi}{\partial x} \text{ and } v_p = \frac{\partial \phi}{\partial r}$$

$$\text{and } u = U + u_p , \quad v = v_p$$

$$u_p \text{ and } v_p \ll U, \quad u_p \text{ and } v_p \ll a$$

Lighthill[40,41] derived expressions for pressure coefficients on slender bodies with both continuous and discontinuous variations in body slope. Fraenkel[42] extended this to open nosed bodies of revolution and obtained expressions for drag of both conical and parabolic cowl shapes. Willis and Randall[43] applied slender body theory to a family of curved profiles defined by:

$$R = R_m - (R_m - R_c)\left(1 - \frac{x}{L}\right)^n \text{where } n > 1$$

which includes the conical (n = 1) and the parabolic cowl (n = 2) (Fig 61) to obtain a general expression for drag (if n is an integer and greater than unity) as:

$$C_D \left(\frac{L}{R_m}\right)^2 = 2 \left(1 - \frac{R_c}{R_m}\right)^2 n^2 \left\{\alpha_n + \beta_n \frac{R_c}{R_m} + \gamma_n \frac{A_c}{A_m} + \frac{A_c}{A_m}\log_e \frac{2}{\frac{\beta R_c}{L}}\right\}$$

where α_n, β_n and γ_n are functions of n and are plotted in Fig 62.

The conical profile (n = 1) has two discontinuities in slope (at the beginning and end of the profile) and the expression for drag is:

$$C_D \left(\frac{L}{R_m}\right)^2 = 2 \left(1 - \frac{R_c}{R_m}\right)^2 \left\{\frac{R_c}{R_m} - \frac{1}{2} - \frac{1}{2}\frac{A_c}{A_m} + \left(1 + \frac{A_c}{A_m}\right)\log_e \frac{2}{\frac{\beta R_m}{L}} - \frac{A_c}{A_m}\log_e \frac{R_c}{R_m}\right\}$$

A simpler expression for the wave drag of conical cowls was deduced by Ward[44] using quasi-cylinder rather than slender body approximations as:

$$C_D = \frac{D}{\pi \bar{R}^2} = 4 \delta_c^2 U_1 \left(\frac{L}{\beta \bar{R}}\right)$$

where $U_1(x)$ is shown plotted in Fig 63 and δ_c is the cone semi-angle in radians and $\bar{R}$ is a mean radius. Warren and Gunn[45] showed that the simplest mean radius $\bar{R} = (R_c + R_m)/2$ does not give plausible results when R_c becomes much smaller than R_m and the open nose body tends towards a solid cone. A weighted mean radius $\bar{R}^2 = (R_c^2 + R_m^2)/2$ gives a better result for area ratios R_c^2/R_m^2 from 1.0 to 0.2 so that the expression for drag coefficient based on maximum area becomes:

$$C_D = \frac{D}{\pi R_m^2} = 2\delta_c^2 \left[1 + \frac{R_m^2}{R_c^2}\right] U_1 \left[\frac{\sqrt{2}}{\delta_c \beta} \cdot \frac{\left(1 - \frac{R_m}{R_c}\right)}{\sqrt{1 + \left(\frac{R_m}{R_c}\right)^2}}\right]$$

Fraenkel[46] used quasi-cylinder approximations to derive the following expression for the drag of parabolic profiles:

$$C_D \left(\frac{L}{R_m}\right)^2 = \frac{8}{(L/R_m)^2} \cdot \frac{\left(\frac{\bar{R}}{R_m}\right)^4}{\left(L_b/L\right)^4} T \left(\frac{L}{\beta \bar{R}}\right)$$

where $T(x)$ is also plotted in Fig 63.

L_b is the length of the full body and L is the length of the open nosed body which is a part of the full length body.

slender body and quasi-cylinder approximations for conical and parabolic profiles are given in Ref 46. Fraenkel[47] gives a similar presentation combining slender body (for $\beta R_m/L = 0.05$ to 0.3) and quasi-cylinder (for $\beta R_m/L = 0.6$ to 1.0) values modified by the introduction of exact values for conical and parabolic pointed bodies at $A_c/A_m = 0$.

Values from Ref 47 are compared to the slender body results of Willis and Randall and results from characteristics calculations for conical profiles[48] in Fig 64.

Both first order and Van Dyke's second order theory become increasingly inaccurate as initial angle of the cowl approaches the freestream Mach angle. Cowls for centrebody intakes are usually inclined initially near to the local flow direction from the conical compression surfaces and hence their initial slopes can be close to or in excess of the freestream Mach angle and other methods for the evaluation of wave drag have to be used. The most accurate of these is the method of characteristics followed by (in order of decreasing accuracy and increasing simplicity) the methods of second order shock-expansion, generalised shock-expansion, tangent-wedge, and impact theory. In all these methods it is convenient to divide the cowl into a number of straight line segments and to evaluate the pressure coefficient on each segment before summing to obtain the wave drag. Fig 65 illustrates the essentials of each method. Appendix B of Ref 49 contains all the information necessary to calculate the geometry of points on the input ray 1-6, at the field points 3-11 (defined as the intersection points of first and second family Mach lines that are equally inclined to the streamline direction) and at body and shock wave points 7 and 12.

Presley and Mossman in Ref 49 give results of applying all these methods to the same family of cowl profiles studied by Willis and Randall for one length and one area ratio A_c/A_m.

Experimental values from a series of pressure plotted elliptic profile cowls that can be approximated by the Willis and Randall family are given by Samanich in Ref 50. These values of wave drag are shown plotted in Fig 66 in the linear theory form of $C_D(L/R_m)^2$ versus $\beta R_m/L$ which effectively collapses all the results from different initial slope cowls and Mach numbers for a given area ratio. Values from shock-expansion calculations for the same profiles are not quite so well collapsed. The same values for wave drag together with results from the Presley and Mossman characteristics calculations are plotted in Fig 67 using the hypersonic similarity parameters $0.7\,C_D\,M_\infty^2$ and $M_\infty\,\delta_0$.

The parameters also effectively collapse both measured and characteristics values into curves that appear to be only functions of area ratio. However variation with area ratio is different for the characteristics and the measured values as illustrated in Fig 68 probably because fineness ratio does not occur explicitly in the hypersonic similarity parameters. Although fineness ratio does occur in the supersonic similarity parameters, Fig 69 shown that characteristic values are not properly collapsed for variation of both Mach number and fineness ratio.

For the fineness ratios 0.4-2.3 and area ratios 0.5-0.8 of the experimental measurements the shock-expansion method is probably sufficiently accurate for most purposes until the Mach number at which the cowl shock wave becomes detached is approached. Under these conditions if the cowl initial angle is not too high, linear theory appears to give a reasonable result (Fig 70).

6.2.2 PRE-ENTRY AND SPILLAGE DRAG

Pre-entry drag can be evaluated either by computing the change in pressure forces and momentum for the flow in the ingested streamtube from freestream conditions to the intake entry plane or by integrating the pressure multiplied by projected area along the stagnation streamline from freestream to intake cowl lip.

Evaluation of pre-entry drag due to supersonic forespillage by integrating the pressure along the stagnation streamline is particularly simple for a two wedge or cone compression surface:

$$D_{pre_0} = (p_1-p_\infty)(A_1-A_\infty) + (p_2-p_\infty)(A_c-A_1)$$

Some typical values for cone, wedge and double wedge compression surfaces with compression surface shock waves focussed on the cowl lip at M_∞ 2.4 are shown in Fig 71(a).

When the intake is operating with subsonic forespillage and the cowl lip shock is detached evaluation of pre-entry drag (Fig 71(b)) for a two wedge or cone compression surface becomes:

$$D_{pre} = (p_1-p_\infty)(A_1-A_\infty) + (p_2-p_\infty)(A_2-A_1) + \int_{NS}^{stagnation\ pt} (p-p_\infty)dA$$

and is more difficult because the variation of pressure along the stagnation streamline from the detached normal shock to the cowl lip is not known. However as was stated in Section 6.1 increased pre-entry drag due to subsonic forespillage is accompanied by

$$D_{spill} = \int_{NS}^{\text{stagnation point}} (p-p_\infty)dA + \Delta D_{cowl} = (p_{NS}-p_\infty)(A_c-A_\infty)$$

ie the underestimate of pre-entry drag obtained by not accounting for the rise in static pressure from the value behind the normal shock to the stagnation point value compensates for the decrease in cowl drag (ΔD_{cowl} is negative). This can be written alternatively as:

$$C_{D_{spill}} = \frac{D_{spill}}{q_\infty A_c} = \frac{10}{6}\left(1 - \frac{A_\infty}{A_c}\right)\left(1 - \frac{1}{M_\infty^2}\right)$$

This method of estimation obviously does not take account of differences in ΔD_{cowl} due to differences in the shape of sharp lipped cowls. It is found, generally, that above M_∞ 1.6-1.7 the ΔD_{cowl} term is small and for spillage up to 20-30% the effect of variation of cowl shape is very small.

The pitot intake assumption obviously applies directly for compression surface intakes when the compression surface shocks are on or inside the cowl lip and spillage drag evaluated on this basis at M_∞ 2.4 is shown in Fig 71(c). If the compression surface shocks are outside the cowl lip and their intersection point with the detached normal shock also remains outside the entering streamtube as the intake spills, then on the same basis (Fig 71(d))

$$D_{spill} = (p_1-p_\infty)(A_1-A_\infty) + (p_2-p_\infty)(A_2-A_1) + (p_{NS}-p_\infty)(A_c-A_2)$$

The position of the normal shock has to be found to evaluate A_1 and this is done by assuming a linear movement of the cowl lip shock from attached at full flow to the shock position that would be obtained for a blunt body equivalent to the intake at zero flow[52]. The shock wave geometry can be treated in differing ways for a multiple shock compression surface and analytical expressions for two-wedge intakes are given in Ref 53.

6.2.3 DIVERTER AND BLEED DRAG

The boundary layer on the body can be prevented from entering the intake by raising the intake from the surface of the body and then diverting or ducting away the boundary layer in the space between the intake and the body surface. In both cases the boundary layer diversion or extraction will be associated with a drag.

BLEED DRAG

A ram scoop bleed may be preferable to a diverter if the main flow duct has to turn into the body immediately downstream of the entry plane so that the angle of the diverter wedge has to be large or if air is needed for some purpose such as cooling electronic components. The bleed duct will perform in the same manner as the main engine air duct. A correct choice of exit area will enable the intake to run full ie in a critical or supercritical condition and at supersonic speeds the exit area to the bleed duct will be choked unless the bleed pressure recovery is very low. A divergent nozzle can be added downstream of the choked throat to expand the bleed flow to freestream or possibly base static pressure and discharge the bleed air at supersonic velocity if sufficient bleed total pressure is available.

Bleed internal drag can be written as:

$$C_{D_{BL_{int}}} = \frac{D_{BL_{int}}}{q_\infty A_c} = \frac{2A_{BL_\infty}}{A_c} - \left\{\left(\frac{P_{ex}}{P_\infty}-1\right)\frac{P_\infty}{q_\infty} + \frac{2q_{ex}}{P_{ex}}\frac{r_{ex}}{P_\infty}\frac{P_\infty}{q_\infty}\right\}\frac{A_{BL_{ex}}}{A_c}$$

If the bleed air is choked at exit

$$C_{D_{BL_{int}}} = \frac{2A_{BL_\infty}}{A_c} - \left\{\left(0.5283\frac{P_{BL_{ex}}}{P_\infty}\cdot\frac{P_\infty}{P_\infty}-1\right)\frac{P_\infty}{q_\infty} + 0.7396\frac{P_{BL_{ex}}}{P_\infty}\frac{P_\infty}{q_\infty}\right\}\frac{A_{BL_{ex}}^*}{A_c}$$

where the choked exit area for the bleed flow is:

$$\frac{A_{BL_{ex}}^*}{A_c} = \frac{A_{BL_\infty}/A_c}{\frac{P_{BL_{ex}}}{P_\infty}\left(\frac{A_\infty}{A_\infty^*}\right)}$$

If the bleed air is discharged at supersonic speed where $\dfrac{P_{BL_{ex}}}{} = 1$

$$C_{D_{BL_{int}}} = 2 \left\{ \frac{A_{BL_\infty}}{A_c} - \left(\frac{q_{BL_{ex}}}{P_{BL_{ex}}} \right) \frac{P_{BL_{ex}}}{P_\infty} \cdot \frac{P_\infty}{q_\infty} \cdot \frac{A_{BL_{ex}}}{A_c} \right\}$$

where $M_{BL_{ex}}$ and hence $\frac{q_{BL_{ex}}}{P_{BL_{ex}}}$ and $\left(\frac{A^*}{A} \right)_{BL_{ex}}$ follow from:

$$\frac{P_{BL_{ex}}}{P_{BL_{ex}}} = \frac{p_\infty / P_\infty}{P_{BL_{ex}} / P_\infty}$$

and

$$\frac{A_{BL_{ex}}}{A_c} = \left(\frac{A}{A^*} \right)_{BL_{ex}} \frac{A_{BL_{ex}}^*}{A_c}$$

Values for $C_{D_{BL_{int}}}$ calculated from these two equations are shown in Fig 72[54] as functions of M_∞, bleed intake pressure recovery $P_{BL_{ex}}/P_\infty$ and bleed flow A_{BL_∞}/A_c. For a normal shock ram scoop bleed, bleed pressure recovery values are shown typically in Fig 73[54].

The same equations can be used to calculate bleed drag for a compression surface throat bleed (Fig 74). For a flush throat bleed, total pressure is found to be roughly equal to the static pressure behind the final normal shock of the main intake and this pressure recovery p_{NS}/P_∞ is shown calculated for a 10°-10° wedge compression surface in Fig 73.

DIVERTE . DRAG

The wave drag of wedge shaped boundary layer diverters (Fig 75) has been presented in a correlation shown in Fig 76 (from Ref 55) for three different diverter heights h/δ 0.75, 1.0 and 1.25. The same basic data (derived from NASA reports of the 1950s)[56],[57],[58] has been smooth and plotted in carpet form for h/δ 1.0 in Fig 77(a). Change of diverter drag with change in h/δ is shown in Fig 77(b) and illustrates some of the scatter of the data.

Compressible flow flat plate boundary layer data gives a good estimate of diverter skin friction drag if the skin friction coefficient is based on total wetted area inside the diverter passage and the Reynolds number is based on the length of the diverter passage. Alternatively Ref 55 gives diverter skin friction drag as:

$$C_{D_{fw}} = C_{fw} \times \frac{C_{D_f}}{C_{fw}} \times \frac{A_w}{A_p}$$

where C_{fw} and the multiplication factor C_{D_f}/C_{fw} are obtained from Fig 78. The Reynolds number in this case is based on frestream conditions and length of boundary layer upstream of the diverter entry. A_p is the frontal area of the diverter and A_w the wetted area of the diverter passage.

7   CONCLUDING REMARKS

Although the internal flow efficiency of nose intakes and underbody intakes (when combined with a bank-to-turn control system) will always be superior to body mounted multi-intakes, the overall efficiency taking into account external flow forces, volume utilisation and control reaction time may not be so clearly demonstrable. The considerable interaction effects of the body flow field on multi-intake performance and nacelle contributions to external forces have been illustrated. Effects of body cross flow and vortex ingestion have been highlighted. At the present time it is not clear what type of intake (rectangular, half axisymmetric or axisymmetric) or orientation is best suited to these unfavourable flow fields at matched engine and intake airflows.

ACKNOWLEDGEMENTS

REFERENCES

1   M. Webster.   Engine airframe integration.   Royal Aeronautical Society Journal.

3 M.R. Nichols. Aerodynamics of airframe-engine integration of supersonic aircraft. AGARD CP No 9, Pt I.

4 Integration of propulsion systems in airframes. AGARD CP No 27.

5 W.F. Davis, R. Scherrer. Aerodynamic principles for the design of jet-engine induction systems. NACA RM A55F16.

6 L.E. Hasel, J.L. Lankford and A.W. Robins. Investigation of a half conical scoop inlet mounted at five alternate circumferential locations around a circular fuselage. Pressure recovery results at a Mach number of 2.01. NACA L53D30.

7 L.E. Hasel. The performance of conical supersonic scoop inlets on circular fuselages. NACA L53I14a.

8 J.L. Lankford. Preliminary results of flow surveys about an inclined body of revolution. NAVORD Report 6708.

9 W.C. Ragsdale. Flow field measurements around an ogive cylinder at angles of attack up to 15 degrees for Mach numbers 3.5 and 4.0. NOL TR 72-198.

10 L.H. Jorgensen, E.W. Perkins. Investigation of some wake vortex characteristics of an inclined ogive-cylinder body at Mach number 1.98. NACA RM A55E31.

11 B.E. Tinling, C.Q. Allen. An investigation of the normal force and vortex wake characteristics of an ogive cylinder body at supersonic speeds. NASA TN D-1297.

12 M. Cooper, P. John and L.E. Hasel. A pressure distribution investigation of a fineness ratio 12.2 parabolic body of revolution (RM10) at M = 1.59 and angles of attack up to 36°. NACA RM L52G14a.

13 J.F. Mello. Investigation of normal force distributions and wake vortex characteristics of bodies of revolution at supersonic speeds. Journal of the Royal Aeronautical Society, Vol 26, No 3, March 1959.

14 T.E. Chamberlain. Aerodynamic forces, separation lines and vortex trajectory on slender bodies with several nose shapes. Massachusetts Institute of Technology Thesis, June 1966.

15 M.R. Mendenhall, J.N. Nielsen. Effect of symmetrical vortex shedding on the longitudinal aerodynamic characteristics of wing-body-tail configurations. NASA CR-2473.

16 C.S. Brown, E.L. Goldsmith. Measurement of the internal performance of a rectangular air intake with variable geometry, Part II. The affect of incidence. RAE Technical Report 71159.

17 C.S. Brown, E.L. Goldsmith. Measurement of the internal performance of a rectangular air intake mounted on a fuselage at Mach numbers from 1.6 to 2.0. RAE Technical Report 72136.

18 M.A. Beheim. A preliminary investigation at Mach number 1.91 of a diffuser employing a pivoted cone to improve operation at angle of attack. NACA RM E53I30.

19 M.A. Beheim, T.G. Piercy. Preliminary investigation of a shield to improve angle of attack performance of a nacelle type inlet. NACA RM E57G25a.

20 J.F. Connors, R.C. Meyer. Performance characteristics of axisymmetric two-cone and isentropic nose inlets at Mach number 1.9. NACA RM E55F29.

21 J.F. Connors, G.A. Wise and J.C. Lovell. Investigation of translating double-cone axisymmetric inlets with cowl projected areas 40 and 20 per cent of maximum at Mach numbers from 3.0 to 2.0. NACA RM E57C06.

22 R. Hawkins. The effects of incidence upon the performance of 24°-31° double cone intakes. Bristol Siddeley Engines Report AP 5081.

23 J.E. Hawkins. YF16 inlet design and performance. AIAA Paper No 74-1062.

24 J.A. Ross, I. McGregor and A.J. Priest. Some RAE research on shielded and unshielded fuselage mounted air intakes at subsonic and supersonic speeds. Aerodynamics of power plant installation. AGARD CP 301.

25 J.G. Bendot, A.E. Heins. Ramjet air induction system design for tactical missile application. 5th International Symposium on Airbreathing Engines, Feb 1981.

26 M.A. Beheim. A preliminary investigation at Mach number 1.91 of an inlet configuration designed for insensitivity to positive angle of attack operation.

28   N.E. Samanich. R.W. Cubbison. A pivoting cowl and spike technique for efficient
      angle of attack operation of supersonic inlets. NASA RM E 301la.

29   J.F. Connors, R.R. Woollett. Preliminary investigation of an axisymmetric swept
      nose inlet of circular projection at Mach number 3.85. NASA RM E54G26.

30   A.S. Valerino, C.B. Pennington and D.J. Vargo. Effect of circumferential location
      on angle of attack performance of twin half conical scoop type inlets mounted
      symmetrically on the RM10 body of revolution. NACA RM E53G09.

31   E.J. Kremzier, R.C. Campbell. Angle of attack supersonic performance of a
      configuration consisting of a ramp-type scoop inlet located either on top or bottom
      of a body of revolution. NACA RM E54C09.

32   E.J. Kremzier, R.C. Campbell. Effect of fuselage fences on the angle of attack
      supersonic performance of a top inlet-fuselage configuration. NACA RM E54J04.

33   G.A. Mitchell, B.G.Chiccine. Investigation of high angle of attack performance of
      a 14° ramp type inlet in various circumferential body locations. Mach number range
      1.5 to 2.0. NACA RM E57C12a.

34   D.J. Vargo, P.N Parks and O.H. Davis. Investigation of a high performance top
      inlet to Mach number of 2.0 and at angles of attack to 20°. NASA RM E57A21.

35   R. Hurd. Ramjet engine intake performance data. Rolls Royce GN 18687.

36   C. Hayes. Aerodynamic characteristics of a series of single-inlet air breathing
      missile configurations. NASA TM 84557.

37   C. Hayes. Aerodynamic characteristics of a series of twin-inlet air-breathing
      missile configurations I. Axisymmetric inlets at supersonic speeds.
      NASA TM 84558.

38   C. Hayes. Aerodynamic characteristics of a series of twin-inlet air-breathing
      missile configurations II. Two-dimensional inlets at supersonic speeds.
      NASA TM 84559.

39   G. Laruelle. Prises d'air four missile probatoire de statofusee. L'Aeronautique
      et l'Astronautique No 98 1983-1.

40   M.J. Lighthill. Supersonic flow past bodies of revolution. R&M 2003, Jan 1945.

41   M.J. Lighthill. Supersonic flow past slender bodies of revolution the slope of
      whose meridian section is discontinuous. Quarterly Journal of Mechanics and
      Applied Maths, Vol I, Part I, March 1948.

42   L.E. Fraenkel. The theoretical wave drag of some bodies of revolution.
      R&M 2842, May 1951.

43   J.H. Willis, D.G. Randall. The theoretical wave drag of open nose axisymmetrical
      forebodies with varying fineness ratio, area ratio and nose angle.
      RAE TN Aero 2360.

44   G.N. Ward. Supersonic flow past slender pointed bodies. Quarterly Journal of
      Mechanics and Applied Maths, Vol 2, Part I, March 1949.

45   C.H.E. Warren, R.E.W. Gunn. Estimation of external drag of an axially symmetric
      conical nose entry for jet engine at supersonic speeds. RAE TN Aero 1934.

46   L.E. Fraenkel. The theoretical wave drag of some bodies of revolution.
      RAE Report Aero 2420.

47   L.E. Fraenkel. Curves for estimating the wave drag of some bodies of revolution
      based on exact and approximate theories. RAE TN Aero 2184.

48   E.F. Valentine. External drag estimation for slender conical ducted bodies at high
      Mach numbers and zero angle of attack. NASA Technical Note D648, March 1961.

49   L.L Presley, E.A. Mossman. A study of several theoretical methods for computing
      the zero-lift wave drag of a family of open nosed bodies of revolution in the Mach
      number range of 2.0 to 4.0. NACA Technical Note 4368, September 1958.

50   N.E. Samanich. Pressure drag of axisymmetric cowls having large initial lip angles
      at Mach numbers from 1.90 to 4.90. NASA Memo 1-10-59E.

51   L.E. Fraenkel. The external drag of some pitot-type intakes at supersonic speeds,
      Part I. RAE Report Aero 2380.

52   W.E. Moeckel. Approximate method for predicting form and location of detached

53   I. McGregor. Some theoretical parameters relevant to the performance of rectangular air intakes with double-ramp compression surfaces at supersonic speeds. RAE TR 71232.

54   E.L. Goldsmith. Boundary layer bleed drag at supersonic speeds. R&M 3529.

55   K.F. Little et al. Internal aerodynamics manual. North American Rockwell Corporation NR-68-H-434, Vol I-III.

56   T.G. Piercy, H.W. Johnson. An experimental investigation at Mach numbers 1.88, 3.16 and 3.83 of pressure drag of wedge diverters simulating boundary layer removal systems for side intakes. NACA RM E53L14.

57   H.W. Johnson, T.G. Piercy. Effect of wedge type boundary layer diverters on performance of half conical side intakes at a Mach number of 2.96. NACA RM E54E20.

58   P.C. Simon, K.L. Kowalski. Charts of boundary layer mass flow and momentum for inlet performance analysis. Mach number range 0.2 to 5.0. NACA TN 3583.

59   R.C. Campbell, E.J. Kremzier. Performance of wedge type boundary layer diverters for side inlets at supersonic speeds. NACA RM E54C23.

60   L.E. Stitt, B.H. Anderson. Friction and pressure drag of boundary layer diverter systems at Mach number 3.0. NASA TM X-147.
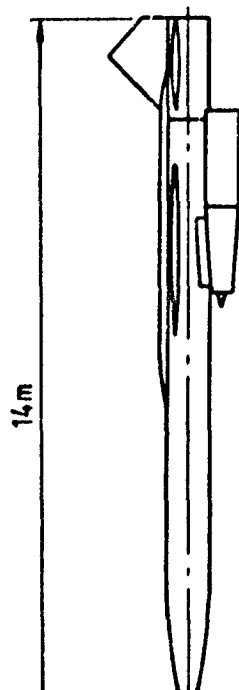
FIG 1 BOMARC (7250 KG)

14m

45°
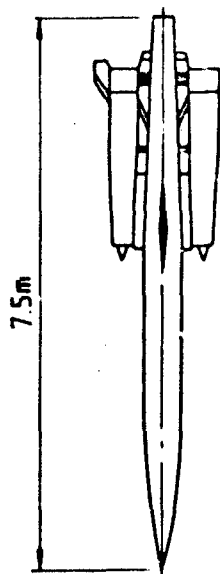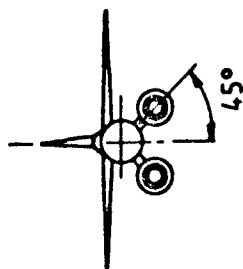
FIG 2 BLOODHOUND (2000 KG APPROX)

7.5m

FIG 3 TALOS (3175 KG)

6.45m
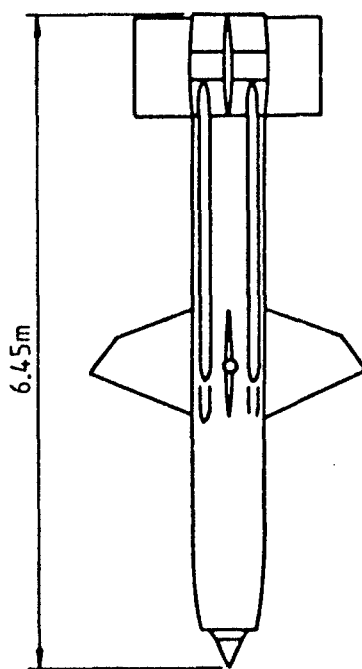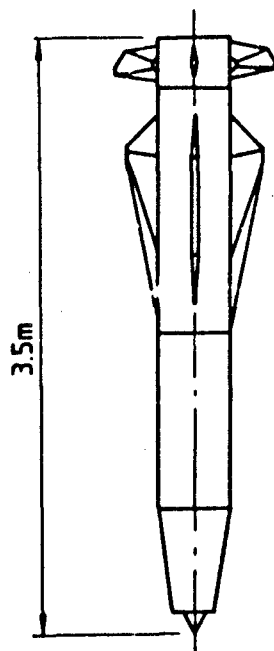
FIG 4 SEA DART (500 KG)

3.5m
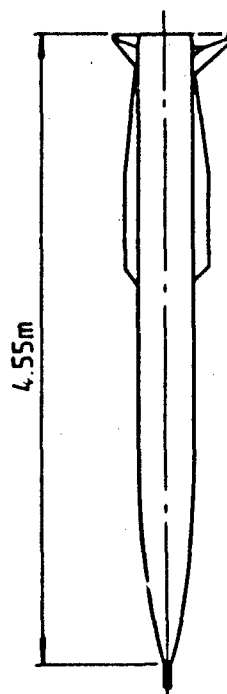
FIG 5 ADVANCED LOW VOLUME RAMJET

4.55m

FIG 6 ADVANCED STRATEGIC AIR
LAUNCHED MISSILE

FIG 7 VARIATION OF SURFACE MACH
NO WITH CHANGE OF NOSE SHAPE (REF 5)

FIG 8 VARIATION OF LOCAL MACH NUMBER
WITH RADIAL & LONGITUDINAL POSITION
AT M_∞ 1.7 & 2.5

FIG 9 CHANGE OF LOCAL MACH NO WITH
LONGITUDINAL POSTION AT $\alpha 3^\circ$ & 6° & $M_\infty 2.0$

FIG 10 DISTRIBUTION OF BOUNDARY LAYER
THICKNESS AROUND CIRCUMFERENCE OF BODY
AT $M_\infty 2.01$ (REF 6)

FIG 11 FORMATION OF VORTICES ON LEE
SIDE OF BODY (REF 7)
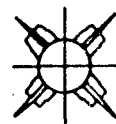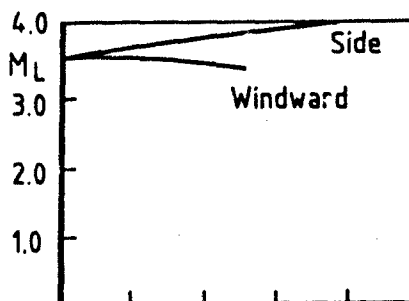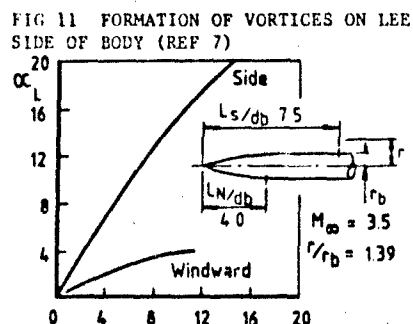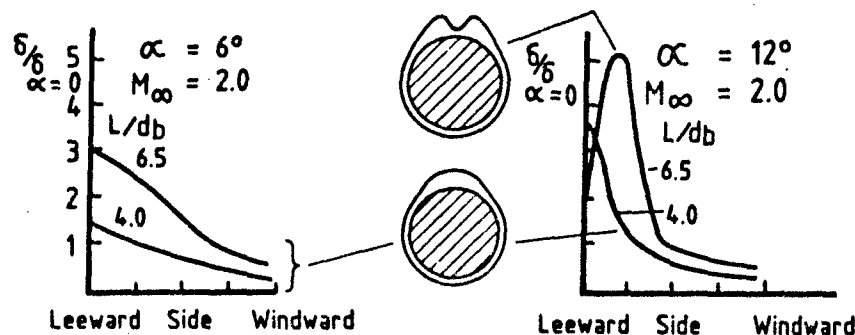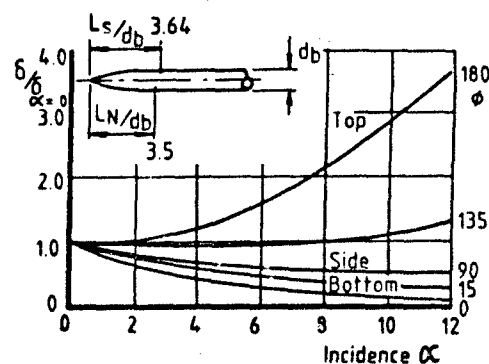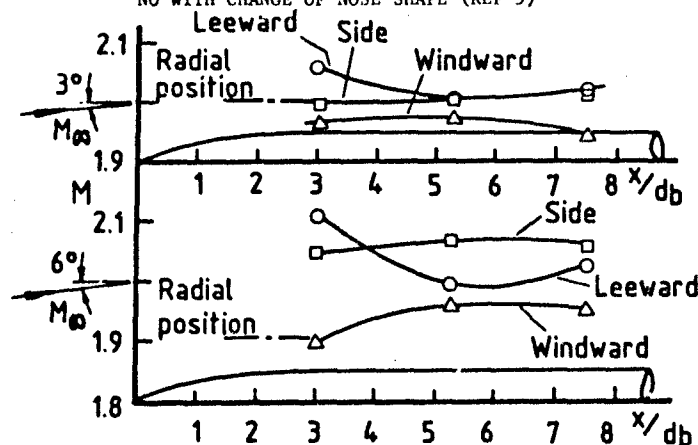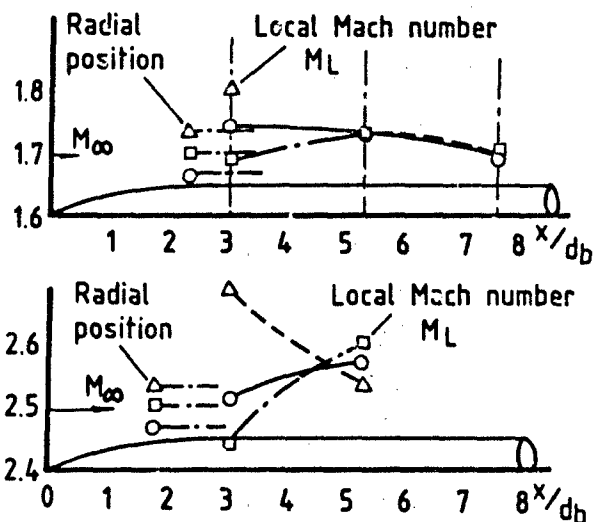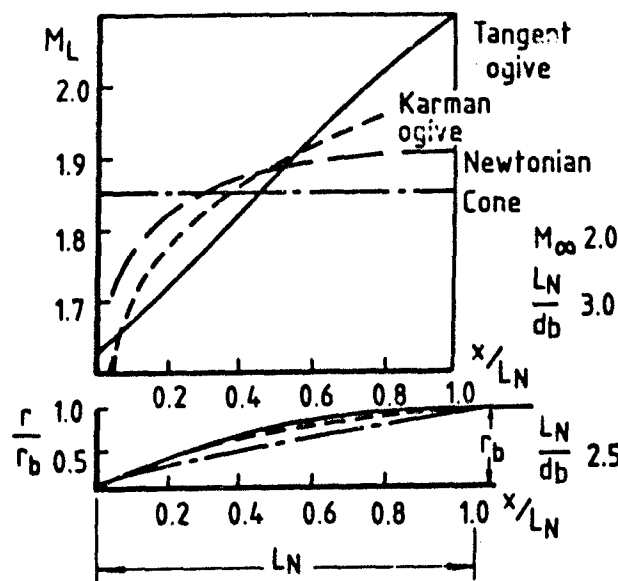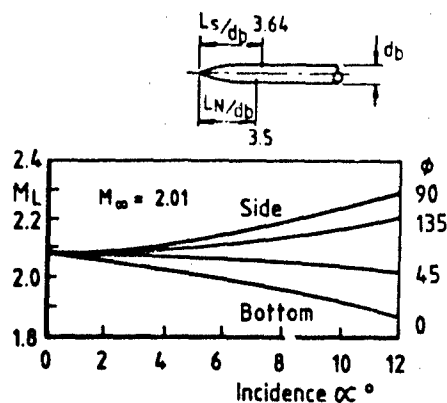
FIG 13 VARIATION OF LOCAL MACH NO
WITH ANGLE OF INCIDENCE (REF 6)

FIG 15 LONGITUDINAL LOCATION OF VORTEX
SEPARATION POSITION

FIG 14 PREDICTED & MEASURED FLOWFIELDS AT
$M_\infty 3.5$ (REF 9)
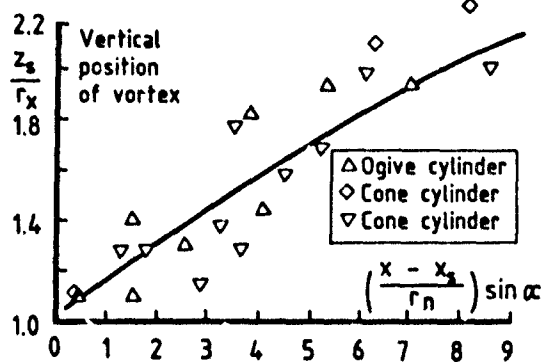
FIG 16 VERTICAL LOCATION OF VORTEX CORES
(REF 15)
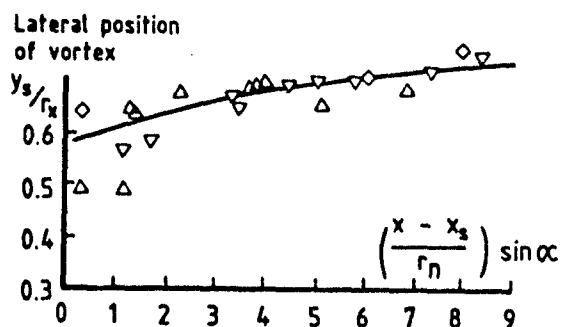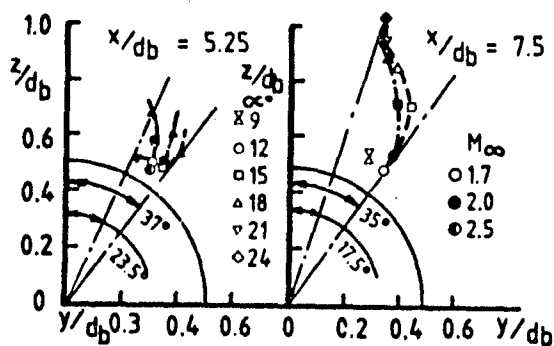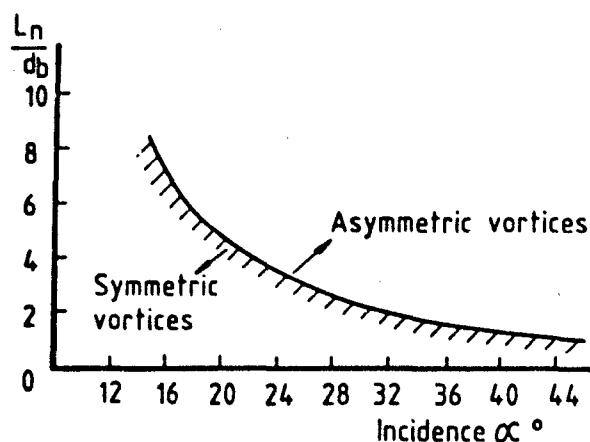
FIG 19 CONDITIONS FOR FORMATION
OF ASYMMETRIC VORTICES (REF 15)

Based on vapour screen
measurements

Diagrammatic
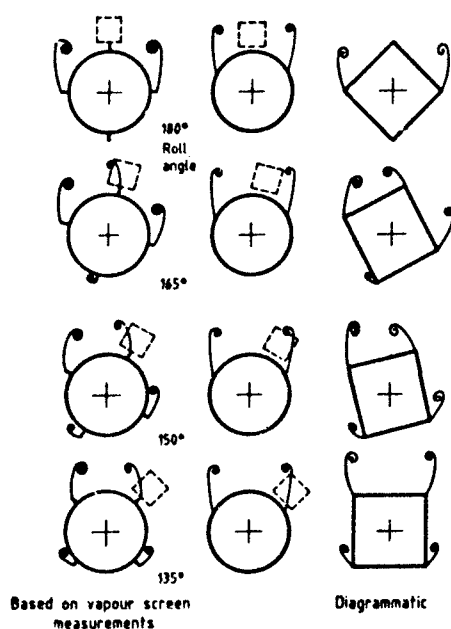
FIG 20   VORTEX POSITION FOR CIRCULAR
BODY WITH & WITHOUT STRAKE & FOR SQUARE
SECTION BODY
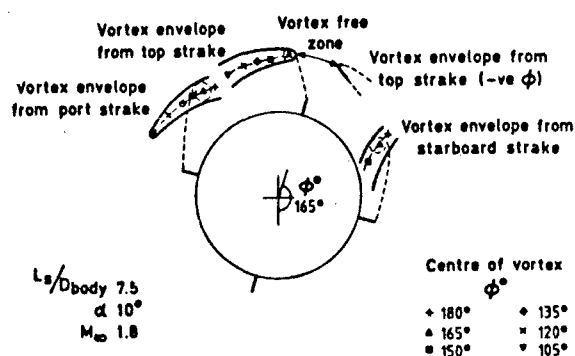
FIG 21   VORTEX POSITIONS VIEWED UPSTREAM
FROM THE TOP RAKE POSITION AS THE BODY
IS ROLLED
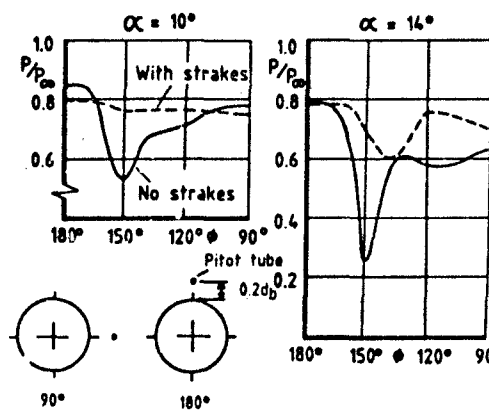
FIG 22   VARIATION OF PITOT PRESSURE WITH
ROLL ANGLE WITH & WITHOUT STRAKE

Pressure recovery

Stability
limit

Critical
point

Constant
engine
demand

$\alpha 0$
$\alpha 1$
Critical
point
$\alpha 2$
$\alpha 3$
$\alpha 4$

Mass flow ratio

Pressure recovery

Recovery penalty incurred at
zero incidence as a function
of required incidence capability

η utilisable
η operating
η limiting $\alpha 3$
η limiting $\alpha 2$
η limiting $\alpha 4$

α_0 α_1 α_2 α_3 α_4
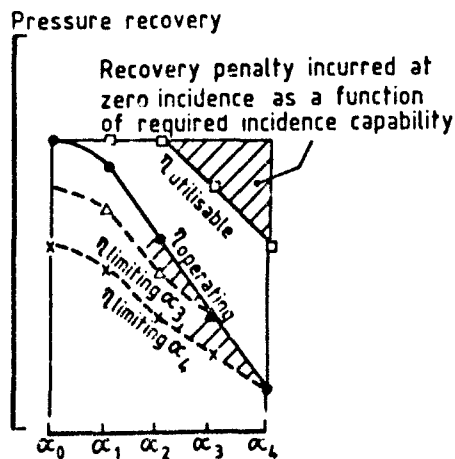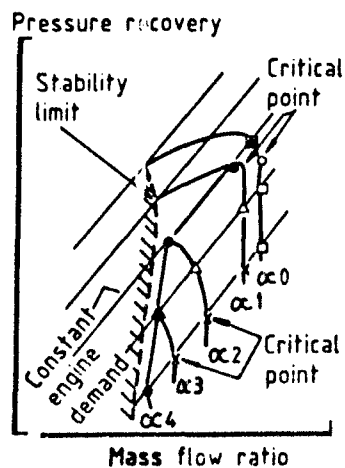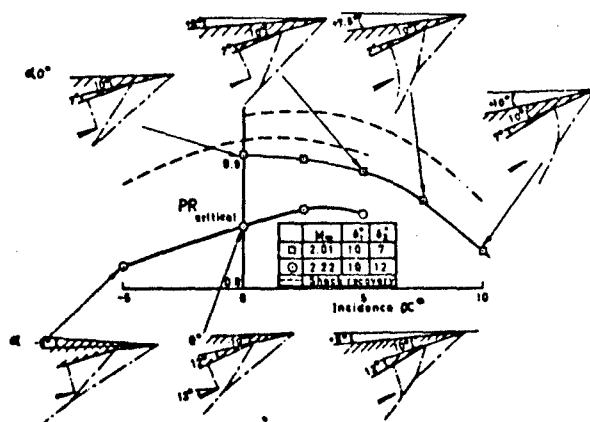
FIG 24 VARIATION OF CALCULATED SHOCK & MEASURED
RECOVERY WITH INCIDENCE FOR RECTANGULAR INTAKE (REF 16)

FIG 25 VARIATION WITH INCIDENCE OF RECOVERY
RELATIVE TO RECOVERY AT ZERO INCIDENCE FOR
RECTANGULAR INTAKE WITH DIFFERENT ENDWALLS (REF 17)

FIG 26(a) VARIATION WITH INCIDENCE OF RECOVERY
RELATIVE TO RECOVERY AT ZERO INCIDENCE FOR
AXISYMMETRIC INTAKES
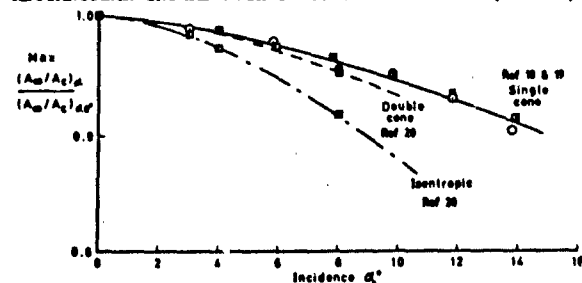
FIG 26(b) VARIATION WITH INCIDENCE OF MAXIMUM
FLOW RELATIVE TO ZERO INCIDENCE VALUE FOR
AXISYMMETRIC INTAKES

FIG 27(a) VARIATION WITH INCIDENCE OF RECOVERY
RELATIVE TO ZERO INCIDENCE VALUE FOR TWO CONE
CENTREBODY INTAKES
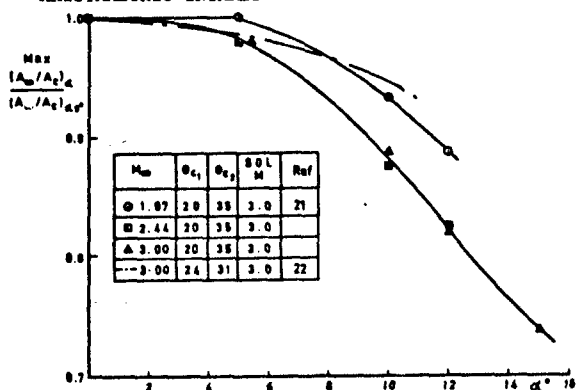
FIG 27(b) VARIATION WITH INCIDENCE OF MAXIMUM
FLOW RELATIVE TO ZERO INCIDENCE VALUE FOR TWO
CONE CENTREBODY INTAKES
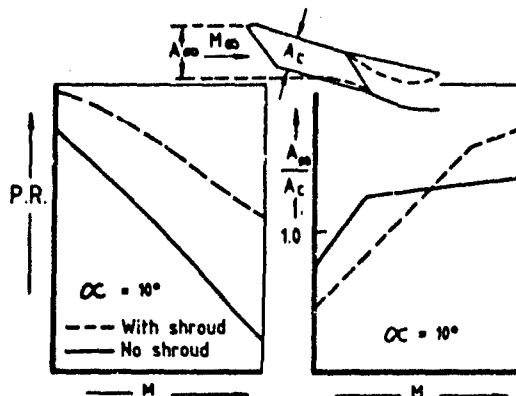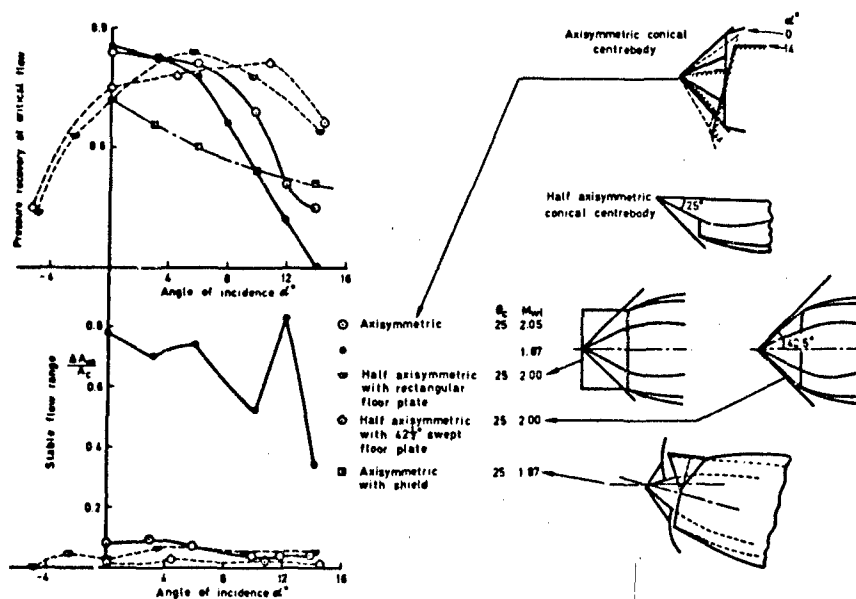
FIG 30 COMPARISON OF PERFORMANCE AT INCIDENCE OF HALF AXISYMMETRIC & AXISYMMETRIC INTAKES WITH & WITHOUT A COWL SHROUD
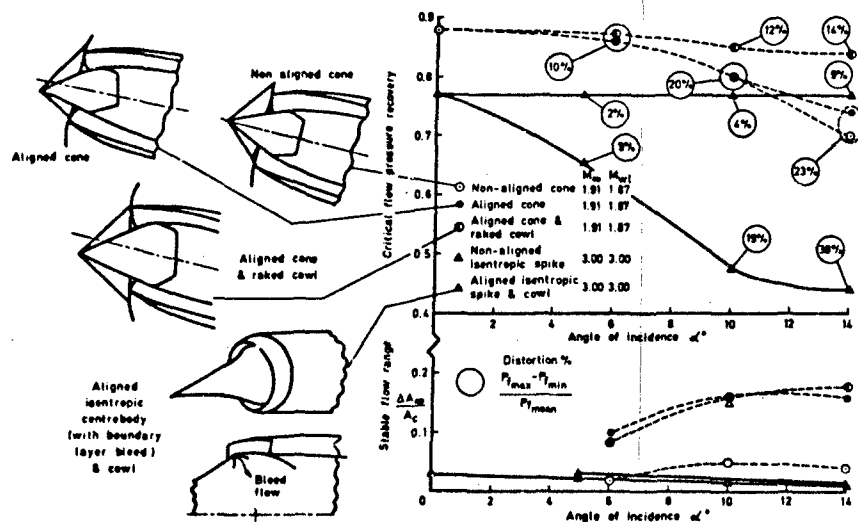
FIG 31 EFFECT OF CENTREBODY PIVOTING & COWL RAKING & PIVOTING ON AXISYMMETRIC INTAKE PERFORMANCE AT INCIDENCE
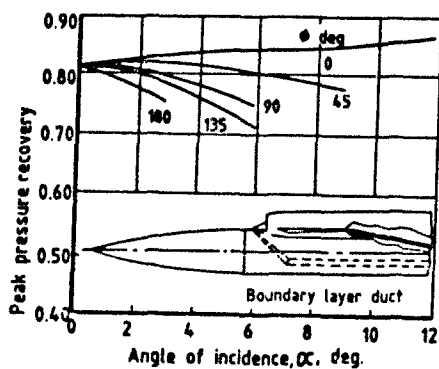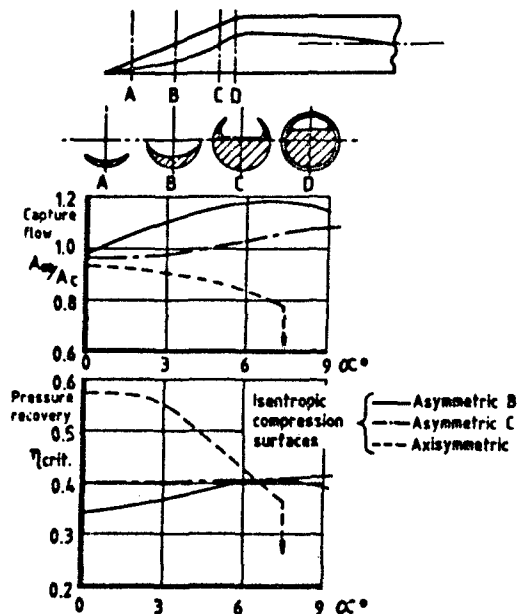
FIG 33 PERFORMANCE OF SINGLE HALF AXISYMMETRIC INTAKE ON A BODY AT $M_\infty 2.0$ (REF 6)
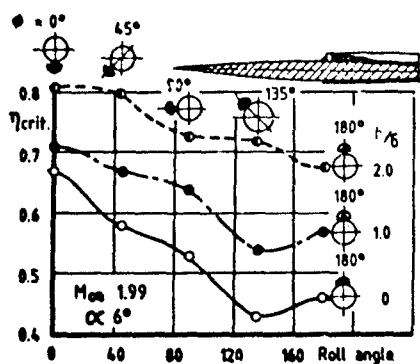
FIG 34 VARIATION OF RECOVERY WITH ROLL ANGLE FOR SINGLE HALF AXISYMMETRIC
INTAKE ON RM10 BODY AT 6° & 10° &
M_∞1.99 (REF 30)
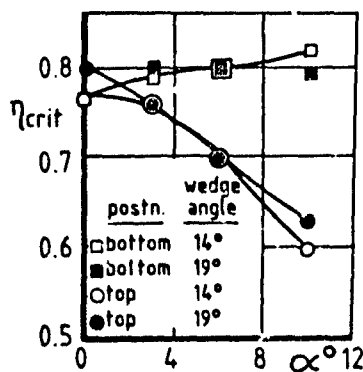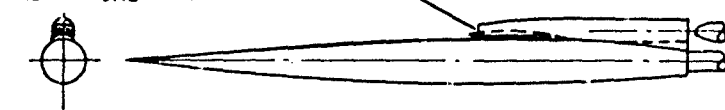
FIG 35 VARIATION OF RECOVERY WITH INCIDENCE
FOR SINGLE RECTANGULAR INTAKE AT TOP & BOTTOM
POSITIONS ON RM10 BODY AT M_∞2.0 (REF 31)
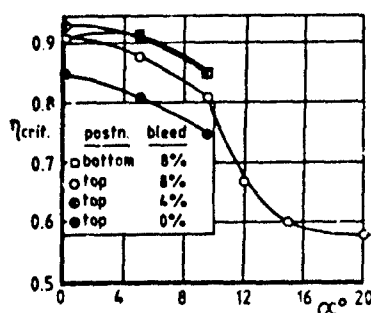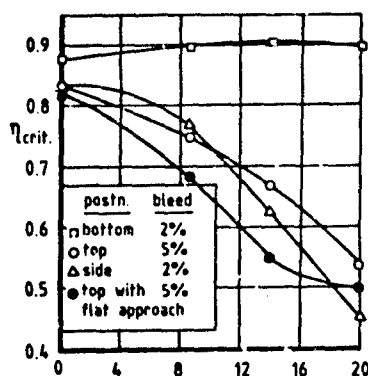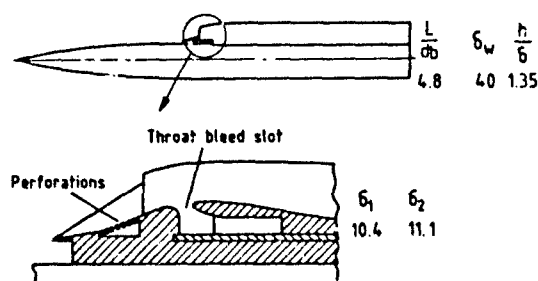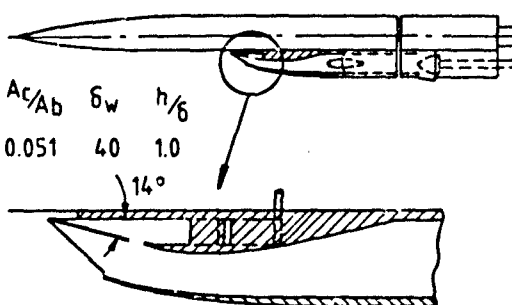
FIG 36 VARIATION OF RECOVERY WITH
INCIDENCE FOR SINGLE RECTANGULAR
INTAKE (WITH COMPRESSION SURFACE
BLEED) ON A BODY AT M 2.0 (REFS
33, 34)

FIG 37 VARIATION OF RECOVERY WITH

	Throat bleed	Body L/db	M_∞
— — Inverted 2 ramp	Yes	5.0	2.3
—·— Half conical	No	7.5	2.0
—··— Half conical	No	7.5	1.8
△ Large half conical	No		1.8
□ Conventional/ramp	Yes		2.0
x Conventional/ramp	No	8.0	2.0
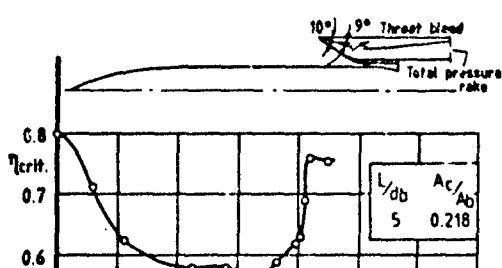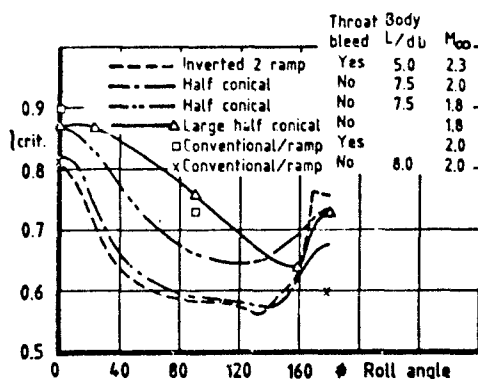
FIG 38 SUMMARY OF RECOVERY VARIATION WITH ROLL ANGLE FOR SINGLE INTAKE AT α=10°

○ ½ Conical centrebody		30	Ref.
● " " "		6	"
□ 14° wedge intake (no swept endwalls)		33	"
△ 10° – 8° wedge (with swept endwall)			
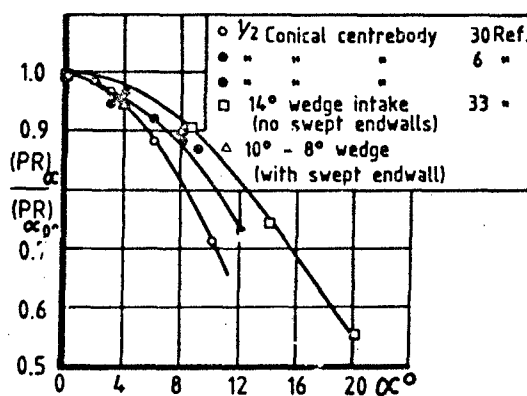
FIG 39 SUMMARY OF RECOVERY VARIATION WITH INCIDENCE FOR SINGLE SIDE (φ90°) INTAKE
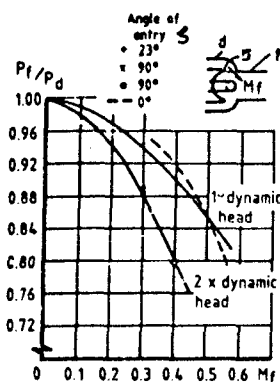
FIG 40 TOTAL PRESSURE LOSS DUE TO MIXING OF FOUR FLOWS (REF 35)
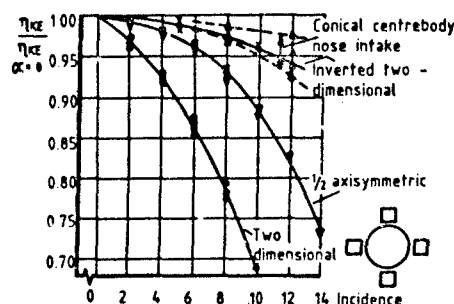
FIG 41 VARIATION OF COMPRESSION EFFICIENCY WITH INCIDENCE FOR FOUR INTAKES IN φ180°/0° POSITION
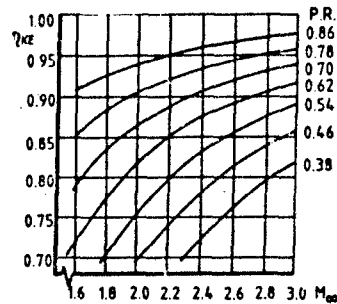
FIG 42 RELATION BETWEEN η_{KE} & PRESSURE RECOVERY
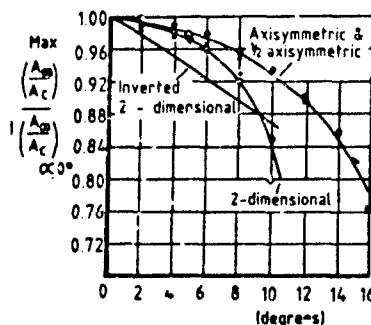
FIG 43 VARIATION OF MAXIMUM CAPTURE FLOW WITH INCIDENCE FOR FOUR INTAKES IN φ180°/0° POSITION
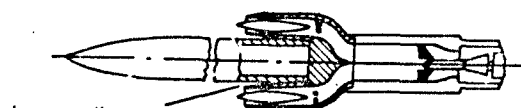
Large diverter height h/d_b = 0.141

Small diverter height h/d_b = 0.066

L/db	Ac/Ab
7.5	0.48
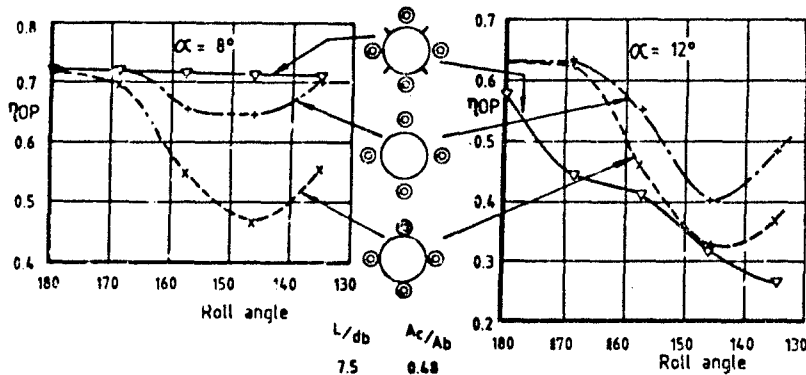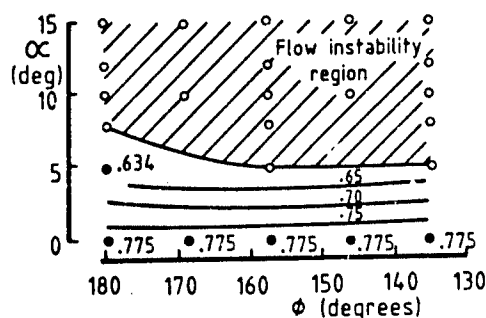
FIG 45 VARIATION OF η_{OP} WITH INCIDENCE & ROLL ANGLE FOR FOUR CONVENTIONALLY MOUNTED RECTANGULAR INTAKES ON A BODY AT $M_\infty 2.3$ ($\frac{L}{d_b}$ 5.0 $\frac{h}{\delta}$ 0.7 $\frac{A_c}{A_b}$ 0.87)

Conventionally mounted intakes

Intake duct flow measuring stn.

Main duct flow measuring stn.

d_b 101.6mm
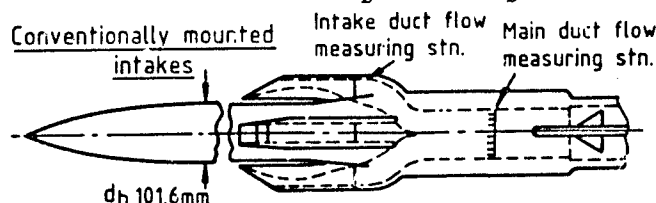
Inverted intake mounting

508mm (medium body)

736mm (long body)
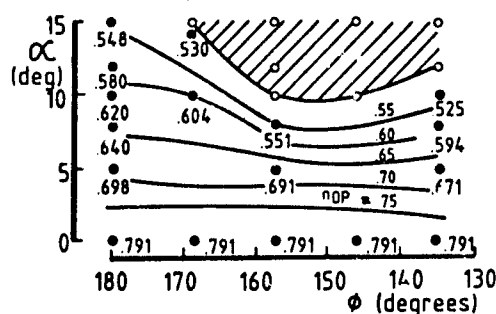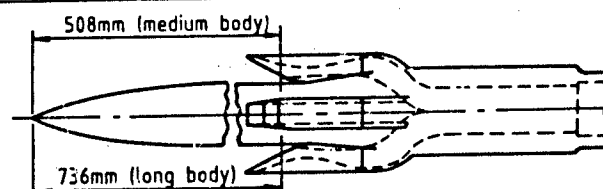
FIG 46(a) INVERTED INTAKE $\frac{L}{d_b}$ 5.0 $\frac{h}{\delta}$ 1.7 $M_{SOL} 2.3$

10° 9° wide slot bleed

30.98

41.55

61.25

Initial cowl undersurface angle = 13°

(a) M = 2.3 Shock on lip design

9.67° 12.33°

38.75

41.55

71.55

(b) M = 2.6 Shock on lip design

FIG 46 VARIATION OF η_{OP} WITH INCIDENCE & ROLL ANGLE FOR FOUR INVERTED RECTANGULAR INTAKES ON A BODY AT M 2.3 A_c/A_b 0.87)

FIG 46(b) INVERTED INTAKE $\frac{L}{d_b}$ 7.24 $\frac{h}{\delta}$ 1.25 $M_{SOL} 2.3$
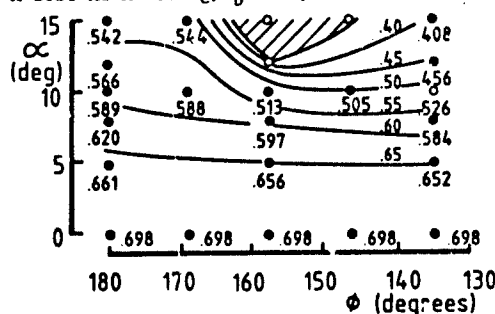
FIG 46(c) INVERTED INTAKE $\frac{L}{d_b}$ 5.0 $\frac{h}{\delta}$ 1.25 $M_{SOL} 2.6$
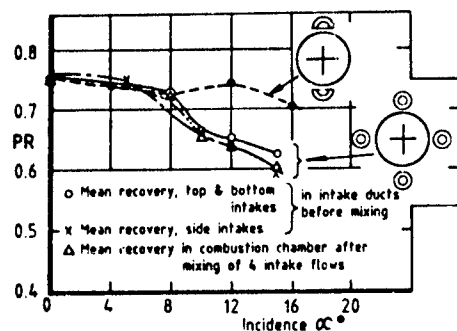
FIG 47 COMPARISON OF TWO & FOUR INTAKE PERFORMANCE AT M_∞ 2.0

o Mean recovery, top & bottom intakes
x Mean recovery, side intakes } in intake ducts before mixing
△ Mean recovery in combustion chamber after mixing of 4 intake flows

Match points at p_d/P_∞
x 0.4
□ 0.5
o 0.525

Single inverted intake at $\propto$ 10° and ϕ90° & 270°(sides)

0° (bottom)

180° (top)
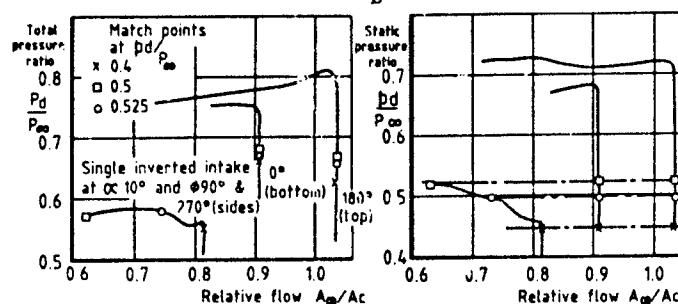
FIG 48 MATCHING OF CHARACTERISTICS FOR SINGLE INVERTED RECTANGULAR INTAKE POSITIONED AT TOP, BOTTOM & SIDES OF A BODY AT $M_\infty 2.3$

Loss due to enforced supercritical operation

FIG 49 VARIATION OF PRESSURE RECOVERY WITH

Single Intake

Twin Axisymmetric Intakes

Axisymmetric   Rectangular

Twin Rectangular Intakes

M_∞	α	Re_{db}	d_b(mm)	L
2.50	-5°	0.5×10^6	76.2	14 d_b
2.95	+20°			
3.50				
3.95				

Axisymmetric Intake   Rectangular Intake
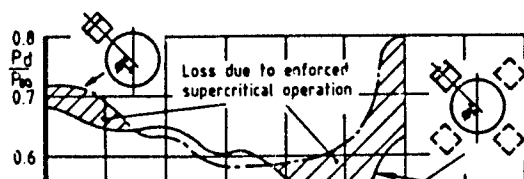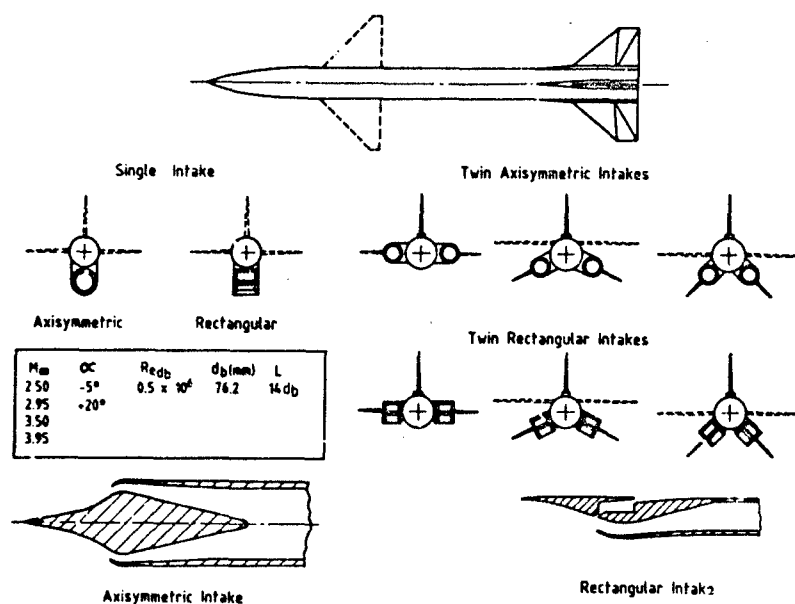
FIG 50   NASA MODEL FOR MEASUREMENT OF FORCES & MOMENTS ON BODY WITH NACELLES

Variations

Number of nacelles

M_∞	α	d_b (mm)	L	Re_{db}
0.6 – 3.4 but mainly 2.0	-6 to +12	60 & 120	14	1 - 2 × 10⁶ 1 - 3 × 10⁶

Type of air intake

Length of nacelle
$\frac{l}{d_n} = 5, 6.17, 8.5$

$L = 19 d_b$

Without boattail   With boattail
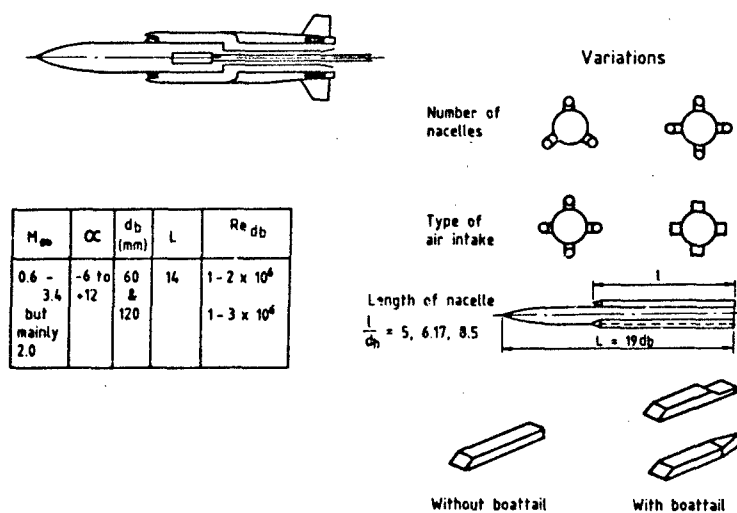
FIG 51   ONERA MODEL FOR MEASUREMENT OF FORCES & MOMENTS ON BODY WITH NACELLES

Half conical centrebody intakes

Sting & balance shield

$\frac{L_N}{d_b}$ 2.5 tangent ogive nose

63.43°

12 arm (4 pitot tubes and 1 static tube per arm) attached to sting

Optional base flow shield

6 component balance

Wings A,B,C,D & E in line with nacelles or interdigitated

4 body mounted controls (one strain gauged)

Sliding cone throttle

12 base pressure pitot tubes

Wing	$\frac{Span}{d_b}$	Plan area for one wing $\frac{}{A_b}$	A.R.	Taper ratio
A	1.0	2.505	1.017	0.326
B	0.721	1.546	0.854	0.401
C	0.673	1.403	0.821	0.418
D	0.633	1.288	0.791	0.433
E	0.556	1.074	0.730	0.465
Control	0.642	0.296	3.524	0.25

Parabolic profile

Rectangular intakes

Parabolic profile

Body alone
Body + wings A,B,C,D and E
Body + wings + controls

Large (A_c/A_{body} 0.5) half axisymmetric intakes in two longitudinal positions, in line wings and controls

Large (A_c/A_{body} 0.5) rectangular intakes, interdigitated wings and controls

M_∞	Intake type	A_c/A_{body}	$\frac{x}{d_b}$	b/d_b	Reynolds No. (on body dia of 1524mm)	Reynolds No. on intake height/radius
1.8	Half conical centrebody	0.225	6.25	1.278	1.25×10^6	0.221×10^6
2.0		0.375		1.653		0.271
2.3		0.5		1.733		0.313
		0.5				
	Rectangular double wedge compression surface	0.5		1.885		0.392

FIG 53   RAE MODEL GEOMETRIES & TEST CONDITIONS
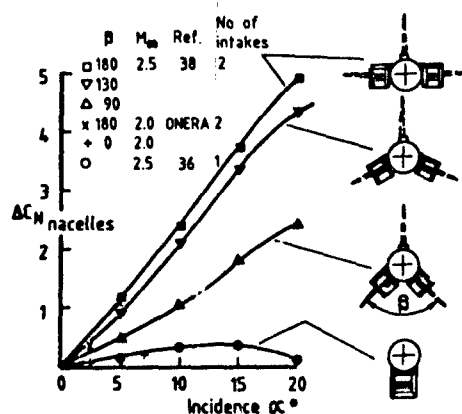
FIG 54   VARIATION WITH INCIDENCE OF INCREMENTAL NORMAL FORCE & CENTRE OF PRESSURE POSITION DUE TO THE ADDITION OF SINGLE & TWIN RECTANGULAR NACELLES TO A BODY
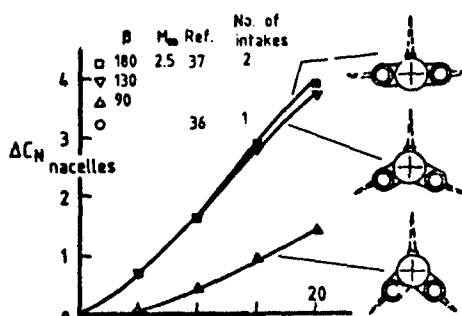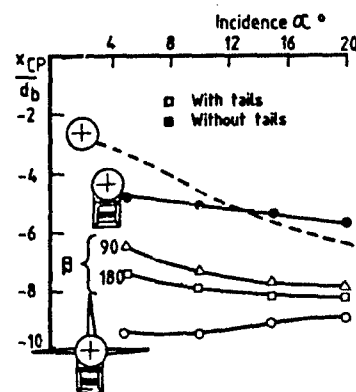
FIG 55   VARIATION WITH INCIDENCE OF INCREMENTAL NORMAL FORCE & CENTRE OF PRESSURE POSITION DUE TO THE ADDITION OF
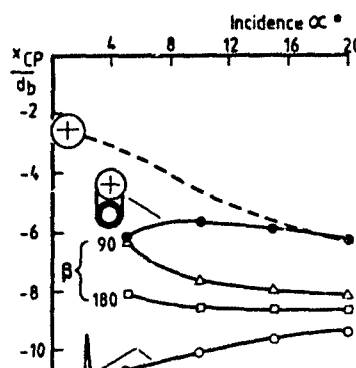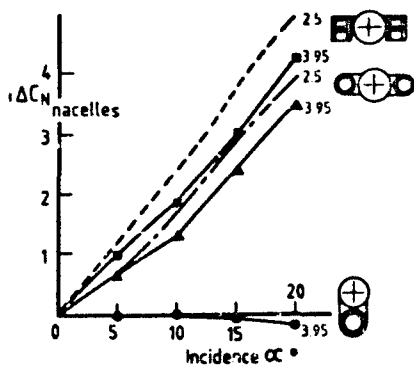
FIG 56 EFFECT OF MACH NUMBER CHANGE ON NACELLE NORMAL FORCE INCREMENT

No	b/d	$\frac{A_{en}}{A_b}$	M_∞	$\alpha°$
◻4	1.885	0.5	2.3	8
◼4	1.830		2.0	
△4	1.885	0.5	2.3	12

FIG 57 VARIATION WITH INCIDENCE OF NORMAL FORCE INCREMENT & OF CENTRE OF PRESSURE POSITION FOR 4 INTAKE CONFIGURATIONS
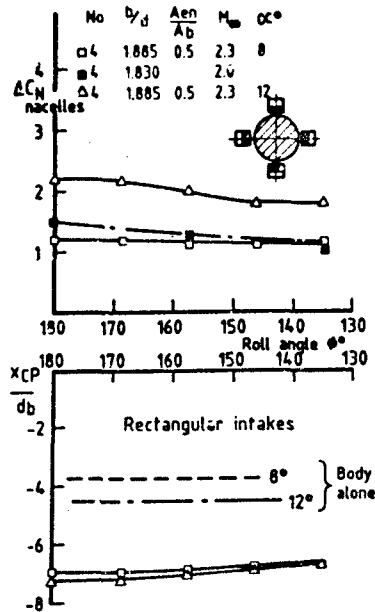
FIG 58 VARIATION WITH ROLL ANGLE OF NORMAL FORCE INCREMENT & CENTRE OF PRESSURE POSITION FOR 4 RECTANGULAR INTAKES

	Intakes	M_∞	Ref.
◯4	Half axisymm	2.3	RAE
△4	Rectangular	2.3	
◻2	Rectangular	2.5	37
◯2	Axisymmetric	2.5	38
+4	Wings	2.3	RAE
×4	Wings	2.3	
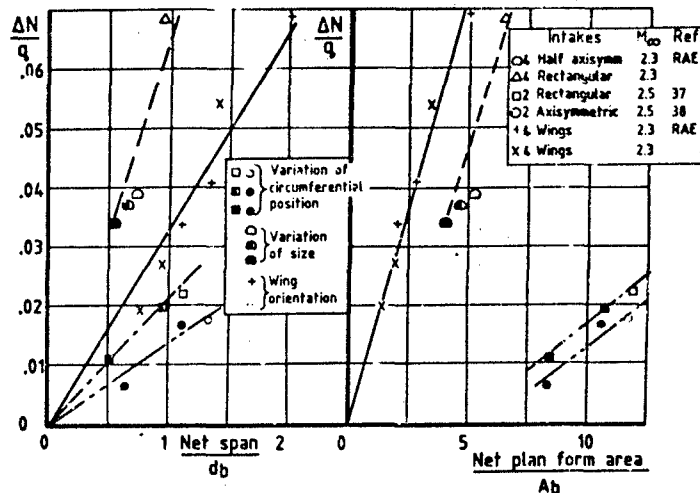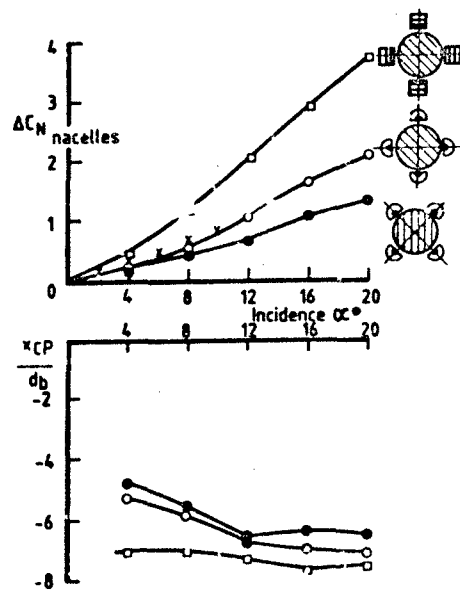
FIG 59 VARIATION OF NORMAL FORCE INCREMENT WITH NET SPAN & NET PLANFORM AREA

Compression surface
Bleed drag
Diverter drag
Afterbody & base drag

Intake at full flow ie with supersonic forespillage

Intake with subsonic forespillage at $M_\infty < M_{SOL}$

(b)

(c)

Increased pre entry drag
Reduced cowl drag

Pre entry or additive drag
$C_{D_{pre_0}}$ or $C_{D_{add}}$
Cowl drag
$C_{D_{cowl_0}}$

Wedge/Cone shock on lip
M_{SOL}

Intake at datum flow

Cowl drag only

(a)

Intake with subsonic forespillage at $M_\infty > M_{SOL}$

C_D
$\Delta C_{D_{cowl}}$
$C_{D_{spill}}$
$C_{D_{pre}}$
$C_{D_{pre_0}}$
$C_{D_{cowl_0}}$
Capture

FIG 61 COWL PROFILES

Cowl profile equation: $R = R_m - (R_m - R_c)\left(1 - \frac{x}{\ell}\right)^n$
(Ref 43)

$\tan \delta = \frac{nR_m}{\ell}\left(1 - \frac{R_c}{R_m}\right)$

FIG 62 VARIATION OF FUNCTIONS α_n & β_n WITH n

FIG 63 VARIATION OF FUNCTIONS $U_1(x)$ & $T(x)$ WITH 'X'

FIG 64 COMPARISON OF LINEAR THEORY & CHARACTERISTICS VALUES FOR CONICAL COWLS

FIG 65 METHODS FOR CALCULATING COWL PRESSURE DISTRIBUTIONS

Characteristics
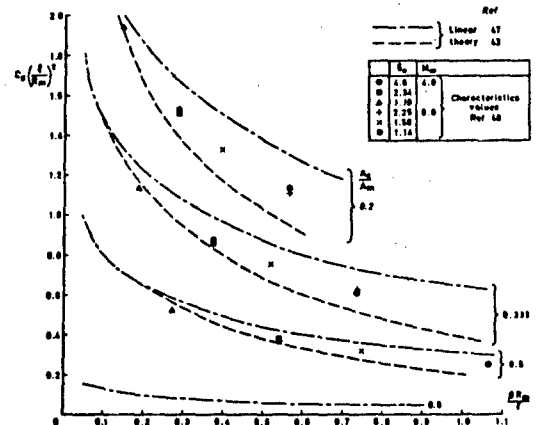
Generalised shock-expansion
1st segment: p_1 is static pressure behind oblique shock for $M = M_\infty$ and deflection δ_1
2nd segment: M_1 defines Prandtl-Meyer angle v_1
$v_2 = v_1 - (\delta_0 - \delta_1)$ defines M_2 and p_2

2nd order shock expansion
After Prandtl-Meyer expansion, pressure on segment falls exponentially towards cone surface pressure (cone angle δ_n, $M = M_\infty$) - Ref 12

Tangent wedge: p_n is static pressure behind oblique shock for $M = M_\infty$ and deflection $= \delta_n$

Impact theory: $C_{p_n} = 2 \sin^2 \delta_n$
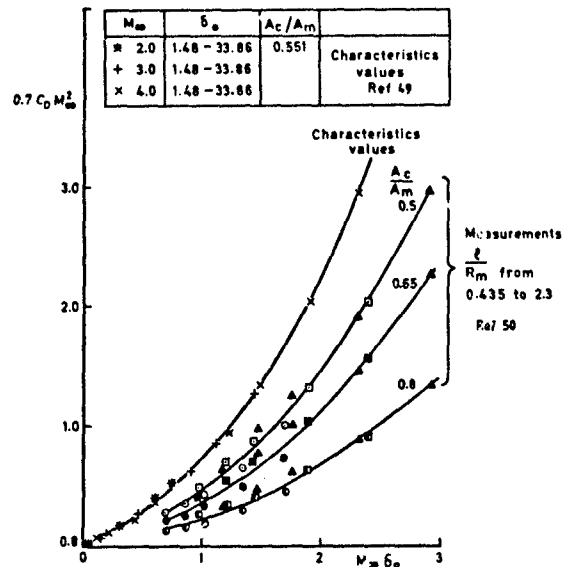
FIG 67 VARIATION OF COWL WAVE DRAG
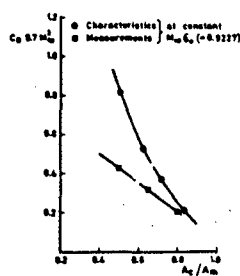
FIG 68   LIMITATIONS OF
HYPERSONIC SIMILARITY PARAMETERS

FIG 70   COMPARISON OF LINEAR
THEORY, SHOCK EXPANSION &
MEASUREMENT FOR ELLIPTIC
COWLS OF REF 50
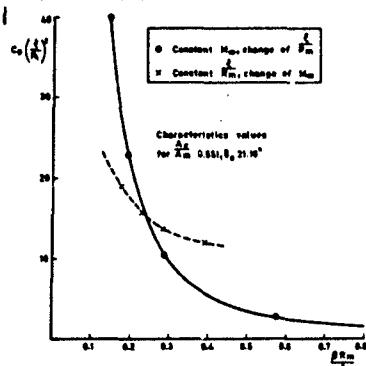
FIG 69   LIMITATIONS OF LINEARISED
SUPERSONIC PARAMETERS

(a) Sonic exit velocity

(b) Supersonic exit velocity
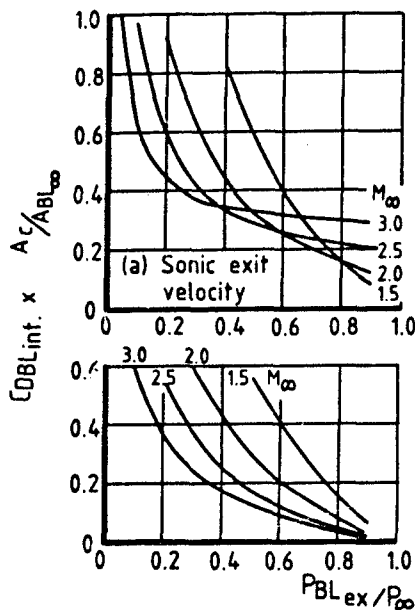
FIG 72   VARIATION OF BLEED INTERNAL
DRAG WITH BLEED PRESSURE RECOVERY
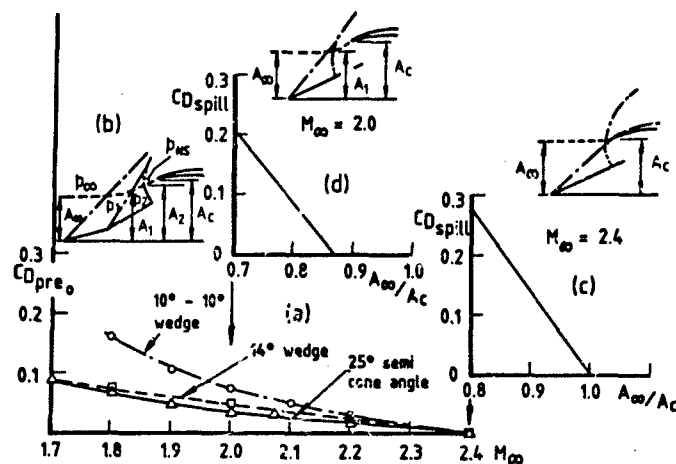
FIG 71   VARIATION OF $C_{D_{PRE_0}}$ WITH
FREESTREAM MACH NUMBER AND
$C_{D_{SPILL}}$ WITH RELATIVE FLOW

FIG 74   WEDGE COMPRESSION SURFACE
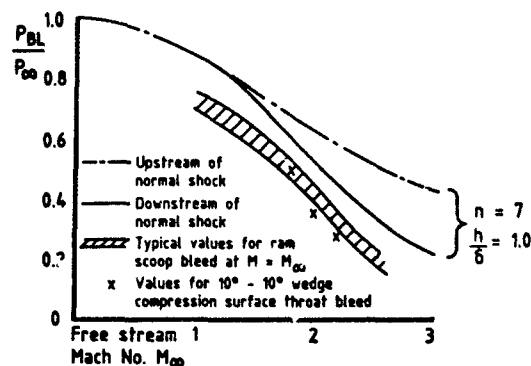
FIG 73   BLEED PRESSURE RECOVERY

Wedge diverter
straight splitter

Wedge diverter
swept splitter

Cowl lip diverter

FIG 75 HALF CONICAL
CENTREBODY DIVERTERS

$h/\delta = 1.0 \quad S/\delta = 0$

Wedge in
supersonic
flow

$\dfrac{C_{D_p}}{\sin^2 \frac{\delta_w}{2}}$

M_β

$\sqrt{M^2 - 1}\ \sin \delta_w/2$

$h/S = 1.25 \quad S/\delta = 0$

Wedge in
supersonic
flow
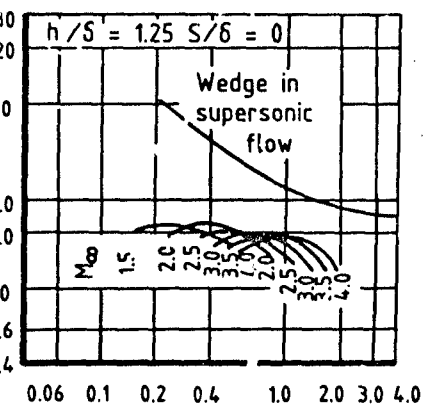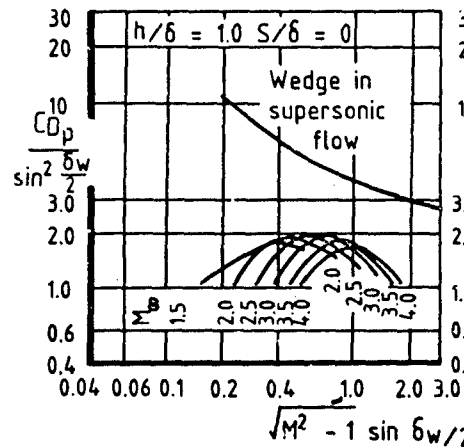
FIG 75(a), (b) & (c) WEDGE
DIVERTER WAVE DRAG (REF 55)

$h/\delta = 0.75 \quad S/\delta = 0$

Wedge in
supersonic
flow

$\dfrac{C_{D_p}}{\sin^2 \frac{\delta_w}{2}}$

$h/\delta = 1.0; \quad 0 < S/\delta < 1.0; \quad 60° < \delta_s < 180°$
Re 1.6 to 16.4 × 10^6 per metre

M_∞

C_{D_p}

$1.5 \quad 2.0 \quad 2.5 \quad 3.0 \quad 3.5 \quad 3.83$

$60 \quad 50 \quad 40 \quad 30 \quad 20 \quad 10 \quad 0$

δ_w deg.

(a)

$0.75 \leqslant h/\delta \leqslant 1.5$
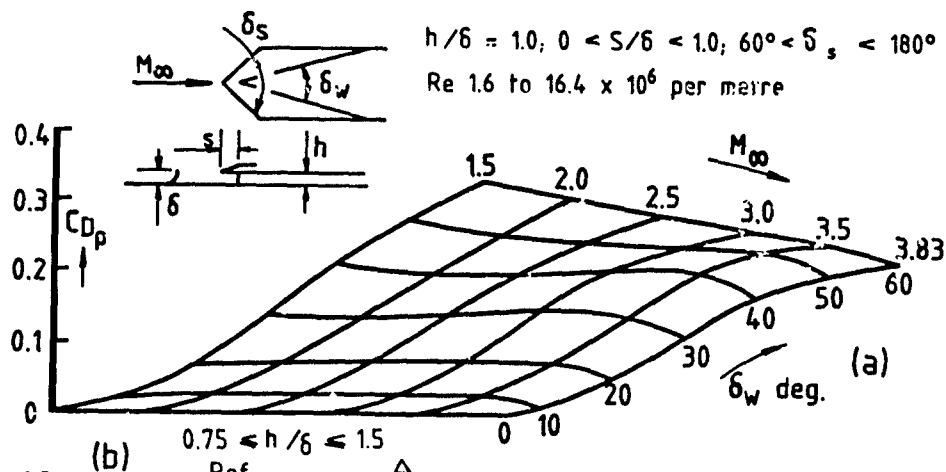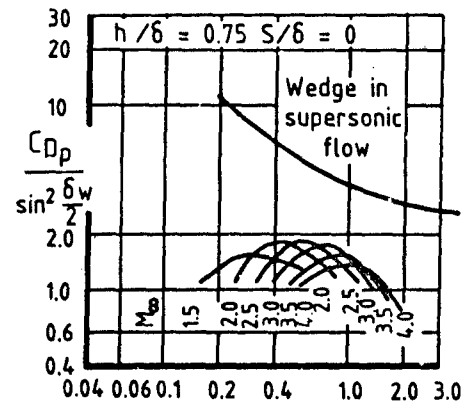
FIG 77(a) & (b)
WEDGE DIVERTER
WAVE DRAG

(b)

$\dfrac{\delta C_{D_p}}{\delta h/\delta}$

Ref.
○ 56
△ 57

M = 3.83

M = 3.16

M = 2.96

M = 1.88

C_{D_f}

$\dfrac{C_{D_f}}{C_{f_w}}$

Ref.
□ 56
△ 59
○ 60

Skin friction multiplication

Reynolds No.- area ratio
parameter $\dfrac{A_W}{A_D}(Re)_L^{-0.2}$

Skin friction
coefficient
C_{f_w}

From Ref. 58

Mach No = 0 1
2 3
4 5

Reynolds No. Re_L
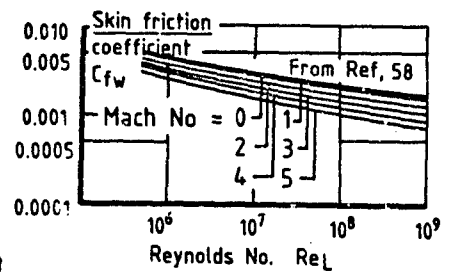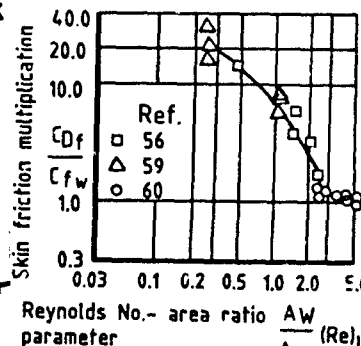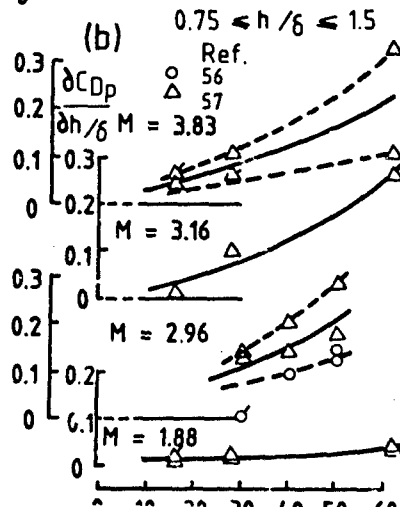
FIG 78 WEDGE DIVERTER
SKIN FRICTION DRAG

INTEGRAL BOOST, HEAT PROTECTION, PORT COVERS AND TRANSITION
by
T. D. Myers
United Technologies/Chemical Systems Division
P.O. Box 50015
San Jose, California 95150-0015

SUMMARY

The integral rocket ramjet (IRR) employs a dual-purpose combustor that serves initially as a rocket combustion chamber for the integral booster and subsequently as a ramjet combustor. The subjects of this lecture are the requirements and basic design approaches for the integral booster motor, heat protection for the integral booster motor, heat protection for the combustor case and nozzle, port cover and transition systems. These requirements and design approaches for the integral booster motor will include the special considerations that must be made for the various types of integral rocket ramjet propulsion systems that include the liquid fuel ramjet, solid fuel ramjet and ducted rocket engines.

The integral boost motor includes the solid propellant grain, igniter, ejectable nozzle and release mechanism and interface bond system. The integral boost motor must accelerate the missile from the Mach number and altitude conditions at launch to a suitable velocity for ramjet takeover, typically Mach 1.5 to 2.5. The integral boost motor weight is very important since it is typically 20 percent of the missile weight for air launched and 25 percent for ground launch missiles. Furthermore, the combustor volume required for the integral boost motor generally exceeds the size required for high performance ramjet operation. Thus minimum booster length yields the highest ramjet fuel load and thereby range.

Since gravity drag losses are a significant factor in establishing the integral boost motor performance, it is also desirable to use the highest thrust compatible with the vehicle structural design and radome temperature constraints to minimize burn time. These three primary integral boost motor design requirements lead to the need for high burn rate propellants with good physical properties to permit high volumetric loading efficiencies. Typical integral boost motor design approaches are discussed that provide these capabilities. The use of nozzleless motors as a design solution to simplify the integral booster is also discussed.

Heat protection for the integral rocket ramjet combustor case must provide for long duration with a high temperature, oxidizing environment. The material selected for heat protection of the IRR combustor must also provide a good structural and bonding interface for the integral boost motor. The heat protection material must withstand both the high temperature and pressure boost motor environment as well as the long duration, low pressure ramjet operating conditions. Several heat protection materials have been investigated for application to IRR combustors that include silica phenolic, quartz phenolic and a silicone elastomer material, DC 93-104, that was specially formulated for IRR applications. The requirments for the heat protection and general lessons learned from development testing with the various materials is discussed.

The IRR propulsion system requires port covers to seal the interfaces between the combustor and air inlet. Depending on the IRR configuration the port cover may be a large unit covering a single air inlet or several small units covering multiple air inlets. The port covers must be designed to structurally support the high integral boost pressure between 1000-2000 psia and still be capable of being easily ejected by the ram air inlet pressure in a reproducible and reliable manner without damaging the heat protection materials lining the combustor case and nozzle. Depending on the IRR configuration, the port cover may have a direct structural and bond interface with the integral boost grain. Typical design solutions to the port cover requirements are presented, including monolithic and segmented designs. A novel solution that has been conceived for solving the port cover design problem, employing a hinged concept will also be discussed.

Design and analyses of the transition sequence from rocket to ramjet modes of operation represent one of the most interesting and challenging aspects of the IRR propulsion system. The transition sequence typically begins with ejection of the port covers from the IRR combustor and includes boost nozzle ejection, ramjet fuel valve opening, initiation of ram air turbine operation and ramjet igniter actuation. All of these events must be carefully sequenced to ensure successful transition in a very short time, typically 300-500 msec. Moreover one of the major considerations in achieving a successful transition is an accurate accounting of all energy sources, including residual boost grain sliver, heat protection material ablation products, ramjet igniter gases and the ramjet fuel transient flow rate. The heat protection material ablation gases frequently include methane, hydrogen and other combustible hydrocarbons. The heat release from these gases can contribute 30-40 percent of the energy needed for normal ramjet operation at takeover. Since inlet design margins are typically minimum at takeover, failure to consider these important energy sources can and has led directly to IRR flight failures.

INTEGRAL BOOST MOTOR

The integral rocket ramjet (IRR) propulsion systems represent a sophisticated technology objective for advancing tactical and strategic missile applications. The three basic ramjet types shown in figure 1 represent the typical engine configurations. Integration of the solid rocket booster motor with the

and volume advantages when compared to the podded or tandem ramjet configurations. When compared to conventional boost/sustain solid rocket motors with the same weight and envelope, the IRR can provide a 200% to 300% increase in powered range.

Naturally, the advantages for the IRR configuration do not come free. In this instance, the price is primarily related to the unique complexities associated with the interfaces between the solid booster motor and the ramjet engine.

The booster motor for the integral rocket ramjet must:

1. Accelerate the missile from ground or air launch speed to a Mach No. satisfactory for ramjet takeover.

2. Provide high volumetric loading to minimize combustor volume.

3. Provide required ΔV gain within 4 to 6 sec to minimize gravity drag losses.

4. Provide minimum motor residuals to allow rapid transition to ramjet operation.

5. Provide ejectable boost nozzle to permit ramjet engine to operate at low ramair pressures.

6. Cause minimum damage to the ramjet engine TPS.

A typical integral booster motor is seen in figure 2. Operation of the IRR begins with ignition of the integral booster motor after the missile has been ejected from the aircraft. The booster motor must accelerate the missile from the Mach number-altitude condition at launch to a velocity suitable for ramjet takeover, typically a Mach number from 1.5 to 2.5. The booster must operate over a wide range of launch conditions, ranging from ground launch to air launch at Mach number of 0.5 at low altitude up to 0.7 to 0.8 at midaltitudes. The booster motor propellant weight is typically 20% of the missile weight for air launched applications. For ground launch application the booster fraction is approximately 25%.

The booster motor burns for approximately 4 to 6 sec at chamber pressures between 1,000 to 2,000 psia. During the tailoff transient of the booster motor, a chamber pressure transducer signals a control mechanism which releases the booster nozzle under the force of the residual booster pressure. A port cover plug, installed at the interface between the combustor case and the turn and dump section of the inlet diffuser, is subsequently ejected by the force of the ram air pressure when it exceeds the decaying booster chamber pressure. The port cover is ejected aft through the combustor case and ramjet nozzle.

After the port cover has been released, ram air is free to flow through the combustor case and nozzle. Since the vehicle drag forces are high at the transition from rocket to ramjet, it is desirable to minimize the time from rocket shutdown to ramjet steady state operation. Typical transition times are from 500 to 1,000 msec. A grain design with minimum slivers and minimum residual or combustible materials is critical to avoid either an excessive loss in system performance capability or an undue risk of inlet unstart which could cause a failure in ramjet takeover. The quantity and rate of heat release from the booster motor residual materials has a direct impact on the design of the ramjet fuel control system and indirectly upon the inlet if pressure control probes which must be installed in the inlet are required. Design of a booster motor having no combustible residual materials, for instance, could significantly simplify the design and cost of the ramjet fuel control system.

High Volumetric Loading

Maximum IRR range is obtained with a solid propellant boost grain of minimum volume since the solid propellant volume required for an optimum ramjet takeover velocity is larger than the chamber required for satisfactory ramjet combustion efficiency. Thus, a high density solid propellant in a grain configuration of high volumetric efficiency is an important design objective for the booster motor. A 1% increase in propellant grain length and combustor length could cause a 5 to 10% loss in IRR vehicle range due to loss of ramjet fuel storage.

Short Burn Time

Since the booster motor volume requirement is a key controller in establishing the maximum IRR range, it is also necessary to minimize gravity drag losses and thereby reduce the required booster motor size. The approach is to minimize the booster motor burn time within the structural limits of the vehicle. Typically this approach results in integral booster motor burn times on the order of 4 to 6 sec to maintain vehicle acceleration limits of 15 to 30 g. The maximum thrust limit required for the booster due to missile structural limitations, in turn, influences the size of the booster motor.

The ramburner case must be fabricated from high temperature alloys such as L-605 or I-718 to withstand both the high external aerodynamic and internal ramjet combustion heat loads. The ramjet operates at a maximum combustor pressure of approximately 150 psia at wall temperatures up to 2,000°F. Generally, the case wall thickness for this design condition permits operation of the booster at pressures up to the MEOP of 1,500 to 2,000 psia. Since these high temperature alloys are heavier than typical solid rocket case materials, the booster motor must operate as efficiently as possible within the specified maximum MEOP limit to avoid undesirable penalties in case weight or booster performance. Therefore, a neutral chamber pressure trace and a propellant with minimum value of π_K will yield a booster motor with highest performance.

Propellant Selection

generally within the range shown in Table 1. The ARCO R-45M HTPB polymer provides outstanding processability and pot life with the 87% to 89% solids propellants currently being developed for booster applications, provided that curing agents and pot life extenders are selected to minimize the catalytic effect of burn rate modifiers on the isocyanate-hydroxyl cure reactions.

As Table 1 shows, the required burn rates of 0.8 to 1.3 in/sec at 1,000 psi are in the medium-high range and require use of burn rate catalysts to achieve these rates. Catalyst selection is one of the key formulation tradeoffs at the present time. Iron oxide, Fe_2O_3, is the most widely used catalyst in solid propellants, but it has the disadvantage of yielding pressure exponents above 0.5 and temperature coefficients, π_K, of 0.20%/$^\circ$F or greater. Since high pressure and temperature sensitivities result in performance penalties, there is current interest in the utilization of anhydrous ferric fluoride as a replacement for iron oxide. This additive provides n and π_K values at the lower end of the range shown in Table 1. However, studies have indicated that HTPB propellants using FeF_3 may have poorer aging characteristics than counterparts formulated with Fe_2O_3. More work is required to evaluate these tradeoffs and investigate approaches to improved aging stability.

The high web fractions characteristic of IRR booster grain designs coupled with the broad -65° to 165°F environmental temperature range require propellants with excellent mechanical properties. Typical requirements include greater than 20% multiaxial strain capability at -65°F measured in strain evaluation cylinders. Table 2 shows mechanical properties of an 88.5% solids IRR booster propellant candidate tested at Chemical Systems Division which meets the established requirements for this type of propellant.

Grain Design

The primary objective in selecting a grain design for an IRR propulsion system is to achieve maximum volumetric loading within the structural limits of the propellant. There are, in addition, several considerations which are unique to an integral booster motor:

- High volumetric loading
- Neutral pressure trace
- No boots in forward closure which must act as ramjet recirculation zone
- Short burn time
- Minimum sliver and residuals

Figure 3 will be used to illustrate the design considerations to be made to the sample grain design. The keyhole grain design provides the following key features.

1. High volumetric loading of 92%

2. Keyhole slot provides stress relief without boot in forward combustor closure.

3. Nearly neutral pressure/thrust profile (1.055)

4. Theoretically sliverless

5. Minimum boost residuals as large exposed area of liner is consumed.

Propellant Grain/Liner

The propellant grain/liner interface with ramburner is a critical interface which has presented a unique new set of technology requirements. The propellant grain/liner interface with the liquid fueled and ducted rocket combustor are very similar as seen in figure 4. The solid fueled IRR presents a completely different interface since the booster grain/liner must interface directly with the solid ramjet fuel. In many solid fuel ramjet (SFRJ) IRR designs a dual boost grain is required for maximum volumetric efficiency. Each of the two grains may require different propellant burn rates as well.

In the liquid fuel ramjet (LFRJ) IRR and ducted rocket the interface is with the TPS which lines the case wall. Three primary TPS materials are currently being used in IRR combustors:

1. A silicone elastomer DC 93-104

2. Silica phenolic

3. Quartz phenolic

The structural and chemical interfaces are vastly different between the silicone elastomer and silica or quartz-phenolic materials.

The propellant/grain liner structural and chemical interface considerations are summarized in Tables 3 and 4. The structural interfaces between the booster grain/liner interface with DC 93-104 presents no problems relative to support of the grain. The major structural problem is to achieve satisfactory bond strengths with the silicone elastomer material. Many interface material bond systems have been evaluated for the DC 93-104 material.

Booster Igniter

closure as well as the need to install a port cover at this interface. In addition, the booster igniter must provide fast, uniform ignition of the internal grain surface to avoid nonuniform burning and undesired slivers at booster grain burnout. An igniter material such as MAG-TEF is highly desirable to avoid overpressure during the ignition transient which could result in an undesirable weight penalty for the ramjet case or excessive pressure rise rates with the cold L605 case material.

Nozzleless Motors

The primary advantage of the so-called nozzleless solid rocket motor lies in the elimination of the ejectable booster nozzle and its attendant complexity and cost. Nozzleless solid rocket motors employ simple circular port grain designs as seen in figure 5 and are characterized by highly regressive pressure-time curves but nearly neutral thrust-time histories. Figure 6 shows a typical set of pressure and thrust curves for a nozzleless motor design. Although nozzleless motors have much lower specific impulse values than conventional motors using the same propellant, this loss can be largely compensated by packaging additional propellant in the volume usually occupied by the nozzle. In addition, a divergent aft conical surface serves to accelerate the exiting combustion products, yielding a small improvement in delivered performance.

Nozzleless motors normally require significantly higher propellant burn rates than conventional motors designed for the same mission. In addition, propellant pressure exponents should be less than 0.50 in order to obtain designs which are competitive with nozzled booster configurations. These additional requirements and constraints add further difficulty to the problems inherent in formulating satisfactory booster propellants.

Table 5 summarizes the outlook for various categories of nozzleless booster propellants. Feasibility studies of nozzleless ramjet boosters using high burn rate aluminized propellants are currently being conducted under Air Force contract. Since these propellants use liquid ferrocene burn rate catalysts, some problems in long term aging may be expected. However, there is no reason that high density-impulse zirconium propellants should not be as satisfactory for nozzleless designs as the aluminized propellants, and the same performance advantages noted earlier for conventional motors can be expected. Up to this time, no effort has been expended in adapting low signature propellants to nozzleless IRR booster concepts. Because of their inherent high burn rates, such propellants will be particularly susceptible to acoustic combustion instability. Very probably, some compromise will be necessary in requirements for smokelessness in order to develop nozzleless boosters with these types of propellants.

HEAT PROTECTION

Thermal protection of the integral rocket ramjet engines requires new materials and construction to withstand the difficult thermal, structural and chemical environment. A comparison of the thermal protection system (TPS) design consideration for rockets and integral rocket ramjets is shown in Table 6. The unique aspect of the thermal protection design is that all of the virgin and charred material properties required either by a solid rocket or liquid rocket must be combined for the integral rocket ramjet engine. In particular, the requirements for a high strain capability, chemical/structural booster compatibility, high charred material mechanical strength and oxidation/erosion resistance make thermal protection a significant IRR design challenge.

The requirements for the thermal protection systems for rockets and ramjets are compared in Table 7. Because of the lower chamber pressure levels of the ramjet the heat fluxes and combustion temperature are significantly lower than the rocket. The ramjet, on the other hand, operates for significantly longer durations with external aerodynamic heating in an oxidizing/high viscous drag environment. Steady state combustor operation with a fully charred insulation material is a unique requirement of the ramjet.

Early podded ramjet combustors employed air cooling to thermally protect the combustor and nozzle. The advent of the integral rocket ramjet with the dump combustors and high L/D combustors made it generally impractical to apply air cooling. Ablation cooling is the most attractive solution to thermal protection of ramjet engines. A large number of candidate ablative materials were evaluated as potential ramjet insulation materials.

Thermal Analysis

The thermal analysis model recommended for use in analyzing the integral rocket ramjet thermal protection systems is the two zone model shown in figure 7.

Combustor State

The combustor environment is defined by a chemical equilibrium calculation based on measured fuel-

to-air ratio (f/a), fuel composition and enthalpy, and air temperature. Calculations are performed using the ACE chemical equilibrium program.[1] Corrections for combustion inefficeincy, when known from test data, are applied as enthalpy losses. Gas emissivity is based on the calculated equilibrium CO_2 and H_2O concentrations.

Boundary-Layer Model

The convective transport of heat and mass to the surface is modeled using a boundary-layer computer code developed by R. J. Flaherty.[2] This model predicts convective heat transfer coefficients that are comparable to values calculated by other boundary-layer programs.[3,4] The boundary-layer program incorporated the effect of axial combustor length into the analysis and provided a continuous model down through the ramjet nozzle. Nozzle heat transfer correlations do not have this length effect explicitly included. The boundary-layer model also considers the effects of pressure Mach number, wall contour, wall temperature and gas properties.

Charring Lining Heat Transfer Model

The actual thermal response of the charring wall and Inconel case is modeled by the CMA computer code.[5] This program is a one-dimensional, transient, charring heat transfer model. It includes convective heat and mass transport with corrections for blowing effects, radiation to and from the surface, and heat conduction into the solid wall material. Pyrolysis of the wall material is described by three independent Arrhenius-type equations; pyrolysis product gases were permitted to react at the surface of the char. The program can consider multiple materials with intermaterial gaps transmitting heat by radiation and gas conduction. The material properties uses the same properties as those reported for MX 2600 silica phenolic.[6] Separate sets of temperature-dependent thermal conductivity and specific heat were input for virgin and char material, respectively.

The reaction of the pyrolysis gas with the ramjet combustion products is assumed to proceed to equilibrium at the char surface, with the resultant enthalpy change included in the solution for the surface temperature. The net enthalpy change then appears as a reactive "heat" flux in addition to the convective, radiative and solid conduction components of the surface heat transfer. Since the pyrolysis gas products are fuel-rich, the reaction is strongly exothermic whenever unreacted oxygen is in the combustion products, and is usually the case in ramjets. There has been some question as to whether the pyrolysis gas-ramjet reaction actually occurs at the surface as this model suggests. Experimental results show that it does occur in some sitations.

Two-Zone Modeling

It has long been accepted that a recirculation zone exists downstream of the step expansion from the inlet. This recirculation zone is characterized by higher fuel-to-air (f/a) ratios and higher flame temperatures than the overall combustor. To apply the charring heat transfer model to this zone, both the local f/a ratio and the local temperature must be predicted.

An extensive study of recirculation zone f/a enrichment showed a correlation between overall equivalence ratio ϕ and recirculation zone equivalence ratio ϕRZ for center dump combustors. While the correlation is not precise (and especially for charring linings) it gives a first approximation to the recirculation zone state. The correlation can be used to determine a new local f/a ratio, and the equilibrium chemistry calculations can be used to determine a new local gas temperature for the recirculation zone.

As a first approximation to convective heat transfer, a short reverse boundary layer is assumed to develop within the recirculation zone similar to that in the aft region.

The starting point for the aft boundary-layer becomes a semiempirical parameter in the two-zone model. However, the aft predictions are in general not sensitive to the exact location of the boundary-layer start. The remaining unspecified parameter is the recirculation zone gas emissivity, which becomes the main point of empiricism in the present approach. Gas emissivity is determined from the charred engine firing and then applied to the values derived are consistent with those derived from other fuel-rich ramjets.

Two-Zone Correlation with Test Results

Full Charred Lining. The conventional boundary-layer model still matches the aft region thermocouple response. The aft zone can be considered to prevail in the region downstream of the 0.45 combustor station (see figure 8).

The forward recirculation zone prediction is significantly higher because of increased fuel concentration. The local equivalence ratio is approximately 1.5 for all phases of the duty cycle. Equilibrium flame temperatures are singificantly higher. The best fit to average forward case temperatures over the entire test duration of 175 sec corresponds to a local efrective emissivity of 0.2, a not unreasonable value considering the highly rich fuel mixture. This recirculation zone model extends across approximately the first quarter of combustor length.

Virgin Lining. When the same two-zone model is applied to the actively charring lining, a reasonable match is still obtained at both zones. The aft region boundary layer again shifts to the right. The midlength peak in the thermocouple band suggests a slightly further aft starting point than for the fully charred lining.

The forward zone is similarly modeled to the fully charred lining; however, a temporarily higher f/a ratio is used during active pyrolysis due to the addition of fuel-rich pyrolysis gases. The overall

The two-zone model is able to fit both locations in both tests because the charring heat transfer model considered reactive as well as convective and radiative heat fluxes. In the actively charring lining, the forward and aft heat fluxes are similar in total magnitude, but quite different in nature. The aft region is mainly reactive because of the exothermic pyrolysis gas reactions and is only secondarily convective. In the forward region, the higher temperatures and emissivity raises the convection and radiation but the reactive term is reduced a comparable amount because of the local lack of excess oxygen. The net result is a similar total heat flux, both forward and aft.

When the lining is fully charred, the reactive flux disappears. This reduces the aft heating considerably, but has little effect in the forward zone when the flux was convective and radiative. Under these conditions, forward-to-aft variation become characteristic. If the initial run continues long enough, this effect will be apparent. The hot forward zone is also seen in metal wall combustors where again no reactive flux is present. Thus, the flat axial temperature profiles, which are seen with all of the pyrolyzing lining materials, result from a hot, fuel-rich forward zone and a comparable, cooler, but more reactive, aft zone. Table 8 summarizes these differences in heat flux and resultant temperatures for the two zones of both tests.

More precise modeling of most of the present approximations should not change the validity of this approach. Any recirculation zone f/a correlation that would give a fuel-rich forward zone would be consistent with this model. Any aft boundary-layer starting point in the midregion of the engine would also be consistent. Changes in recirculation zone convective heat transfer coefficient would result in a revised empirical emissivity for both forward zones. Material property changes would also apply to both zones of both tests.

In conducting preliminary design studies of a ramjet propulsion system it is important to consider the relative effect of different configurations on thermal protection requirements. An an example, in figure 9, two candidate combustors having the same nozzle area ratio (A_5) but with significantly different L/D ratios can satisfy the basic mission requirement. Tne high L/D combustor, however, has 50% higher heating and 100% higher combustor gas velocities. This significantly more severe thermal environment could result in a longer and more costly flight engine development effort.

Several general conclusions can be drawn from recent thermal protection system development efforts that have involved bench test, subscale test and fullscale durability testing of several thermal protection systems. These general conclusions are summarized below.

Bench/lab tests useful as qualitative indicators

  . Can identify unsatisfactory TPS material/construction

  . Cannot be directly scaled to full size

Analysis required to identify requirements

Fundamental TPS laboratory/subscale test data acceptable.

Testing required to demonstrate specific requirements, such as

  . Weight loss vs temperature and time

  . Strain capability of virgin/charred TPS material

Correlation of information from various tests

Prohibitive cost/schedules for F/S IRR TPS durability tests systematic approach

Improved thermal/structural desired TPS modeling techniques are needed

PORT COVERS

Among the key elements in the IRR concept is the air inlet port cover. The port cover design requirements are summarized below. Depending upon the configuration of the ramjet combustor, the port cover may be a large unit covering a single axial inlet or several smaller units covering multiple air inlets. The cover, or covers, must withstand booster chamber pressures of 1,000 to 2,000 and still be capable of being ejected reproducibly, reliably and without damage to the ramjet combustor, nozzle, or thermal protection system. To minimize the need for active control devices, it is desirable for the port covers to be self ejected due to ram air pressure during booster tailoff. Finally, the port covers must be suitably insulated from heat generated by burning of the booster propellant.

The integral rocket ramjet port cover design problem is illustrated in figure 10. In the top inset the overall transition sequence from rocket to ramjet operation is depicted. In the example shown the booster propellant is cast over the multiple side mounted inlet dump openings. In this configuration the boost propellant retains the port cover during captive flight (if inlet covers are not used). In alternate center dump configurations, for example, the boost propellant may not be directly cast against the port cover and special retaining devices must be used to prevent the port cover from being prematurely ejected by the ram air loads during captive carry.

The apparent simplicity of the basic port cover operation belies the true complexity of the design engineer's challenge. The port cover interfaces with many of the other major IRR subsystems, creating several specific interface design problems. These port cover design problems are defined in figure 9. In addition to the basic port cover structural, seal and design problems, some additional design requirements are frequently imposed. These are associated with providing signals to the flight vehicle controller to initiate ramjet operation.

Design concepts currently in use include: the monolithic cover, the segmented cover, and the frangible cover. The simplest type of cover (a monolithic metal cover) is found on the Supersonic Tactical Missile (STM). The STM utilizes four smaller covers (figure 11A) over the combustor size wall air inlets. In the design, ejection of the cover(s) necessitates the expulsion of fairly large metal pieces, creating the possibility of damage to the combustor or nozzle. Although numerous tests proved these designs do not damage the ramjet combustor, other designs are being investigated to decrease the damage potential by reducing the size of the ejected material.

The Modern Ramjet Engine (MRE) used a segmented inlet port cover (figure 11B) to reduce the size of the ejected particles. This cover was made up of several structural beams placed across the air inlet and held together by a rubber-like retention boot. At ejection, the boot released the "beams" and allowed them to individually exit the combustor.

Both monolithic and segmented port covers have been successfully employed. However, several newer concepts are of considerable interest because they offer the possibility of further reducing the size of ejected pieces or eliminating them entirely. One approach is to mechanize the port cover so that it can be opened without being ejected. For example, the cover could be hinged (figure 11C), louvered or sliding. These approaches would be particularly good for small dump openings. Moreover, the port structural elements could potentially be designed to act as flameholders.

Another means of reducing the size of the ejector is the frangible cover. This cover is made from high-strength chemically treated or heat-treated frangible glass. When the glass is broken (by a hard metallic pin that penetrates the hard outer surface or by a small detonating device), it breaks into rock salt shaped granules about the size of the original glass thickness. This method seems best suited for combustors with center dump.

TRANSITION

The transition sequence in the integral rocket ramjet propulsion system created new design requirements, unique to this system.

During rocket operation, the combustor must function as a conventional rocket combustor, closed at the forward end and with a suitable "rocket" nozzle at the aft end. During transition, the combustor must reconfigure itself to a ramjet combustor, open at the forward end to allow air to enter the combustor, and with a large throat nozzle, suitable for ramjet operation at the aft. Two schemes are employed to permit this dual operation of the combustor chamber - the "blow-in" port cover and the ejectable rocket nozzle.

In addition to their steady-state functioning, the port cover and ejectable nozzle design must consider the ability of these components to quickly and reliably allow transition from rocket to ramjet operation. After tailoff of the booster, drag forces acting on the airframe with engine off quickly slow the forward speed of the ramjet vehicle, typically losing on the order of 0.1 Mach No. per sec. Longer transition times require increased booster loading which in turn causes undesirable ramjet fuel losses and consequently significant range loss. Transition to ramjet takeover must, therefore, be done very quickly. Although transition sequences may vary, the basic transition operations following booster tailoff remain the same. When the booster rocket chamber pressure decays to a value where positive vehicle acceleration approaches zero, which is approximately equal to ramjet takeover combustor pressure, the rocket nozzle release mechanism is activated, and the residual booster pressures force the nozzle rearward, ejecting it freely through the ramjet nozzle. During this same time period, the air inlet port covers are forced inward when the inlet ram air pressure exceeds the residual chamber pressure. The covers are expelled through the ramjet nozzle by the force from incoming ram air flow. Ramjet fuel control and ignition systems then sequence the ramjet fuel and igniter. Ramjet fuel ignition is further aided by the remaining burning residuals of both the rocket grain and the thermal protection system combustibles. All this must take place in a few hundred milliseconds or excessive forward velocity will be lost to drag forces.

The propulsion transition sequence for the Supersonic Tactical Missile illustrates a typical transition design (figure 12).

A typical propulsion transition sequence is shown in figure 13. The design transition sequence is initiated during booster tailoff when inlet ram air pressure exceeds booster combustor pressure (ΔP = 5 psi nominal) forcing the air inlet port covers inward. Movement of any one of the four port covers actuates a port cover sensing switch which energizes the nozzle snapring retention system relay. Upon relay closure, voltage is applied across the propagation cord initiator bridgewires, firing the initiator squib which in turn ignites the propagation cord. Closure of the port cover sensing switch also initiates a nominal 300-ms time delay relay that is subsequently used to open the ramjet fuel valve and fire the ramjet igniter. Upon firing the propagation cord, the booster nozzle snapring is released and residual chamber pressure, in conjunction with incoming air pressure, ejects the booster nozzle. Residual propellant slivers and liner continue to burn until the slivers are essentially consumed at the end of the 300-ms delay. Closure of the time delay relay initiates fuel valve opening and ramjet igniter firing current which is followed by fuel flow, ramjet ignition, and steady-state ramjet operation. The ramjet igniter fires for approximately 1 sec, releasing 1,500 Btu/sec of energy.

While the transition sequence must be accomplished quickly, it must also be timed very carefully with the other sources of energy release during the transition period. Early ramjet light-off can cause excessive chamber pressure, resulting in inlet "unstart". Late light-off allows excessive vehicle slow down, also resulting in unstarted inlets.

The primary integral rocket-to-ramjet transition interface considerations are shown in Table 9. Critical interfaces exist with the inlet, fuel control, combustor/nozzle and booster motors. Maintaining a supercritical design margin or, if necessary, stable subcritical inlet operation during transition is a primary requirement. Several early IRR flight tests resulted in failures due to failure to anticipate the energy release during transition. Careful analysis and resolution of this problem during the early 1970's cleared a major technical obstacle for IRR systems. The interface with the fuel control frequently involves providing pressure control signals to limit maximum combustor pressure, in thereby maintaining the desired inlet margins. Another solution may be to pre-program the fuel flow rate during transition so that inlet margins cannot be exceeded.

During transition, combustor operation must account for energy sources from the ramjet igniter, ramjet fuel and combustible pyrolysis gases from the thermal protection system.

Residual booster motor energy sources that must be accounted for during transition include the propellants sliver, residual propellant liner and, if present, stress relief boots.

A typical account of the total ramjet energy sources during transition is seen in Table 10. The energy contributions from each potential source are identified as a function of transition time. The heat release from each one of these energy sources is shown also as a function of time, leading to the predicted combustion pressure (P_4) rise. During the first 50 msec of the transition sequence the residual energy sources provide 7100 BTU/sec compared to 16,200 BTU/sec expected from the ramjet fuel flow. Failure to accommodate this high energy release could easily cause an inlet unstart.

EJECTABLE BOOSTER NOZZLE

Several designs for the ejectable nozzle have developed and at least three nozzle release concepts have been successfully tested: the use of multiple explosive bolts, the use of a Marman type clamping device, and the use of a snapring retention system.

The use of multiple explosive bolts on the Low Altitude Supersonic Ramjet Missile (LASRM) represented a conventional approach to nozzle retention as does the Marman type clamp (figure 14) used on the Air Launched Low Volume Ramjet (ALVRJ). Both systems attain booster nozzle alignment by direct mechanical interfaces provided by the fasteners and the use of explosive bolts (common in aerospace use) to release the booster nozzle. The systems are reliable and due to the use of ordnance common to aerospace use are easily adapted for use in ramjet vehicles. They also share a common disadvantage - relatively high weight and complexity.

A later concept incorporated on the Modern Ramjet Engine (MRE) and the Supersonic Tactical Missile (STM) is the snapring retention system (figure 15). The advantage of this system is significant weight savings over the other systems and it was demonstrated to be extremely fast, repeatable, and reliable by several test programs. The system was successfully flight tested on the STM in 1979.

The snapring retention system utilizes a high strength snapring to restrain rearward movement of the booster nozzle. Booster nozzle alignment is attained by close tolerance alignment surfaces machined into the nozzle assembly. Replacing the explosive bolts used in the other systems is a length of mild detonating cord positioned in a groove beneath the snapring. Ignition of this cord releases large quantities of combustion gas which compress the ring and force it from the retention groove. As in other systems, the booster nozzle is thrust rearward by residual chamber pressure. Tests have shown this system to release in less than 10 msec without imparting rotational or tumbling motion to the booster nozzle.

While the snapring and other concepts offer promise for the IRR of today, advanced concepts are in development. Several concepts that have been advanced to eliminate the ejectable booster nozzle include a nozzle fabricated to erode at a rate predetermined to give near maximum performance for boost and ramjet combustor pressures. Such nozzles may be designed to "step" from one throat size to another as the chamber pressure decreases or they may be designed to erode in a continuous manner approximating the chamber pressure decay from boost to ramjet operation.

CONCLUSIONS/RECOMMENDATIONS

After expending a significant development effort over the past decade, a solid engineering data base exists for the design and analysis of the integral boost motor, thermal protection system, port cover and transition devices.

High performance and reliable operation of these components can be assured through knowledgeable application of this comprehensive data base.

Further development efforts in this area should concentrate on: (1) extending the data base on the shelf life of the integral boost motor and (2) further simplification of the IRR transition sequence, leading to a totally passive (no vehicle controls required) transition system design to reduce cost.

REFERENCES

1. Kendall, R. M., "A Gene⋯ ⋯roach to the Thermochemical Solution of Mixed Equilibrium-Nonequilibrium Homogeneous or Heteroge⋯ ⋯stems," NASA CR-1064, Aerotherm Acurex Corp. Report (1967).

2. Private communication with R. J. Flaherty, United Technologies Research Center, East Hartford, CT (1971).

3. Flaherty, R. J., "Arbitrary Pressure Gradient Integral Technique for Predicting Boundary Layer and Thermal Parameters," J. Aircraft, Vol, 11, 243 (1974).

4. Elliot, D. B. et al., "Calculation of Turbulent Boundary Layer Growth and Heat Transfer in Axisymmetric Nozzles," JPL Tech. Report No. 32-387.

5. Moyer, C. R. and Rindal, R. A., "Finite Difference Solution for the In-Depth Response of Charring Materials Considering Surface Chemical and Energy Balances," NASA CR-1061, Aerotherm Acurex Corp. Report (1967).

6. Schaefer, J. W. et al., "Studies of Ablative Material Performance for Solid Rocket Nozzle Applications," NASA CR 72429, Aerotherm Acurex Corp. Report (1968).

TABLE 1   TYPICAL PROPELLANT FORMULATIONS FOR CURRENT IRR BOOSTER DESIGN

T11285

Formulation Range	Property	Nominal Value
87 to 89% solids HTPB	I^o_{sps}, sec	262
17 to 18% Al	Density, lb/in.^{3}	0.064
1 to 3% fine-ground AP	Burning rate at 1,000 psi, in./sec	0.8 to 0.3
Fe_2O_3 or FeF_3 catalyst	Pressure exponent	0.40 to 0.55
	π_K, %/F	0.16 to 0.21
	Hazards	Class 1.3
Structural Characteristics		
● Mechanical properties suitable for -65 to 165 F environment		
● Tradeoffs of ballistic properties versus aging stability being studied		

TABLE 2   MECHANICAL PROPERTIES OF TYPICAL HTPB TACTICAL PROPELLANTS

T11286

Propellant No. 1				Propellant No. 2			
	Temperature, F				Temperature, F		
Property	165	70	-65	Property	165	70	-65
Tm^C, psi	110	148	581	Tm^C, psi	102	147	822
Em^C, %	35	42	22	Em^C, %	27	29	12
E_R, %	37	44	36	E_R, %	28	31	15
E_0, psi	512	628	9220	E_0, psi	455	671	11,800

TABLE 3   PROPELLANT GRAIN/LINER STRUCTURAL INTERFACE CONSIDERATIONS

T11296

- Provide suitable structural support for grid to avoid excessive strain

- Booster pressure loads must not cause TPS liner failure, particularly at low temperatures

- Propellant boots in forward combustor recirculation zone are unacceptable

- Port cover in side-dump combustor must not cause grain/liner movement

- Booster motor MEOP must exceed structural margins of combustor case, which is sized by ramjet loads at high temperature and pressure

- Booster motor must not cause structural damage to SFRJ fuel grains

TABLE 4   PROPELLANT GRAIN/LINER CHEMICAL INTERFACE CONSIDERATIONS

T11296

- Interface material system must provide strong chemical bond with TPS: BIT > 100 psi, peel > 5 pli

- Propellant constituents must have long-term chemical compatibility with TPS

- TPS constituents must not degrade interface material bond strength

TABLE 5   PROPELLANT CATEGORIES FOR ADVANCED IRR BOOSTERS
NOZZLELESS MOTOR DESIGNS

T11288

Propellant Type	Characteristics	Status	Problem Areas
High-rate HTPB with Al	86 to 88% solids HTPB with liquid ferrocene catalysts to achieve burn rate >1.5 in./sec, pressure exponents <0.5	Feasibility demonstration in process	Ballistic properties and reproducibility; propellant aging
High-rate HTPB with Zr	91 to 93% solids HTPB with ~40% Zr and liquid ferrocene or FeF_3 catalysts	Propellant development in process	Propellant aging; Zr purity and cost
Reduced smoke class 1.3	86 to 88% solids HTPB without Al; catalyzed to high burn rate	No work in burn rate regime of interest	Combustion instability; aging
Minimum smoke class 1.1	High energy binder with HMX/RDX and rate enhancing additives	No work in process; may require new ingredient technology	Achieving burn rate and pressure exponent; combustion stability; low temperature properties

TABLE 6   THERMAL PROTECTION SYSTEM DESIGN CONSIDERATIONS

T11289

Property	Solid Rockets	Liquid Rockets	Integral Rocket Ramjets
Virgin material			
High strain capability	X		X
Light weight	X	X	X
Low thermal conductivity	X	X	X
Oxidation resistant		X	X
Erosion resistant	X		X
Chemically/structurally compatible with booster liner materials	X		X
High gas temperature capability	X	X	X
Charred material			
High mechanical strength		X	X
Light weight		X	X
Low thermal conductivity		X	X
Oxidation resistant		X	X
Erosion resistant			X

TABLE 7   REQUIREMENTS FOR THERMAL PROTECTION SYSTEMS

T11290

Rocket Type	Duration, sec	Pressure, psi	Heat Flux, Btu/ft^2-sec	Temperature, F	Environment	External Aerodynamic Heating
Solid	60 to 120	500 to 1,000	500 to 1,500	6,300	Oxidizing particle versions	None
Liquid	100 to 600	100 to 500	700 to 2,000	5,000 to 5,500	Oxidizing	None
Ramjets	100 to 1,000	10 to 150	10 to 30	2,500 to 4,000	Oxidizing/	500 to 1,200 F

TABLE 8   PREDICTED AND MEASURED THERMAL RESPONSE

T11293

Property	Forward Recirculation Zone	Aft Boundary-Layer Zone
Typical boundary conditions		
● f/a	0.10	0.039
● Tc, R	4,300	3,700
● HTC, boundary-layer relative length	0.075	0.05 to 0.60
● HTC, blowing effect reduction, %	5 (maximum)	6 (maximum)
● Effective emissivity	0.15	0.036
Charring lining		
● Typical heat flux (predicted), Btu/ft²-sec	13.5	13.0
● Convective, %	50	30
● Radiative, %	50	10
● Reactive, %	0	60
● Inconel case temperature		
● Predicted/measured	1.043	1.006
Fully charred lining		
● Typical heat flux (predicted), Btu/ft²-sec	13.6	8.0
● Convective, %	60	90
● Radiative, %	40	10
● Reactive, %	0	0
● Inconel case temperature		
● Predicted/measured	0.974	0.992

TABLE 9   INTEGRAL ROCKET RAMJET TRANSITION INTERFACE CONSIDERATIONS

T11294

Parameter	Consideration
Inlet	● Pressure margin ● Supercritical design margin ● Subcritical stability limit
Fuel control	● Fuel flow control accuracy ● Pre-programmed fuel flow rate and time
Combustor/nozzle	● Ramjet igniter ● Fuel flow rate ● Thermal protection system
Booster motor	● Propellant sliver ● Residual propellant liner ● Boot

TABLE 10   IRR BOOSTER RESIDUAL ENERGY RELEASE DURING TRANSITION

Energy Source	Mass Flow Rate, lb/sec			Heat Release, Btu/sec			P_4, psi		
	0 to 50 msec	50 to 1000 msec	1000 msec	0 to 50 msec	50 to 1000 msec	1000 msec	0 to 50 msec	50 to 1000 msec	1000 msec
Booster residuals									
Propellant liner	0.45	0.45	0	4000	4000	0	6.0	6.0	0
Propellant slivers	0.5	0	0	1000	0	0	1.5	0	0
HTPB insulation	0.06	0.06	0.06	500	500	500	0.8	0.8	0.8
Ramjet									
Fuel (η_c = 90%)	1.0	1.0	1.0	16,200	16,200	16,200	40.1	40.1	40.1
Ramjet igniter	0.5	0.5	0	1500	1500	0	2.6	2.6	0
TPS pyrolysis gases	0.006	0.003	0.003	100	50	50	0.2	0.2	0.2

T11295

Booster

Ramjet fuel

Podded combustor
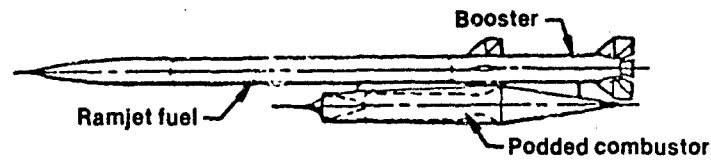
A. Initial Podded Ramjet Configuration

Booster

Ramjet combustor
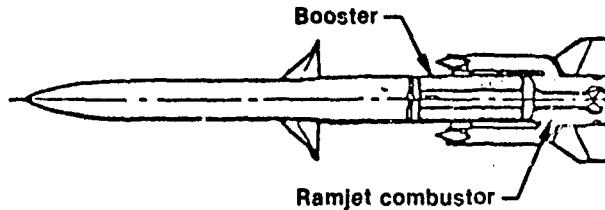
B. Tandem Rocket Ramjet with Submerged Nozzle

Integral booster

Integral rocket ramjet combustor
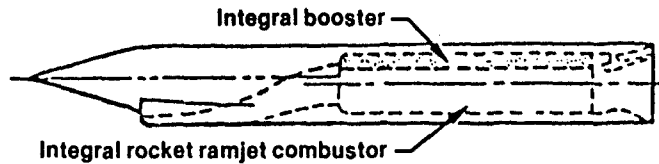
C. Internal Rocket Ramjet

Figure 1.   Evolution of Integral Rocket Ramjet Configuration

33057

Port cover (four places)

O-ring

Wire mesh

Igniter assembly (MAG-TEG)

Frangible forward support ring

Aft igniter safe and arm support ring

Propellant grain, 89% solids HTPB

Case insulation, DC 93-104 silicone elastomer

Ejectable booster nozzle assembly, snap ring release mechanism

Wire mesh

Safe and arm device

Boot

Propellant liner/ bond system

Pressure transducer boss

Fuel manifold boss (four places)

Combustor case

Inlet turn and dump (four places)

Fin actuator boss (four places)

View B-B
Port Cover,
Top View

Figure 2.   Typical Integral Boost Motor

33054
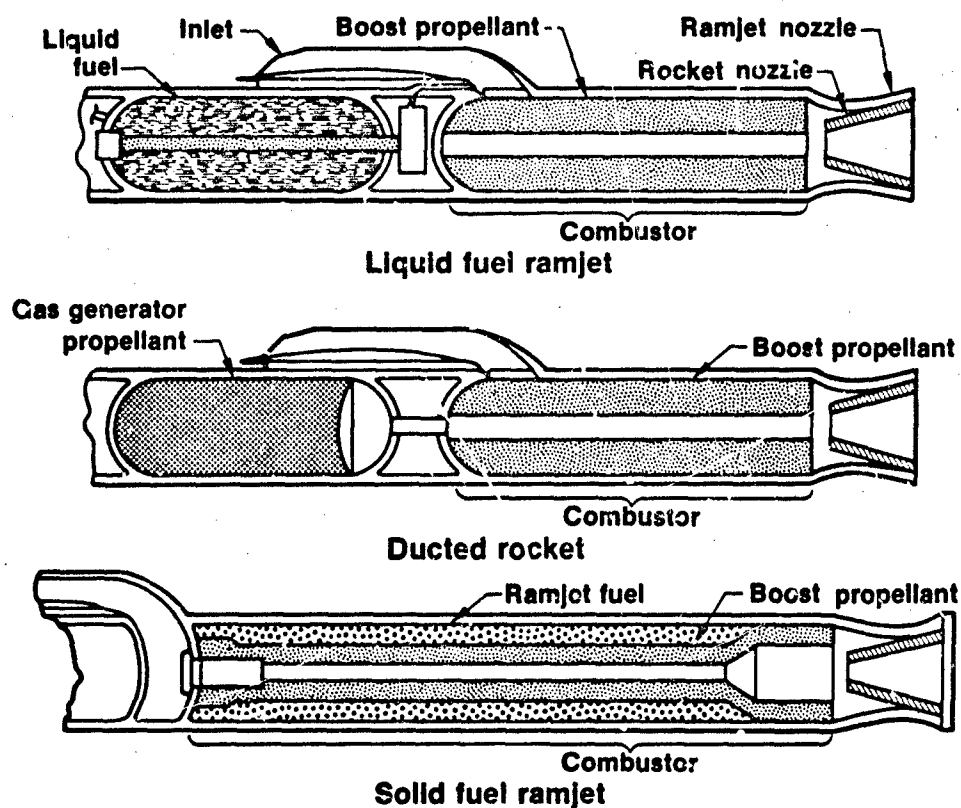
Figure 3. Types of Integral Rocket Ramjets

V- 08171-R1
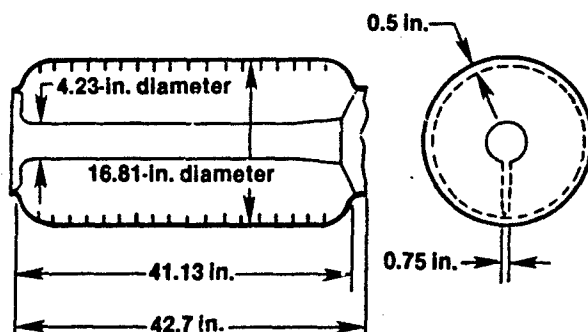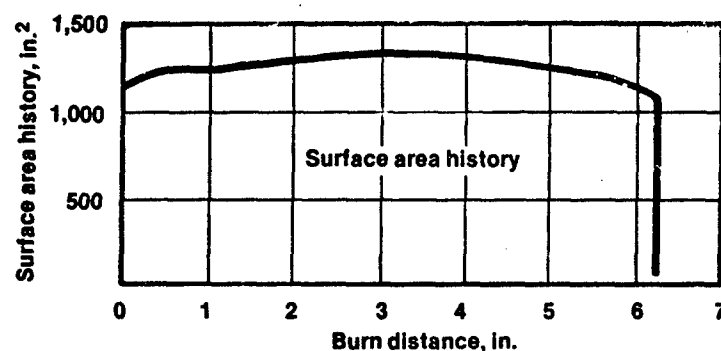
Property	Unit of Measurement
Web thickness, in.	4.31
Propellant weight, in.	538.25
Grain length diameter, in.	2.53
Port/throat ratio (geometric)	1.84
b/a ratio (outer to inner radius ratio)	4.0
Volumetric loading	0.92
Neutrality (maximum to average area ratio)	1.055
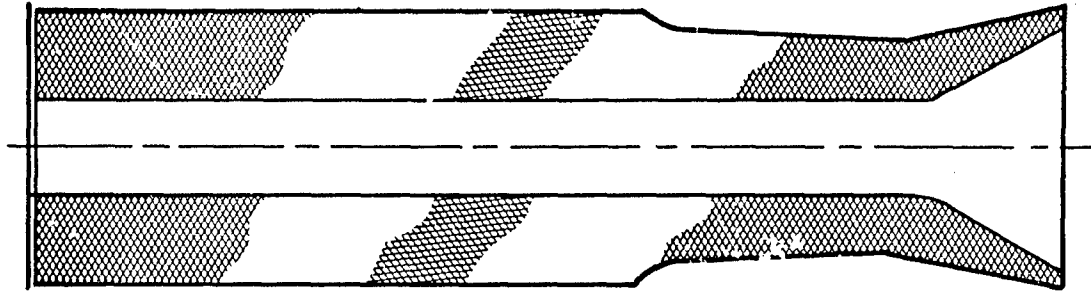
Figure 5. Nozzleless Motor

33056
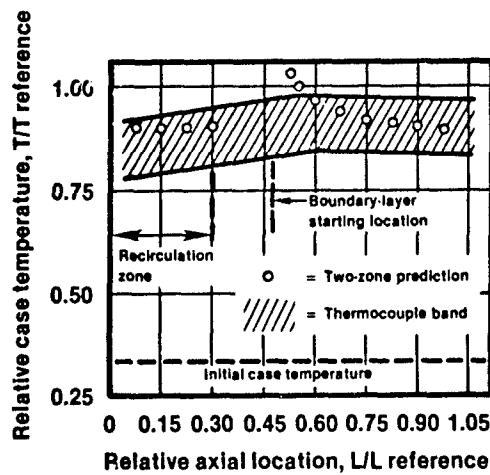
A. Virgin Lining, Two-Zone Correlation
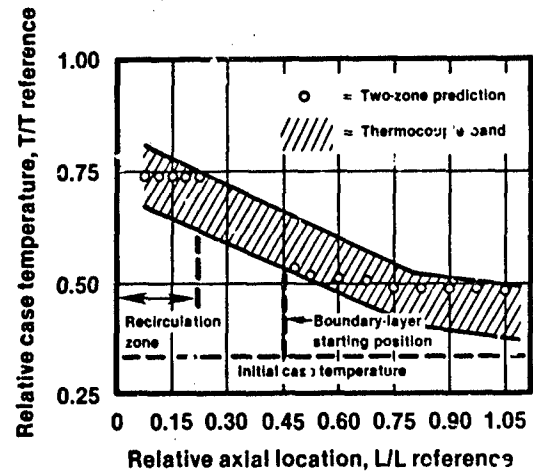
B. Fully Charred Lining, Two-Zone Correlation

Figure 6. Two Zone Thermal Model Data Correlation

33057
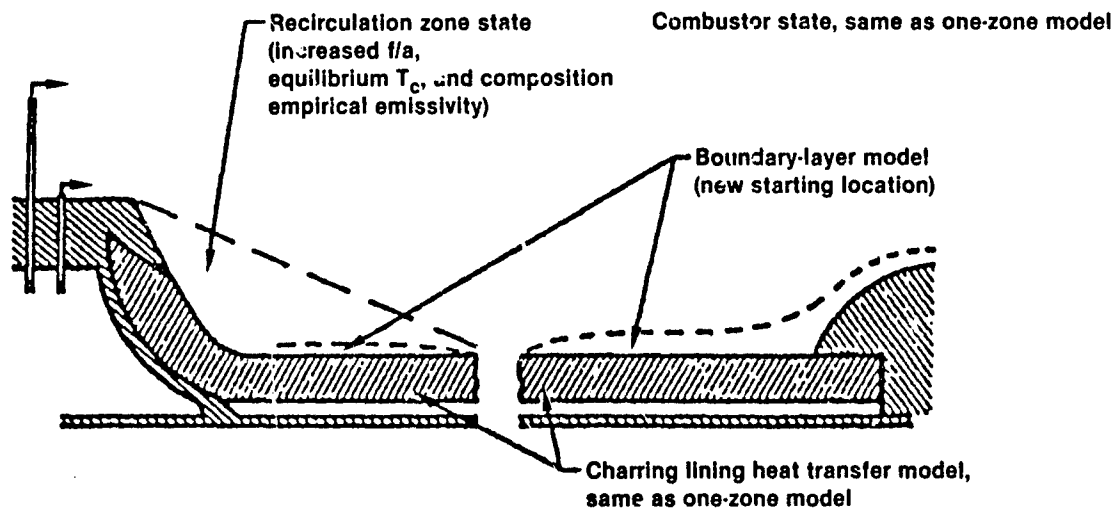
A. Forward Recirculation Zone   **B. Aft Combustor and Nozzle**
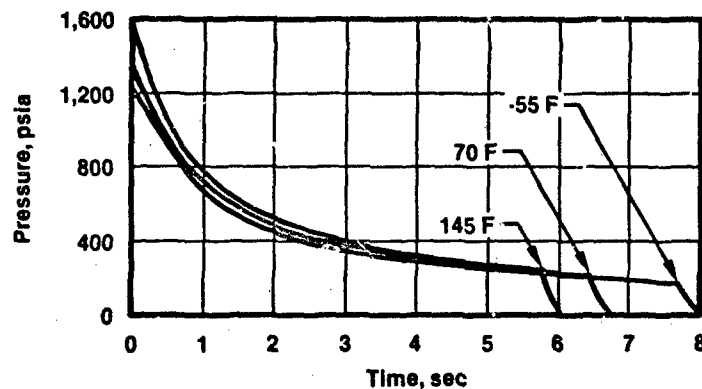
A. Forward Head Chamber Pressure vs Time
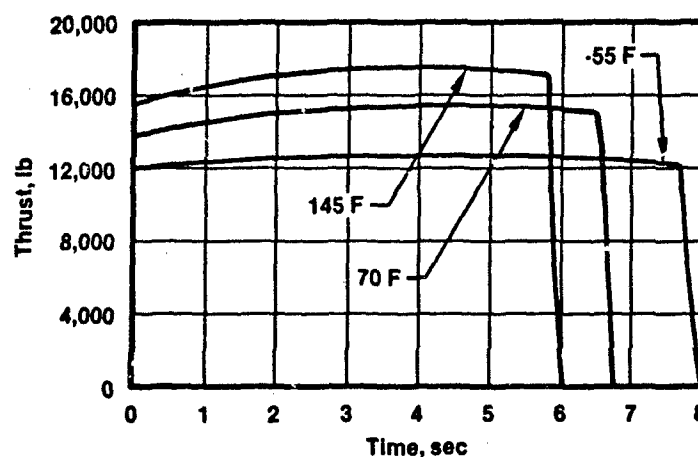
B. Thrust vs Time

Figure 8. Nozzleless Motor Ballistics

33059
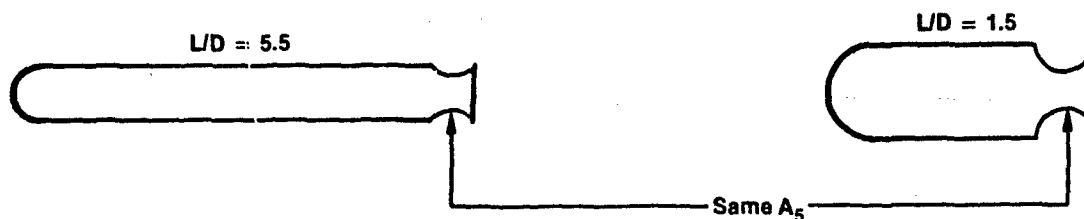
Parameter	High L/D	Low L/D
Cruise chamber pressure, psia	10.5	13.5
Combustor Mach No.	0.43	0.21
Cruise heat transfer coefficient (H/CP)	0.0195	0.0135
Integrated surface heat flux at end of identical trajectory, Btu/ft^2	7640	5025
Combustion chamber gas velocity, ft/sec	1210	600

Conclusions:
(1) High L/D combustor has 50% higher heating
(2) High L/D combustor sees 100% higher gas velocity

Port Cover Design Problems	Special Nonejectable Port Cover Problems
• Must seal interface between combustor and air inlet over −65 to 165 F environmental range (2100 psia)	
• Must be opened rapidly (< 300 msec) with minimum pressure differential	• Must not affect basic combustor flameholding and mixing processes
• First priority must be given to self-actuation vs. commanded port cover opening for simplicity, low cost and reliability	• Must not cause significant (> 3%) pressure loss

• Must provide suitable bonding/structural interface for integral solid booster grain
  • Mandatory for side dump
  • Optional for center dump*
	• Must not eject any particles greater than 0.03 in. in diameter for launch/chase aircraft safety
	
	Additional Problems

• Must be lightweight and not damage ramjet insulation	• May be required to provide control signals for ramjet engine start
	  • Open fuel isolation valve
	  • Fire signal to turbine start cartridge
	  • Fire signal to ramjet igniter
	  • Fire signal to ducted rocket gas generator

• Must be able to withstand ram air external loads (< 100 psi) during captive flights	
*If booster grain does not cover port cover, insulation is required during boost operation	

Figure 10. IRR Port Cover Design Problem

V-25292

A. Monolithic Port Cover

B. Segmented Port Cover

C. Hinged Port Cover
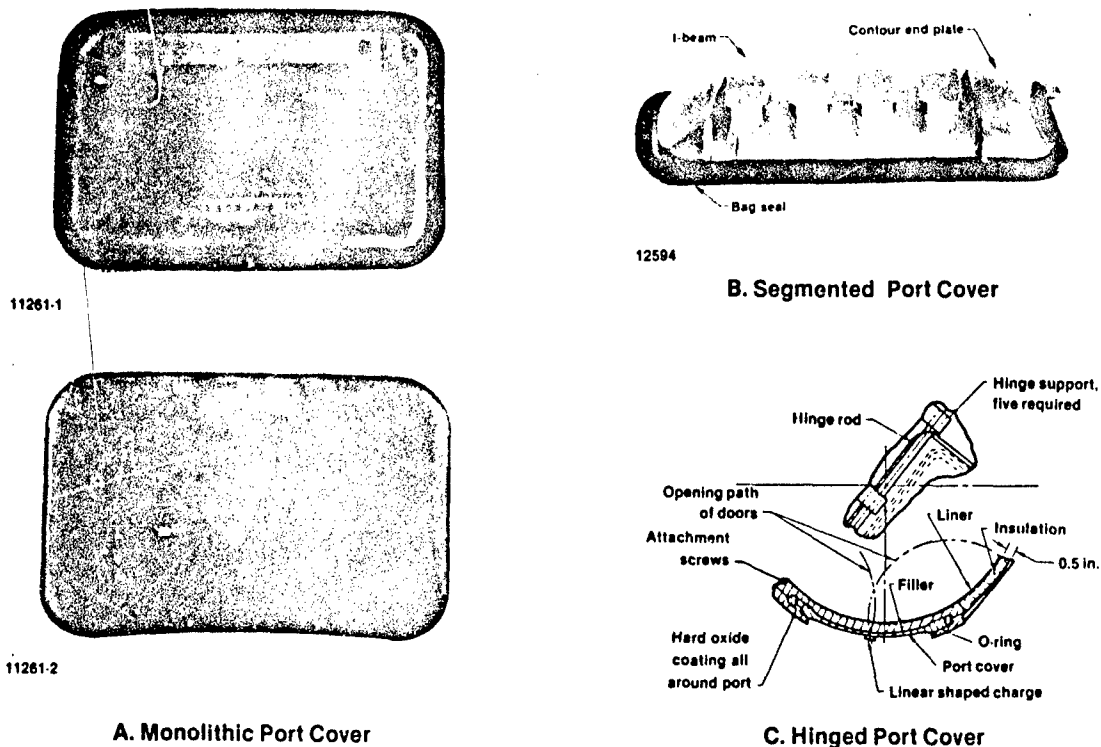
Figure 11. Port Cover Types

33061

Dual purpose combustion chamber — Booster grain

Ramjet fuel — Air — Nozzle clamp

Air

Inlet port cover —

Ramjet nozzle —

A. Boost

Dual purpose combustion chamber —

Inlet port cover —

Air

Air

Ramjet fuel — Ramjet nozzle — Booster nozzle

Nozzle clamp

Booster nozzle

B. Transition

Dual purpose combustion chamber —

Ramjet fuel — Air

Air

Ramjet nozzle —

C. Ramjet Operation
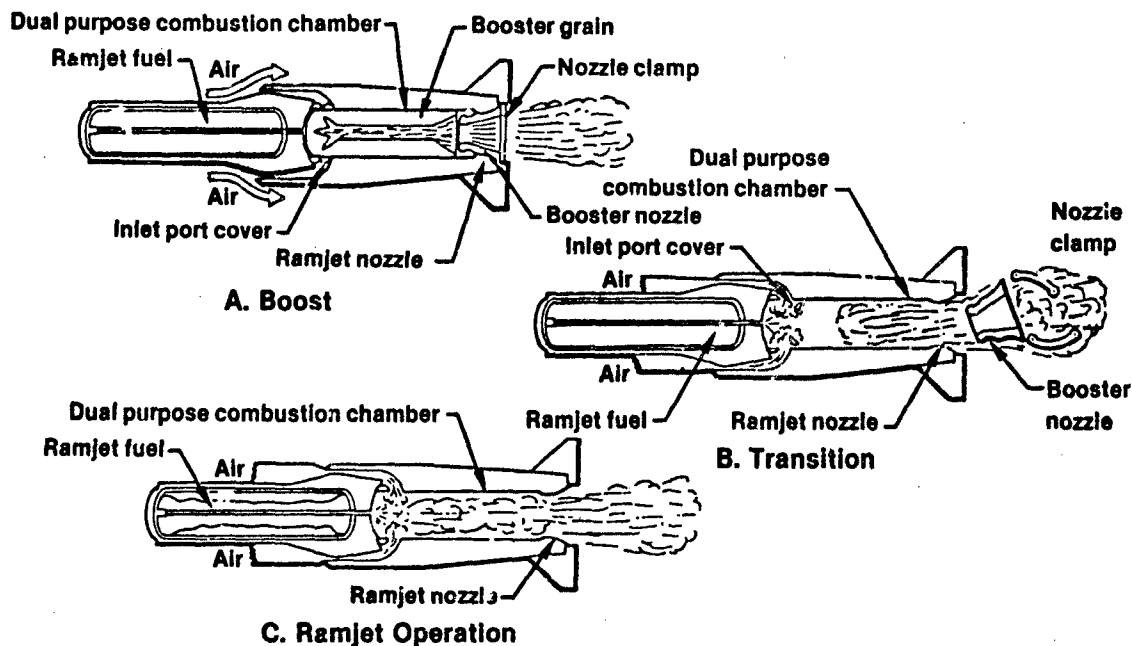
Figure 12. Integral Rocket Ramjet Combining Booster and Ramjet in One Combustor Chamber

33062

Booster grain web B.O.

P.C. sensor setting signals nozzle trigger mechanism

Trigger mechanism fires release device squib

Boost nozzle fully ejected
Port cover blows in

Port cover fully ejected

Steady state cold flow combustor pressure

t, 220

t,t 100 msec

Ramjet igniter on

$\leftarrow$ 150 msec. $\rightarrow$

Total fuel flow rate · 2.64 lb/sec

$W_T = W_{air} + W_{liner}$
$W_{liner} = 0.60$ lb/sec
$W_{air} = 60.7$ lb/sec

t, 530 msec

Ramjet igniter off

Nominal ramjet ignition transient

Chamber pressure, psia

ΔP due to combustion of residuals

Chamber pressure, psia

Time, msec.

Figure 13. Typical Transition Sequences for High Altitude Launch

V-28398

Segment (four each)

Explosive bolt assembly

Band assembly

Figure 14. Marman Type Booster Nozzle Retention System

33063

Booster nozzle

Metal insert

Detonator (alternate location)

Detonator (proposed location)

Snapring

Nozzle shell

Pyrocore ejection cord

Ramjet nozzle

Figure 15. Snapring Type Booster Nozzle Retention System

33064

LES STATOREACTEURS A COMBUSTIBLE LIQUIDE

par Ph. CAZIN
Coordinateur Missiles

Office National d'Etudes et de Recherches Aérospatiales (ONERA)

29 Avenue de la Division Leclerc
92320   Chatillon
FRANCE

RESUME

Les statoréacteurs à combustible liquide, utilisés pour propulser les missiles supersoniques, permettent de répondre à certaines spécifications opérationnelles, telles que la recherche de portées élevées, jointes à une grande flexibilité des trajectoires. Ces moteurs trouvent ainsi leur emploi dans un créneau particulier, qui se distingue de celui des statofusées ou des turboréacteurs supersoniques : leur domaine est celui des missions qui requièrent de fortes variations d'altitude ou de vitesse.

Les performances énergétiques élevées de ces machines sont obtenues au moyen de techniques ou de technologies spécifiques que l'on se propose d'examiner, à savoir :

* Les combustibles liquides : kérosène, combustibles liquides très denses, combustibles boueux, ...

* Systèmes d'alimentation : par pressurisation, par turbopompe. Avantages et inconvénients de chaque système. Conception des réservoirs.

* Régulation et injection : lois de régulation requises suivant les missions. Différents types d'injecteurs.

* Chambre de combustion : conception, dessin général, zones de recirculation, localisation de l'injection, protection thermique, contraintes dues à la présence d'un accélérateur intégré.

* La combustion : performances, rendements et instabilités. On étudie plus particulièrement les causes des instabilités de combustion, leurs conséquences et les remèdes envisageables pour y remédier.

* Les bancs d'essai des statoréacteurs à combustible liquide, avec leurs caractéristiques spécifiques.

En conclusion, un aperçu sur les possibilités de ces moteurs suivant les missions, sur les principales étapes d'un développement et sur l'avenir de ces techniques, est proposé.

SUMMARY

Liquid-fueled ramjets provide a means of satisfying certain performance requirements in supersonic missile propulsion, such as combining long range with a large flight path flexibility. These power plants thus have a particular application quite distinct from that of ramrockets or supersonic turbojets : missions requiring major altitude or velocity variations.

The high energy efficiency of these engines is obtained by specific techniques and technologies which we propose to investigate :

* Liquid fuels : kerosene, very dense liquid fuels, fuels in suspension, etc..

* Fueling system : Advantages and disadvantages of pressure vs. turbopump systems, tank design.

* Regulation and injection : Regulation laws required for different missions, various injector types.

* Combustion chamber : Design, general chape, recirculation zones, injector location, thermal insulation, stresses due to integrated booster.

* Combustion : Performance, efficiency and instability. In particular, we will go into the causes, consequences an possible remedies for combustion instabilities.

* Test stands : Specific characteristics of test stands for liquid-fueled ramjets.

NOMENCLATURE

A, Section

Indices : 0 infini amont
1 section de captation de la prise d'air
2 diffuseur prise d'air
2' chambre de combustion, avant front de flamme
3 chambre de combustion, après front de flamme
4 col de la tuyère
5 sortie tuyère
i conditions d'arrêt

D, diamètre missile (chambre de combustion)

1 - INTRODUCTION

Le moteur fusée à propergol solide a été et restera encore longtemps le principal moyen de propulsion des missiles tactiques : bien adapté aux courtes portées, il est capable de fortes accélérations et surtout il est relativement bon marché.

Mais il a aussi certains inconvénients : par exemple, pour augmenter sensiblement la portée d'un missile à moteur fusée, il faut, soit lui faire suivre une trajectoire balistique à haute altitude, avec les problèmes de guidage et de détection que cela suppose, soit, pour des trajectoires à basse altitude, augmenter fortement sa masse et son encombrement.

C'est pourquoi, pour les missiles lancés à une certaine distance de leur objectif, il faut se tourner vers d'autres systèmes de propulsion plus efficaces, c'est à dire plus économiques et capables de produire une poussée continue : c'est le domaine de la propulsion aérobie, avec le turboréacteur, le statofusée à combustible solide et le statoréacteur à combustible liquide. Après une rapide comparaison entre les possibilités de ces trois familles, qui ont chacune un domaine particulier auquel elles sont bien adaptées, on se propose d'examiner les techniques et les technologies requises pour la propulsion des missiles par statoréacteur à combustible liquide.

2 - LES DIFFERENTS CONCEPTS

Découvert en 1911 par le Français R. LORIN, le principe de la propulsion par statoréacteur est extrêmement simple : il consiste à tirer parti de la recompression réalisable en vol dans une prise d'air, pour obtenir, après combustion, une force de poussée résultant de l'évacuation du débit d'air capté, à une vitesse supérieure à celle du vol. Mais il a un inconvénient : n'étant pas autonome, le statoréacteur ne peut fonctionner qu'après une mise en vitesse par un propulseur auxiliaire ou "accélérateur".

2.1. - Rappel historique

Depuis la fin de la Deuxième Guerre Mondiale, jusqu'à 1965 environ, il y eut dans plusieurs pays un effort de recherche important qui aboutit à de nombreux essais en vol de missiles expérimentaux et à quelques développements opérationnels, principalement pour des missions surface-air ou sol-sol.

De cette époque très fertile, on peut citer tout d'abord les missiles opérationnels américains BOMARC et TALOS, britanniques BLOODHOUND et SEA DART et soviétique SA4. En France, malgré plus de 200 essais eu vol qui ont permis d'acquérir de solides connaissances techniques et technologiques, il n'y eut aucun développement opérationnel : c'est de cette époque que datent les missiles expérimentaux CT 41 et VEGA de Nord Aviation, R431 de MATRA-NORD- AVIATION, STATALTEX de l'ONERA, etc...

Tous ces missiles avaient des configurations voisines, à savoir
(Fig. 1) :

- prise d'air axisymétrique située à l'avant

- accélérateurs largables, montés en tandem ou latéralement

- chambre de combustion à accroche-flammes métalliques (gouttières, cônes percés de trous ...)

- combustible liquide kérosène.

Puis entre les années 1965 et 1970, se produisit une décroissance des recherches sur le statoréacteur classique, modérément supersonique, au profit du statoréacteur hypersonique à combustion supersonique (kérosène ou hydrogène). Les applications alors envisagées étaient : l'avion Mach 6/7, le lanceur atmosphérique récupérable, le missile tactique sol-air ou air-air à vitesse supérieure à Mach 6.
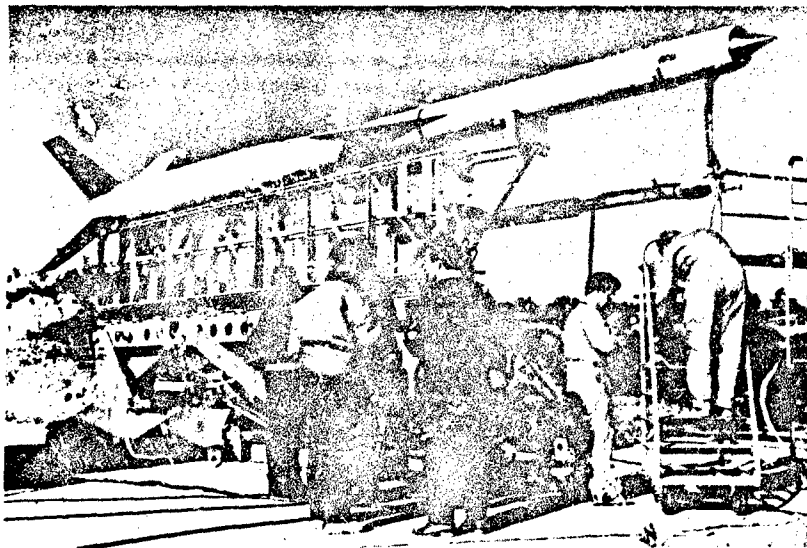
Fig. 1 : Configuration des années 1960/1970 : missile expérimental
français STATALTEX (ONERA)

2.2. - Tendances actuelles

Vers les années 1970, on a assisté, surtout aux Etats-Unis et en France, à l'apparition de nouvelles
configurations aérodynamiques et à la mise au point de technologies destinées à rendre le statoréacteur plus
attractif et plus compatible avec les exigences opérationnelles. De plus, c'est en 1973, lors de la guerre
du Kippour, que le missile SA.6 soviétique propulsé par statofusée à accélérateur intégré, a montré sur le
terrain, l'efficacité des formules nouvelles. Enfin les progrès effectués dans le domaine des équipements de
guidage, de pilotage et des calculateurs embarqués permettent maintenant d'envisager de façon plus réaliste
une extension sensible du domaine de vol des missiles (portée, vitesse, dénivelée, diversification des
trajectoires, manoeuvrabilité, ...).

C'est ainsi que, sous l'impulsion de ces nouvelles contraintes opérationnelles, sont apparus depuis
les années 70, les concepts suivants :

* __Configurations aérodynamiques à prises d'air latérales__ (et non plus frontales) afin de rendre le missile
  modulaire (structures simplifiées et maintenance facilitée) et dégager l'ogive (montage possible de tout
  type d'autodirecteur électromagnétique).

* __Statoréacteur avec accélérateur intégré__ : cette technologie permet de concevoir un missile beaucoup plus
  compact et surtout __monoétage__ et ainsi d'éliminer les problèmes de sécurité liés à la retombée d'un
  accélérateur d'appoint.

* __Chambre de combustion "tourbillonnaire"__ , c'est à dire dans laquelle la flamme n'est plus stabilisée par
  des accroche-flammes métalliques mais par des dispositifs purement aérodynamiques, laissant ainsi la
  liberté de remplir la chambre avec le propergol d'accélération.

* __Statofusée à combustible solide__ : dans ce concept, on a recherché à simplifier encore le système
  propulsif, de telle sorte que le stockage et la maintenance s'apparentent à ceux d'une munition ou d'un
  missile classique à propulseur fusée. Il en existe deux variantes principales :

  - la plus simple est le statofusée à générateur intégré ("Solid-fueled ramjet"), dans laquelle le
    combustible solide du statoréacteur est placé directement dans la chambre de combustion.

  - le statofusée à générateur séparé ("Ducted rocket") qui est plus ou moins simple selon la nature du
    combustible et l'existence ou non d'un système de modulation.

Ces nouvelles technologies ont rendu ce système propulsif très attractif, du point de vue militaire,
en supprimant ou en atténuant ses principaux inconvénients. C'est pourquoi de nombreux pays se sont lancés
dans cette voie depuis les années 1970 ; on peut ainsi citer, en se limitant aux missiles essayés en vol en
Occident :

- aux Etats Unis, des prototypes ou missiles expérimentaux : l'Advanced Strategic Air-Launched Missile
  (ASALM), l'Advanced Low Volume Ramjet (ALVRJ).

- en France, l'activité est très importante puisqu'elle concerne, non seulement des missiles expérimentaux,
  tels que le statofusée à générateur séparé ("Ducted rocket") essayé en vol en 1976/77 et le statofusée
  "rustique" à générateur intégré ("Solid fueled ramjet") essayé en vol en 1983/84, mais surtout l'ASMP
  (Air-Sol Moyenne Portée) qui sera bientôt le premier missile __operationnel__ de ce type dans le monde
  occidental (Fig. 2) ; il utilise un statoréacteur à combustible liquide.

- enfin la France et l'Allemagne préparent le missile ANS (Anti-Navires Supersonique) destiné à succéder
  à la famille EXOCET. Deux systèmes propulsifs sont en compétition : un statoréacteur à combustible
  liquide (Aérospatiale/ONERA) et un statofusée à combustible solide dopé au bore (MBB), dont un modèle à

Fig. 2 : Configuration récente : missile
français Air-Sol (Aérospatiale)

Il faut noter que l'intérêt marqué des Européens, en particulier de la France, pour ces formules nouvelles, s'explique, notamment pour les missions air-surface, par les faibles dimensions des avions Européens : lorsque l'on compare les possibilités d'emport d'un B1 ou d'un F15, à celles d'un Mirage IV ou d'un Super-Etendard, il est bien évident que les exigences d'amélioration de la compacité du missile sont plus élevées en France qu'aux Etats-Unis !

2.3. - Possibilités des statoréacteurs à combustible liquide, par rapport à celles des statofusées et des turboréacteurs supersoniques

Chaque type de moteur a des avantages et des inconvénients selon l'emploi opérationnel auquel il est destiné. Ainsi, pour mieux cerner les possibilités du statoréacteur à combustible liquide il faut le comparer aux moteurs qui sont les plus proches, le statofusée à générateur séparé et le turboréacteur supersonique. En effet, le statofusée à générateur intégré ("Solid fueled ramjet"), plus spécifique des petits missiles ou des courtes portées, entre beaucoup moins en concurrence avec le statoréacteur à combustible liquide.

2.3.1. Statoréacteur et statofusée à générateur séparé

Les domaines d'emploi, à savoir les trajectoires de moyenne portée, sont assez proches : c'est pourquoi les industriels européens envisagent les deux formules pour propulser le futur missile ANS.

Le tableau ci-dessous montre les possibilités de ces moteurs :

	AVANTAGES	INCONVENIENTS
Missile à stato-réacteur à combustible liquide	* Taux de modulation élevé , donc fortes variations d'altitude ou de vitesse * Régulation précise et souple (manoeuvres rapides) * Performances massiques élevées	* Complexité (stockage et alimentation du combustible) * Coût plus élevé
Missile à stato-fusée à générateur séparé	* Simplicité (surtout si absence de modulation) * stockage aisé * compacité éventuelle-ment plus élevée	* Performances moins élevées (surtout à cause du taux de modu-lation limité)

Pour illustrer la proximité des domaines d'emploi, la figure 3 compare l'encombrement et la masse de quatre missiles supersoniques air-surface (portée à basse altitude : 100 km) :

* deux sont propulsés par statoréacteur à combustible liquide (kérosène de densité 0,8 et combustible liquide de densité 1,0).

* deux sont propulsés par des statofusées à combustible solide discret (densité 1,2) et à combustible solide dopé au bore (densité 1,7).
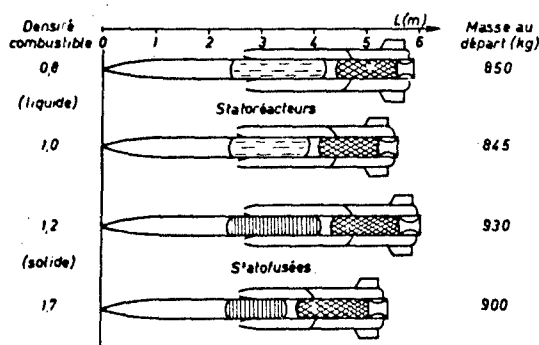
Fiç. 3 : Comparaison statoréacteur/statofusée. Mission : Air-Surface-Mach 2 - Z = 0 - D = 0,35 m

Bien que les écarts de masse et de longueur soient relativement modérés, on constate l'intérêt des combustibles denses pour la compacité du missile.

Mais, une comparaison plus précise entre ces deux formules doit tenir compte d'autres critères complémentaires tels que :

- diversification des trajectoires,

- discrétion optique du jet,

- coût du développement et coût du missile en série,

- possibilités industrielles,

- etc...

Elle dépend donc fortement de la mission envisagée.

2.3.2. Statoréacteur et turboréacteur supersonique

Les domaines d'emploi ne sont pas aussi proches. Mais puisque, pour les missiles tactiques subsoniques de type air-mer ou mer-mer, on trouve une cohabitation entre des moteurs très différents, à savoir la fusée à propergol solide (EXOCET, KORMORAN, GABRIEL, ...) et le turboréacteur (HARPOON, OTOMAT, SEA EAGLE, ...), on peut penser qu'elle puisse se poursuivre en supersonique, en particulier pour des raisons industrielles.

C'est pourquoi, le tableau suivant montre les principales possibilités de ces deux moteurs :

	AVANTAGES	INCONVENIENTS
Missile à statoréacteur à combustible liquide	* plus rapide * plus manoeuvrant * dénivelées plus élevées	* plus lourd et plus encombrant pour les portées supérieures à 150 km (vol à basse altitude)
Missile à turbo-réacteur supersonique	* faible consommation * éventuellement monomoteur pour missions depuis avion	* complexité du système propulsif * coût élevé * domaine moins étendu en : - vitesse maximale - altitude - dénivelée - manoeuvrabilité

La figure 4 qui présente, suivant le moteur adopté, la poussée et la trainée du missile en fonction de la vitesse de vol, éclaire le domaine d'emploi :

- le statoréacteur est apte aux grandes vitesses (plus de Mach 2) et aux trajectoires diversifiées.

- le turboréacteur supersonique basse altitude restera limité à des vitesses sensiblement inférieures à Mach 2 (Mach 1,6 ?). Il prendra son essor d'autant mieux que les portées augmenteront et qu'il sera capable de voler en sub-, trans- et supersonique.
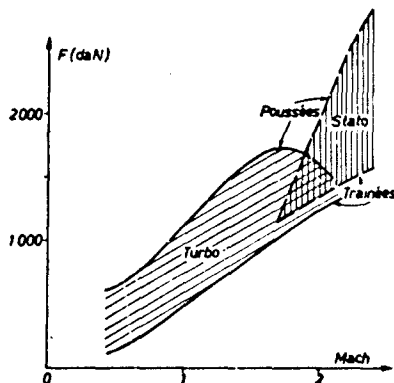
Fig. 4 : Poussée et Trainée de missiles à turboréacteur et à statoréacteur (Z = 0)

2.4. Domaine d'emploi du statoréacteur à combustible liquide

En résumé, pour la propulsion des missiles, le statoréacteur est particulièrement bien adapté aux missions à moyenne portée (jusqu'à 150 kilomètres à basse altitude et plusieurs centaines de kilomètres à haute altitude), à vitesse hautement supersonique ,avec de fortes variations d'altitude et de vitesse .

Dans ce document, on s'intéresse exclusivement au statoréacteur à combustion subsonique qui est capable de fonctionner depuis Mach 1,5 (*) jusqu'à Mach 6, mais qui est surtout utilisé opérationnellement dans le domaine de Mach 2 à Mach 4 : en effet, comme le montre la figure 5, il est possible d'obtenir dans cette zone des performances quasi-optimales, en simplifiant le moteur par utilisation d'une géométrie fixe (référence 1). Dans cet exemple où le Mach de vol d'adaptation est égal à 3,2, la perte d'impulsion spécifique du moteur à géométrie fixe n'est que 10% à Mach 4, mais elle dépasse 20% à Mach 5.
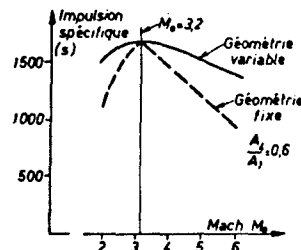
Fig. 5 : Performances optimales d'un statoréacteur au kérosène. (richesse : 1, A_5/A_1 = 3)

Pour utiliser un tel moteur, il faut maîtriser des techniques ou technologies particulières, examinées ci-après, à savoir :

- la mise au point d'une famille de combustibles liquides

- les réservoirs, et les systèmes d'alimentation, de régulation et d'injection

- les chambres de combustion

3 - LES COMBUSTIBLES LIQUIDES

Les missions qui font appel à un combustible liquide sont caractérisées :

- soit par une longue portée, le combustible liquide permettant une meilleure impulsion spécifique que celle des combustibles solides (car ces derniers contiennent généralement des produits oxydants).

- soit par un domaine de vol étendu (en particulier en altitude), le combustible liquide étant plus apte que les combustibles solides à de fortes variations de débit .

Le combustible liquide le plus utilisé est bien entendu le kérosène −de type aviation− en raison de son faible coût et de son approvisionnement aisé.

_____

(*) Note : En fait, le statoréacteur peut délivrer une poussée substantielle à des vitesses nettement

Mais pour l'utilisation sur missile, le problème du coût est beaucoup moins aigu que pour les applications aux avions ou hélicoptères, puisque le moteur ne sert qu'une fois. A titre indicatif, le prix d'un kilogramme de propergol classique est fréquemment plus de 100 fois plus élevé que celui d'un litre de kérosène !

C'est pourquoi, dans plusieurs pays, des recherches ont été menées dans le but de développer des combustibles liquides plus efficaces que le kérosène, c'est à dire ayant les caractéristiques suivantes :

a) Si possible, pouvoir calorifique massique égal ou supérieur à celui du kérosène

b) Essentiellement, masse volumique nettement supérieure

Certains de ces combustibles peuvent être utilisés aussi bien sur turboréacteurs que sur statoréacteurs. Mais l'emploi sur missile répond à des critères de choix très spécifiques.

3.1. Critères de choix

Selon la mission, on choisira un combustible qui réponde en priorité à tel ou tel critère. Parmi ceux-ci, on peut citer :

* Performances énergétiques : recherche de combustibles à haut pouvoir calorifique massique (ou à forte impulsion spécifique), c'est à dire un pouvoir calorifique inférieur, au moins égal à 10 000 K Cal/kg (soit 18 000 BTU/lb)

* Masse volumique et impulsion volumique . Pour augmenter la compacité d'un missile, ou à volume donné pour améliorer sa portée, on recherche une augmentation de l'impulsion volumique : le procédé le plus efficace est généralement un accroissement de la masse volumique. Des combustibles liquides de masse volumique comprise entre 1 000 et 1 100 kg/m3 ont ainsi déjà été mis au point en vue d'une utilisation sur missile tactique.

* Fonctionnement à haute altitude : certains combustibles boueux, tels ceux qui contiennent des particules de bore, brûlent plus difficilement à basse pression. Ils peuvent donc ne pas être retenus pour des missions à haute altitude.

* Dilatation : la masse volumique varie avec la température. Ainsi sur un missile devant fonctionner à des températures extrêmes, un kérosène classique se dilatera en volume d'environ 7 à 8% pour un écart de 100 degrés centigrades : le réservoir devra donc être conçu pour permettre cette libre dilatation.

* Viscosité : la recherche de combustibles de plus en plus denses s'accompagne généralement d'une augmentation de la viscosité, en particulier aux basses températures. C'est ce phénomène qui limite l'utilisation de combustibles très denses sur missiles tactiques, en particulier pour les versions air-sol ou air-surface non stockées en soute, en raison des conséquences pratiques sur les systèmes de chasse ou les pompes.

A titre indicatif, des viscosités supérieures à 150 centistokes posent des problèmes ou nécessitent une technologie adaptée.

Mais certains combustibles boueux peuvent être utilisés malgré une viscosité statique beaucoup plus forte, car dotés de propriétés thixotropiques : au repos, ces boues possèdent une viscosité élevée qui chute considérablement dès qu'elles sont soumises à une force de cisaillement, c'est à dire au moindre mouvement.

* Point d'éclair : pour faciliter l'allumage et la combustion, en particulier lorsque le combustible est porté à très basse température (missile en charge externe d'un avion effectuant un vol prolongé à haute altitude), le choix se portera plutôt vers un combustible ayant un point d'éclair à basse température.

Mais parfois ce choix ne peut être fait pour des raisons de sécurité, par exemple pour limiter les risques d'incendie à bord des navires (référence 2). Une telle contrainte peut obliger à choisir un point d'éclair supérieur à 60°C.

* Point de congélation : il est bien évident que celui-ci doit être inférieur aux températures les plus basses rencontrées au cours du stockage ou de l'emport.

* Discrétion : certaines missions opérationnelles nécessitent l'utilisation de combustibles assurant une bonne discrétion du jet propulsif, soit dans le domaine électromagnétique, soit surtout dans le domaine optique (visible et infra-rouge). Une telle contrainte peut conduire à préférer des combustibles ne contenant que des hydrocarbures (uniquement carbone et hydrogène), plutôt que certains métaux (aluminium, magnésium) ou métalloïdes (bore).

* Stockabilité : les combustibles pour missiles tactiques doivent être aptes à un stockage de longue durée à l'intérieur du réservoir. Or, il ne s'agit jamais d'un produit chimique simple : par exemple, le kérosène, pourtant très courant, est un dérivé du pétrole dont la composition chimique est très variable suivant les différents traitements effectués en raffinerie et la provenance du brut. C'est pourquoi certaines normes ont été établies pour les carburants à stockage de longue durée.

Les principaux problèmes rencontrés sont les suivants :

- oxydation en présence d'air dissout, ce qui peut avoir une action corrosive ou favoriser l'apparition de gommes. Il en résulte certaines précautions à prendre au remplissage du réservoir et l'adjonction

- corrosion de certains matériaux plastiques ou de joints d'étanchéité, ce qui conditionne la conception du réservoir. Par ailleurs, il existe des additifs qui limitent les risques de corrosion.

- présence de micro-organismes (bactéries, champignons, moisissures, levures) qui peuvent se développer au contact du combustible. Ils peuvent alors former des boues et des amas de filaments qui risquent d'obstruer différents organes. La présence d'eau dans le combustible en favorise la prolifération.

* Décantation : certains combustibles de haute densité sont préparés à partir d'une suspension de particules solides lourdes pulvérisées dans un support organique liquide ; la stabilité de la suspension étant alors assurée par la gélification du support de façon à bloquer le mouvement des particules. Il faut donc s'assurer qu'après un stockage prolongé il n'y ait pas de risque de décantation des particules solides susceptibles de modifier les caractéristiques du combustible au niveau des injecteurs.

* Autres propriétés : cette liste n'est pas exhaustive : suivant les applications, d'autres propriétés spécifiques peuvent être souhaitées. A noter en particulier :

  - la présence d'additifs anti-glace pour éviter la formation de cristaux pouvant obstruer les filtres ou les canalisations

  - l'adjonction de dissipateurs d'électricité statique pour rendre le combustible plus conducteur

  - les contraintes de coût du combustible qui n'influent pas uniquement sur le coût du missile de série mais aussi sur le coût du développement en raison du grand nombre d'essais effectués (voir paragraphe 6)

  - l'absence de toxicité, non seulement du combustible, mais des produits de sa combustion avec l'air. Cette contrainte est imposée aussi par le développement du missile plutôt que par son utilisation opérationnelle.

3.2. Principaux combustibles liquides

De nombreuses recherches sont effectuées dans plusieurs pays, en particulier aux Etats-Unis (référence 2), afin de mettre au point des combustibles liquides, soit plus énergétiques que le kérosène, soit surtout beaucoup plus denses.

Ainsi trois principales familles sont apparues :

a) carburants à base d'hydrocarbures provenant du pétrole ou de la houille : kérosènes TRO, JP4, JP5, décaline, tétraline, ...

b) carburants à base de produits chimiques de synthèse : RJ4, RJ5, JP9, JP10... Pour de tels produits, la proportion d'atomes de carbone par rapport aux atomes d'hydrogène est plus élevée, de façon à augmenter l'impulsion volumique.

c) combustibles gélifiés injectables ou "boueux" : il s'agit de liquides, tels les précédents, dans lesquels on ajoute une forte proportion de particules solides très fines en suspension ; par exemple : carbone ou hydrocarbure aromatique, bore, aluminium, magnésium (le béryllium étant éliminé car toxique et coûteux).

Comme l'indique le tableau I, le bore est intéressant par son fort pouvoir calorifique volumique, alors que l'Aluminium et le Magnésium permettent plutôt d'augmenter la poussée spécifique (référence 1 et 3).

Elément	Point de fusion °C	Point ébullit. °C	Densité	Pouvoir calorifique KCal/kg	KCal/Dm3	KCal/kg air	Rapport de mélange (avec air)
Aluminium	660	2465	2,70	7 350	19 845	1940	0,264
Beryllium	1280	2970	1,85	15 900	29 410	2100	0,132
Bore	2300	2530	2,34	13 800	32 300	1450	0,105
Carbone	3650	4200	2,25	7 830	17 620	630	0,080
Magnésium	648	1104	1,74	5 910	10 270	2080	0,352

TABLEAU I : Additifs pour combustibles liquides boueux

Du point de vue énergétique, il y a intérêt à ajouter le plus possible de particules solides dans le liquide. Mais pratiquement, cette tendance est freinée par :

- le souci de conserver un produit fluide et injectable

- la capacité des particules solides à brûler dans la chambre de combustion (en particulier, pour celles de bore, il faut qu'elles rencontrent suffisamment de zones chaudes issues de la combustion du support liquide)

A titre d'exemple, le tableau II donne les caractéristiques de quelques combustibles liquides. Sans être exhaustif, car certaines données ne sont pas accessibles dans la littérature, il illustre la recherche de combustibles à fort pouvoir calorifique volumique. On peut constater en particulier que :

- l'augmentation du pouvoir calorifique volumique est souvent liée à une proportion élevée d'atomes de carbone

- pour les applications aéroportées, on privilégie un bas point de congélation

- pour les applications sur navire, ce sont plutôt les problèmes de sécurité incendie qui guident le choix (point d'éclair élevé)

- certains combustibles "boueux" permettent d'obtenir des pouvoirs calorifiques très élevés. Deux exemples de ces produits, objets de recherches en France sont indiqués. Dotés de fortes propriétés thixotropiques, ils ont une faible variation du comportement à l'injection, dans un grand intervalle de température.

	Hydrocarbures			Corps de Synthèse			Combustibles boueux	
	TRO (ou JP1)	JP5	Tétraline +5%hexane	RJ4	JP9	CSD 15T	AK 70-30	BK 55-45
Formulation	$C_{10}H_{20}$	$C_{11}H_{19}$	$C_{98}H_{141}$	$C_{12}H_{20}$	$C_{10,6}H_{16,2}$	$C_{14}H_{18}$	Anthracène $(C_{14}H_{10})$ + kérosène	Bore+kérosène
Pouvoir calorifique inférieur volumique (KCal/dm3)	8180	8324	9247	9323	9456	10400	10300	12000
Densité à 15°C	0,79	0,83	0,95	0,94	0,94	1,04	1,06	1,25
Viscosité cinématique à - 40°C (Cst)	9	17	11	60	24	105	Produits thixotropiques	
Point de congélation (°C)	-53°	<-46°	-40°	<-40°	<-54°	<-60°	<-40°	<-40°
Point d'éclair (°C)	>38°	65°	10°	65°	24	36°	-	-
Applications et Observations	Air Force - avions -missiles carburant classique	Navy Avions et missiles carburant classique	Non opérationnel	Navy - Talos - SLCM Tomahawk - GORJE	Air Force ALCM	* Non opérationnels * essayés en France sur turboréacteur et statoréacteur	* fait l'objet de recherches en France	

TABLEAU II : Combustibles liquides à fort pouvoir calorifique volumique

4 - ALIMENTATION, REGULATION ET INJECTION DU COMBUSTIBLE

L'utilisation de combustible liquide sur missile conduit à des technologies particulières, en raison de contraintes opérationnelles spécifiques, telles que :

- Stockage de très longue durée (≫ 10 ans), avec cycles thermiques, sans modification de l'état du combustible et de l'étanchéité du réservoir.

- Expulsion du combustible assurée dans toutes les conditions de facteur de charge (jusqu'à 10 ou 20 g en transversal), en évitant le ballottement du liquide ; en effet, il ne faut pas secouer les équipements embarqués, ni surtout désamorcer les pompes ou les vannes , avec le risque d'extinction du statoréacteur qui s'en suivrait. C'est pourquoi il est préférable de recourir à un dispositif "actif" d'expulsion du combustible (piston ou vessie pressurisée).

- Système de régulation capable d'assurer une grande plage de variation de débit À titre indicatif, un missile devant évoluer dans une gamme étendue d'altitude, avec des trajectoires diversifiées, aura pratiquement besoin d'une régulation de débit dans un rapport de 1 à 15 ou 1 à 20 pour couvrir l'ensemble du domaine de vol.

Par ailleurs, d'autres contraintes plus générales sont à prendre en compte :

- recherche d'une grande compacité , ce qui conduit à optimiser le système de chasse du combustible et la conception du réservoir,

- recherche d'une réduction de la vulnérabilité du missile à des impacts de balles ou d'éclats, ce qui peut conduire à un fractionnement du réservoir,

- etc...

4.1. Systèmes d'alimentation

Il existe de nombreuses techniques pour expulser le combustible du réservoir et alimenter le moteur. Si l'on se limite à celles développées ces dernières années, on peut dire qu'elles se groupent en deux familles :

* les systèmes de chasse à partir d'un gaz sous pression

* les systèmes à turbo-pompe.

Ces deux techniques ont été développées avec succès : schématiquement, la première est particulièrement bien adaptée aux problèmes de stockage de longue durée, tandis que la seconde est préférable pour les vols de longue portée.

4.1.1. Chasse par gaz sous pression

Les missiles les plus anciens, ou certains prototypes ont utilisé un réservoir d'air ou d'azote comprimé sous plusieurs centaines de bar. Ce gaz, après passage dans un détendeur était envoyé dans un réservoir à piston ou à vessie.

Mais cette technologie est mal adaptée aux conditions opérationnelles des longs vols à basse altitude : dès que la portée s'accroît, la masse et l'encombrement deviennent prohibitifs. C'est pourquoi on utilise maintenant un gaz fourni par un générateur pyrotechnique, soit à propergol solide, soit à ergols liquides. Dans les deux cas, les gaz produits doivent être suffisamment froids pour ne pas dégrader les matériaux du piston ou de la vessie.

La figure 6 illustre une telle technique : les gaz "froids" délivrés par le générateur poussent un piston qui chasse le combustible vers les injecteurs. Cette configuration est bien adaptée au stockage de longue durée, car le combustible peut être totalement isolé et sans contact avec des matériaux organiques ou plastiques, une membrane métallique claquable scellant complètement le réservoir. Il faut, bien sûr, prévoir à l'arrière du réservoir une enceinte d'expansion pour assurer la libre dilatation du combustible. Cette formule supprime totalement les risques de ballottement ; mais elle est incompatible avec l'utilisation de réservoirs multiples ou de forme irrégulière.
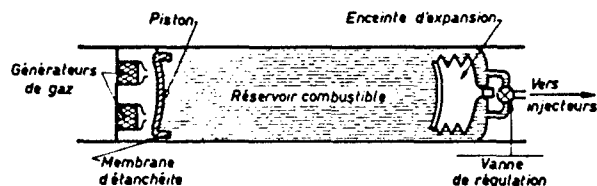
Fig. 6 : Alimentation par générateur de gaz et piston

L'utilisation d'un générateur de gaz présente des avantages opérationnels, mais elle conduit aussi à certaines contraintes pour la régulation du débit. En effet, ce dernier est fonction de l'écart entre la pression dans le réservoir et celle qui règne dans la chambre de combustion. Il existe donc :

- une pression minimale dans le réservoir, suffisante pour une injection correcte lorsque la pression dans la chambre est élevée (par exemple vol à grande vitesse à basse altitude)

- une pression maximale afin de limiter les contraintes, ou les déformations, dans la structure du réservoir.

C'est pourquoi, dans le cas de missions de longue durée, comportant de grandes variations d'altitude ou de vitesse, c'est à dire de grandes variations de débit de combustible, un tel système suppose :

* un fractionnement en plusieurs générateurs de gaz fonctionnant successivement (limitation de la pression maximale)

* l'utilisation d'injecteurs à section variable (voir paragraphe 4.3.1.)

4.1.2. Systèmes à turbo-pompe

Le transfert du combustible du réservoir vers les injecteurs peut être assuré par une turbo-pompe. Celle-ci aspire le combustible et fournit la pression nécessaire à une bonne injection. La turbine qui entraîne la pompe est alimentée par un prélèvement d'air dans la manche (de l'ordre de 1% du débit d'air qui traverse le moteur), son échappement s'effectuant à la pression atmosphérique. On arrive ainsi à un système beaucoup plus léger que dans le cas où la pompe serait entraînée par un moteur électrique alimenté par des batteries.

Dans cette formule, le combustible est généralement stocké à l'intérieur d'une vessie souple ; celle-ci est pressurisée à la pression de l'air entrant dans la chambre (fig. 7), cette pressurisation permettant de "gaver" la turbo-pompe et ainsi d'éviter les risques de cavitation.

Une telle configuration est bien adaptée aux missions de longue durée, ou à l'utilisation de

* la mise au point de la turbo-pompe qui doit, après des années de stockage, faire preuve d'une grande fiabilité dans des conditions opérationnelles d'emploi très variables, par exemple en température.

* la conception du réservoir et le choix des matériaux permettant un stockage de longue durée. En particulier, le matériau de la vessie doit :

    - assurer une étanchéité parfaite au stockage

    - ne pas se dégrader au contact du combustible

    - être apte à une pressurisation par de l'air chaud prélevé en amont des injecteurs (température pouvant être supérieure à 400°C suivant la vitesse de vol)

Fig. 7 : Alimentation par turbo-pompe et vessie souple
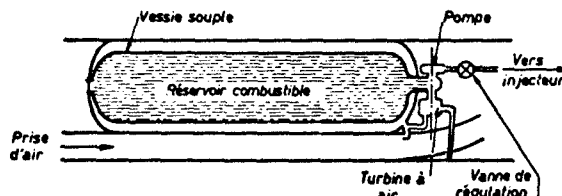
    - avoir une bonne tenue mécanique pour résister aux efforts dus aux facteurs de charge et néanmoins être suffisamment souple pour expulser presque tout le combustible (par exemple rendement d'expulsion supérieur à 96%).

    C'est pourquoi des vessies métalliques sont parfois utilisées.

4.2. Principe de la régulation

    Le système de régulation doit fournir à chaque instant le débit de combustible nécessaire au programme de vol (réf. 4). Il doit donc, dans tout le domaine (caractérisé par la variation du nombre de Mach, de l'altitude, de l'incidence, de la température de l'atmosphère, ...) :

* assurer un fonctionnement correct du moteur ; pour cela le débit de combustible doit toujours être compris entre deux valeurs limites :

    - une valeur maximale correspondant à la poussée maximale compatible avec la limite d'extinction riche et le fonctionnement stable des entrées d'air,

    - une valeur minimale correspondant à la poussée minimale compatible avec la limite d'extinction pauvre.

* permettre de régler la vitesse du missile aux valeurs demandées par le programme de vol, en fonction du temps, de l'altitude, ...

    Une chaîne de régulation comprend donc une vanne de réglage du débit, un ensemble de capteurs, un calculateur et un système d'asservissement (figure 8).

    La position de la vanne de régulation est asservie de façon à ce que la valeur d'un paramètre caractéristique de la poussée, calculée à partir de mesures faites sur le statoréacteur en fonctionnement, soit égale à la valeur de commande.

    Il faut noter que la régulation d'un combustible liquide peut se faire avec un temps de réponse beaucoup plus bref que celui d'un combustible gazeux (pour un statofusée avec générateur de gaz séparé, il faut en effet tenir compte de la réponse du propergol et du volume du générateur) et donc peut être utilisée même au cours de manoeuvres très rapides (mises en incidence brutale, par exemple). Le moteur peut alors fonctionner avec une marge supercritique plus réduite et donc des performances optimales.
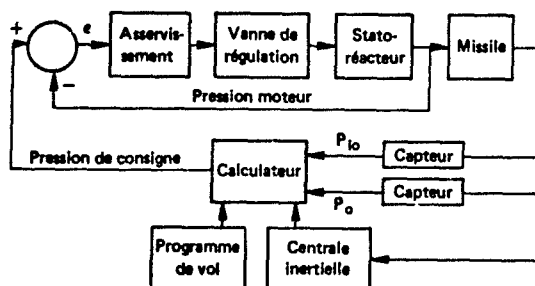
Fig. 8 : Schéma d'une chaîne de régulation

4.3. Injection

4.3.1. Technologie des injecteurs

Celle-ci est fonction de la mission du missile et de son domaine de vol. Par exemple, pour un missile air-sol capable de voler à très haute et très basse altitude, ou d'un missile mer-mer avec croisière à moyenne altitude, et accélération au niveau de la mer pour des évasives finales, le débit de combustible nécessaire peut varier au moins dans un rapport 1 à 15 .

Dans ce cas, la différence de pression à travers un injecteur à section d'injection fixe devra varier dans un rapport 1 à 225 (*). Or, pour bien pulvériser un combustible liquide, surtout s'il est un peu visqueux (pour mémoire certains combustibles denses sont visqueux à froid), il faut une différence de pression minimale à travers l'injecteur. Supposons que celle-ci soit de 1 bar à haute altitude, cette différence de pression devrait varier alors de 1 à 225 bars, ce qui correspond à basse altitude à une pression d'injection trop élevée, de l'ordre de 235 bars.

C'est pourquoi, pour de telles missions, on utilise :

- soit plusieurs circuits équipés d'injecteurs à section constante, coupés successivement lorsque le débit diminue (figure 9).

- soit un seul circuit équipé d'injecteurs à section, ou à coefficient de débit, variable permettant d'exploiter au mieux les possibilités du système d'alimentation.

Les technologies mises en oeuvre sont très diverses : injecteurs à boisseau tournant, à boisseau coulissant, à membrane, ...(figure 10).

En dehors des problèmes classiques, de mécanique, de lubrification et d'usinage, la mise au point de tels injecteurs consiste à vérifier que l'homogénéité du panache et la qualité de la pulvérisation se conservent malgré la variation :

- de la section d'injection
- de la pression d'injection
- de la pression du courant d'air.

1 et 2 Vannes de laminage à positionnement proportionnel
3 Electrovanne de barrage
Circuits 1 et 2 : basse à moyenne altitude
Circuits 1 vanne 3 fermée : moyenne à haute altitude
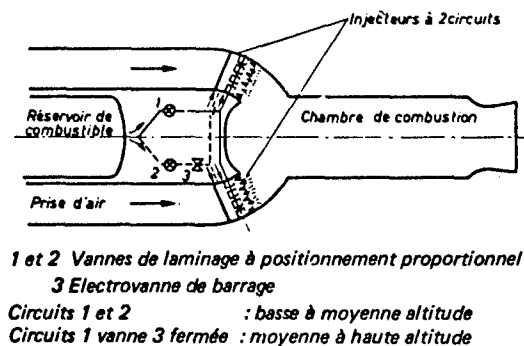
Fig. 9 : Injection à circuits séparés

1) à boisseau tournant
2) à clapet mobile
3) à fente déformable
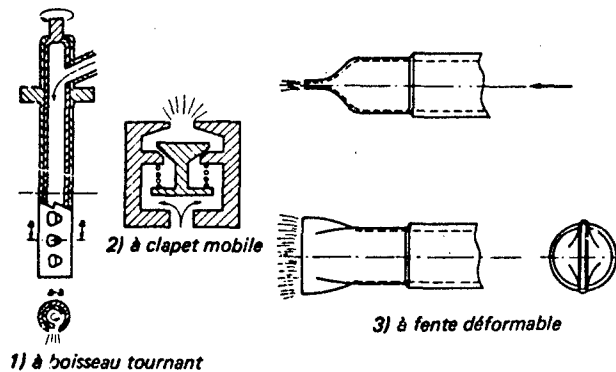
Fig. 10 : Injecteurs à section variable

(*) Rappel : $q = C_D S_c \sqrt{2 \rho \Delta p}$

q : débit massique
C_D : coefficient de débit caractérisant la géométrie de l'injecteur
S_c : section d'injection
ρ : masse volumique du combustible
Δp : différence de pression à travers l'injecteur

4.3.2. Localisation de l'injection

La localisation précise de chaque injecteur est un problème difficile et qui reste probablement pour de nombreuses années, essentiellement empirique . C'est pourquoi la mise au point complète d'un moteur nécessite plusieurs années d'essais au banc, surtout si le domaine de vol est étendu. En effet, le nombre de paramètres de réglage est élevé :

- type d'injecteurs
- nombre et position
- orientation du jet de combustible : dans le sens du courant, à contre-courant, etc...

Pour chaque configuration d'injection, il faut optimiser, dans toutes les conditions du vol (Mach, altitude, incidence/dérapage, ...) :

- le rendement de combustion
- les limites d'extinction riche et pauvre
- les pertes de charge internes
- les instabilités de combustion

5 - CHAMBRES DE COMBUSTION

La chambre de combustion d'un statoréacteur est un des éléments du missile dont le développement est le plus long. En effet, elle doit assurer un grand nombre de fonctions, principalement sur les versions modernes où l'accélérateur est intégré. Ces fonctions sont les suivantes :

* assurer une combustion avec un bon rendement, tout en minimisant la trainée aérod·iamique du missile : ceci conduit à une réduction des sections frontales, donc à des ·itesses internes très élevées (fréquemment 100 à 150 mètres/sec dans les entrées d'air et 300 mètres/sec. dans la chambre). C'est pourquoi la flamme doit être stabilisée par des moyens particuliers, mécaniques ou aérodynamiques.

* contenir le propergol de l'accélérateur intégré et par conséquent les contraintes qui résultent de son fonctionnement : trappes assurant l'étanchéité à l'amont en phase accélérée, tuyère maintenant la pression de l'accélérateur (70 à 140 bars) puis s'éjectant en fin de séquence.

* contribuer à l'endurance du moteur, surtout pour les vols de longue durée avec des conditions de température et de pression interne très variables.

Il faut noter que ces fonctions ainsi que les contraintes qui en résultent, sont pratiquement indépendantes de la nature physique du combustible, qu'il soit liquide ou gazeux (statofusée).

5.1. Conception

La conception d'une chambre de combustion dépend de la configuration aérodynamique du missile et de la mission qui lui est assignée. D'une façon générale, on peut distinguer :

5.1.1. Les configurations avec accélérateur séparé , celui-ci pouvant être monté en tandem, latéralement ou coulissant dans la chambre de combustion. Dans ce cas, la chambre n'a pas à subir les contraintes d'un accélérateur intégré :

- elle peut contenir des accroche-flammes métalliques pour faciliter la combustion

- elle fonctionne à basse pression (inférieure de 10 bars environ) et ne comporte pas d'obturateurs éjectables

- sa structure peut être optimisée par les conditions d'endurance en vol de croisière, avec un choix beaucoup plus large de technologies. Par exemple, on peut envisager des solutions où les parois sont refroidies par film d'air prélevé à l'amont, comme pour les post-combustions des turboréacteurs

- la séquence d'allumage du statoréacteur n'est pas critique, puisque celui-ci peut être allumé y compris pendant le fonctionnement de l'accélérateur

- la longueur de la chambre est déterminée par l'obtention d'un bon rendement de combustion. Elle peut être plus courte que pour les versions à accélérateur intégré (soit 1 mètre au maximum).

Exemple de calcul de la longueur minimale d'une chambre de combustion (figure 11) :

Considérons un mélange précarburé pénétrant dans une chambre de combustion. La longueur minimale de la chambre est celle à partir de laquelle la combustion peut être considérée comme complète, avant que l'écoulement ne pénètre dans la tuyère d'éjection.

A partir du point B, zone où la flamme s'accroche, se détache un front de flamme BA à la traversée duquel la combustion se produit ; si elle était instantanée, il est clair que la combustion serait complète à partir de A, point où se rencontrent les fronts de flamme. Mais en réalité, il faut tenir compte d'une distance supplémentaire qui est fonction d'un temps caractérisant la durée des réactions chimiques.
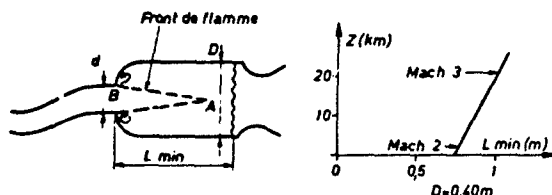
Fig. 11 : Longueur minimale d'une chambre de combustion.

La longueur minimale est alors la somme de ces deux termes :

$$L_{min} = \frac{d}{2} \times \frac{V}{V_b}2' + V_3 \cdot t_c$$

V_2, et V_3 étant les vitesses dans la chambre, avant et après combustion. La vitesse de progression du front de flamme étant :

$$V_b = V_r \left(\frac{P_2}{Pr}\right)^{0,1} \times \left(\frac{T12}{Tr}\right)^{0,2}$$

Avec les conditions de références :

$$V_r = 15 \text{ mS}^{-1} \text{ pour } Pr = 1 \text{ bar}$$
$$\text{et } Tr = 288°K$$

tc, temps caractéristique des réactions chimiques, est donné par :

$$tc \times (P_3)^{0,25} \times (T_{12})^{1,8} = 50$$

La figure 11 montre que la longueur de la chambre de combustion est dé . inée par l'altitude maximale de vol. Bien entendu, d'autres configurations géométriques que celles c cette figure permettraient de réduire cette longueur si cela s'avérait nécessaire.

Cette configuration est celle de la plupart des missiles à statoréacteur conçus dans le passé. Mais il est probable qu'elle reviendra dans l'avenir pour les vols de longue durée (plus de 10 minutes par exemple).

5.1.2. **Les configurations avec accélérateur intégré** dans la chambre, qui sont actuellement les plus étudiées pour les missions de courte ou moyenne portée, en raison de leur excellente compacité. Les contraintes qui guident leur conception sont les suivantes :

* la longueur est généralement déterminée par le volume occupé par le bloc de propergol, cette condition étant dimensionnante, même dans le cas où le missile est tiré depuis un avion rapide

* la flamme est stabilisée principalement par des moyens purement aérodynamiques, car il faut éliminer tout dispositif accroche-flammes au contact avec les gaz du propergol. Néanmoins, si les volumes de recirculation sont insuffisants, il est possible d'améliorer la combustion par de petits accroche-flammes situés en amont des obturateurs éjectables.

* la technologie de la protection thermique est un élément déterminant car les parois sont soumises à des écoulements de gaz à forte température et grande vitesse, entraînant des échanges thermiques importants ; de plus elle doit résister à des conditions très différentes :

Dans la phase d'accélération, les gaz du propergol sont réducteurs, à des températures élevées, jusqu'à 3 600°K, à des pressions de l'ordre de 100 bars, mais avec de faibles vitesses à la paroi et des durées de fonctionnement courtes (4 à 10 secondes environ).

Les gaz du statoréacteur sont plutôt oxydants et à beaucoup plus faible température (2 000°K au maximum, sauf dans les noyaux de recirculation) et pression (inférieure ou égale à 10 bars environ), mais les vitesses peuvent atteindre 300 à 350 mS^{-1} et les durées de fonctionnement plusieurs centaines de secondes.

Bien entendu, la protection thermique doit être de faible épaisseur afin de ne pas réduire la poussée du statoréacteur (en effet, à tuyère donnée, la poussée maximale diminue avec l'augmentation du nombre de Mach dans la chambre).

Ces problèmes techniques peuvent être assez facilement résolus pour les missions de courte durée avec des conditions de fonctionnement relativement peu variables (par exemple mission sol-air de durée inférieure ou égale à 30 secondes). Par contre, si le vol dure plusieurs centaines de secondes, avec des conditions très variables (trajectoires diversifiées à basse et haute altitude) le problème devient plus difficile, d'autant plus qu'il est parfois accentué par la présence d'instabilités de combustion (voir 5.3.).

Les solutions envisageables sont diverses, suivant la durée de la mission :

5.1.2.1. Protections thermiques fonctionnant en régime transitoire : il s'agit de matériaux composites peu conducteurs qui pyrolisent et se céramisent progressivement en surface. Une faible conductivité thermique permet non seulement de conserver la paroi externe "froide", mais aussi de réduire le flux de chaleur qui pénètre dans le matériau, grâce à une élévation rapide de la température de paroi T_{pi} au contact avec la flamme :

$$Q = C_h \, \rho \, V \, C_p \, (Ta - T_{pi})$$

C_h, coefficient de transfert de chaleur (de 0,001 à 0,005 suivant la zone de la chambre de combustion)

ρ, V, Cp, Ta, caractéristiques des gaz de combustion.

De plus, les réactions d'ablation ou de pyrolyse qui se produisent en surface refroidissent la paroi. Mais lorsque le matériau est entièrement ablaté ou céramisé, la conductivité du résidu est la seule propriété qui agisse sur le gradient thermique dans la paroi. C'est pourquoi, un tel procédé est limité en durée : de l'ordre de 10 ou 15 minutes pour des épaisseurs inférieures ou égales à 15 mm.

Deux types de produits ont donné satisfaction :

- rigidimères à base de résines thermodurcissables (phénolique) chargés de produits réfractaires et structurés avec un très fort pourcentage de tissus de silice disposés non parallèlement à la paroi. Cette structuration doit être telle qu'elle permette les déformations radiales et

- élastomères à base de résine silicone chargés en matériaux et fibres réfractaires qui peuvent être moulés in situ dans la chambre de combustion. Cette solution est performante (car faible conductivité) et de mise en oeuvre en principe simple. Mais la couche pyrolysée étant plus fragile, il est parfois nécessaire d'armer la protection thermique au moyen d'une armature métallique ou en matériau composite (référence 5 et figure 12).
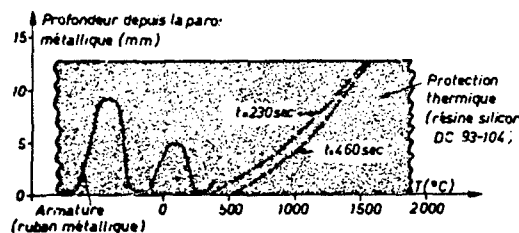
Fig. 12 : Gradient thermique dans l'épaisseur d'une protection thermique isolante

5.1.2.2. Protections thermiques fonctionnant en régime permanent . Pour des temps de vol encore plus longs il faudrait faire appel à des techniques de refroidissement, par convection forcée de l'air, par rayonnement des parois ou ,localement, par circulation du combustible. Tous ces procédés sont complexes ou coûteux.

Un autre concept peut être proposé : il s'agit de réaliser la protection thermique en matériaux "thermostructuraux", c'est à dire qui ne perdent pas leurs propriétés mécaniques, même à haute température : ceci peut être obtenu en associant une structure résistante (fibres de carbone, de carbure de silicium, d'alumine, ...) avec une matrice stable à haute température (carbone, carbure de silicium, alumine, ...). L'avantage est que l'épaisseur du matériau est faible et pratiquement indépendante de la durée de vol. Par contre, la température élevée de la paroi externe et la nécessité d'évacuer les calories par convection ou par rayonnement compliquent l'aménagement du missile. A titre d'exemple, la figure 13 indique le gradient thermique dans un matériau thermostructural, d'épaisseur 8 mm et de conductivité k = 10 W/m.K ; deux missions sont envisagées : croisières à Mach 3,5 à une altitude de 25 km, et à Mach 2,6 à une altitude de 10 km.
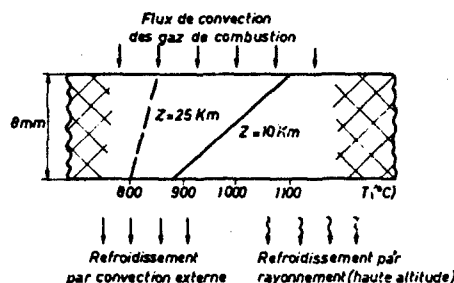
Fig. 13 : Gradient thermique dans la paroi d'une chambre de combustion en matériau thermostructural

Les hypothèses de calcul sont les suivantes :

Coefficient de transfert de chaleur :

$$C_h = 0,0010 \text{ à l'extérieur du moteur}$$

$$= 0,0025 \text{ à l'intérieur du moteur}$$

Emissivité de la paroi externe : 0,7
Richesse du moteur : 0,6

5.2. Performances et modélisation

Les performances recherchées sont les suivantes :

* bon fonctionnement dans une large plage de richesse ; celle-ci peut aller d'une valeur minimale de 0,2 (manoeuvres à haute altitude, décélération) jusqu'à une limite riche souvent supérieure au stoechiométrique (forte poussée pour accélérer ou monter à haute altitude, manoeuvres, ...).

* rendement de combustion (rapport du débit de combustible brûlé au débit injecté) supérieur à 0,9 en phase de croisière.

* efficacité en pression (rapport de la pression totale au col à la pression totale en fin de diffuseur) supérieure à 0,85 malgré les pertes de charge de combustion ou d'origine aérodynamique (obstacles divers dans les manches à air : injecteurs, stabilisateurs de flamme, ...).

Ces performances ne sont acquises qu'au prix de nombreux essais effectués sur des maquettes en vraie grandeur. Un tel développement est coûteux en raison du grand nombre de paramètres à faire varier. C'est pourquoi il est préférable d'optimiser à priori la géométrie et le fonctionnement du moteur grâce à l'exploitation de modèles mathématiques approchés. La démarche est alors la suivante (réf 6 et 7) :

5.2.1. Des essais de visualisation, en écoulement froid, sont réalisés au moyen d'une maquette transparente (Fig. 14). Deux méthodes sont employées :

* méthode du tunnel hydrodynamique : par injection de microbulles, on observe l'écoulement dans la chambre de combustion, afin de situer les zones de recirculation, les décollements, les tourbillons. L'utilisation d'un traceur coloré et de techniques vidéo permet d'obtenir des résultats quantitatifs : volume des zones de recirculation, carburation locale pour chaque position d'injection, etc...

* méthode en veine forcée aérodynamique : grâce à des mesures différentes (vitesse locale de l'écoulement d'air, concentration locale d'un traceur gazeux, ...), il est possible de compléter la description qualitative et quantitative de l'écoulement dans la chambre de combustion.
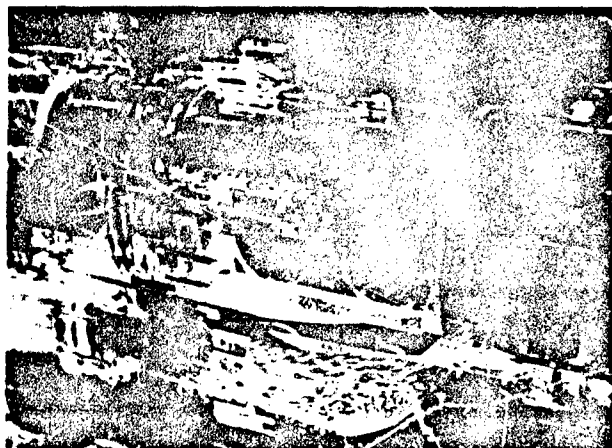
Fig. 14 : Visualisation hydrodynamique de l'écoulement dans une chambre de combustion

5.2.2. A partir des résultats expérimentaux obtenus précédemment, une modélisation simplifiée de la combustion est effectuée, en considérant globalement les zones principales de la chambre, par exemple les réacteurs R1, R2 et la zone de jet J (Fig. 15). Pour chacune de ces zones, les essais ont permis de déterminer le volume occupé dans la chambre et les fractions de débit d'air et de débit de combustible qui les traversent.

En assimilant les réacteurs R1 et R2 à des foyers homogènes, il est possible de prévoir les limites de stabilité de la combustion dans tout le domaine de vol (Fig. 16).

Bien que la méthode ci-dessus soit sommaire et ne rende sans doute compte qu'imparfaitement des phénomènes, elle permet d'effectuer une optimisation paramétrique de la configuration, ce qui facilite et réduit le coût de la mise au point de la chambre de combustion.
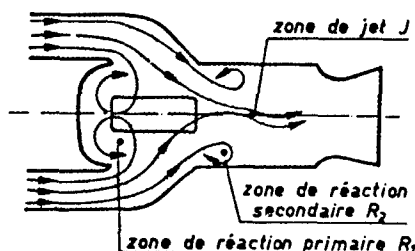
Fig. 15 : Modélisation d'une chambre de combustion
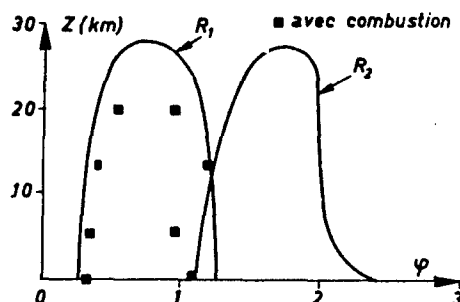
Fig. 16 : Prédiction du domaine de stabilité

5.3. Instabilités de combustion

Tout moteur thermique auquel on demande d'excellentes performances dans un domaine de fonctionnement très étendu risque de rencontrer en quelques points de ce domaine des phénomènes vibratoires gênants. Ce n'est pas une particularité du statoréacteur, et l'on sait que de graves déboires peuvent apparaître sous forme d'instabilités de combustion, aussi bien sur les fusées à propergol solide que sur les fusées à liquide, dès que l'on recherche des performances élevées (exemples : instabilités du 1er étage de SATURNE V, instabilités tangentielles du moteur ARIANE, etc...).

Toute bonne combustion étant assortie de vibrations, il faut donc s'assurer que celles-ci ne s'amplifient pas de telle sorte qu'elles aient des conséquences néfastes, soit sur l'intégrité du moteur, en particulier de sa protection thermique, soit sur le fonctionnement des prises d'air, soit sur le comportement des équipements.

Enfin, l'acuité de ces problèmes n'apparaît parfois qu'au cours d'un développement, c'est à dire lorsque le moteur est testé dans toutes ses conditions de fonctionnement opérationnel, car les méthodes de

5.3.1. Types d'instabilités et conséquences

Schématiquement, il existe deux types d'instabilités de combustion dont les spectres sont bien définis ; elles produisent :

* des vibrations de <u>basse fréquence</u> (100 ou quelques centaines de Hertz). Il s'agit d'instabilités qui apparaissent aux limites thermodynamiques de la combustion et qui sont entretenues par des résonances, soit des jets pénétrant dans la chambre, soit de l'ensemble chambre de combustion + prises d'air. Elles sont plus sensibles aux basses températures génératrices.

Si leur niveau est élevé, ces instabilités de basse fréquence risquent :

- de fatiguer et de détériorer les structures et les équipements du missile

- de provoquer des phénomènes de couplage aérodynamique avec la prise d'air et ainsi de limiter la poussée maximale (Fig. 17).

* des vibrations de <u>haute fréquence</u> (1 000 et quelques milliers de Hertz). Celles-ci se déclenchent pour certaines plages de richesse. Ces vibrations risquent de détériorer la protection thermique et de faire subir de fortes accélérations aux équipements embarqués.
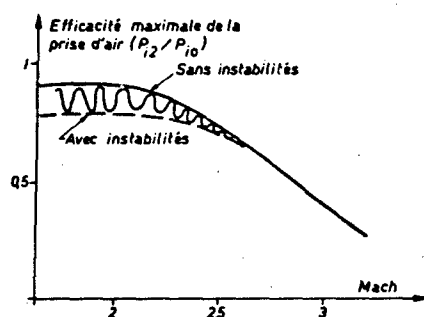
Fig. 17 : Limitation de la poussée maximale par suite d'instabilités de combustion de basse fréquence

Application : calcul des fréquences des principaux modes acoustiques (figure 18)

La fréquence F de chaque mode peut être estimée à partir de la relation suivante, valable pour une cavité cylindrique :

$$F = \frac{a}{2}\sqrt{\left(\frac{2\,k}{D}\right)^2 + \left(\frac{n}{L}\right)^2}$$

a, vitesse du son dans la chambre de combustion
D, diamètre intérieur
L, longueur
k et n, coefficients dont les valeurs pour les principaux modes sont indiquées ci-dessous :

	k	n
1er mode longitudinal	0	1
1er mode tangentiel	0,586	0
2è mode tangentiel	0,972	0
1er mode radial	1,220	0
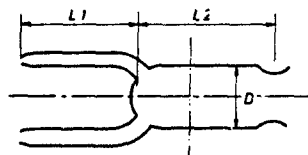
Fig. 18 : Modes acoustiques transversaux
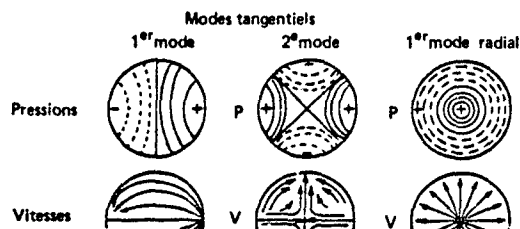
A titre d'exemple, avec les valeurs numériques,

$$a = 750 \text{ mS}^{-1} \quad D = 0,40 \text{ m} \quad L_1 = 1,20 \text{ m} \quad L_2 = 1,10 \text{ m}$$

les fréquences des principaux modes sont alors :

$$\begin{array}{l}
\text{(1er mode longitudinal (chambre seule) : } F = 340 \text{ Hz} \\
\text{"Basses" fréquences(1er mode longitudinal (chambre + prises d'air) :} \\
\hspace{8cm} F = 160 \text{ Hz}
\end{array}$$

$$\begin{array}{ll}
\text{(1er mode tangentiel} & F = 1100 \text{ Hz} \\
\text{"Hautes" fréquences(2è mode tangentiel} & F = 1820 \text{ Hz} \\
\text{(1er mode radial} & F = 2290 \text{ Hz}
\end{array}$$

5.3.2. Origine et remèdes

Comme la plupart des phénomènes instationnaires, les instabilités de combustion des statoréacteurs font appel à des phénomènes physiques complexes. Bien que des travaux approfondis aient été entrepris depuis dix ans, en particulier aux Etats Unis et en France, ils restent encore mal élucidés.

Les instabilités de combustion peuvent être engendrées par différents mécanismes agissant comme source excitatrice et qui peuvent être amplifiés par apport d'énergie lié à la combustion et couplé avec les modes acoustiques du moteur. Si ces derniers peuvent être assez facilement identifiés, il n'en est pas de même pour les mécanismes d'excitation et d'amplification : détachement périodique des tourbillons de Von Kármán existant dans les prises d'air et à l'entrée de la chambre, distorsions instables dans le diffuseur des prises d'air, et surtout comportement dynamique des zones de recirculation.

La complexité de ces phénomènes rend difficile le travail du scientifique qui cherche à comprendre et à prévoir les instabilités, ... mais il favorise la multiplicité des remèdes que l'ingénieur peut apporter expérimentalement.

Ainsi, quelques exemples concrets peuvent illustrer l'efficacité de ces remèdes :

1er exemple : l'injection d'air aux sommets d'un accroche-flamme permet de repousser la valeur de la richesse limite pour laquelle les instabilités de haute fréquence (ou "screech") apparaissent (réf 8). En effet, cette injection d'air perturbe la couche cisaillée où se forment les tourbillons qui se détachent de l'accroche-flamme, phénomène aérodynamique périodique qui, dans ce cas, était la cause des instabilités (Fig. 19).

Injection d'air aux sommets d'un
accroche-flamme
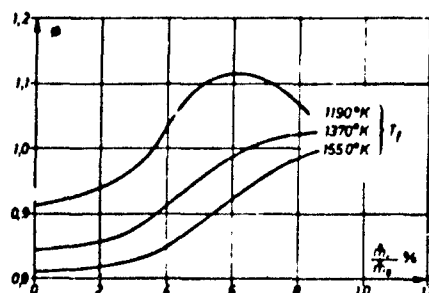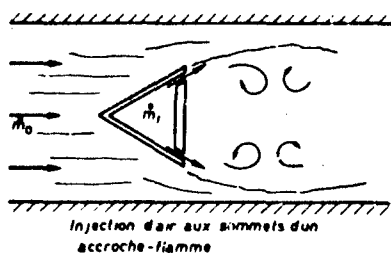
Fig. 19 : Variation de la richesse limite d'apparition des instabilités en fonction du débit d'air injecté (réf. 8)

2ème exemple : la manière dont le combustible est injecté, vaporisé et carbure les différentes zones de la chambre de combustion, a un rôle très important. Ainsi la figure 20 montre que suivant le débit de chaque injecteur, on peut faire apparaître ou disparaître des instabilités de haute fréquence.

L'explication physique de ces phénomènes est un problème difficile et controversé, bien que très étudié : il semble qu'en agissant sur l'injection, on modifie la combustion dans les zones de recirculation, principales sources d'énergie acoustique (réf 9 et 10).

Répartion de l'injection en %		Niveau des instabilités de haute fréquence $\Delta p/P$ (en %)
en A	en B	
30	70	0
40	60	0 à 2
50	50	8 à 10
60	40	12 à 30
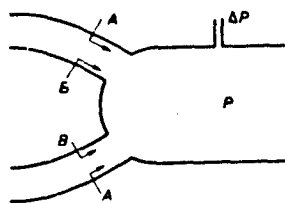
Fig. 20 : Apparition d'instabilités de combustion en
fonction de la répartition du débit d'in-
jection

3ème exemple : d'autres remèdes peuvent agir, non pas en supprimant la cause des instabilités, mais en modifiant la structure spatiale du champ de pression et les fréquences. C'est le cas des cloisons longitudinales disposées à la paroi de la chambre (Fig. 21) et qui sont susceptibles d'amortir certains modes de vibration (modes tangentiels)-réf 9. Ce remède est d'ailleurs bien connu des utilisateurs de moteurs fusées à ergols liquides et à propergol solide.

Cloisons longitudinales
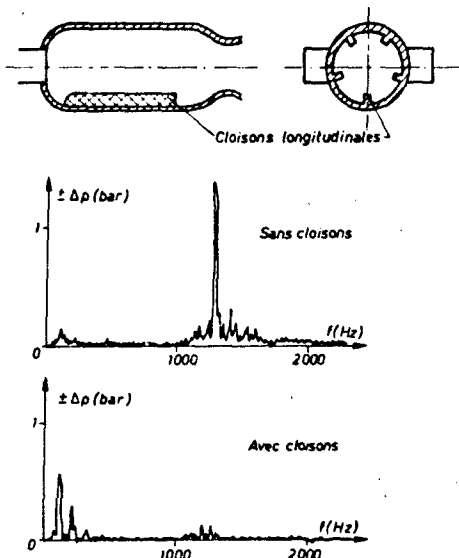
Fig. 21 : Amortissement des instabilités de haute
fréquence par cloisons longitudinales

5.3.3. Quelques réserves

Il est indéniable que, dans le cas de missions de longue durée, le problème du risque d'apparition d'instabilités de combustion doit être sérieusement pris en compte. C'est une étape importante dans un développement.

Chambre percée
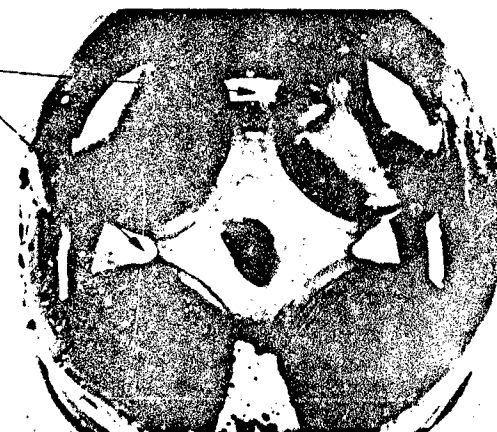
Fig. 22 : Conséquences des instabilités de haute
fréquence sur une chambre de combustion
de statofusée

Toutefois, quelques réserves doivent inciter à la prudence le responsable d'un programme :

a) il n'y a pas, à priori, de configuration "miracle" permettant à coup sûr de s'affranchir de ces difficultés. Des échanges franco-américains faits en 1982 sur des géométries très diverses (une, deux, trois et quatre entrées d'air) l'ont montré.

moteur à 4 entrées d'air alimenté avec du kérosène, un combustible liquide dense, du propane à 50°C et du gaz issu d'un générateur de gaz (700°C) : dans ces quatre cas, on a pu constater sensiblement le même type d'instabilité, avec des niveaux équivalents. Comme le montre la figure 22, ces instabilités peuvent parfois avoir des conséquences catastrophiques !

6 – INSTALLATIONS D'ESSAIS ET PRINCIPALES ETAPES D'UN DEVELOPPEMENT

Comme pour tout propulseur, l'élaboration d'un moteur à statoréacteur passe par des phases successives, de mise au point détaillée, puis de recette dans toutes les conditions du vol, qui nécessitent des travaux expérimentaux importants.

De la même façon que pour les avions, la tendance actuelle consiste à qualifier le missile au sol, dans un environnement le plus réaliste possible, afin d'entreprendre les essais en vol, toujours très onéreux, avec une forte probabilité de succès.

C'est pourquoi la France s'est équipée depuis dix ans d'installations modernes bien adaptées à ces développements, à savoir :

* Centre d'essais de l'ONERA à Palaiseau et à Modane pour les essais en conduite forcée et en jet semi-libre de statoréacteur à combustible liquide ou de statofusée (Fig. 23). On y traite des recherches, des développements exploratoires et des développements opérationnels avec simulation de toutes les conditions de vol (vitesse, altitude, température, conditionnement du combustible, incidence, échauffement cinétique, etc...) (réf 11).

* Installations de l'Aérospatiale (Bourges Le Subdray). De création plus récente, ce centre a des capacités voisines de ceux de l'ONERA. Bien équipé pour les problèmes de sécurité, il est plutôt axé vers les essais de qualification industrielle et de recette (réf 6).

* Centre d'essais des propulseurs à Saclay. Cette installation très puissante permet des essais en jet libre d'un missile complet (simulation de haute altitude).
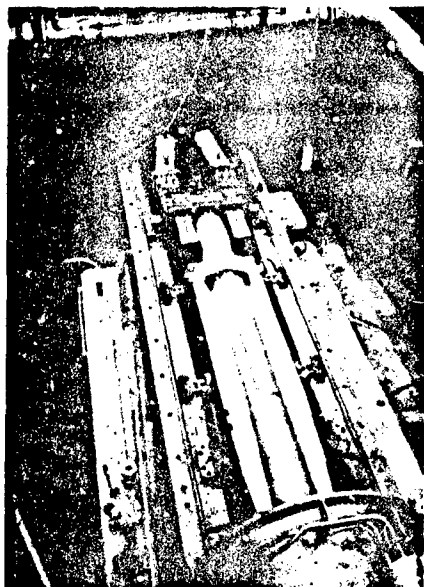
Fig. 23 : Essai d'un statoréacteur avec accélérateur intégré en soufflerie (ONERA/Modane)

Le délai de développement d'un missile opérationnel à statoréacteur n'est pas supérieur à celui d'un autre type de missile (à propulseur fusée ou à turboréacteur). A titre d'exemple, voici le calendrier de développement d'un missile français de ce type :

to   : Lancement du programme

to + 1 an   : Début de la mise au point du moteur

to + 2 ans : 1er essai en vol depuis une rampe terrestre
              (sans accélérateur intégré)

to + 3 ans : 1er essai au banc du système propulsif complet

to + 5 ans : 1er essai en vol depuis avion

to + 8 ans : Mise en service opérationnel.

Pour un tel programme (domaine de vol étendu), les principales qualités demandées aux installations sont la disponibilité et la fiabilité . A titre indicatif, pour mettre au point le statoréacteur et le qualifier avec ses équipements dans toutes les conditions de vol, il faudra 600 rafales par an pendant 7 ans (90% des rafales durent environ 30 secondes et 10% ont une durée supérieure) et l'utilisation d'environ 80 tonnes de combustible liquide. Un développement analogue avec un statofusée à générateur séparé devrait être nettement plus lourd (malgré des performances moins

7 - CONCLUSION : L'AVENIR DES STATOREACTEURS A COMBUSTIBLE LIQUIDE

La progression de l'efficacité des défenses adverses et le souci de maintenir la plate-forme de lancement à une bonne distance de sécurité de sa cible, laissent à penser que le statoréacteur à combustible liquide a un avenir assuré (Fig. 24). Mais le spécialiste sait très bien que ce n'est pas une machine aussi simple que le laisserait supposer son schéma de principe ! C'est pourquoi son utilisation restera tournée vers des missiles à hautes performances et donc relativement complexes.
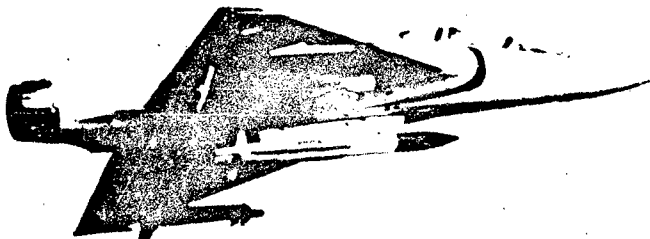
Fig. 24 : Missile Air-Sol sous Mirage 2000

Il faut noter que ces techniques et technologies sont de mieux en mieux maîtrisées par les industriels : par exemple, en France, l'Aérospatiale qui a fait d'importants efforts intellectuels et financiers à l'occasion du développement du missile ASMP, bientôt opérationnel, dispose de nombreux atouts pour entreprendre avec le minimum de risques la réalisation des missiles futurs de ce type.

Or cette expérience acquise semble indiquer que ce mode de propulsion n'a pas encore donné toutes ses possibilités. C'est pourquoi des recherches et études sont menées pour mieux répondre aux exigences du futur.

Ainsi d'ici la fin du siècle, on verra apparaître des améliorations des techniques et technologies décrites dans le présent document. Parmi celles-ci :

* nouveaux combustibles de plus en plus énergétiques,

* amélioration de l'endurance des moteurs et des chambres de combustion (structures, protections thermiques, systèmes de refroidissement),

* mise au point de modèles permettant de mieux prévoir le fonctionnement des chambres de combustion, en régime stationnaire et instationnaire, et ainsi de réduire le nombre des essais au banc,

* amélioration des performances et de la précision des systèmes de régulation, compte tenu des progrès des calculateurs et des senseurs.

* géométrie variable des entrées d'air et éventuellement de la tuyère de sortie.

La figure 25 illustre ces variations géométriques, en prenant pour exemple un missile capable d'une croisière à Mach 4 à haute altitude. Pour accélérer franchement et ainsi réduire la durée de la montée, le rapport des sections $\frac{A_1}{A}$ doit être grand ; mais c'est exactement l'inverse qui est nécessaire pour réduire la consommation en croisière. L'optimisation des performances conduit alors à utiliser des entrées d'air et un col variables, ce qui correspond à une technologie sophistiquée et coûteuse. C'est pourquoi des solutions intermédiaires, telles que la variation de section des entrées d'air seules, méritent d'être étudiées.

Bien sûr, un changement très important des techniques et technologies décrites dans le présent document se produirait avec l'utilisation de la combustion supersonique pour propulser les missiles à des vitesses hypersoniques (mach 6 et plus). Mais ce sujet, passionnant, est traité par ailleurs (F. BILLIG).
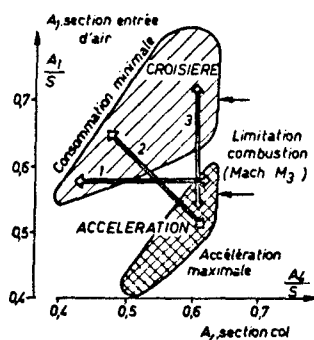
Fig. 25 : Variations de géométrie permettant d'optimiser les phases d'accélération et de croisière

REFERENCES

(1) P. CARRIERE et R. MARGUET
Aérodynamique interne des réacteurs - 3ème partie : statoréacteurs
Cours à l'ENSAE (1975)

(2) G.W. BURDETTE, HR. LANDER et J.R. Mc COY
High energy fuels for cruise missiles - AIAA 78-267

(3) I. PELEG et Y.M. TIMNAT
Investigation of slurry fuel performance for use in a ramjet combustor.
Israel Annual Conference on Aviation and Astronautics (Tel Aviv et Haifa - 1982)

(4) M. RAVEL
Conception d'un statoréacteur à accélérateur intégré
AGARD CP 307 (Octobre 1981)

(5) W.E. ROBERTS, E.R. BOWMAN et S. WASSERBERG
Test and analysis of the ASALM-PTV insulated combustion chamber
ASME Paper 79 - ENAs - 21

(6) P. BERTON et Ph CAZIN
Méthodes et moyens d'essai des statoréacteurs et statofusées.
Comparaison des résultats obtenus au sol et en vol
AGARD CP 307 (1981)

(7) P. CALVET, A. GIOVANNINI, P. HEBRARD, G. TOULOUSE
Quantitative interpretation of recirculated flow visualization by the analysis of video pictures.
International Symposium on flow visualization - Bochum (September 1980)

(8) C.L. BARKER
Experiment concerning the occuring and mecanism of high frequency combustion instability
Ph.D. Thesis - California Inst. of Tech. 1958

(9) A. LAVERDANT
Instabilités de combustion de haute fréquence dans les foyers de statoréacteurs.
Etudes documentaire et expérimentale. Document ONERA non publié

(10) R.C. WAUGH, R.S. BROWN, T.S. HOOD, G.A. FLANDRO, G.C. OATES,
F.H. REARDON
Ramjet combustor instability investigation literature survey and preliminary design study
UTC/CSD - 2770 - IR - 1 (1982)

(11) P. BERTON et D. REGARD
Installations d'essais de statoréacteurs à l'ONERA
T.P. ONERA n°1980-132.

SPECIAL PROBLEMS OF RAMJET WITH SOLID FUEL
by
T D Myers
United Technologies/Chemical Systems Division
P.O. Box 50015
San Jose, California   95150-0015

SUMMARY

Ramjet propulsion systems that use a solid fuel have been of interest to missile design engineers since the 1930's. The operational simplicity of the solid fuel ramjet is of great interest since it does not require fuel tanks, fuel pumping devices or fuel controls to operate. The potential for a highly reliable and storable ramjet propulsion system exists at a cost only slightly higher than a solid rocket motor. The solid fuel ramjet can provide specific impulse in the 900 - 1000 second range, resulting in typically a 200 - 400 percent range increase over a comparable size and weight solid rocket motor.

The "self-throttling" characteristics of the solid fuel ramjet permits high performance operation from sea level to high altitude conditions. Thus, early beliefs that the solid fuel ramjet would only be used for constant altitude and speed missions have proved to be erroneous as a greater understanding of the solid fuel ramjet engine operation was developed.

Another unanticipated benefit of the solid fuel ramjet engine that evolved during 10 years of development tests at the Chemical Systems Division was the high degree of combustion stability experienced with a wide variety of combustion types and sizes. The basic diffusion-controlled solid fuel ramjet combustion process results in a distributed energy release throughout the combustion. This uniform energy release in the solid fuel ramjet engine is believed to be the basic reason why no combustion instability problems have been encountered in over 2500 combustion test firings with many different combustion configurations.

Given all of these attributes of the solid fuel ramjet it is interesting to consider why the solid fuel ramjet engine has not yet been selected for an operational missile. The probable reason is a lack of understanding of the special problems of ramjets with solid fuel that cause the potential missile developer to have concerns about its satisfactory operation over a full flight envelope and with the "off-design" effects that result from environmental conditions and manufacturing tolerances. Unfortunately, the basic operational simplicity of the solid fuel ramjet conversely requires a relatively complex analysis to select a grain design for a given set of mission requirements.

The special problems that are associated with ramjets using a solid fuel include:

- Selection of a fuel type
- Flameholding requirements that limit maximum fuel loading
- Fuel regression rate behavior as a function of flight speed and altitude
- Diffusion controlled combustion process that requires special mixing section
- Inlet/combustor matching.

Considerable insight has been acquired with these special solid fuel ramjet design problems over the past 15 years. Over 2500 ground test firings have been successfully conducted that have included direct connect, semi-freejet and freejet tests. Moreover, in the last few years several hundred experimental flight tests have been successfully conducted that confirm the operational flight characteristics of the solid fuel ramjet. In this lecture we will briefly examine each of these special design problems associated with the solid fuel ramjet.

SOLID FUEL RAMJET TYPES

Two types of solid fuel ramjet engines have evolved in the course of recent development testing. These two basic types are shown in figure 1. The top schematic shows the non-bypass combustor type with a special vane mixing device installed aft of the solid fuel grain. In this solid fuel engine all of the inlet air flows through the solid fuel grain. The lower schematic shows a bypass combustor where a fraction of the inlet air is bypassed to the aft mixing section where combustion of the fuel-rich combustion gases from the fuel grain section is completed. Bypass air ratios from 25% to 80% are typically used to match a specific set of mission requirements.

Both of these solid fuel ramjet combustor types can be used with single or multiple inlets, using an air mixing manifold to provide a uniform air flow to the combustor.

Because of the special operating features of the solid fuel ramjet, additional station locations have been added to the standard ramjet stations as shown in figure 2. These special solid fuel ramjet engine station designations include:

- 2a - entrance to inlet air manifold
- 2b - entrance to air flow injector

These special station designations are used to help analyze the solid fuel ramjet engine combustion efficiency and pressure losses.

There are a wide variety of solid fuel binder materials that have been investigated to date. Depending on the mission requirements, the best gravimetric or volumetric heat release fuel binder can be selected. One of the best performing solid fuels developed to date consists of a blend of PB and polystyrene, providing high gravimetric heat release, good mechanical properties, good regression characteristics, and high combustion efficiency over a wide range of conditions.

It is possible to increase both the gravimetric heat release and the volumetric heat release of the solid fuels by use of metal additives. The boron family of metal additives offer the highest potential increases in both gravimetric heat release and volumetric heat release. Aluminum, boron and boron carbide are all attractive additives for solid fuels.

With the solid fuel ramjet casting the metal fuel directly in the combustor case eliminates the difficult problem associated with storing, pumping, and injecting liquid slurry fuels. Attaining high combustion efficiency with the boron fuels, however, presents a challenging design problem.

SOLID FUEL REGRESSION RATE

The fuel flow rate in the solid fuel ramjet engine is a function of the surface area of the grain, the regression rate of the particular solid fuel formulation, and the flight speed and altitude of the missile. Basically, heat from the combustion gases cause the temperature of the fuel grain to increase to a point where the fuel is vaporized. The hot, vaporized fuel then diffuses in the boundary layer until a combustible mixture of oxygen from the air stream is established. A diffusion flame within the boundary layer is established and steady state combustion is released.

The basic model of the regression rate for solid fuels is shown in figure 3. The solid fuel grain is heated by convective and radiative heat transfer from the diffusion flame. The vaporized fuel diffuses from the grain surface into the boundary layer. The convective heat transfer component is dependent on the air mass flux through the fuel grain port, the air temperature, and air pressure. Thus at low altitude where the air mass flux is high, a large convective heat transfer takes place, causing a high fuel regression rate. Conversely, at high altitudes the air mass flux is low and the solid fuel regression rate is lower. While the resulting fuel-to-air ratio is not perfect, this self-throttling feature of the solid fuel permits good performance over a wide range of altitudes and flight speeds.

The radiative heat transfer function is typically lower than the convective heat transfer, but is significant. Radiation from carbon particles, water vapor, and carbon monoxide from the combustion products are the primary contributors to the radiative heat flux.

An approximate expression for the convective heat transfer function is shown in figure 3 where:

$$\dot{Q}_{convective} \propto G^X, \ T_a^Y, \ D^{-Z}$$

The strong dependence of convective heat flux to the fuel port mass flux (G) is the major contributor to the self-throttling characteristic of the solid fuel ramjet.

The resulting solid fuel regression rate is basically then a balance between the heat transfer to the solid fuel grain and the heat required to vaporize the fuel:

$$\dot{r}_{fuel} \propto G, \ \Delta Q, \ h_v, \ \rho f$$

where: G = fuel port mass flux

ΔQ = heat of combustion
h_v = fuel heat of vaporization
ρ_f = fuel density

A typical effect of flight altitude on the fuel flow in a solid fuel ramjet engine is shown in figure 4. Here the resulting equivalence ratio (ϕ) that occurs as a function of flight altitude at a constant speed climb is shown. The inlet air flow rate drops and the air temperature increases as the missile climbs. The equivalence ratio varies from a ϕ = 0.95 at 30K ft. to ϕ = 1.15 at 40K ft. While the fuel flow is still higher than desired at high altitude, the "self-throttling" characteristic of the solid fuel ramjet reduced the fuel flow rate to a sufficiently low value that a significant range was achieved.

The relative effect of port size and axial position on fuel regression rate is seen in figure 5. In this figure the relative fuel regression rate along the length of the grain is plotted for a 2.5-in.-diameter motor. The experimental values were then compared to theoretical regression rate, with and without considering air acceleration effects. The experimental data fell approximately equally between the theoretically

2500 tests with engine sizes, ranging from 2.5 in. to 10-in.-diameter.

SOLID FUEL RAMJET FLAMEHOLDING/COMBUSTION EFFICIENCY

The solid fuel ramjet engine uses a rearward facing step to produce a recirculation zone that forms the basic flame stabilization region. This flame stabilization region is depicted in figure 6. A critical step height, h, is required for combustion to occur in a solid fuel ramjet engine. The required value of the step height is a function of the inlet air mass flow and temperature. Each particular solid fuel formulation requires a minimum step height for sustained combustion to occur. The importance of the minimum step height limitation ultimately limits the maximum fuel grain loading and thus range in a solid fuel ramjet engine. Thus it is highly desirable to minimize the required step height.

Studies at CSD have shown that combustion in the SFRJ is governed by the degree of mixing between the fuel and air. Within the combustion boundary layer along the grain, the mixing rate is controlled by turbulent diffusion and there exists a natural degree of separation between the fuel and air. Calculations of mixing within the fuel port based on turbulent boundary layer theory showed that only about 50% of the fuel had mixed and burned at the chamber exit plane. The calculations indicated the importance of additional mixing aft of the grain and are in general agreement with combustion efficiencies observed in motors with low L/D mixers.

Analysis showed that the parameters controlling combustion efficiency are the mixer L/D, equivalence ratio, and port-to-injector area ratio. Equivalence ratio is important because it determines the relative thickness of the fuel-rich layer which must be mixed; and port-to-injector area ratio controls the turbulence level introduced at the injector, thereby influencing mixing throughout the combustor. Correlations of combustion efficiency in terms of these three parameters has been successful.

Early attempts to evaluate SFRJ combustion efficiency at low pressure indicated that a reduction in efficiency could be expected at pressures below 25 psia. This conclusion was based on seven tests at pressures from 7.5 to 16.4 psia. More recently, CSD has conducted a series of 13 tests at pressures ranging from 7.6 to 35 psia and found that combustion efficiency does not degrade at pressures down to 12 psia. At pressures below 12 psia, some of the individual test points indicate a lower combustion efficiency.

The combustion efficiency of the solid fuel ramjet engine has been correlated for both circular and spoked type grains, ranging from 2.5-in.-diameter to 10-in.-diameter. The correlating factor, designated burned factor (BF) correlates the combustion efficiency as a function of the equivalence ratio (ϕ), L/D of the engine, and fuel port-to-air injector (A_3/A_i) ratio. Good agreement between combustion efficiencies predicted by the burner factor (BF) and a large number of combustion test firings and configurations has been found.

The effect of combustor size on combustion efficiency has been studied. The highest efficiencies are achieved with the smaller 2.5-in.-diameter combustors with decreasing efficiency levels at the higher motor diameters. The combustion efficiency increases from approximately 70% for a $\phi = 1$ to a value of approximately 85% for a value of $\phi = 0.5$. This trend is typical for all motor sizes and is probably due to mixing limitations since perfect mixing becomes more important as ϕ approaches a value of 1.

Thus combustor designs and devices that promote mixing tend to improve combustion efficiency in the solid fuel ramjet. In nonbypass combustors the use of special vaned mixers at the aft end of the solid fuel grain are effective in increasing overall engine performance. In the bypass combustor radial injection of the bypass air in the secondary combustor promotes improved mixing and thus increases combustion efficiency.

SOLID FUEL RAMJET INLET-COMBUSTOR MATCHING

Matching the inlet and combustor in a solid fuel ramjet engine requires special attention since not only inlet/combustor pressure matching must be analyzed but inlet flow distortion effects could potentially result in nonuniform fuel regression. To study these effects the inlet-combustor simulator shown in figure 7 was fabricated. The objective was to establish a baseline engine performance base for a well-stirred combustor. The design permitted installation of turbulence screens at the inlet-combustor dump to also evaluate the potential effect of local turbulence on the SFRJ combustor performance. Having established the baseline SFRJ performance, test firings were conducted with: (1) a single side-mounted inlet dumping into the plenum chamber, (2) dual side-mounted inlets at 180° dumping into the plenum chamber, (3) the single side-mounted inlet in combination with a special tube-in-hole injector in the dump plane and (4) a screen at the inlet dump to increase the turbulence level. The effects of the various inlet-combustor combinations on SFRJ operating limits are shown in figure 8. The single inlet required a much larger forward dump area and lower combustor Mach number that would limit maximum range and engine thrust, respectively. The dual inlet results showed that only small maximum range and thrust penalties would result. Incorporation of the tube-in-hole air injector reduced the effect of the single inlet on performance, resulting in only a small range and thrust degradation. The effect of increasing turbulence level on fuel regression characteristics was also very small, causing a minor change in the flameholding limits.

The results of these tests showed that with careful design of the inlet air dump to the combustor, using devices such as the tube-in-hole injector that satisfactory inlet-combustor matching was possible. Thus the inlet could be designed to best fit the missile envelope and performance requirements.

The pressure loss characteristics of various inlet air injectors is in figure 9, using the dual inlet configuration as a baseline. Total pressure ratio through the inlet-combustor section is plotted as a function of the inlet dump Mach number. The tube-in-hole injector shown schematically in the left hand figure has the smallest pressure loss of all the types tested. Over the typical range of inlet dump Mach numbers between 0.2 and 0.3 the tube-in-hole injector provides inlet total pressure ratios in excess of 90%. Fortunately, the device that proved best for uniform fuel regression in the solid fuel ramjet also provides the lowest pressure loss, superior even to a straight orifice.

It is generally desirable to design the ramjet engine so that the inlet is operating with a small supercritical pressure margin to ensure stable inlet operation and avoid inlet air spillage drag losses. The liquid fuel ramjet engine can operate with a very close supercritical margin control (3-5%) by varying the fuel flow rate around a closed loop inlet pressure controller. The SFRJ, however, has a fixed grain geometry and the fuel flow rate is determined uniquely by the missile flight conditions, i.e., altitude, speed, and angle of attack. Therefore, the SFRJ must use either a higher supercritical inlet margin and/or select an inlet design that will operate stably at inlet subcritical flow conditions. Both of these choices result in some range penalty. The repeatability of both the SFRJ fuel regression rate and combustion efficiency determine the required inlet matching condition. Based on current state-of-the art it is recommended to either design the solid fuel ramjet engine with a 10% supercritical inlet margin or use an inlet with a stable subcritical operating capability.

The bypass SFRJ combustor presents a special problem for matching the inlet to the combustor. This occurs because either separate inlets or a diffuser bleed system is used to introduce the inlet air both upstream and downstream of the SFRJ fuel grain. The inlet pressure upstream of fuel grain is higher than the downstream pressure since the dump loss and Rayleigh heat addition pressure loss occurs in the primary combustor section. Thus special attention must be given to match both the forward and aft inlets to avoid coupling as well as to match the inlet air pressure with the SFRJ primary and secondary combustor sections.

A typical solution to the forward and aft inlet design matching is as follows. In this application the forward inlet used more inlet flow turning compared to the aft inlet to achieve the desired pressure match. The forward inlet in this manner provided a higher pressure recovery to compensate for the higher dump and Rayleigh losses that occurred in the fuel grain sections. There was no flow coupling between the inlets in any of the installed inlet wind tunnel or freejet tests of the solid fuel ramjet engine.

CONCLUSIONS

The functional simplicity of the solid fuel ramjet combined with high performance makes this engine type quite attractive for many future tactical missions. Conversely, the complexity of the analysis of the fuel regression behavior, combustion efficiency, and inlet-combustion matching has caused vehicle designers concern over the ability of the solid fuel ramjet to be able to operate satisfactorily at all the off design conditions required of a tactical missile propulsion system.

A large engineering data base has been developed for the solid fuel ramjet over the past 15 years that provides answers to all of the special design problems of the solid fuel ramjet. This technology base includes over 2500 ground test firings as well as several hundred successful flight tests. This broad technology base provides confirmed solutions to the special design problems of the solid fuel ramjet.

Mixer vane
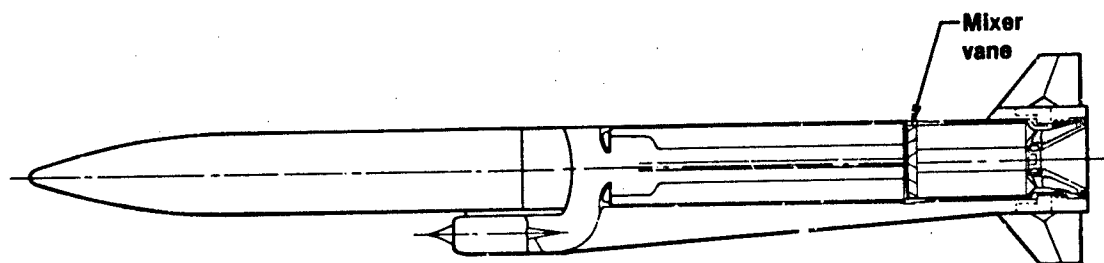
Nonbypass with vane mixing device

Aft bypass inlet

Forward inlet   Mixer plate
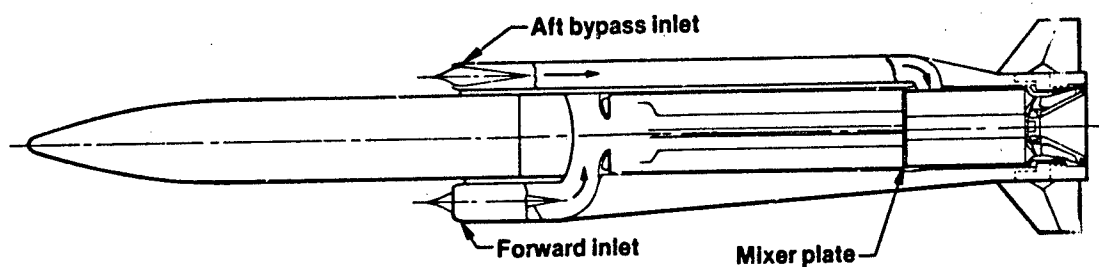
Bypass with simple orifice mixing device

Figure 1.   SFRJ Combustor Configurations

V08113

- FLAME STABILIZATION

- FUEL REGRESSION

- COMBUSTOR PERFORMANCE
    - COMBUSTION EFFICIENCY
    - FUELS

2c
2b
Sta. 2a
3b
4 5   6
① ©

Fuel
Section

Mixing
Chamber
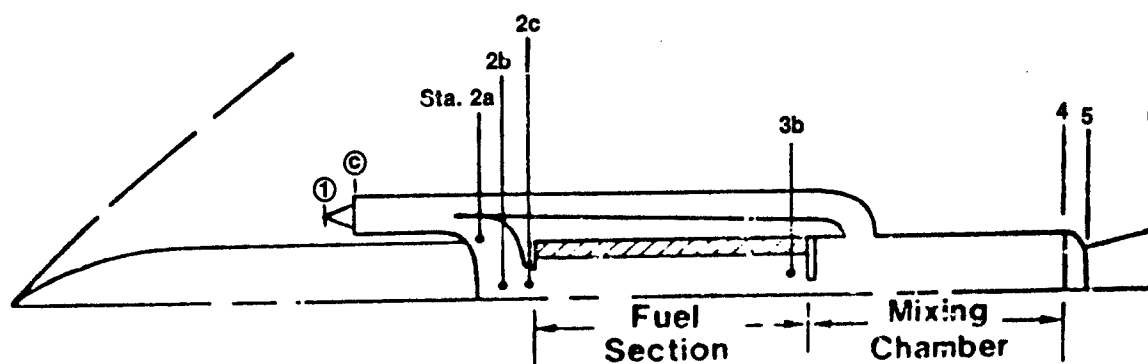
Figure 2.   Solid Fuel Ramjet Combustor Phenomena
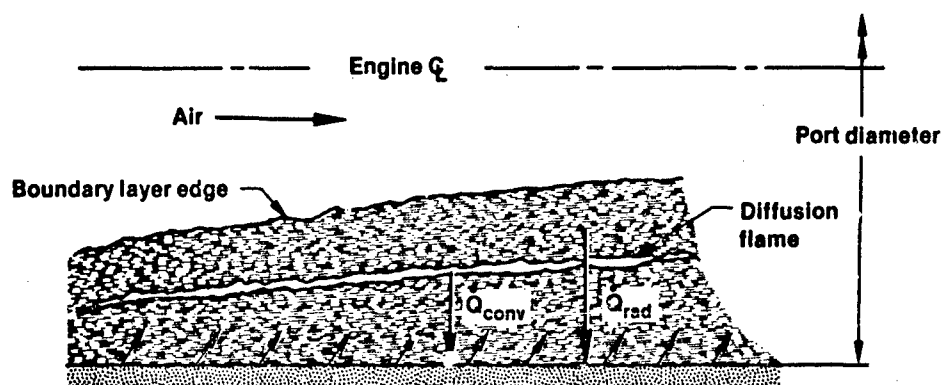
$$\dot{r} \propto \dot{Q}_{conv} + \dot{Q}_{rad}$$

$$Q_{conv} \propto G^x T^y D^{-z}$$

$$Q_{rad} \propto a, P, \delta, T$$

$\dot{r}$ = regression rate
$\dot{Q}_{conv}$ = convective heat transfer
$\dot{Q}_{rad}$ = radiative heat transfer
G = fuel port mass flux
T_a = air temperature
D = port diameter
a = constant of proportionality
P = combustor pressure
T_f = flame temperature
δ = combustion zone thickness

Figure 3. Regression Rate Model for SFRJ Fuel

33210
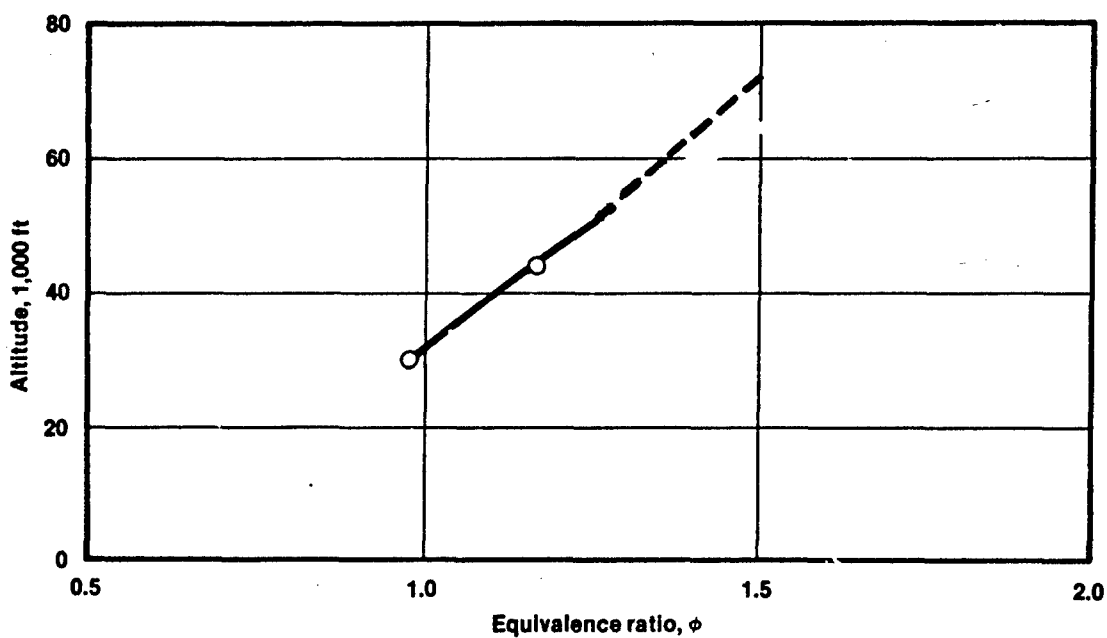
Figure 4. Effect of Flight on Fuel Flow

33211
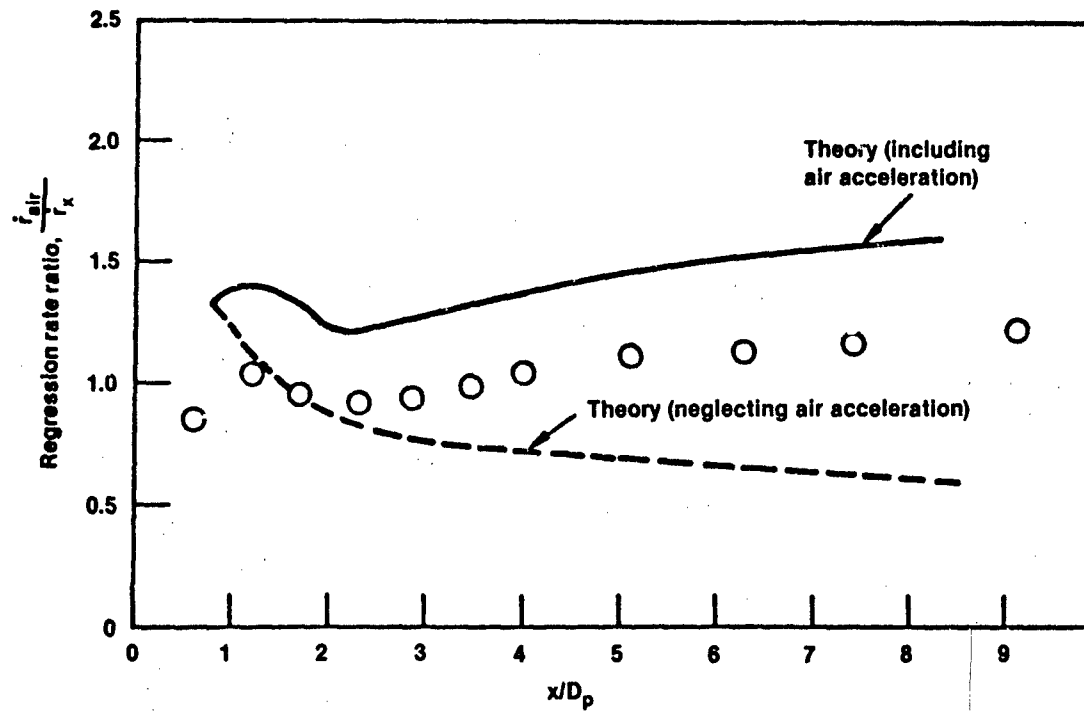
Figure 5.   Regression Rate Distribution in 2 1/2-in.-Diameter Motor

33212
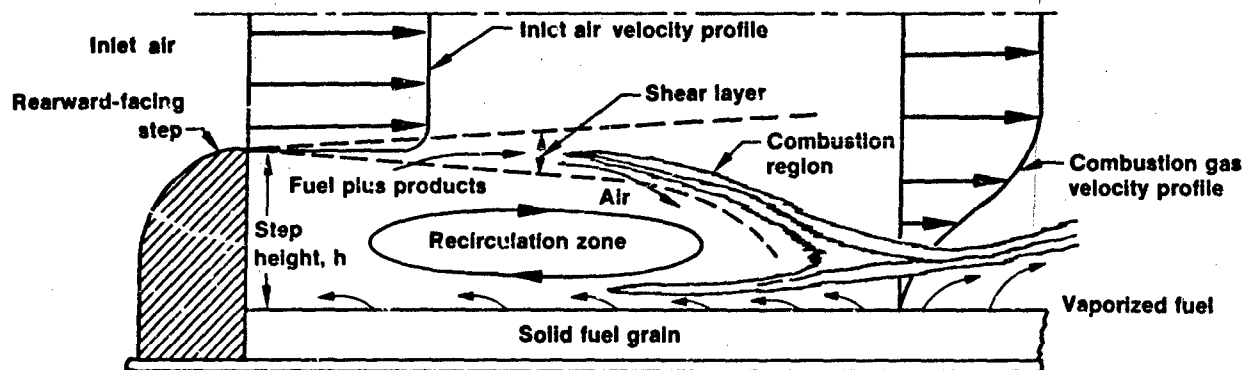
Schematic representation of SFRJ combustion
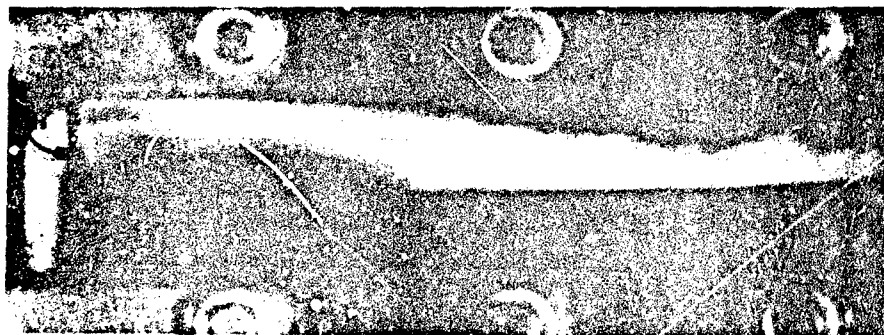
Photograph of two-dimensional Plexiglas combustion

Figure 6.   Flow Field in the Flame Stabilization Region

V06146-R1
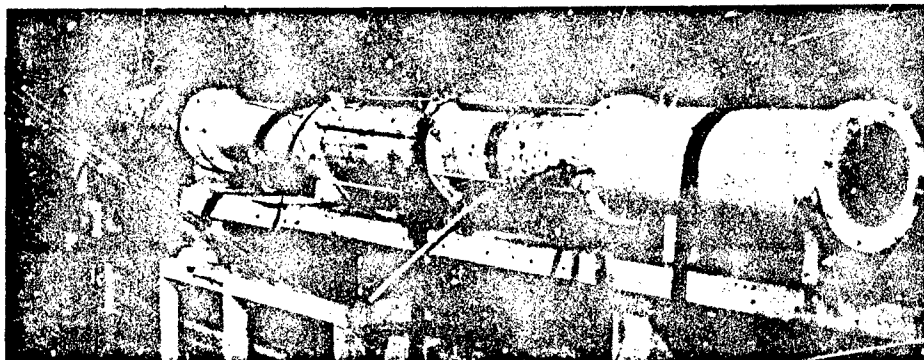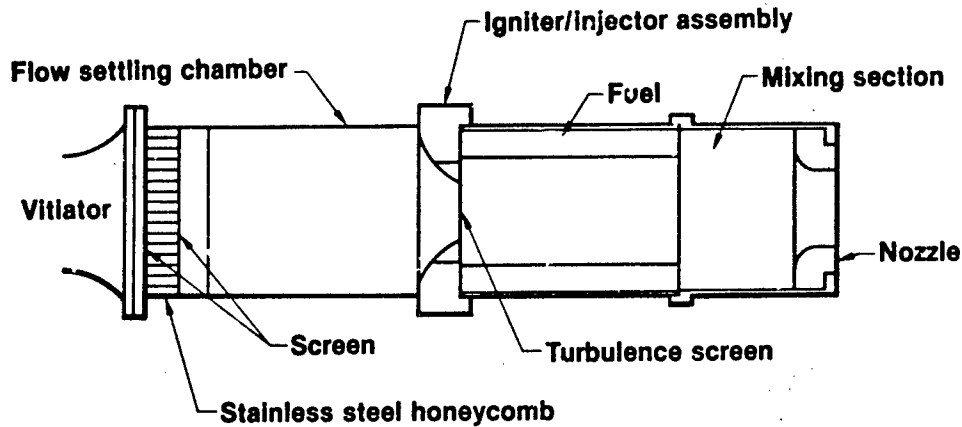
Figure 7. Inlet-Combustor Simulator

V08563
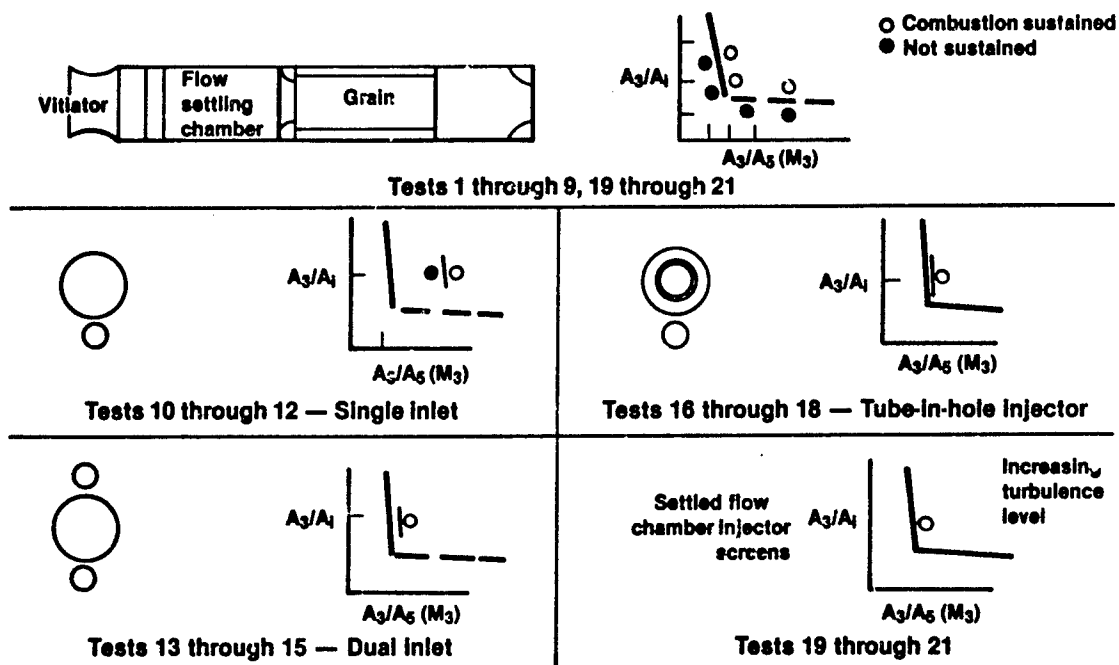
Figure 8. Inlet-Combustor Flameholding Studies

V08441
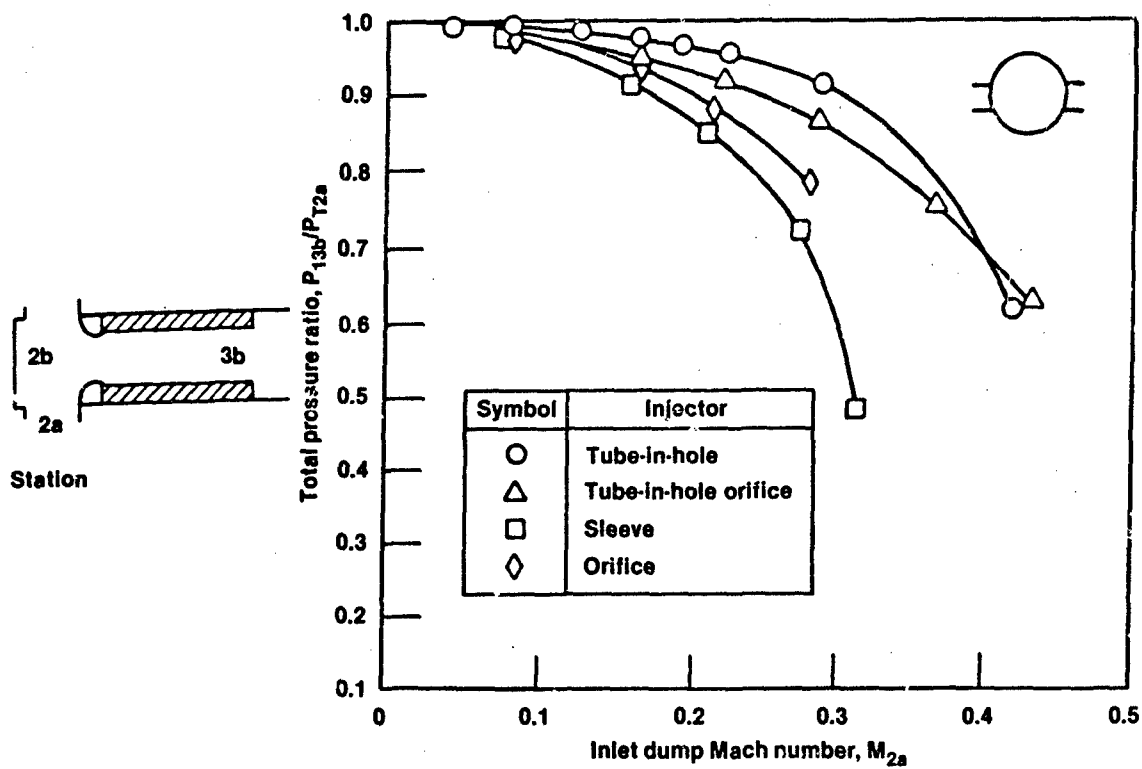
Figure 9 . Effect of Inlet Configuration on Pressure Loss

33216

SOLID PROPELLANT RAMROCKETS

Hans-L. Besser
Messerschmitt-Bölkow-Blohm GmbH
Unternehmensbereich Apparate
Postfach 80 11 49
8000 München 80

SUMMARY

The solid propellant ramrocket (SPR) is very suitable for military applications because of its high values of performance and reliability. The capability of fuel flow modulation, however, is a precondition for various applications. The subject of burn rate modulation has been intensively investigated for SPR propellants and presently can be considered to be state of the art.

The lecture introduces basic design principles of the SPR. The main components of the SPR propulsion system as propellant, fuel flow control, control valve and ram-combustor are discussed in detail.

Finally the lecture reviews the present state of technology and dicusses possible future applications for the SPR.

LIST OF SYMBOLS

A	Area		r	Burn rate
c^*	Characteristic velocity		R	Gas constant
ΔH_c	Heat of Combustion		T	Temperature
ΔH_f	Heat of Formation		γ	Ratio of specific heats
K	K-ratio		η	Efficiency
n	Pressure exponent		σ_p	Constant pressure coefficient for temperature sensitivity of burn rate
p	Pressure			
			ρ	Density

SUBSCRIPTS

b	Burning
c	Combustion
t	Throat

1. INTRODUCTION

The solid propellant ramrocket (SPR), also known as ducted rocket, is an airbreathing propulsion system which belongs to the family of ramjets. The origins of the SPR date back to the 1950's. A considerable effort was made in the USA between the mid 1950's and the late 1960's to investigate this propulsion system. Even flight demonstration programs were included in these activities. This was followed by a phase of lower activities in the 1970's.

In the USSR, SPR development was probably carried out since the late 1950's leading to the propulsion module of the SAM 6 "Gainful" antiaircraft missile which became operational in 1967. Technological and application orientated development work in the field of solid propellant ramrockets has been carried out in France and especially in Germany since the end of the 1960's.

Since several years SPR development activities are stimulated in the USA and Europe due to the growing interest for the application of this propulsion system to tactical missiles of the next generation. Its high volumetric impulse and thrust density make the SPR a preferable candidate to meet high velocity, range and maneuverability requirements even at low altitude flight as well as volume limitations being frequently imposed on missile design.

During recent development programs, flight demonstrations of SPR propulsions systems were carried out by the French ONERA in 1976 (missile outer diameter 0.4 m/16 in) and the German aerospace company Messerschmitt-Bölkow-Blohm GmbH (MBB) in 1981 (missile outer diameter 0.24 m/9.5 in). By now, a high-energy SPR propulsion system is under development at MBB for application in a joint German-French anti-ship missile project. In the USA, the DRED-program (Ducted Rocket Engine Development) has been conducted since several years. A flight demonstration, originally scheduled for 1981 has been delayed. Nevertheless, a follow-on program has already been initiated in 1982.

2. CHARACTERISTICS OF THE SOLID PROPELLANT RAMROCKET

The basic design of a solid propellant ramrocket is illustrated by fig. 2.1. For comparison, sketches of a conventional liquid fuel ramjet (CRJ) and a solid fuel ramjet (SFRJ) are included in this figure. An oxygen deficient solid propellant burns within the primary combustion chamber (gasgenerator). The fuel-rich combustion products are exhausted into the secondary combustion chamber (ramcombustor). There they mix and afterburn with the ram-air supplied by the air intakes.

The precombustion of the fuel is the main characteristic of the SPR. The oxidizer incorporated in the propellant of course reduces the specific impulse compared with a system using the corresponding pure fuel. This somewhat hypothetical disadvantage is more than compensated by various advantageous characteristics which are highly favorable to the application of a SPR.

Performance:

o The SPR allows the incorporation of great portions of high energy/high density ingredients such as carbon, aluminum, magnesium, boron etc. in the propellant, the application of which is not practicable in CRJ's and SFRJ's at the present state of technology.

   CFR with slurries: pumping and combustion performance problems
   SFRJ with great portions of high energy ingredients: combustion performance problems

o The high temperature of the combustible products injected into the ram-combustor

   - allows to achieve a high combustion efficiency for high energy fuel ingredients which are difficult to burn, e.g. boron.

   - reduces or eliminates flame-out problems and may eliminate the need for an additional device to ignite ram-combustion

   - makes the SPR fairly insensitive to cold environment operation (where problems may be anticipated for CRJ's using high-density hydrocarbon fuels)

o The SPR has a potential to allow higher maximum thrust levels than it is possible using CRJ's or SFRJ's. This is due to the higher temperatures achieved at stoichiometric combustion as it is illustrated by fig. 2.2, which compares curves of combustion temperature vs. equivalence ratio (air : fuel) for different fuels and SPR propellants.

o The SPR has a fuel flow modulation capability by using a solid propellant with a pressure sensitive burn rate. This is very important to fulfil the requirements of a wide mission envelope (e.g. flight at different altitudes, different flight velocities, maneuvering). Obviously achievable turndown ratios (TDR) are lower than using a CRJ. Nevertheless, TDR's of SPR propellants up to 18 were demonstrated, while values between 5 and 10 should be considered state of the art for medium to high energy gasgenerator propellants.

Design:

o The SPR is very suitable for volume limited propulsion modules, due to its capability to incorporate ingredients of high density (i.e. high volumetric heating value) in the solid propellant.

o Especially the SPR with fixed fuel flow offers a very simple design without movable parts. The simplicity of design is comparable to a solid rocket or a SFRJ.
   The SPR with variable fuel flow customarily uses a pressure sensitive propellant and a valve for the variation of the gasgenerator throat. The basic design complexity of this control valve, being the only movable part of the variable flow SPR, is more adequately comparable to a fin actuator being present in every modern missile, than to the fuel-feeding devices of a CRJ. Nevertheless, this should mainly be understood to be an argument for the favorable storage characteristics of a SPR system. High gasgenerator temperatures and particle-laden gas flow may induce sophisticated design and the use of exotic (thermally resistant) materials for the control valve.

o The SPR has the capability to accommodate an integrated booster in the ram-combustor in the same way as the CRJ.

Logistics:

o Storage and maintenance requirements and long duration storage characteristics of the SPR are corresponding to the solid propellant rockets being presently operational.

o The SPR induces no additional fire hazard for storage and handling by leaking fuel. This is especially important for naval weapon systems.

o SPR systems having a low optical signature (a requirement sometimes stated for air-to-air missiles) are feasible. This requirement, however, puts some limits to the performance level that can be attained with such systems.

3. DESIGN PRINCIPLES OF THE SPR

All major components of a SPR are indicated in the schematic view given by fig. 3.1.
Main design aspects for these components

- propellant formulation

are discussed in detail in the following paragraphs. The subjects of air intakes and structural design are not specially treated in this lecture since both are corresponding to customary missile or ramjet design, respectively. Where the design of a SPR component requires the application of special material, this item will be included in the discussion of that component. The integrated booster and the boost sustain transition phase are treated very shortly, because the inherent problems are common to all ram-type propulsion systems.

3.1 PROPELLANT FORMULATION [2, 3, 4, 5]

A complex interrelationship exists between the propellant formulation and the performance and characteristics of the SPR propulsion system. Fig. 3.2 illustrates the influence of the propellant formulation on parameters which directly or indirectly affect the figures of merit usually required for a propulsion system.

Main performance related parameters directly depending on the propellant formulation will be discussed in detail. These parameters are indicated in fig. 3.2 by bold frame lines. Additionally, indications will be given where the selection of propellant ingredients has a major influence on cost, aging or handling charact-eristics and optical signature of the propulsion system. Two further parameters are discussed which are not performance related, but which are indispensable to consider in propellant design. These are

- processability which must allow a reproducible industrial product

- mechanical properties which must be compatible with the selected grain configuration and anticipated environmental loads.

3.1.1 Basic Aspects

Usually the main requirements established for a propulsion module to be designed for a certain missile application are concerned with

- range
- mission envelope (flight trajectories, maneuverability)
- missile handling
- missile signature
- design restrictions (length, weight)
- system cost

The range requirement essentially means a required energy content of the propellant while the mission envelope determines the required burn-rate level and turndown ratio for a chosen propellant having a fixed heating value. Besides these two main items, various system related aspects have to be considered in prop-ellant formulation selection to achieve an overall optimum SPR propulsion system [2].

A high SPR performance requires:

o A volumetric heating value sufficient to meet possible volume restrictions for the propulsion module, but always going along with a high gravimetric heating value.
The required total energy to be contained in the gasgenerator should mainly be attained by means of a high gravimetric heating value with secondary importance laid on density with respect to the propulsion module weight. This is very important because the propulsion-module weight influences

  - the required total impulse and volume of the boost motor
  - missile maneuverability and

  may be a restricted figure for airborne missile applications.

o A high expulsion efficiency to make use of the propellants energy content. This parameter refers to the fact that usually a small portion of the combustible is not injected into the ram-combustor but is re-tained in the gasgenerator. Expulsion efficiency depends on the burn-rate level, the primary combustion temperature, the portion of condensed phases in the primary combustion products, the geometry of the gas-generator outlet, and the volume of the empty gasgenerator at burnout.

o A high secondary (ram)-combustion efficiency to get a high degree of conversion of the propellants energy content into heat release in the secondary combustion chamber. Secondary combustion problems are frequently inherent in the use of high energy/high density propellant ingredients.

o An adequate turndown ratio, with an upper limit determined by the maximum thrust level required by the mission envelope and with a desirable lower limit according to economic fuel consumption at the minimum required thrust level. A low figure is desirable for the upper limit of the pressure bracket used to achieve the fuel flow modulation. A high primary combustion pressure leads to the need of heavy gas-generator structure and increases propulsion-module weight.

Good handling, aging and storage properties of a SPR require to exclude as far as possible propellant ingredients which are

- toxic materials

- explosive materials leading to a high degree of propellant hazard classification (e.g. greater portions of high energy oxidizers like HMX and RDX)

- materials undergoing a temperature dependent change of their properties (e.g. the phase change of ammonium-nitrate)

A low signature of a SPR propulsion module requires:

- A low metal content of the propellant due to the visibility of condensed metallic oxide exhaust.
- A low content of otner fuel ingredients which are difficult to burn under ram-combustor operating conditions (e.g. graphite or carbon black) and consequently may induce soot formation in the engine exhaust.
- A sufficient turndown ratio to avoid excess fuel flow at any operating condition.
- The exclusion of ammonium-perchlorate (AP) as oxidizer if minimum signature is a strict requirement. (A visible contrail of the missile is formed as a result of the hygroscopic reaction of hydrogen chloride with water vapor in the exhaust plume.) This argument to exclude AP is only valid for low to medium altitude flight conditions since a visible contrail of water crystals is inevitable at high altitudes greater than 9000 m/27000 ft even without AP.

The compatibility of a SPR system with possible design restrictions essentially requires:

- The favoring of propellant ingredients with high volumetric heating value if range and low propulsion module length are the predominant requirements.
- The favoring of propellant ingredients with high gravimetric heating value if the propulsion module weight is restricted.

Desired moderate cost of the SPR system induce the following considerations for the propellant formulation:

- Some applicable high energy fuel components (mainly metal or metal compounds) are relatively expensive and may boost propellant cost if major portions are included in the formulation.
- Physical and chemical properties of the ingredients included in the propellant may require sophisticated or time consuming and consequently expensive processing procedures for propellant mixing and grain manufacturing. Here the use of ingredients with a very fine particle size or arrangements to avoid migration effects may be quoted as examples. ·
- Characteristics of the propellant like very high combustion temperature or very high particle loading of the combustion products may indirectly contribute to an increase of system cost by inducing the need for sophisticated design or exotic materials.

The processability of a SPR propellant

- is mainly depending on the balance of liquid and solid components in the formulation and
- is strongly influenced by the particle size distribution of the solid propellant ingredients.

All processability problems inherent in the manufacturing of SPR gasgenerator propellant are similar to those of conventional solid composite propellants. Basically the processability features of gasgenerator propellants tend to be inferior compared with conventional solid propellants.

The aspects stated concerning the processability are also true for the mechanical properties of a SPR propellant. Usually, depending on the grain configuration, required figures for mechanical properties of gasgenerator propellant are significantly lower than for conventional solid propellants. Since an endburning grain and a cartridge loaded configuration are preferable for a SPR (cf. para. 3.2) only minor stress loads may arise due to

- the propellants own weight
- pressurizing during ignition
- mismatch of the cartridge properties (thermal expansion etc.)

3.1.2 Ingredient Selection Trade

In the following, major aspects for the selection of the different type of propellant ingredients
- oxidizer
- binder
- carbon and hydrocarbon fuels
- metallic fuels
- catalysts

are reviewed.

Oxidizer

Selection criteria for a SPR propellant oxidizer may be summarized as follows:

o High gas output in order to achieve good expulsion efficiency of the solid organic/inorganic particles from the gas generator

o High gas output in order to minimize deposits within valve and injector orifices as well as to minimize expansion losses in the thrust nozzle due to particle flow

o High combustion temperature, high oxygen content, and high oxygen balance

o High density in order to minimize the oxidizer volume content in the propellant, since heating values of oxidizers are negligible unless they are monopropellants like cyclotetramethylene tetranitramine (HMX)

chlorides (primary smoke), and hydrogen chloride (secondary smoke enhancement)

o Compatibility with other propellant ingredients

o Low hazard classification

o Minimization of risk and cost of the oxidizer as an ingredient as well as overall propellant manufacturing cost

o Availability.

Due to general considerations to be discussed in para. 3.2, the selection of an endburning grain configuration appears to be most favorable for a SPR. Consequently, required burn rates (influencing oxidizer selection) may be localized between 3 mm/s and 30 mm/s (0.15 in/s to 1.2 in/s). Twelve oxidizer candidates are listed along with their pertinent properties in the table of figure 3.3a. Figure 3.3b illustrates the selection trade for these oxidizers.

Nitronium perchlorate and nitrosyl perchlorate cannot be regarded to be feasible oxidizer candidates because of their extremely severe hygroscopicity and their incompatibility with common binders. Sodium perchlorate and potassium perchlorate are unfavorable because of their insufficient gas production and condensed reaction products (low expulsion efficiency). The same argument applies to lithium nitrate, sodium nitrate and potassium nitrate, since they form a high portion of condensed products. Ammonium nitrate in turn yields only marginal burn rates, is hygroscopic, and undergoes a phase change at 305 K/ 550 R. The latter does not apply to the expensive phase-stabilized ammonium nitrate.

As far as combustion characteristics are concerned, HMX and cyclotrimethylene trinitramine (RDX) are comparable. However, HMX has a higher density. The advantage of HMX is that it has a moderate heating value, lacks hydrogen chloride, and thus exhibits minimum smoke. The heating value improves the propellant energy level by 80 KJ/dm³ (1.24 Btu/in³) when 1 % ammonium perchlorate (AP) is replaced with 1 % HMX. Less advantageous is the negative oxygen balance of HMX, which tends to inhibit satisfactory decomposition and combustion of any kind of binder (marginal expulsion).

Further drawbacks of a SPR propellant containing HMX as the principal oxidizer can be summarized as follows:

o The burn rate is low. Compared to AP there is no known burn rate catalyst that can significantly increase the marginal burn rate. Also, unlike AP, the particle size of HMX does not have a major influence on burn rate.

o Raw material costs are about four to six times higher than those for AP.

o A desired low hazard classification may prohibit the use of RDX or HMX in greater amounts in the formulation.

Thus, of the 12 oxidizers considered, AP and lithium perchlorate (LP) appear to be favorable as principal oxidizers with HMX as a potential co-oxidizer. Whereas LP has the higher density, AP has the advantage of being the most frequently used oxidizer in composite propellants. Since LP has a more favorable oxygen balance compared to AP, one may be tempted to conclude that less LP produces the same total propellant energy. However, the amount of condensed lithium chloride formed by the decomposition of LP (according to calculations with NASA's Chemical Equilibrium Code [6]) is high even at temperatures up to 1860 K/3350 R. The liquid lithium chloride may pose problems for the valve flow passages and injector orifices. In addition, the hygroscopic character of LP poses problems in both propellant manufacturing and aging. Finally, LP is about seven times more expensive than AP.

To conclude, AP may be recommended as the principal oxidizer for a SPR gasgenerator propellant. However, the addition of lesser amounts of HMX, chlorates, or nitrates as co-oxidizers in AP-oxidized formulations should be considered if necessary as a means of tailoring the burn rate and pressure exponent.

Binder

At the present state of technology, there are two binder systems currently used for castable composite propellants. These are polyurethenes and polybutadienes. The more modern polybutadiens include

- Carboxy-terminated polybutadiene (CTPB)

- Hydroxy-terminated polybutadiene (HTPB)

- polybutadiene-acrylic acid (PBAA)

- polybutadiene-acrylic nitrile-polymer (PBAN)

While PBAA and PBAN certainly will remain in use for the next decade, future systems will mainly apply CTPB or HTPB. The preferred application of these two binders is based on the following characteristics:

o Low viscosity of the prepolymer in order to facilitate loading with a high content of solid particles while maintaining processability and castability

o Good mechanical properties over a wide temperature range in oder to ensure the mechanical integrity of the propellant

o Low oxygen content

o Secured availability.

The functional groups (carboxyl or hydroxyl group) at the ends of the prepolymer chain are used to cure

Carbon and Hydrocarbon Fuels

A selection of liquid and solid carbon and hydrocarbon fuel candidates is listed in the table of fig. 3.4. Desired properties for the fuel components are:

o High heat of combustion

o High density

o Combustion products that are gaseous (or at least in a state to facilitate expulsion).

The binder polymers (HTPB and CTPB) are exhibiting favorable figures in terms of gravimetric heating value. Due to the low density,however, there is a relatively poor performance on a volumetric basis. Liquid plasticizers like IDP and Oppanol may replace part of the binder to reduce the viscosity of the propellant slurry during mixing, or to allow higher portions of solid ingredients to be incorporated. The use of certain plasticizers (e.g. Oppanal) may be interesting also from the energetic view, since their energy content is superior to that of the binder. Liquid burn rate catalysts (like organic iron compounds) also act as a plasticizer and exhibit high volumetric heating values.

Regarding the solid non-metallic fuel candidates, elementary carbon (as carbon black or graphite) has the highest volumetric heating value while the hydrocarbons (Zecorez, CLPS, PAMS) are superior with respect to the gravimetric heating value.

Two additional aspects should be considered for the selection of non-metallic solid fuel components.

o the use of carbon black and especially of graphite may impose problems for ram-combustion efficiency and consequently contribute to soot formation and visible signature of the exhaust contrail.

o Lower expulsion efficiency can be anticipated for the application of elementary carbon fuels compared with the use of solid hydrocarbons,where portions of the decomposition products are gaseous.

Metallic Fuels

Metallic fuels may be incorporated in a SPR gasgenerator propellant mainly for two reasons:

o to increase the volumetric heating value

o to increase primary combustion temperature in order to achieve autoignition of the ram-combustion and possibly to enhance combustion efficiency in the ram-combustor.

On the other hand, the following problems inherent in the use of metallic fuels have to be considered:

o High primary combustion temperatures may pose problems to valve and injector design

o Metallic fuels contribute to the particle loading of the gasgenerator combustion products which may be detrimental to expulsion efficiency and enhance the risk of deposits being formed in valve passages or injectors.

o High ram-combustion efficiencies are not easily attained using some highly energetic metal-compounds like boron.

o Metallic oxide exhaust contributes to the optical signature of the engine contrail.

o Some metallic fuel components (e.g. boron) are very expensive compared with other, more customary fuel ingredients.

Gravimetric and volumetric heating values of some interesting metallic fuels are presented in a bar-chart by figure 3.5. The corresponding values of carbon and Kerosene are included for comparison. The table of figure 3.6 gives data about density and heating value of various metallic fuel components.

Boron has most favorable energetic features but is difficult to burn under ram-combustor conditions. This is due to the high temperatures required to evaporate boron-oxide which otherwise forms a layer around the boron particles and terminates combustion. Boron combustion has been intensively investigated and high combustion efficiencies can be attained at present state of technology.

Comparatively little experience exists concerning the application of boron carbide which is not included in fig. 3.5. Boron carbide has a gravimetric heating value of 52 MJ/kg (22350 Btu/in³) and a density of 2,5 g/cm³ (0.09 lb/in³)leading to a volumetric heating value insignificantly lower than boron. Combustibility behavior can be considered similar or worse than for elementary boron. Aluminum provides a reasonably high volumetric and gravimetric heating value and yields less combustion problems. However, the use of this metal is limited to small quantities because of its strong tendency to form deposits.

Magnesium provides no significant improvement over carbon or hydrocarbon fuels from the energetic point of view. On the other hand, magnesium is easily burned with high efficiency and yields an increase in primary combustion temperature. Other metals not included in figure 3.5, like zirconium or titanium, are sometimes discussed as fuel ingredients. These are exhibiting a very high density and a volumetric heating value comparable to aluminum, but consequently a low gravimetric heating value which is not favorable for overall performance as outlined before.

The use of metal compounds (e.g. borides) or metal alloys have been also proposed to increase the heat content of SPR gas generator propellants. Since there is very little experience with the application of these ingredients a valuation can be hardly given.

Catalysts

Usually the application of a burn rate catalyst is required to adjust the burn rate of an oxygen-deficient

of the propellant).

There exists a vast number of catalysts used in conventional composite propellants which are also applicable for gas generator propellants. Only one type of catalysts being frequently used in gas generator propellants (with AP as oxidizer) shall be presented here. These catalysts effect an increase in burn rate by fine iron oxide particles which either are incorporated in the propellant as an ingredient or are formed during combustion of an iron containing catalyst.

Iron containing catalysts are

- ferrocene (sol , rarely used)
- n-butylferrocene
- catocene   } (liquid; strong catalyst; frequently used)

The use of liquid burn rate catalysts is desirable with respect to the processability of the propellant. The liquid catalysts are exhibiting a considerable heat content as mentioned before at the discussion of hydrocarbon fuels. Iron-oxide (Fe_2O_3) itself is also frequently used as burn rate catalyst. Its catalyzing properties are relatively weak and depending on the applied particle size. Iron oxide, of course, has a zero heating value.

Iron-oxide is a cheap commercial product which is commonly used as a pigment. The aforementioned liquid catalysts are produced in small quantities and consequently are very expensive.

3.1.3 Examples for Formulation Screening

To complete the consideration of propellant formulation some examples for formulation screening are added below.

Figure 3.7 compares density and gravimetric and volumetric heating values of five hypothetical formulations with different amounts and types of fuel components. These formulations are

1. 25% AP + 75% HTPB
2. 25% AP + 25% HTPB + 50% PAMS
3. 25% AP + 25% HTPB + 50% carbon black
4. 25% AP + 25% HTPB + 50% Mg
5. 25% AP + 25% HTPB + 40% B + 10% Al

The portion of binder in these formulations should be understood to include approximately 5% of curing and burn rate additives in a real propellant.

The bar chart of fig. 3.7 illustrates the stepwise increase of energy content when hydrocarbon, carbon, and metallic fuels are introduced into the propellant formulation.

To compose an appropriate propellant formulation for any given application, firstly a decision must be made to use a metallized or non-metallized propellant. This decision has to be based on the requirements for energy content, gas generator temperature and possibly optical signature. Additionally, a proper balance has to be found between fuel components with low or high energy content and good or marginal combustibility properties to get an overall good performance.

Figure 3.8 presents an example for the screening of a non-metallized propellant formulation. The volumetric heating value is plotted versus the AP content for the following variable formulation:

AP	:	variable (10 to 40%)
binder	:	25 %
carbon black	:	0 to 40 %
PAMS	:	75 % - % AP - % CB

Lines of constant primary combustion temperature (according to chemical equilibrium calculations) are also indicated in fig. 3.8. The predominant influence of the oxidizer content on the heating value is quite evident. However, burn rate requirements impose a lower limit for the oxidizer content, rarely allowing oxidizer portions lying significantly below 25 percent.

Furthermore, fig. 3.8 shows that the increasing of carbon black by forty percent and reducing PAMS by the same amount results in an increase of the volumetric heating value by about six percent. Only an increase of the density is effected by this variation of the formulation while the gravimetric heating value even decreases when PAMS is replaced by carbon black. Gasgenerator temperatures for a fixed AP content are decreasing when the portion of carbon black is increased. Besides the theoretical consideration of energy content it must be reminded that good afterburning efficiency is presumably much easier to achieve using a hydrocarbon than a carbon fuel. Consequently, only lower portions of carbon fuel can be recommended if volumetric restrictions are given for the propulsion module and severe requirements for the optical signature do not allow the application of metallic fuels.

Gas generator temperatures which are calculated for the propellants of fig. 3.8 will be probably insufficient to achieve autoignition of ram-combustion.

thermo chemistry are again indicated in the figure. The propellants considered in fig. 3.9 are based on the following formulation:

AP   :   variable 1C to 32 %

binder   :   25 %

metal   :   7.5 to 15 %

PAMS   :   75 % - % AP - % metal

The portion of metal included in the figure has the following composition:

boron   :   80 %

aluminum   :   20 %

Three major aspects can be concluded from the comparison of figures 3.8 and 3.9:

o   Replacing part of the solid hydrocarbon fuel by metals leads to a moderate increase of the gravimetric heating value (while carbon fuels reduce the gravimetric heating value)

o   The incorporation of the mentioned metallic fuel effects a significant increase of the volumetric heating value (which only could be achieved by much higher quantities of carbon fuels)

o   Primary combustion temperatures are much higher than for the propellants of figure 3.8 and by far sufficient to attain autoignition of ram-combustion. It has to be added that measured gasgenerator temperatures are below the calculated equilibrium temperatures indicating a reaction rate of the metallic ingredients below equilibrium. However, this does not affect the aforementioned statement concerning autoignition.

Afterburning of metallic fuels is not easily done but poses no greater problems than for the compared carbon fuels. This is especially true since much more experience exists for the application of metallized than for carbon loaded propellants.

To summarize, the application of metal fuel can be recommended to increase the energy content of the propellant if optical signature is no severe requirement or is inevitable anyway due to the characteristics of other propellant ingredients as for example AP. State of the art propellant formulations and overall performances will be discussed later on in para. 4.

3.2 GRAIN DESIGN [3, 5]

The gas generator propellant grain configuration must be selected early in SPR design since it drives such key propellant characteristics as burn rate as well as other system aspects such as valve sizing. Experience gained in fixed and variable flow SPR programs leads to the conclusion that an endburner grain configuration is optimum for the following reasons:

o   Any internal burning configuration (star, rod and tube et. al.) requires very low regression rates which usually can be achieved only by pyrolysis rather than by flame front combustion. Pyrolysis in turn implies the danger of unacceptably high residues in the gas generator as well as a gas temperature that is too low for autoignition in the ram combustor.

o   Depending on the internal-burning configuration, there is a more or less pronounced variation in burning surface which has a direct impact on the variable flow valve size as well as on the maximum/minimum gas generator pressure range.

o   The volumetric propellant loading of an internal-burning grain is inferior to that of an endburner.

A cartridge configuration is the appropriate design for an end-burning grain especially for long burning times. Severe problems are inherent in a case-bonded configuration of a long end-burning grain concerning the considerable axial elongation of the grain between commonly required low and high operational temperature limits. Using a cartridge design, a radial gap between grain liner and gas generator insulation may occur at low temperature which has to be sealed or filled by elastic material since a variable empty volume of the gas generator will pose ignition problems.

Different from customary solid rockets, aerodynamic heating occurring during long flight duration at high Mach numbers may warm up the propellant and at least may provoke conical burning. Therefore, not only heat flux to the gas generator wall downstream of the burning surface but also heat flux from the structure into the propellant has to be considered for insulation design of a SPR gas generator. Aspects of liner formulation concerning adhesion or migration problems are similar for SPR and conventional composite propellants.

3.3 FUEL FLOW MODULATION

Fuel flow modulation for a SPR is usually achieved by using a propellant with a pressure sensitive burn rate and a valve to vary the gas generator throat. This concept and the inherent problems are discussed in detail. Some remarks are added concerning alternative, more exotic concepts for fuel flow modulation.

3.3.1 Fuel Flow Modulation Using Pressure Sensitive Propellants

The characteristics of fuel flow control using a pressure sensitive propellant are discussed below. Additionally, basic aspects of valve design are reviewed.

for SPR gas generator propellants is corresponding to conventional composite propellants and may be described by the following formula

$$r = a \cdot p^n \qquad (3.1)$$

Where a and n are empirical parameters which are not necessarily independent from pressure over a utilized wide pressure bracket. Consequently mass production may be written as

$$\dot{m}_{prop} = \rho_{prop} \cdot A_b \cdot a \cdot p_c^n \qquad (3.2)$$

The mass flow ejected through the gas generator throat, a critical pressure ratio being provided, is given by

$$\dot{m}_{eje} = \frac{A_t \cdot P_c}{c^*} \qquad (3.3)$$

with

$$c^* = \frac{1}{\Gamma} \cdot \sqrt{R \cdot T_c} \qquad (3.4)$$

and

$$\Gamma = \sqrt{\gamma} \left(\frac{2}{\gamma+1} \right)^{\frac{\gamma+1}{2(\gamma-1)}} \qquad (3.5)$$

according to fundamental fluid dynamics.

Equilibrium exists when the produced mass flow equals the ejected mass flow. Consequently, the equilibrium pressure is given by

$$P_c = (a \cdot \rho_{prop} \cdot c^* \cdot K)^{\frac{1}{1-n}} \qquad (3.6)$$

where K is defined as the area ratio $\frac{A_b}{A_t}$

Pressure and burn rate variations are depending on a variation of the K ratio as follows:

$$\frac{d_{P_c}}{P_c} = \frac{1}{1-n} \frac{dK}{K} \qquad (3.7)$$

and

$$\frac{d_r}{r} = \frac{n}{1-n} \frac{dK}{K} \qquad (3.8)$$

Fig. 3.10 illustrates the influence of n on the ratio of burn rate variation and K variation. It is quite evident from fig. 3.10 that the application of propellants exhibiting very high pressure exponents above .75 may be very hazardeous from the stability point of view.

Fuel flow control using pressure sensitive solid propellants is especially complicated by the inverse response of the fuel flow to the actuation of the control valve. This characteristic is illustrated by figure 3.11 showing traces of the valve throat area, pressure and fuel flow for a control action to increase or decrease fuel flow, respectively. To increase fuel flow means to reduce the valve throat area and consequently to increase pressure to the values which stationarily correspond to the desired fuel flow. When the valve closes, first the ejected mass flow decreases corresponding to the reduced throat area. Now the pressure rises since the produced mass flow is greater than the ejected mass flow. Mass production and ejected mass flow increase corresponding to the pressure rise until the new equilibrium is reached. The inverse occurs when the valve opens to decrease fuel flow.

The magnitude of the fuel flow over- or undershoot depends on

- the turndown ratio of the control action
- logic of the control loop and velocity of valve displacement

The time span required to change from one fuel flow rate to another depends on

- gas generator empty volume
- the turndown ratio of the control action
- logic of the control loop
- pressure exponent within the pressure bracket used for the control action

The achievable turndown ratio depends on various factors which are related to the propellant characteristics as well as to system aspects. One main limiting parameter for the TDR is the pressure bracket allowed for the burn rate modulation. The upper pressure limit is imposed by the design of the gas generator structure. The lower pressure limit depends on the pressure level in the ram-combustor and on system requirements to include or not a second sonic nozzle downstream of the control valve to evaluate the fuel flow. Evidently, the other main parameter affecting TDR is the pressure exponent of the propellant within the allowed pressure bracket. Since the burn rate of solid propellants is more or less temperature sensitive, the maximum achievable TDR is also limited by the upper and lower operational temperature required for the propulsion system.

Figure 3.13 summarizes the parameters limiting the maximum achievable TDR. Lines of constant TDR are indicated as a function of pressure exponent n and temperature sensitivity σ_p [% / $^\circ$ K]. The left figure is related to a configuration where the control valve forms the only sonic throat whereas a second sonic nozzle is added in the right figure which increases the lower pressure limit. The calculations for figure 3.13 are based on a 103 bars/1500 psia pressure bracket and a 128 K/230°F temperature bracket.

Essentially two types of control logic may be applied to solid propellant burn rate control.

o   A sonic nozzle is installed downstream of the control valve. Pressure and possibly temperature are measured upstream of this nozzle allowing to evaluate the actual fuel flow if gas properties are known with sufficient accuracy. The control valve is adjusted to a position where the desired fuel flow is stationarily evaluated at the second sonic throat. The applied control algorithm must take into consideration the mass flow overshoot during the control action, the pressure sensitivity of the propellant (for stability reasons) and a possible dependency of the c* figure on pressure (which is mainly according to a variation of gas temperature)especially if no temperature measurement is provided.

This control logic which appears to be simple and evident at the first look has several disadvantages.

-   The installation of a second sonic nozzle downstream of the control valve and possibly still upstream of the injector (a simple sonic throat configuration for the fuel injector may not be compatible with combustion efficiency requirements) is space-consuming and may not be compatible with design restrictions given for a modern SPR system.

-   Pressure measurement shortly downstream of the irregularly shaped valve cross section, a tube turn etc. may be of poor accuracy.

-   The dicussed control logic is restricted to propellants which predominantly produce gaseous combustion products with a minimum of condensed species, since two phase flow effects and deposits possibly formed in the second throat are highly detrimental to control accuracy.

o   Another control logic which may also be applied to solid propellants forming combustion products with high loading of condensed phases only relates to the predetermined ballistic data (including c* variability) of the propellant and the calibrated throat area variation of the valve. The control algorithm adjusts the valve to a position where the K ratio corresponds to the desired burn rate. A comparison of the actual and the expected pressure allows to correct disturbances caused by grain temperature, coning effects or clogging of the valve. The essential control variable for this kind of control logic is the required thrust level or flight velocity. The fuel flow not being explicitly known is adjusted until the desired performance of the propulsion system is achieved.
This control logic requires a more complex and skilful control algorithm but is capable to handle highly particle-laden flows with moderate depositing characteristics.

Any control logic must take into consideration that the overshoot of the fuel flow during control action may induce operational conditions for the ram engine which may be off-limits for air intake operation. A sudden increase in fuel flow and heat release in the ram-combustor will cause a pressure rise which may blow off the final shock forcing the air intake into subcritical operation. If the air intake exhibits no stable subcritical operation the air intake will go into inverse flow leading to the destruction of the missile. On the other hand, a long lasting undershoot of the fuel flow (occurring for high modulation ratios, big gas generator empty volume, low n) may lead to thrust deficiency and deceleration of the missile and consequently also may pose problems concerning air intake operation.

3.3.1.2 Control Valve Design [3, 9, 10, 12]

The subject of control valve design, due to its complexity cannot be treated completely in this context. Major aspects of valve design and some basic valve design principles will be discussed below.

All customary valve design principles are applicable to a gas generator control valve as long as primary combustion temperature is low (e.g. below 1000 K/1800 R) and the portion of condensed species in the primary combustion products is low, too. Problems arise for high temperatures and highly particle-laden flows. Problems may also arise from high pressure ratios across the valve if the configuration is not adequate.

The following aspects have to be considered for gas generator valve design:

(1)   space requirement for valve and actuator
(2)   compatibility with other components, e.g. injectors
(3)   sealing problems
(4)   actuation loads (determining type and size of the actuator)
(5)   mechanical and thermal stress arising for the components
(6)   heat flux into the control valve and to the actuator
(7)   clogging risk
(8)   overall functional safety
(9)   cost

The significance of several aforementioned items depends,of course,on the required endurance time. The consideration of the items (1) to (5) and (8) leads to the conclusion that a rotating motion of the control valve is preferable to a translatory motion. In most cases a rotating valve and its actuator may be accommodated in a smaller volume than a translatory valve. Sealing problems of the rotating valve are inferior to that of translatory valves. Rotary sealing surfaces usually stay clean of deposits while any translatory valve component may draw deposits up into the bore on which it seals. Rotary seals may be composed more easily of heat resistant materials like graphite foils or wool. Translatory seals on the other hand usually apply elastomeric materials which must be thermally protected. Actuation loads tend to be greater for translatory valves compared with rotary configurations. A load balance at the control element may also be attained

actuator are low. Problems may arise from dividing the fuel flow to be fed into the ram-combustor by several injectors. Where narrow bending of the flow is prohibited due to the clogging risk, a valve configuration with several throats actuated by one unit may be the only adequate solution. This, however, is not feasible with every valve type.

Referring to the items (5) and (6), probably less problems arise if the valve is installed in an environment with low flow velocity. If the valve is installed in a region of higher flow velocity, e.g. in a gas pipe, thermal stress will be great and possibly non-uniform around the control element. Consequently, heat flux into the valve and the actuating unit will be greater for a high flow velocity than a low flow velocity environment.

A clogging risk (item (7)) only exists for particle-laden flows. Deposits are predominantly formed at

- stagnation points
- deadwater regions

which cannot be completely avoided by valve design. If depositing is expected, any valve configuration exhibiting a small valve lift or narrow slots for the valve throat should be discarded. Further on, it must be considered that additional valve actuation loads may arise from stripping off deposited material.

The overall functional safety (item (8)) summarizes the remaining risks of the items (3) to (7). Cost of the valve may be boosted by the need for sophisticated design and complex manufacturing procedures, by using exotic temperature resistant material, and by type and size of the actuation unit.

Figure 3.14 presents six basic valve configurations which will be shortly discussed below, referring to the aforementioned design aspects. A temperature bracket of 1000 K to 1700 K (1800 R to 3100 R) an upper pressure limit of 100 bars (1500 psia) and particle loadings from 0 to 50 percent are implicitly assumed as possible operational conditions for the gas generator control valve. The qualitative estimation of the characteristics and the applicability of the presented valve design variants are based on available state of the art experience.

(1) Rotary Blade / Butterfly Valve

- Space requirement is small for valve and actuator
- Feasible but infavorable, if more than one throat is desired
- Rotary sealing poses no major problems
- Low actuation loads due to ideal force balance
- Moderate mechanical load but high thermal load due to high flow velocity around the valve element
- High heat flux to the actuator, thermal insulation of the actuator may be problematic
- Unfavorable for use with highly particle-laden flow due to the depositing risk
- Excellent functional safety for gas flow with moderate temperature and low particle loading; hardly applicable to highly particle-laden flow.
- Moderate cost, if applied to an adequate fuel flow environment
  Expensive material may be required for the blade if the valve is used in high temperature flow.

(2) Translatory Plunger

- Little space is needed for the valve but considerable volume may be required for the actuator
- Feasible but unfavorable if more than one throat is desired
- Translatory seal may pose severe problems when the valve is applied to high temperature particle-laden fuel flow
- High actuation loads
- High mechanical loads due to a non-uniform force distribution around the control element; high thermal load due to high gas flow velocity around the control element
- High heat flux into valve and actuator; thermal insulation of the actuator may be problematic
- High depositing risk when used in particle-laden flow
- Medium functional safety for the application to gas flow with moderate temperature and low particle loading, due to the mechanical and thermal loads at the control element as well as to the high actuation loads. Low functional safety for the application to high temperature or highly particle-laden flow
- Costly because of the power requirement of the actuator and the need for sophisticated design and the use of expensive materials for the control element if the valve is used in high temperature flow.

(3) Needle Valve - Opposite to Flow Direction

- Highly space-consuming for the uni-axial configuration of valve and actuator. Alternative configurations with lateral actuation are feasible but exhibit a complex design. High space requirement of the actuator.
- Feasible but unfavorable if more than one throat is desired
- Extreme sealing problems since the rod housing inevitably forms a stagnation point for the flow
- High actuation loads
- Moderate mechanical load but high thermal load due to high flow velocity around the valve
- High heat flux into valve and actuator; thermal insulation of the actuator is highly problematic
- High risk that deposits are formed at the rod and the orifice when used in particle-laden flow
- Medium functional safety for the application to gas flow with moderate temperature and low-to-zero particle loading. Hardly applicable to high temperature, highly particle-laden flow
- Costly, because of the power requirement of the actuator and the complex design of rod guide and sealing. Expensive material is required for the rod, if the valve is used in high temperature flow.

(4)   Needle Valve - Parallel to Flow Direction

- Reasonable configuration only, when accommodated in the gas generator.
  Medium to high space requirement for the valve installation; high volume requirement for the actuator; lateral actuation is mandatory and feasible but includes complex design using lever bars. Even a rotary actuation is feasible.
- Configuration with several throats are feasible
- Sealing is difficult but feasible
- High actuation loads
- Moderate mechanical load but partially high thermal load due to high flow velocity around the control element
- Potentially high heat flux into valve installation and the actuator
- Thermal insulation of the actuator may be more easily accomplished than for configuration (3)
- Deposits may be formed at the orifice and less likely at the rod. Deposits are not necessarily detrimental to valve function if the throat gap is wide and sufficient valve lift is provided.
- Medium to high functional safety even for the application to high temperature, highly particle-laden flow.
- Costly, because of the high power requirement of the actuator and the complex design of the act-uating lever system. The use of expensive material may be mandatory for the control element and the actuating lever system.

(5)   Gate Valve

The gate valve in some kind is a variant of the translatory plunger accommodated in the gas generator. The translatory gate covers part of the gas generator outlet forming a variable throat. The translatory motion has usually to be transformed into a rotary motion to accomplish a feasible and compact actuation. Alternatively, the translation of the gate may be accomplished more favorably by rotating an eccentrically shaped disk.

- Medium space requirement for valve installation and actuator
- Configurations with several throats are feasible
- Sealing is feasible for rotary actuation
- Comparatively low actuation loads
- Moderate mechanical and thermal load. Partially low flow velocity around the control element
- Medium heat flux into valve and actuator. Thermal insulation of the actuator is feasible.
- Deposits may be formed at the deadwater region of the downstream side of the gate. Stripping off deposits when the valve moves may increase actuating loads.
- Medium to high functional safety even for the application to high temperature, highly particle-laden flow.
- Moderate cost referring to actuator and design complexity. The use of expensive thermally resistant material may be mandatory for the gate element

(6)   Disk Valve

The basic arrangement of the disk valve is similar to the needle valve parallel to flow direction (4). The valve is accommodated in the gas generator and laterally activated by means of a lever system.

- Medium to high space requirement for the valve installation; high space requirement for the actuator
- Configurations with several throats are feasible
- Sealing is difficult but feasible
- High actuation loads
- High mechanical load; partially high thermal load due to high flow velocity at the downstream side of the control disk.
- Medium heat flux into valve and actuator; thermal insulation of the actuator is feasible
- Comparatively small valve lift (depending on the diameter of the gas generator outlet) leads to a narrow throat gap of the valve. High clogging risk at narrow gaps excludes the disk valve from the application to gas flow with considerable particle loading.
- Medium to high functional safety for the application to gas flow with low-to-zero particle loading (where another valve design like (1) may be the better choice). Hardly applicable to highly particle-laden flow.
- Costly, because of the high power requirement of the actuator, the complex design of the actuating lever system. The use of expensive material may be mandatory for the disk element.

The selection of an appropriate actuator for the control valve depends strongly on the actuation load of the valve. An electrical actuation is frequently desirable due to aspects of the missile system. However, electrical actuation is restricted to moderate actuation loads because of

- limited power supply of the missile system
- volume requirement of high power electromotors
- thermal problems.

High actuation loads may be handled using pneumatical or hydraulical actuators. If a pressurizing system does not exist in the missile an air turbine fed by tap air from the intakes may be applied. However, a pneumatical or hydraulical actuation is space-consuming due to the required auxiliary valves and power supply.

Several types of thermally resistant materials may be applied to valve components:

- high melting metals like molybdenum or tungsten
- ceramic material

The application of high melting metals is a customary and safe approach but it includes a considerable weight penalty. Ceramic materials are exhibiting a lower density and are highly temperature resistent. However, some ceramics are sensitive to the thermal shock occurring at the ignition of the propellant. The manufacturing of ceramic components of complex shape is very expensive. Components made of graphite or CFC exhibit medium to low densities und high thermal resistance. If such components will be exposed to particle-laden flow, usually an impregnation or coating of ceramic material at the surface is needed to avoid erosion.

Surface coating may also be considered to protect thermally stressed valve components. Spinels and zirconium-oxide can be quoted as examples of coating materials.

3.3.2 Alternative Concepts for Fuel Flow Modulation

Some alternative, somewhat exotic concepts for fuel flow modulation shall be presented below.

Retractable Silver Wires

This concept is illustrated by figure 3.15. It is based on a burn rate increase around a silver wire embedded in the propellant which is due to increased conductive heat flux into the propellant effected by the wire. A local increase in burn rate leads to a conical shape of the combustion surface. When several silver wires are axially embedded at regular intervals in an endburning propellant (as shown by fig. 3.15), a cone will be formed around each silver wire leading to an increased burning surface and an increased fuel flow. When the siver wires are retracted behind the burning surface by a skilful mechanism and a locally increased heat flux into the propellant does no more exist, the burning surface equalizes after some time due to the uniform burn rate. Consequently, this concept for fuel flow modulation means a controlled variation of the burning surface instead of a variation of the burn rate. The logic of the control loop may be based on the evaluation of the ejected mass flow through a constant sonic throat (measurement of gas generator pressure and temperature).

Various disadvantages and hardly estimable risks are inherent in this concept:

- The achievable burn rate increase by means of silver wires is limited to a ratio of 3 to 4, consequently (according to geometrical considerations), the ratio of surface increase being effected by the coning is limited to about 4. The resulting narrow cones (cone angle ≈ 30 degrees) will pose problems concerning burning characteristics.

- The response time of the system may be poor depending on the time needed for the formation of the cones and the equalization of the burning surface, respectively. The response time will improve, if the number of silver wires and cones is increased.

- The response time problem of pressurizing or depressurizing the empty gas generator volume when gas production changes and has to be fed through a constant throat, is also inherent for this control concept. However, no fuel flow overshoot will occur during a control action.

- The axial bores in which the wires are drawn , probably need to be insulated to avoid conical burning induced by entering combustion gases when the silver wire is withdrawn.

- Since pressure is a fairly insensitive input parameter for the control loop to adjust wire drawing to the actual burn rate, control accuracy and control stability are questionable.

- The overall functional safety of a wire drawing mechanism is questionable either. The space needed for the accommodation of this mechanism may be considerably greater than for a control valve.

- The manufacturing of the propellant and the embedded wire system will be highly complex and expensive.

The concept of retractable silver wires for fuel flow modulation exhibits no favorable features. Its realization seems to be hardly feasible.

Longitudinal Tubes

An increase of the burning surface by coning is also effected by a concept proposed by Thiokol. The THERMATROL® (Thiokol Heat Exchange Rocket Motor Augmented Rate Control) concept employs small diameter metal tubes embedded longitudinally in an endburning grain. The forward tube ends (at the bottom of the grain) are connected to a flow rate control system. Hence for this concept the heat flux into the propellant (to effect coning) is delivered by the combustion gas flowing through the longitudinal pipes.

Most statements brought up concerning the silver wire system do also apply to this concept. Feasibility of the THERMATROL concept may be somewhat superior to the silver wire concept.

Matrix Propellant

Another concept (cf. fig. 3.16) proposes to compose two different propellants to a so-called matrix grain. According to this concept, preproduced granules of one propellant would be added to the mix of the other propellant. By this way, a high energy propellant which is not pressure sensitive could be embedded in a highly pressure sensitive propellant exhibiting a low energy content. Fuel flow modulation would be effected by burn rate variation of the pressure sensitive propellant according to para. 3.1.3. The granules of the high energy propellant would be ejected from the burning surface by the combustion gases of the pressure sensitive propellant, somewhat similar to erosive burning.

Basically, this alternative concept for fuel flow modulation may be feasible. Nevertheless, two objections

will not reach very high values.

- A possibly low degree of decompositon of the ejected high energy propellant granules may be highly unfavorable for afterburning efficiency.

- Propellant processing will be highly complex and expensive. Poor mechanical and aging properties of the matrix propellant can be anticipated.

Coaxial Endburning Propellants

This concept (cf. fig. 3.17) acts somewhat similar to the application of silver wires. Here, a central rod made of a pressure sensitive low energy propellant is embedded in a tubular high energy propellant which is not pressure sensitive (a configuration similar to a candle). The core propellant is embedded in the tubular propellant without insulation. The gas generator pressure is controlled by a valve. The core propellant needs to exhibit the same burn rate as the tubular propellant at the lowest required burn rate level. When the valve closes and pressure rises, the burn rate of the core propellant increases and effects a more or less significant coning depending on the burn rate ratio $r_{rod} : r_{tube}$. Fuel flow modulation again is done by a variation of the burning surface.

Of course, several axial propellant rods embedded at regular intervals may be used instead of one core propellant. Reviewing this concept, the following critical remarks shall be added:

- The loss of energy content of the overall propellant is lower than for the matrix propellant but is not negligible, especially if more than one low energy rod is used.

- The achievable TDR is limited since the area ratio of a plane and conically shaped burning surface equals to $\sin(\alpha/2)$ where α is the cone angle. Consequently, an area ratio of 5 corresponds to a cone angle of 23 degrees. Obviously, the accurate handling of such narrow cone angles can hardly be estimated to be feasible (erosion, mechanical properties of the propellant).

- The control logic corresponds to the one applied for pressure sensitive propellants (cf. para. 3.3.1) while the control accuracy may be inferior.

- The system response to a control action and inherent problems correspond to the silver wire system.

- Complex and costly manufacturing procedures can be anticipated for the propellant, mechanical and aging properties are questionable.

No advantages can be stated for this concept concerning simplicity, control accuracy or volume requirement (since a control valve is mandatory). The feasibility may be estimated to be superior to the silver wire system. The concept of coaxial propellant may be applied when pressure sensitivity of the high energy propellant cannot be effected by variation of the propellant formulation and the requirements stated for TDR, control response and control accuracy are moderate.

Staged Propellants

If only two (or a maximum of three) fixed levels are required for fuel flow and if sequence and duration are predetermined for these mass flow levels, the application of propellants with different burn rate levels offers a simple and reliable concept.

Different propellant types may be cast one on another or the gas generator may be divided into different chambers which are ignited and operated independently. The use of several primary combustion chambers leads to a low volume efficiency and an increase in structure weight. Usually, mission requirements are prohibitive to the application of this simple concept.

3.4 RAM-COMBUSTOR

Three topics have to be discussed concerning ram-combustor design:
- optimization of the geometry to achieve high combustion efficiency
- thermal protection of the combustion chamber
- thrust nozzle design and thermal protection

Especially, the first item is reviewed in some detail in the next paragraph, since there are characteristic aspects inherent in the SPR system. Insulation problems and thrust nozzle design are similar to other ram type engines and are only shortly discussed.

3.4.1 RAM-COMBUSTOR CONFIGURATION [4, 15, 16, 17, 18, 19]

The basic design of the ram-combustor (secondary combustion chamber) is mainly determined by the missile configuration. Different air intake configurations are presented by figure 3.18. A lateral arrangement of two or more air intakes usually leads to a side dump configuration of the ram-combustor. A chin ar ventral intake or a non-integrated design of the propulsion module are favorable to the application of a coaxial ram-combustor configuration.

Possible ram-combustor configurations are schematically schown by fig. 3.19, along with some examples of detailed design patterns.

are predetermined by the required mission envelope of the propulsion system. These are:

- equivalence ratio
- chamber pressure
- thrust nozzle throat area (i.e. combustion chamber contraction ratio)
- chamber length

The figures for total mass flow through the ram-combustor, the equivalence ratio and the chamber contraction ratio result from the required thrust level. All three parameters together determine the chamber pressure. The chamber length usually corresponds to the required length of an integrated boost motor.

The equivalence ratio (determining combustion temperature) and the chamber pressure have a strong influence on the combustibility characteristics of most types of fuel components. The chamber length and the chamber contraction ratio determine the residence time of the combustion products in the ram-combustor which is a very important parameter for the efficiency of particle combustion.

As a consequence, the optimization of the ram-combustor geometry is restricted to the following subjects:

- To provide proper mixing of the fuel-rich primary combustion products and the ram air (possibly for a wide range of operating conditions)

- To provide local variations of the equivalence ratio different from the overall figure which may be favorable to the combustion of high energy fuel components exhibiting marginal combustibility character- istics. Variations of the equivalence ratio are effected by special flow patterns like recirculation zones.

- To provide a uniform pressure and temperature profile upstream of the thrust nozzle to get optimum use of the expansion flow in the divergent part of the nozzle.

Beside a high combustion efficiency, it is a main objective of the ram-combustor optimization to provide autoignition of the secondary combustion (if the temperature of the primary combustion products is adequate).

Since the usually required accommodation of an integrated booster is prohibitive to any installation (e.g. flameholders) in the ram-combustor, the aforementioned optimization goals must be achieved by proper design of

- the air injection into the ram-combustor
- the fuel injection.

It is obvious that there is no general approach to the optimization of these geometrical parameters. Optimiz- ation depends on the predetermined overall ram-combustor configuration (coaxial or lateral air injection) and the applied fuel components (particle loading, combustibility). Consequently, only some major aspects can be discussed in this place.

Air Injection

Generally, three major parameters are available to optimize air injection:

- air injection angle
- air injection velocity (i.e. area of air inlet into the ram-combustor)
- shape of the air inlet

Additionally, vanes or similar installation may be inserted in the air inlet in order to effect flow deviation or swirl.

A high angle of air injection applied to a lateral combustor configuration or swirl applied to a coaxial geometry may be favorable to combustion efficiency due to efficient mixing of air and fuel within a short distance. This is especially true for gaseous primary combustion products. If major portions of condensed phases are included in the primary combustion products and the equivalence ratio is on the lean side however, rapid and complete mixing of air and fuel-rich gas and the resulting cooldown of the condensed phases may be detrimental to combustion efficiency. The last statement also applies to autoignition. A penalty in terms of an impulse loss is inherent in any flow deviation of the ram air. The magnitude of the impulse loss is proportional to the sine of the flow deviation angle.

A high air injection velocity may improve mixing and combustion characteristics for lateral combustor configurations. It may be helpful to break up highly particle-laden jets of primary combustion products. However, the objection stated for the air injection angle concerning rapid and complete mixing of air and fuel applies to the air-injection velocity. A high air injection velocity is effected by throttling at the intake port to the ram combustor. Throttling of the air flow leads to a loss of total pressure. Total pressure loss being a performance related parameter should be kept low.

A particular shape of the air inlet(s) may be designed to induce high local turbulence or to adjust the circum- ferential or axial extension of air injection (e.g. using rectangular instead of circular intake ports). An appropriate geometry of the air inlet may be important for the combustion of fuel gas containing high portions of condensed phases. A sophisticated shape of the intake ports poses severe problems to the design of the port covers which seal the air ducts during the operation of the integrated booster.

The axial position of the air injection is a geometrical parameter which applies only to lateral air intake configurations. A downstream positioned side dump configuration of air injection has to use a high injection angle to get advantage of a recirculation to be formed in the combustor dome.

Fuel Injectors

duct near the intake port of the combustor by upstream or downstream orientated injectors similar to customary configurations of CRJ's. Primary combustion products of high temperature or with significant particle loading have to be fed into the dome of the ram-combustor. This being the case, the following geometrical parameters are available to optimize fuel injection:

- fuel injection angle relative to air injection
- number of fuel injectors
- angular and radial position of the fuel injectors
- fuel injection velocity
- shape of the fuel injector

A wide angle included by air and fuel gas injection (e.g. a perpendicular configuration) is desirable to provide proper mixing. On the other hand, a high amount of particle loading in the primary combustion products may be prohibitive to wide angles included by fuel injectors and ram-combustor axis. Significant erosion can be effected by particle-laden fuel flow directed to the ram-combustor wall. As a consequence, proper mixing of air and particle-laden fuel gas is not easily achieved for a coaxial ram-combustor configuration. The lateral combustor design usually allows an almost perpendicular injection of air and fuel gas.

The number of fuel injectors depends on the overall combustor configuration. One central fuel injector is frequently applied to a coaxial ram-combustor. This injector, however, may feed through several nozzles or ports ejecting to different directions. An impinging injector consisting of several injector nozzles installed at regular intervals in the air intake port is also applicable to a coaxial combustor configuration if particle loading is low for the primary combustion products.

For lateral configurations the number of fuel injectors usually is related to the number of air inlets into the ram-combustor. The angular and radial position of the fuel injectors are parameters mainly applying to the lateral ram-combustor configuration. Corresponding angular positions of air and fuel injection are desirable to ensure break up of particle-laden fuel flow. Furthermore, it is evident that fuel injection at an outer radial position is more favorable to mixing than a central fuel injection.

The optimization of fuel injection velocity depends on the composition of the primary combustion products, and the configuration selected for fuel injection. Plume expansion downstream of a sonic nozzle may provide sufficient distribution of gaseous primary combustion products. Particles needing time and distance for velocity relaxation possibly are not properly distributed by a sonic injector. Any sophisticated shape of the fuel injectors designed to induce particular flow patterns for mixing will only be effective for gaseous primary combustion products. A rapid deviation of particle-laden flow (e.g. by a vortex) will more likely result in a separation of gaseous and condensed phases than in an improved distribution of the particles due to the aforementioned two phase flow problems.

One important aspect has to be added concerning fuel injector optimization which is not related to combustion efficiency. While no major design restrictions are imposed when the primary combustion products are predominantly gaseous and have a low temperature, any sophisticated design of the fuel injectors will be highly complex if not infeasible for high temperature particle-laden fuel flow. Remembering that depositing and erosion risks are inherent in particle-laden flow and high heat flux exists in narrow gas pipes and bends, there should be two additional objectives for fuel injector design:

- To minimize the duct length between gas generator and ram-combustor

- To avoid complex flow patterns

The use of thermally resistant materials may be required for fuel injector components. For this purpose, all materials quoted in para. 3.3.1.2 referring to control valve components can be applied.

3.4.2 Thermal Insulation [10, 11]

Obviously, an insulation of the ram-combustor is required to protect the structure from the hot combustion gas. The application of an ablative layer is customary for the SPR system as well as for CRJ's. This material usually consists of a silicon rubber filled with different portions of carbonaceous or ceramic fibers or powder. Fillers are added to improve insulating properties to adjust ablation rate and to ensure sufficient mechanical properties of the pyrolized material. The ablative layer may be applied to the combustor by centrifugal action or by pressing depending on the viscosity of the uncured material.

Insulation thickness should be kept low since it determines the diameter being allowed for the integrated booster. An increase in insulation thickness results in an increase of booster length referring to a fixed booster mass and volume. The required thickness of the insulation depends on

- heat flux into insulation (depending on ram-combustor operating conditions)

- maximum temperature allowed for the structure

- operation time of the engine

- ablation rate

- insulating properties of the pyrolized matrix

- rigidity of the pyrolized matrix

Problems have been experienced concerning the last item with CRJ's. The pyrolized insulator was damaged by combustion instabilities occuring for equivalence ratios near the stoichiometric figure. Although the risk of combustion instabilities appears to be inferior for the SPR (according to available experience), the mentioned problem has to be considered for the design of the ram-combustor insulation.

3.4.3 Thrust Nozzle / 10, 11 /

All main aspects of thrust nozzle design for a SPR correspond to CRJ design. However, two problems have to be considered additionally which may arise when the combustion products of the ram-combustor include a significant portion of condensed material. This will occur when metals are used as high energy fuel components. In this case

- there will be a moderate risk of erosion or depositing which both may degrade the contour of the thrust nozzle

- two phase flow effects will increase expansion losses.

Both effects are not very detrimental to engine performance and may be minimized by adequate design of the convergent and divergent nozzle contours. The thrust nozzle is exposed to high thermal stress for a long duration. Consequently, the application of temperature resistant materials is mandatory. High melting metals cannot be used for the thrust nozzle due to the unacceptable weight penalty. Since large ceramic parts are extremely expensive and still imply a considerable manufacturing risk these are not exhibiting a proper solution either. Consequently,

- steel nozzles with thermally resistent coatings (spinels, zirconium-oxide)

- graphite nozzles } with ceramic coating or impregnation
- CFC nozzles

should be applied.

3.5 INTEGRATED BOOSTER AND TRANSITION

The subject and the inherent problem of integrated booster and boost-sustain transition phase are common to all ram-type engines. The ignition of the sustain propellant and the subsequent pressurizing of the gas generator are the only particular characteristics of the SPR transition. Since a short time span (usually below 200 milliseconds) is needed for this action it has to be included adequately in the transition sequence of

- booster burn-out
- booster nozzle separation
- opening of the port covers
- ignition of ram-combustion.

An additional device to ignite ram-combustion will not be needed for the high energy SPR, due to its auto-ignition feature. If an ignition device is required for a low or medium energy SPR system the same install-ation may be applied as for the CRJ.

4. DEVELOPMENT HISTORY AND STATE OF THE ART / 1, 2, 4, 12, 13, 14, 20 /

At the end of this lecture, some historical highlights of SPR development shall be presented along with a short summary of the present state of the art and anticipated future applications. Several SPR systems of different size were flight tested since 1955. One SPR system is operational in the Soviet SAM 6 missile. These flight vehicles are shown by figure 4.1. Available technical data are summarized below.

o   1954/1955:   Four SPR flight tests carried out by Thiokol

  - flight vehicle: diam: 2 in (50 mm); length: approx. 28 in (710 mm)
  - SPR engine: annular scoop air intake; fixed flow gas generator
  - tandem booster; ground launched

o   1958:   Three flight tests of FDR3 by Thiokol

  - flight vehicle: diam: 6,62 in (168 mm); length: approx. 4 ft 7 in (1,4 m)
  - SPR engine: conical nose air intake; coaxial ram-combustor configuration, fixed flow gas
                     generator
  - tandem booster; ground launched

o   1966:   Two flight tests of SPARM (solid propellant augmented rocket motor)

  - flight vehicle: modified airframe of the AQM37A drone
                     diam.: 13 in (330 mm), length approx. 12 ft (3,65 m)
                     (length without pitot probe and booster nozzle)
  - SPR engine: 2-dim ventral air intake; side dump ram-combustor; staged propellant to
                     demonstrate two level sustained thrust.
  - integrated booster, air launched
  - flight envelope: Mach 2.5; flight altitude 45000 ft (13 km); burn time 182 sec; range 74 nm (135 km)

o   1967:   Soviet SAM 6/Gainful becomes operational

  - type: Surface-to-air tactical anti-aircraft weapon
  - configuration: Slender cylindrical body with pointed nose, small cruciform wings near mid-
                     length and cruciform tail fins, four air inlet ducts between wings
  - length: 20 ft 4 in (6.2 m)
  - diameter: 1 ft (33 cm), span (max): 4 ft 1 in (1.24 m)
  - weight: 1212 lb (550 kg)
  - SPR engine: four lateral trailing shock air intakes; side dump ram-combustor; fixed

o   1976:   Two flight tests of an SPR experimental missile carried out by
                              the French ONERA

-   flight vehicle: diam.: 15,75 in (400 mm), length 18 ft (5.5 m), weight 1430 lb (650 kg)
-   SPR engine: four lateral bi-conic air intakes; side dump ram-combustor, rod and tube
                     grain configuration; medium energy self-pyrolizing propellant, fixed flow
                     gas generator
-   tandem booster, ground launched
-   flight envelope: ballistic flight; culmination 8600 ft (3 km) with Mach 2.1, approx. 50 sec of
                     sustained flight; range 19 nm (35 km)

o   1982:   Two test flights of the EFA experimental missile carried out by the
                              German MBB (Messerschmitt-Bölkow-Blohm GmbH) company

-   flight vehicle: diam.: 9.45 in (240 mm), length 12 ft (4.2 m)
-   SPR engine: four lateral half-axisymmetric air intakes, side dump ram-combustor configuration;
                     endburning grain; high energy propellant (40 % boron loading); fixed flow
                     gas generator
-   tandem booster, ground launched
-   flight envelope: one ballistic and one guided flight; altitude approx. 4300 ft (1500 m);
                     Mach 2.5; high g side maneuvers during second flight

o   scheduled: DR-PTV (ducted rocket propulsion test vehicle) by Hughes

-   flight vehicle: diam.: 7 in (178 mm)
-   SPR engine: two 2-dim lateral air intakes; side dump ram-combustor configuration;
                     endburning grain, medium energy propellant; fixed flow gas generator

-   integral nozzleless booster; air-launched
-   in the VFDR (variable flow ducted rocket) program, initiated in 1982, a throttleable propellant
                     of increased energy content will be developed for use in the DR-PTV system.

The present state of SPR technology shall be illustrated by some figures referring to

-   propellant energy content
-   propellant throtteability
-   ram-combustion efficiency

Concerning the energy content of the propellant, a hypothetical highly metallized formulation containing

50 %	boron
5 %	aluminum
20 to 25 %	AP
25 to 20 %	binder

and exhibiting heating values of

-   $1700 - 1800 \ \frac{Btu}{lb} \ / \ 40 - 42 \ \frac{MJ}{kg}$

-   $1050 \ \frac{Btu}{in^3} \ / \ 68 \ \frac{MJ}{dm^3}$

may be considered to be the present feasibility limit referring to processability, burning characteristics
and expulsion efficiency. Assuming reasonable parameters for performance calculation, a flight Mach number
of 2.5 and sea-level flight, a specific impulse of 14000 m/s can be attributed to a SPR using the afore-
mentioned propellant. This figure should only be understood as a rough hint for performance level.

As already mentioned in para. 2, turndown ratios up to 18 have been demonstrated for SPR gas generator
propellants. Nevertheless, referring to high energy propellant formulations, available information indicates
that turndown ratios between 5 and 10 more likely present the current state of the art.

Referring to afterburning, there exists considerable experience with low energy propellants without solid
fuel additives and with highly metallized high energy propellants (up to 40 percent boron loading). Less
experience is available for medium energy propellants with solid carbon or hydrocarbon additives and low
to zero metallic loading. However, increasing emphasis is placed on the investigation of this type of SPR
propellants. Summarizing the available experience, the following figures may be indicated as state of the
art (temperature rise) afterburning efficiencies:

-   low energy propellants   :   > 90 %
-   medium energy propellants
    (carbon or hydrocarbon fuel additives   :   85 to 95 % (depending on ram-combustor operating conditions)
    low to zero metal content)
-   high energy propellant   :   80 to 95 % (depending on ram-combustor operating conditions)

Problems concerning the design of control valves, injectors and thrust nozzles that arise from high temperature
particle-laden combustion products can be handled for state of the art propellants. However, sophisticated
design and ultimate use of modern materials and manufacturing technology are required for the construction
of these components.

Finally, some possible future applications of the solid propellant ram rocket shall be reviewed. As already
indicated in the introduction, the SPR is a favorable candidate for the propulsion system of medium to high
range tactical missiles of the next generation. In this field of course, the SPR competes with CRJ's and SFRJ's

The SPR provides the general advantages of ram-type propulsion referring to range, sustained supersonic speed and the capability to perform high g maneuvers even in the terminal flight phase. While the CRJ may be preferred for extreme range requirements and for reusable vehicles and the SFRJ may be preferably applied where simplicity, small size and low cost are the predominant requirements, there is a considerable domain of mission profiles where the SPR features are equivalent or superior to those of its competitors. These features are:

- direct control capability along with relative simplicity
- autoignition capability - reduced or eliminated flame out problems
- all solid fuels
- high volumetric heating value, application of high density fuels

The SPR may replace the solid rocket propulsion unit of operational missiles to upgrade their performance. Here the SPR is preferable when tne CRJ is incompatible with logistic considerations (e.g. liquid fuel) and the performance and system flexibility of the SFRJ are insufficient.

By now, SPR systems are in discussion or under development for the following applications:

Surface-to-surface/antiship: A high energy SPR propulsion unit (40 percent boron loading) is under development at MBB/FRG for use in the ANS (anti-navire-supersonique) missile. ANS (cf. fig. 4.2) is a French-German cooperative project carried out by SNIAS (societé nationale industrielle aérospatiale) and MBB. ANS shall replace missiles like Exocet, Otomat or Harpoon in the 1990's.

Surface-to-air: SPR application to future medium range SAM systems is discussed in the European part of NATO. Even for the short range low altitude surface-to-air mission, the application of the SPR provides advantages. A study considering a SPR Roland missile (cf. fig. 4.3) provides a significant potential for range increase and a tailchase capability which does not exist for the rocket-powered missile.

Air-to-surface: In this field, SPR application is considered in the USA. An air-to-surface mission with cruise flight at high altitude and terminal dive to the target may be accomplished using a simple fixed flow SPR system.

Air-to-air: Medium range air-to-air applications for the SPR are discussed in Europe and in the USA. Possibly, a throtteable variant of the DR-PTV may lead to a future AMRAAM (advanced medium range air-to-air missile) propulsion unit.

5. CONCLUDING REMARKS

This lecture reviewed design and performance characteristics of the solid propellant ram rocket. The advanced technical standard that has been presently achieved for this propulsion system allows its application with moderate development expense and relatively low technical risk.

While no general design or selection criteria can be provided for a missile propulsion system, the lecture tried to indicate major advantages as well as problematic aspects of the SPR system to be considered for propulsion system selection and to present a rough guide to performance tailoring and component design.

The author wishes to express his particular thanks to all members of the MBB-UA airbreathing propulsion group for their advice and assistance to compile all the information that formed the basis of this lecture.

REFERENCES

[1] Anonymous
Presentation to FMOD/MBB
United Technologies - Chemical Systems Division, Sunnyvale Calif. Juli 1980

[2] Besser, H.L.; Strecker, R; Weinreich, H.-L.
Advanced Variable Flow Ducted Rocket Propellart Development
Final Report - MBB TN-RT31-7/83, Nov. 1983

[3] Anonymous
Advanced Ducted Rocket Gas Generator
Volume I, Technical Proposal
United Technologies - Chemical Systems Division, Sunnyvale Calif. May 1982

[4] Besser, H.-L.
Investigation of Boron Solid Propellant Combustion in Ducted Rockets
AGARD-CP-307, Ramjets and Ramrockets für Military Applications
London, Oct. 1981

[5] Strecker, R.
Private communication about gas generator propellants

[6] Gordor, S; McBride, B.
Computer Program for Calculation of Complex Chemical Equilibrium Compositions,
Rocket Performance, Incident and Reflected Shocks and Chapman-Jouguet-Detonations

[7]   Thomaier, D.
        Untersuchung eines nicht-linearen Regelkonzepts für den Gasgenerator des Feststau-Antriebs
        MBB-TN-RT31-18/78, June 1978

[8]   Thomaier, D.
        Private communication about fuel flow control concepts for the solid propellant ramrocket

[9]   Engl, E.; Engel, H.
        Private communication about control valve design

[10] Henkel, H.
        Private communication about temperature resistant materials and ablators

[11] Crispin, B. et al
        Feststau-Raketenantrieb
        MBB-Präsentation vor dem BMVg und BWB, June 1976

[12] Weinreich, H.-L.
        Skriptum der Vorlesung "Raketen- und Stauantriebe"
        Hochschule der Bundeswehr, 8014 Neubiberg, 1984

[13] Anonymous
        History of the Ducted Rocket
        Thiokol

[14] Marguet, R; Ecary, C; Cazin, P.
        Studies and Tests of Rocket Ramjets for Missile Propulsion
        4th Int. Symp. on Air-Breathing Engines
        Lake Buena Vista, Orlando, Florida, April 1 - 6, 1979

[15] Henkel, H.
        Experimentelle Untersuchung von Gasverteilern und Brennkammererprobung plasmabeschichteter
        Schubdüsen für die Feststoff-Staustrahlrakete als Vorbereitung der Funktionsuntersuchungen
        des Windkanal-Versuchstriebwerks
        MBB TN-RC1-35/71, Nov. 1971

[16] Engl, E.
        Gasverteiler und Mischsysteme bei Staustrahlraketen mit vier Diffusoren
        MBB TN-RT34-6/76, May 1976

[17] Thomaier, D.
        Feststau-Brennversuche mit 226 Ø Triebwerken im "Connected-pipe"- und Freistrahl-Betrieb
        MBB TN-RT31-20/76, Nov. 1976

[18] Besser, H.-L.
        Untersuchungen zur Optimierung der Luft- und Brennstoffzuführung am Feststau-Antrieb bei
        Verwendung von Bor-Treibstoffen
        MBB TN-RT31-20/80, Nov. 1980

[19] Jell, C.S.
        Air Intake Aerodynamics and Operational and Installation Effects on Missile Powerplant
        Performance
        AGARD LS-98/14 Supplement , Missile Aerodynamics, March 12-16, 1979

[20] Jane's
        Pocket Book 10 - Missiles

Fuel Tank | Ram Combustor | Conventional Liquid Fuel Ramjet (CRJ)

Air Intake — Fuel Flow Control and Injection
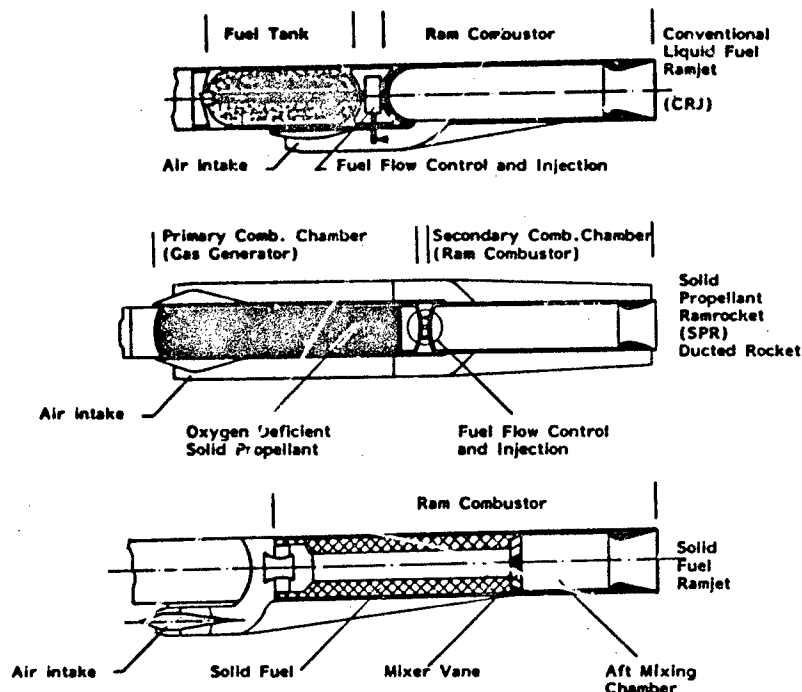
Fig. 2.1: Comparison of Different Ram-Type Propulsion Systems

Primary Comb. Chamber (Gas Generator) | Secondary Comb. Chamber (Ram Combustor)

Solid Propellant Ramrocket (SPR) Ducted Rocket

Air intake

Oxygen Deficient Solid Propellant | Fuel Flow Control and Injection

Ram Combustor

Solid Fuel Ramjet

Air intake — Solid Fuel | Mixer Vane | Aft Mixing Chamber
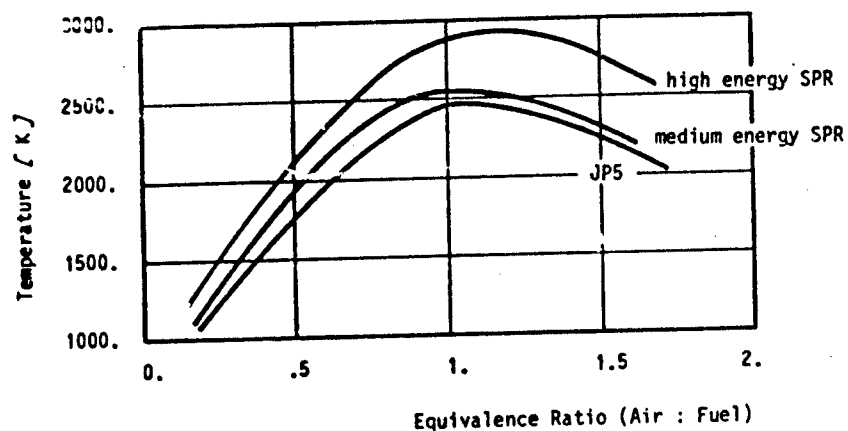
Fig. 2.2: Combustion Temperatures of Different Propellants and Fuels

Equivalence Ratio (Air : Fuel)

Temperature [K]

high energy SPR
medium energy SPR
JP5

- Propellant
- Grain Configuration | Ram Combustor

Air Injection | Thrust Nozzle
Thermal Protection
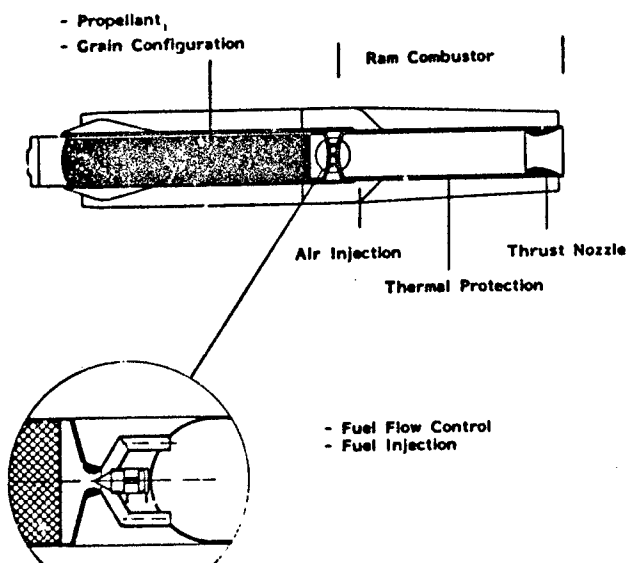
Fig. 3.1: Components of a Solid Propellant Ramrocket (SPR)

- Fuel Flow Control
- Fuel Injection

LEGEND:
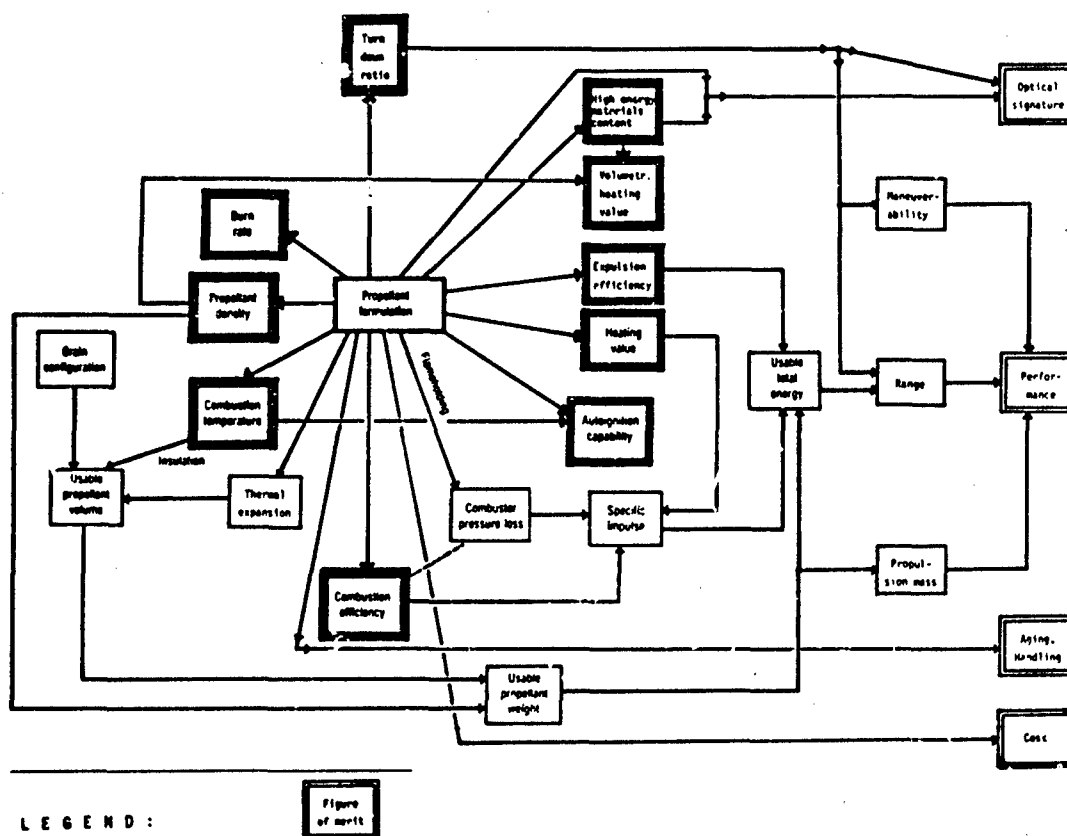
Fig. 3.2: Interrelationship Between the Propellant Formulation and Different Aspects of the SPR Propulsion System

Oxidizer	Chemical Formula	Reaction Products	Specific Gravity, g/cm³	Oxygen Content, %	Melting Point/ Boiling Point of Reaction Product, R
Nitronium perchlorate	NO_2ClO_4	..	2.22	66.0	-
Nitrosyl perchlorate	$NOClO_4$	-	2.17	61.8	-
Lithium perchlorate	$LiClO_4$	LiCl	2.43	60.1	1397/2903
Ammonium perchlorate	NH_4ClO_4	N_2, HCl, H_2O	1.95	54.5	-
Sodium perchlorate	$NaClO_4$	NaCl	2.54	52.2	1933/3035
Potassium perchlorate	$KClO_4$	KCl	2.53	46.1	1883/3191
Lithium nitrate	$LiNO_3$	Li_2O	2.38	69.6	3317
Ammonium nitrate	NH_4NO_3	N_2, H_2O	1.73	60.0	-
Sodium nitrate	$NaNO_3$	Na_2O	2.26	56.5	-
Potassium nitrate	KNO_3	K_2O	2.11	47.5	>3600
HMX	$(CH_2N_2O_2)_4$	-	1.90	43.2	-
RDX	$(CH_2N_2O_2)_3$	-	1.70	43.2	-

Note: HMX = cyclotetramethylene tetranitramine, RDX = cyclonite (cyclotrimethylene trinitramine)

Oxidizer	Amount of Uncondensed Species	Performance	Burn Characteristics	Manufacturing Aging	Experience	Overall
Nitronium perchlorate	++	++	+	--	-	-
Nitrosyl perchlorate	++	++	+	--	-	-
Lithium perchlorate	-	++	+	-	0	0
Ammonium perchlorate	++	+	+	+	++	+
Sodium perchlorate	--	+	+	-	0	--
Potassium perchlorate	--	0	+	+	0	-
Lithium nitrate	--	++	+	--	-	-
Ammonium nitrate	++	+	+	--	0	-
Sodium nitrate	--	0	-	-	0	-
Potassium nitrate	--	0	-	-	0	-
HMX	++	+	0	--	0	0
RDX	++	0	0	--	0	-

Legend: ++ very good, + good, 0 fair, - marginal, -- bad

Note: HMX = cyclotetramethylene tetranitramine, RDX = cyclonite (cyclotrimethylene trinitramine)

Fig. 3.3b: Oxidizer Selection Trade

Ingredient	Oxygen Requirement gram oxygen/gram fuel	Density lb/in³	Density g/cc	Heat of Combustion Btu/lb	Heat of Combustion kJ/kg	Heat of Combustion Btu/in³	kJ/dm³	State at ambient condition
Hydroxyl-terminated polybutadiene (HTPB)	3.19	0.0336	0.930	18045.	41972.	606.3	39036.	l
Carboxyl-terminated polybutadiene (CTPB)	3.20	0.0347	0.960	1791?.	41664.	621.5	40014.	l
Isodecylpelargonat (IDP)	2.95	0.0311	0.860	16126.	37508.	501.5	32288.	l
Polyisobutylene (Oppanol)	3.42	0.0329	0.910	18713.	43526.	615.6	39634.	l
Catocene	2.54	0.0466	1.29	14257.	33161.	664.4	42776.	l
Carbon amorphous	2.66	0.0587	1.625	14095.	32784.	827.4	53271.	s
Graphite	2.66	0.0813	2.250	14095.	32784.	1145.9	73777.	s
Polydicyclopentadiene (Zecorez)	3.15	0.0397	1.100	17535.	40786.	696.1	44817.	s
Cross-linked polystyrene (CLPS)	3.07	0.0381	1.054	17139.	39865.	653.	42042.	s
Poly-(alpha-methylstyrene) (PAMS)	3.11	0.0387	1.07	17317.	40279.	670.2	43150.	s

Fig. 3.4: Properties of Carbon and Hydrocarbon Fuels
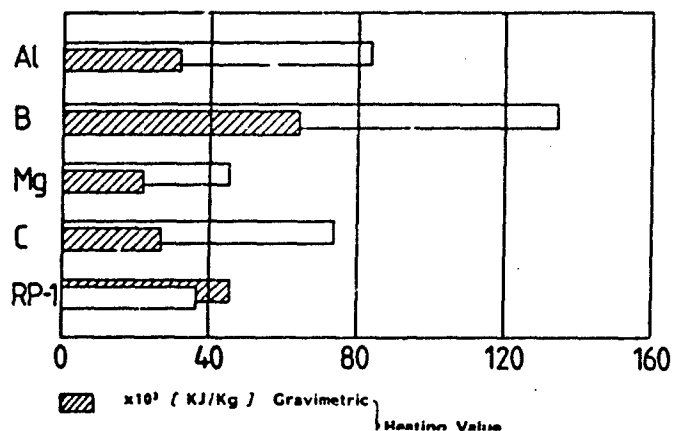
Fig. 3.5: Heating Values of Different Metallic Fuels

Fuel Additive	Density		Heat of Combustion			
	lb/in³	g/cm³	Btu/lb	kJ/kg	Btu/in³	kJ/dm³
B (amorphous)	0.0802	2.22	25 486.	59 280.	2044.	131 602.
Al	0.0975	2.70	13 356.	31 056.	1302.	83 878.
Mg	0.0629	1.74	10 636.	24 739.	669.	43 046.
Zr	0.2345	6.49	5 177.	12 043.	1214.	78 162.
Ti	0.1626	4.5	8 487.	19 744.	1380.	88 849.
B₄C	0.0903	2.5	22 159.	51 532.	2001.	128 831.

Fig. 3.6: Properties of Different Metallic Fuels
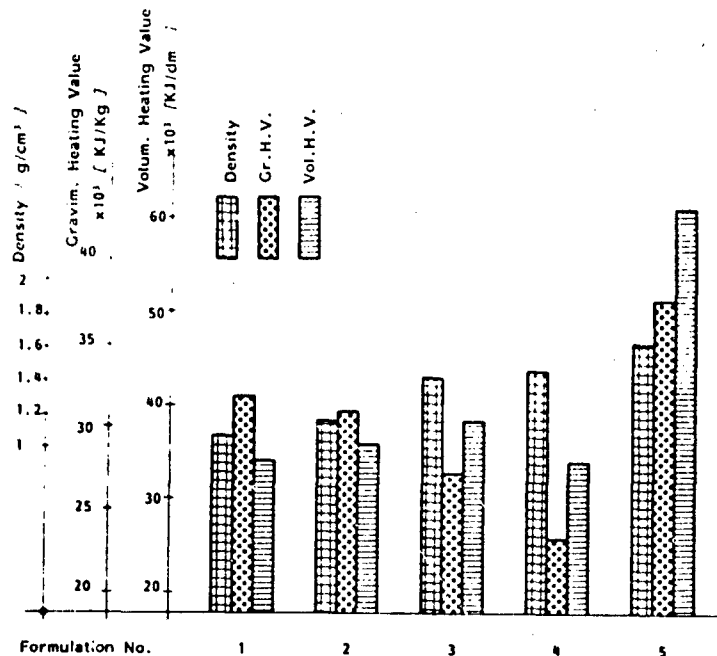
Fig. 3.7: Density and Heating Values of Different Metallized and Non-Metallized Propellant Formulations
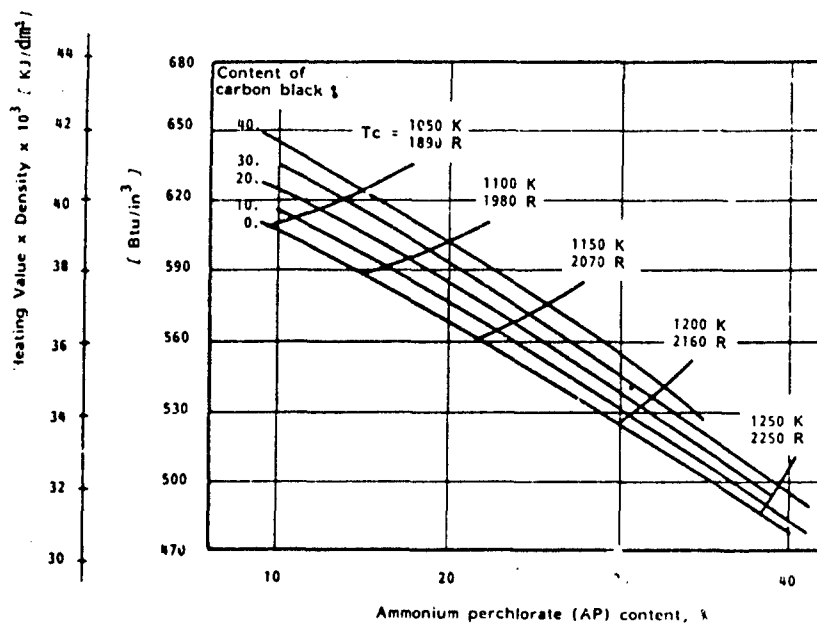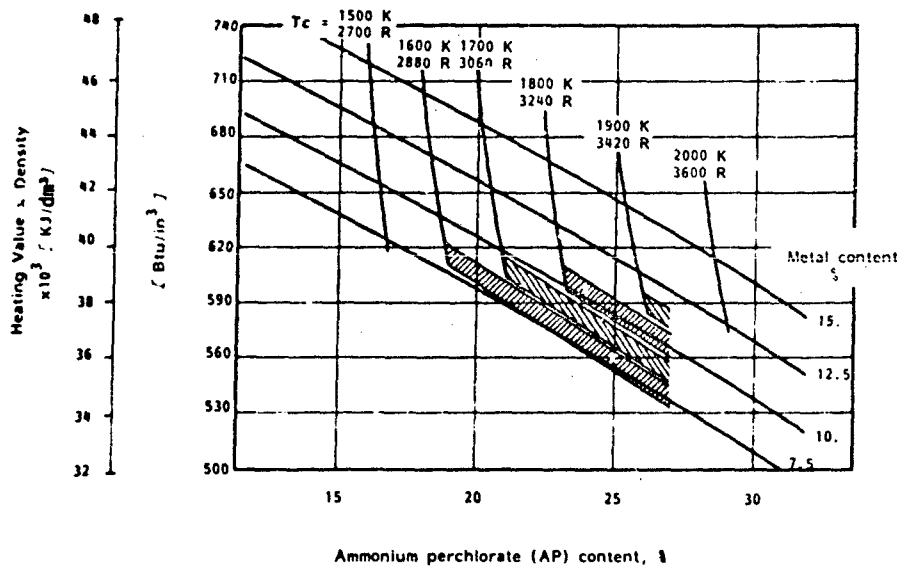
Fig. 3.9: Screening of a Metallized Propellant
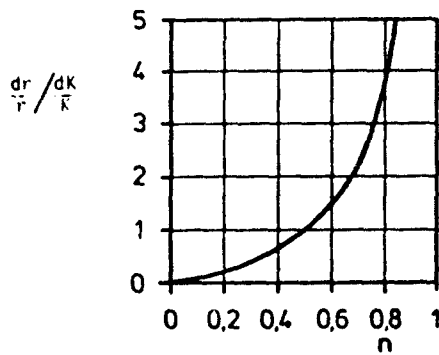
Fig. 3.10: Influence of the Pressure
Exponent on the Variation of K-Ratio
and Burn Rate
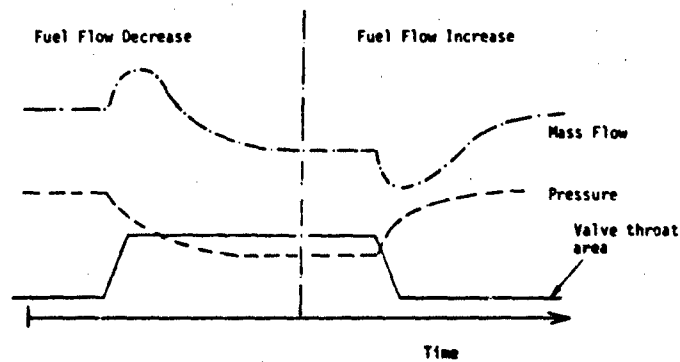
Fig. 3.11: Control Characteristic of Pressure
Sensitive Propellants
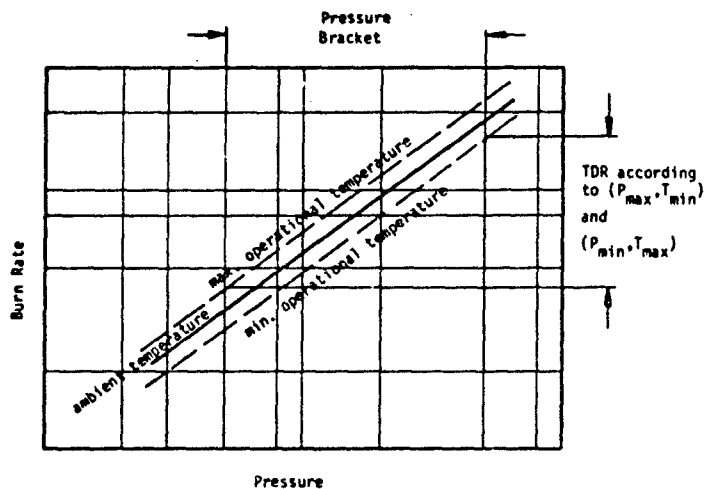
Fig. 3.12: Dependence of the Achievable TDR on Pressure and Temperature Brackets

Propellant Temperature Sensitivity σp
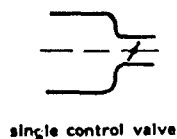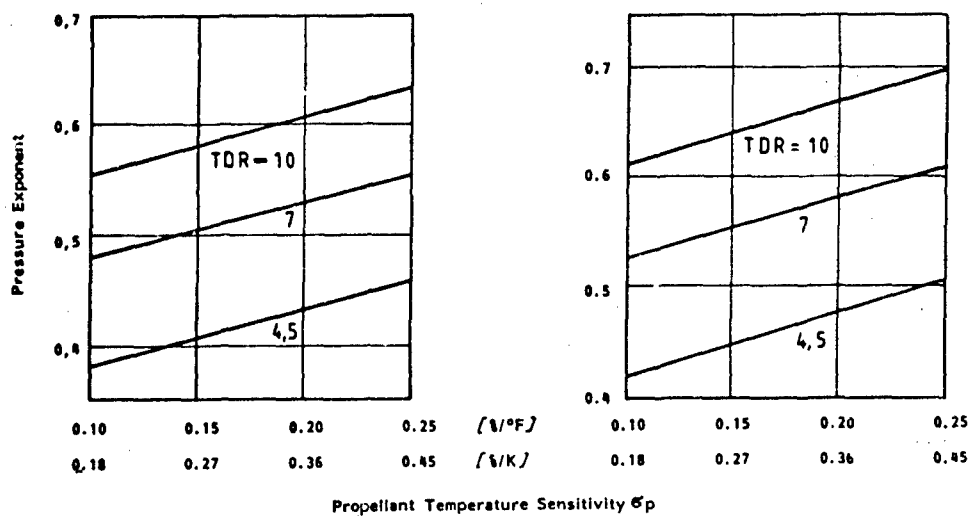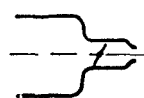
single control valve   control valve · second sonic nozzle

Fig. 3.13: Parameters Limiting the Achievable TDR
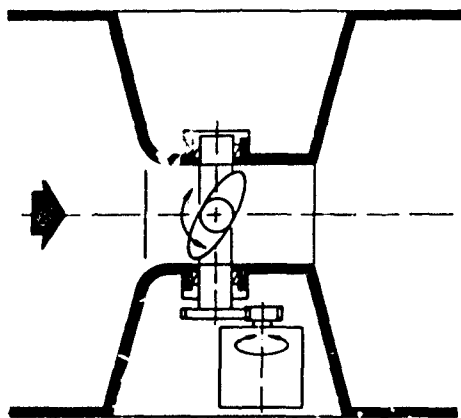
Fig. 3.14: (1) Rotating Blade/Butterfly Valve   (2) Translating Plunger
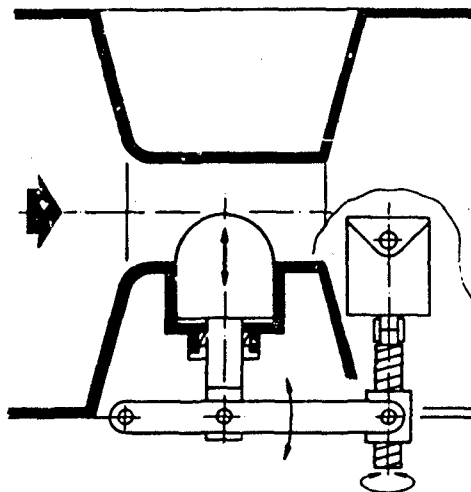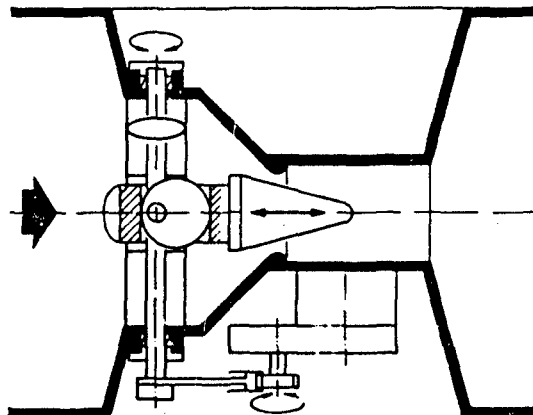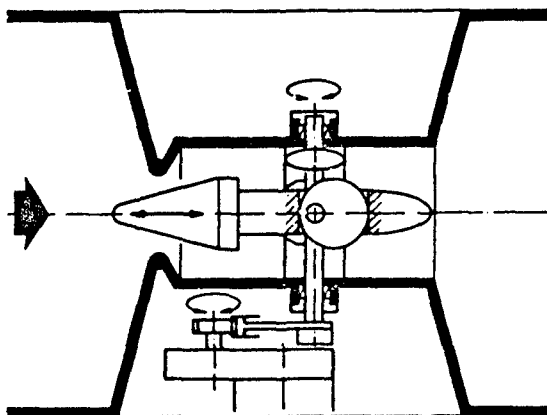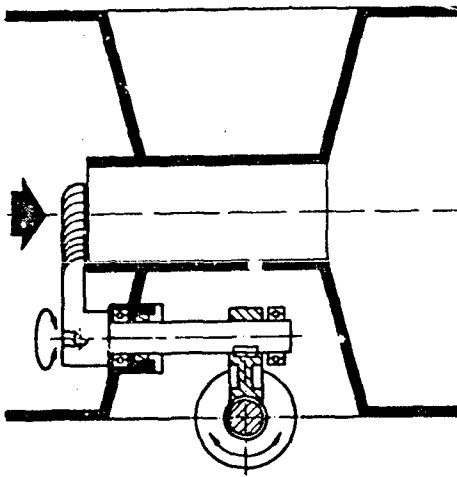
Fig. 3.14: (5) Gate Valve
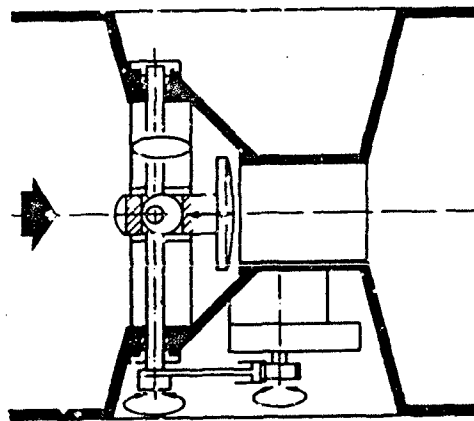
(6) Disk Valve
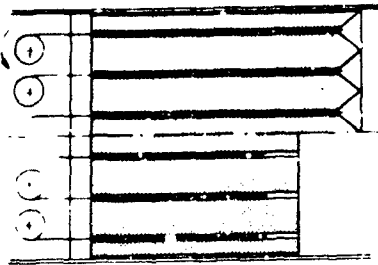
Fig. 3.15: Retractable Silver Wires
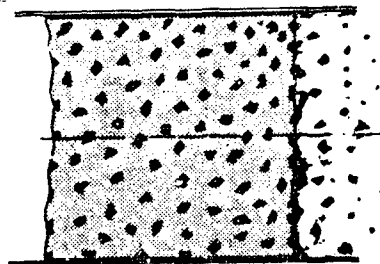
Fig. 3.16: Matrix Grain
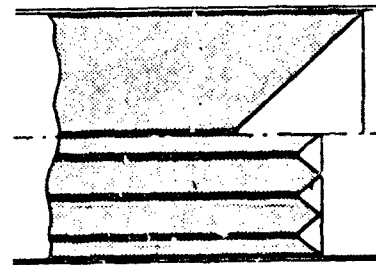
Fig. 3.17: Coaxial Propellants

Four Inlet Side Dump

(MBB Design Study)

Two Inlet Side Dump

Gas generator
igniter

Gas generator

Booster/gas generator arm fire device

Port cover

(DR PTV Ramcombustor
[1])

Inlet

Injector

Booster
Propellant

Coaxial

(MBB Windtunnel-tested
Engine; Half-Integrated
Configuration)
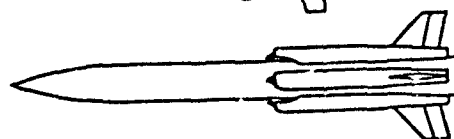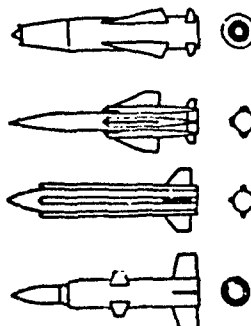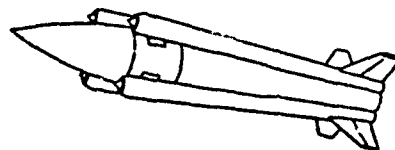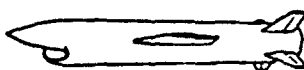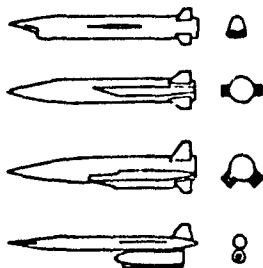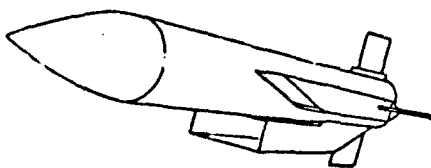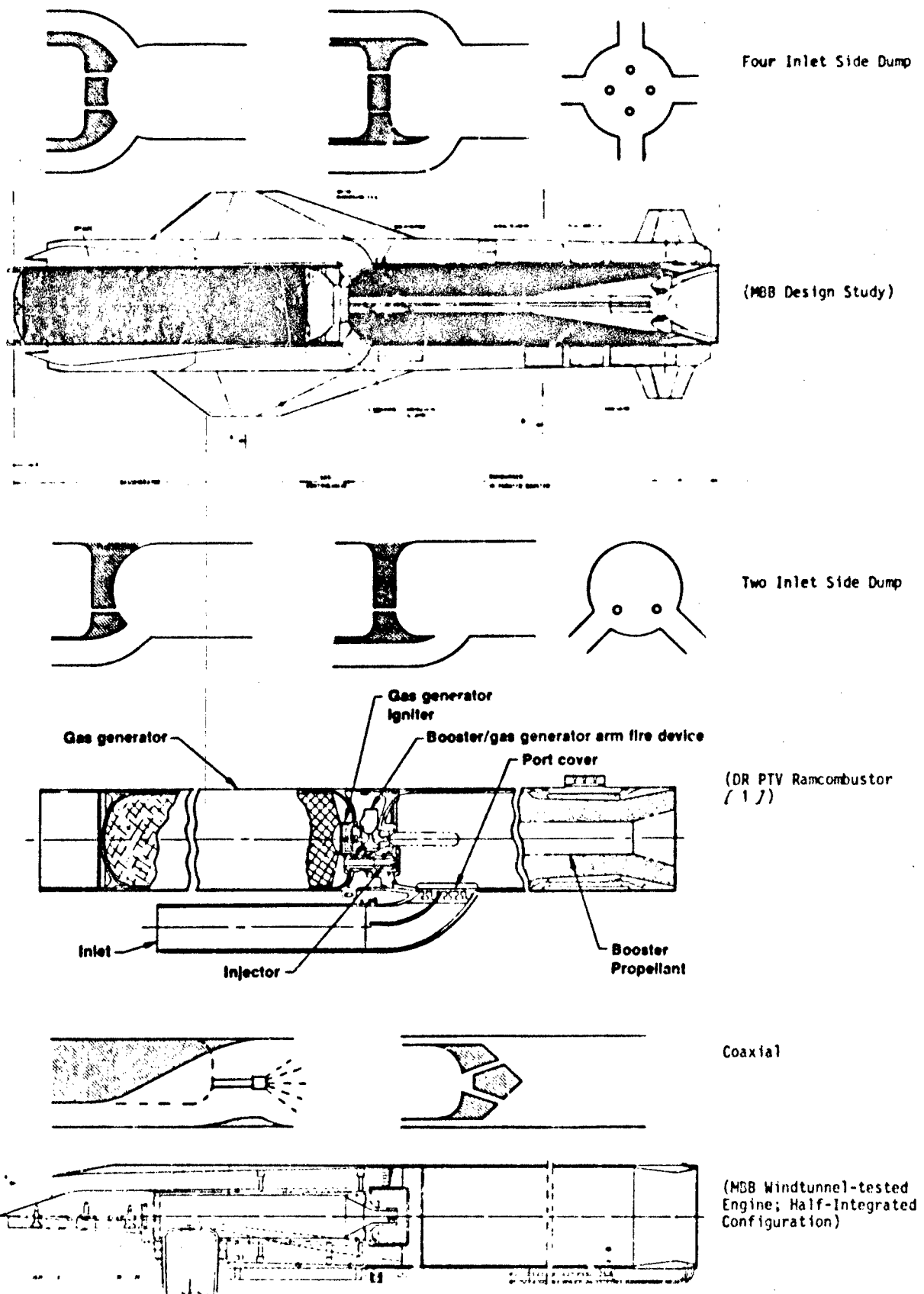
Fig. 3.19: Ramcombustor Configurations
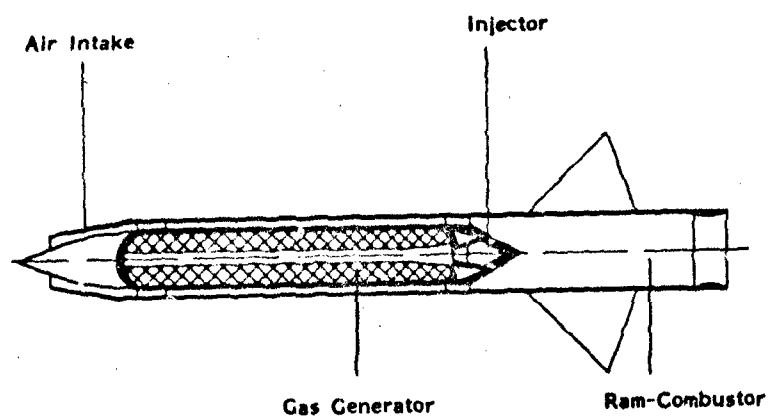
THIOKOL - FDR3 (1958) [13]
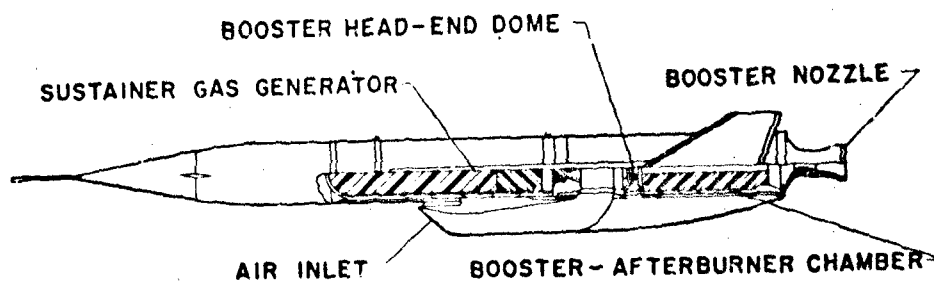
THIOKOL - SPARM (1966) [13]
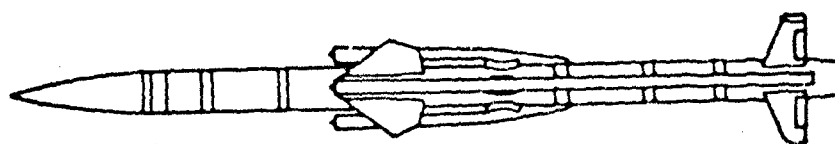
USSR - SAM 6 (1967) [20]
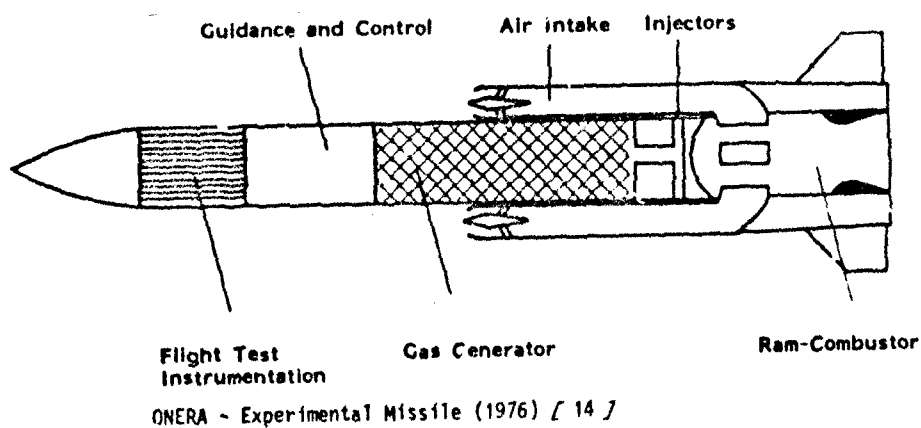
ONERA - Experimental Missile (1976) [14]

Fig. 4.1a: Operational or Flight Tested SPR Systems
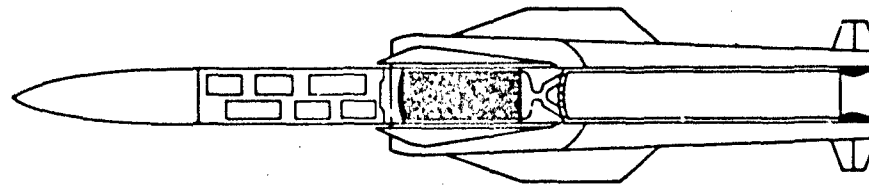
| Nose Cone
Recovery System | Electronics Module
(Guidance and
Control, Telemetry) | Ramrocket Propulsion Unit |

MBB - EFA Experimental Missile (1981) [4]
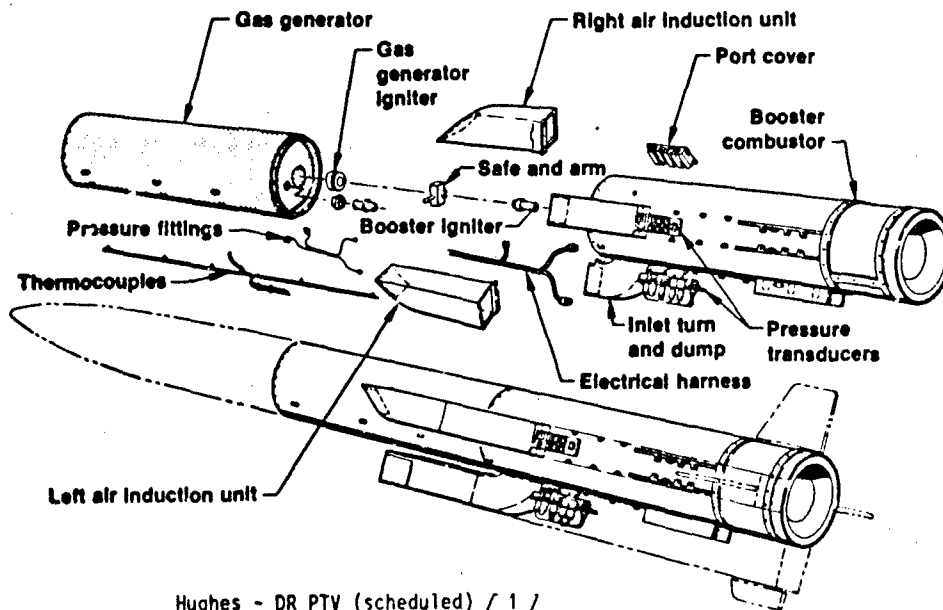
Hughes - DR PTV (scheduled) [1]

Fig. 4.1b: Operational or Flight Tested SPR System (no uniform scale)
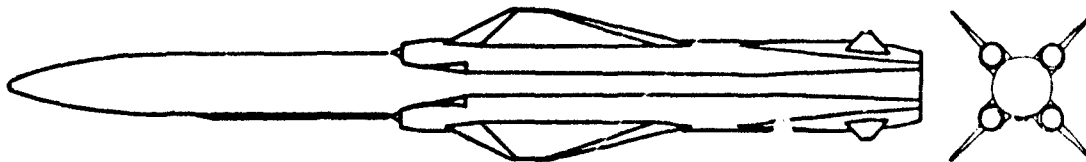
Fig. 4.2: SNIAS/MBB Anti-Navire-Supersonic (ANS),
Anti-Ship Missile Project
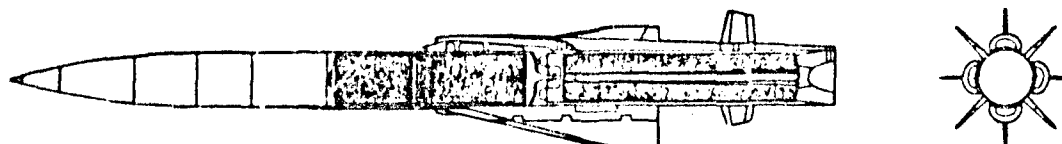
Fig. 4.3: SPR Powered Roland Missile; MBB Design Study

RAMJETS WITH SUPERSONIC COMBUSTION

Frederick S. Billig
The Johns Hopkins University
Applied Physics Laboratory
Johns Hopkins Road
Laurel, Maryland 20707

SUMMARY

A terse look at the requirements for high speed-long endurance missiles and the virtues of airbreathing propulsion are presented to support arguments for developing ramjets that employ supersonic combustion. A review of general classes of inlet configurations leads to the selection of multiple inward turning scoop (ITS) configurations to serve as the basis for engine cycle analysis. A fixed geometry ITS inlet is shown not only to have an attractive performance potential, but to be quite versatile for use in a variety of engine configurations. When it is designed to have full air capture at a flight Mach number M_0 somewhat below the cruise Mach number, it can produce high pressure recovery over a wide M_0 range with high air capture during climbout at low angle of attack α as well as during cruise at near optimal α. The geometry of a family of ITS inlets is examined to determine optimal configurations for various constraints and to provide quantitative values for the flow properties for entering the combustor analysis.

A flow model for the combustion process that includes the major features that have been observed in experiments serves as the basis for determining the pressure rise in the shock train that precedes combustion and the conditions at the combustor exit. Calculations for simplified frictionless flow with constant specific heats show that 1) the combustor area ratio is set by the acceleration requirements at the end of boost; 2) the combustor operates in a subsonic mode at low M_0 and in a supersonic mode at high M_0; and 3) optimal performance occurs when the combustor inlet conditions correspond to moderate inlet contraction ratios. Computed values for the net engine force coefficient show that forebody drag must also be considered to determine the optimal overall engine configuration.

NOMENCLATURE

A	cross-sectional area
A_e	effective flow area
A_s	physical area
A_i	projected area of inlet
A_w	surface area
C_D	forebody drag coefficient $= D/q_0 A_R$
C_{DADD}	additive drag coefficient $= D_{ADD}/q_0 A_R$
C_F	net force coefficient
$\bar{C}_f$	mean skin friction coefficient
C_T	thrust coefficient
D	drag
D_{ADD}	additive drag
D_4	diameter or hydraulic diameter at station 4
ER	equivalence ratio
ER_{eff}	effective equivalence ratio $= ER \cdot \eta_c$
f	fuel/air weight ratio
f_s	stoichiometric fuel/air weight ratio
F	net force $= T-D-D_{ADD}$
ϑ	stream thrust $= pA + \rho Au^2$
k_1	constant in Eqns. 10, 11
L	lift
M	Mach number
M_{FC}	Mach number at which inlet obtains full capture at $\alpha = 0°$
η	molecular weight
p	pressure
q	dynamic pressure
R	gas constant
s	axial distance from origin of shock train
s_d	axial distance between fuel ports and end of shock train
T	temperature

α	angle of attack
β	inner scoop angle with respect to missile axis
γ	ratio of specific heats
δ	boundary layer thickness
δ^*	boundary layer displacement thickness
δ_c	half-angle of conical compression surface
ϵ	Crocco parameter for pA processes
$\tilde{\epsilon}$	Crocco parameter for processes between stations s and e
η_c	combustion efficiency
η_{KE}	inlet kinetic energy efficiency
η_N	nozzle efficiency
θ	boundary layer momentum thickness
$\bar{\theta}$	flight path angle
θ_w	angle between cone axis and ray passing through scoop leading edge
ρ	density
τ_w	wall shearing stress
ϕ	roll angle
ψ	smile angle of ITS scoop
$\tilde{\psi}$	sector angle of scoop duct
ψ_w	flow angle along conical ray

Subscripts

0	free stream conditions
1	conditions ahead of scoop lip shock
2	conditions in plane of crotch in side plate
3	conditions at end of supersonic compression processes
3'	conditions corresponding to downstream of a normal shock at station 3
4	conditions ahead of shock train
5	conditions at combustor exit
6	conditions at nozzle exit
c	conditions on cone surface
CR	flight conditions corresponding to cruise
e	effective; conditions at origin of ϵ = constant heat addition
EOB	flight conditions corresponding to end of boost
f	fuel
s	conditions at downstream end of shock train
w	wall

Superscript

$-$	mean value
$'$	conditions downstream of normal shock
$*$	conditions at the sonic point

INTRODUCTION

The attractiveness of the supersonic combustion ramjet as the powerplant for a high-speed missile has been recognized for more than twenty-five years. Arguments supporting the use of the scramjet cycle for a missile and comparison of performance with engines using subsonic combustion were presented in Ref. 1. The effective defense against future air-to-surface missiles, on-the-deck attacks, and IRBM attacks will require major reduction in time-to-intercept of the defense missiles, compared with presently available surface-to-air missiles. For the foreseeable future, effective intercept of ballistic missile warheads, as well as air-supported attacks, will occur within the atmosphere, because the atmosphere provides the best means for distinguishing between the ballistic warhead which must be destroyed and extraneous re-entering material accompanying the warhead to which firepower must not be diverted. The margin of superiority of ramjet missiles to rockets increases rapidly as missile speed increases. To provide equivalent perfor-mance to a Mach 7 supersonic combustion ramjet vehicle at sea level, a rocket would have to have roughly three times as much weight. Included in the open literature (see e.g., Ref. 2-4) are a number of super-sonic combustion ramjets that have progressed through the stage of free-jet engines tests.

Before proceeding into the main discussion of this paper, some clarification in semantics is needed to differentiate between the conventional subsonic combustion ramjet (CRJ), the scramjet and a hybrid cycle, the dual-combustion ramjet (DCR). As used herein, the CRJ is an engine cycle wherein there is a normal shock structure in the inlet compression system for all operating conditions and all of the heat addition takes place in subsonic flow. All of these ramjets must be boosted to some supersonic end-of-boost Mach

number (M_{EOB}) by a rocket engine. Scramjet will refer to an engine cycle which over at least som⸱ ⸱rt of
the Mach (M_0) altitude (Z) equivalence ratio (ER) operating envelope, heat is released in superso⸱ ⸱ tlow.
Most practical scramjet engines for missile applications must operate at high ER upon the ramjet tai⸱⸱⸱⸱⸱ at
an $M_{EOB} \leq 4$, and at this modest speed a normal shock structure will be present and some, if not all, ⸱ ⸱e
heat will be released in subsonic flow. This cycle is often referred to as a dual-mode engine, but ⸱⸱ ⸱⸱⸱
paper no distinction w'll be made from the scramjet. Dual-mode should not be confused with the DCR, ⸱ ⸱⸱⸱
is a hybrid engine cycle that combines a CRJ with a scramjet (Ref. 5). The moderate M_{EOB} for the scra⸱ ⸱⸱
or DCR is a consequence of the optimization of a tandem or integral-rocket-boosted, fixed-geometry scram⸱⸱
system which dictates that $0.55 \, M_{CR} \leq M_{EOB} \leq 0.6 \, M_{CR}$, where M_{CR} is the Mach number during high-altitude
cruise. Typically, $6 \leq M_{CR} \leq 8$; thus $M_{EOB} \approx 3-4$. Since cost and complexity are key considerations in
determining missile feasibility, variable geometry and active cooling of the airframe are not practical.

Schematic illustrations of the scramjet and DCR are shown in Fig. 1. Nose entry configurations are
shown, but aft entry configurations such as the so-called underslung engine (Ref. 6) have also received
considerable attenticn. Inlets for these engines are of the external-internal compression type wherein the
pressure rise is obtained via a series of weak shocks and regions of isentropic compression, a portion of
which occurs in the internal ducting. Typical inlet contraction ratios, A_1/A_3, vary from 4 to 8 (see Ref.
7). Whereas the inlet flow is fully contracted at station 3, additional length must be added in an isolator
section to prevent combustion-induced disturbances from causing adverse interactions in the inlet (Ref. 8).
The combustor generally has a diverging area to permit high heat release at low M_0. In some configurations,
a step increase in cross-sectional area at the combustor entrance has been used (see e.g., Refs. 9, 10) to
help mitigate combustor-inlet interactions and to enhance flame-holding. The exhaust nozzle has either a
straight or a contoured shape and the demarcation between combustor and nozzle is the change in shape rather
than the point of completion of heat release. All of the fuel can be added at the combustor entrance or
fuel injectors can be staged at several axial stations. The latter method can be used as a means of adjusting
the effective area ratio of the combustor thereby enhancing p rformance, but at the expense of weight,
complexity and cost. Instream injectors have been given consideration, but with some trepidation due to the
difficulty in providing adequate structural integrity. Injection from ports in the wall is preferred.

If the scramjet must operate at $M_0 < 4.5$, which is generally the case, the static temperature in the
combustor is below the autoignition point of conventional hydrocarbon fuels such as JP-5 and RJ-5. For
these, some type of piloting system is needed and piloting has proven difficult. Even when ignition has
been obtained, flame spreading has been minimal and reaction rates slow compared with typical residence times
of 1-2 ms. Highly reactive fuels such as HiCal 3-D (a blend of mono and higher ethyldecaboranes) and penta-
borane-hydrocarbon blends autoignite and burn rapidly at static temperatures at least as low as that corres-
ponding to $M_0 \approx 3.5$ and have been used in free-jet engine test demonstrations of the scramjet (Ref. 2).
Unfortunately, these fuels are expensive, toxic, pyrophoric at room conditions, and no longer in production.
It was these limitations which led to the concept of the DCR.

The DCR is conceptually a scramjet with a large pilot burner. The inlet airflow is split so that 20-
25 percent is directed into a "dump-type" subsonic combustor, herein called the gas generator. Because the
flow is subsonic, the static temperatures are higher and ignition and combustion can be obtained as in any
well designed CRJ. From both an engine cycle efficiency standpoint and a design simplicity standpoint, it is
advantageous to add all of the fuel in the gas generator and eliminate the need for a fuel injection system
for the main supersonic combustor. This means that for all overall engine fuel/air equivalence ratio (ER)
requirements greater than the value corresponding to the fractional air flow split (gas generator/total), the
gas generator operates in excess of stoichiometric. The bulk of the air captured by the inlet is ducted
supersonically around the gas generator to the main combustor entrance. Refer to Fig. 1b. The downstream
portion of this duct serves as a combustor-inlet isolator. The hot, generally fuel-rich effluent from the gas
generator mixes and reacts with the main flow before passing through the exhaust nozzle. Presuming that the
gas generator can operate efficiently over a wide ER range, the designer can tailor the air split and the area
of the discharge port of the gas generator to obtain optimal performance for a given application.

INLET DESIGN

Before presenting in detail the current understanding of the physical processes and the state-of-the-art
of the analytical tools that are used to analyze supersonic combustion, various concepts for scramjet and DCR
inlet designs will be discussed. The literature is rich (see e.g., Ref. 11) with the results of engine cycle
calculations that give the requirements for air capture, inlet compression ratio and efficiency that result in
a competitive propulsion cycle. Some general guidelines are: the inlet contraction ratio should be sufficient
to provide $0.35 \leq M_3/M_0 \leq 0.50$; at M_{EOB} the air capture ratio A_0/A_1 should be no less than 0.6 to 0.7 of the
maximum air capture ratio; the inlet kinetic energy efficiency prior to any shock structure in the isolator
should be no less than 0.95; the cowl lip and wave drag must be low; and operation at angles-of-attack, α, of
12° or greater should be tolerated without causing engine unstart. These requirements have been paramount in
the design strategies employed in the development of the three types of inlets shown in Fig. 2.

Figure 2a is a modular or Busemann-type inlet wherein the flowfield into each inlet module is in effect a
section of a fully internally contracting flowfield that has been cut along streamlines and turned inside out.
The swept "cowl" leading edges are shaped to follow the intersection of the first compression wave with the
captured free streamtube when the inlet is operating at its design M_0 and at $\alpha = 0°$. The sweep angles are
typically greater than 60°, therefore the leading edge drag and heat transfer rates are minimal. Theoretical
tools have been developed (see e.g., Ref. 12) which can provide contours for compression surfaces for any
desired contraction ratio up to that corresponding to $M_3 = 1$. Practical designs are limited to contraction

a) Supersonic combustion ramjet (scramjet)

b) Dual combustion ramjet.
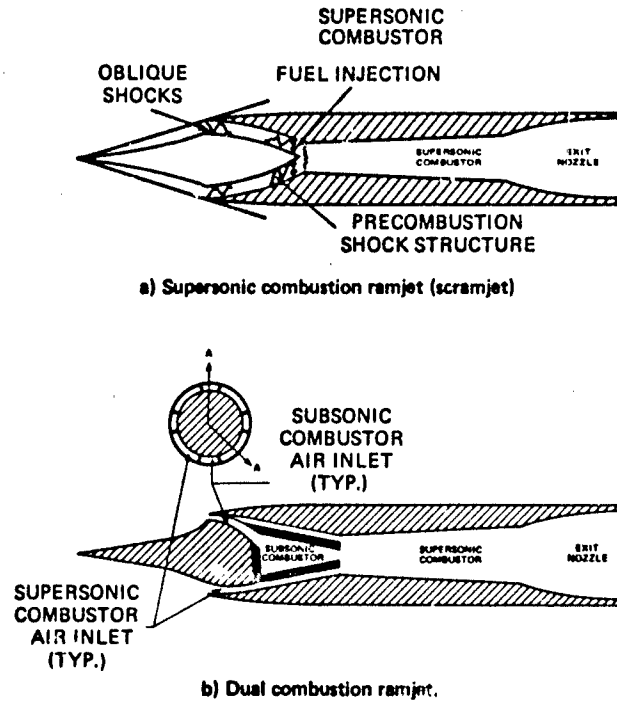
Fig. 1   Schematic illustrations of hypersonic ramjet engines.

a) SECTIONAL VIEW OF MODULE ON BUSEMANN TYPE INLET

b) SIDE VIEW OF SHOCK TRAP TYPE INLET
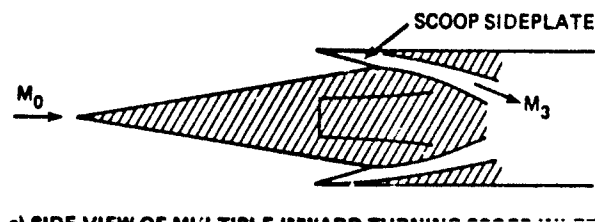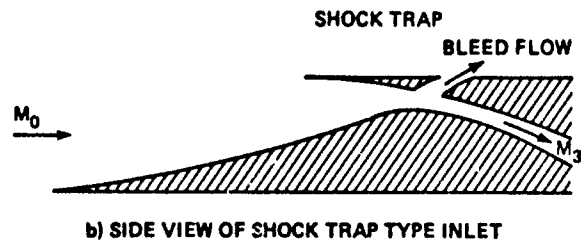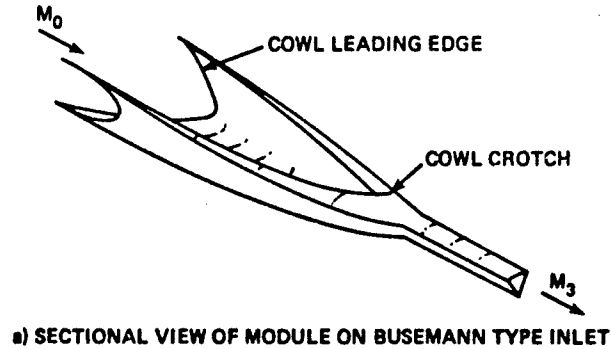
contraction than would be allowable in the fully internally contracting counterpart because the controlling area to meet the starting criterion is the cross-sectional area of the duct at the crotch station rather than the cross-sectional area at the cowl leading edge station.

Designs can be developed to bring a cylindrical capture tube into any number of modules, but most attention has been given to three and four module designs, as typified by the photographs shown in Fig. 3 of inlets tested over the range of Mach 4-10. The modular design brings the flow to the periphery of the engine and

SCRAM INLETS
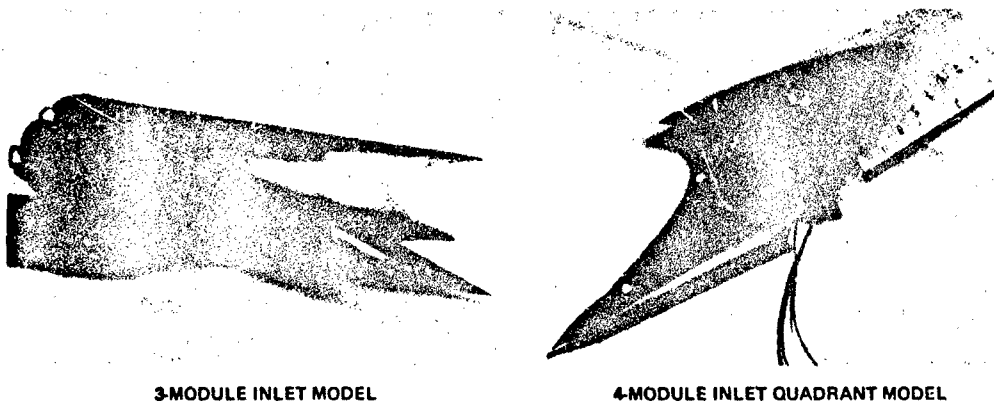
3-MODULE INLET MODEL   4-MODULE INLET QUADRANT MODEL

3-MODULE INLET EVALUATED IN 7 WIND TUNNEL TESTS AT M_0 = 4.0, 5.3, 6.0, 7.8 AND 8.1
4-MODULE INLET EVALUATED IN 6 WIND TUNNEL TESTS AT M_0 = 4.0, 5.3, 7.8, 8.1 AND 10.0

Fig. 3 Photographs of Busemann type hypersonic inlets.

cannot in supersonic flow practically be brought back to a central duct combustor. Thus, the designer has two choices: either each inlet can be used to supply a separate modular scramjet combustor, or the flow from each module can be spread circumferentially in a contoured duct to bring the flow to a common annular combustor. In the free jet test previously cited (Ref. 2), a three-module inlet was used to supply three separate combustors, and the exhaust nozzle was shaped as the inverse of the inlet to bring the three streams together in the nozzle exit plane. For such a design the modules function separately as three independent engines and by using differential fuel-flows it becomes possible to obtain thrust vector control.

Figure 2b shows the so-called "shock trap" inlet that has been examined for use in both the CRJ and the scramjet. Annular and chin-type nose and half annular aft designs have been examined. In these configurations, the flow is first turned outward on the external compression surface and then turned toward the axis through a relatively strong shock emanating from the cowl lip. Ideally, the external surface of the cowl lip is aligned with the body axis to eliminate cowl wave drag at α = 0. To mitigate the adverse effects that are caused when the strong shock strikes the boundary layer that has built up on the compression ramp, a large bleed slot is added. When used in the CRJ cycle, the bleed acts as an "educated" slot to provide additional inlet margin. The slot's intelligence is ascribed to its self-regulating flow characteristics. When the disturbance in the region of the slot is weak, the local pressure is low, and the bleed flow is minimal, thereby matching a low mass flow requirement. When the disturbance is strong, as is the case when the inlet approaches critical operation with the normal shock positioned in the region of the cowl lip plane, the pressure is high and the bleed flow is correspondingly high as required. Whereas bleed can increase the maximum pressure recovery and inlet margin, it generally reduces the effective air capture of the inlet, requires additional ducting, and incurs a loss in momentum (bleed drag). Various bleed configurations, including slots, holes and scoops, have also been used to vent low energy air in other inlet configurations. An alternative technique for boundary layer control is the diverter. Here, the inboard surface of the inlet duct is raised above the boundary layer on external compression surface, or above the body boundary layer in an aft entry configuration, and the low energy air is diverted laterally. This method is restricted to segmented or fractional entry inlets such as the chin, where lateral spill is possible. In all cases, a detailed composite design and performance analysis is needed to assess whether the benefits derived outweigh the penalties incurred.

Figure 2c shows an innovative inlet concept that has been given the name "inward turning scoop" (ITS). Multiple scoops, each capturing a sector of the flow are used and the area between the scoops is used for venting during starting and for diverting boundary layer air when appropriate. Three or more scoops can be arranged symmetrically to produce overall inlet characteristics that are quite insensitive to roll angle, thereby permitting the use of skid-to-turn control. On the other hand, two or more scoops located on the windward side provide an alternative configuration to the chin-type inlet for a bank-to-turn vehicle. In the latter case, maneuvering is made in the meridional plane of the inlet and the designer can take advantage of the additional compression on the windward surface. As in the shock-trap design, the external cowl lip surface is aligned with the missile axis. Consequently, in configurations with the cowl located in the fore-

to permit starting is moved from the plane of the cowl lip to the end of the venting slot and lateral spill is prevented at $M_0 > M_{EOB}$ with $\alpha = 0°$. Within limits, the designer can change the circumferential "smile" angle ψ of the scoops to accommodate different maximum air capture ratio requirements. For nose entry configurations, such as shown in Fig. 2c, the forebody angle can be reduced aft of the sideplate to reduce drag. Although a conical forebody is shown, other shapes can be used, albeit to accommodate a more optimal radome shape or to improve the inlet efficiency by including some isentropic turning.

Aft of the plane of the end of the sideplate vent, the designer has a number of options for ducting the flow. They are typified in Fig. 4 for the particular case of a 4-scoop symmetric inlet in a conical forebody flowfield. In this figure, CRJ, scramjet and DCR engine options are considered. Figure 4a depicts the

a) Annular or modular scramjet.   b) 4 duct dump type ramjet

c) Center dump ramjet   d) Center duct scramjet   e) Dual combustor ramjet
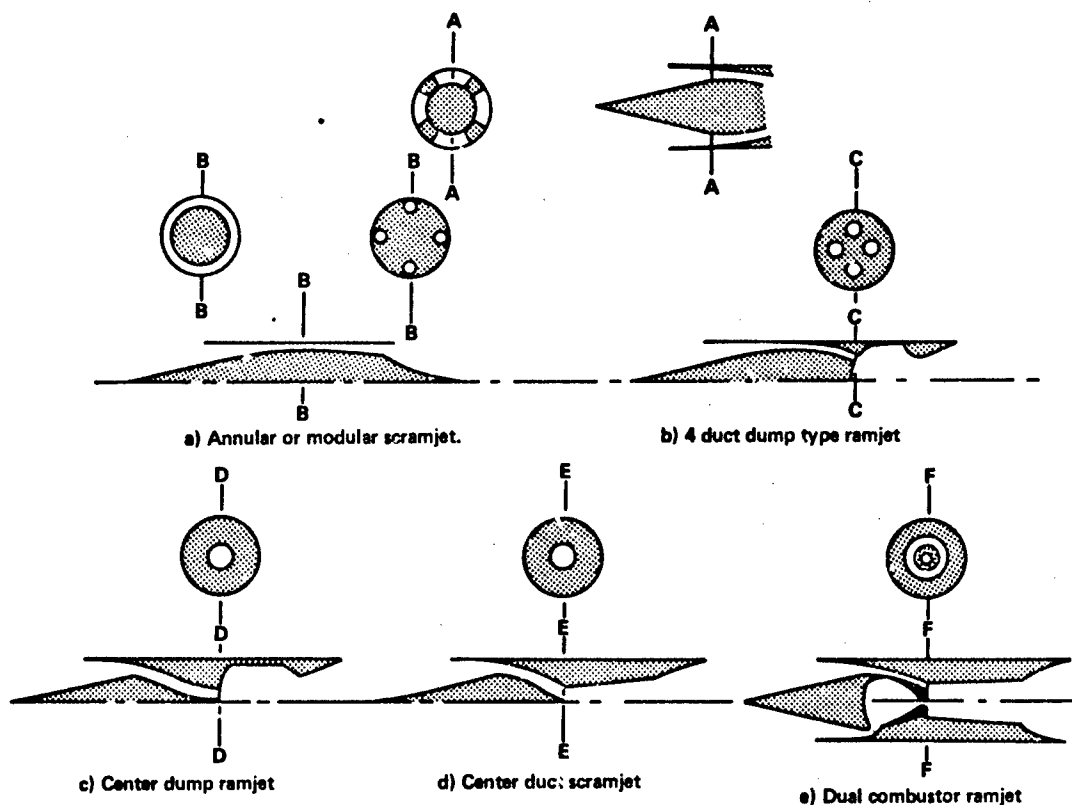
Fig. 4   Engine options with inward turning scoop inlets.

option for an annular or modular scramjet. In the annular design, the flowfield from the truncated sectors at station A-A is spread circumferentially to form a complete annulus at the scramjet combustor inlet. Alternatively, the flow can either be distributed by shaped transition sections into 4 circular modular ducts or "dumped" into 4 circular scramjet combustors, the presumption being that circular cross-sections in the high pressure-thermal loading combustor are desirable, i not mandatory.

In configuration b, the quadrant flowfields are blended into circular cross-sections and brought partially inboard after the flow has "shocked down" to subsonic. As shown, the four ducts supply a subsonic "dump type" CRJ. Similarly, the flow could simultaneously be spread circumferentially and be directed to the missile axis to provide a central duct dump combustor as shown in Fig. 4c, or a central duct scramjet as shown in Fig. 4d. Finally, the flow from the inlets can be split to supply two combustors as would be needed for the DCR. Here, two inlets supply the subsonic dump combustor as depicted in the lower half of Fig. 4e, and the flow from the other two inlets is spread circumferentially to form an annular concentric supersonic flow in the plane of the gas generator exit. In practice, it has been shown that more than two scoops are required to provide a reasonably uniform flow in the supersonic annulus, thus the configuration shown is only illustrative.

Given that the ITS inlet is potentially attractive for a variety of engine concepts, it is an appropriate choice for describing a strategy for designing the inlet for a scramjet engine. The first step in the design process is to examine the effects that changes in geometry have on inlet performance using simplified inviscid flowfield solutions. Then for a few geometries, perhaps only one, the inviscid flow solutions are used as edge conditions for a boundary layer analysis to yield the displacement thickness, δ^*, and the surface geometry is accordingly adjusted by δ^*. With the revised geometry, fully viscous solutions of the flowfield are obtained either using the parabolized approximation of the Navier-Stokes equations (PNS) or, if subsonic
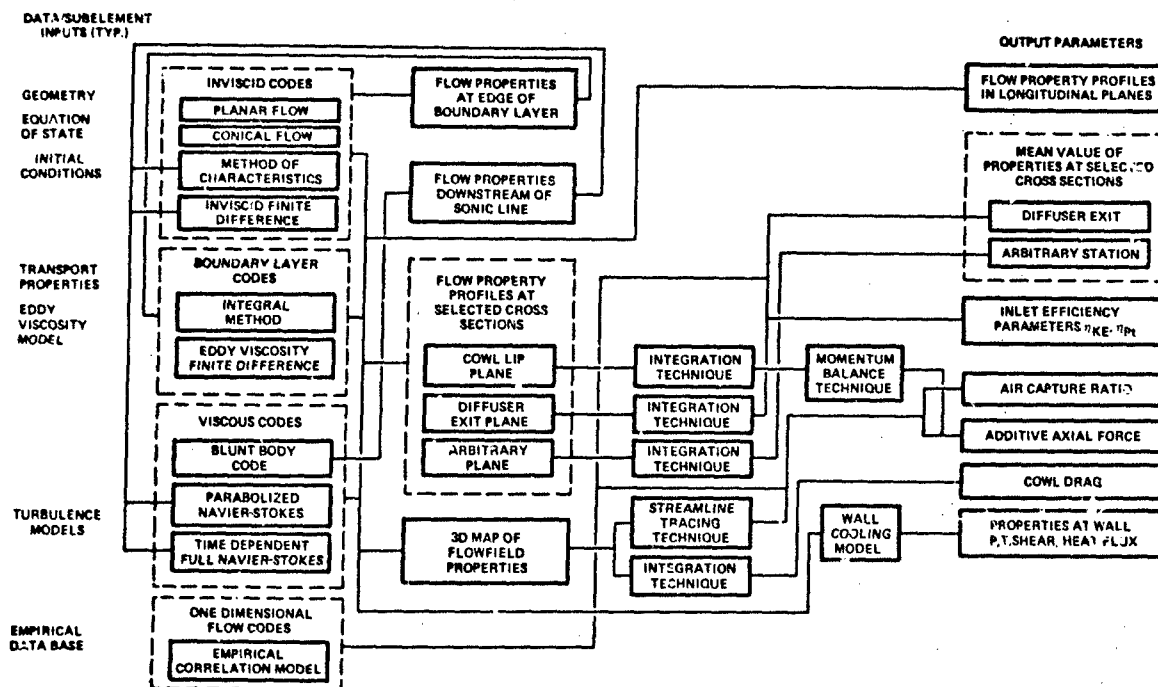
Fig. 5   Block diagram of computational procedures for design of hypersonic inlets.

In this example it is assumed that $M_{EOB} = 4$ and the missile will climb and accelerate to cruise at $M_{CR} = 7$. To minimize fuel consumption during the climb phase, it is necessary to control both the rate of acceleration and the flight path angle $\tilde{\theta}$, having entered the climb phase at an optimal θ_{EOB}. The determination of the optimal climb-out trajectory is a formidable task but for a relatively high thrust-to-weight ratio missile, optimal climb-outs generally require $\alpha \approx 0°$ until an altitude $Z \approx 0.7\ Z_{CR}$ is reached, at which time M_0 has nearly reached M_{CR}. Thus, inlet operation at angle of attack and low M_0 is not a significant design consideration. On the other hand, during cruise at high altitude, maximum range results when the missile is flying just below the α corresponding to maximum L/D. Typically, α at $(L/D)_{MAX}$ lies between 7° and 12° for missiles with $M_{CR} = 6-8$. So, inlet operation at α, particularly with respect to air capture ratio, is important for $M_0 \approx M_{CR}$. Arguments are presented in Ref. 13 showing that for symmetrical inlet geometries it is advantageous to design $M_{FC} = M_{CR} - \Delta M$, where $\Delta M \approx 0.5-1.0$ to obain optimal performance. Consequently, in this example $M_{FC} = 6$.

Figure 6a is a schematic illustration of the flowfield in the inlet under consideration at $M_0 = M_{EOB}$. The conical shock lies ahead of the cowl lip, since $M_0 < M_{FC}$, and the air entering the inlet is represented by A_0 and the last captured streamline. A_i is the projected area of the entire sector of the circle bounded by the smile angle of the scoop. The conical compression field is turned toward the missile axis by the cowl lip shock. Internal cowl lip angles β of 0° to 20° will be examined. Inlet sideplates follow the cowl shock to prevent lateral spillage at $\alpha = 0$, and no further turning of the flow is introduced ahead of the plane of the sideplate crotch (Station 2). Thus, the innerbody is turned approximately parallel to the inner cowl surface along the line of the shock intersection with the conical surface. Downstream of the station of the sideplate crotch a "boundary layer recovery" section is shown. Unless the boundary layer has been removed from the inlet innerbody, the shock from the cowl lip distorts the boundary layer to a profile that is nearing separation. Length at constant pressure is required to restore the profile to a shape more tolerable to exposure to the adverse pressure gradient in the isentropic compression region 2-3. In region 2-3 the flow is compressed by gentle turning of the cowl side of the internal duct. The innerbody also curves inwardly to provide cancellation of the weak compression waves. This section can have an arbitrary length greater than a minimal value corresponding to a centered wave compression focused on the innerbody. Engine packaging considerations and perhaps viscid-inviscid interactions such as those just mentioned would govern the length selection. In this example, the length was chosen such that the inner duct contour is the middle streamline in a centered compression field. The amount of allowable internal contraction is governed by the starting area ratio criterion, i.e. that is, A_3/A_2 can be no smaller than the ratio corresponding to sonic

flow at station 3 when a normal shock is positioned in the plane of the sideplate crotch. The internal compression is assumed to be isentropic. For the engine configurations shown in Fig. 4 that require transition from a sector of having a smile angle ψ to, say, a quadrant of a circle or annulus, circumferential spreading of the duct aft of sideplate crotch can be incorporated. Providing circumferential spreading while maintaining either constant pressure as in the "boundary layer recovery" section and downstream of Section 3, or providing a "shock-free expansion-wave-free" compression as in Section 2-3, is a challenging design problem that is beyond the scope of this paper. Suffice it to say that generally the desired longitudinal variation
... ... area of the duct is obtained by prescribing the shape of the inner and outer duct walls

a) DESIGNED FOR $A_0/A_i = 1$ AT $M_{FC} = 6$

b) DESIGNFD FOR $A_0/A_i = 1$ AT $M_0 = 4$
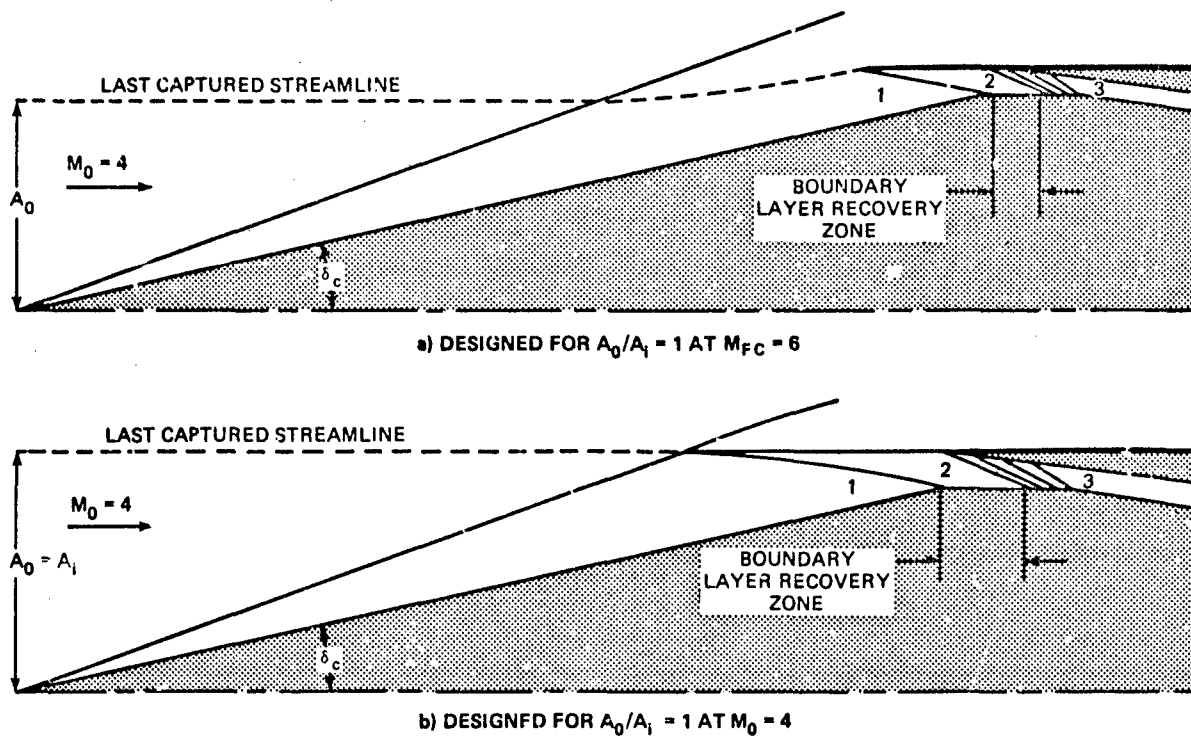
Fig. 6   Geometrics and flowfields of two ITS inlets.

The cowl reflected shock has a slight inward curvature due to the decreasing gradient in Mach number from the cowl lip to the conical surface and due to flow convergence downstream of the shock. The waves in the isentropic compression region are similarly curved due to the persistence of the outward to inward decreasing Mach number gradient downstream of the cowl reflected shock as well as flow convergence. In the numerical examples of the inviscid flowfield solutions that follow, two simplifying assumptions were made aft of the cowl lip station: 1) a mean Mach number that satisfied conservation of mass was used to represent the flow at major stations and 2) the pressure rise and total pressure loss across the cowl reflected shock were taken equal to those for a planar flow with the same turning angle.

Other scoop geometries could have been considered. For example, the external compression surface could have comprised a cone followed by an outward turning isentropic compression surface. For the same amount of external compression, viz $\bar{p}_1/p_0$, the efficiency would be slightly greater, but the inlet would be longer. Presuming that the innerbody houses an RF seeker, this shape would be less favorable from the point of view of minimization of radome boresight error. Likewise, the cowl inner surface ahead of the sideplate crotch plane could be shaped to provide isentropic compression for cases corresponding to $\beta > 0$. For the same compression $(\overline{p_2/p_1})$, the efficiency would be higher but the subsequent amount of allowable internal contraction, A_3/A_2, would be slightly less. For most designs, the curved inner cowl lip gives better inviscid performance but the issue would be moot unless the inlet incorporates boundary layer control. If no boundary layer control is provided, the subsequent discussion will show that $\beta = 0$ is optimal.

Figure 6b is used for exemplary purposes to show the general utility of the inviscid flowfield analysis. This inlet has the same cone angle δ_c, and cowl angle $\beta = 0°$, and it is operating at the same M_0 as the inlet shown in Fig. 6a but it is designed for $M_{FC} = 4$. All of the other constraints regarding internal contraction, etc. remain the same. It can be shown that the static pressure increases and total pressure losses through the shock and isentropic compressions are nearly identical for the two cases (Figs. 6a and 6b). This is because the average Mach number of the flow ahead of the cowl reflected shock is only weakly dependent on M_{FC}, e.g. for $\delta_c = 15°$ $\bar{M}_1 = 3.230$ for $M_{FC} = 6$ and $\bar{M}_1 = 3.255$ for $M_{FC} = 4$. The internal duct is, of course, larger for the $M_{FC} = 4$ case, but A_3/A_0, A_3/A_2, p_c/p_0 and $\bar{p}_{t_3}/p_{t_0}$ are nearly the same for both cases. It is also apparent that the inlet contraction ratio A_1/A_3 is smaller for the $M_{FC} = 4$ case, which means that for $M_0 > 4$ the $M_{FC} = 4$ case will have lower p_3/p_0 and therefore the cycle performance will be lower. Thus, as in a number of other situations in well designed fixed geometry inlets, a loss in air capture is, in part, compensated by increased compression and vice versa. The loss in air capture at $\alpha = 0$ can be obtained from solutions of the conical flowfield to yield ψ_w, the flow angle and M_w, the Mach number along the conical ray θ_w that strikes the cowl lip and the total pressure loss across the conical shock p_{t_w}/p_{t_0}, together with the relationship

$$\cdot = \frac{\gamma + 1}{2(\gamma-1)} \text{ n}$$
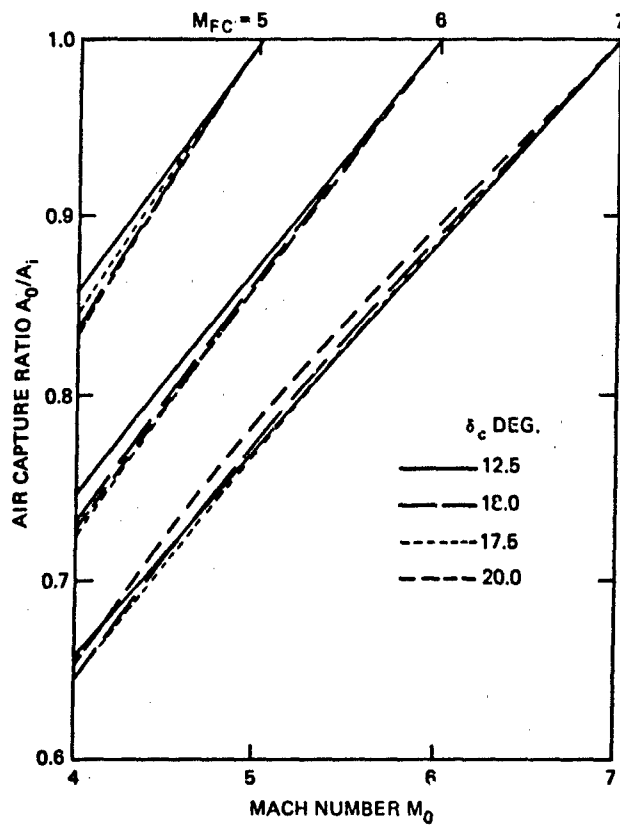
Fig. 7   Air capture ratio for inlets with conical forebodies.
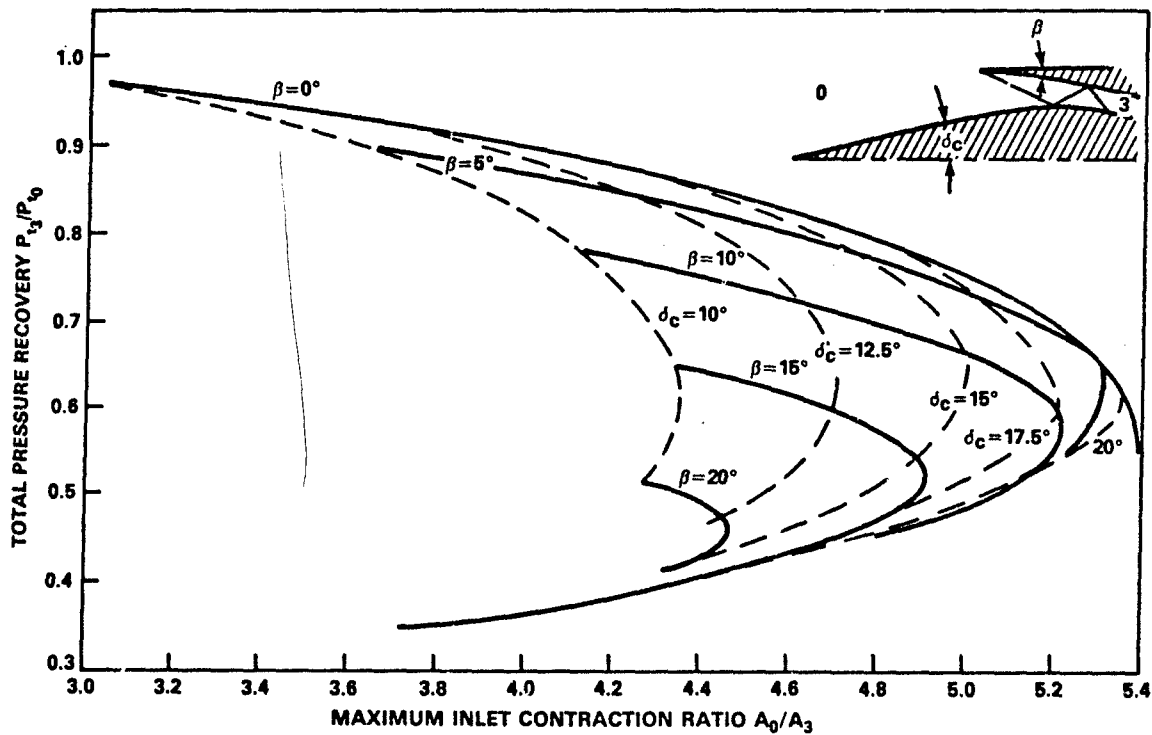
Fig. 8   Total pressure recovery for family of inward turning scoop inlets at $M_0 = 4$.
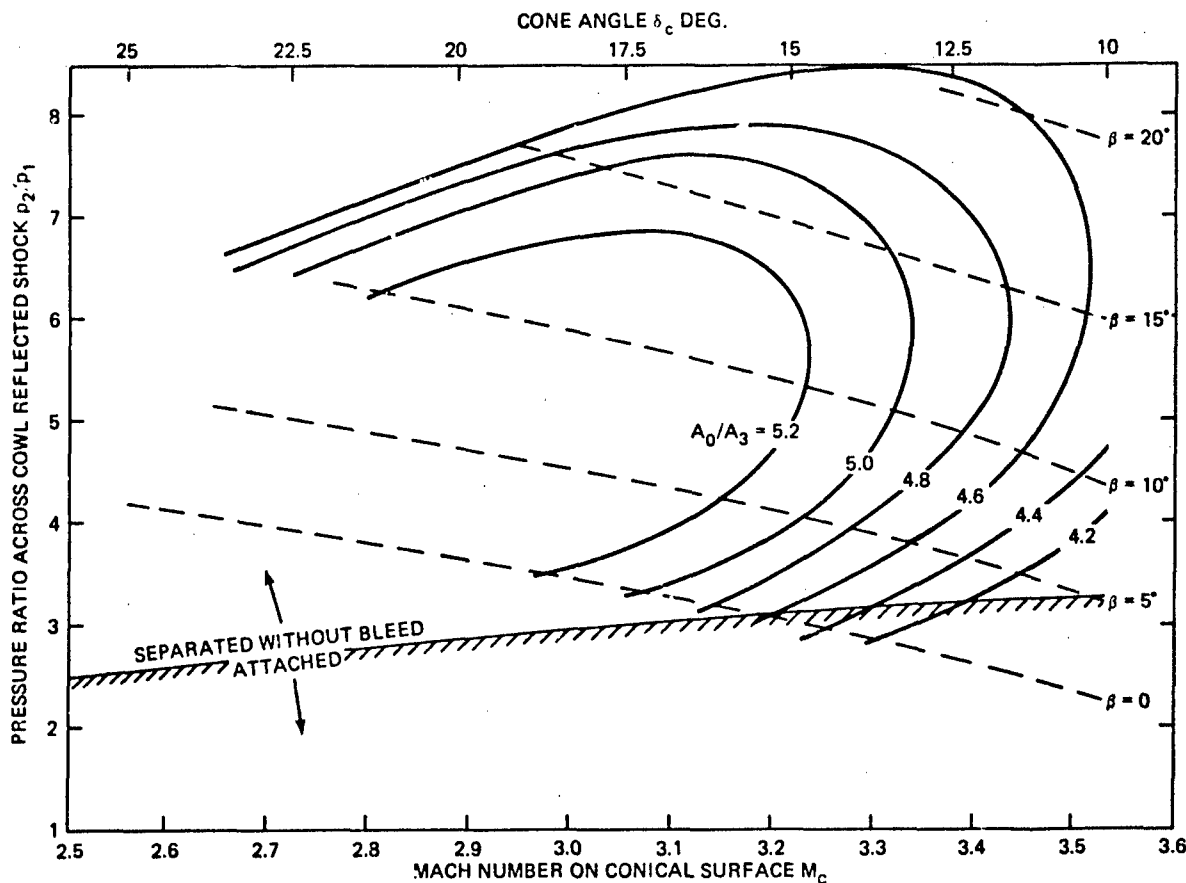
Fig. 9 Maxium contraction ratio contours on grid of shock pressure ratio at $M_0 \approx 4$ for inward turning scoop inlets.

Figure 7 shows A_0/A_1 for M_{FC} 5, 6 and 7 inlets with $\delta_c = 12.5$, 15, 17.5 and 20° over the range $4 \leq M_0 \leq 7$. Air capture is only weakly dependent on δ_c. At $M_0 = 4$, $M_{FC} = 6$, $A_0/A_1 \approx 0.73$, so the inlet contraction ratio can be about 37% greater for a $M_{FC} = 6$ versus a $M_{FC} = 4$ design.

Figures 8 and 9 show the method for determining the preferred geometry of the ITS inlet for this example. Total pressure recovery p_{t_3}/p_{t_0} is shown as a function of A_0/A_3 for cone angles δ_c from 10° to 20° and cowl angles β of 0° to 20° in Fig. 8. Three important points can be learned from these results.

1) There is a maximum allowable inlet contraction ratio A_0/A_3 that is considerably smaller than would occur if the compression was isentropic and the internal contraction was not limited for starting, i.e., ~ 5.4 vs. 10.7 for $M_0 = 4$, the Mach number at which the scoop lip shock is designed to strike the knee in the innerbody surface.

2) For a constant δ_c and increasing β, or with β constant and increasing δ_c results in a monotonically decreasing p_{t_3}/p_{t_0} and a corresponding monotonically decreasing value of M_3, but a maximum occurs in A_0/A_3. Scramjet cycle performance increases with increasing M_3 for a given A_0/A_3, so only the upper branches of the curves are of interest.

3) Small or negligible internal cowl lip angles result in the best performance, i.e., maximum p_{t_3}/p_{t_0} for a given A_0/A_3. Indeed, for any value of $A_0/A_3 < 5.3$, $\beta = 0°$ is optimal.

Contours for constant values of A_0/A_3 are mapped in a plane of cowl shock pressure rise, p_2/p_1 vs. the Mach number on the conical surface, M_c, to examine the problem of boundary layer separation on the innerbody surface in Fig. 9. The separation criterion used to establish the demarcation between separated and attached flow is in accordance with the values suggested in Ref. 16 for turbulent boundary layers. Additional experimental data are needed to establish the veracity of the values so derived. Nonetheless, this figure shows that geometries having A_0/A_3 values greater than 4.6 would be expected to have separated flow at the sideplate crotch station even with $\beta = 0°$. A local separation would cause unwanted compression and expansion waves and

At $M_0 = 4$ for most scramjet engine operating conditions there will be a normal shock preced'ng the com-
ustion (dual mode operation) and since the ITS inlet is also attractive for use in the CRJ, it is useful to
ramine conditions corresponding to those with a normal shock located downstream of station 3 with no addi-
ional diffusion. Figure 10 shows the total pressure recovery p'_{t_3}/p_{t_0} for this family of inlets at $M_0 = 4$.

aximum values occur for a given δ_c when the total turning of the flow in the compression process is approxi-
ately 40°. If there were no design consideratio.s other than inlet recovery and drag on the portion of the
orebody not wetted by the air captured in the inlet, a design with $\delta_c = 17.5°$ and $\beta = 5°$ would be optimum.
oreover, since the optimum occurs with inward turning at the scoop lip, somewhat higher recovery could be
btained by curving this surface through the 5 degree turn. On the other hand, if the constraint to avoid
oundary layer separation is operative and $\delta_c \leq 15°$, a 10% lower inviscid recovery would have to be accepted.

At this point in the discussion all but a narrow range of geometries can be eliminated from further
onsideration. Four cases have been selected. Case A with $\delta_c = 12.5°$, $\beta = 0$ is a conservative geometry, and
ase B with $\delta_c = 15.0°$, $\beta = 0°$ is the optimal geometry for inlets without boundary layer control at $\alpha = 0°$.
ases C and D with $\delta_c = 17.5°$ and $\beta = 0$ and 5° are near optimal if boundary layer separation is not a problem.
able 1 lists inlet parameters and flow properties for these $M_{FC} = 6$ design inlets at $M_0 = 4$, 5, 6 and 7. In
ll designs the scoop lip shock strikes the knee on the innerbody at $\alpha = 0$, $M_0 = 4$. For $M_0 > 4$, the lip shock
alls downstream of the knee and a far more complex wave structure exists in the duct. Whereas these flow-
ields can be obtained using the computer routines shown in Fig. 5, a good approximation of average properties
t station 3 can be obtained with the assumption that the total pressure loss is the sum of the loss across

TOTAL PRESSURE RECOVERY OF INWARD TURNING
SCOOP INLETS AT $M_0=4$
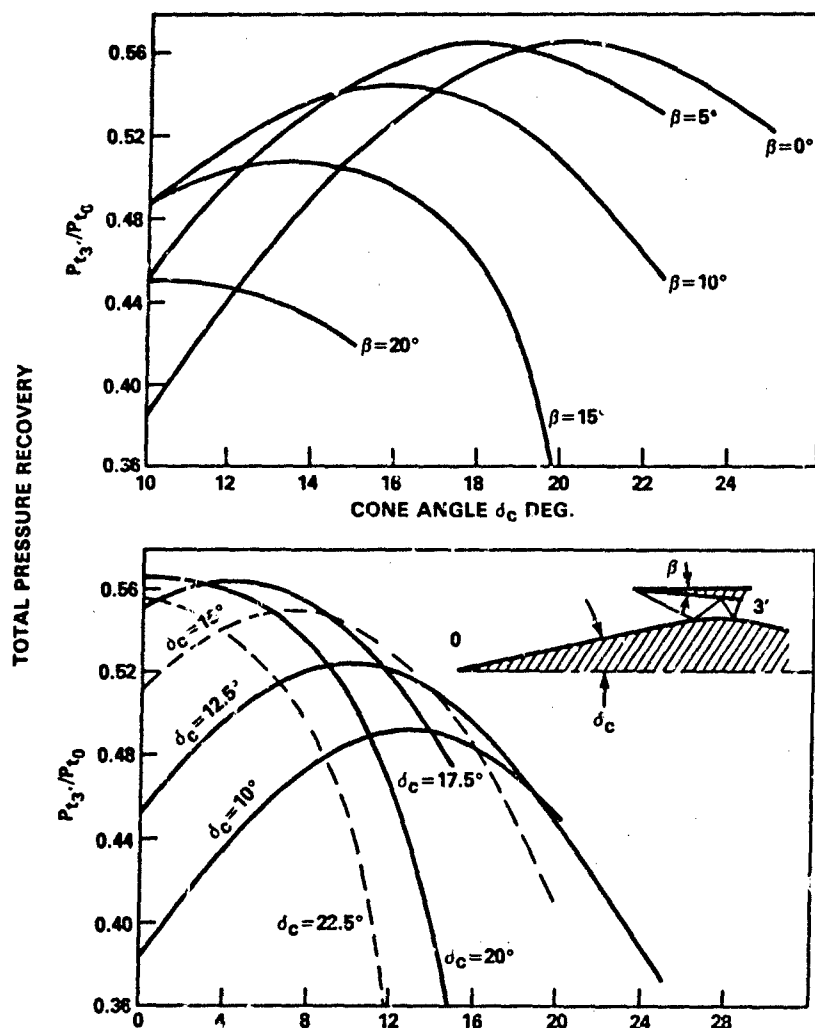
Table 1

Inlet Parameters and Flow Properties for Four ITS $M_{FC} = 6$ Inlet Geometries

Inviscid Flow

Case	δ_c Deg.	β Deg.	A_1/A_3	M_0	A_0/A_3	M_3	P_{t_3}/P_{t_0}	P_3/P_0	$M_{3'}$	$P_{t_{3'}}/P_{t_0}$	$P_{3'}/P_0$
A	12.5	0	4.934	4	3.682	2.522	0.9245	7.938	0.511	0.4531	57.6
				5	4.305	3.140	0.8346	9.750	0.467	0.2427	110.6
				6	4.934	3.670	0.7373	12.019	0.445	0.1356	186.9
				7	4.934	4.232	0.6230	12.532	0.429	0.0712	259.7
B	15.0	0	5.881	4	4.297	2.280	0.8632	10.813	0.537	0.5113	63.8
				5	5.040	2.828	0.7335	13.692	0.486	0.2789	125.5
				6	5.811	3.272	0.6069	17.445	0.461	0.1570	215.0
				7	5.811	3.744	0.4797	18.519	0.443	0.0828	299.7
C	17.5	0	6.667	4	4.842	2.045	0.7886	14.598	0.570	0.5516	68.8
				5	5.787	2.523	0.6235	18.632	0.511	0.3055	135.3
				6	6.667	2.909	0.4866	24.002	0.481	0.1728	232.9
				7	6.667	3.314	0.3650	25.888	0.459	0.0913	327.3
D	17.5	5	7.160	4	5.200	1.806	0.6983	18.284	0.615	0.5656	66.5
				5	6.215	2.259	0.5253	23.702	0.539	0.3160	137.2
				6	7.160	2.596	0.3883	30.929	0.504	0.1793	237.9
				7	7.160	2.945	0.2762	33.823	0.479	0.0951	336.5

the conical shock and the loss across a scoop reflected shock thet would turn all of the flow to an angle With the air capture characteristics given in Fig. 7 and the contraction ratio A_1/A_3 set by $M_{FC} = 6$, all properties at station 3 can be obtained. The trend of improving performance with increased compression th was previously shown at $M_0 = 4$, is present for $M_0 = 5-7$.

Whereas these results provide a basis for selecting the compression field, viscous effects must be in troduced to define the geometry and provide a basis for proceeding into the combustor and overall engine c analysis.

Using flow properties from the inviscid flow solution as input for conditions on the edge of the boun layer, the displacement thickness δ^* is obtained by one of several possible techniques (Ref. 17). All con tours are adjusted by the local value of δ^* and fully viscous solutions of the flowfield are made, δ^* is adjusted and the process repeated until the core of the flowfield is approximately the same as that of the initial inviscid analysis. For the asymmetric portion of the flow, e.g., in the internal ducts, δ^* varies circumferentially as well as longitudinally. The resulting cross-sectional area A_g, the physical area, is therefore defined. Additionally, the local static pressure in the boundary layer at a given location is th same as in the inviscid flow. Superficially, it would appear that A_{g3} and p_3, together with the continuit equation, could be used to define a set of mean flow properties that would be appropriate for a cycle anal sis. If this is done, however, the deduced mean value of the total pressure is artificially low. In effe the mean value of the momentum, which is directly related to the thrust, would not be well represented.

A more appropriate method, albeit more rigorous to obtain, is to calculate the mass averaged value of total pressure $\bar{P}_{t_3}$, and with the local static pressure, p_3, define an effective flow area A_{3e} that also satisfies the continuity equation. The resulting area lies between A_3 and A_{g3}. A numerical example will to clarify this point. Let us suppose that the viscous solution of the flowfield for Case A at $M_0 = 4$ sho that $(A_g/A)_3 = 1.2$ and that the profile in the turbulent boundary layer can be represented by $u/u_3 = (y/\delta)$ For an adiabatic wall the mass averaged total pressure in the viscous layer is 59% of the value in the in viscid core. The resulting mass averaged total pressure for the entire flow is 83% of the inviscid value, which leads to $\bar{P}_{t_3}/P_{t_0} = 0.7689$, $(A_e/A)_3 = 1.079$, and a corresponding effective Mach number $M_{e3} = 2.404$.

These effective flow properties now become the values to be used in an simplified one-dimensional analysis Accordingly, the conditions corresponding to those downstream of a normal shock at station 3 are $M_{3'e} = 0$. $P_{t_{e'}}/P_{t_0} = 0.414$.

Since the boundary layer parameters are dependent on the geometry, M_0, the altitude, and the wall cooling of each case, each flight condition would produce a different A_{g3}/A_3. At first glance it would ap that the geometry selected for one flight condition would not yield the compression field previously compu at other flight conditions. However, it turns out that for a given geometry and altitude, δ^* is only weak dependent on M_0, changing only about 10% from $M_0 = 4$ to $M_0 = 7$. Moreover, changes with altitude at a give are also not too great, e.g., a 30,000-ft increase in altitude Z increases δ^* by about 20%. Mach number a altitude also have only a small effect on the ratio of mass averaged total pressure to core flow total pre sure. Thus, even though the boundary layer thickness, δ, can vary by more than a factor of 2 over a typic flight envelope, the changes in A_e/A are quite small. Thus, the design strategy is to base the geometry c the conditions at the end of boost and accept the relatively minor changes in the flowfield at $M_0 > M_{EOB}$.

Table 2

Inlet Parameters for Four ITS $M_{FC} = 6$ Inlets

Viscous Losses Based on $(A_g/A)_3 = 1.2$ at $M_0 = 4$

Case	δ_c Deg.	β Deg.	M_0	M_{e3}	P_{e3}/P_0	$P_{t_{e3}}/P_{t_0}$	A_0/A_{e3}	$\eta_{KE_{e3}}$	$M_{e3'}$	$P_{e3'}/P_0$	$P_{t_{e3'}}/P_{t_0}$
A	12.5	0	4	2.404	7.938	0.7689	3.414	0.9756	0.523	52.2	0.4140
			5	2.999	9.750	0.6771	3.992	0.9764	0.475	100.7	0.2224
			6	3.512	12.019	0.5905	4.574	0.9774	0.451	170.9	0.1244
			7	4.055	12.532	0.4943	4.574	0.9772	0.434	238.4	0.0655
B	15.0	0	4	2.159	10.813	0.7148	3.960	0.9685	0.553	57.0	0.4624
			5	2.688	13.692	0.5921	4.645	0.9684	0.497	113.1	0.2533
			6	3.116	17.445	0.4825	5.356	0.9679	0.469	194.7	0.1433
			7	3.571	18.519	0.3770	5.356	0.9672	0.449	277.4	0.0755
C	17.5	0	4	1.921	14.598	0.6493	4.425	0.9590	0.592	60.4	0.4920
			5	2.380	18.632	0.4989	5.289	0.9560	0.525	120.0	0.2737
			6	2.751	24.002	0.3825	6.093	0.9561	0.492	207.9	0.1553
			7	3.141	25.888	0.2831	6.093	0.9557	0.467	293.8	0.0823
D	17.5	5	4	1.652	18.284	0.5531	4.604	0.9424	0.653	55.2	0.4840
			5	2.081	23.702	0.3976	5.503	0.9397	0.564	115.8	0.2716
			6	2.400	30.929	0.2865	6.340	0.9404	0.523	202.7	0.1547
			7	2.731	33.823	0.1996	6.340	0.9403	0.493	288.3	0.0824

Moreover, it is possible to adjust the inviscid flow results to values suitable for cycle calculations by obtaining only a few viscous flow solutions and applying a constant value of A_e/A over a suitable range of conditions. The value of 1.2 for A_{g3}/A_3 would be representative for engines of about two foot diameter for Cases B-D, as well as Case A at $M_{EOB} = 4$, $Z = 5,000$ ft. A_{e3}/A_3 would be different for each case, increasing from 1.079 for Case A to 1.129 for Case D. Maintaining these values of A_{e3}/A_3 constant at higher M_0 results in effective flow properties at station 3, as shown in Table 2. The kinetic energy efficiency of the inlet, η_{KE}, at station 3 has been added to the Table since this parameter, rather than P_{t_3}/P_{t_0}, is generally used as the basis of empirical correlations. For a calorically perfect gas, η_{KE} and P_{t_3}/P_{t_0} are related by the simple expression

$$\eta_{KE} = 1 - \frac{2}{(\gamma-1)M_0^2}\left[\left(\frac{P_{t_0}}{P_{t_3}}\right)^{\frac{\gamma-1}{\gamma}} - 1\right] \qquad (2)$$

The same trends with M_0 that were present in the inviscid flow results are maintained, but a few additional points can be made. Total pressure recovery is lower but the effective inlet contraction ratio is higher. Moreover, η_{KE_3} is nearly invariant with M_0 for a given case. This result lends credence to the results of simplified analyses of performance that are based on holding η_{KE} constant.

There are many situations when the rigor of the foregoing approach is not warranted, i.e. for preliminary engine performance evaluations. Reference 7 gives the details of a method that uses a strategy similar to the one just described, viz. it is based on the premise of a uniquely defined effective inlet contraction ratio. The method is based on an empirical relationship

$$\eta_{KE_3} = 1 - 0.4(1-M_{e3}/M_0)^4 \qquad (3)$$

and an inlet air capture ratio characteristic similar to that shown in Fig. 7. It is of interest to add the "data" from Table 2 to the Figures from Ref. 7 as a further test of the adequacy of Eqn. 3. Figure 11 shows that for inlets with high values of M_{e3}/M_0, e.g. Case A, Eqn. 3 yields η_{KE_3} values that are somewhat high, but the agreement improves at low M_{e3}/M_0. Note also the near independence of M_{e3}/M_0 with M_0 for each of the cases. Figure 12 from Ref. 7 shows the corresponding values of $\overline{P}_{t_3}/P_{t_0}$ versus A_0/A_{e3}, and to complete the picture, Fig. 13 shows P_3/P_0 versus M_{3e}/M_0. For clarity, the values from Table 2 have not been added to these figures.

The design feature of the ITS inlet that remains to be substantiated is the favorable inlet air capture characteristics at angle of attack at $M_0 > M_{CR}$. Figure 14 shows this effect for the $\delta_c = 15°$ conical fore-body, symmetrical ITS inlet with four scoops, each having a smile angle ψ of 45°. Curves of air capture are shown for three values of the roll orientation angle ϕ of 0°, 22.5° and 45°. The decrease in air capture of < 9% at $\alpha = 10°$ in the least favorable roll orientation is remarkably small.
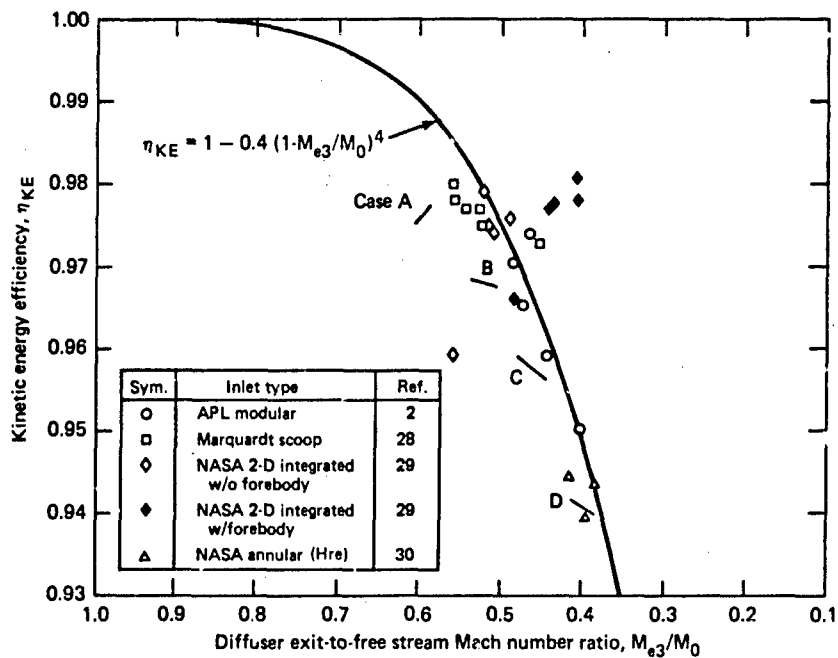
Fig. 11 Kinetic energy efficiency as a function of diffuser exit-to-free stream Mach number ratio.
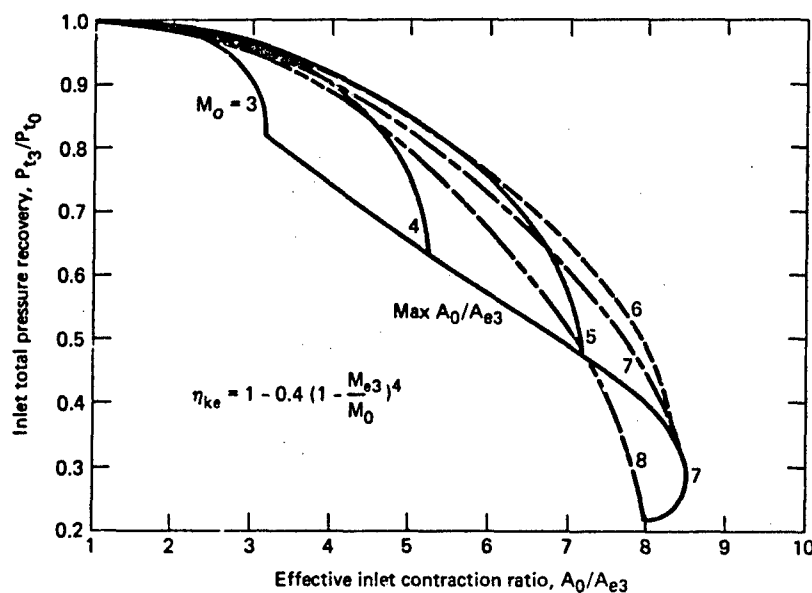
Fig. 12 Inlet total pressure recovery as a function of effective contraction ratio.

COMBUSTOR ANALYSIS

Treatment of the combustor of the scramjet varies in complexity from relatively simple, one-dimensional integral solutions to relatively complex finite difference solutions that include wall shear and non equilibrium chemistry. The key to the successful adaptation of any of the theoretical descriptions of the combusto flowfield is the adoption of models that take into consideration the ever growing base of experimental observations. The schematic illustration of the combustor flowfield shown in Fig. 15 will help to develop this point. The combustor is a simple diverging cone frustum. The qualitative features of the flow for other diverging shapes such as those containing step increases in area just downstream of the fuel injection statio are the same, but the details of the flow are different and must be considered even in a simplified integral analysis. The subsequent discussion will show that constant-area or converging shapes are not practical for the types of missile applications that have been postulated.

For all but the highest Mach number and lowest equivalence ratio conditions, the blockage due to the combined effects of the injection and heat release generates a "shock train" disturbance that originates in the isolator section and extends downstream of the injection ports into the combustor. In general, the pressure rise associated with the shock train is sufficiently great to separate the boundary layer. In a well designed engine, the isolator is of sufficient length to prevent the combustion-induced disturbances from

$$\eta_{KE} = 1 - 0.4 \left(1 - M_3/M_0\right)^4$$
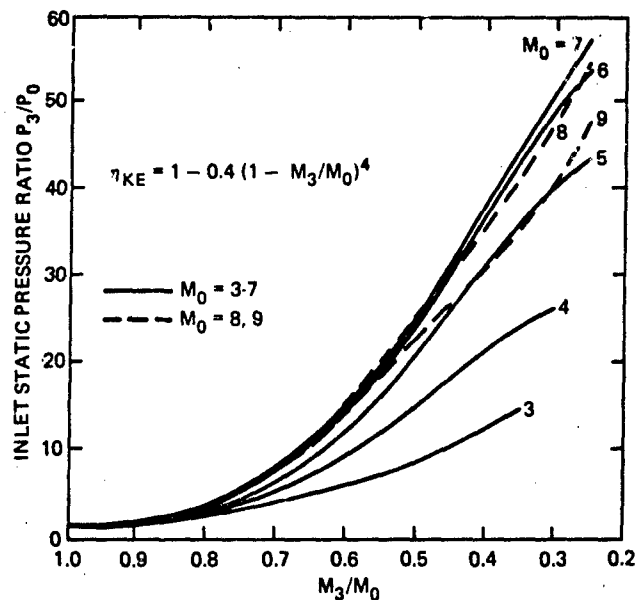
Fig. 13 Inlet pressure ratios based on data correlation.

$M_{FC} = 6$
$M_0 = 7$
$\Psi = 45°$
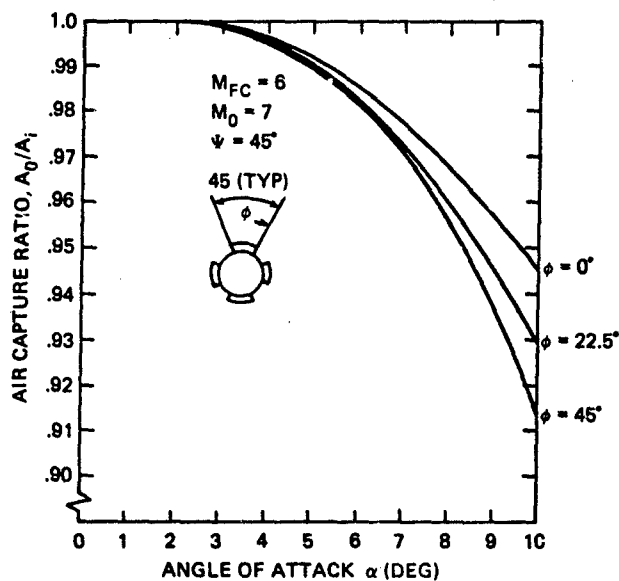
Fig. 14 Effect of angle of attack and roll angle on the air capture of 4 ITS inlets.
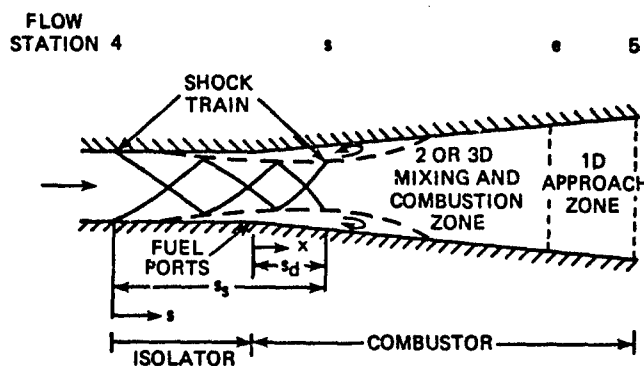
Fig. 15 Schematic illustration of flow processes in isolator and combustor sections.

disrupting the flow in the inlet. Generally, combustors with step increases in area require less isolator length because the strength of the shock train is diminished. Downstream of the shock train mixing and combustion are intensive, with large radial, axial and, perhaps, circumferential gradients in flow properties and chemical composition. Further downstream, the mixing and combustion is less intense and the gradients are considerably weaker, and the flow can be reasonably approximated by one-dimensional mean flow properties at each axial station.

A similar shock train structure can be generated in a duct of this shape by placing a physical blockage, such as a partially closed valve, downstream of the duct, or by simply increasing the back pressure in a direct-connect testing apparatus. Several investigators have exploited this fact to study the shock train in an unheated, nonreacting air stream that is more conducive to measurement. In particular, Waltrup, et al. (Ref. 18) made sufficient measurements to model the pressure rise over a range of conditions typifying those in the entrance of the scramjet combustor. Figure 16 from Ref. 18 is a data correlation that shows that the shape of the pressure rise curves for various p_s/p_4 values of 1.6 to 6.9 with initial Mach numbers of 1.53 to
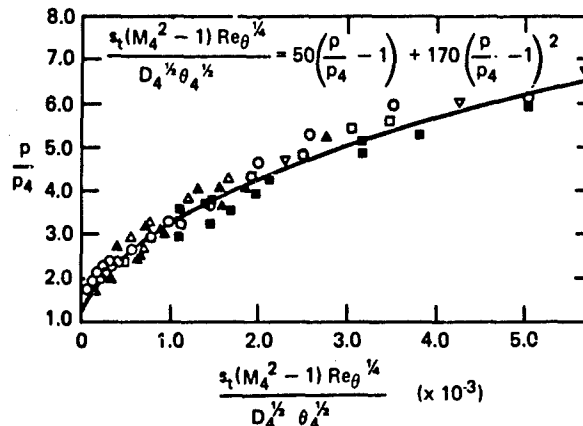
Fig. 16   Normalized pressure distributions in shock train flow structures.

2.72 can be collapsed to a single correlating curve. Here, p_s is the pressure downstream of the shock train and p_4 is the initial pressure. The correlating equation is

$$\frac{s(M_4^2 - 1)Re_{\theta_4}^{1/4}}{D_4^{1/2}\theta_4^{1/2}} = 50\left(\frac{p}{p_4} - 1\right) + 170\left(\frac{p}{p_4} - 1\right)^2 \tag{4}$$

Equation (4) can be used to obtain the total length of the shock train s_s shown in Fig. 15 for given shock pressure rises and then used to find $p = f(s)$. The nondimensionalizing length scale of $(D^{1/2}\theta^{1/2})_4$ was based on a regression analysis of data taken over a limited range of these parameters and could, therefore, be subject to revision with the compilation of additional data. Until additional experiments are conducted, it is necessary to use the hydraulic diameter in place of D_4 for isolators having non circular cross-sections.

Experiments are currently underway (Ref. 19) to develop similar data correlations in co-annular isolators typified by Fig. 4e. The overall pressure ratios in Fig. 14 correspond to a range of shock strengths equivalent to either oblique or normal shocks. It has been found that the mean value of other flow properties downstream of shock trains correspond to conditions downstream of the equivalent single shock. This suggests that wall shear contributes only a small part to the total pressure loss in this strongly coupled viscous-inviscid interaction zone. The static pressure distribution downstream of a shock train depends on the duct shape and on whether the flow is separated at the end of the shock train. In separated zones the pressure would be nearly constant. For attached flow in constant area or diverging sections and subsonic initial conditions, the pressure decreases monotonically. For supersonic initial conditions and either constant area or very small divergence the static pressure rises slightly, but in the geometries of most interest that have moderate divergence, i.e., area ratios of about two, the pressure decreases monotonically.

Combustor analysis based on integral solutions of the x momentum equation require that the wall stress be well posed. Therefore, it is evident that not only must the shape of the pressure rise in the shock train be known, but its position relative to the fuel ports must be defined.

In Ref. 10, the relationship

$$s_d/D_4^{1/2}\theta_4^{1/2} = 0.5\left(\frac{p_s}{p_4} - 1\right) \tag{5}$$

was derived from hueristic arguments and limited data to define the distance, s_d, that the shock train extend downstream of the fuel ports as shown in Fig. 15. Thus, for a given set of initial conditions M_4, θ_4, Re_{θ_4} and the shock train pressure rise p_s/p_4, the pressure distribution to the end of the shock train or the re-

attachment point is defined. No ambiguity exists if a step increase in area is present because the pressure is given as a function of x rather than A. Downstream of the shock train, it turns out that the pressure distribution can be well represented by a pressure-area relationship first suggested by Crocco (Ref. 20) if the area is taken as the local cross-sectional area of the duct. Crocco noted that the relationship $pA^{\epsilon/\epsilon-1}$ = constant, where ϵ is an arbitrary constant, embraced the particular solutions: 1) ϵ = 1 corresponding to the Rayleigh process, i.e., one-dimensional constant area heat addition, and 2) ϵ = 0 corresponding to constant pressure process. Reference 21 added to the attributes of this formulation by noting that ϵ = $-\gamma M^2$ corresponds to a one-dimensional heat addition with constant Mach number.

Note that the assumption of the wall pressure distribution does not require unidimensionality of the flow, but the association with the corresponding one-dimensional flow having the same value of ϵ can be informative. It is particularly important to grasp this point if one is to use integral techniques effectively. For a given set of conditions (not necessarily uniform) in a starting plane and heat release, there is a unique set of unidimensional properties in the exit plane for a given total force and heat flux on the boundary (the combustor wall in this case), regardless of the path of the process. The total axial force on the wall is the difference between the integrated pressure on the projected area and the wall shear. Thus, a given solution of the integral equations is valid for an infinite number of combinations of axial pressure force and wall shear. To exploit this reality, one needs a shear model for reacting ducted flows. Although considerable progress has been made in the development of analytical models (see e.g. Ref. 22), these efforts have not progressed to the point of practical application; consequently empirical correlations still must form the basis of scramjet combustor analyses.

In Refs. 9 and 23 heat flux data from six different supersonic combustor geometries, with both gaseous and liquid fuels and M_4 from 1.6 to 3.2 were correlated and used to obtain a deduced combustor shear parameter. Figure 17 shows this shear parameter $\overline{C}_f = 2\overline{\tau}_w/\rho_4 u_4{}^2 = 2\overline{\tau}_w$ ($A_4/\dot{w}_a u_4$) versus ER_{eff}, where $\overline{\tau}_w$ is the mean

EQUIVALENCE RATIO, ER (TYP. LIQUID FUEL)

HEAT RELEASE PARAMETER (f · ΔH_f · η_c)
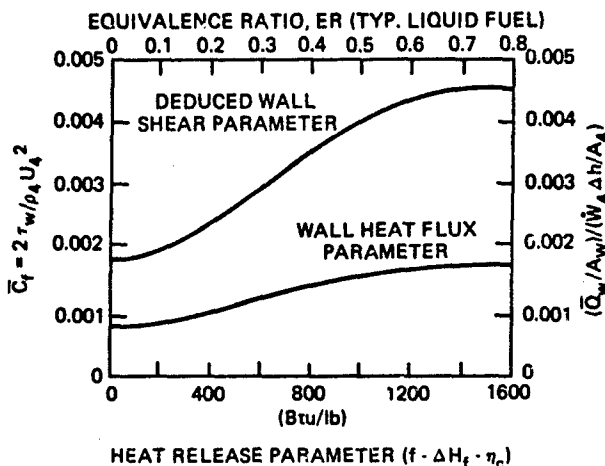
Fig. 17 Combustor wall heat transfer and skin friction coefficient as a function of equivalence ratio.

shearing stress, $\dot{w}_a$ the weight flow of air entering the combustor. Here, $ER_{eff} = ER\cdot\eta_c$ for typical liquid hydrocarbon fuels and η_c is the combustion efficiency. The form of the parameter was intentionally selected to enhance combustor calculations by giving the mean value of shear in terms of combustor inlet conditions. Preliminary results from the aforementioned theoretical analysis confirm the qualitative trend of increasing shear with increasing heat release.

With this modeling of the wall stresses the solution of the integral form of the conservation equations can be carried out. In particular, the x momentum equation can be expressed as

$$\int_{x=0}^{x=x_t} p dA_x + \int_{x=x_t}^{x=x_e} p dA_x + (1-\epsilon)\left[p_5 A_5 - \left(\frac{p_e A_e}{p_4 A_4}\right) p_4 A_4\right] - \int_{x=0}^{x=x_5} \tau_w dA_w = p_5 A_5 + \rho_5 u_5{}^2 A_5 - p_4 A_4 - \rho_4 u_4{}^2 A_4 - \rho_f u_f{}^2 A_f$$

(6)

where the subscript 5 refers to conditions at the combustor exit, subscript e to conditions corresponding to the point where the pressure variation with area can be represented by the Crocco parameter and subscript f refers to the fuel. For normal injection, the fuel momentum term is zero and for other injection angles the term is small and usually is neglected. In all of the data that have been examined to date, either $x_s = x_e$, i.e., immediately following the shock train the pressure-area distribution can be represented by $\epsilon = c$ process or $A_s = A_e$, i.e., the downstream end of the shock train is in a constant area section. Thus, the second integral has been set = 0 in the analysis of data currently available. In the latter case, it still would be necessary to relate p_s to p_e to obtain solutions rigorously, but considering the approximate nature of the shear modelling, p_e is frequently taken equal to p_s. With these assumptions, a set of initial conditions, including the fuel specification (atom balance, flow rate and enthalpy) and a value for η_c and a procedure for

relating the state variables, the integral form of the conservation equations can be solved for selected values of p_s/p_4. Generally, local thermodynamic equilibrium is assumed at the combustor exit, where the composition is assumed to be products of combustion at $ER_{eff} = \eta_c ER$ and unreacted fuel in the amount $(1 - \eta_c)ER$. References 24 and 25 provide the basis for computing the state relationships. Of course, the application of this analysis is limited to either the determination of the global heat release and combustor exit conditions given a wall pressure distribution or the prediction of the wall pressure and exit conditions given an assumed heat release. If neither the heat release nor the pressure distribution is known a priori, then suitable kinetic rate equations must be introduced and solved simultaneously with the aforementioned conservation equations. A discussion of this subject is beyond the scope of this paper. Conversely, if both the pressure distribution and the global heat release are known from experiments, the veracity of this analysis can be examined.

Equation (6) can be simplified to

$$(1 - \epsilon)\left[\frac{p_5 A_5}{p_4 A_4} - \left(\frac{p_e A_e}{p_4 A_4}\right)\right] = \frac{p_5 A_5}{p_4 A_4}\left(1 + \frac{\rho_5 u_5^2}{p_5}\right) - \left(1 + \frac{\rho_4 u_4^2}{p_4}\right) - z \qquad (7)$$

where

$$z = \frac{\rho_f u_f^2 A_f}{p_4 A_4} + \int_{x=0}^{x=x_s} \frac{p}{p_4}\, d\left(\frac{A}{A_4}\right) + \int_{x=x_s}^{x=x_e} \frac{p}{p_4}\, d\left(\frac{A}{A_4}\right) - 2\, \overline{C}_f\, \frac{\rho_4 u_4^2}{p_4}\, \frac{A_w}{A_4} \qquad (8)$$

and the procedure for obtaining all terms in Eq. (8) has been described.

For a given combustor and shock train pressure ratio, there are two solutions for every fuel flow rate, one of which can be eliminated because either the pressure increases downstream of the shock or the second law of thermodynamics is violated, or both. In effect then, for a given heat release there is one candidate solution for each value of p_s/p_4, and an additional constraint must be imposed to yield a unique solution.

Reference 26 introduced the constraint $(\partial p/\partial A)_{\epsilon=c} = (\partial p/\partial A)_{s=c}$ as $A \rightarrow A_5$ and $(dT_t/T_t) \rightarrow 0$, which simply states that the slope of the pressure area relationship for a constant ϵ process at the combustor exit, where the derivative of the total temperature approaches zero, should be equal to the slope of an isentropic process. More rigorously, the slope should match that of an adiabatic process that includes wall shear. However, if the shear terms are added, no simple analytic relationship has been found, and indeed, when typical experimental results are examined, the effects do not significantly affect this constraint.

With this constraint the additional condition

$$M_5 = \left[\frac{\epsilon}{\epsilon + \gamma_5(1-\epsilon)}\right]^{1/2} \quad \text{or} \quad \epsilon = \left[\frac{\gamma_5 M_5^2}{1 + (\gamma-1)M_5^2}\right] \qquad (9)$$

must also be met, and a unique solution for each heat release can be obtained. That is, there is a specified shock train pressure rise for a given heat release. This result represents an analogous situation to the well recognized thermal choking point in a Rayleigh heating process. Reference 21 gave the name "entropy limit" to solutions of the conservation equations that were so constrained. One caveat remains, viz for low area ratio combustors and high heat release rates, the solutions to the equations would yield shock train pressure rises which would exceed that of a normal shock. For those cases, the slope constraint is relaxed, the normal shock pressure ratio is held, and the combustor exit Mach number, M_5, is permitted to decrease. The limiting heat release for a combustor operating in this mode corresponds to $M_5 = 1$. Analysis of free-jet tests of scramjet engines verifies this mode of engine operation.

The steps in the procedure for determining the wall pressure distribution, wall shear and flow properties in the exit plane for a given combustor and heat release rate are as follows:

1) The shear term in Eq. (8) is computed directly using the relationship from Fig. 17, A_w, and the initial conditions.

2) An initial value of p_s/p_4 is estimated from previous calculations or from a calorically perfect solution, which will subsequently be discussed.

3) Equation (5) is solved for s_d; then Eq. (4) is solved for s_s and values of p/p_4 vs x in the region $x = 0$ to $x = s_s - s_d$. These values, together with the geometry of the combustor, permit the evaluation of the left hand integral in Eq. (8) and define A_s/A_4.

4) The energy, continuity and state equations are combined to obtain $p_5 A_5/p_4 A_4$ which, for fluids that can be treated as calorically perfect at a given flow station, yields

$$\frac{p_5}{p_4}\frac{A_5}{A_4} = (1 + f)\frac{M_4}{M_5}\left(\frac{\gamma_4 m_5}{\gamma_5 m_4}\right)^{1/2}\left[\frac{2 + (\gamma_4-1)M_4^2}{2 + (\gamma_5-1)M_5^2}\right]^{1/2}\left(\frac{T_{t_5}}{T_{t_4}}\right) = \frac{k_1}{M_5[2 + (\gamma_5-1)M_5^2]^{1/2}} \qquad (10)$$

5) Equation (9) is substituted into Eq. (7) and set equal to Eq. (10) to yield

$$\frac{p_e}{p_4} = \frac{A_4}{A_e(1-M_5^2)}\left\{\left[1 + (\gamma_5-1)M_5^2\right](1 + \gamma_4 M_4^2 + z) - \frac{k_1\gamma_5^2 M_5}{[2 + (\gamma_5-1)M_5^2]}\right\} \qquad (11)$$

For cases where $p_s \approx p_e$, as has been observed in many experimental results, the computed value of p_e/p_4 is compared to the initially selected value of p_s/p_4, a new value assumed and steps 2 through 5 repeated until the suitable agreement is reached. When $p_s \neq p_e$ and the values are known a priori and $A_s = A_e$, the above matching is carried out for the known value of p_s/p_e, which could simply be an iterant in a $p_s = p_e$ solution. When $p_s \neq p_e$ and the respective values are not known a priori, or if $A_s \neq A_e$, or both, a joining process is required. The joining process necessitates the adoption of an additional constraint, viz, that the flow at stations s and e can be represented as unidimensional at those stations. Again, the integral method does not require one-dimensional flow between these stations. Between stations s and e it is again assumed that the pressure distribution can be represented by another value of the Crocco parameter, i.e., $\bar{\epsilon}$. Solutions can now be found for any other imposed constraint within limits. For example, it could be assumed that the variation in heat release is known as a function of distance or residence time, thereby the values of T_{t_s}/T_{t_e} would be known. Solutions for the upstream portion, i.e., from 4 to s would be joined to the downstream portion, i.e., from s to e by an $\bar{\epsilon}$ = constant process, and from e to 5 by an ϵ = constant process.

6) For the converged value of p_e/p_4 and the corresponding values of M_5 and γ_5, Eq. (7) is solved for ϵ and

$$\frac{p_5}{p_4} = \frac{p_5}{p_e}\frac{p_e}{p_4} = \frac{p_e}{p_4}\left(\frac{A_e}{A_5}\right)^{\frac{\epsilon}{\epsilon-1}} = \frac{p_e}{p_4}\left(\frac{A_e}{A_4}\right)^{\frac{\epsilon}{\epsilon-1}}\left(\frac{A_4}{A_5}\right)^{\frac{\epsilon}{\epsilon-1}} \qquad (12)$$

7) For cases where the converged solution for p_s/p_4 yields a value greater than that corresponding to a normal shock at station 4, the normal shock p_s/p_4 value is held, and the constraint imposed by Eq. (7) is relaxed. A value for M_5 less than that corresponding to the entropy limit case is assumed, and Eq. (10) is solved for $A_5 p_5/A_4 p_4$, which is substituted into Eq. (7) to find ϵ and into Eq. (12) to obtain a calculated value of A_5/A_4, which is compared to the actual A_5/A_4. The process is repeated until convergence is obtained or the limiting value of $M_5 = 1$ is reached.

Results from this analysis are peculiar to a particular combustor and operating conditions. On the other hand, a number of important qualitative features of the analysis can be examined by considering the idealized case of a calorically perfect gas with $\gamma = 1.4$, and neglecting shear and the mass and momentum contributions of the fuel. Figure 18 shows a typical set of solutions for the case of $M_4 = 2.5$, $s_s - s_d = 0$ and $p_e = p_s$. The solid lines show the p_5/p_4 values as a function of the combustor area ratio for the entropy limit solutions at selected shock train pressure ratios of 1, 2, 4, 6 and 7.125. The dashed curves for M_5 values of 1.0, 1.2, 1.4, 1.6 and 1.8 are solutions that correspond to the normal shock pressure rise, $p_s/p_4 = 7.125$ but

$$M_4 = 2.50$$
$$\gamma = 1.4$$
$$\tau_w = 0$$
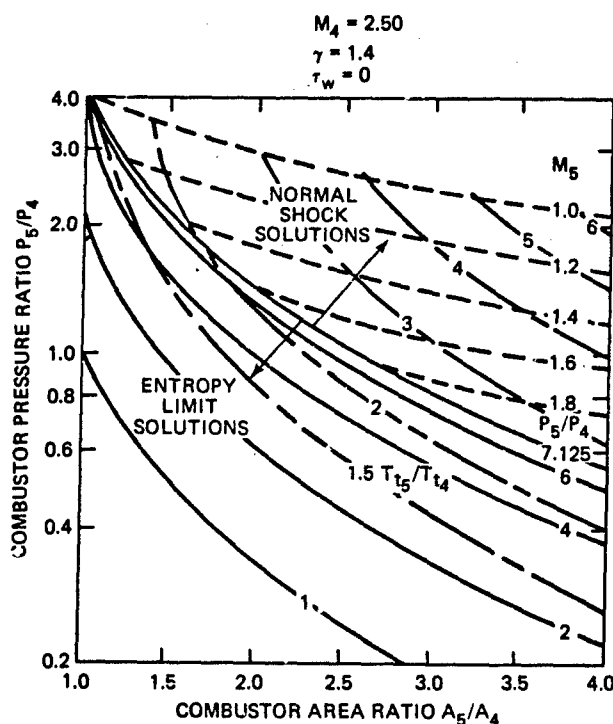
Fig. 18 Combustor exit pressure ratios for selected heat release rates.

with the slope constraint at the combustor exit relaxed. Superposed on these solutions are curves corresponding to total temperature ratios of 1.5, 2, 3, 4, 5 and 6. For all $A_5/A_4 > 1$, $p_5 < p_8$, but this does not preclude the possibility of pressures within the combustor being greater than p_8. In fact, if the combustor comprised a cylindrical or slowly diverging area section followed by a more rapidly diverging section, $p > p_8$ would be expected.

The distinction between solutions resulting from this modeling and those for flows that are constrained to be unidimensional throughout is clearly evident for the particular case of $A_5/A_4 = 1$. As shown in Fig. 18, the $p_8/p_4 = 1$, 2 and 4 curves intersect the $A_5/A_4 = 1$ axis at $p_5/p_4 = 1$, 2 and 4, respectively. Upon closer examination it can be shown that for all values of $p_8/p_4 \leq 4.0625$, $p_5 = p_8$, whereas for all values of $p_8/p_4 > 4.0625$ there are no solutions at $A_5/A_4 = 1$. It can be rigorously proved that every combustor exit solution of $p_5/p_4 \leq 4.0625$ corresponds to an end point state on the supersonic leg of a Rayleigh heating process, i.e., a one-dimensional frictionless heat addition process in a constant area duct. Moreover, the M_5 values are identical to those of the corresponding Rayleigh heating process. However, from Eq. (9) the slope constraint at station 5 requires $\varepsilon > 1$ for $M_5 > 1$. From a physical standpoint, this would imply that for all $T_{t_5}/T_{t_4} \leq 1.4083$, the value corresponding to $p_5/p_4 = 4.0625$, $M_5 = 1$, shock trains having strengths corresponding to single oblique waves would be present and not the shock-free all supersonic Rayleigh process. Note, too, that these results would also hold for cases where the shock train extends into the duct as long as wall friction is negligible. When wall friction is included, the same qualitative features are present, but the values of p_5/p_4 and p_8/p_4 shift for given values of T_{t_5}/T_{t_4}. Also note that as A_5/A_4 is increased slightly above 1 in the wall-shear-free case, solutions for p_8/p_4 up to the normal shock value at M_4 are possible, but p_5/p_4 is always < 4.0625. This can also be seen in Fig. 19 where p_8/p_4 instead of p_5/p_4 is the ordinate.

$$M_4 = 2.5, \gamma = 1.4, \tau_w = 0$$
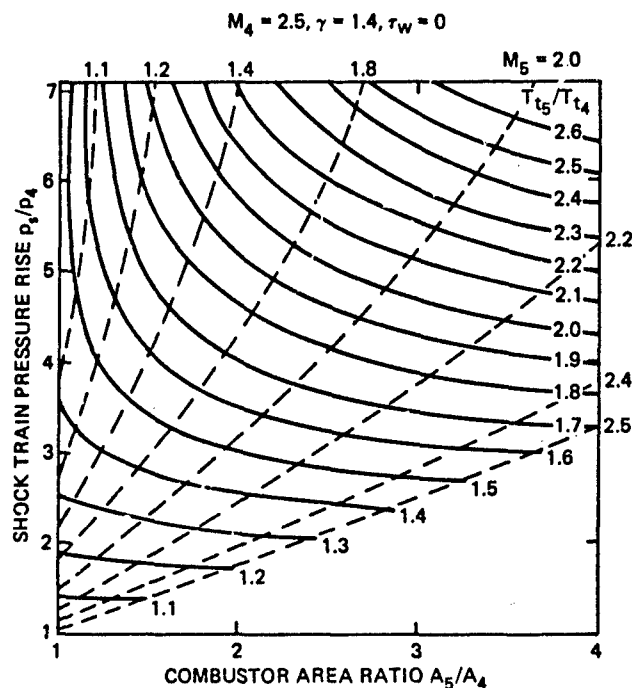
Fig. 19 Pressure ratios across precombustion shock train.

Curves for constant T_{t_5}/T_{t_4} values from 1.1 to 2.6 are given in Fig. 19 as $f(A_5/A_4, p_8/p_4)$ for solutions constrained by the slope condition at the combustor exit. For values of $T_{t_5}/T_{t_4} \leq 1.4083$ the curves intersect the $A_5/A_4 = 1.0$ axis and, indeed, there are valid solutions for $A_5/A_4 < 1$, i.e., for combustors with converging areas. The curves for $T_{t_5}/T_{t_4} > 1.4083$ are cusped at $A_5/A_4 \rightarrow 1$, i.e., there are also solutions for $A_5/A_4 < 1$, and those T_{t_5}/T_{t_4} curves also become asymptotic to the $A_5/A_4 = 1$ axis. Overlaid on this grid are dashed curves for constant M_5 values of 1.1 to 2.5. The entropy limit solutions for $p_8/p_4 = 7.125$ are limited to a maximum $T_{t_5}/T_{t_4} = 2.813$ for combustors with $A_5/A_4 \leq 4$. However, if the exit slope condition is relaxed and M_5 is permitted to equal unity, the maximum T_{t_5}/T_{t_4} is 6.293.
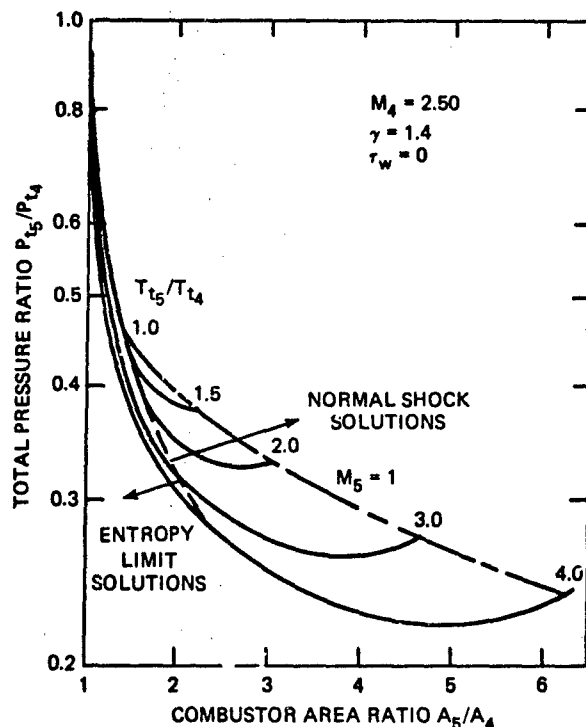
Fig. 20 Total pressure ratio for selected heat release rates.

Figure 20 shows the important effect of combustor area ratio on the total pressure recovery in the heat addition process, P_{t_5}/P_{t_4}. Curves for total temperature ratios T_{t_5}/T_{t_4} of 1, 1.5, 2, 3 and 4 are shown.

Points to the left of the dashed line correspond to entropy limit solutions and those to the right of the dashed line are for shock trains with normal shock pressure ratios. The T_{t_5}/T_{t_4} curves terminate at $M_5 = 1$.

For $T_{t_5}/T_{t_4} > 1$, the P_{t_5}/P_{t_4} curves decrease rapidly with increasing A_5/A_4, but reach a minimum at M_5 slightly > 1. Whereas larger values of A_5/A_4 permit more heat to be released, the expense in total pressure loss is insignificant. For the same T_{t_5}/T_{t_4} more heat can be added in a given A_5/A_4 combustor as M_4 increases. As shown in Table 2, $M_4 = M_{e3}$ increases with M_0, but T_{t_5}/T_{t_4} decreases with M_0 for a given ER, which is, un-fortunately, the opposite of the desired trend. For this reason the designer generally selects the smallest possible A_5/A_4 that provides sufficient thrust to climb out at M_{EOB} and then accepts the loss in P_{t_5}/P_{t_4} that occurs at $M_0 > M_{EOB}$ where A_5/A_4 is greater than the optimal value.

Similar curves to Figs. 18-20 can be generated for values of $Z \neq 0$ (Eq. 8) to provide a means for assessing the effects of shear, combustor shape and of the shock train extending into the combustor. Of course, for a precise calculation, the actual properties of the flow at the combustor entrance, the fuel type and injector configuration, etc., must be known, together with the appropriate state equation and solutions must be done on a computer.

As previously stated, when the bulk value of the heat release is known, experimental measurements can be compared to the results of this analysis. Over a period of about twenty years at the Johns Hopkins University Applied Physics Laboratory, bulk heat release rates have been obtained from a steam calorimeter attached to the exit of supersonic combustors. One of the first reported experiments (Ref. 21) remains as a benchmark to index the veracity of analytical solutions due primarily to the atypical test configuration. In this test, the boundary layer of the incoming air was removed just ahead of the fuel injector ports (see Fig. 21a), thus providing the unique situation where the shock train can collapse to a simple normal wave as $s_s \to 0$. For the $ER_{eff} = 0.424$ with hydrogen fuel and combustor entry conditions of $M_4 = 1.95$ and $T_{t_4} = 2188°R$, the foregoing analysis would predict a normal shock-entropy limit solution. For this $A_5/A_4 = 2.28$ combustor using a value for Z in Eq. (8) deduced from the measured heat transfer and a modified Reynold's analogy (see Ref. 23), the entropy limit solution corresponds to $\epsilon = 2.004$, $p_s/p_4 = 4.28$, $p_5/p_4 = 0.835$ and $M_5 = 1.676$. Figures 21b and c show the excellent agreement between theory and measurement of the wall static and combustor exit pitot pressures P_{t_5}, and exit Mach number deduced from p_5 and P_{t_5}.

In all other available experimental data there has been a boundary layer of finite thickness at the combustor entrance, thus it has been necessary to compute s_s, s_d and $p = f(x)$ from $x = 0$ to $x = s_s - s_d$.

Figure 22 compares measured and computed wall pressure distributions for three different combustor geometries (see Refs. 9 and 10 for details). In each case M_4, θ_4, D_4 and A_5/A_4 are 3.23, 0.0146 in, 2.74 in, and 2.0,

COMBUSTION AND FLOW
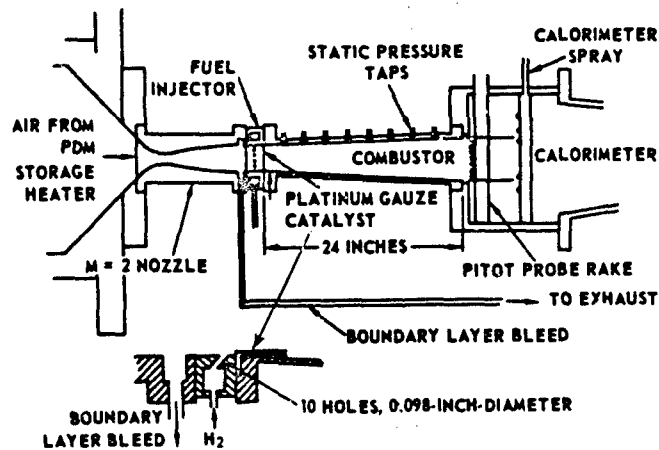
a) Schematic of test apparatus.

b) Experimental and theoretical combustor pressure distribution.
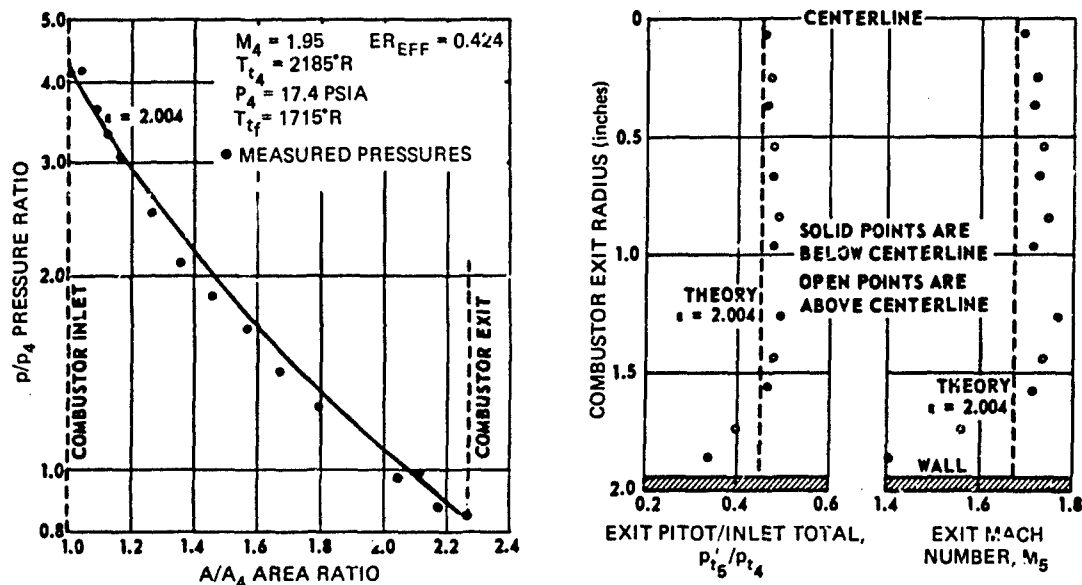
c) Experimental and theoretical combustor-exit profiles.

Fig. 21   Comparison of experimental measurements with theoretical
analysis for combustor with normal shock at entropy limit.

respectively. Since these data were used to obtain the empirical relationship for s_d given in Eq. (5), the positioning of the shock train with respect to the fuel injectors is reasonably well represented. Some changes in the theoretical pressure distributions from those presented in Ref. 10 have been made due to the improved modeling of the "Z" term in Eq. (8). For the conical combustor, no joining process is warranted since it appears that station s and e are about coincidental. In the short cylinder-cone and the step cylinder cone, the constant area sections necessitated a joining procedure to complete the theoretical analysis. In the absence of any well posed theory or experimental correlation, the simple assumption of a linearly increasing total temperature with distance was assumed to hold between the shock train and the $\varepsilon = c$ region. This zone is so short in the short cylinder case that no judgment on the appropriateness of the modeling can be made. In the step cylinder cone, both the analysis and the experimental pressure distributions show that the flow is "overcompressed" with respect to the duct area by the shock train, i.e., the effective cross-sectional area of the flow is smaller than the duct area at station s. The theoretical pressure distribution in the joining region was based on the assumption that the total heat release was evenly split between the cylindrical and conical stations and station e was located at the entrance to the 0.7° half-angle cone. With these assumptions, the pressure is predicted to decrease by about 10–15% in the constant area section.

A much larger data base will have to be analyzed before any conclusive arguments can be made to improve the modeling. Nonetheless, the general agreement between theory and experiment is considered to be quite good.

a) CONICAL COMBUSTOR

b) SHORT CYLINDER CONE COMBUSTOR

c) STEP CYLINDER CONE COMBUSTOR
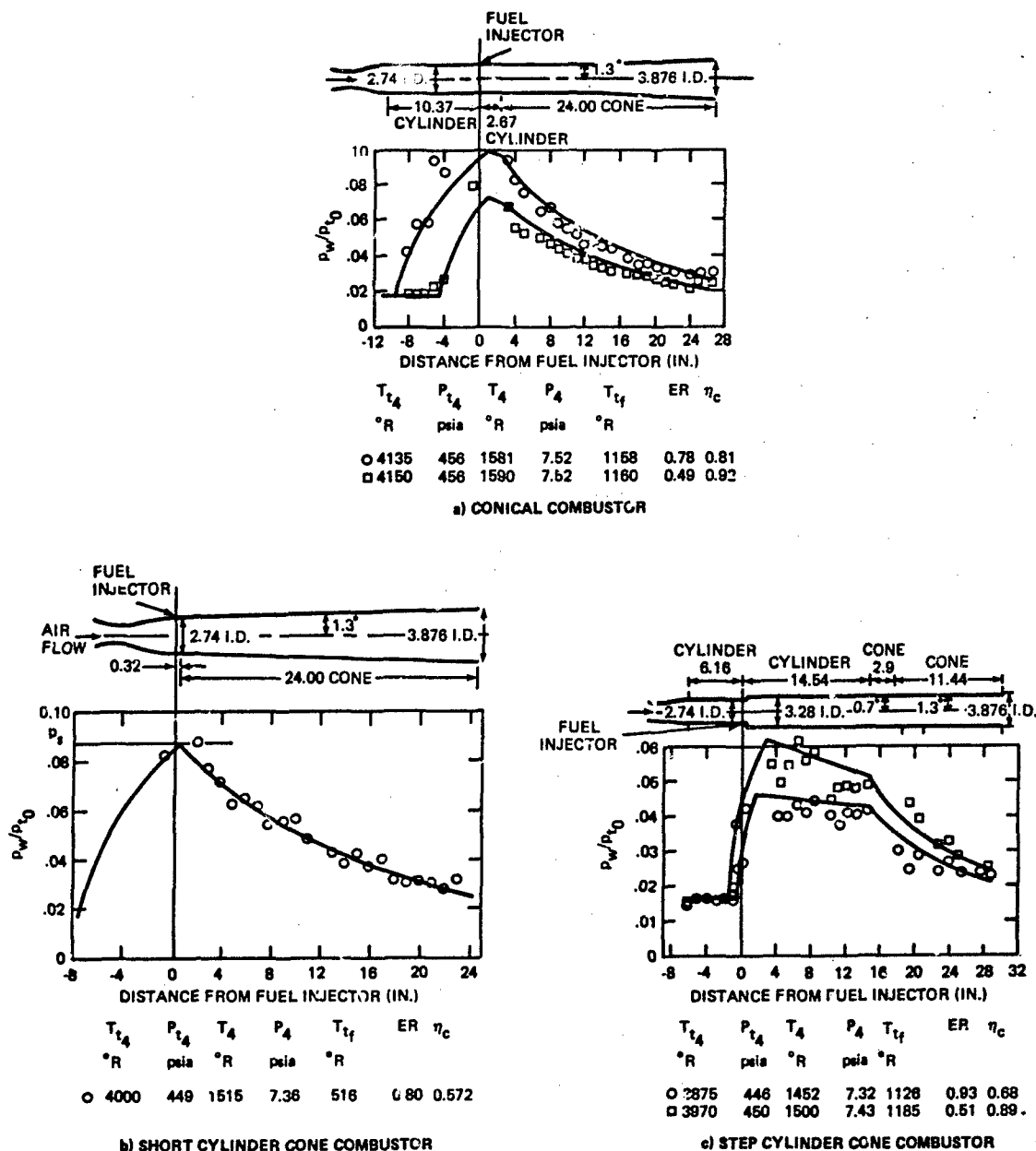
Fig. 22 Comparison of theoretical and experimental wall pressure distributions in supersonic combustors.

Since in the design of a fixed geometry engine A_5/A_4 must be specified, a procedure for selection must be developed. Each application imposes different constraints, e.g., the available length will directly affect the combustor wall shear, whereas a change in combustor area ratio may or may not cause a change in the allowable fuel volume, therefore there is no one design strategy. Nonetheless, some of the steps in the process that can be generalized are as follows.

Generally, as mentioned, the maximum thrust requirement occurs at M_{EOB}, and A_5/A_4 is selected to meet the requirement and provide some margin to assure that the missile will climb out and accelerate when anomalous conditions arise. However, an overly conservative value for A_5/A_4 is not a judicious choice, because provision for additional thrust margin invariably leads to engine inefficiency during cruise. The following example should help clarify these points. Consistent with the general nature of this discussion, the simplified assumptions that were adopted to develop Figs. 18-20 are the basis for the curves shown in Fig. 23. Here, the maximum values of T_{t_5}/T_{t_4} for the normal shock, $M_5 = 1$ limit are shown as a function of M_4 for

values of A_5/A_4 from 1 to 3. The aforementioned trend of increasing $(T_{t_5}/T_{t_4})_{max}$ with increasing M_4 is characteristic of all of the A_5/A_4 curves. Overlaid on these curves are curves drawn through points corresponding to the combustor requirements for the four ITS inlets (Cases A through D) that were previously discussed (Table 2). Here, $M_4 = M_{e3}$ and the values of the required T_{t_5}/T_{t_4} assume that the engines are opera-
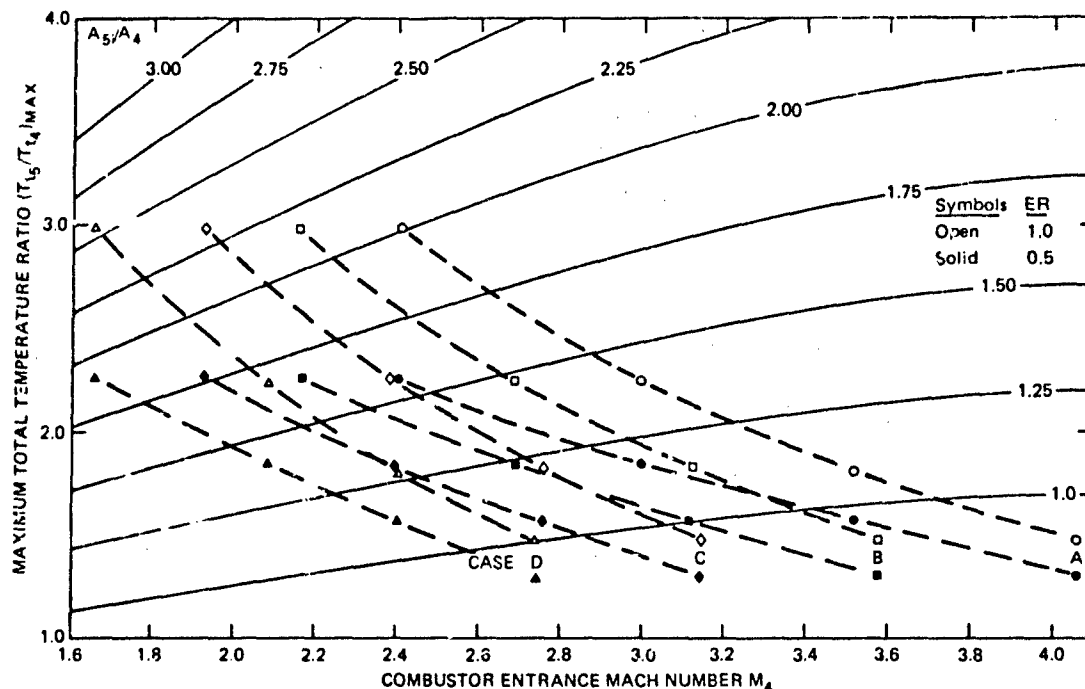
Fig. 23   Maximum total temperature in diverging combustors normal shock pressure rise, $M_5 = 1$.

ting in the tropopause with $T_0 = 390°R$ and that the fuel is Shelldyne H (RJ-5) with a heating value of 17 Btu/lb$_m$ and a stoichiometric fuel/air ratio (ER = 1) of 0.07284. The required T_{t_5}/T_{t_4} values are based on real gas in thermodynamic equilibrium, but all other parameters are consistent with the simplifying assumptions of a calorically perfect gas with $\gamma_4 = \gamma_5 = 1.4$ and no mass or momentum of the fuel.

The open symbols are for T_{t_5}/T_{t_4} values that correspond to ER = 1.0. The required A_5/A_4 vary from 2 2.55 at $M_0 = 4$ to below 1 at $M_0 = 7$ for this ER. The solid symbols are for ER = 0.5 and the required $A_5/$ are correspondingly reduced, varying from 1.58 to 1.91. To size the combustor, the thrust requirements would have to be known, but in this example it is assumed that at $M_0 = M_{EOB} = 4$, $T_{t_5}/T_{t_4} = 2.5$. The corr ponding ER would be 0.639 and the values of A_5/A_4 for the four engine designs are listed in Table 3. For maximum acceleration in the climbout, the fuel control could be programmed to increase ER to the allowabl limit as M_0 increased. This would occur at M_0 from 4.3 to 4.4 for the four cases. In this example, it is also assumed that the engines would accelerate at ER = 1 until $M_0 = M_{CR} = 7$ at which point they would be throttled back to ER = 0.5 for cruise.

With A_5/A_4 and T_{t_5}/T_{t_4} specified, solutions can be found for each set of initial conditions. Result from these calculations are summarized in Table 3. At $M_0 = 4$ all cases correspond to normal shock pressu rises with $M_5 = 1$. As M_0 increases, M_5 also increases until a condition is reached where it is possible obtain an entropy limit solution. Normal shock and entropy limit processes are labeled N.S. and S.L., re spectively, under "Type" in Table 3. For all points other than Case D at $M_0 \geq 6$, the static pressure at combustor exit is higher than it is prior to the shock train. In the absence of a more detailed analysis the viscous layer at station 5, it is usually assumed that $(A/A_e)_5 = (A/A_e)_4$. This assumption was made t obtain the values of A_0/A_{e5} shown in the Table. Total pressure recovery in the combustor, p_{t_5}/p_{t_4}, incre as the inlet compression increases because the beneficial effects of reduced initial Mach number more tha compensate for the detrimental effect of larger A_5/A_4. Combining the pressure recovery in the inlet with combustor results in the values of p_{t_5}/p_{t_0} shown in the last column. An extremely important trend is sho in the values of p_{t_5}/p_{t_0}. Case C yields higher total pressure recovery than Case D, even though there is less compression than for Case D. Thus, there would be no reason to select D and exacerbate the possible problems of boundary layer separations due to shock reflections from the inward turning scoop inlet. The ranking of Cases A, B and C must also take into consideration forebody forces and additive drag before a final ranking can be established.

Table 3

Combustor Parameters for Four Engines with ITS $M_{FC} = 6$ Inlets

Case	M_0	A_5/A_4	M_4	ER	Type[a]	T_{t_5}/T_{t_4}	M_5	P_s/P_4	ϵ	P_5/P_4	A_0/A_{e5}	P_{t_5}/P_{t_4}	P_{t_5}/P_{t_0}
A	4	1.717	2.404	0.639	N.S.	2.500	1.000	6.58	3.12	2.968	1.989	0.3819	0.2936
	5	"	2.999	1.000	S.L.	2.241	1.479	9.33	1.63	2.467	2.329	0.2396	0.1622
	6	"	3.512	1.00?	S.L.	1.805	1.799	6.64	1.97	2.215	2.665	0.1638	0.0967
	7	"	4.055	1.000	S.L.	1.463	2.342	4.40	2.40	1.744	2.665	0.1427	0.0705
	7	"	4.055	0.500	S.L.	1.290	2.773	3.00	2.64	1.258	2.665	0.2005	0.0991
B	4	1.822	2.159	0.639	N.S.	2.500	1.000	5.27	4.05	2.378	2.174	0.4489	0.3209
	5	"	2.688	1.000	N.S.	2.241	1.493	8.26	1.70	1.925	2.580	0.3059	0.1811
	6	"	3.116	1.000	S.L.	1.805	1.793	5.80	1.97	1.715	2.941	0.2230	0.1077
	7	"	3.571	1.000	S.L.	1.463	2.292	3.84	2.37	1.361	2.941	0.1994	0.0752
	7	"	3.571	0.500	S.L.	1.290	2.675	2.67	2.59	1.006	2.941	0.2672	0.1007
C	4	1.954	1.921	0.639	N.S.	2.500	1.000	4.74	6.39	1.871	2.255	0.5117	0.3321
	5	"	2.380	1.000	N.S.	2.241	1.478	6.44	1.85	1.503	2.707	0.3773	0.1882
	6	"	2.751	1.000	S.L.	1.805	1.800	5.04	1.98	1.298	3.119	0.2961	0.1133
	7	"	3.141	1.000	S.L.	1.463	2.249	?.38	2.34	1.051	3.119	0.2677	0.0758
	7	"	3.141	0.500	S.L.	1.290	2.583	2.40	2.55	0.798	3.119	0.3423	0.0969
D	4	2.154	1.652	0.639	N.S.	2.500	1.000	3.02	44.56	1.377	2.129	0.5674	0.3138
	5	"	2.081	1.000	N.S.	2.241	1.477	4.89	2.08	1.117	2.555	0.4467	0.1776
	6	"	2.400	1.000	S.L.	1.805	1.827	4.31	2.00	0.931	2.940	0.3814	0.1093
	7	"	2.731	1.000	S.L.	1.463	2.223	2.97	2.32	0.774	2.940	0.3511	0.0701
	7	"	2.731	0.500	S.L.	1.290	2.509	2.16	2.51	0.603	2.940	0.4279	0.0854

[a] N.S. = normal-shock processes; S.L. = entropy-limit processes

Solutions for the flowfield in the combustor based on the use of finite difference solutions of the differential form of the conservation equations are also in an active state of development. The deficiencies in these techniques are in the formulations for modeling turbulence and kinetics and in incorporating boundary constraints that are not in opposition to experimental observations. Indeed, it has been found that the most successful approach has been to impose a wall pressure distribution governed by the foregoing integral analysis. References 13 and 27 discuss this methodology for the particular case of the DCR engine cycle. The practical limitation of the cost of the computations still precludes the use of the finite difference approach as an effective design tool, but the value of having the capability to examine the entire flowfield in detail for a few selected cases cannot be underestimated. As reductions in the cost of CPU time accrue and better techniques for adaptive grid point spacing evolve, these techniques will play an important role in design.

NOZZLE ANALYSIS

The analytical tools that are required for the design of the exit nozzle and the analysis of the flow-fields for the supersonic combustion engine are not significantly different than those for the CRJ. The principal difference is that the throat station in the converging-diverging nozzle provides a reference plane in which sufficient constraints are present to describe the flow properties, albeit with certain assumptions regarding the chemical composition of the gas. In the scramjet, the distinction between nozzle and combustor can be obscure and as the previous discussion suggested, station 5 can, in fact, change with changing conditions at the combustor entrance. Moreover, significant gradients in flow properties in the initial plane are much more likely to be present in the scramjet.

As in the case in the combustor, both integral analyses and finite difference techniques have been developed. Emphasis shifts from properly modeling the mechanisms that contribute to the losses in total pressure to adequate representation of flow angularity, especially in the nozzle exit plane. The greatest deficiency in nozzle flow analysis, as in the combustor, is in the modeling of the chemistry. In the combustor the processes during the early phases of reactions, e.g., chain breaking, cause the greatest difficulties. In the nozzle, modeling of the recombination reactions and, in the case of some specialized fuels, phase changes of metal oxides are problems.

Much of the work in the development of useful design approaches based on finite difference techniques is still in progress, but Refs. 31 and 32 give some insight into these methods. The integral analyses are at present quite rudimentary. Given a unidimensional representation of the flow at station 5, calculations of isentropic expansion corresponding to the effective nozzle area ratio A_6/A_{5e} are made for two cases: one assuming thermodynamic equilibrium and the other assuming a constant chemical composition "frozen" at station 5. Two empirical constants, r and η_N, are then introduced, the first to account for the loss in nozzle exit stream thrust that is attributable to finite rate reactions (and phase changes) and the second to account for friction, divergence and non-uniformity. Thus,

$$\mathfrak{F}_6 = \eta_N [r \mathfrak{F}_{6_{EQ}} + (1 - r) \mathfrak{F}_{6_{FZ}}] \qquad (13)$$

where

$$\mathfrak{F}_6 = P_6 A_6 + \rho_6 u_6^2 A_6 \qquad (14)$$

and typical values are $r = 1/3$, $\eta_N = 0.97-0.99$. An adequate data base to substantiate the validity of this modeling has not yet been forthcoming.

With $\mathfrak{F}_6$ defined, the thrust and net engine force can be determined for specific values of A_i/A_R, when A_R is the frontal area of the engine. In Fig. 14, $\psi = 45°$ for each of four inward turning scoop inlets, thus $A_i/A_R = 0.5$. By changing either ψ or the number of scoops, or both, A_i/A_R can be varied with an upper bound that is governed by starting. The relative performance of engines corresponding to Cases A-D can be obtained by examining a single value of A_i/A_R, e.g. 0.5, and then the effects of changing A_i/A_R can be studied independently.

The thrust coefficient is given as

$$C_T = \frac{1}{q_0 A_R}\left[\mathfrak{F}_6 - \mathfrak{F}_0 - p_0(A_R-A_0)\right] = \frac{2}{\gamma M_0^2}\left[\frac{p_6}{p_0}(1 + \gamma M_6^2) - 1\right] - 2\frac{A_0}{A_R} \tag{1}$$

and the drag coefficient due to the pressure acting on that portion of the conical forebody not wetted by the air captured in the inlet is

$$C_D = \frac{2}{\gamma M_0^2}\left(\frac{p_c}{p_0} - 1\right)\left(1 - \frac{A_i}{A_R}\right) \tag{1}$$

The additive drag for $M_0 < M_{FC}$ is given as

$$C_{DADD} = \frac{2}{\gamma M_0^2}\left\{\frac{p_w}{p_0}\left[1 + \frac{\gamma M_w^2 \sin(\theta_w-\psi_w)\cos\psi_w}{\sin\theta_w}\right] - 1\right\} - 2\frac{A_0}{A_i} \tag{:}$$

Therefore, the resulting net force coefficient is

$$C_F = C_T - C_D - C_{DADD} \tag{(}$$

Table 4 lists the Mach number and pressure ratio at the nozzle exit plane and the calculated force co efficients for Cases A-D. Again, for clarity, the simplifying assumption of $\gamma = 1.4$ was adopted, thus $r =$ and η_N was taken as 0.985. At $M_0 = 4$, the exit pressure is somewhat below the ambient pressure, but the values are not low enough to suggest separation in the nozzle. The gross thrust coefficients, C_T, exhibit the same general trend as the p_{t_5}/p_{t_0} values discussed earlier. However, when additive drag is subtracted it turns out that Case B yields the highest values, and if the forebody drag is subtracted, Case A is best. If other values of A_i/A_R between the limits $0.4 \leq A_i/A_R \leq 0.8$ are examined, the trend is toward higher re lative values of C_F with greater inlet contraction as A_i/A_R increases. Nonetheless, over the entire range reasonable values for A_i/A_R, the optimal conical forebody angle is $\delta_c \leq 12.5°$. These results clearly show need to consider additive drag and forebody drag if a true optimum is to be identified.

Typical values of the ratio of missile weight to maximum cross-sectional area are from 4 to 7 lbs/in². For a value of 5 lb/in² and flight at $M_0 = 4$, $Z = 5000$ ft, a value of $C_F = 0.26$ would correspond to 7.1 "g" of accelerative capability.

It is of interest to compare the results obtained from these dual mode engines with those from a set (engines having the same inlets but with dump-type subsonic combustors. As in the case of the scramjet, acceleration requirements at the end of boost prescribe the combustor-nozzle area ratio. To obtain maximum performance in the CRJ, the nozzle throat is sized to produce critical flow in the inlet at this condition. In an inlet having internal contraction such as the ITS, the critical condition corresponds to locating a normal shock (in actuality, a shock-train having a pressure rise equal to a normal shock) at station 3. These conditions are shown in Table 3 and are labelled 3'. As M_0 increases and/or ER decreases, the total temperature ratio in the combustor decreases and the normal shock seeks a location where $A > A_{3e'}$. Para doxically, the inlet must throw away pressure recovery in order to satisfy the sonic flow conditions impose at the nozzle throat. For the example cases, this area is set by the $M_0 = 7$, ER $= 0.5$ operating condition

Larger duct areas would be possible, which would lead to smaller duct and dump losses but with a loss in th internal volume available for packaging. The minimal duct area was used to obtain conditions at the com bustor dump plane. Total pressure losses during heat addition vary inversely with combustor entrance Mach number, so to obtain minimal loss the combustor area was taken as A_R. Again, to simplify the calculations, $\gamma = 1.4$ was assumed, the duct flow was frictionless, the dump was considered as an isobaric area expansion, and the heating was taken as a Rayleigh process. With these assumptions, the total pressure loss from station 3e' to the nozzle throat and the throat size for the $M_0 = 4$, ER $= 0.639$ operating conditions can be calculated for each of the four engines. These losses vary from 16% for Case A to 21.1% for Case D which, when coupled with the inlet losses (Table 3) give the values of p_t^*/p_{t_0} at $M_0 = 4$ shown in Table 5 and pre scribe the nozzle throat size A^*/A_{3e} that is also listed in this table. For the $M_0 = 5$, 6 and 7 condition p_t^*/p_{t_0} is deduced from the continuity equation using the lower values of total temperature rise in the co bustor given in Table 3. Proceeding backwards through the engine cycle computing first the total pressure

loss in the Rayleigh heat addition and the isobaric dump loss provides a means of verifying that the inlet must indeed operate supercritically at all but the $M_0 = 4$ condition. Had total temperature ratios below 2.5 (ER = 0.639) been prescribed at the end of boost, A^*/A_{je} would have been set by the $M_0 = 5$ conditions with critical inlet operation. The static pressure ratios p^*/p_0 at the sonic point listed in Table 5 are about one-half of the maximum value in the combustor. When compared with the maximum pressure ratios (p_s/p_0) that occur in the scramjet at the same operating point, a significant difference is present at high M_0. For example, taking case B at $M_0 = 7$, ER = 1.0, the maximum pressure in the subsonic combustor is $103.79 \div 0.5302 = 195.8$, whereas in the scramjet combustor it is $3.84 \times 17.445 = 67.0$. The implications with respect to the structural design of the combustor and nozzle are obvious.

With A^*/A_e prescribed and $A_6 = A_R$ the nozzle exit conditions p_6/p_0 and M_6 and the force coefficients can be calculated by the same method used in the scramjet analysis. The values of C_{DADD} and C_D are the same as for the comparable scramjet at the same operating conditions and therefore are not re-listed from Table 4. Comparing C_F values from Table 5 for the CRJ with those for the scramjet from Table 4 shows that the CRJ has somewhat higher performance at $M_0 = 4$ and 5, about equal performance at $M_0 = 6$, and significantly lower performance at $M_0 = 7$. For most applications of engines operating over this M_0 range, overall performance would favor the scramjet. A superficial examination of the listed results will help to support this argument. For example, if the CRJ engine for Case B was required to produce the same C_F as its scramjet counterpart, the ER, or fuel flow rate, would be reduced by about 9% at $M_0 = 4$, 5% at $M_0 = 5$, but would have to be increased by 50% during cruise at $M_0 = 7$. Both cycles exhibit the same trends in performance with inlet contraction ratio and the conclusions previously stated for the scramjet therefore hold.

Table 4

Exit Parameters and Force Coefficients for Four Engines
with ITS $M_{FC} = 6$ Inlets
(Supersonic Combustion)

Case	M_0	ER	M_6	p_6/p_0	C_T	C_{DADD}	$C_T - C_{DADD}$	C_D	C_F
A	4	0.639	3.246	0.848	0.3370	0.0124	0.3246	0.0584	0.2663
	5	1.000	3.402	1.293	0.3219	0.0059	0.3160	0.0555	0.2605
	6	1.000	3.631	1.668	0.2291	0	0.2291	0.0538	0.1753
	7	1.000	4.141	1.257	0.1173	0	0.1173	0.0527	0.0647
	7	0.500	4.611	1.237	0.0631	0	0.0631	0.0527	0.0105
B	4	0.639	3.347	0.795	0.3530	0.0188	0.3342	0.0804	0.2538
	5	1.000	3.515	1.228	0.3402	0.0089	0.3313	0.0771	0.2542
	6	1.000	3.733	1.610	0.2500	0	0.2500	0.0752	0.1748
	7	1.000	4.202	1.573	0.1328	0	0.1328	0.0739	0.0588
	7	0.500	4.617	1.247	0.0756	0	0.0756	0.0739	0.0016
C	4	0.639	3.409	0.772	0.3565	0.0257	0.3307	0.1057	0.2250
	5	1.000	3.570	1.182	0.3283	0.0120	0.3163	0.1021	0.2142
	6	1.000	3.802	1.538	0.2373	0	0.2373	0.0999	0.1374
	7	1.000	4.224	1.542	0.1209	0	0.1209	0.0986	0.0223
	7	0.500	4.584	1.250	0.0623	0	0.0623	0.0986	-0.0363
D	4	0.639	3.348	0.777	0.3248	0.0257	0.2991	0.1057	0.1934
	5	1.000	3.507	1.220	0.3250	0.0120	0.3130	0.1021	0.2109
	6	1.000	3.763	1.567	0.2354	0	0.2354	0.0999	0.1355
	7	1.000	4.132	1.605	0.1185	0	0.1185	0.0986	0.0199
	7	0.500	4.434	1.327	0.0575	0	0.0575	0.0986	-0.0412

$$\eta_N = 0.985 \qquad r = 1$$

Table 5

Nozzle Throat and Exit Parameters and Force Coefficients for Four Engines

with ITS $M_{FC} = 6$ Inlets

(Subsonic Combustion)

Case	M_0	ER	A^*/A_{3e}	p_t^*/p_{t_0}	p^*/p_0	M_6	p_6/p_0	C_T	$C_T - C_{DADD}$	C_F
A	4	0.639	1.293	0.3898	31.27	3.544	0.729	0.3562	0.3438	0.2855
	5	1.000	"	0.1853	51.79	"	1.207	0.3366	0.3307	0.2752
	6	1.000	"	0.0894	74.53	"	1.737	0.2225	0.2225	0.1687
	7	1.000	"	0.0411	89.84	"	2.094	0.0886	0.0886	0.0360
	7	0.500	"	0.0386	84.35	"	1.966	0.0203	0.0203	-0.0323
B	4	0.639	1.325	0.4412	35.39	3.689	0.674	0.3742	0.3554	0.2750
	5	1.000	"	0.2126	59.43	"	1.131	0.3528	0.3439	0.2668
	6	1.000	"	0.1035	86.57	"	1.648	0.2518	0.2518	0.1767
	7	1.000	"	0.0475	103.79	"	1.976	0.1085	0.1085	0.0346
	7	0.500	"	0.0446	97.47	"	1.855	0.0392	0.0392	-0.0347
C	4	0.639	1.408	0.4612	36.99	3.764	0.635	0.3480	0.3223	0.2165
	5	1.000	"	0.2249	62.87	"	1.080	0.3406	0.3286	0.2265
	6	1.000	"	0.1093	91.15	"	1.565	0.2347	0.2347	0.1348
	7	1.000	"	0.0502	109.87	"	1.887	0.0995	0.0995	0.0008
	7	0.500	"	0.0472	103.18	"	1.772	0.0307	0.0307	-0.0679
D	4	0.639	1.496	0.4518	36.24	3.740	0.643	0.3477	0.3220	0.2163
	5	1.000	"	0.2202	61.55	"	1.093	0.3402	0.3286	0.2262
	6	1.000	"	0.1071	89.31	"	1.585	0.2355	0.2355	0.1355
	7	1.000	"	0.0492	107.69	"	1.912	0.0838	0.0838	-0.0148
	7	0.500	"	0.0462	101.12	"	1.795	0.0305	0.0305	-0.0681

$$\eta_N = 0.985 \quad r = 1$$

$$A_1/A_R = 0.5$$

CONCLUSIONS

A summary of the contemporary approaches to the design and analysis of scramjet engines has been presented. Where possible, comparisons with data have been made and judgments made regarding the adequacy of the modeling. In many instances the treatment herein is superficial and only in conjunction with a thorough knowledge of the ever-growing base of reference material can the designer properly assess the state-of-the-art.

REFERENCES

1. G. L. Dugger, "Comparison of Hypersonic Ramjet Engines with Subsonic and Supersonic Combustion," Fourth AGARD Colloquium, Milan, Italy; also Combustion and Propulsion-High Mach Number Air Breathing Engines, Edited by Jaumotte, Rothrock, and Le Febvre, Pergamon Press, New York, 1960.

2. P.J. Waltrup, G.Y. Anderson, F.D. Stull, "Supersonic Combustion Ramjet (Scramjet) Engine Development in the United States," Proceedings of 3rd ISABE, Deutsch Gesellschaft für Luft und Raumfahrt, Cologne, West Germany, Rept. No. A77-17266-05-07, pp. 835-861, 1976.

3. "Hypersonic Research Engine Project - Phase II, Aerothermodynamic Integration Model Development - Final Technical Data Report," (AP 75-11133, AiResearch Manufacturing Company of California; NAS1-6666) NASA CR-132654, 1975.

4. T.D. Burnette, "Dual Mode Scramjet," The Marquardt Corp., Van Nuys, CA, AFAPL-TR-67-132, June 1968.

5. F.S. Billig, P.J. Waltrup and R.D. Stockbridge, "Integral-Rocket Dual-Combustion Ramjets: A New Propulsion Concept," Journal of Spacecraft and Rockets, Vol. 17, No. 5, Sept.-Oct. 1980, p. 416.

6. J.L. Hunt, P.J. Johnston, J.M. Cubbage, J.L. Dillion, C.B. Richie, and D.C. Marcum, Jr., "Hypersonic Airbreathing Missile Concepts Under Study at Langley", presented at AIAA 20th Aerospace Sciences Meeting, Jan. 11-14, 1982, Orlando, FL, AIAA paper No. 82-0316.

7. P.J. Waltrup, F.S. Billig and R.D. Stockbridge, "Engine Sizing and Integration Requirements for Hypersonic Airbreathing Missile Applications," AGARD Propulsion and Energetics Panel, 58th Symposium, Ramjets and Ramrockets for Military Applications, London, England, Oct. 26-30, 1981. Also, The Johns Hopkins University Applied Physics Laboratory Preprint PEP-58-8, Oct. 1981.

8. F.S. Billig, G.L. Dugger and P.J. Waltrup, "Inlet-Combustor Interface Problems in Scramjet Engines," 1st International Symposium on Air Breathing Engines, June 19-23, 1972, Marseille, France, Johns Hopkins University Applied Physics Laboratory preprint, June 1972.

9. F.S. Billig, R.C. Orth and J.A. Funk, "Direct-Connect Tests of a Hydrogen-Fueled Supersonic Combustor," NASA-CR-1904, August 1971.

10. P.J. Waltrup and F.S. Billig, "Prediction of Precombustion Wall Pressure Distributions in Scramjet Engines," Journal of Spacecraft and Rockets, Vol. 10, No. 9, September 1973, pp. 620-622.

11. P.J. Waltrup, F.S. Billig, R.D. Stockbridge, "Procedure for Optimizing the Design of Scramjet Engines," Journal of Spacecraft and Rockets, Vol. 16, No. 3, May-June 1979, p. 163.

12. S. Mölder and E.J. Szpiro, "Busemann Inlet for Hypersonic Speeds," J. of Spacecraft and Rockets, Vol. 3, No. 8, 1966.

13. M.D. Griffin, F.S. Billig and M.E. White, "Applications of Computational Techniques in the Design of Ramjet Engines," 6th ISABE, Paris, France, June 1983.

14. F.S. Billig, M.E. White and D.M. Van Wie, "Application of CAE and CFD Techniques to a Complete Tactical Missile Design," AIAA 22nd Aerospace Sciences Meeting, January 9-12, 1984, Reno, NV, AIAA paper No. 84-0387.

15. A. Kumar, "Numerical Analysis of the Scramjet-Inlet by Using Two-Dimensional Navier-Stokes Equations," NASA TP-1940, Dec. 1981.

16. A. Mager, "On the Model of the Free, Shock-Separated Turbulent Boundary Layer," Journal of the Aeronautical Sciences, Vol. 23, No. 2, Feb. 1956.

17. J. Persh, "A Theoretical Investigation of Turbulent Boundary Layer Flow with Heat Transfer at Supersonic and Hypersonic Speeds," U.S. Naval Ordnance Laboratory, White Oak, MD, NAVORD Report 3854, May 1955.

18. P.J. Waltrup and F.S. Billig, "The Structure of Shock Waves in Cylindrical Ducts," AIAA Journal, Vol. 2, No. 10, Oct. 1973, pp. 1404-1408.

19. R.D. Stockbridge, "Experimental Results from the HDCR Combustor/Inlet Interaction Test Program," The Johns Hopkins University Applied Physics Laboratory, Laurel, MD, June 1982.

20. L. Crocco, "One-Dimensional Treatment of Steady Gas Dynamics, Fundamentals of Gas Dynamics, Vol. III of High Speed Aerodynamics and Jet Propulsion, Princeton University Press, 1958.

21. F.S. Billig, "Design of Supersonic Combustors Based on Pressure-Area Fields," Eleventh Symposium (International) on Combustion, The Combustion Institute, 1967, pp. 755-769.

22. E. C. Anderson and C. H. Lewis, "Laminar or Turbulent Boundary-Layer Flows of Perfect Gases or Reacting Gas Mixtures in Chemical Equilibrium," NASA CR-1893, Oct. 1971.

23. F.S. Billig and S.E. Grenleski, "Heat Transfer in Supersonic Combustion Processes," presented at Fourth International Heat Transfer Conference, Versailles, France, August 1971.

24. S. Gordon and B. McBride, "Computer Program for Calculation of Complex Equilibrium Compositions," NASA SP-273, 1971.

25. D.R. Cruise, Notes on the Rapid Computation of Chemical Equilibria, J. Phys. Chem. 68, 3797 (1964).

26. F.S. Billig and G.L. Dugger, "The Interaction of Shock Waves and Heat Addition in the Design of Supersonic Combustors," Twelfth Symposium (International) on Combustion, The Combustion Institute, Pittsburgh, PA, 1969, pp. 1125-1134.

27. J.A. Schetz, F.S. Billig and S. Favin, "Flowfield Analysis of a Scramjet Combustor with a Coaxial Fuel Jet," AIAA Journal, Vol. 20, No. 9, September 1982, pp. 1268-1274.

28. L.C. Dunsworth and K.E. Woodgrift, "Dual Mode Scramjet, Part I: Inlet Design and Performance Characteristics," The Marquardt Corp., AFAPLTR-67-132, Part I, December 1967.

29. C.A. Trexler, "Inlet Performance of the Integrated Langley Scramjet Module (Mach 2.3 to 7.6)," presented at the AIAA/SAE 11th Propulsion Conference, Anaheim, CA, Sept. 29-Oct. 1, 1975, AIAA Preprint 75-1212.

30. L.F. Jilly (Ed.), "Hypersonic Research Engine Project - Phase II: Aerothermodynamic Integration Model Development Final Technical Data Report," Garrett Airesearch Manufacturing Company of California, NASA-CR-132654, May 1975.

31. V. Agosta and S. Hammer, "Scramjet Nozzle Analysis, PSI Report 70-1, Propulsion Sciences, Inc., Melville, N.Y., February 1970.

32. D. Migdal, "Supersonic Annular Nozzles," AIAA 9th Aerospace Sciences Meeting, January 1971, Preprint 71-43.

BIBLIOGRAPHY

TYPE 19/4/1
84A20222 NASA ISSUE 7 Category 18
Tactical missile structures and materials technology
CAYWOOD, W. C.; RIVELLO, R. M.; WECKESSER, L. B.
830900 Johns Hopkins APL Technical Digest (ISSN 0270-5214), vol. 4, July-Sept. 1983, p. 166-174. AC(Johns Hopkins University, Laurel, MD) 9 p. Refs. 7 Jpn. 876

While some of the advancements in missile structures and materials technology have come as a result of improvements in design concepts and materials properties, others derive from the development of novel materials and fabrication techniques as well as the introduction of computer-based structural analysis methods. Attention is presently given to the structural design requirements of next-generation tactical missiles, which must be able to cruise at Mach 5-8 at 80,000 ft, in view of such considerations as thermal and loading environments, and range and launching requirements. An assessment is made of technology readiness for these requirements in the fields of homogeneous metallic materials, composites, ablative and insulating thermal protection systems, sensor windows, and radomes. The incorporation of advanced resin, metal matrix, and carbon composites into missile airframes will increase structural efficiency through improved weight and volume control. O.C.

Controlled Terms: COMPOSITE MATERIALS / *CONSTRUCTION MATERIALS / CRUISING FLIGHT / *MISSILE DESIGN / *MISSILE STRUCTURES / RADOME MATERIALS / *STRUCTURAL DESIGN / SUPERSONIC COMBUSTION RAMJET ENGINES / TECHNOLOGY ASSESSMENT / THERMAL PROTECTION

TYPE 19/4/2
84A20220 NASA ISSUE 7 Category 20
Tactical missile design concepts
BILLIG, F. S.
830900 Johns Hopkins APL Technical Digest (ISSN 0270-5214), vol. 4, July-Sept. 1983, p. 139-154. AA(Johns Hopkins University. Laurel, MD) 16 p. Refs. 5 Jpn. 878

A detailed discussion is presented of the design features, relative merits, performance characteristics, and operational consequences of subsonic and supersonic combustion ramjet, and integral rocket-ramjet tactical missile propulsion systems. Attention is given to accumulated hypersonic wind tunnel test data for advanced ramjet inlet and combustor designs, together with comparisons of the downrange and altitude performance envelopes projected for pure rocket and airbreathing propulsion systems. Significant performance divergence between the two types of missile propulsion system are largely predicated on the fact that, while rocket specific impulses are typically 20-30 percent those of ramjets, the propellant mass fraction for a tactical missile rocket is of the order of 50-70 percent of initial weight, as opposed to 25-35 percent for a ramjet. O.C.

Controlled Terms: COMBUSTION CHAMBERS / *ENGINE INLETS / MACH NUMBER / *MISSILE DESIGN / *PROPULSION SYSTEM PERFORMANCE / RAMJET ENGINES / *ROCKET ENGINE DESIGN / THRUST-WEIGHT RATIO

TYPE 19/4/3
84N18170# NASA ISSUE 9 Category 2
Air intakes for a probative missile of rocket ramjet
LARUELLE, G.
National Aeronautics and Space Administration, Washington, D. C. !
NC452981)

NASA-TM-77407, NAS 1.15:77407 840100 NASW-3541 Transl. into ENGLISH from L'Aeron. et L'Astronautique (France), no. 98, 1983 p 47-59 Original language document was announced as A83-31824 Transl. by Kanner (Leo) Associates, Redwood City, Calif. 33 p. Jpn. 1251 HC A03/MF A01

The methods employed to test air intakes for a supersonic guided ramjet powered missile being tested by ONERA are described. 30th flight tests and wind tunnel tests were performed on instrumented rockets to verify the designs. Consideration as given to the number of intakes, with the goal of delivering the maximum pressure to the engine. The S2, S4, and S5 wind tunnels were operated at Mach nos. 1.5-3 for the tests, which were compartmentalized into fuselage-intake interaction, optimization of the intake shapes, and the intake performance. Tests were performed on the length and form of the ogive, the presence of grooves, the height of traps in the boundary layer, the types and number of intakes and the lengths and forms of diffusers. Attention was also given to the effects of sideslip, effects of the longitudinal and circumferential positions of the intakes were also examined. Near optimum performance was realized during Mach 2.2 test flights of the prototype rockets. M.S.K.

Controlled Terms: AERODYNAMIC CHARACTERISTICS / BALLISTIC MISSILES / *ENGINE INLETS / HYPERSONIC WIND TUNNELS / INLET AIRFRAME CONFIGURATIONS / INLET FLOW / INLET NOZZLES / INLET PRESSURE / *MISSILE DESIGN / MISSILE TESTS / *RAMJET MISSILES / *ROCKET ENGINE DESIGN / SOLID PROPELLANT ROCKET ENGINES / *SUPERSONIC INLETS / SUPERSONIC WIND TUNNELS / *WIND TUNNEL TESTS

TYPE 19/4/4
84A17862 NASA ISSUE 6 Category 5
Synthesis and performance of an Air-TurboRamjet-propelled supersonic target vehicle
BRIGGS, M. M.; CAMPBELL, J. V.; ANDRUS, S. R.; BURGNER, G. R.
AIAA PAPER 84-0075 840100 N60530-82-C-0315 American Institute of Aeronautics and Astronautics, Aerospace Sciences Meeting, 22nd, Reno, NV, Jan. 9-12, 1984. 8 p. AA(Integrated Systems, Inc., Missile, Div., Palo Alto, CA) AC(Aerojet TechSystems Co., Sacramento, CA) AD(U.S. Naval Weapons Center, China Lake, CA) 8 p.

A modified version of the AQM-37 target vehicle was used in this study in expectation that integrating an Air-TurboRamjet (ATR) propulsion subsystem would provide safety and performance benefits relative to the existing AQM-37A target. The ATR propulsion subsystem allows utilization of relatively benign fuel 'OTTO II) in place of the inhibited red fuming nitric acid/mixed amine fuel NO. 4 (IRFNA/MAF no. 4) bipropellant combination used in the current version of the AQM-37. Otto II provides more than twice the currently delivered specific impulse. Performance evaluations of the ATR-propelled target vehicle designs show capability for sustained low-altitude flight at Mach 1.5 and a powered flight range of more than 200 NM cruising at Mach 3.0, 80,000 ft. altitude when launched at Mach 1.5, 50,000 ft. altitude. Author

Controlled Terms: AERODYNAMIC CHARACTERISTICS / ENGINE AIRFRAME INTEGRATION / ENGINE DESIGN / ENGINE INLETS / *MISSILE CONTROL / PERFORMANCE PREDICTION / *PROPULSION SYSTEM PERFORMANCE / AIRCRAFT / TARGETS / *TURBORAMJET ENGINES

TYPE 19/4/5
84A17194 NASA ISSUE 5 Category 26
Large thin walled titanium castings
SCHWEDT, S. J.; GULLEY, L. R.
830000 IN: Materials and processes - Continuing innovations; Proceedings of the Twenty-eighth National SAMPE Symposium and Exhibition, Anaheim, CA, April 12-14, 1983 (A84-17101 05-23). Azusa, CA, Society for the Advancement of Material and Process Engineering, 1983, p. 1318-1328.

with two degrees of freedom. Tests can be run on aerodynamics, air intakes, ablation or radome deformation, heat transfer, and the performance of complete engines at Mach 6. Full engine trials have included solid fueled ramjets, with adaptations permitting connected pipe and semi-free jet testing in conjunction with the hot gas generator. The ramjet trials have been limited to a simulation of Mach 2.7 at ground level conditions and Mach 3.35 at altitudes over 11 km. M.S.K.

Controlled Terms: *ENGINE TESTS / FREE JETS / HEAT TRANSFER / *HYPERSONIC WIND TUNNELS / MACH NUMBER / *MISSILE TESTS / RAMJET ENGINES / *RAMJET MISSILES / *WIND TUNNEL TESTS

TYPE 19/4/8
83A36389 NASA ISSUE 16 Category 20
Analytical characterization of flow fields in side-inlet dump combustors
VANKA, S. P.; STULL, F. D.; CRAIG, R. R.
AIAA PAPER 83-1399 830600 AIAA, SAE, and ASME, Joint Propulsion Conference, 19th, Seattle, WA, June 27-29, 1983. 12 p. AA(Argonne National Laboratory, Argonne, IL) AC(USAF, Wright Aeronautical Laboratories, Wright-Patterson AFB, OH) 12 p. Refs. 8

Side-inlet dump combustors are being investigated as a design alternative to coaxial dump combustors. In a side-inlet dump combustor, the ducted rocket missile applications. A side-inlet dump combustor, the main air flow enters the combustor through multiple side inlets. The fuel may be injected at the side arms in case of a liquid fueled ramjet. The flow fields resulting from the side injection are highly three-dimensional and complex. The present paper attempts to analytically characterize these flow fields through numerical solution of the governing partial differential equations. The effects of turbulence are represented through a two equation (k-epsilon) model in which additional equations are solved for the kinetic energy of turbulence and its dissipation rate. Results of four different calculations are presented in which the position of the dome plate and the angle of injection have been varied to study their influences. The computed flow patterns are in general agreement with flow visualization photographs. Author

Controlled Terms: *COMBUSTION CHAMBERS / *COMPUTATIONAL FLUID DYNAMICS / ENERGY DISSIPATION / *FINITE DIFFERENCE THEORY / *FLOW DISTRIBUTION / FLOW VISUALIZATION / KINETIC ENERGY / MISSILE DESIGN / *RAMJET ENGINES / *ROCKET ENGINE DESIGN / TURBULENCE EFFECTS / WATER TUNNEL TESTS

TYPE 19/4/9
83A35805 NASA ISSUE 16 Category 7
Cruise flight of a tail mounted ramjet
HATTINGH, H. V.; ARENS, D. R. M.; VAN WYK, J. S.
830000 IN: International Symposium on Air Breathing Engines, 6th, Paris, France, June 6-10, 1983, Symposium Papers (A83-35801 16-07). New York, American Institute of Aeronautics and Astronautics, 1983, p. 25-34. AC(Stellenbosch, University, Stellenbosch, Republic of South Africa) 9 p. Refs. 9

A program has been developed for the calculation of the cruise regime flight time, for a given altitude and supersonic Mach number, of a tail-mounted integral ramjet (short range) cruise missile. The mass available for the engine and its fuel is a required input. The suboptimization of the exhaust nozzle, to yield maximum propulsive force, resulted in a nozzle possessing both unnecessarily low drag and excessive length and weight. Factors taken into account by the computational method presented include internal flow modeling, fuel/air mixing, flame stabilization, combustion, boundary layer flow, engine geometry, and friction and pressure drag. O.C.

AA(McDonnell Douglas Astronautics Co., St. Louis, MO) AB(USAF, Materials Laboratory, Wright-Patterson AFB, OH) 11 p.

It is pointed out that titanium castings offer a low-cost approach for producing efficient, complex-shaped parts for high temperature applications. A chin inlet duct for a Mach 4 ramjet missile represents an example for such an application. A research program has been conducted to evaluate the properties of thin gage Ti-6242S parts cast in a simulated inlet duct geometry. The program has the objective to determine the efficiency of Ti-6242S alloy for thin gage structural applications, evaluate the effect of oxygen content on mechanical properties, and determine the postcasting processing necessary to optimize the short time elevated temperature properties of the cast alloy. The results of the program show that titanium castings are a viable alternative to built-up structures. G.R.

Controlled Terms: AIR INTAKES / *CASTINGS / CREEP TESTS / DUCTS / FATIGUE TESTS / *INVESTMENT CASTING / MICROSTRUCTURE / RAMJET MISSILES / *THIN WALLS / *TITANIUM

TYPE 19/4/6
84N13195# NASA ISSUE 4 Category 7
Preliminary scramjet design for hypersonic airbreathing missile application
Final Report
CARLSON, C. H.
Marquardt Corp., Van Nuys, Calif. (MH569990)
NASA-CR-3742; NAS 1.26:3742; S-1585 831100 NAS1-15434 71 p. Washington
NASA Jpn. 486 HC A04/MF A01

A conceptual design study of a scramjet engine was conducted for a hypersonic surface to air missile (HYSAM). The definition of the engine was based upon the requirements of accelerating the HYSAM from Mach 4 at 20,000 feet to Mach 6 at 100,000 feet and the cruise conditions at Mach 6. The resulting external and internal environmental conditions were used by various engineering disciplines performing design, stress and heat transfer analysis. A detailed structural analysis was conducted along with an indepth thermal analysis. Structurally all the components within the system exhibit positive margins of safety. A feasible concept was defined which uses state-of-the-art materials and existing TMC technology. The engine basically consists of a three dimensional carbon/carbon combustor/nozzle secured to an FS-85 columbium inlet. The carbon/carbon liner is sheathed with carbon felt insulation to thermally protect the FS-85 structure and skin. The thermal analysis of the engine indicates that a thermally viable configuration exists. Author

Controlled Terms: CARBON-CARBON COMPOSITES / ENGINE DESIGN / *HYPERSONIC VEHICLES / NIOBIUM / *SUPERSONIC COMBUSTION RAMJET ENGINES / *SURFACE TO AIR MISSILES / THERMAL PROJECTION

TYPE 19/4/7
83A36433 NASA ISSUE 16 Category 9
New transformations of S4 Modane hypersonic wind tunnel for ramjet missiles tests
CHRISTOPHE, J.
ONERA, TP NO. 1983-24 830000 (Supersonic Tunnel Association, Semi-Annual Meeting, 59th, Colorado Springs, CO, Apr. 6, 7, 1983) ONERA, TP, no. 1983-24, 1983, 14 p. AA(ONERA, Chatillon-sous-Bagneux, Hauts-de-Seine, France) 14 p. Refs. 11

The capabilities, equipment, and performance of the Modane S4 hypersonic wind tunnel are described. The tunnel has a Mach 6 nozzle, storage facilities for dry air at 400 bars, a heater bed of aluminum pebbles capable of raising the air temperature to 1850 K, and a mounting table

Controlled Terms: ALTITUDE / BOUNDARY LAYER FLOW / COMPUTATIONAL FLUID DYNAMICS / *CRUISE MISSILES / *ENGINE INLETS / *FLIGHT TIME / FRICTION DRAG / FUEL COMBUSTION / INLET FLOW / *MACH NUMBER / NOZZLE FLOW / RAMJET ENGINES / *RAMJET MISSILES

TYPE 19/4/10
83A31824 NASA ISSUE 14 Category 2
Air intakes for an experimental rocket ramjet
Prises d'air pour missile probatoire de^statofusee
LARUELLE, G.
B30000 L'Aeronautique et l'Astronautique (ISSN 0001-9275), no. 9B, 1983, p. 47-59. In French. Research supported by the Direction Technique des Engines. AA(ONERA, Chatillon-sous-Bagneux, Hauts-de-Seine, France) 13 p. Refs. 6

The methods employed to test air intakes for a supersonic guided ramjet-powered missile being tested by ONERA are described. Both flight tests and wind tunnel tests were performed on instrumented rockets to verify the designs. Consideration as given to the number of intakes, with the goal of delivering the maximum pressure to the engine. The S2, S4, and S5 wind tunnels were operated at Mach nos. 1.5-3 for the tests, which were compartmentalized into fuselage-intake interaction, optimization of the intake shapes, and the intake-intake interaction. Tests were performed on the length and form of the ogive, the presence of grooves, the height of traps in the boundary layer, the types and number of intakes and the lengths and forms of diffusers. Attention was also given to the effects of sideslip, flow separation, the forward intake tip, and the intake drag. Finally, the effects of the longitudinal and circumferential positions of the intakes were also examined. Near-optimum performance was realized during Mach 2.2 test flights of the prototype rockets. M.S.K.

Controlled Terms: AERODYNAMIC CHARACTERISTICS / BALLISTIC MISSILES / *ENGINE INLETS / HYPERSONIC WIND TUNNELS / INLET AIRFRAME CONFIGURATIONS / INLET FLOW / INLET NOZZLES / INLET PRESSURE / *MISSILE DESIGN / MISSILE TESTS / *RAMJET MISSILES / *ROCKET ENGINE DESIGN / SOLID PROPELLANT ROCKET ENGINES / *SUPERSONIC INLETS / SUPERSONIC WIND TUNNELS / *WIND TUNNEL TESTS

TYPE 19/4/11
83N26791M NASA ISSUE 16 Category 7
Coaxial dump combustor investigations
Final Report
CRAIG, R. R.; DREURY, J. E.; STULL, F. D.
Air Force Aero Propulsion Lab., Wright-Patterson AFB, Ohio. (AH661913)
B20600 Ramjet Technology Branch. In AFWAL A Collection of Papers in the Aerospace Sci p 145-156 (SEE N83-26787 16-01) 12 p. Jpn. 2510 HC A99/MF A01

An experimental investigation was conducted involving coaxial dump combustors with two different types of flameholders (annular and V) installed at the dump station in an attempt to correlate combustor performance with previous nonreacting flowfield results. Flameholder blockage, combustor length, exit area ratio, inlet temperature, and chamber pressure were varied for both wall injection and premixed fuel conditions. Lean blowout limits, combustion efficiency, combustor total pressure drop, and wall static pressure distributions were obtained from these runs using JP-4 fuel. In addition, a limited amount of surface heating patterns and combustion oscillation data were obtained. Author

Controlled Terms: *BLOWOUTS / *COAXIAL FLOW / *COMBUSTION CHAMBERS / COMPUTER GRAPHICS / COMPUTER PROGRAMS / DATA ACQUISITION / *FLAME HOLDERS / FLOW VELOCITY / FUEL INJECTION / *INLET TEMPERATURE / *INTERNAL PRESSURE / *JP-4 JET FUEL / MATHEMATICAL MODELS / PRESSURE DISTRIBUTION / *RAMJET MISSILES

TYPE 19/4/12
83N26023M NASA ISSUE 15 Category 34
Design of choking cascade turns
M.S. Thesis
BAIRD, J.
Air Force Inst. of Tech., Wright-Patterson AFB, Ohio. (A174479)
AD-A124792; AFIT/GAE/AA/82D-3 821200 School of Engineering. 79 p. Jpn.
2395 HC A05/MF A01

Five different shock-positioning cascades, for short-radius turns in ramjet inlet diffusers, were designed and tested on the AFIT water table. The flow controllers were to perform the same function as the conventional arrangement of an aerodynamic grid and a long-radius turn. The tests were to determine the suitability of the water table for such experimentation, in addition to determining the flow-control capabilities and pressure recovery of the cascades. All five designs accomplished the flow-control function as designed, and two designs exhibited the same or better pressure recovery than the aerodynamic grid. The water table proved to be an excellent means of testing these cascades, primarily due to the ease of flow visualization in the tests done. The shock-positioning cascade, short-radius turn concept shows promise and should be tested further in gas-dynamic apparati. Author (GRA)

Controlled Terms: *AIR FLOW / *AIR LAUNCHING / AIRCRAFT MANEUVERS / *CASCADE FLOW / *COMBUSTION CHAMBERS / *FLOW VISUALIZATION / INLET FLOW / MISSILE CONTROL / PROPULSION SYSTEM PERFORMANCE / RAMJET ENGINES / *WATER TABLES / WATER TUNNEL TESTS

TYPE 19/4/13
83N18843 NASA ISSUE 9 Category 20
Airbreathing missile propulsion: A bibliography
REEDY, T. L.
Applied Physics Lab., Johns Hopkins Univ., Laurel, Md. (AU080119)
AD-B995104; CPIA-LS82-31 821100 N00024-81-C-5301 Chemical Propulsion Information Agency. 477 p. Jpn. 1327 Avail: Issuing Activity

This bibliography presents 1430 citations of reports dealing with all aspects of airbreathing missile propulsion concerning the 1969-1981 time period. Corporate source, personal author and subject indexes are provided. Author

Controlled Terms: *AIR BREATHING ENGINES / *BIBLIOGRAPHIES / COMBUSTION CHAMBERS / COMPUTER PROGRAMS / FEED SYSTEMS / FUEL COMBUSTION / *PROPULSION / RAMJET MISSILES / *ROCKET ENGINES

TYPE 19/4/14
83A14542 NASA ISSUE 3 Category 2
Problems concerning the external aerodynamics of air-breathing missiles
Problemes lies a l'aerodynamique externe des^missiles aerobies
CHAMPIGNY, P.
ONERA, TP NO. 1982-93 B20000 (NATO, AGARD, Symposium sur l'Aerodynamique des Missiles, Trondheim, Norway, Sept. 20-22, 1982.) ONERA, TP no. 1982-93, 1982. 13 p. In French. AA(ONERA, Chatillon-sous-Bagneux, Hauts-de-Seine, France) 13 p.

The influence of the inlet on the external aerodynamics of air-breathing missiles is investigated as part of a study of new configurations for air-breathing missiles from both the internal and external point of views. Since the theoretical calculation of the aerodynamic coefficients is very difficult, tests are instead conducted in several wind tunnels (S3Ch, S5Ch, S3MA, and S2MA) over a wide range of Mach numbers (0.6-3.4) and angles of attack of up to 12 degrees. The influences of the shape, and the

number and position of the inlets on the aerodynamic coefficients, in
particular the drag and the life, are examined. N.B.

Controlled Terms: *AERODYNAMIC COEFFICIENTS / AERODYNAMIC DRAG /
AERODYNAMIC STABILITY / *AIR BREATHING ENGINES / *INLET AIRFRAME
CONFIGURATIONS / LIFT / *MISSILE CONFIGURATIONS / MISSILE TESTS / *RAMJET
MISSILES / WIND TUNNEL TESTS

TYPE 19/4/15
83A12858 NASA ISSUE 2 Category 17
The Talos guidance system
GULICK, J.; HYATT, W. C.; MARTIN, D. M., JR.
820600 Johns Hopkins APL Technical Digest, vol. 3, Apr.-June 1982, p.
142-153. AC(Johns Hopkins University, Laurel, MD) 12 p.

A description is given of the design principles and performance
capabilities of the Talos surface-to-air missile's homing system, which
over the course of its development came to be virtually unjammable, as
well as the associated antiradiation seeker, which enables the Talos to
operate against radar signal-emitting targets. The interferometric homing
system chosen employs widely spaced, airframe-fixed antennas compatible
with ramjet inlet geometry and simpler than the alternative gimballed dish
antenna. Early Talos missile guidance systems used scanning
interferometry, but for subsequent models a continuous wave interferometer
was developed, followed by a monopulse seeker. Attention is given to the
use of the Talos system as a long range antiradiation missile for radar
suppression in the Vietnam conflict. O.C.

Controlled Terms: ANTIRADIATION MISSILES / *BEAM RIDER GUIDANCE /
BUMBLEBEE PROJECT / *FLIGHT CONTROL / FLIGHT TESTS / HOMING DEVICES /
*MIDCOURSE GUIDANCE / *RAMJET MISSILES / *TALOS MISSILE

TYPE 19/4/16
83A12857 NASA ISSUE 2 Category 20
The Talos propulsion system
SHIPPEN, W. B.; GARTEN, W., JR.; HARDGRAVE, E. J., JR.; BERL, W. G.
820600 Johns Hopkins APL Technical Digest, vol. 3, Apr.-June 1982, p.
126-134. AC(Johns Hopkins University, Laurel, MD) 9 p.

After giving a historical account of ramjet development in the years
following 1945, a description is given of the design features and
performance characteristics of the Talos surface-to-air missile's ramjet
propulsion system. Attention is given to the can-like flameholder devised
to sustain efficient combustion for extended periods at an altitude of
60,000 ft and an airspeed of 2000 ft/sec, under which conditions the
combustor would have to operate at a pressure of 1/3 atmosphere. The
evolution of inlet diffuser geometry and fuel composition are also
considered, along with the pumping and metering of fuel and the protection
of the combustor from burnout at 3500 F by means of zirconia coatings.
O.C.

Controlled Terms: ANTIAIRCRAFT MISSILES / *ASCENT PROPULSION SYSTEMS /
BUMBLEBEE PROJECT / COMBUSTION CHAMBERS / COMBUSTION EFFICIENCY / FUEL
COMBUSTION / HISTORIES / *JET PROPULSION / *RAMJET MISSILES / *SUPERSONIC
COMBUSTION RAMJET ENGINES / *TALOS MISSILE

TYPE 19/4/17
83N11893M NASA ISSUE 2 Category 64
Solid body equations to calculate the trajectory of ramjet
IMAI, K.
National Defence Academy, Tokyo (Japan). (NHB77499)
AD-A118241; NPS67-82-001CR 820400 N62271-82-M-1221; DARPA ORDER 4035 25
p. Naval Postgraduate School Jpn. 279 HC A02/MF A01

Six degree-of-freedom trajectory equations for a ramjet propelled, gun
launched projectile are formulated. An outline for FORTRAN computer
program flow charts also appears in the report. Special emphasis is given
to the effect of wind on trajectory errors. Author (GRA)

Controlled Terms: DEGREES OF FREEDOM / FORTRAN / *GUN LAUNCHERS /
HYPERSONIC FLIGHT / *MISSILE TRAJECTORIES / *PROJECTILES / *RAMJET ENGINES
/ *TRAJECTORY ANALYSIS / WIND EFFECTS

TYPE 19/4/18
82A41412 NASA ISSUE 20 Category 12
Design considerations for relativistic antimatter rockets
CASSENTI, B. N.
820900 British Interplanetary Society, Journal (Interstellar Studies),
vol. 35, Sept. 1982, p. 396-404. AA(United Technologies Research Center,
East Hartford, CT) 9 p. Refs. 16

Matter annihilation, by combining equal amounts of matter and
antimatter, provides the greatest energy output for a given mass input,
and is energetic enough to send vehicles to the stars. Proton-antiproton
annihilation produces a spray of mesons, consisting primarily of positive,
negative and neutral pions. The decay products of the pions are muons,
neutrinos, and gamma rays. The muons decay into electrons or positrons,
and neutrinos. In order to determine the usefulness of using the energy of
the pions, muons or electrons the energy spectrum of each has been
evaluated. Two major difficulties associated with antimatter propulsion
(i.e., production and storage) would be reduced if the amount of
antimatter required could be minimised. For this purpose a solution which
minimises the amount of required antimatter has been extended to
relativistic velocities. (Author)

Controlled Terms: *ANNIHILATION REACTIONS / *ANTIMATTER / ANTIPROTONS /
ENERGY SPECTRA / *INTERSTELLAR TRAVEL / LIQUID HYDROGEN / NEUTRINOS /
PARTICLE ENERGY / PARTICLE MASS / *RAMJET MISSILES / *RELATIVISTIC
PARTICLES / *ROCKET ENGINE DESIGN / *SPACECRAFT PROPULSION

TYPE 19/4/19
82N32270# NASA ISSUE 22 Category 20
Design of hydrogen fueled ramjets and ramrockets
DINI, D.
Pisa Univ. (Italy). (PT043364)
820300 1st. di Macchine. In AGARD Ramjets and Ramrockets for Mil. Appl.
5 p (SEE N82-32256 22-99) 5 p. Jpn. 3224 HC A12/MF A01

Problems arising from high energy fuels, particularly hydrogen which
impose remarkable changes in interface components, geometry and control,
of current ramjets and ramrockets design are discussed. Starting from
typical missions scenarios, advanced configurations are established for
military applications. Variable geometry nozzles and combustion chambers
because of their combined effect with the intake to give good performance
and flexibility are considered. A numerical example of overall design is
given for very high flight Mach numbers which considers the problems
arising from engine/airframe integration and cryogenic fuel storage.
Features effecting installation of such engines in aircraft are examined.
EAK

Controlled Terms: COMBUSTION CHAMBERS / CRYOGENIC FLUID STORAGE / FUEL
TANKS / *HYDROGEN FUELS / *LIQUID ROCKET PROPELLANTS / MACH NUMBER /
MATHEMATICAL MODELS / *PROPELLANT CHEMISTRY / *RAMJET ENGINES

TYPE 19/4/20
82N33268M NASA ISSUE 22 Category 25

ramjet. The reliability of the ramjet propulsion system in many practice firings of service maintained missiles by service crews is discussed and compares well with that of rocket systems. E.A.K.

Controlled Terms: *CLOSURES / ENVIRONMENT EFFECTS / *LIQUID ROCKET PROPELLANTS / MAINTAINABILITY / MARINE ENVIRONMENTS / *MILITARY TECHNOLOGY / PERFORMANCE TESTS / RAMJET ENGINES / *RAMJET MISSILES / *SOLID ROCKET PROPELLANTS / *SURFACE TO AIR MISSILES

TYPE 19/4/23
82N32263# NASA ISSUE 22 Category 15
Range maximization method for ramjet powered missiles with flight path constraints
SCHOETTLE, U. M.
Stuttgart Univ. (West Germany). (S4355674)
820300 Inst. fuer Raumfahrtantriebe. In AGARD Ramjets and Ramrockets for Mil. Appl. 19 p (SEE N82-32256 22-99) Sponsored in part by the German Ministry of Defense 19 p. Jpn. 3223 HC A12/MF A01

Mission performance of ramjet powered missiles is strongly infuenced by the trajectory flown. The trajectory optimization problem considered is to obtain the control time histories (i.e. propellant flow rate and angle of attack) which maximize the range of ramjet powered supersonic missiles with preset initial and terminal fight conditions and operational constraints. The approach chosen employs a parametric control model to represent the infinite-dimensional controls by a finite set of parameters. The resulting suboptimal parameter optimization problem is solved by means of nonlinear programming methods. Operational constraints on the state variables are treated by the method of penalty functions. The presented method and numerical results refer to a fixed geometry solid fuel integral rocket ramjet missile for air-to-surface or surface-to-surface missions. The numerical results demonstrate that continuous throttle capabilities increase range performance by about 5 to 11 percent when compared to more conventional throttle control. Author

Controlled Terms: *ANGLE OF ATTACK / *DISTANCE / *FLIGHT PATHS / *FLOW VELOCITY / *FUEL FLOW / *MISSILE TRAJECTORIES / NONLINEAR PROGRAMMING / OPTIMIZATION / PARAMETERIZATION / *RAMJET MISSILES / SOI ID PROPELLANT ROCKET ENGINES / SUPERSONIC COMBUSTION RAMJET ENGINES / VARIABLE THRUST

TYPE 19/4/24
82N32261# NASA ISSUE 22 Category 15
Multiple intakes for ramrockets
KROHN, E. O.; TRIESCH, K.
Deutsche Forschungs- und Versuchsanstalt fuer Luft- und Raumfahrt, Cologne (West Germany). (D0696939)
820300 In AGARD Ramjets and Ramrockets for Mil. Appl. 14 p (SEE N82-32256 22-99) 14 p. Jpn. 3223 HC A12/MF A01

Several ramrocket missiles under development have a central combustion chamber and more than one side mounted intake in general four. The junction of different inlet flows in a common chamber causes, in certain cases, flow instability and flow reversal in single ducts. The flow mechanism will be explained by examples. A computer program was developed which calculates the overall performance of the system from single inlet data. The results are compared with wind tunnel measurements. Methods for reducing the negative effects of combining multiple intakes with a common chamber are discussed. Author

Controlled Terms: COMBUSTION CHAMBERS / COMPUTERIZED SIMULATION / *ENGINE INLETS / FLOW GEOMETRY / *INLET FLOW / PERFORMANCE PREDICTION / *PROPULSION SYSTEM CONFIGURATIONS / PROPULSION SYSTEM PERFORMANCE / *RAMJET ENGINES / *ROCKET ENGINES

Boron combustion in ducted rockets
SCHADOW, K. C.
Naval Weapons Center, China Lake, Calif. (NU452890)
020300 In AGARD Ramjets and Ramrockets for Mil. Appl. 12 p (SEE N82-32256 22-99) 12 p. Jpn. 3224 HC A12/MF A01

The qualitative effect of inlet and combustor parameter on mixing and overall performance for solid boron propellant gas generator ramjets with two opposing 45 deg side air inlets were studied. Highest combustion efficiencies were achieved at lowest air injection momentum and lowest fuel injection momentum. The decrease of the combustion efficiency with increasing air injection was underlined explaining the observed combustion efficiency decrease with decreasing ramjet combustor pressure and increasing air to fuel ratio, which at constant air inlet geometry results in increasing air injection momentum. It is shown that optimum plume ignition at the fuel injector is more difficult to achieve at decreasing fuel mass flow per fuel injector. The importance of the combustor aerodynamics for achieving efficient boron combustion is shown. EAK

Controlled Terms: AERODYNAMIC CHARACTERISTICS / *BORON CARBIDES / *COMBUSTION EFFICIENCY / *DUCTED ROCKET ENGINES / *FUEL COMBUSTION / FUEL INJECTION / RAMJET ENGINES / *RAMJET MISSILES / SOLID PROPELLANT IGNITION / *SOLID ROCKET PROPELLANTS

TYPE 19/4/21
82N32267# NASA ISSUE 22 Category 20
Experimental investigation of a hydrocarbon solid fuel ramjet
MEINKOEHN, D.; BERGMANN, J. W.
Deutsche Forschungs- und Versuchsanstalt fuer Luft- und Raumfahrt, Hardthausen (West Germany). (D0696975)
820300 Inst. fuer Chemische Antriebe und Verfahrenstechnik. In AGARD Ramjets and Ramrockets for Mil. Appl. 11 p (SEE N82-32256 22-99) 11 p. Jpn. 3224 HC A12/MF A01

A solid fuel ramjet motor in a connected pipe air supply under simulated in flight operating conditions was investigated. Diffuser losses based on empirical efficiencies were considered and a set of states of the air upstream of the ramjet combustor was theoretically derived to simulate certain in flight conditions of a ramjet-powered missile. Internal ballistics, combustion efficiency and overall combustor performance which covers a range of Mach numbers between 1.5 and 3.0 for altitudes between sea level are investigated and 6000 m Polyethylene was the hydrocarbon fuel used in most of the tests. It is found that a suitable regression can be established for varying peformance requirements even by providing for trajectory dependent combustion efficiencies. EAK

Controlled Terms: *COMBUSTION EFFICIENCY / DUCTED FLOW / DUCTED ROCKET ENGINES / FLIGHT SIMULATION / FUEL FLOW / *HYDROCARBONS / PROPULSION / RAMJET ENGINES / *RAMJET MISSILES / *SOLID ROCKET PROPELLANTS

TYPE 19/4/22
82N32266# NASA ISSUE 22 Category 20
Service experience with three generations of ramjets
FLETCHER, C. F.; LANE, D. R.
Rolls-Royce Ltd., Bristol (England). (RZ028870)
820300 In AGARD Ramjets and Ramrockets for Mil. Appl. 9 p (SEE N82-32256 22-99) 9 p. Jpn. 3224 HC A12/MF A01

The development of three generations of ramjets for use in operational surface to air missiles is discussed. Operation and maintenance in tropical, arctic and marine environment was tested. The precautions taken during design to achieve reliability and a low level of mantenance effort are reported. In the third generation, design progressed to the establishment of wooden round status for a factory filled liquid fuelled

TYPE 19/4/25
82N32259# NASA ISSUE 22 Category 20
Design consideration and analytical comparison of different types of ramjets and ramrockets
BENKMANN, P.; KRAMER, P. A.
Stuttgart Univ. (West Germany). (SA355674)
820300 Inst. fuer Raumfahrtantriebe. In AGARD Ramjets and Ramrockets for Mil. Appl. 14 p (SEE N82-32256 22-99) Sponsored in part by the German Ministry of Defense 14 p. Jpn. 3223 HC A12/MF A01

Several types of ramjet and ramrocket (or ducted rocket) propulsion systems with hydrocarbon fuels for high sub- to supersonic missile application are theoretically analyzed and compared. Design considerations are discussed with respect to their performance impacts. Fundamental physical connections as well as mission and internal design variables are investigated in order to give some insight into the ramjet's and ramrocket's performance and application potential. The results are presented in graphical form. Author

Controlled Terms: COMBUSTION CHAMBERS / DESCRIPTIVE GEOMETRY / DESIGN ANALYSIS / *ENGINE DESIGN / HYDROCARBON FUELS / *LIQUID PROPELLANT ROCKET ENGINES / *PROPULSION SYSTEM PERFORMANCE / *RAMJET ENGINES / *RAMJET MISSILES / SUBSONIC SPEED / SUPERSONIC SPEEDS

TYPE 19/4/26
82N32257# NASA ISSUE 22 Category 20
Low-cost combustor for a supersonic tactical missile
MYERS, T. D.; PETERS, A. P.
United Technologies Corp., Sunnyvale, Calif. (UU302247)
820300 Chemical Systems Div. In AGARD Ramjets and Ramrockets for Mil. Appl. 15 p (SEE N82-32256 22-99) 15 p. Jpn. 3222 HC A12/MF A01

Development of a low cost advanced low volume ramjet (ALVRJ) propulsion system for the supersonic tactical missile (STM) and other tactical mission application is summarized. A series of propulsion system performance/cost vehicle systems trades were conducted. Key propulsion system requirements that most strongly influenced cost were: (1) fuel flow rate accuracy, (2) inlet pressure recovery, and (3) required combustor operational life. From these trade studies specific low cost ramjet component designs were selected, including: (1) inlet, (2) fuel controller, (3) rocket booster motor nozzle release mechanism, and (4) combustor/thermal protection system (TPS). The low cost combustor/TPS development effort is stressed. The low cost combustor for the STM propulsion system was successfully demonstrated through a series of ground tests and a flight test. The 5:1 combustor cost reduction for the ALVRJ propulsion system compared to the ALVRJ propulsion sytem was achieved with no performance penalty. J.D.

Controlled Terms: *COMBUSTION CHAMBERS / COST REDUCTION / DISCONNECT DEVICES / ENGINE DESIGN / ENGINE PARTS / FLIGHT TESTS / FUEL FLOW / GROUND TESTS / INLET PRESSURE / INTAKE SYSTEMS / *LIQUID PROPELLANT ROCKET ENGINES / *LOW VOLUME RAMJET ENGINES / *PROPULSION SYSTEM PERFORMANCE / ROCKET NOZZLES / *SUPERSONIC COMBUSTION RAMJET ENGINES / THERMAL PROTECTION

TYPE 19/4/27
82N32255# NASA ISSUE 22 Category 99
Ramjets and Ramrockets for Military Applications
Advisory Group for Aerospace Research and Development, Neuilly-Sur-Seine (France). (AD455458)
AGARD-CP-307; ISBN-72-835-0312-X 820300 Mostly in ENGLISH; One in FRENCH Proceedings of 58th Propulsion and Energetics Symp., London, 26-29 Oct. 1981 266 p. Jpn. 3222 HC A12/MF A01

A comprehensive survey of ramjet and ramrocket technology and its application to missile propulsion is presented. For individual titles, see N82-32257 through N82-32274

Controlled Terms: AFTERBODIES / COMBUSTION CHAMBERS / *CONFERENCES / *DRAG REDUCTION / *DUCTED ROCKET ENGINES / ENGINE DESIGN / HYDROGEN FUELS / *LIQUID ROCKET PROPELLANTS / PROPULSION SYSTEM PERFORMANCE / *PULSEJET ENGINES / *RAMJET ENGINES / *RAMJET MISSILES / *ROCKET ENGINES / *SOLID ROCKET PROPELLANTS / SUPERSONIC DIFFUSERS

TYPE 19/4/28
82N31392M NASA ISSUE 22 Category 15
Performance of solid fuel ramjet guided projectile for USN 5 inch/54 caliber gun system
AMICHAI, O.
Naval Postgraduate School, Monterey, Calif. (NS368219)
AD-A115108; NPS67-82-002CR 820300 N00228-81-C-H231; DARPA ORDER 4035 220 p. Jpn. 3092 HC A10/MF A01

This report covers work done on performance analysis of a 5 inch, 54 caliber gun-launched guided projectile with solid fuel ramjet (SFRJ). A computer program (TRAJET) was developed. The program contains ramjet and trajectory analysis. The ramjet part considers conical shock wave losses, inlet boundary layer losses, normal shock losses, subsonic diffuser recovery, expansion into combustor losses, heat losses at the combustor and nozzle losses. A flat earth trajectory with drag and thrust was considered. The various drag coefficients which were considered are: cowl drag coefficient, skin drag coefficient, wing (or fin) wave drag coefficient and wing (or fin) friction drag coefficient. The 5'/54 solid fuel ramjet has a capability to produce fuel specific impulse in the order of 400 - 900 sec. depending mostly on the flight altitude. The thrust coefficient varies in the range of 0.3 + or - 0.1 depending on the internal areas. A range in the order of 50 miles can be achieved with the ramjet operation compared to only 13 miles achieved by the conventional projectile. At low-altitude launch, a range of over 18 miles can be reached in Air-Defense Scenario. The ramjet propelled projectile reaches the ranges mentioned above at high Mach numbers (MO 1.8). GRA

Controlled Terms: AERODYNAMIC COEFFICIENTS / *GUN LAUNCHERS / MISSILE TRAJECTORIES / *PRECISION GUIDED PROJECTILES / *RAMJET ENGINES / SHOCK WAVES / *SOLID PROPELLANT ROCKET ENGINES / SPECIFIC IMPULSE

TYPE 19/4/29
82N27693M NASA ISSUE 18 Category 34
Performance of an Oswatisch inlet with hemispherical centerbody at zero angle of attack
M.S. Thesis
MORAN, J. F.
Naval Postgraduate School, Monterey, Calif. (NS368219)
AD-A107439; NPS67-81-009 810600 ARPA ORDER 4035 Dept. of Aeronautics. 87 p. Jpn. 2557 HC A05/MF A01

This thesis analyzes the performance of a ramjet with an Oswatisch inlet using a blunt centerbody and compares performance to a baseline ramjet using an inlet with a conical spike at Mach 3.0. Inlet performance as a ratio of inlet tip to nose centerbody ratio, r sub L/r sub n, is developed. The capture streamline for each ratio is determined and the coefficient of additive drag is calculated as a function of r sub L/r sub n. Setting thrust coefficient equal to coefficient of drag, the performance of two ramjets is determined. One ramjet is the baseline with a spike inlet; the other ramjet uses the blunt centerbody. Ramjets and inlets are compared on the basis of specific fuel consumption, exress thrust coefficient and specific thrust. For the ramjet with blunt

centerbody, performance parameters were calculated as a function of inlet lip radius to nose centerbody radius. Also compared is the effect of the ramjets, the detection range is reduced by approximately 66%. Performance of the ramjet with blunt nosed centerbody is severly handicapped due to high additive drag and poor pressure recovery. Specific fuel consumption is approximately 50% greater for the ramjet with the blunt centerbody compared to the ramjet with the spike inlet. Author (CRA)

Controlled Terms: *ANGLE OF ATTACK / *BLUNT BODIES / COMPUTER PROGRAMS / DRAG / *ENGINE INLETS / FUEL CONSUMPTION / NOSES (FOREBODIES) / *PRESSURE RECOVERY / *RAMJET ENGINES / *RAMJET MISSILES / THRUST

TYPE 19/4/30 NASA ISSUE 16 Category 7
New developments in the field of ramjet missile propulsion
(Neue entwicklungen auf dem gebiet der^flugkoerper-stauantriebe)
WEINREICH, H. L.
Messerschmitt-Boelkow-Blohm G.m.b.H., Ottobrunn (West Germany). (MT620643)
MBB-UR-516-81-0 B11112 Unternehmensbereich Raumfahrt. 65 p. Jpn. 2202 HC A04/MF A01

Various supersonic ramjets are discussed which were proposed for the propulsion systems of tactical missiles with higher average velocities. Design and general operating characteristics of ramjet engines are reviewed. The interaction between intake system and ramjet combustion chamber performance is treated with reference to throttling schemes. Ramjet engines, using liquid or solid propellant, as well as solid fuel ramrockets are studied. Experimentally proven performance of ramjet designs is cited and technological trends are identified. Development results concern fuel, inlet systems, variable thrust chokes; and ramjet combustion chamber/integral booster configurations. Author (ESA)

Controlled Terms: INLET NOZZLES / NOZZLE DESIGN / *PROPULSION SYSTEM CONFIGURATIONS / *RAMJET MISSILES / *ROCKET ENGINE DESIGN / ROCKET PROPELLANTS / *SUPERSONIC COMBUSTION RAMJET ENGINES / SUPERSONIC INLETS / THROTTLING / VARIABLE THRUST

TYPE 19/4/31 NASA ISSUE 15 Category 20
Demonstration of a simple device to start an overcontracted mixed compression inlet
DUNN, B. M.; FINK, L. E.
Boeing Aerospace Co., Seattle, Wash. (BR113710)
B10500 In APL The 1981 JANNAF Propulsion Meeting. Vol. 2 p 1-19 (SEE
N82-25149 15-99) 19 p. Jpn. 2184 HC $60.50/MF $60.50

A simple concept which also serves as a non-ejectable inlet cover was conceived (and patent applied for) that allows starting of an overcontracted mixed compression inlet. Two-dimensional, inviscid internal flow analyses of this concept indicate its workability. A small scale inlet model was designed and fabricated, and the feasibility of this concept was demonstrated during a series of IR&D funded wind tunnel tests performed at Mach 3.0 and 2.73. Other major test variables were boundary layer bleed flow amount and location, and cowl lip geometry. The design analysis, test results, and the impact of the concept on mission performance of a typical air-to-air missile are discussed. A.R.H.

Controlled Terms: AIR TO AIR MISSILES / BASE PRESSURE / COMPRESSIBLE FLOW / *CONTRACTION / DRAG REDUCTION / *INTERNAL COMPRESSION INLETS / INVISCID FLOW / *MECHANICAL DEVICES / RAMJET MISSILES / *STARTING / *SUPERSONIC INLETS / *WIND TUNNEL TESTS

TYPE 19/4/32 NASA ISSUE 12 Category 28
Firebrand ramjet propulsion system development
JONES, U. R.; RANSLEM, G. R.
Marquardt Corp., Van Nuys, Calif. (MH569990)
B11000 In APL The 18th JANNAF Combust. Meeting. Vol. 3 p 415-4 ? (SEE
N82-21378 12-28) 29 p. Jpn. 1641 HC A20.

The development of the Navy/Teledyne Ryan Aeronautical FIREBRAND vehicle which is an antiship missile target used to evaluate current and future onboard weapon system effectiveness against a group of enemy threats is discussed. The cruise propulsion thrust for the FIREBRAND vehicle is supplied by two identical normal shock inlet ramjet engines. The review of pressure recovery and combustion efficiency with respect to fuel-air ratio at various altitudes and Mach numbers was tested. Durability of the flightweight hardware is discussed. The integrated fuel control performance is also reported. Plans for the PFRT/Qual test are outlined. E.A.K.

Controlled Terms: *ANTISHIP MISSILES / *COMBUSTION CHAMBERS / COMBUSTION EFFICIENCY / *FUEL COMBUSTION / FUEL CONSUMPTION / MACH NUMBER / PROPULSION SYSTEM PERFORMANCE / *RAMJET ENGINES

TYPE 19/4/33 NASA ISSUE 12 Category 28
A technique for rapid analysis of interactions between SFRJ fuel requirements and missile mission performance
DUNN, B. M.; FINK, L. E.
Boeing Aerospace Co., Seattle, Wash. (BR113710)
B11000 In APL The 18th JANNAF Combust. Meeting. Vol. 3 p 377-401 (SEE
N82-21378 12-28) 13 p. Jpn. 1640 HC A20

The integral rocket solid fuel ramjet propulsion system is ideally suited for missile applications because of its all solid fuel and boost propellant features. While conceptually simple, it is difficult to analyze and design because of complex sizing and performance interactions among the fuel, engine, trajectory, and missile size. Fundamental solid fuel ramjet sizing considerations and mission performance considerations are reviewed. The use of analytical technique, ARES, to provide a rapid assessment of these interactions is discussed. Examples are presented which emphasize the interactions between solid fuel characteristics and missile mission performance. E.A.K.

Controlled Terms: FUEL TANKS / NUMERICAL ANALYSIS / PERFORMANCE TESTS / *PROPULSION SYSTEM PERFORMANCE / *RAMJET ENGINES / *RAMJET MISSILES / *SOLID PROPELLANT COMBUSTION / SOLID PROPELLANTS / SPACE MISSIONS

TYPE 19/4/34 NASA ISSUE 1 Category 7
Air-film cooling returns to ramjets
ROBERTS, W. E.; WASSERBERG, S.
ASME PAPER 81-ENAS-8 810700 American Society of Mechanical Engineers, Intersociety Conference on Environmental Systems, San Francisco, CA, July 13-15, 1981. 5 p. AB(Marquardt Co., Van Nuys, CA) 6 p. Jpn. 13 MEMBERS, $2.00; NONMEMBERS, $4.00

A ramjet engine was configured for the Navy Firebrand program to propel an antiship target missile. After years of using insulation to thermally protect engine combustor/nozzle assemblies, air-film cooling was used in the Firebrand engine. A combustor liner causes a layer of cool air to be injected between the combustion gas and combustor/nozzle structural shell. As this film flows downstream, mixing and reaction with combustion gas

causes its cooling effectiveness to deteriorate. A satisfactory structural design requires shell temperature prediction. Using three film cooling correlations, a method of defining the Firebrand film cooling effectiveness is shown. Thermal models are presented which utilize this effectiveness and provide shell temperature predictions under- ground test conditions. This analytical method is shown to be sufficient when predicted temperatures are compared with shell temperatures measured during these ground tests. (Author)

Controlled Terms: *AIR COOLING / *AIRCRAFT ENGINES / *ANTISHIP MISSILES / COMBUSTION CHAMBERS / *ENGINE COOLANTS / ENGINE TESTS / EXHAUST NOZZLES / *FILM COOLING / GAS INJECTION / GROUND TESTS / PREDICTION ANALYSIS TECHNIQUES / *RAMJET ENGINES / SHELLS (STRUCTURAL FORMS) / TURBULENT MIXING

TYPE 19/4/35
81A40904 NASA ISSUE 19 Category 7
Firebrand ramjet propulsion system development
RAMJEM, G. R.
AIAA PAPER 81-1486 810700 AIAA, SAE, and ASME, Joint Propulsion Conference, 17th, Colorado Springs, CO, July 27-29, 1981, AIAA 12 p. AA(Marquardt Co., Van Nuys, CA) 12 p.

Test results for the first two development phases of the Navy Firebrand antiship target vehicle's ramjet powerplant are reported. Cruise propulsion thrust for the vehicle is supplied by two identical, normal shock inlet ramjet engines, whose simulated flight test performance with integrated fuel controls is reported. Among the other topics covered are: (1) basic mission description for the target vehicle; (2) development objectives; (3) test program plan; (4) engine design; (5) test installation; (6) heavy duty engine test results; (7) fuel control system; and (8) propulsion system performance. Among the program accomplishments are to be counted a ramburner drag coefficient of 4.0, high altitude cruise performance insensitivity to fuel temperature variation, and the obtaining of engine ignition with flares at a variety of simulated speed/altitude conditions. O.C.

Controlled Terms: AIR TO SURFACE MISSILES / *CRUISE MISSILES / FLIGHT TESTS / FUEL CONTROL / MACH NUMBER / *MISSILE TESTS / PERFORMANCE PREDICTION / *PROPULSION SYSTEM PERFORMANCE / *RAMJET ENGINES / *RAMJET MISSILES / ROCKET ENGINE DESIGN / SURFACE TO SURFACE MISSILES / TEST FACILITIES

TYPE 19/4/36
81A39134 NASA ISSUE 17 Category 2
A survey of heating and turbulent boundary layer characteristics of several hypersonic research aircraft configurations
LAWING, P. L.
National Aeronautics and Space Administration. Langley Research Center, Hampton, Va. (ND210491)
AIAA PAPER 81-1145 810600 American Institute of Aeronautics and Astronautics. Thermophysics Conference, 16th, Palo Alto, CA, June 23-25, 1981. 11 p. AA(NASA, Langley Research Center, Transonic Aerodynamics Div., Hampton, VA) 11 p. Refs. 26

Four of the configurations investigated during a proposed NASA-Langley hypersonic research aircraft program were selected for phase-change-paint heat transfer testing and forebody boundary layer pitot surveys. In anticipation of future hypersonic aircraft, both published and unpublished data and results are reviewed and presented with the purpose of providing a synoptic heat-transfer data base from the research effort. Engineering heat-transfer predictions are compared with experimental data on both a global and a local basis. The global predictions are shown to be

predictions can be adequate when interpreted in light of the proper flow field. In that regard, cross flow in the forebody boundary layers was examined for significant heating and aerodynamic effect on the scramjet engines. A design philosophy which evolved from the research airplane effort is used to design a forebody shape that produces thin, uniform, forebody boundary layers on a hypersonic airbreathing missile. Finally, heating/boundary layer phenomena which are not predictable with state-of-the-art knowledge and techniques are shown and discussed. (Author)

Controlled Terms: *AIRCRAFT CONFIGURATIONS / CROSS FLOW / FLOW DISTRIBUTION / FOREBODIES / *HEAT TRANSFER / *HYPERSONIC AIRCRAFT / LEADING EDGES / NASA PROGRAMS / *PERFORMANCE PREDICTION / *RESEARCH AIRCRAFT / SUPERSONIC COMBUSTION RAMJET ENGINES / *TURBULENT BOUNDARY LAYER

TYPE 19/4/37
81A33285 NASA ISSUE 14 Category 9
O.N.E.R.A. ramjet test facilities
BERTON, P.; REGARD, D.
800900 (La Recherche Aerospatiale, July-Aug. 1980, p. 241-258.) La Recherche Aerospatiale (English Edition), Aug.-Sept. 1990, p. 25-44. Translation. ABIONERA, Chatillon-sous-Bagneux, Hauts-de-Seine, France) 20 p.

(For abstract see issue 24, p. 4320, Accession no. A80 52915

Controlled Terms: *ENGINE TESTING FACILITIES / FRANCE / PROTOTYPES / *RAMJET MISSILES / *ROCKET TEST FACILITIES / SOLID PROPELLANT ROCKET ENGINES / *SUPERSONIC COMBUSTION RAMJET ENGINES / SUPERSONIC WIND TUNNELS

TYPE 19/4/38
81A32535 NASA ISSUE 14 Category 18
Air intake for a ramjet propelled test missile
Prise d'air pour missile probatoire de statofusee
LARUELLE, G.
ONERA, TP NO. 1981-5 810000 (Israel Annual Conference on Aviation and Astronautics, 23rd. Haifa, Israel, Feb. 11, 12, 1981.) UNERA, TP no. 1981-5, 1981. 22 p. In French. AAIONERA, Chatillon-sous-Bagneux, Hauts-de-Seine, France) 22 p.

Methods and aerodynamic tests for definition and optimization of air intake for a test missile powered by a solid propellant ramjet during cruise, developed by ONERA, are presented. Results for scale model testing in the supersonic wind tunnels S2 and S5 and the hypersonic S4 are given for various conditions of height, flow, air intake rate, placement and height of boundary layer intake of ducts, influence of longitudinal position, and effect of duct position during roll maneuvers. It was found that the Mach adaptation number must be slightly higher than the nominal Mach number to compensate for shock induced on the missile body by the air intakes. Predictions based on the wind tunnel tests are found to compare favorably with data gleaned from the first two nonguided ballistic test flights made in June 1976. D.H.K.

Controlled Terms: *AIR INTAKES / *ENGINE DESIGN / FLIGHT TESTS / HYPERSONIC WIND TUNNELS / MACH NUMBER / *MISSILE TESTS / *RAMJET MISSILES / SUPERSONIC WIND TUNNELS / WIND TUNNEL TESTS

TYPE 19/4/39
81N30164# NASA ISSUE 21 Category 15
European missile aerodynamics and developments
GREGORIOU, G: ...

MT620643)
MBB-UA-531/80-OE B00421 Unternehmensbereich Apparate. Presented at Short Course on Missile Aerodyn., Tenn., 7-11 Apr. 1980 54 p. Jpn. 28/5 HC A04/MF A01

The joint development of new generation missiles by many European countries not only minimizes the costs and the technological risks for each individual country, but also increases the degree of research in recent years standardization within NATO. Focal points of research in recent years include: (1) jet influence on the dispersion of artillery rockets; (2) problems associated with the vertical launch of missiles; and (3) air intakes of ramjets. These areas are examined with respect to their significance in missile design. Some characteristic theoretical and measurement results are given. A.R.H.

Controlled Terms: *AERODYNAMIC COEFFICIENTS / AIR INTAKES / *ARTILLERY / FINNED BODIES / JET IMPINGEMENT / LONGITUDINAL STABILITY / MISSILE CONTROL / *MISSILE DESIGN / *RAMJET MISSILES / *ROCKET LAUNCHING / *WEAPONS DEVELOPMENT

TYPE 19/4/40
81A29065 NASA ISSUE 12 Category 7
An approach to ramjet trajectory simulation test
CHIANG, S.-S. In: International Symposium on Air Breathing Engines, 5th, Bangalore, India, February 16-22, 1981, Proceedings. (A81-29051 12-07) Bangalore, National Aeronautical Laboratory, 1981, p. 23-1 to 23-7. AA(China Precision Machinery Corp., Beijing, Communist China) 7 p.

A ground simulation test (conducted in a direct-connect test facility) has been developed for a ramjet trajectory in the boost and the ascent phases. The simulation process is presented in detail. The test results have been verified in flight tests with very good results. The inlet flow parameter, the overshoot problem, the temperature and pressure simulation and the exhaust environment parameters are also covered. K.S.

Controlled Terms: EXHAUST FLOW SIMULATION / *FLIGHT SIMULATION / FUEL CONTROL / FUEL PUMPS / *FUEL SYSTEMS / *GROUND TESTS / *INLET FLOW / INLET TEMPERATURE / *MISSILE TRAJECTORIES / OPERATING TEMPERATURE / PRESSURE DISTRIBUTION / *RAMJET MISSILES / *ROCKET EXHAUST

TYPE 19/4/41
81N25003# NASA ISSUE 16 Category 14
ONERA ramjet test facilities --- supersonic combustion ramjet engines
BENTON, P.; REGARD, D.
Office National d'Etudes et de Recherches Aerospatiales, Paris (France).
(QF368396)
810300 In its La Rech. Aerospatiale, Bi-Monthly Bull. No. 1980-4 (ESA-TT-672) p 25-44 (SEE N81-26000 16-99) Transl. into ENGLISH of la Rech. Aerospatiale, Bull. Bimestriel (Paris), no. 1980-4, Jul.-Aug. 1980 p 241-258 Original report in FRENCH previously announced as A80-52915/4 20 p. Jpn. 2279 HC A05/MF A01

Wind tunnel requirements and facilities for testing integrated rocket ramjet missiles and motors for solid or liquid fuel ramjets are obtained obtained rate measurements for solid or liquid fuel ramjets are obtained with water cooled probes, ultrasonic flowmeters, and an analogy method involving the weighing of a gas generator on a continuous weighing device. Test benches are described for solid fuel tests and for rocket and integrated rocket connected pipe or semifree jet tests. Wind tunnel facilities are indicated and capabilities are described for the S4 supersonic tunnel which permits testing of full scale ramjet missiles with solid propellant boosters. Author (ESA)

Controlled Terms: *ENGINE TESTING LABORATORIES / PROTOTYPES / *RAMJET MISSILES / *ROCKET TEST FACILITIES / SOLID PROPELLANT ROCKET ENGINES / *SUPERSONIC COMBUSTION RAMJET ENGINES / SUPERSONIC WIND TUNNELS

TYPE 19/4/42
81N24089# NASA ISSUE 15 Category 7
Free-jet testing of powerplants for aircraft and missiles
ASHWOOD, P. F.; PHIL, P. D.
National Gas Turbine Establishment, Farnborough (England). (N1420960)
810100 Engine Test Dept. In AGARD Turbine Engine testing 24 p (SEE N81-24071 15-07) 24 p. Jpn. 2013 HC A21/MF A01

The free-jet test facilities available at the National Gas Turbine Establishment for testing complete aircraft propulsion systems (the air intake, engine, and exhaust system) at conditions reproducing those encountered during flight are described. Supersonic and subsonic flight conditions can be simulated, both steady state and transient; the latter aspect including the effects of time-variant changes in aircraft flight speed, attitude, and engine power. The scope of free-jet testing is reviewed and compared with what can be achieved using direct-connect facilities. Subsonic free-jet tests made under the extreme conditions encountered in an icing cloud are discussed. The tests are designed to determine the effectiveness of intake and engine anti-icing equipment and the ability of the powerplant to operate satisfactorily following the shedding of ice that may have accreted on the inlet duct surfaces. M.G.

Controlled Terms: *AIRCRAFT ENGINES / ENGINE INLETS / *ENGINE TESTING LABORATORIES / *ENGINE TESTS / EXHAUST SYSTEMS / *FREE JETS / HELICOPTERS / ICE FORMATION / RAMJET ENGINES / *ROCKET ENGINES / SUBSONIC SPEED / SUPERSONIC SPEEDS

TYPE 19/4/43
81A29061 NASA ISSUE 9 Category 24
Application of composites to missile structures - A review
BAILIE, J. A.
810100 SAMPE Quarterly, vol. 12, Jan. 1981, p. 1-8. AA(Lockheed Missiles and Space Co., Inc., Sunnyvale, Calif.) 8 p. Refs. 22

A brief survey of current and potential future uses of composites in missiles was conducted by extracting typical samples of data from the generally available literature. Use of fiber reinforcement composites to solid rocket motors and nozzles, missile body structures and sensor windows are discussed in very general terms. Differences in the demands made upon composite missile structures, relative to those on aircraft are outlined. (Author)

Controlled Terms: AIRCRAFT STRUCTURES / AIRFRAME MATERIALS / CARBON-CARBON COMPOSITES / COMPRESSION TESTS / EPOXY RESINS / *FIBER REINFORCED COMPOSITES / GLASS FIBER REINFORCED PLASTICS / GRAPHITE-EPOXY COMPOSITE MATERIALS / HONEYCOMB CORES / LAMINATES / METAL MATRIX COMPOSITES / *MISSILE BODIES / *MISSILE STRUCTURES / HX MISSILE / RADOME MATERIALS / RAMJET MISSILES / *RENTRY VEHICLES / ROCKET ENGINE CASES / *ROCKET NOZZLES / *SOLID PROPELLANT ROCKET ENGINES

TYPE 19/4/44
81A22616 NASA ISSUE 8 Category 5
ASALM/PTV propulsion system development and flight test program --- Advanced Strategic Air Launched Missile Propulsion Technology Validation
GARNER, A. M.; WEBSTER, F. F.
800000 In: Association for Unmanned Vehicle Systems, Annual Technical Symposium, 7th, Dayton, Ohio, June 16-18, 1980, Proceedings. (A81-22602 08-01) Dayton, Ohio, Association for Unmanned Vehicle Systems, 1980, p. 135-141. AB(Martin Marietta Aerospace, Orlando, Fla.) 7 p.

The ASALM Propulsion Technology Validation (PTV) contract is for a liquid fueled integral rocket/ramjet propulsion system. The ground development portion of the program was completed and the flight testing phase is nearing the end. To date, five flights have successfully demonstrated functional operation and performance capability during boost, rocket-to-ramjet transition, and ramjet operation. Both subsystem performance and overall system performance are in good agreement with the results obtained during the ground test program. During the ground test program, development problems were encountered with the booster dome port cover, the ejectable booster nozzle, and the ramburner thermal protection system. None of these problems has been encountered during any of the flights. (Author)

Controlled Terms: *AIR LAUNCHING / AVIONICS / BOOSTER ROCKET ENGINES / *FLIGHT TESTS / FUEL SYSTEMS / *LIQUID PROPELLANT ROCKET ENGINES / MISSILE CONTROL / *PROPULSION SYSTEM PERFORMANCE / *RAMJET MISSILES / RESEARCH AND DEVELOPMENT / TECHNOLOGY ASSESSMENT / TELEMETRY

TYPE 19/4/45
81A20729 NASA ISSUE 7 Category 1
Aerodynamic properties of an advanced indirect fire system /AIFS/ projectile
FINK, M. R.
AIAA PAPER 81-0287 810100 DAAK10-80-C-0114 American Institute of Aeronautics and Astronautics, Aerospace Sciences Meeting, 19th, St. Louis, Mo. Jan. 12-15, 1981, 7 p. AA(Norden Systems, Inc., Norwalk, Conn.) 7 p. Refs. 6 Jpn. 985

Aerodynamic compromises in the design of an advanced artillery projectile are discussed. This Advanced Indirect Fire System has solid-fuel ramjet propulsion for increased range and reduced sensitivity to winds. Folding aft fins provide static stability during powered flight. Maneuverability is needed only during the terminal maneuver phase near the target. At that time, thrust is terminated by removing the sharp inlet spike ahead of the blunt seeker dome. The canards are then extended to provide maneuverability and to compensate for increased stability caused by the forward shift of center of gravity as fuel is burned. Interaction of body vortexes and the initially designed small-span aft fins produced a nonlinear increase of lift and static stability at small and moderate incidence. Thus the canards could not trim the airframe at sufficiently high lift coefficients to achieve the required maneuver footprint. Fin redesign to delay onset of the nonlinear airloads was needed. (Author)

Controlled Terms: *AERODYNAMIC CONFIGURATIONS / ANGLE OF ATTACK / *ARTILLERY / BLUNT BODIES / *FORCE DISTRIBUTION / LIFT / MACH NUMBER / PITCH (INCLINATION) / *PROJECTILES / *RAMJET MISSILES / SOLID PROPELLANT ROCKET ENGINES / TERMINAL BALLISTICS

TYPE 19/4/46
81A15017 NASA ISSUE 4 Category 5
Application of an advanced trajectory optimization method to ramjet propelled missiles
PARIS, S. W.; FINK, L. E.; JOOSTEN, B. K.
Boeing Aerospace Co., Seattle, Wash. (BR113710)
801200 Optimal Control Applications and Methods, vol. 1, Oct.-Dec. 1980, p. 319-334. AB(Boeing Aerospace Co., Seattle, Wash.) AC(NASA, Johnson Space Center, Houston, Tex.) 16 p. Refs. 10 Jpn. 482

The mission performance characteristics of ramjet-propelled missiles are highly dependent upon the trajectory flown. Integration of the trajectory profile with the ramjet propulsion system performance characteristics to achieve optimal missile performance is very complex. Past trajectory optimization methods have been extremely problem dependent and require a high degree of familiarity to achieve success. A general computer code (CTOP) has been applied to ramjet-powered missiles to compute open-loop optimal trajectories. CTOP employs Chebyshev polynomial representations of the states and controls. This allows a transformation of the continuous optimal control problem to one of parameter optimization. With this method, the trajectory boundary conditions are always satisfied. State dynamics and path constraints are enforced via penalty functions. The presented results include solutions to minimum fuel-to-climb, minimum time-to-climb, and minimum time-to-target intercept problems. (Author)

Controlled Terms: CHEBYSHEV APPROXIMATION / COMPUTER PROGRAMS / *MISSILE CONTROL / *MISSILE TRAJECTORIES / PENALTY FUNCTION / POLYNOMIALS / *PROPULSION SYSTEM PERFORMANCE / *RAMJET MISSILES / *TIME OPTIMAL CONTROL / *TRAJECTORY OPTIMIZATION

TYPE 19/4/47
81N12106# NASA ISSUE 3 Category 7
Effects of advances in propulsion technology on missile effectiveness
--- solid fuel ramjets
LIMAGE, C. R.; FIELDS, J. L.
Atlantic Research Corp., Gainesville, Va. (A6416051)
AD-A090545 800905 26 p. Jpn. 306 HC A03/MF A01

This paper presents the effects of propulsion technology evolution on the performance capability of advanced missile systems. The evolution of the missile propulsion system from rocket to ramjet with increased emphasis on advanced airbreathing missile cycles, has significantly extended missile operational capabilities. The development of these new areas of ramjet technology, specifically in solid fuel propellants, offers the advantages of large increases in heating value, density, burning efficiency and improves system packaging. Application of these technology advancements to potential mission scenarios produces impressive increases in overall mission performance. These large performances gains provide a basis for improvements in mission effectiveness in terms of kill probability and survivability. Kill probability is increased by application of shorter intercept times, improved multi-shot capability and reductions in individual system size to improve weapon carrier payload cap-bility. Survivability is enhanced by increased standoff distances and higher penetration velocities. Demonstration of these improved capabilities, over a variety of tactical mission are provided by a direct comparison of missile performance for a variety of missile propulsion systems. The systems studied range from the conventional solid rocket system to the advanced highly energetic boron solid fuel ramjet concept. GRA

Controlled Terms: BORON / MILITARY OPERATIONS / *MISSILE SYSTEMS / PROPULSIVE EFFICIENCY / *RAMJET ENGINES / *SOLID PROPELLANTS / SURVIVAL / *SYSTEM EFFECTIVENESS / TERMINAL BALLISTICS

TYPE 19/4/48
80N33409# NASA ISSUE 24 Category 7
Conceptual model of turbulent flameholding for scramjet combustors
HUBER, P. W.
National Aeronautics and Space Administration. Langley Research Center, Hampton, Va. (ND210491)
NASA-TP-1543; L-13600 801000 36 p. Jpn. 3235 HC A03/MF A01

New concepts and approaches to scramjet combustor design are presented. Blowoff was from failure of the recirculation-zone (RZ) flame to reach the dividing streamline (DS) at the rear stagnation zone. Increased turbulent exchange across the DS helped flameholding due to forward movement of the flame anchor point inside the RZ. Modeling of the blowoff phenomenon was

TYPE 19/4/51
80N30420 NASA ISSUE 21 Category 20
Optimized propulsion/guidance analysis of ramjet powered vehicles
GOLDSTEIN, F.; CALISE, A.
Dynamics Research Corp., Wilmington, Mass. (D9080510)
B00300 F33615-79-C-2088 In APL The 1980 JANNAF Propulsion Meeting, Vol.
5 p 621-633 (SEE N80-30381 21-20) A8(Drexel Univ.) 13 p. Jpn. 2812 Avail:
Issuing Activity

An evaluation of the use of singular perturbation methods for developing computer algorithms for on-line optimal control of ramjet powered vehicles is presented. Optimal control solutions using singular perturbation theory (SPT) are derived which incorporate optimal aerodynamic control of turn rate and optimal thrust magnitude control of velocity. Maximum lift coefficient, maximum load factor, minimum and maximum velocity and thrust, and instrumentation related constraints are enforced. Particular attention is given to identifying quantities that can be precomputed and stored (as a function of total energy), thus reducing the onboard computational load. Numerical results are given that illustrate the nature of the optimal intercept flight paths, and which demonstrate the impact on trajectory shaping through use of optimal control techniques. J.M.S.

Controlled Terms: AIRBORNE/SPACEBORNE COMPUTERS / ALGORITHMS / BOUNDARY VALUE PROBLEMS / *GUIDANCE (MOTION) / OPTIMAL CONTROL / PERTURBATION THEORY / *PROPULSION SYSTEM PERFORMANCE / *RAMJET MISSILES / *THRUST CONTROL / *TRAJECTORY OPTIMIZATION

TYPE 19/4/52
80N27512# NASA ISSUE 18 Category 28
Carbon slurry fuels for volume limited missiles
Annual Report, Sep. 1978 - Oct. 1979
SALVESEN, R. H.; RIGANO, D. C.; BLAZOWSKI, W. S.; TAYLOR, W. F.
Exxon Research and Engineering Co., Linden, N.J. (E9814224)
AD-A084710; EXXON/PLUS.1KWX.79; AR-1; AFAPL-TR-79-2122 791100
F33615-78-C-2025; AF PROJ. 3048 219 p. Jpn. 2395 HC A10/HF A01

The Air Force has contracted with ER E to develop a carbon slurry fuel with a minimum of 180,000 BTU/gal. This report provides results of the first year's effort of this twenty-seven month program. Initial results indicate that a dispersion of carbon black in JP-10 with select dispersing agents can be made that meets the BTU requirements. Preliminary results look promising. Combustion tests using a specially developed Liquid Fuel Jet Stirred Combustor (LFJSC) have demonstrated that carbon burnout efficiencies greater than 90% are achievable with 300 nm particles in residence times down to 4 ms. Homogeneous iron, lead, manganese, and zirconium catalysts at concentrations up to 1000 ppm proved ineffective as accelerators of carbon burnout. Further tests are in progress to optimize the composition of the most promising formulations and to test these materials under more vigorous conditions in order to determine their suitability for missile applications. GRA

Controlled Terms: *CARBON / CATALYSTS / CHEMICAL REACTIONS / COMBUSTION / *CRUISE MISSILES / JET ENGINE FUELS / *RAMJET ENGINES / *SLURRY PROPELLANTS

TYPE 19/4/53
80N22396# NASA ISSUE 13 Category 15
The use of ram rockets for high altitude missiles
RIESTER, E.
European Space Agency, Paris (France). (E9854803)
ESA-TT-505; DLR-FB-77-47 781200 Transl. into ENGLISH of ''Die Anwendung von Staustrahlraketen bei Flugkoerpern in Groesseren Hoehen'', Rept.

based on a mass conservation concept involving the traverse of a flame element across the RZ and a flow element along the DS. The scale required to achieve flameholding, predicted by the model, showed a strong adverse effect of low pressure and low fuel equivalence ratio, moderate effect of flight Mach number, and little effect of temperature recovery factor. Possible effects of finite rate chemistry on flameholding and flamespreading in scramjets are discussed and recommendations for approaches to engine combustor design as well as for needed research to reduce uncertainties in the concepts are made. Author

Controlled Terms: BACKFIRE / COMBUSTION CHAMBERS / *COMBUSTION PHYSICS / *ENGINE DESIGN / *FLAME HOLDERS / *FLAME PROPAGATION / FLAME STABILITY / *FLAMEOUT / FUEL COMBUSTION / RAMJET MISSILES / *SUPERSONIC COMBUSTION RAMJET ENGINES

TYPE 19/4/49
80N32422# NASA ISSUE 23 Category 15
Guidance and control of tactical missiles
GROTE, T. A.
M.S. Thesis
Naval Postgraduate School, Monterey, Calif. (NS368219)
AD-A085147 791200 174 p. Jpn. 3098 HC A08/HF A01

The functioning program used to investigate the impact miss distance for the Supersonic Tactical Missile was modified. When the initial y-displacement error exceeded 1800 feet, the missile did not acquire the target. All errors smaller than this resulted in miss distances within 0.5 feet of the target. The midcourse guidance reference altitude was changed to reflect a sea-skimming missile. This simulation ran and impact was recorded. An attempt at adding random noise to the homing seeker was tried, but revealed that more information is required on this topic. The computer program was successfully converted and altered to run using the simplified ramjet model. T.M.

Controlled Terms: ACCURACY / *ALTITUDE CONTROL / ANALOG COMPUTERS / *COMPUTER PROGRAMS / *COMPUTERIZED SIMULATION / *HOMING / MATHEMATICAL MODELS / *MISS DISTANCE / *MISSILE CONTROL / *MISSILES / SUPERSONIC COMBUSTION RAMJET ENGINES / *TARGET ACQUISITION

TYPE 19/4/50
80N30421 NASA ISSUE 21 Category 20
Application of an advanced trajectory optimization method to ramjet propelled missiles
PARIS, S. W.; JOOSTEN, B. K.; FINK, L. E.
Boeing Aerospace Co., Seattle, Wash. (BR113710)
B00300 In APL The 1980 JANNAF Propulsion Meeting, Vol. 5 p 635-650
(SEE N80-30381 21-20) 16 p. Jpn. 2812 Avail: Issuing Activity

The mission performance characteristics of ramjet propelled missiles are highly dependent upon the trajectory flown. Integration of the trajectory profile with the ramjet propulsion system performance characteristics to achieve optimal missile performance is very complex. A general computer code (CTOP) is applied to ramjet powered missiles to compute open-loop optimal trajectories. The CTOP employs Chebychev polynomial representations of the states and controls, allowing a transformation of the continuous optimal control problem to one of parameter optimization. With this method, the trajectory boundary conditions are always satisfied. State dynamics and path constraints are enforced via penalty functions. The presented results include solutions to minimum fuel to climb, and minimum time to target intercept problems. J.M.S.

Controlled Terms: COMPUTER PROGRAMS / CONTROL THEORY / FLIGHT PATHS / OPTIMAL CONTROL / *PROPULSION SYSTEM PERFORMANCE / *RAMJET MISSILES / *TRAJECTORY OPTIMIZATION

The conditions under which a ram rocket is superior to a rocket as a power plant for the cruising phase of high altitude supersonic missiles are analyzed and defined. The influence of mission and power plant parameters on the payload of both kinds of engine units is investigated. The advantages of a booster-ram rocket combination over a two-stage rocket are pointed out. This advantage can be increased if the booster acceleration is terminated before the cruise velocity is reached and the ram rocket then continues the acceleration. In that case, the payload attains a maximum at a particular final booster velocity. The working regimes in the ram rocket combustion chamber needed to obtain these optimal conditions are deduced. Author (ESA)

Controlled Terms: ACCELERATION (PHYSICS) / BOOSTER ROCKET ENGINES / CRUISING FLIGHT / GAS GENERATORS / *HIGH ALTITUDE / *MISSILES / *RAMJET ENGINES / *SUPERSONIC FLIGHT

TYPE 19/4/54
80N19123# NASA ISSUE 10 Category 7
Demonstration program for a flexible duct valve for ramjet engine fuel controls
Final Report, 15 Nov. 1978 - 28 Feb. 1979
ROUNDY, J. S.
AiResearch Mfg. Co., Phoenix, Ariz. (AL681511)
AD-A078529; AIRESEARCH-41-2226; NADC-77136-60 790914 N62269-77-C-0352 67 p. Jpn. 1244 HC A04/MF A01

A demonstration program was conducted to develop a flex duct-type metering valve for use in the fuel control of ramjet engines for Navy missiles. This type valve has inherent advantages of simplicity, low cost, and high reliability that make it particularly attractive for this application. This type valve functions best when the leakage flow from the metering gap is bypassed back upstream of the fuel pump. GRA

Controlled Terms: DUCTS / FLEXIBLE BODIES / *FUEL CONTROL / FUEL SYSTEMS / *FUEL VALVES / LOW COST / *MISSILES / *RAMJET ENGINES / RELIABILITY

TYPE 19/4/55
80N17100 NASA ISSUE 8 Category 15
ALVRT flight test program summary
PEARSON, L. E.
Vought Corp., Dallas, Tex. (V9759601)
790300 In APL The 1979 JANNAF Propulsion Meeting, Vol. 1 p 63-82 (SEE N20-17097 08-12) 20 p. Jpn. 761 Avail: Issuing activity

An advanced development flight test program of the Navy's air launched low volume ramjet (ALVRJ) was completed in 1976. The program resulted in five highly successful flight tests of an integral rocket ramjet (IRR) missile configuration through various simulated tactical flight profiles. The program successfully demonstrated the ALVRJ configuration and provided performance capability of the ... technology, established the environmental data operating in this high temperature, high dynamic pressure sustained flight regime. The flight test program is discussed including preparations and conduct of the tests, flight characteristics of the vehicle, performance math model simulation used for flight prediction, and data analysis techniques and routines used to define the performance capability of the subsystems as well as the total vehicle system. R.E.S.

Controlled Terms: *AIR LAUNCHING / COMPUTERIZED SIMULATION / *FLIGHT CHARACTERISTICS / FLIGHT TESTS / MATHEMATICAL MODELS / *MISSILE

TYPE 19/4/56
80N17097 NASA ISSUE 8 Category 12
The 1979 JANNAF propulsion meeting, volume 1
STRANGE, K. L.
Applied Physics Lab., Johns Hopkins Univ., Laurel, Md. (AU080119)
AD-A075262; CPIA-PUB-300-VOL-1 790300 N00024-78-C-5384 Meeting held at Anaheim, Calif., 6-8 Mar. 1979 643 p. Jpn. 960 Avail: Issuing Activity

A collection of papers dealing with various aspects of ballistic missile propulsion is presented. Topics discussed include research, development, test, and engineering advancements in solid, liquid, ramjet, and gun propulsion systems

Controlled Terms: *BALLISTIC MISSILES / *CONFERENCES / MX MISSILE / PROPELLANT COMBUSTION / *PROPULSION SYSTEM CONFIGURATIONS / PROPULSION SYSTEM PERFORMANCE / RAMJET MISSILES / SMOKE ABATEMENT / *SOLID PROPELLANT ROCKET ENGINES / SOLID ROCKET PROPELLANTS / *SPACE TRANSPORTATION SYSTEM / *WEAPON SYSTEMS

TYPE 19/4/57
80A52915 NASA ISSUE 24 Category 9
ONERA ramjet test facilities
Installations d'essais de statoreacteur a l'O.N.E.R.A
BERTON, P.; REGARD, D.
800800 La Recherche Aerospatiale, July-Aug. 1980, p. 241-258. In French. AB(ONERA, Chatillon-sous-Bagneux, Hauts-de-Seine, France) 18 p. Jpn. 4320

Complementary ramjet test facilities have been built at Palaiseau near Paris (basic tests and component development) and at Modane in the Alps (industrial and synthesis tests). At Palaiseau, five benches are devoted to tests ranging from new configurations to technical assistance to industry in developing an operational missile. At Modane, the S4 supersonic wind tunnel has been modified to allow the testing of an actual ramjet missile scale model with its solid propellant booster. B.J.

Controlled Terms: *ENGINE TESTING LABORATORIES / FRANCE / PROTOTYPES / *RAMJET MISSILES / *ROCKET TEST FACILITIES / SOLID PROPELLANT ROCKET ENGINES / *SUPERSONIC COMBUSTION RAMJET ENGINES / SUPERSONIC WIND TUNNELS

TYPE 19/4/58
80A51066 NASA ISSUE 22 Category 5
Optimized guidance and propulsion control for ramjet propelled vehicles based on singular perturbation methods
CALISE, A.; GOLDSTEIN, F.
790000 F66315-77-C-2072 In; Annual Allerton Conference on Communication, Control, and Computing. 17th, Monticello, Ill., October 10-12, 1979, Proceedings. (A80-51051 22-59) Urbana, Ill., University of Illinois, 1979, p. 725-734. AA(Drexel University, Philadelphia, Pa.) AB(Dynamics Research Corp., Wilmington, Mass.) 10 p. Refs. 6

This paper presents an optimal component integration and effectiveness analysis of ramjet powered air-to-air missiles. The approach is based on the simultaneous optimization of the propulsion and guidance, where classically these have been treated separately. To accomplish this, an optimal control approach is required that can determine the optimal propulsion/guidance control algorithm which is in feedback form for the nonlinear ramjet problem, and which can be mechanized on board the missile. Optimal control solutions using singular perturbation techniques are derived for ramjet controlled missiles which incorporate optimal aerodynamic control of turn rate and optimal thrust magnitude control of

velocity. Maximum lift coefficient, maximum load factor, minimum and maximum velocity and thrust, and instrumentation related constraints are enforced. The control solutions are nonlinear and in a feedback form suitable for on-board implementation. (Author)

Controlled Terms: *AIR TO AIR MISSILES / ALGORITHMS / BOUNDARY LAYER CONTROL / CONSTRAINTS / DRAG / EFFICIENCY / FEEDBACK / *GUIDANCE (MOTION) / LIFT / *OPTIMAL CONTROL / *PERTURBATION THEORY / *PROPULSION / *RAMJET MISSILES / TRAJECTORY CONTROL

TYPE 19/4/59
80A44212 NASA ISSUE 17 Category 7
Propulsion integration considerations for advanced boron powered ramjet
LIMAGE, C. R.; SARGENT, W. H.
AIAA PAPER 80-1283 800600 AIAA, SAE, and ASME, Joint Propulsion Conference, 16th, Hartford, Conn., June 30-July 2, 1980, AIAA 10 p. Jpn. 3122
AB(Atlantic Research Corp., Gainesville, Va.) 10 p.

The current emphasis on increased missile performance in terms of range, intercept velocity, and maneuverability has renewed interest in the use of boron as a ramjet fuel. When burning boron, severe constraints are placed on the combustor design to meet the boron fuel particle residence times, stoichiometry, and particle diameter requirements. The impact of these combustor constraints on the ramjet design are shown to have minimum influence on the minimum missile take over Mach number. As a result, the full potential of the large volumetric heating value of boron is available for improvements in missile performance. (Author)

Controlled Terms: *AIRCRAFT FUELS / *BORON / COMBUSTION CHAMBERS / COMBUSTION EFFICIENCY / FLAME TEMPERATURE / *FUEL COMBUSTION / *MISSILE SYSTEMS / PARTICLE SIZE DISTRIBUTION / *RAMJET ENGINES / *SOLID PROPELLANT IGNITION

TYPE 19/4/60
80A41211 NASA ISSUE 20
Nozzleless boosters for integral rocket ramjet missile systems
PROCINSKY, I. M.; MCHALE, C. A.; SMITH, W. R.
AIAA PAPER 80-1277 800600 AIAA, SAE, and ASME, Joint Propulsion Conference, 16th, Hartford, Conn., June 30-July 2, 1980, AIAA 11 p. Refs. 5 Jpn. 3140
AC(Atlantic Research Corp., Gainesville, Va.) 11 p.

The concept of a nozzleless solid propellant booster for an integral-rocket-ramjet missile system offers a number of advantages over the conventional ejectable nozzle design. These advantages include elimination of the debris hazard, simplicity of design, reliability, and performance. Experience with both subscale and fullscale motor designs shows that with a grain length to diameter ratio of 3.5, a nozzleless booster will match the performance of an ejectable nozzle system, and that at larger ratios, the nozzleless motor can be configured to produce up to 15% more performance. General design rules and limitations are also presented. (Author)

Controlled Terms: *BOOSTER ROCKET ENGINES / COMBUSTION EFFICIENCY / COMPUTER PROGRAMS / INTERIOR BALLISTICS / *NOZZLE DESIGN / *NOZZLELESS ROCKET ENGINES / PERFORMANCE TESTS / PROPELLANT TESTS / *RAMJET MISSILES / SOLID PROPELLANT COMBUSTION / *SOLID PROPELLANT ROCKET ENGINES

TYPE 19/4/61
80A41199 NASA ISSUE 20
Future trends in solid rocket technology in Germany
SCHNUCKER, R. H.; STRECKER, R. A. H.
AIAA PAPER 80-1220 800600 AIAA, SAE, and ASME, Joint Propulsion Conference, 16th, Hartford, Conn.,

Research sponsored by the Bundesministerium der Verteidigung. AB(Bayern-Chemie GmbH, Aschau, West Germany) 11 p. Jpn. 3139

Present situation in the field of solid propellant rockets in West Germany is discussed with consideration given to criteria for technology program selection and comparison with foreign countries. Status and trends in component technology, rocket motors, and analytical and design procedures are outlined. Emphasis is placed on application to missile propulsion and non-rocket areas. V.T.

Controlled Terms: GERMANY / RAMJET MISSILES / *ROCKET ENGINE DESIGN / *SOLID PROPELLANT ROCKET ENGINES / SOLID ROCKET PROPELLANTS / *TECHNOLOGICAL FORECASTING / THRUST VECTOR CONTROL

TYPE 19/4/62
80A39003 NASA ISSUE 16 Category 2
Aero-propulsion interactions of a modular missile
FRONING, H. D., JR.; HERR, F. M.
AIAA PAPER 80-1280 800600 AIAA, SAE, and ASME, Joint Propulsion Conference, 16th, Hartford, Conn., June 30-July 2, 1980, AIAA 8 p.
AA(McDonnell Douglas Astronautics Co., Huntington Beach, Calif.)
AB(Marquardt Co., Van Nuys, Calif.) 8 p.

Wind tunnel investigation of a modular missile configuration is considered. The aerodynamic force and moment characteristics of a highly maneuverable rocket-powered missile are analyzed, the changes in the missile's force and moment characteristics due to replacement of its rocket propulsion by rocket-ramjet propulsion are discussed, and the effects of the missile forebody and wings on the operation of a ramjet inlet are outlined. V.I.

Controlled Terms: AERODYNAMIC CHARACTERISTICS / AERODYNAMIC CONFIGURATIONS / AERODYNAMIC FORCES / FLIGHT TESTS / FLOW DISTRIBUTION / LONGITUDINAL CONTROL / MISSILE CONTROL / *PROPULSION SYSTEM PERFORMANCE / *RAMJET ENGINES / *RAMJET MISSILES / *ROCKET ENGINES / *WIND TUNNEL TESTS

TYPE 19/4/63
80A38926 NASA ISSUE 16 Category 7
A fluidic fuel control for advanced ramjet engines
CHAPIN, D. W.; SCHEFR, L. E.; WALDON, B. E.
AIAA PAPER 80-1122 800600 AIAA, SAE, and ASME, Joint Propulsion Conference, 16th, Hartford, Conn., June 30-July 2, 1980, AIAA 10 p.
AB(AiResearch Manufacturing Company of Arizona, Phoenix, Ariz.) ACCU.S. Navy, Naval Weapons Center, China Lake, Calif.) 10 p.

This technical paper summarizes the development of a fluidic fuel control for application to ramjet-powered, air-to-air missiles. The basic control mode is achieved by maintaining a constant fuel-to-air ratio, with overrides as necessary to maintain supercritical operation of the ramjet inlet and to control the velocity of the vehicle. Without an override, fuel is scheduled as a function of pressure at the inlet diffuser which approximates airflow. Inlet supercritical margin control is implemented by direct comparison of inlet total and cowl pitot pressures. An electrofluidic transducer provides an interface between the fuel control and the vehicle flight control system to provide velocity control for the missile. Unique features of this control concept include its capability for operation without a regulated fluidic supply and the use of a high sensitivity fluidic signal comparator for control of inlet supercritical margi. (Author)

Controlled Terms: *AIR TO AIR MISSILES / AIRSPEED / FIGHTER AIRCRAFT / FLIGHT CONTROL / *FLUIDICS / *FUEL CONTROL / FUEL-AIR RATIO / INLET FLOW / MISSILE CONTROL / PRESSURE EFFECTS / PRESSURE SENSORS / *RAMJET ENGINES / RAMJET MISSILES / RESEARCH AND DEVELOPMENT / *ROCKET ENGINE DESIGN

TYPE 19/4/64
80A37481 NASA ISSUE 15 Category 7
New generation ramjets - A promising future
THOMAS, A. N., JR.
800600 Astronautics and Aeronautics, vol. 18, June 1980, p. 36-41, 71. AA(Marquardt Co., Van Nuys, Calif.) 7 p. Refs. 6 Jpn. 2678

Four ramjet variants are under investigation for next generation missiles: the liquid fuel ramjet offers the best performance, the solid ducted rocket offers simplicity, and the solid fuel ramjet offers simplicity and good performance; above Mach 5 the scramjet performs best. It is shown that the combination of high speed, continuous thrust, and low fuel consumption uniquely suits the ramjet to next-generation atmospheric missiles. It is argued that ramjet technology must be doubled to maintain a healthy industrial technical base for expected full-scale engineering development. B.J.

Controlled Terms: FUEL CONSUMPTION / HIGH SPEED / LIQUID ROCKET PROPELLANTS / MACH NUMBER / PROPULSION SYSTEM PERFORMANCE / *RAMJET MISSILES / *RESEARCH AND DEVELOPMENT / ROCKET THRUST / SOLID ROCKET PROPELLANTS / SUPERSONIC COMBUSTION RAMJET ENGINES

TYPE 19/4/65
80A35093 NASA ISSUE 14 Category 5
Elevated temperature structural testing of advanced missiles
OTTO, D. R.; INUKAI, G. J.
AIAA 80-0812 800000 In: Structures, Structural Dynamics, and Materials Conference, 21st, Seattle, Wash., May 12-14, 1980, Technical Papers. Part 2. (A80-34993 14-39) New York, American Institute of Aeronautics and Astronautics, Inc., 1980, p. 902-907. AB(McDonnell Douglas Astronautics Co., St. Louis, Mo.) 6 p. Jpn. 2494

Structural tests at room and elevated temperature were conducted on a full-scale aft airframe section of the Advanced Strategic Air-Launched Missile (ASALM). Loads applied at room temperature represented conditions during captive carry and ejection. Test data are shown to agree well with theory. Loads applied at temperatures up to 1200 F represented conditions during ramjet flight. The high heating rates and temperature levels produced unanticipated and invalid response from some instrumentation. These events will be described and guidelines for high temperature testing will be presented. Although limited elevated-temperature test data were obtained, structural verification of the airframe was achieved. (Author)

Controlled Terms: *AIRFRAMES / *HIGH TEMPERATURE TESTS / LOAD DISTRIBUTION (FORCES) / *LOAD TESTS / *MISSILE STRUCTURES / *MISSILE TESTS / RAMJET MISSILES / ROOM TEMPERATURE / *STRUCTURAL STABILITY

TYPE 19/4/66
80A18302 NASA ISSUE 5 Category 25
Liquid fuel jet injection in a simulated subsonic 'dump' combustor
OGG, J. C.; SCHETZ, J. A.
AIAA PAPER 80-0298 800100 American Institute of Aeronautics and Astronautics, Aerospace Sciences Meeting, 18th, Pasadena, Calif., Jan. 14-16, 1980, 10 p. USAF-supported research. AB(Virginia Polytechnic Institute and State University, Blacksburg, Va.) 10 p. Refs. 10

Basic experimental studies of injection of liquid fuel into a subsonic, sudden-expansion, 'dump' combustor were performed under cold-flow conditions. Short duration photographs, pressure surveys, and surface flow visualization methods were used to investigate area expansion ratios of 1.33 and 1.17. It was found that liquid jet penetration height was essentially independent of injector location and area expansion ratio. Injectant accumulation on the combustor wall was found to be substantial under some conditions, and the amount accumulated was shown to be a strong function of liquid jet penetration height. (Author)

Controlled Terms: *COMBUSTION CHAMBERS / FLOW DISTRIBUTION / FLOW VISUALIZATION / FUEL COMBUSTION / *FUEL INJECTION / INLET FLOW / JET FLOW / *LIQUID INJECTION / *LIQUID ROCKET PROPELLANTS / PHOTOGRAPHIC RECORDING / *RAMJET MISSILES / SHADOWGRAPH PHOTOGRAPHY / *SUBSONIC FLOW

TYPE 19/4/67
80A18293 NASA ISSUE 5 Category 2
Aerodynamic prediction rationale for advanced arbitrarily shaped missile concepts
GREGOIRE, J. E.; KRIEGER, R. J.
AIAA PAPER 80-0256 800100 American Institute of Aeronautics and Astronautics, Aerospace Sciences Meeting, 18th, Pasadena, Calif., Jan. 14-16, 1980, 9 p. AB(McDonnell Douglas Astronautics Co., St. Louis, Mo.) 9 p. Refs. 8

An aerodynamic prediction rationale has been developed for advanced cruise and maneuvering missile concepts using the Mark IV Supersonic/Hypersonic Arbitrary Body Program (HABP). Methods are selected to predict lift, drag, stability and control for advanced missile concepts in the Mach 3 to 5 speed range. Wind tunnel data are shown versus predictions for shapes that have flat bottoms, spatular noses, elliptic, blended and planar cross-sections, two-dimensional and axisymmetric inlets and movable fins and flaps. The techniques employed include various HABP windward and leeward side inviscid pressure methods, the Van Driest II skin friction method and the HABP routine identifying shielding of one part of a vehicle by another. (Author)

Controlled Terms: AERODYNAMIC DRAG / AERODYNAMIC STABILITY / *COMPUTERIZED DESIGN / GRAPHS (CHARTS) / LIFTING BODIES / *MISSILE CONFIGURATIONS / *MISSILE DESIGN / *PERFORMANCE PREDICTION / PRESSURE DISTRIBUTION / PROPULSION SYSTEM CONFIGURATIONS / *RAMJET MISSILES / *SUPERSONIC FLIGHT / TECHNOLOGY UTILIZATION

TYPE 19/4/68
80A18282 NASA ISSUE 5 Category 2
Aerodynamic and inlet flow characteristics of several hypersonic airbreathing missile concepts
DILLON, J. L.; MARCUM, D. C., JR.; JOHNSTON, P. J.; HUNT, J. L.
National Aeronautics and Space Administration. Langley Research Center, Langley Station, Va. (ND210491)
AIAA PAPER 80-0255 800100 American Institute of Aeronautics and Astronautics, Aerospace Sciences Meeting, 18th, Pasadena, Calif., Jan. 14-16, 1990, 10 p. AD(NASA, Langley Research Center, High-Speed Aerodynamics Div., Hampton, Va.) 10 p. Refs. 8

Four conceptual hypersonic missile configurations were examined experimentally and theoretically. Two of the concepts employed twin module bottom-mounted engines and two were designed for upper surface inlets or engines with the intent of reducing the vehicle observables. The tests were conducted at Mach 6 and Reynolds numbers of 6 to 7.5 x 10 to the 6th per foot. Flow field surveys in the vicinity of the engine inlet were made on all configurations and force and moment tests were conducted on three of the vehicles. Stability and control characteristics of the bottom-mounted engine configurations which incorporated slender, low wings were dominated by strong vortices that promoted severe pitchup tendencies. The shock layer and flow quality in the vicinity of the bottom-mounted engine inlets were dependent on nose shape. The spatula-like upper surface engine concept demonstrated good performance and had uniform flow entering the engine inlet, while the upper surface inlet concept with a highly swept forebody incurred large gradients due to interactions with leading

VOSS, N.
Messerschmidt-Boelkow G.m.b.H., Ottobrunn (West Germany). (MT624400)
740000 In Von Karman Inst. for Fluid Dyn. Missile Aerodyn., Vol. 2 49 p (SEE N79-27211 16-15) 49 p. Jpn. 2375 HC A12/MF A01

Air intake problems, fuels, and performance characteristics of ram-type engines were discussed. A comparison of several kinds of ram-type engines with the conventional rocket propulsion system was presented. The efficiency of ram-type engines for long ranges and high speeds was also demonstrated. R.E.S.

Controlled Terms: AIR INTAKES / MISSILE SYSTEMS / *MISSILES / PROPULSION SYSTEM PERFORMANCE / *RAMJET ENGINES / ROCKET PROPELLANTS / *SUPERSONIC FLIGHT

TYPE 19/4/72
79N27211N NASA ISSUE 18 Category 15
Missile Aerodynamics, volume 2
Von Karman Inst. for Fluid Dynamics, Rhode-Saint-Genese (Belgium). (V9672648)
VKI-LECTURE-SERIES-67-VOL-2 740000 Lecture Ser. held at Rhode-Saint-Genese, Belgium, 22-26 Apr. 1974 273 p. Jpn. 2374 HC A12/MF A01

Lecture notes are presented on the following areas of missile aerodynamics: (1) missile trajectories, (2) aerodynamic interference, (3) missile control, (4) target simulators, and (5) ramjet engines and supersonic flight

Controlled Terms: AERODYNAMIC INTERFERENCE / *AERODYNAMICS / *FLIGHT MECHANICS / MISSILE CONTROL / *MISSILE SYSTEMS / MISSILE TRAJECTORIES / RAMJET ENGINES / SUPERSONIC FLIGHT / TARGET SIMULATORS

TYPE 19/4/73
79N21437M NASA ISSUE 12 Category 39
Structures for hypersonic airbreathing tactical missiles
CAYWOOD, W. C.; RIVELLO, R. M.
Applied Physics Lab., Johns Hopkins Univ., Laurel, Md. (AW080119)
780000 In NASA. Langley Res. Center Recent Advan. in Structures for Hypersonic Flight, Pt. 2 p 577-599 (SEE N79-21435 12-39) Sponsored in part by Navy 22 p. Jpn. 1574 HC A18/MF A01

The studies to date were encouraging and indicated that materials were available or could be developed to satisfy scramjet requirements. Some of the more promising materials for the critical components were indicated. This information is summarized as follows: (1) radome - Slip cast fused silica is the current candidate, but others are being investigated. One shortcoming of slip cast fused silica is its susceptibility to rain damage. (2) inlet leading edges - A refractory metal with a good oxidation protective coating will be required. Tantalum T222 with a Hafnia coating looks promising. (3) inlet ducts - An uninsulated refractory alloy will be required. Columbium F-85 was the best of those considered for the noncircular ducts. (4) external body - The external body temperatures are sufficiently low to permit the use of super alloys. (5) combustor and nozzle - The pyrolytic graphite/silicon carbide coating is very attractive for use in the combustor and nozzle areas. J.A.M.

Controlled Terms: *AIR BREATHING ENGINES / COMBUSTION CHAMBERS / HYPERSONIC FLIGHT / INTAKE SYSTEMS / LEADING EDGES / *MISSILES / PAYLOADS / PROTECTIVE COATINGS / RADOMES / *RAMJET ENGINES / ROCKET NOZZLES / *SUPERSONIC COMBUSTION

TYPE 19/4/74

---

edge shocks. (Author)

Controlled Terms: *AERODYNAMIC CHARACTERISTICS / AIRCRAFT CONTROL / AIRCRAFT STABILITY / FLOW DISTRIBUTION / GRAPHS (CHARTS) / *HYPERSONIC FLIGHT / HYPERSONIC WIND TUNNELS / *MISSILE CONFIGURATIONS / *PROPULSION SYSTEM CONFIGURATIONS / *SUPERSONIC COMBUSTION RAMJET ENGINES / *WIND TUNNEL TESTS

TYPE 19/4/69
80A15245 NASA ISSUE 3 Category 7
Test and analysis of the ASALM-PTV insulated combustion chamber
ROBERTS, W. E.; BOWAN, E. R.; WASSERBERG, S.
ASME PAPER 79-ENAS-21 790700 F33657-76 C-0355 American Society of Mechanical Engineers, Intersociety Conference on Environmental Systems, 9th, San Francisco, Calif., July 16-19, 1979, 6 p. AC(Marquardt Co., Van Nuys, Calif.) 6 p. MEMBERS, $1.50; NONMEMBERS, $3.00

Direct-connect ground test simulations of climb-cruise-dive flight trajectories were made on the Advanced Strategic Air Launched Missile - Propulsion Technology Validation (ASALM-PTV) ramjet engine to check structural durability. Thermal protection of the metal shell was provided by a filled, silicone elastomer (DC93-104) with welded CRES 321 stainless steel metal ribbon and radial vent holes. Excessive temperatures caused initial test failure by eroding the DC93-104 insulation. A thermal model of the DC93-104, incorporating internal insulation heating from combustion gas temperature using a forced connection heat transfer coefficient, temperature nodes with constant heat capacity, internodal heat conduction utilizing an effective conductivity as a function of local insulation temperature, and including shell external aerodynamic heating and backside heating air shroud heat rejection, was concluded to be a satisfactory analytical tool to evaluate a corrective design, after actual test conditions were applied to the model. Dual height ribbon, a change to CRES 310 stainless steel, and elimination of the vent holes showed satisfactory results. J.P.B.

Controlled Terms: AERODYNAMIC HEATING / *COMBUSTION CHAMBERS / ELASTOMERS / *FLIGHT SIMULATION / *GROUND TESTS / HEAT TRANSFER COEFFICIENTS / METAL SHELLS / *MISSILE TRAJECTORIES / *RAMJET ENGINES / SILICON / STAINLESS STEELS / *STRUCTURAL ANALYSIS / TEMPERATURE CONTROL / THERMAL PROTECTION / VENTS

TYPE 19/4/70
80A11188 NASA ISSUE 1 Category 7
Speed control of a missile with an airbreathing ramjet engine
KREUZER, W.; SCHWELLINGER, U.
790000 In: Military Electronics Defence Expo '78; Proceedings of the Conference, Wiesbaden, West Germany, October 3-5, 19/8. (A80-11151 01-04) Geneva, Interavia, S.A., 1979, p. 729-742. AB(Messerschmitt-Boelkow-Blohm GmbH, Ottobrunn, West Germany) 14 p.

A dual structure control system, which comprises small-range and large-range speed control, is proposed for a missile whose thrust is generated by a solid-propellant airbreathing ramjet engine. Speed control is programmed for a digital computer. V.P.

Controlled Terms: BLOCK DIAGRAMS / COMPUTER SYSTEMS DESIGN / DATA PROCESSING / DIGITAL SYSTEMS / *ENGINE CONTROL / MATHEMATICAL MODELS / *MISSILE CONTROL / MISSILE DESIGN / MISSILE TRAJECTORIES / *NUMERICAL CONTROL / PERFORMANCE PREDICTION / *RAMJET ENGINES / *SPEED CONTROL

TYPE 19/4/71
79N27215M NASA ISSUE 18 Category 15
The application of ram-type engines to long-range supersonic missiles

79N17809# NASA ISSUE 9 Category 2
An experimental wind-tunnel investigation of a ram-air-spoiler roll-control device on a forward-control missile at supersonic speeds
BLAIR, A. B., JR.
National Aeronautics and Space Administration. Langley Research Center, Hampton, Va. (ND210491)
NASA-TP-1353; L-12518 781200 191 p. Jpn. 1071 HC A09/MF A01

A parametric experimental wind-tunnel investigation was made at supersonic Mach numbers to provide design data on a ram-air-spoiler roll-control device that is to be used on forward-control cruciform missile configurations. The results indicate that the ram-air-spoiler tail fin is an effective roll-control device and that roll control is generally constant with vehicle attitude and Mach number unless direct canard and/or forebody shock impingement occurs. The addition of the ram-air-spoiler tail fins resulted in only small changes in aerodynamic-center location. For the ram-air-spoiler configuration tested, there are large axial force coefficient effects associated with the increased fin thickness and ram-air momentum loss. Author

Controlled Terms: AERODYNAMIC CHARACTERISTICS / *CANARD CONFIGURATIONS / *CRUCIFORM WINGS / DESIGN ANALYSIS / FINS / JET FLOW / *LATERAL CONTROL / *RAMJET MISSILES / *SPOILERS / *SUPERSONIC SPEEDS / TAIL ASSEMBLIES / *WIND TUNNEL TESTS

TYPE 19/4/75
79A50443 NASA ISSUE 22 Category 9
FIREBRAND anti-ship missile target wind tunnel test program /Phase I/
LEHMAN, L. O.
780000 In: Why flight test; Proceedings of the Ninth Annual Symposium, Arlington, Tex., October 4-6, 1978. (A79-50426 22-01) Lancaster, Calif., Society of Flight Test Engineers, 1978, p. 25-1 to 25-16. AA(U.S. Naval Material Command, Naval Air Development Center, Warminster, Pa.) 16 p.

Wind tunnel testing of the FIREBRAND supersonic anti-ship missile target system at NASA Ames and data which led to the selection of the S6 configuration for this system are presented. The FIREBRAND system includes a boost assisted, ramjet propelled, supersonic aerial target capable of simulating the performance and emission characteristics of future anti-ship cruise missile threats. Its mission profile, speed-altitude envelope, command guidance loop, avionics and payload are discussed. The wind tunnel tests were conducted to select the aerodynamic design among the candidate configurations S4, S5, and S6 for defining the aerodynamic stability and control characteristics of the selected configuration, and for conducting trade-off studies toward the optimization of the configuration. It was concluded that the S6 aerodynamic model was selected because of its stability characteristics, and the S4 and S5 configurations were eliminated because of poor roll control at subsonic and supersonic speeds. A.T.

Controlled Terms: *AERODYNAMIC CONFIGURATIONS / CONFIGURATION MANAGEMENT / *CONTROL STABILITY / FLIGHT CHARACTERISTICS / GRAPHS (CHARTS) / *MISSILE CONTROL / *MISSILE DESIGN / MISSILE SYSTEMS / RAMJET ENGINES / *RAMJET MISSILES / WIND TUNNEL TESTS

TYPE 19/4/76
79A49222 NASA ISSUE 22 Category 20
Ramjet renaissance imminent -- ramjet engine technology assessment
BULLOCH, C.
790900 Iteravia, vol. 34, Sept. 1979, p. 854-856. 3 p.

Current programs for development of ramjet propulsion missiles are described and similar programs underway in Europe, including the Anglo-Franco-German project for an advanced anti-surface-ship missile, are

discussed. Operation principles such as design calculations for long-range missions and the necessary fuel or propellants for these missions are examined. The practical speed range of ramjet powered vehicles was found to lie between 1.5 and 5 M with maximum flying altitudes of 120,000 ft. Various propulsion systems employing both liquid and solid fuel are presented, emphasizing the problem of maintaining complete and stable combustion. C.F.W.

Controlled Terms: AIR TO AIR MISSILES / GRAPHS (CHARTS) / MISSILE COMPONENTS / *MISSILE DESIGN / *PERFORMANCE PREDICTION / *RAMJET ENGINES / *RAMJET MISSILES / ROCKET ENGINES / *ROCKET PROPELLANTS / SURFACE TO AIR MISSILES / TECHNOLOGY ASSESSMENT / *TECHNOLOGY UTILIZATION

TYPE 19/4/77
79A47963 NASA ISSUE 21 Category 13
Trajectory optimization of a ramjet-powered missile using singular perturbation methods
SRIDHAR, B.
790000 In: 1978 Conference on Decision and Control, 17th, San Diego, Calif., January 10-12, 1979, Proceedings. (A79-47930 21-63) New York, Institute of Electrical and Electronics Engineers, Inc., 1979, p. 387-389. AA(Systems Control, Inc., Palo Alto, Calif.) 3 p.

A nonlinear optimal control law is derived for a ramjet powered missile using singular perturbation theory. The singular perturbation analysis, together with multiple time scaling converts the solution of the two point boundary value problem into the extremization of nonlinear algebraic equations. The derivation of the control law takes into account the various operational constraints and an algorithm is outlined describing the various steps in the computation of the control law. The control law has a feedback form and is a good candidate for real-time implementation. (Author)

Controlled Terms: ALGORITHMS / BOUNDARY VALUE PROBLEMS / ENGINE CONTROL / FEEDBACK CONTROL / *MISSILE CONTROL / *MISSILE TRAJECTORIES / NONLINEAR EQUATIONS / *OPTIMAL CONTROL / *PERTURBATION THEORY / *RAMJET MISSILES / REAL TIME OPERATION / *TRAJECTORY OPTIMIZATION

TYPE 19/4/78
79A39049 NASA ISSUE 16 Category 7
Air breathing missile fuel control - A unique solution
CRAVEN, D.
AIAA PAPER 79-1354 790600 AIAA, SAE, and ASME, Joint Propulsion Conference, 15th, Las Vegas, Nev., June 18-20, 1979, AIAA 8 p. AA(Lucas Aerospace, Ltd., Wolverhampton, Staffs., England) 8 p. Jpn. 2935

The paper reports on an electronic fuel control unit being developed for air breathing missile fuel control applications. The electronic fuel control system combines the well-proven features of hydromechanical controls with the flexibility and performance advantages of electronic control. The hydromechanical features discussed include stoichiometric flow schedule to the primary burners at all conditions combined with electronically controlled modulation of main burner flow. The electronic features include reversion to a preferred fuel/air ratio in case of electronic failure. S.D.

Controlled Terms: *AIR BREATHING ENGINES / COMBUSTION CHAMBERS / ELECTRONIC CONTROL / *FUEL CONTROL / FUEL SYSTEMS / FUEL-AIR RATIO / GRAPHS (CHARTS) / HYDROMECHANICS / *MISSILES / *RAMJET ENGINES / STOICHIOMETRY

TYPE 19/4/79
79A38998 NASA ISSUE 16 Category 2

ASALM-PTV chin inlet technology overview -- Advanced Strategic Air Launched Missile Propulsion Technology Validation of integral rocket/ramjet
WEBSTER, F. F.; BUCY, J. A.
AIAA PAPER 79-1240 790600 AIAA, SAE, and ASME, Joint Propulsion Conference. 15th, Las Vegas, Nev., June 18-20, 1979, AIAA 12 p. A8(Martin Marietta Aerospace, Orlando, Fla.) Jpn. 2926

The ASALM Propulsion Technology Validation (PTV) vehicle is intended to demonstrate the flight feasibility of the integral rocket/ramjet propulsion system. This paper addresses the PTV chin inlet, its design and performance evolution, and its relationship to other missile systems. The three-dimensional nature of the chin inlet and its resulting effects on such parameters as subcritical stability and pressure distortions are addressed. The phenomenon of inlet resonance that occurs during boost due to a blocked inlet duct is treated. Performance results from full scale freejet testing are compared with subscale wind tunnel testing. Finally, the interactions with the ramburner, fuel management system (FMS), and overall vehicle are assessed. (Author)

Controlled Terms: AERODYNAMIC CONFIGURATIONS / BOOSTER ROCKET ENGINES / DIFFUSERS / *ENGINE INLETS / *ENGINE TESTS / FULL SCALE TESTS / GRAPHS (CHARTS) / *INLET FLOW / *RAMJET ENGINES / *RAMJET MISSILES / SOLID PROPELLANT ROCKET ENGINES / *SUPERSONIC INLETS

TYPE 19/4/80
79A29420 NASA ISSUE 11 Category 20
The integral-rocket, dual-combustion ramjet - A new propulsion concept
BILLIG, F. S.; WALTRUP, P. J.; STOCKBRIDGE, R. D.
AIAA 79-7044 790000 N00024-78-C-5384 In: International Symposium on Air Breathing Engines, 4th, Orlando, Fla., April 1-6, 1979, Proceedings. (A79-29376 11-07) New York, American Institute of Aeronautics and Astronautics, Inc., 1979, p. 433-444. AC(Johns Hopkins University, Laurel, Md.) 12 p. Refs. 15 Jpn. 1963

A new propulsion concept, the integral-rocket, dual-combustion ramjet (IRDCR), for hypersonic, volume-limited missiles is described. In essence, a 'dump-type'-subsonic-combustion ramjet is embedded within the main supersonic-combustion ramjet (scramjet) system to act as a fuel-rich, hot-gas generator for the latter and thus permit use of a hydrocarbon fuel rather than highly reactive borane based fuel. By packaging rocket-boost-phase propellant in the scramjet combustor, the volumetric efficiency of the propulsion system is improved. The new propulsion system required to design the IRDCR engine cycle and evaluate its performance are developed and discussed in the framework of exemplary calculations for a particular family of inlet designs and for flight at Mach numbers 4 through 7 at a constant flight dynamic pressure of 5000 lbf/sq ft. (Author)

Controlled Terms: COMBUSTION CHAMBERS / DYNAMIC PRESSURE / ENGINE INLETS / GAS GENERATORS / HYDROCARBON FUELS / *HYPERSONIC FLIGHT / *MISSILE DESIGN / *PROPULSION SYSTEM PERFORMANCE / PROPULSIVE EFFICIENCY / *RAMJET MISSILES / *ROCKET ENGINE DESIGN / *SUPERSONIC COMBUSTION

TYPE 19/4/81
79A29412 NASA ISSUE 11 Category 20
The single throat ramjet and its application to cruising and accelerating systems -- cruise missile ramjet engine performance
ANGELUCCI, S. B.; ROFFE, G.; BARONTI, P. O.
AIAA 79-7043 790000 In: International Symposium on Air Breathing Engines, 4th, Orlando, Fla., April 1-6, 1979, Proceedings. (A79-29376 11-07) New York, American Institute of Aeronautics and Astronautics, Inc., 1979, p. 337-346. AA(Snia Viscosa, Rome, Italy) AC(General Applied Science Laboratories, Inc., Westbury, N.Y.) 10 p. Jpn. 1963

The single throat ramjet, characterized by a single converging-diverging chamber, employs the heat released by combustion to produce thermal choking at some intermediate station within the expanding part of the channel. Subsequent expansion of the exhaust gases produces supersonic exit velocities. By changing the fuel/air mixing rates, the physical location of the section where thermal choking occurs, and which is equivalent to the second throat of a conventional ramjet, can be varied, thereby changing the 'throat' area of the exhaust nozzle. The paper describes the operational features of the engine and presents a method of analysis to evaluate engine performance. P.T.H.

Controlled Terms: ACCELERATION (PHYSICS) / *CRUISE MISSILES / ENGINE INLETS / *ENGINE TESTS /FLIGHT TESTS / FUEL COMBUSTION / GRAPHS (CHARTS) / MACH NUMBER / *PERFORMANCE TESTS / *RAMJET ENGINES / SPECIFIC IMPULSE

TYPE 19/4/82
79A29408 NASA ISSUE 11 Category 20
Studies and tests of rocket ramjets for missile propulsion
MARGUET, R.; CAZIN, P.; ECARY, C.
ONERA, TP NO. 1979-26, AIAA 79-7037 790000 In: International Symposium on Air Breathing Engines, 4th, Orlando, Fla., April 1-6, 1979, Proceedings. (A79-29376 11-07) New York, American Institute of Aeronautics and Astronautics, Inc., 1979, p. 297-306. A8(ONERA, Chatillon-sous-Bagneux, Hauts-de-Seine, France) AC(ONERA, Chatillon-sous-Bagneux, Hauts-de-Seine) Ministere de la Defence, Paris, France) 10 p. Jpn. 1962

The use of a ramjet burning a gas produced by pyrolysis of a dense solid fuel is the central concept for a compact propulsive system called the rocket ramjet with integrated booster. The paper discusses some rocket ramjet configurations in relation to different missions. The characteristics of self-pyrolyzing fuels are reviewed, and work on a nonguided test ramjet rocket without integrated booster is reported. Inflight characteristics such as thrust, specific impulse, pressure in combustion chamber and gas generator, air intake pressure recovery, and vibration levels for two test flights are given. P.T.H.

Controlled Terms: AERODYNAMIC CONFIGURATIONS / AIR INTAKES / BOOSTER ROCKET ENGINES / COMBUSTION CHAMBERS / *ENGINE TESTS / FLIGHT TESTS / FRANCE / *MISSILE CONFIGURATIONS / *PROPULSION SYSTEM PERFORMANCE / PYROLYSIS / *RAMJET MISSILES / SOLID PROPELLANT ROCKET ENGINES / SPECIFIC IMPULSE

TYPE 19/4/83
79A29407 NASA ISSUE 11 Category 20
A low cost rocket ramjet for air-to-ground missile applications
HALL, P. H.
AIAA 79-7036 790000 In: International Symposium on Air Breathing Engines, 4th, Orlando, Fla., April 1-6, 1979, Proceedings. (A79-29376 11-07) New York, American Institute of Aeronautics and Astronautics, Inc., 1979, p. 291-296. AA(U.S. Naval Weapons Center, China Lake, Calif.) 6 p. Jpn. 1962

The paper describes a low-cost rocket ramjet propulsion system suitable for air-to-ground missile applications. The low-cost approach is based on parallel packaging of the rocket and ramjet which eliminates the complexity of rocket to ramjet transition experienced by integral rocket ramjets. A low cost air induction system utilizing axisymmetric inlets and a fuel management system based on an open loop fuel controller and gas generator expulsion system are also described. Advantages and disadvantages of the low cost approach are discussed. Some technical highlights from the development program are presented. These include the demonstration of a low cost alternative to freejet testing as well as the

role of combustion induced pressure oscillations in the determination of real supercritical inlet margin. Data are presented which show that oscillation effects can be significant. (Author)

Controlled Terms: *AIR TO SURFACE MISSILES / COMBUSTION CHAMBERS / EXPULSION / FUEL CONTROL / FUEL SYSTEMS / FULL SCALE TESTS / GAS GENERATORS / INTAKE SYSTEMS / *LOW COST / PACKAGING / PRESSURE OSCILLATIONS / *PROPULSION SYSTEM PERFORMANCE / *RAMJET ENGINES / *RAMJET MISSILES

TYPE 19/4/84

79A24103 NASA ISSUE 8 Category 37
Hot isostatic pressing structural materials for ramjet applications
BANTA, F. L.
780000 In: Materials synergisms; Proceedings of the Tenth National Technical Conference, Kiamesha Lake, N.Y., October 17-19, 1978. (A79-24076 08-31) Azusa, Calif., Society for the Advancement of Material and Process Engineering, 1978, p. 330-339. AA(United Technologies Corp., Chemical Systems Div., Sunnyvale, Calif.) 9 p. Jpn. 1414

Complex ramjet inlet turn and dump configurations were cast by the investment process from 17-4 pH stainless steel and treated by a secondary operation (hot isostatic pressing) to enhance mechanical and fracture toughness properties. The effects of this treatment were evaluated by microstructural examination, tensile tests, and fracture toughness properties determinations in benign (KIc) and hostile (KIscc) environments. Mechanical properties tests were made on weldments produced by the gas tungsten arc process, which was used to assemble these castings into a ramjet combustion chamber. (Author)

Controlled Terms: COMBUSTION CHAMBERS / ENGINE INLETS / *ENGINE PARTS / FRACTURE STRENGTH / *HOT PRESSING / *ISOSTATIC PRESSURE / *MECHANICAL PROPERTIES / *RAMJET ENGINES / RAMJET MISSILES / SOLID PROPELLANT ROCKET ENGINES / STRESS CONCENTRATION / STRESS CORROSION CRACKING

TYPE 19/4/85

79A12561 NASA ISSUE 2 Category 18
An approach to solving controls compartment heating problems on air-launched missiles
GONZALEZ, J. I.
ASME PAPER 78-ENAS-12 780700 American Society of Mechanical Engineers, Intersociety Conference on Environmental Systems, San Diego, Calif., July 10-13, 1978. 7 p. AA(Martin Marietta Aerospace, Orlando, Fla.) 7 p. Jpn. 192 MEMBERS, $1.50; NONMEMBERS, $3.00

The Advanced Strategic Air Launched Missile (ASALM) Control Actuator System (CAS) is tightly packaged around the ramjet nozzle and is subject to high heat loads from several sources. This combination of diverse heat loads and complicated geometry requires detailed analytical models to accurately predict the structural thermal response. In view of the uncertainties involved in these predictions, a test program was conducted. Results indicate that the major heat paths to the uninsulated actuator are from the air vane pad (60 percent) and the nozzle (25 percent). The most effective way to protect the actuator is to insulate it from the nozzle and from the pad. The effects of contact resistances across interfaces are discussed. (Author)

Controlled Terms: *ACTUATORS / *AIR LAUNCHING / COMPARTMENTS / *MISSILE CONTROL / *MISSILE TESTS / NOZZLE EFFICIENCY / RAMJET MISSILES / *TEMPERATURE CONTROL / THERMAL PROTECTION

TYPE 19/4/86

78N32168M NASA ISSUE 23 Category 15

Hypersonic airbreathing missile
Patent Application
HUNT, J. L.; LAUING, P. L.; MARCUM, D. C., JR.
National Aeronautics and Space Administration. Langley Research Center, Hampton, Va. (ND210491)
NASA-CASE-LAR-12264-1; US-PATENT-APPL-SN-943087 /C0918 21 p. Jpn. 3048
HC A02/MF A01

A hypersonic airbreathing missile using dual mode scramjet engines for propulsion is described. The fuselage is constructed of a material with a high heat sink capacity and is covered with a thermal protective shield and lined with an internal insulating blanket. The engine airframe integration uses the flat lower portion of the lower fuselage to precompress the air entering the scramjet engines. The precompression of air entering the scramjet inlets increases as the angles of attack. This feature results in a highly maneuverable missile which can accelerate as it banks into a turn. NASA

Controlled Terms: AIRFRAMES / ANGLE OF ATTACK / *HEAT SINKS / *HYPERSONIC FLIGHT / HYPERSONIC SPEED / *MISSILES / PATENT APPLICATIONS / *RAMJET ENGINES / SHIELDING / *SUPERSONIC COMBUSTION / *SUPERSONIC INLETS / THERMAL PROTECTION

TYPE 19/4/87

78N31153M NASA ISSUE 22 Category 15
The use of ram rockets for high altitude missiles
RIESTER, E.
Deutsche Forschungs- und Versuchsanstalt fuer Luft- und Raumfahrt, Brunswick (West Germany). (DD696666)
DLR-FB-77-47 77111B Abt. Flugkoerperantrieb. In GERMAN; ENGLISH summary Report will also be announced as translation (ESA-TT-505) 60 p. Jpn. 2905
HC A04/MF A01; DFVLR, Cologne DM 29,60

The applicability of ram rockets for the propulsion of high altitude missiles was investigated. As a power plant for the cruising phase of high altitude supersonic missiles, rockets and ram rockets are competing with each other. The conditions are shown, under which the ram rocket is superior. The influence of mission and power plant parameters on the payload of both kinds of power plants is investigated. The advantage of the combination booster - ram rocket over a two stage rocket under altitude conditions is pointed out. The advantage may increase, if the booster acceleration is finished before reaching the cruise velocity, and the ram rocket is continuing the acceleration. At a definite booster and velocity the payload becomes a maximum. The control regimes of the ram rocket combustion chamber, being necessary to maintain the maximum conditions, are shown. Author (ESA)

Controlled Terms: ACCELERATION (PHYSICS) / BOOSTER ROCKET ENGINES / CRUISING FLIGHT / GAS GENERATORS / *HIGH .. .DE / *MISSILES / *RAMJET ENGINES / *SUPERSONIC FLIGHT

TYPE 19/4/88

78A49462 NASA ISSUE 21 Category 37
Status of an ultra-low-cost turbojet engine
BAERST, C. F.; HUGHES, N. M.
AIAA PAPER 78-965 780700 American Institute of Aeronautics and Astronautics and Society of Automotive Engineers, Joint Propulsion Conference, 14th, Las Vegas, Nev., July 25-27, 1978, AIAA 10 p. AB(AiResearch Manufacturing Company of Arizona, Phoenix, Ariz.) 10 p. Refs. 7 Jpn. 3316

This application of turbojet engines to tactical missiles and expendable drones has placed significant importance on reducing engine acquisition cost. This paper reviews such an effort - a series of research and

development programs wherein a high-production-rate truck engine turbocharger was the basis for the design of a low-cost, expendable turbojet. An integral part of this effort was the adaptation of a low-cost thrust augmentor based on ramjet, sudden-expansion burner technology. Specifically, the design, performance predictions, and test program results are presented. (Author)

Controlled Terms: DRONE AIRCRAFT / *LOW COST / MISSILE STRUCTURES / *PERFORMANCE PREDICTION / RAMJET ENGINES / *RESEARCH AND DEVELOPMENT / STRUCTURAL DESIGN / TECHNOLOGY UTILIZATION / *THRUST AUGMENTATION / *TURBOJET ENGINES

TYPE 19/4/89
78A48456 NASA ISSUE 21 Category 7
Center-loaded duct integral rocket-to-ramjet transition testing
READEY, H. J., JR.; COBB, E. R.
AIAA PAPER 78-937 780700 American Institute of Aeronautics and Astronautics and Society of Automotive Engineers, Joint Propulsion Conference, 14th, Las Vegas, Nev., July 25-27, 1978, AIAA 9 p. AB(Martin Marietta Aerospace, Orlando, Fla.) 9 p. Jpn. 3757

This paper describes the facility test equipment and techniques that have been developed for efficient integral rocket-to-ramjet transition testing. The facility and test procedures were successfully demonstrated with the use of representative advanced cruise missile test hardware and test conditions to establish the feasibility of the high-performance center-loaded duct propulsion concept. This concept requires that the ramjet flameholder and fuel injectors be stationed between two solid propellant rocket grains. The transition test method was elected because it produces the true thermal/time history for both the test hardware and the environment. The test series included component checkout tests, ramburner firings to establish baseline performance, simulated transition tests to verify facility operation, and full rocket-to-ramjet transition firing for design verification. (Author)

Controlled Terms: *AIR DUCTS / *CRUISE MISSILES / *ENGINE TESTS / FLAME HOLDERS / FUEL INJECTION / MEASURING INSTRUMENTS / *MISSILE DESIGN / *RAMJET ENGINES / *ROCKET ENGINES / SCALE MODELS / TEST FACILITIES

TYPE 19/4/90
78A43604 NASA ISSUE 19 Category 7
Coaxial dump combustor investigations --- ramjet engine design with booster rocket
CRAIG, R. R.; DREWRY, J. E.; STULL, F. D.
AIAA PAPER 78-1107 780700 American Institute of Aeronautics and Astronautics and Society of Automotive Engineers, Joint Propulsion Conference, 14th, Las Vegas, Nev., July 25-27, 1978, AIAA 12 p. AC(USAF, Aero Propulsion Laboratory, Wright-Patterson AFB, Ohio) 12 p. Refs. 5 Jpn. 3416

An experimental investigation was conducted involving coaxial dump combustors with two different types of flamcholders (annular and V) installed at the dump station in an attempt to correlate combustor performance with previous non-reacting flowfield results. Flam-holder blockage, combustor length, exit area ratio, inlet temperature, and chamber pressure were varied for both wall injection and premixed fuel conditions. Lean blowout limits, combustion efficiency, combustor total pressure drop, and wall static pressure distributions were obtained from these runs using JP-4 fuel. In addition, a limited amount of surface heating patterns and combustion oscillation data were obtained. (Author)

Controlled Terms: *COMBUSTION CHAMBERS / COMBUSTION VIBRATION / FLAME HOLDERS / FUEL INJECTION / *MISSILE DESIGN / *RAMJET MISSILES / *ROCKET ENGINE DESIGN

TYPE 19/4/91
78A43506 NASA ISSUE 19 Category 7
Ramjet ground and flight test performance correlations
DOHERTY, J. F.
AIAA PAPER 78-936 780700 N00019 68 (0605, American Institute of Aeronautics and Astronautics and Society of Automotive Engineers, Joint Propulsion Conference, 14th, Las Vegas, Nev., July 25-27, 1978, AIAA 6 p. AA(Vought Corp., Dallas, Tex.) 6 p. Jpn. 3414

The paper deals with the development and testing of the Navy's Air-Launched Low-Volume Ramjet (ALVRJ) missile. Ground tests were conducted on propulsion system components and subsystems, and integrated vehicle freejet tests were carried out in which functional verification and flight readiness were proven. The culmination of the program was the flight testing of five vehicles to demonstrate satisfactory achievement of the following objectives: capability of the system to be air-launched at altitudes from sea level to 10,670 m; launch from Mach-0.7 and higher speed aircraft; rocket motor ignition and operation; rocket to ramjet transition; ramjet operation at above Mach 2 at sea level and higher Mach numbers at 10,670 m; and angle-of-attack capability consistent with a tactical air-to-surface weapon system. V.P.

Controlled Terms: AIR LAUNCHING / COMPUTER PROGRAMS / *FLIGHT TESTS / *GROUND TESTS / *LOW COST / MATHEMATICAL MODELS / *MISSILE TESTS / *PERFORMANCE PREDICTION / *PROPULSION SYSTEM PERFORMANCE / *RAMJET MISSILES / SUPERSONIC SPEEDS

TYPE 19/4/92
78A35978 NASA ISSUE 14 Category 5
Full scale correlation of an effective thermal model for air launched supersonic missile applications.
GONZALEZ, J. I.; ELIAS, J. M.
AIAA PAPER 72-842 780500 American Institute of Aeronautics and Astronautics and American Society of Mechanical Engineers, Thermophysics and Heat Transfer Conference, 2nd, Palo Alto, Calif., May 24-26, 1978, AIAA 6 p. AB(Martin Marietta Aerospace, Orlando, Fla.) 6 p.

The analytical correlations used are based on extensive data obtained in connection with a full scale missile integration test. The test article consisted of a fuel tank/inlet, an interstage compartment, a flight weight ramjet combustor, and an aft compartment. A significant number of geometrical and mass simulated components were included in the various compartments. The integration test simulated the flight of an operating missile through a trajectory which included a low level accelerat on stage with a climbout to high altitude and a high velocity cruise. Attention is given to fuel tank and insulation backside temperature distributions, predicted versus measured data, and the variation in the overall heat transfer coefficient as a function of thickness. The investigation shows that the transient performance of an insulation system for a fuel tank, bladder, and fuel subsystem of an air launched ramjet missile can be analytically described for design purposes with a two-dimensional model that includes convection and radiation between insulation and bladder. G.R.

Controlled Terms: *AERODYNAMIC HEATING / *AIR LAUNCHING / COMPUTERIZED SIMULATION / CORRELATION / *FUEL TANKS / FULL SCALE TESTS / HEAT TRANSFER COEFFICIENTS / MATHEMATICAL MODELS / *RAMJET MISSILES / *SUPERSONIC FLIGHT / TEMPERATURE DISTRIBUTION / *THERMAL INSULATION

TYPE 19/4/93
78A25128 NASA ISSUE 9 Category 20
Propulsion systems for missiles --- using air breathing engines

Flugkoerper-Antriebe
MACH, U.
780200 VDI-Z, vol. 120, no. 3, Feb. 1978, p. 121-124. In German.
AA(Messerschmitt-Boelkow-Blohm GmbH, Ottobrunn, West Germany) 4 p. Refs.
34 Jpn. 1323

Systems for the propulsion of military missiles utilize to a very large degree rocket motors. The rocket motors employed are generally based on a use of solid propellant. Missiles for tactical applications are currently mainly propelled by two-stage solid-propellant rockets. The first stage is used for acceleration, while the second stage provides thrust during the cruise. Disadvantages of this type of propulsion system are related to a rapid decrease in missile speed after the propellant has been consumed. Better possibilities with regard to range and maneuverability are provided by air-breathing propulsion systems. New developments related to cruise missiles and missiles for naval warfare applications are, therefore, equipped with gas turbines and ramjet engines. Attention is given to specific developments concerning gas turbines, ramjet engines, a hypergolic liquid propellant system for air-to-air missiles, solid-propellant rockets, and hybrid rockets in which a solid fuel is employed with liquid nitric acid as oxidizer. G.R.

Controlled Terms: *AIR BREATHING ENGINES / AIR TO AIR MISSILES / CRUISE MISSILES / GAS TURBINE ENGINES / HYBRID PROPELLANTS / HYPERGOLIC ROCKET PROPELLANTS / MANEUVERABILITY / *MISSILES / *PROPULSION SYSTEM CONFIGURATIONS / PROPULSIVE EFFICIENCY / RAMJET ENGINES / *ROCKET ENGINES / SOLID ROCKET PROPELLANTS

TYPE 19/4/94

78A20628 NASA ISSUE 7 Category 5
Conceptual study of hypersonic airbreathing missiles
HUNT, J. L.; LAWING, P. L.; MARCUM, D. C.; CUBBAGE, J. M.
National Aeronautics and Space Administration. Langley Research Center, Langley Station, Va. (ND210491)
AIAA PAPER 78-6 780100 American Institute of Aeronautics and Astronautics. Aerospace Sciences Meeting, 16th, Huntsville, Ala., Jan. 16-18, 1978, 15 p. AD(NASA, Langley Research Center, High-Speed Aerodynamics Div., Hampton, Va.) 15 p. Refs. 22 Jpn. 1118

The purpose of this paper is to report recent results of an in-house conceptual study to evaluate the performance potential and research needs of airbreathing hypersonic missiles. An alkylated-borane (noncryogenic) fueled, dual-mode, ramjet/scramjet propulsion system structured with a Rene 41 inlet and a carbon-carbon combustor was assumed along with a Lockalloy heat sink fuselage structure and beryllium wings and control surfaces. Performance for an air-launched baseline missile with a 961 pound staging weight containing a 100 pound payload indicated excellent long range cruise. A sizing study indicates that Mach 6 cruise ranges of the order of 2500 nautical miles for payloads of 300 pounds can be achieved with moderate size missile carry weights (9000 lbs.). Aerodynamic heating analyses indicate that unprotected heat-sink structures with internal insulation are feasible for ranges of several hundred miles. For ranges of several thousands of miles a multiwall radiation shield (Inconel/titanium) was selected for protection of the internally insulated heat sink structure. (Author)

Controlled Terms: DUAL THRUST NOZZLES / HEAT RESISTANT ALLOYS / HEAT SINKS / *HYPERSONIC VEHICLES / INCONEL (TRADEMARK) / MANEUVERABILITY / MISSILE STRUCTURES / MISSILE TRAJECTORIES / PAYLOADS / *PROPULSION SYSTEM PERFORMANCE / RADIATION SHIELDING / *RAMJET MISSILES / *SUPERSONIC COMBUSTION RAMJET ENGINES / TITANIUM

TYPE 19/4/95

78A18918 NASA ISSUE 6 Category 7
Optimization of ramjet cruise performance
Ottimizzazione delle prestazioni in crociera di un autoreattore
GALASSO, A.
770600 L'Aerotecnica - Missili e Spazio, vol. 56, June 1977, p. 41-69.
In Italian. AA(Aeritalia S.p.A., Naples, Italy) 9 p. Refs. 16

An optimal design (i.e., one involving minimum fuel consumption) is formulated for a ramjet missile with a cruise speed of Mach 3. The low cost, high thrust-to-weight ratio and simplicity of design of the ramjet engine motivate this investigation of its use as a missile propulsion system. In studying the ramjet missile performance, attention is given to the thermodynamic properties of the combustion products, the nozzle geometry, pressure losses due to the flameholder, and pressure recovery in the combustion chamber. In addition, the thrust coefficient and the specific impulse of the proposed ramjet engine are analyzed quantitatively as a function of the nozzle throat geometry. J.M.B.

Controlled Terms: CRUISE MISSILES / *ENGINE DESIGN / *FUEL CONSUMPTION / NOZZLE GEOMETRY / OPTIMIZATION / *PROPULSION SYSTEM PERFORMANCE / *RAMJET ENGINES / *ROCKET ENGINES / THERMODYNAMIC PROPERTIES

TYPE 19/4/96

77N30156W NASA ISSUE 21 Category 15
A Kalman filter application to the advanced tactical inertial guidance system of the air-launched low volume ramjet cruise missile
M.S. Thesis
VANDEVENDER, J. A.
Naval Postgraduate School, Monterey, Calif. (NS368219)
AD-A039338 761200 94 p. Jpn. 2763 HC A05/MF A01

A Montecarlo simulation is conducted to ascertain performance of the ATIGS system which is a proposed air-launched cruise missile configuration. The simulation is conducted within a local-level inertial frame consisting of down-range, cross-range, and up as primary reference vectors. Efforts are made to measure the relative effects associated with the intended pure position reset provided by a MICRAD sensor as compared with those effects which could be expected from a linear suboptimal Kalman filtering scheme used in conjunction with the MICRAD sensor. Author (GRA)

Controlled Terms: *AIR TO AIR MISSILES / CRUISE MISSILES / *KALMAN FILTERS / MATHEMATICAL MODELS / *MISSILE CONTROL / MONTE CARLO METHOD / *RAMJET MISSILES / SIMULATION / *STRAPDOWN INERTIAL GUIDANCE

TYPE 19/4/97

77N13147M NASA ISSUE 4 Category 20
Considerations for hybrid gas generators for a ramjet-rocket --- metal propellant performance
WEILER, M.
European Space Agency, Paris (France). (E6854803)
ESA-TT-251; DLR-MITT-74-37 760200 Transl. into ENGLISH of "Ueberlegungen zu lithergolen Gasgeneratoren fuer eine Staustrahlrakete", DFVLR, Lampoldshausen, West Ger. Report DLR-Mitt-74-37, 9 Oct. 1974 Original German report available from DFVLR, Porz, West Ger. DM 12.60 25 p. Jpn.
438 HC A02/MF A01

The performance of ramjet rockets using metallized fuels was investigated. The specific impulse of pure metals and metal-containing hybrid gas generators in airbreathing propulsion was calculated and plotted for equilibrium thermochemical conditions. The factors affecting the metal combustion are discussed for several metals and oxidizers. Nonequilibrium calculations were made for temperature and exhaust gas composition in the primary chamber in order to evaluate the conditions for metal ignition. Author (ESA)

Controlled Terms: EXHAUST GASES / *GAS GENERATORS / METAL COMBUSTION /
*METAL PROPELLANTS / *PROPULSION SYSTEM PERFORMANCE / *RAMJET ENGINES /
*RAMJET MISSILES / *ROCKET ENGINES / SPECIFIC IMPULSE / THROTTLING

TYPE 19/4/98
77A42264 NASA ISSUE 20 Category 17
Real-time trajectory control using augmented energy management
GLAROS, L. N.; CRIGLER, S. N.
AIAA 77-1052 770000 In: Guidance and Control Conference, Hollywood,
Fla., August 8-10, 1977, Technical Papers. (A77-42751 20-35) New York,
American Institute of Aeronautics and Astronautics, Inc., 1977, p.
101-108. A8(Martin Marietta Aerospace, Orlando, Fla.) 8 p. Refs. 8 Jpn.
3372

A real-time near-optimal trajectory controller has been formulated and
optimized for implementation onboard an advanced integral rocket ramjet
missile. This controller, called Augmented Energy Management (AEM), is
based in form on a feedback control law which results from the application
of extended energy management (EEM). The AEM controller is developed by
modifying the EEM law to include an approximation to the optimal altitude
profile, and a density correction filter and energy rate feedback to
account for vehicle performance. Numerical examples demonstrate that AEM
results in range benefits over a suboptimal controller. Further examples
show that when off-nominal conditions are present, AEM is less range
sensitive, assuring greater targetable range. (Author)

Controlled Terms: ALTITUDE CONTROL / ENERGY REQUIREMENTS / *FEEDBACK
CONTROL / FLIGHT CONTROL / FLIGHT PATHS / MANAGEMENT METHODS / *MISSILE
CONTROL / *OPTIMAL CONTROL / *RAMJET MISSILES / *REAL TIME OPERATION /
*TRAJECTORY CONTROL

TYPE 19/4/99
77A38594 NASA ISSUE 17 Category 9
The ramburner - A versatile and economical facility base for thermal and
propulsion experimental work
READEY, H. J., JR.
AIAA PAPER 77-915 770700 American Institute of Aeronautics and
Astronautics and Society of Automotive Engineers, Propulsion Conference,
13th, Orlando, Fla., July 11-13, 1977, AIAA 10 p. AA(Martin Marietta
Aerospace, Orlando, Fla.) 10 p. Jpn. 2828

The ramburner is an airbreathing test facility that uses two combustors
connected in series to generate a wide range of thermal conditions. This
paper describes the development, functional description, performance
ranges, operational modes and operating methods for this thermal test
facility. Significant and sophisticated experiments requiring severe
thermal environments, and ramjet motor simulations requiring some
innovative techniques are described. Techniques discussed are those for
integral rocket-to-ramjet transition experiments, duplication of heating
rate histories of external aerodynamic heating and internal combustor
heating for an ASALM trajectory, and free jet testing of gas cooled nose
tips. Control and data measurement systems are also discussed. (Author)

Controlled Terms: AERODYNAMIC HEATING / *AIR BREATHING ENGINES /
AUTOMATIC TEST EQUIPMENT / COMBUSTION CHAMBERS / *COST EFFECTIVENESS /
DATA ACQUISITION / *ENGINE TESTS / *FREE JETS / *MISSILE TESTS / RAMJET
ENGINES / *TEST FACILITIES

TYPE 19/4/100
77A27031 NASA ISSUE 11 Category 20
Advanced propulsion systems for missiles
GEODES, J. P.

770300 Interavia, vol. 32, Mar. 1977, p. 250-252. 3 p. Jpn. 1786

In connection with studies concerning the most suitable approaches for
the propulsion of high altitude stand-off range tactical missiles,
propulsion systems are considered for which ramjet technology is combined
with liquid and solid rocket technology. A description is presented of the
hybrid rocket for the High Altitude Supersonic Target (HAST) program. The
integral Rocket Ramjet represents the most promising propulsion concept
for future high performance missiles with extended range. A summary is
provided concerning the advantages of ramjet propulsion in a new
long-range tactical missile to be carried by a U.S. Navy air superiority
fighter. G. R.

Controlled Terms: AIR LAUNCHING / F-14 AIRCRAFT / *HIGH ALTITUDE /
*HYBRID ROCKET ENGINES / *MISSILE DESIGN / MISSILE RANGES / *PROPULSION
SYSTEM PERFORMANCE / *RAMJET MISSILES / ROCKET VEHICLES / SUPERSONIC
FLIGHT / TARGET ACQUISITION

TYPE 19/4/101
77A22709 NASA ISSUE 8 Category 63
Optimal switching criteria for two-position configuration controls
GLAROS, L. N., JR.
770200 Journal of Spacecraft and Rockets, vol. 14, Feb. 1977, p. 124,
125. AA(Martin Marietta Aerospace, Orlando, Fla.) 2 p.

Optimal switching criteria for two-position configuration controls in
aerospace vehicles are developed. Performance criteria to be optimized
include: minimum time-to-climb, minimum fuel-to-climb, and maximum range
with a fixed fuel weight. The controls can be applied to afterburners
(on/off), folded wings (deployed/folded), and two-position
variable-geometry nozzles. The switching criteria depend solely on the
point performance capabilities of the vehicle and are totally independent
of boundary conditions. An example is analyzed for maximum range of a
ramjet missile featuring variable-geometry nozzles. R.D.V.

Controlled Terms: *AERODYNAMIC CONFIGURATIONS / *AIRCRAFT CONTROL /
AIRCRAFT PERFORMANCE / *OPTIMAL CONTROL / *MISSILE CONTROL / NOZZLE
GEOMETRY / *OPTIMAL CONTROL / *RAMJET MISSILES / SPACECRAFT CONTROL /
VARIABLE GEOMETRY STRUCTURES

TYPE 19/4/102
77A19774 NASA ISSUE 7 Category 28
Analysis of boron combustion in air-augmented ram-rockets
BESSER, H.-L.
AIAA PAPER 77-13 770100 American Institute of Aeronautics and
Astronautics. Aerospace Sciences Meeting, 15th, Los Angeles, Calif., Jan.
24-26, 1977, 10 p. AA(Muenchen, Technische Universitaet, Munich, West
Germany) 10 p. Refs. 13

This paper contributes to the field of combustion diagnostics. It is
especially concerned with the combustion of elementary boron. The
condensed combustion products were sampled in the secondary combustor
exhaust plume of a ram-rocket motor, which had a propellant containing
boron. The main purpose of the experiments was to evaluate the local boron
combustion efficiency at different regions of the engine cross section.
The boron combustion efficiency was evaluated through the chemical
composition of the samples. The results of the experiments were
satisfying. Some simple and inexpensive sampling methods are presented, in
addition to the error possibilities of sampling techniques. In addition,
it is also explained, how combustion efficiencies, determined by particle
sampling and by thrust measurement, can be compared in order to examine
the reliability of sampling experiment results. (Author)

Controlled Terms: AIR BREATHING ENGINES / *BORON / *COMBUSTION

EFFICIENCY / COMBUSTION PRODUCTS / HYBRID PROPULSION / METAL COMBUSTION / PARTICULATE SAMPLING / *PROPELLANT COMBUSTION / *RAMJET MISSILES / *ROCKET ENGINE DESIGN / THRUST MEASUREMENT

TYPE 19/4/103
77A17267 NASA ISSUE 5 Category 7
Definition and performance of a one-stage rocket ramjet
MARGUET, R.; HUET, C.; LARUELLE, G.
760000 In: International Symposium on Air Breathing Engines, 3rd, Munich, West Germany, March 7-12, 1976, Proceedings. (A77-17226 05-07) Cologne, Deutsche Gesellschaft fur Luft- und Raumfahrt, 1976, p. 863-878. ACOFRA, Chatillon-sous-Bagneux, Hauts-de-Seine, France) 16 p.

A rocket ramjet with an integrated booster and a dual-function annular nozzle has been considered as a propulsion unit for a cruise missile with a 100-km range at Mach 2 and a 200-kg payload. This paper reviews criteria for choosing a fuel, analyzes the performance of the integrated-booster configuration, and presents test results for a 200-mm-diameter model. It is shown that an auto-pyrolizing solid fuel is the best choice because it makes a reduction in overall missile size possible. The operation of a ramjet with an integrated booster is described, and possible integrated dual-function annular nozzle is considered. The thrust produced by a ramjet with a dual-function annular nozzle is computed, and the results are compared with findings of wind-tunnel tests on the model. F.G.M.

Controlled Terms: ANNULAR NOZZLES / *BOOSTER ROCKET ENGINES / *CRUISE MISSILES / DUAL THRUST NOZZLES / MILITARY TECHNOLOGY / PAYLOADS / PROPULSION SYSTEM CONFIGURATIONS / *RAMJET MISSILES / ROCKET ENGINE DESIGN / *SOLID PROPELLANT ROCKET ENGINES / *SUPERSONIC COMBUSTION RAMJET ENGINES / *WIND TUNNEL TESTS

TYPE 19/4/104
76A46257 NASA ISSUE 23 Category 7
Ramjet research payoffs believed near
760913 Aviation Week and Space Technology, vol. 105, Sept. 13, 1976, p. 71, 73-75, 77. 5 p. Jpn. 3581

The status of various missile ramjet propulsion systems is sketched. Supersonic speeds and terminal-phase maneuverability are advantages emphasized. Programs discussed include: an integral rocket-ramjet/torpedo tube missile adaptable to surface firings, a solid fuel ramjet project, a liquid fuel ramjet demonstrator, modern ramjet engine/modern ramjet system synthesis, advanced surface-to-air ramjet projects for medium range and extended range, a supersonic combustion ramjet missile capable of flying at sustained hypersonic speeds around Mach 5.5, Combustor configurations, advantages and drawbacks as weapons systems, improvements required, and program status are indicated. R.D.V.

Controlled Terms: MILITARY TECHNOLOGY / *MISSILE DESIGN / *PROPULSION SYSTEM CONFIGURATIONS / *RAMJET MISSILES / *ROCKET ENGINE DESIGN / SOLID PROPELLANT ROCKET ENGINES / *SUPERSONIC COMBUSTION RAMJET ENGINES / SURFACE TO AIR MISSILES / UNDERWATER TO SURFACE MISSILES / WEAPON SYSTEMS

TYPE 19/4/105
76A30029 NASA ISSUE 13 Category 5
Low cost/optimized performance inlets for ramjets
KOETJE, E. L.
760000 NO0123-73-C-2225 In: Structures, Structural Dynamics, and Materials Conference, 17th, King of Prussia, Pa., May 5-7, 1976, Proceedings. (A76 30004 13 39) New York, American Institute of Aeronautics and Astronautics, Inc., 1976, p. 229-233. AA(Boeing Aerospace Co., Seattle Wash.) 5 p. Jpn. 1908

Procedures have been developed for cost/performance optimization of inlets for supersonic ramjet powered missiles. Several trade studies were conducted and cost/performance sensitivity methods were developed to define the effects of low cost detail features on the final candidates. Formed and welded titanium was selected for the final design. Fabrication techniques were developed and a full scale demonstration part was built. Results show approximately 80% cost reduction and approximately 10% range increase compared to the original titanium sandwich design. (Author)

Controlled Terms: *COST REDUCTION / *ENGINE INLETS / *FABRICATION / FULL SCALE TESTS / *RAMJET MISSILES / *STRUCTURAL DESIGN CRITERIA / *SUPERSONIC COMBUSTION RAMJET ENGINES / TRADEOFFS / WIND TUNNEL TESTS

TYPE 19/4/106
76A26671 NASA ISSUE 11 Category 20
Propulsion systems for earthbound missiles --- Antriebe fuer erdgebundene Flugkoerper
MACH, W.
760300 VDI-Z, vol. 118, no. 6, Mar. 1976, p. 292-295. In German.
AA(Messerschmitt Boelkow-Blohm GmbH, Ottobrunn, West Germany) 4 p. Refs.
47 Jpn. 1608

The majority of the missiles which are currently used have solid-propellant engines. However, a steadily increasing number of missiles employ airbreathing propulsion systems, in particular gas turbines. Gas turbines of simple design and comparatively low cost are developed for remotely piloted vehicles. A description is given of new developments related to gas turbines, ramjet engines, liquid-propellant rocket engines, solid-propellant rocket engines, hybrid rocket engines, and propulsion systems which utilize a combination of different types of engines. G.R.

Controlled Terms: *AIR BREATHING ENGINES / ENGINE TESTS / *GAS TURBINE ENGINES / HYBRID PROPELLANT ROCKET ENGINES / LIQUID PROPELLANT ROCKET ENGINES / LOW COST / *MISSILES / *PROPULSION SYSTEM CONFIGURATIONS / RAMJET ENGINES / REMOTELY PILOTED VEHICLES / *ROCKET ENGINE DESIGN / *SOLID PROPELLANT ROCKET ENGINES

TYPE 19/4/107
76A11260 NASA ISSUE 01 Category 39
Application of limit analysis to structural design of advanced ramjet inlets
MOORE, F. C.; MYERS, G. G.
000575 F33615-72-C-1366 Society for Experimental Stress Analysis, Spring Meeting, Chicago, Ill., May 11-15, 1975, Paper. 31 p. AB(Martin Marietta Aerospace, Orlando, Fla.) Refs. 6 Jpn. 76

Controlled Terms: CYLINDRICAL TANKS / DEFLECTION / *DESIGN ANALYSIS / *ENGINE DESIGN / *ENGINE INLETS / FABRICATION / FINITE ELEMENT METHOD / ITERATIVE SOLUTION / *MISSILE DESIGN / *RAMJET ENGINES / *STRUCTURAL DESIGN / WEIGHT REDUCTION

TYPE 19/4/108
75N29953# NASA ISSUE 17 Category 07
Investigation of surface tension screens for use in ramjet fuel systems/Final Report, Jan. - Jul. 1973/
FULTZ, J. R.
Air Force Aero Propulsion Lab., Wright-Patterson AFB, Ohio. (AH661913)
AD-A004098 AFAPL-TR-74-29 001074 AF PROJ. 3012 69 p. Jpn. 2068

Controlled Terms: ENGINE DESIGN / FLUID FLOW / FUEL CONTROL / *FUEL FLOW REGULATORS / *FUEL SYSTEMS / *JET ENGINE FUELS / MISSILE DESIGN / *RAMJET ENGINES

TYPE 19/4/109
75N12010# NASA ISSUE 03 Category 09
Environmental investigation of pilot propulsion test sled/Final Report/
GLASER, A. R.
Rockwell International Corp., Columbus, Ohio.Missile Systems Div (
RY230857)
AD-785134 AFSWC-TR-73-6 000374 F29601-72-C-0131 Missile Systems Div. 198 p. Jpn. 263
Controlled Terms: *CAPTIVE TESTS / IGNITION / PAYLOADS / PILOTS (PERSONNEL) / *RAMJET ENGINES / *SLEDS / SUPERSONIC SPEEDS / *TEST FACILITIES / VELOCITY

TYPE 19/4/110
75N12006# NASA ISSUE 03 Category 07
Pilot model for aero propulsion test sled/Final Report/
UYKES, R. C.; PETERS, H. J.
Rockwell International Corp., Columbus, Ohio.Missile Systems Div (
RY230857)
AD-785125 AFSWC-TR-72-6 000374 F29601-71-C-0113 AF PROJ. 589 Missile Systems Div. 362 p. Jpn. 269
Controlled Terms: EQUIPMENT SPECIFICATIONS / *NOSE CONES / POWER SPECTRA / *PROPULSION SYSTEM CONFIGURATIONS / *RAMJET ENGINES / *ROCKET PROPELLED SLEDS / SYSTEMS ENGINEERING / TEST FACILITIES

TYPE 19/4/111
75A43836 NASA ISSUE 23 Category 18
Air enriched propulsion system for earth resources rockets
MONTI, R.
IAF PAPER 75-031 000975 International Astronautical Federation, International Astronautical Congress, 26th, Lisbon, Portugal, Sept. 21-27, 1975, 26 p. AA(Napoli, Universita, Naples, Italy) Refs. 5 Jpn. 3376
Controlled Terms: AERODYNAMIC DRAG / APOGEES / ENGINE DESIGN / MASS FLOW RATE / MISSILE TRAJECTORIES / *PROPULSION SYSTEM CONFIGURATIONS / *RAMJET ENGINES / *REMOTE SENSORS / *SOUNDING ROCKETS / VERTICAL DISTRIBUTION

TYPE 19/4/112
75A41675 NASA ISSUE 20 Category 06
Observers for cruise missile autopilots --- control system design
GULLY, S. W.; SKELLEY, E. D.
AIAA PAPER 75-1113 000875 American Institute of Aeronautics and Control Conference, Boston, Mass., Aug. 20-22, 1975, 15 p. AB(Honeywell, Inc., St. Petersburg, Fla.) Refs. 11 Jpn. 2930
Controlled Terms: *AUTOMATIC PILOTS / *CONTROL THEORY / *CRUISING FLIGHT / FLIGHT CONDITIONS / *MISSILE CONTROL / MISSILE DESIGN / OBSERVATION / RAMJET ENGINES / *SYSTEMS ENGINEERING / SYSTEMS STABILITY

TYPE 19/4/113
75A27910 NASA ISSUE 12 Category 07
Ramjet missile research reevaluated
YAFFEE, M. L.
140475 Aviation Week and Space Technology, vol. 102, Apr. 14, 1975, p. 40-43. Jpn. 1711
Controlled Terms: FUEL CONTROL / FULL SCALE TESTS / MISSILE DESIGN / *MISSILE TESTS / *RAMJET MISSILES / RESEARCH PROJECTS / *STATIC TESTS / *SUPERSONIC COMBUSTION RAMJET ENGINES / *SURFACE TO AIR MISSILES / *SURFACE TO SURFACE MISSILES / SYSTEM EFFECTIVENESS / TECHNOLOGY ASSESSMENT

TYPE 19/4/114
75A18051 NASA ISSUE 06 Category 28
An experimental study of combustion of solid-fuel for ramjet
LITUIN, T.; WOJCICKI, S.
000074 Archiwum Procesow Spalania, vol. 5, no. 4, 1974, ; 447-459. AB(Warszawa, Politechnika, Warsaw, Poland) Refs. 6
Controlled Terms: COMBUSTION PHYSICS / DIFFUSION FLAMES / FLAME PROPAGATION / *FUEL COMBUSTION / METAL COMBUSTION / *METAL PROPELLANTS / *PROPELLANT GRAINS / PROPELLANT TESTS / *RAMJET MISSILES / *SOLID PROPELLANT IGNITION / THERMODYNAMIC PROPERTIES

TYPE 19/4/115
74N34710# NASA ISSUE 24 Category 12
Simulation of flow approaching the chin inlet of a ramjet missile/Final Report, 1 Jul. 1972 - 30 Jun. 1973/
BAUER, R. C.; MUSE, W. W.; TINSLEY, C. R.
ARO, Inc., Arnold Air Force Station, Tenn. (A3165097)
AD-783244 AEDC-TR-74-5 000774 Sponsored by AEDC 43 p. Jpn. 2930
Controlled Terms: *AIR BREATHING ENGINES / ANGLE OF ATTACK / INLET NOZZLES / *MISSILES / *RAMJET ENGINES / SUPERSONIC DIFFUSERS / SUPERSONIC FLOW

TYPE 19/4/116
74N18522M NASA ISSUE 09 Category 31
Synthesis of ramjet missile integrated flight control/fuel control/Final Technical Report, 20 Oct. 1972 - 19 Oct. 1973/
MICHAEL, G. J.; DIPIETRO, R. C.
United Aircraft Corp., East Hartford, Conn.Research Labs (UJ140625)
AD-772112 UARL-M941526-4 001173 N00019-73-C-0131 Research Labs. 66 p. Jpn. 1103
Controlled Terms: AIR TO AIR MISSILES / COMPUTERIZED SIMULATION / *FLIGHT CONTROL / *FUEL CONTROL / MISSILE TRAJECTORIES / *RAMJET MISSILES / VERTICAL FLIGHT

TYPE 19/4/117
74A39976 NASA ISSUE 20 Category 28
Ramjet engines - Highlights of past achievements and future promise
CURRAN, E. T.; STULL, F. D.
000074 In: International Symposium on Air Breathing Engines, 2nd, Sheffield, England, March 24-29, 1974, Proceedings. (A74-39964 20-28) London, Royal Aeronautical Society, 1974. 15 p. AB(USAF, Aero Propulsion Laboratory, Wright-Patterson AFB, Ohio) Refs. 18 Jpn. 2905
Controlled Terms: AFTERBURNING / EJECTORS / *ENGINE DESIGN / MISSILE LAUNCHERS / *PROPULSION SYSTEM CONFIGURATIONS / SOLID PROPELLANTS / *SUPERSONIC COMBUSTION RAMJET ENGINES / TECHNOLOGY ASSESSMENT / TURBOROCKET ENGINES

TYPE 19/4/118
74A39371 NASA ISSUE 19 Category 22
Nuclear propulsion - An epilogue
GREY, J.
001273 AIAA Student Journal, vol. 11, Dec. 1973, p. 4-7. AA(American Institute of Aeronautics and Astronautics, Inc., New York, N.Y.) Jpn. 2734

Controlled Terms: AIR BREATHING ENGINES / *AIRCRAFT ENGINES / MISSILE DESIGN / *NUCLEAR PROPULSION / *RAMJET ENGINES / ROCKET ENGINES / SPACECRAFT PROPULSION / *TECHNOLOGY ASSESSMENT

TYPE 19/4/119

74A39207 NASA ISSUE 19 Category 14
Thermal math model development for a resonant-cavity temperature sensor
--- for ramjet engine combustors
HOJNACKI, J. T.; HOGLUND, M. J.
000074 In: Advances in test measurement; Proceedings of the Twentieth International Instrumentation Symposium, Albuquerque, N. Mex., May 21-23, 1974. Volume 11. (A74-39177 19-14) Pittsburgh, Pa., Instrument Society of America. 1974. p. 323-334. AA(USAF. Aero Propulsion Laboratory, Wright-Patterson AFB, Ohio) AB(Honeywell, Inc., Government and Aeronautical Products Div., Minneapolis, Minn.) Refs. 7 Jpn. 2709

Controlled Terms: CAVITY RESONATORS / *COMBUSTION CHAMBERS / ERROR ANALYSIS / FEEDBACK CONTROL / *FUEL CONTROL / FUEL FLOW / GAS PRESSURE / *GAS TEMPERATURE / HEAT TRANSFER COEFFICIENTS / MASS FLOW RATE / *MATHEMATICAL MODELS / MISSILES / *RAMJET ENGINES / *TEMPERATURE SENSORS / THERMAL CONDUCTIVITY

TYPE 19/4/120

74A18184 NASA ISSUE 06 Category 28
Engines for earthbound missiles
MACH, U.
001273 VDI-Z, vol. 115, no. 18, Dec. 1973, p. 1471-1473. In German.
AA(Messerschmitt-Boelkow-Blohm GmbH, Munich, West Germany) Refs. 48

Controlled Terms: ECONOMIC FACTORS / *GAS TURBINE ENGINES / LIQUID PROPELLANT ROCKET ENGINES / MISSILE BODIES / *MISSILE DESIGN / *PROPULSION SYSTEM CONFIGURATIONS / RAMJET ENGINES / *ROCKET ENGINE DESIGN / *SOLID PROPELLANT ROCKET ENGINES / TECHNOLOGY UTILIZATION

TYPE 19/4/121

74A17177 NASA ISSUE 05 Category 28
Comparative study of various flight vehicle propulsion systems, using an air-to-air missile as an example
HEISE, G.
DGLR PAPER 73-058 000973 Oesterreichische Gesellschaft fuer Weltraumforschung und Flugkoerpertechnik and Deutsche Gesellschaft fuer Luft- und Raumfahrt, Gemeinsame Jahrestagung, 6th, Innsbruck, Austria, Sept. 24-28, 1973, DGLR 32 p. In German. Refs. 5 Jpn. 587

Controlled Terms: AFTERBURNING / *AIR TO AIR MISSILES / *COST ANALYSIS / *MISSILE DESIGN / *PROPULSION SYSTEM CONFIGURATIONS / PULSEJET ENGINES / RAMJET ENGINES / SOLID PROPELLANT ROCKET ENGINES / TURBOJET ENGINES

TYPE 19/4/122

74A14519 NASA ISSUE 03 Category 31
Integral rocket/ramjet for tactical missiles
BELDING, J. A.; COLEY, W. B.
001273 Astronautics and Aeronautics, vol. 11, Dec. 1973, p. 20-26.
AA(U.S. Naval Air Systems Command, Washington, D.C.) AB(LTV Aerospace Corp., Dallas, Tex.) Jpn. 442

Controlled Terms: *AIR TO AIR MISSILES / *FLIGHT TESTS / *MILITARY TECHNOLOGY / *MISSILE DESIGN / PROPULSION SYSTEM PERFORMANCE / *RAMJET MISSILES / SYSTEMS ENGINEERING / TECHNOLOGY ASSESSMENT / TECHNOLOGY UTILIZATION / WEAPON SYSTEMS

TYPE 19/4/123

74A11292 NASA ISSUE 01 Category 11
Dynamic simulation of CONFLOW - A facility to provide hot-gas ground testing of air-breathing missiles under simulated flight conditions
MITCHELL, U.
AIAA PAPER 73-1281 001173 American Institute of Aeronautics and Astronautics and Society of Automotive Engineers, Propulsion Conference, 9th, Las Vegas, Nev., Nov. 5-7, 1973, AIAA 10 p. AA(Martin Marietta Aerospace, Aeromechanical Engineering Div., Orlando, Fla.) MEMBERS, $1.50; NONMEMBERS, $2.00

Controlled Terms: *AIR BREATHING ENGINES / AIR FLOW / AIR TO AIR MISSILES / *ANALOG SIMULATION / ENGINE TESTS / *FLIGHT SIMULATION / GAS GENERATORS / *GROUND TESTS / HIGH TEMPERATURE GASES / *MISSILE TESTS / RAMJET ENGINES / TEMPERATURE CONTROL / *TEST FACILITIES / THERMAL ENVIRONMENTS

TYPE 19/4/124

73N32785# NASA ISSUE 23 Category 31
Development of AFT inlets for a ramjet powered missile (Development of aft intake system for ramjet powered missile)
ROSANDER, G.
Volvo Flygmotor A.B., Trollhaettan (Sweden). (V9421371)
000072 Presented at 1st Intern. Symp. on Air Breathing Engines.
Marseille, 19-23 Jun. 1973 47 p. Jpn. 2851 HC $4.50

Controlled Terms: AERODYNAMIC CONFIGURATIONS / CONFERENCES / ENGINE CONTROL / *INTAKE SYSTEMS / PRESSURE SENSORS / *RAMJET ENGINES / *RAMJET MISSILES

TYPE 19/4/125

73N14793N NASA ISSUE 05 Category 28
Characteristics of solid fuel rocket-ramjet engines (Analysis of reaction kinetics, combustion physics, and propellant properties of fuel elements used with rocket and ramjet engines)
ZUEV, V. S; MAKARON, V. S.
Lockheed Missiles and Space Co., Palo Alto, Calif. (L1535051)
000072 Transl. into ENGLISH from the book ""Teoriia Priamotochnykh i Rak-tno-Priamotochnykh Dviagatelei'', Moscow, Mashinostr., 1971 p 310-317
JPN. 590 HC *3.00; National Translations Center, John Crerar Library, Chicago, Ill. 60616

Controlled Terms: *COMBUSTION PHYSICS / PROPELLANT CHEMISTRY / PROPELLANT PROPERTIES / *RAMJET ENGINES / *REACTION KINETICS / *SOLID PROPELLANT ROCKET ENGINES / THERMODYNAMIC PROPERTIES

TYPE 19/4/126

73A14133 NASA ISSUE 03 Category 01
Development of aft inlets for a ramjet powered missile.
ROSANDER, G.
000672 Institut de Mecanique des Fluides, International Symposium on Air Breathing Engines, 1st, Marseille, France, June 19-23, 1972, Paper, 48 p. USAF-sponsored research. AA(Volvo Flygmotor AB, Trollhattan, Sweden)

Controlled Terms: AERODYNAMIC DRAG / AIRCRAFT PERFORMANCE / ANGLE OF ATTACK / ENGINE CONTROL / *ENGINE INLETS / FLOW DISTORTION / FOREBODIES / *INTAKE SYSTEMS / MACH NUMBER / *MISSILE DESIGN / *PROPULSION SYSTEM CONFIGURATIONS / *RAMJET MISSILES

TYPE 19/4/127

72N17795N NASA ISSUE 02 Category 31
Influence of mission and design parameters on the application of ramjet

rockets for low altitude missiles (Influence of velocity, range, and engine design parameters on use of low level ramjet missiles)
RIESTER, E.
Deutsche Forschungs- und Versuchsanstalt fuer Luft- und Raumfahrt, Brunswick (West Germany). (D0695666)
DLR-FB-71-58 000071 Inst. fuer Luftzaugende Antriebe. In GERMAN; ENGLISH summary 31 P. JPN. 256 ; DFVLR, Porz, West Ger.: 9 DM
Controlled Terms: BOOSTER ROCKET ENGINES / BORON / *ENGINE DESIGN / *LOW ALTITUDE / *RAMJET MISSILES / *RANGE (EXTREMES) / SOLID PROPELLANT ROCKET ENGINES / SPECIFIC IMPULSE / STRUCTURAL WEIGHT / THRUST-WEIGHT RATIO / *VELOCITY

TYPE 19/4/128
72A20249 NASA ISSUE 07 Category 28
Structural limitations on interstellar spaceflight. (Structural limitations of interstellar ramjet, investigating operation during travel in high matter number density space)
MARTIN, A. R.
001272 Astronautica Acta, vol. 16, Dec. 1971, p. 353-357. Research supported by the Science Research Council. AA(City University, London, England)
Controlled Terms: ALUMINUM / ERROR ANALYSIS / *INTERSTELLAR TRAVEL / LORAN / MATERIALS SCIENCE / *MECHANICAL PROPERTIES / *RAMJET MISSILES / STAINLESS STEELS

TYPE 19/4/129
72A16741 NASA ISSUE 05 Category 28
Propulsion systems for earthbound missiles (Earthbound missile propulsion systems, reviewing turbojet and ramjet engines, liquid, solid and hybrid propellant rocket engines and composite propulsion systems for special applications)
MACH, U.
001271 VDI-Z, vol. 113, Dec. 1971, p. 1433-1435. In German. AA(Messerschmitt-Boelkow-Bloehm GmbH, Munich, West Germany) REFS. 37
Controlled Terms: HYBRID PROPELLANT ROCKET ENGINES / LIQUID PROPELLANT ROCKET ENGINES / *MISSILE SYSTEMS / *PROPULSION SYSTEM CONFIGURATIONS / RAMJET ENGINES / SOLID PROPELLANT ROCKET ENGINES / TURBOJET ENGINES

TYPE 19/4/130
71N26257# NASA ISSUE 14 Category 28
ROCKET AND JET POWER (AIR BREATHING ENGINE PRINCIPLES FOR IMPROVED GUIDED MISSILES AND ARTILLERY PROJECTILES)
BJOERK, I.; HJERTSTRAND, A.; MARKLUND, T.
FORSVARETS FORSKNINGSANSTALT, STOCKHOLM /SWEDEN/. (F22926/2)
FOA-2-C-2362-1246 001269 DATE- DEC. 1969 COLL- 44 P LANG- IN SWEDISH AVAIL- NTIS
Controlled Terms: AERODYNAMIC CHARACTERISTICS / *AIR BREATHING ENGINES / AMMUNITION / *BALLISTIC TRAJECTORIES / *HYPERVELOCITY PROJECTILES / MISSILE TRAJECTORIES / RAMJET ENGINES / *ROCKET ENGINES

TYPE 19/4/131
71N17055# NASA ISSUE 07 Category 31
ON THE INFLUENCE OF AERODYNAMIC DRAG ON RAMJET DRIVEN HORIZONTAL FLYING MISSILES DURING THE BOOSTER PHASE (AERODYNAMIC DRAG EFFECTS ON RAMJET MISSILE BOOSTER ROCKET ENGINE)
RIESTER, E.
DEUTSCHE FORSCHUNGS- UND VERSUCHSANSTALT FUER LUFT- UND RAUMFAHRT, BRUNSWICK /WEST GERMANY/. (D0696666)
DLR-FB-70-45 000870 DATE- AUG. 1970 COLL- 18 P REFS LANG- IN GERMAN, ENGLISH SUMMARY AVAIL- NTIS, ZLDI MUNICH 7 DM
Controlled Terms: *AERODYNAMIC DRAG / *BOOSTER ROCKET ENGINES / BURNOUT / EQUATIONS OF MOTION / HORIZONTAL FLIGHT / *RAMJET MISSILES

TYPE 19/4/132
71A37189# NASA ISSUE 19 Category 21
DESIGN, SIMULATION, AND EVALUATION OF THE KALMAN FILTER USED TO ALIGN THE ;SRAM MISSILE (KALMAN FILTER FOR COMPUTERIZED OPTIMAL ;SRAM AIR TO SURFACE MISSILE ALIGNMENT, DISCUSSING DESIGN, DIGITAL SIMULATION AND FLIGHT TESTS)
BROWN, J. I.; YAMAMOTO, G. H.
AIAA PAPER 71-948 000871 CONF- AMERICAN INST. OF AERONAUTICS AND ASTRONAUTICS, GUIDANCE, CONTROL AND FLIGHT MECHANICS CONFERENCE, HOFSTRA U., HEMPSTEAD, N.Y., AUG. 16-18, 1971. PLAC- NEW YORK. PUBL- AMERICAN INST. OF AERONAUTICS AND ASTRONAUTICS, DATE- 1971. COLL- 10 P. MEMBERS, DOL- 1.50, NONMEMBERS, DOL- 2.00.
Controlled Terms: *AIR TO SURFACE MISSILES / *AIRBORNE/SPACEBORNE COMPUTERS / COMPUTER TECHNIQUES / CONFERENCES / *DIGITAL SIMULATION / ERROR ANALYSIS / FLIGHT TESTS / INERTIAL GUIDANCE / *LINEAR FILTERS / *MISSILE CONTROL / MISSILE DESIGN / *OPTIMAL CONTROL / *SUPERSONIC COMBUSTION RAMJET ENGINES

TYPE 19/4/133
70N32090# NASA ISSUE 17 Category 33
AN EXPERIMENTAL INVESTIGATION OF THE SUPERSONIC COMBUSTION OF VITIATED AIR HYDROGEN MIXTURES FINAL REPORT. 13 MAY 1968 - 30 JUN. 1969 (SUPERSONIC COMBUSTION OF VITIATED AIR-HYDROGEN MIXTURES)
DAVIS, R. E.
ARO, INC., ARNOLD AIR FORCE STATION, TENN. (A3165097)
AD-705129; AEDC-TR-70-60 000570 F40600-69-C-0001 PUBL- AEDC DATE- MAY 1970 COLL- 36 P REFS AVAIL- CFSTI
Controlled Terms: ARC HEATING / ENTHALPY / *HYDROGEN / *NOZZLE DESIGN / RAMJET MISSILES / *SUPERSONIC COMBUSTION RAMJET ENGINES

TYPE 19/4/134
70A26287 NASA ISSUE 11 Category 31
COMPARISON OF A BOOSTER-RAM ROCKET COMBINATION WITH A TWO-STAGE ROCKET FOR AN ACCELERATION MISSION (TWO STAGE ROCKET BOOSTER-RAM ROCKET LAUNCHER COMBINATION COMPARED TO SINGLE AND TWO STAGE ROCKETS)
SANLIK, H.; RIESTER, E.
000070 CONF- IN- SPACE ENGINEERING, PROCEEDINGS OF THE SECOND INTERNATIONAL CONFERENCE, VENICE, ITALY, MAY 7-10, 1969. P. 323 337. /A70-24276 11-31/ COLL- 15 REFS. PLAC- DORDRECHT, PUBL- D. REIDEL PUBLISHING CO., SERI- /ASTROPHYSICS AND SPACE SCIENCE LIBRARY. VOLUME 15/, DATE- 1970.
Controlled Terms: *BOOSTER ROCKETS / CONFERENCES / *LAUNCH VEHICLE CONFIGURATIONS / *MULTISTAGE ROCKET VEHICLES / PAYLOADS / *RAMJET MISSILES / RECOVERABLE LAUNCH VEHICLES / ROCKET ENGINE DESIGN / STRUCTURAL WEIGHT

TYPE 19/4/135
69A33262 NASA ISSUE 16 Category 29
RAMJETS. (COLLECTION OF ARTICLES ON RAMJETS INCLUDING REACTION PROPULSION, HYPERSONIC INLETS, COMBUSTION PROBLEMS, GRIFFON AIRCRAFT, STORABLE LIQUID FUELS, ETC)
000069 PLAC- NEW YORK. PUBL- AMERICAN INST. OF AERONAUTICS AND ASTRONAUTICS, SERI- /AIAA SELECTED REPRINT SERIES. VOLUME 6/, DATE- 1969.
COLL- 136 P. $2.50.

Controlled Terms: *COMBUSTION PHYSICS / COMBUSTION STABILITY / FLAME PROPAGATION / *HYPERSONIC INLETS / *RAMJET ENGINES / RAMJET MISSILES / *REACTION KINETICS / RESEARCH AND DEVELOPMENT / *STORABLE PROPELLANTS

TYPE 19/4/136
69A25586 NASA ISSUE 11 Category 28
RAMJETS AND AIR-AUGMENTED ROCKETS. (RAMJETS AND AIR AUGMENTED ROCKETS AS PROPULSION SYSTEMS FOR SUPERSONIC ATMOSPHERIC FLIGHT, NOTING INLET DESIGN, COMBUSTORS AND NOZZLES)
DUGGER, G. L.
000668 SERI- IN- JET, ROCKET, NUCLEAR, ION AND ELECTRIC PROPULSION-THEORY AND DESIGN. EDITED BY W. H. T. LOH. <A69-25582 11-28< /APPLIED PHYSICS AND ENGINEERING SERIES. VOLUME 7/, P. 236-273. COLL- 54 REFS. PLAC- NEW YORK, PUBL- SPRINGER-VERLAG NEW YORK, INC. DATE- 1968.

Controlled Terms: *AIR BREATHING ENGINES / AIRCRAFT CONFIGURATIONS / COMBUSTION CHAMBERS / HYDROGEN FUELS / HYPERSONIC INLETS / KEROSENE / MISSILE CONFIGURATIONS / NOZZLE DESIGN / *RAMJET ENGINES / *ROCKET ENGINES / SUPERSONIC COMBUSTION RAMJET ENGINES / SUPERSONIC DIFFUSERS / *SUPERSONIC FLIGHT / *SUPERSONIC INLETS

TYPE 19/4/137
68A45740N NASA ISSUE 24 Category 27
HIGH-DENSITY FUEL TO EXTEND RANGE OF RAMJET MISSILE. (HIGH DENSITY HYDROCARBON FUEL, TETRA HYDRO METHYLCYCLOPENTADIENE DIMER /;T-H-MCPD/ FOR REPLACING ;JP-5 AND INCREASING ;TALOS RAMJET RANGE)
FARRAR, R. B.
AIAA PAPER 68-632 001168 CONF- /AMERICAN INST. OF AERONAUTICS AND ASTRONAUTICS, PROPULSION JOINT SPECIALIST CONFERENCE, 4TH, CLEVELAND, OHIO, JUN. 10-14, 1968./ PLAC- NEW YORK, INIT- JOURNAL OF SPACECRAFT AND ROCKETS, VOL. 5, DATE- NOV. 1968, COLL- P. 1364-1367. REAN- <FOR ABSTRACT SEE ISSUE 17, PAGE 3232, ACCESSION NO. A68- 33816<

Controlled Terms: CONFERENCES / CYCLIC HYDROCARBONS / DENSITY (MASS/VOLUME) / DIMERS / *HYDROCARBON FUELS / JP-5 JET FUEL / *LIQUID ROCKET PROPELLANTS / METHYL COMPOUNDS / *RAMJET MISSILES / *ROCKET FLIGHT / *TALOS MISSILE

TYPE 19/4/138
68A45729M NASA ISSUE 24 Category 28
DEVELOPMENT OF A SPARK IGNITION SYSTEM FOR A RAMJET MISSILE. (SPARK IGNITION SYSTEM FOR RAMJET MISSILE, DISCUSSING DESIGN, DEVELOPMENT AND TESTS)
DE GRACE, L. G.
AIAA PAPER 68-645 001168 CONF- /AMERICAN INST. OF AERONAUTICS AND ASTRONAUTICS, PROPULSION JOINT SPECIALIST CONFERENCE, 4TH, CLEVELAND, OHIO, JUN. 10-14, 1968./ PLAC- NEW YORK, INIT- JOURNAL OF SPACECRAFT AND ROCKETS, VOL. 5, DATE- NOV. 1968, COLL- P. 1325-1328. REAN- <FOR ABSTRACT SEE ISSUE 17, PAGE 3241, ACCESSION NO. A68- 33828<

Controlled Terms: CONFERENCES / GROUND TESTS / *IGNITION SYSTEMS / PROPULSION SYSTEM PERFORMANCE / *RAMJET MISSILES / *ROCKET ENGINE DESIGN / *SPARK IGNITION / TIMING DEVICES

TYPE 19/4/139
68A32P3N NASA ISSUE 17 Category 28
DEVELOPMENT OF A SPARK IGNITION SYSTEM FOR A RAMJET MISSILE. (SPARK IGNITION SYSTEM FOR RAMJET MISSILE, DISCUSSING DESIGN, DEVELOPMENT AND TESTS)
DEGRACE, L. G.
AIAA PAPER 68-645 000668 CONF- AMERICAN INST. OF AERONAUTICS AND

ASTRONAUTICS, PROPULSION JOINT SPECIALIST CONFERENCE, 4TH, CLEVELAND, OHIO, JUN. 10-14, 1968. PLAC- NEW YORK, PUBL- AMERICAN INST. OF AERONAUTICS AND ASTRONAUTICS. DATE- 1968, COLL- 9 P. MEMBERS, $1.00, NONMEMBERS, $1.50.

Controlled Terms: CONFERENCES / GROUND TESTS / *IGNITION SYSTEMS / PROPULSION SYSTEM PERFORMANCE / *RAMJET MISSILES / *ROCKET ENGINE DESIGN / *SPARK IGNITION / TIMING DEVICES

TYPE 19/4/140
68A33816# NASA ISSUE 17 Category 27
HIGH DENSITY FUEL TO EXTEND RANGE OF RAMJET MISSILE. (HIGH DENSITY HYDROCARBON FUEL, TETRA HYDRO METHYLCYCLOPENTADIENE DIMER /;T-H-MCPD/ FOR REPLACING ;JP-5 AND INCREASING ;TALOS RAMJET RANGE)
FARRAR, F. B.
AIAA PAPER 68-632 000668 CONF- AMERICAN INST. OF AERONAUTICS AND ASTRONAUTICS, PROPULSION JOINT SPECIALIST CONFERENCE, 4TH, CLEVELAND, OHIO, JUN. 10-14, 1968. PLAC- NEW YORK, PUBL- AMERICAN INST. OF AERONAUTICS AND ASTRONAUTICS. DATE- 1968, COLL- 8 P. MEMBERS, $1.00, NONMEMBERS, $1.50.

Controlled Terms: CONFERENCES / CYCLIC HYDROCARBONS / DENSITY (MASS/VOLUME) / DIMERS / *HYDROCARBON FUELS , JP-5 JET FUEL , *LIQUID ROCKET PROPELLANTS / METHYL COMPOUNDS / *RAMJET MISSILES / *ROCKET FLIGHT / *TALOS MISSILE

TYPE 19/4/141
68A29625 NASA ISSUE 14 Category 28
DEVELOPMENT AND FLIGHT TESTS OF AN EXPERIMENTAL RAMJET AT MACH 5. (ETUDE ET ESSAIS EN VOL D*UN STATOREACTEUR EXPERIMENTAL A MACH 5. (FLIGHT TESTS OF EXPERIMENTAL RAMJET AT MACH 5, GIVING RESULTS, BALLISTIC RANGE AND ALTITUDE REACHED)
MARGUET, R.
001267 INIT- TECHNIQUE ET SCIENCE AERONAUTIQUES ET SPATIALES, DATE- SEP.-OCT., NOV.-DEC. 1967, COLL- P. 485-488. LANG- IN FRENCH.

Controlled Terms: BALLISTIC RANGES / FLIGHT ALTITUDE / *FLIGHT TESTS / FREE FLIGHT / *LAUNCH VEHICLES / MACH NUMBER / *MISSILE DESIGN / *RAMJET MISSILES / TELEMETRY

TYPE 19/4/142
69A20580 NASA ISSUE 08 Category 31
DESIGN AND FLIGHT TESTS OF A MACH-NUMBER-5 EXPERIMENTAL RAMJET. (FLIGHT TESTS AND DESIGN OF MACH 5 RAMJET MISSILES, NOTING APPLICATIONS TO FUTURE ATMOSPHERIC BOOSTERS)
MARGUET, R.
001067 PUBL- PYRODYNAMICS, VOL. 5, DATE- OCT. 1967, COLL- P. 307-340. 5 REFS. LANG- TRANSLATION.

Controlled Terms: *FLIGHT TESTS / *HYPERSONIC FLIGHT / HYPERSONIC SPEED / *MISSILE DESIGN / MISSILE TESTS / *PROPULSION SYSTEM CONFIGURATIONS / PROPULSION SYSTEM PERFORMANCE / RAMJET ENGINES / *RAMJET MISSILES

TYPE 19/4/143
68A10649M NASA ISSUE 01 Category 28
TRANSIENT CONDENSATION EFFECTS ON FLIGHT EQUIPMENT. (TRANSIENT CONDENSATION OF ATMOSPHERIC WATER CAUSING RAMJET ENGINE IGNITION DELAY SOLVED BY INCREASING VOLTAGE APPLICATION RATE)
WORLEY. W. E.
000067 CONF- IN- ANNUAL NATIONAL CONFERENCE ON ENVIRONMENTAL EFFECTS ON AIRCRAFT AND PROPULSION SYSTEMS, 7TH, PRINCETON, N.J., SEP. 25-27, 1967. PROCEEDINGS. <A68-10642 01-28< SPON- CONFERENCE SPONSORED BY THE U.S.

Controlled Terms: AERODYNAMIC / *AERODYNAMIC CHARACTERISTICS / ALTITUDE / BURNER / CHAMBER / CHARACTERISTICS / COMBUSTION / COOLING / ENGINE / FREE / *FREE JET / IGNITION / JET / LINER / NAVAHO MISSILE / PERFORMANCE / PROPULSION / RAMJET / RAMJET ENGINE / SHELL / TEST / *TEST CHAMBER

TYPE 19/4/148
64N26775M   NASA ISSUE 14 Category 28
DESIGN AND FLIGHT TESTS OF A MACH-5 EXPERIMENTAL RAMJET (DESIGN AND FLIGHT TESTS OF MACH-5 RAMJET FOR ACQUIRING HIGH SPEED ATMOSPHERIC PROPULSION DATA)
MARGUET, R.
OFFICE NATIONAL D ETUDES ET DE RECHERCHES AEROSPATIALES, PARIS /FRANCE/.
(OF368396)
ONERA-NT-94 000066 1966 37 P REFS IN FRENCH, ENGLISH SUMMARY CFSTI-
HC $2.00/MF $0.50

Controlled Terms: ATMOSPHERIC / BOOSTER / *FLIGHT TEST / *MACH NUMBER / MISSILE / PROPULSION / *PROPULSION SYSTEM / RAMJET / *RAMJET MISSILE / ROCKET / SUPERSONIC / SYSTEM / TRAJECTORY / UNMANNED / VELOCITY

TYPE 19/4/149
66A35630M   NASA ISSUE 19 Category 31
VENTING A RAMJET MISSILE TO PREVENT BUZZ DURING BOOST BY TANDEM ROCKET.
(MODEL STUDY OF AERODYNAMIC OSCILLATIONS IN RAMJET DIFFUSER AND COMBUSTION CHAMBER PRIOR TO BOOSTER SEPARATION IN RAMJET MISSILE INDICATES THAT VENTING MAY SOLVE PROBLEM)
BUNT, E. A.
000256 NGU-62-0604-C JOURNAL OF SPACECRAFT AND ROCKETS, VOL. 3, JUL. 1966, P. 1140, 1141.

Controlled Terms: AERODYNAMIC / BOOSTER / CHAMBER / COMBUSTION / *COMBUSTION CHAMBER / DIFFUSER / ENGINE / FLOW / MISSILE / MODEL / NOZZLE / *NOZZLE FLOW / OSCILLATION / RAMJET / *RAMJET ENGINE / SEPARATION / STUDY / VENT

TYPE 19/4/150
66A20667M   NASA ISSUE 09 Category 28
AEROSPACE PROPULSION EQUIPMENT - MACH 2 TO 5. (AIRCRAFT AND MISSILES OPERATING AT MACH 2 TO 5 USING AIR BREATHING PROPULSION SYSTEMS, NOTING ROLES OF RAMJET AND TURBINE ENGINES)
000166 AIRCRAFT ENGINEERING, VOL. 38, JAN. 1966, P. 8-10, 18.

Controlled Terms: AIRCRAFT / CONSTRUCTION / CYCLE / DESIGN / ENGINE / MACH NUMBER / MISSILE / *MISSILE CONSTRUCTION / POWER / PROPULSION / *PROPULSION SYSTEM / RAMJET / *RAMJET ENGINE / RANGE / SUPERSONIC / *SUPERSONIC AIRCRAFT / SYSTEM / TURBINE / *TURBINE ENGINE

TYPE 19/4/151
66A15847   NASA ISSUE 05 Category 28
SOLID PROPELLANT RAMJETS / STATOREATTORI A PROPELLENTE SOLIDO/. (SOLID PROPELLANT RAMJETS FOR TARGET AIRCRAFT, MISSILES AND SPACE VEHICLE BOOSTERS, NOTING ADVANTAGES AS COMPARED TO LIQUID PROPELLANT RAMJETS)
PARTEL, G.
001165 RIVISTA AERONAUTICA, VOL. 41, NOV. 1965, P. 1587-1608. IN ITALIAN.

Controlled Terms: AIR / BOOSTER / BREATHING / ENGINE / LIQUID / MISSILE / PROPELLANT / RAMJET / *RAMJET ENGINE / ROCKET / SOLID / *SOLID PROPELLANT / SPACE VEHICLE

NAVAL AIR PROPULSION TEST CENTER AND THE INST. OF ENVIRONMENTAL SCIENCES.
PLAC- MOUNT PROSPECT, ILL., PUBL. INST. OF ENVIRONMENTAL SCIENCES, DATE- 1967. COL1- P. 71-73.

Controlled Terms: *CONDENSING / CONFERENCES / *IGNITION SYSTEMS / *RAMJET ENGINES / TALOS MISSILE / TIME LAG / TRANSIENT RESPONSE / *WATER

TYPE 19/4/144
67N26146   NASA ISSUE 13 Category 28
A MATHEMATICAL MODEL OF A CLASS OF RAMJET ENGINES (MATHEMATICAL MODEL FOR RAMJET ENGINE PERFORMANCE)
PACKER, T. J.
WEAPONS RESEARCH ESTABLISHMENT, SALISBURY /AUSTRALIA/. (WH7-4278)
WRE-SAD-163 000744 JUL. 1966 96 P REFS CFSTI HC $3.00

Controlled Terms: COMBUSTOR / DIFFUSER / ENGINE / INLET / *MATHEMATICAL MODEL / MATHEMATICS / MISSILE / MODEL / PERFORMANCE / RAMJET / *RAMJET ENGINE / SIMULATION / SUPERSONIC

TYPE 19/4/145
67N18662   NASA ISSUE 06 Category 34
CONTRIBUTION OF FLIGHT EXPERIMENTATION TO AEROSPACE RESEARCH
(CONTRIBUTION OF FLIGHT EXPERIMENTS TO AEROSPACE RESEARCH)
BOUTTES, J.; LYCRISSE, P.
OFFICE NATIONAL D ETUDES ET DE RECHERCHES AEROSPATIALES, PARIS /FRANCE/.
(OF 68996)
000066 IN ITS SCI. SESSIONS OF THE O.N.E.R.A. 1966 P 5 /SEE N67 19451 08-34/ CFSTI- HC $3.00

Controlled Terms: ABSTRACT / AERODYNAMICS / AEROSPACE / *AEROSPACE TECHNOLOGY / CONFERENCE / EUROPE / FLIGHT / *FLIGHT TEST / FRANCE / HYBRID PROPULSION / INFRARED / KINETIC HEATING / MISSILE / ONBOARD / RAMJET ENGINE / REENTRY / SUPERSONIC FLIGHT / TECHNOLOGY / TEST / TRAJECTORY / TUNNEL / WIND / *WIND TUNNEL

TYPE 19/4/146
67N17399*N   NASA ISSUE 07 Category 28
STUDY AND FLIGHT TESTS OF A MACH 5 EXPERIMENTAL RAMJET (FLIGHT TESTS OF MACH 5 EXPERIMENTAL RAMJET MISSILES)
MARGUET, R.
NATIONAL AERONAUTICS AND SPACE ADMINISTRATION, WASHINGTON, D. C. (
N368373)
NASA-TT-F-10318 001165 NOV. 1966 39 P REFS TRANSL. INTO ENGLISH OF OFFICE NATL. DETUDES ET DE RECH. AEROSPATIALES REPT. TR 94, 1966 CFSTI-
HC $3.00/MF $0.65

Controlled Terms: ALTITUDE / ATMOSPHERIC / BOOSTER / COMBUSTION / EUROPE / *EUROPEAN SPACE PROGRAM / EXPERIMENT / FLIGHT / *FLIGHT TEST / LOADING / MACH NUMBER / MISSILE / SPACE / TEST / THRUST / PERFORMANCE / PROGRAM / PROPULSION / RAMJET / *RAMJET MISSILE / SPACE / TEST / THRUST / TRAJECTORY

TYPE 19/4/147
67N36416*M   NASA ISSUE 21 Category 28
PRELIMINARY EVALUATION OF FLIGHT-WEIGHT ;XRJ47-W-5 RAMJET ENGINE AT A MACH NUMBER OF 2.75 (FREE JET INVESTIGATION OF PERFORMANCE, BURNER SHELL COOLING, LINER DURABILITY, AND IGNITION CHARACTERISTICS OF RAMJET ENGINE CONDUCTED IN ALTITUDE TEST CHAMBER AT INLET MACH NUMBER 2.75)
REILLY, D. H.; WEINA, H. T.
NATIONAL AERONAUTICS AND SPACE ADMINISTRATION. LEWIS RESEARCH CENTER, CLEVELAND, OHIO. (ND31575)
NASA-RM-E55622 020055 WASHINGTON, NACA (1955) 43 P REFS CFSTI- HC $2.00/MF $0.50 /DECLASSIFIED/

TYPE 19/4/152

65A19791 NASA ISSUE 09 Category 31
THE CT-41 MISSILE TARGET /LENGIN-CIBLE CT 41<. (LAUNCHING AND CONTROL
OF RAMJET POWERED)CT-41 MISSILE TARGET USED IN DEFENSE SYSTEM TESTING AND
PERFECTING)
POTIER, J.; RAVEL, M.
001064 TECHNIQUE ET SCIENCE AERONAUTIQUES ET SPATIALES, SEP.-OCT. 1964,
P. 409-412. IN FRENCH.

Controlled Terms: ACCELERATION / CANARD / CONTROL / DEFENSE / ENGINE /
*ENGINE CONTROL / LAUNCHER / LAUNCHING / MISSILE / *MISSILE LAUNCHER /
PROPELLANT / RAMJET / *RAMJET MISSILE / ROCKET / SIMULATOR / SOLID /
SPOILER / STRUCTURE / SYSTEM / TARGET / TESTING / WING

TYPE 19/4/153

64N21157N NASA ISSUE 14 Category 18
PRELIMINARY EVALUATION OF FOUR COLUMBIUM BASE ALLOYS FOR COATING
CAPABILITIES AND MECHANICAL PROPERTIES AT ELEVATED TEMPERATURES (
PROTECTIVE COATING FOR NIOBIUM BASE ALLOYS TO BE USED IN RAMJET MISSILE)
REEVES, J. C.
MARQUARDT CORP., VAN NUYS, CALIF. (HH569990)
REPT.-6012 181063 AF 33/657/-10795 18 OCT. 1963 33 P REFS

Controlled Terms: ALLOY / BRAZING / COATING / DISILICIDE / EVALUATION /
MATERIAL / METAL / NIOBIUM / *NIOBIUM ALLOY / PROTECTION / *PROTECTIVE
COATING / RAMJET / *RAMJET ENGINE / *RAMJET MISSILE / REFRACTORY /
STRUCTURE

TYPE 19/4/154

64A11903 NASA ISSUE 04 Category 09
DESIGN AND TEST OF A NUCLEAR RADIATION-TOLERANT SERVO AMPLIFIER. (
AMPLIFIER DESIGN AND COMPONENTS TESTED FOR ACCEPTABILITY IN RELIABLE,
RADIATION RESISTANT SERVO SYSTEM OF NUCLEAR RAMJET MISSILE)
JOHNSON, B. E.; NELSON, R.; SCARBOROUGH, J. R.
001163 AF 33/657/-8686 /NUCLEAR RADIATION EFFECTS CONFERENCE. IEEE
SUMMER GENERAL MEETING, TORONTO, ONTARIO, CANADA, JUN. 16-21, 1963./ IEEE
TRANSACTIONS ON NUCLEAR SCIENCE, VOL. NS-10, NOV. 1963, P. 104-109.

Controlled Terms: AMPLIFIER / COMPONENT / DESIGN / ENVIRONMENT / MISSILE
/ NUCLEAR / *NUCLEAR RADIATION / RADIATION / *RADIATION RESISTANCE /
RAMJET / *RAMJET MISSILE / RESISTANCE / SERVO / *SERVOAMPLIFIER / TEST

TYPE 19/4/155

64A10797M NASA ISSUE 02 Category 27
GUN-LAUNCHING SUPERSONIC-COMBUSTION RAMJETS. (FLIGHT PERFORMANCE OF A
HYPERSONIC COMBUSTION RAMJET LAUNCHED BY A BALLISTIC GUN TO ACHIEVE SPEEDS
IN THE MACH 15 RANGE)
MOLDER, S.; SALTER, G. R.; VALENTI, A. M.
ASTRONAUTICS AND AEROSPACE ENGINEERING, VOL. 1, DEC. 1963, P. 24-29. 13
REFS.

Controlled Terms: *BALLISTIC VEHICLE / BALLISTICS / COMBUSTION / FLIGHT
/ GUN / *HYPERSONIC FLIGHT / HYPERSONICS / LAUNCH / MISSILE / PERFORMANCE
/ PROJECTILE / RAMJET / *RAMJET MISSILE / SUPERSONIC

TYPE 19/4/156

63N20024N NASA ISSUE 19 Category 27
(GUN LAUNCHED HYPERSONIC RAMJET PERFORMANCE STUDY)
MOLDER, S.; SALTER, G. R.; VALENTI, A. M.
MCGILL UNIV., MONTREAL /QUEBEC/. (HP756794)
000663 DRB G-9350-05 N63-20024 MCGILL U., MONTREAL /CANADA/ HYPERSONIC
PROPULSION LAB. PERFORMANCE STUDY OF GUN LAUNCHED HYPERSONIC RAMJETS S.

MOLDER, G. R. SALTER, AND A. M. VALENTI JUNE 1963 60P 9 REFS /DEFENCE
RESEARCH BOARD G?^NT 9550-06/ /REPT. 63-4/

Controlled Terms: AIRCRAFT / BALLISTICS / BOOSTER / DEVICE / ENGINE /
FUEL / GUN / *GUN LAUNCHING DEVICE / *HYPERSONIC AIRCRAFT / HYPERSONICS /
KEROSENE / LAUNCH / PERFORMANCE / RAMJET / *RAMJET MISSILE / TRAJECTORY

TYPE 19/4/157

63A22677 NASA ISSUE 21 Category 07
(ANALYSIS OF DIFFUSER, COMBUSTOR AND NOZZLE DESIGN PROBLEMS OF
HYPERSONIC RAMJETS USING SUPERSONIC COMBUSTION INDICATES HIGH PROPULSION
EFFICIENCIES UP TO MACH 20)
MORDELL, D. L.; SWITHENBANK. J.
000062 A63-22677 HYPERSONIC RAMJETS. DONALD L. MORDELL /MCGILL
UNIVERSITY, DEPT. OF ENGINEERING, MONTREAL, QUEBEC. CANADA/ AND J.
SWITHENBANK /MCGILL UNIVERSITY, HYPERSONIC RESEARCH GROUP, MONTREAL,
QUEBEC, CANADA/. IN- ADVANCES IN AERONAUTICAL SCIENCES. VOL. 4. 2ND
INTERNATIONAL CONGRESS IN THE AERONAUTICAL SCIENCES, PROCEEDINGS, ZURICH,
SWITZERLAND, SEPT. 12-16, 1960. NEW YORK, PERGAMON PRESS, INC., 1962, P.
831-847, DISCUSSION, P. 848.

Controlled Terms: AIRCRAFT / ARTILLERY / BOOSTER / COMBUSTION / DESIGN /
DIFFUSER / EFFICIENCY / HIGH SPEED / *HYPERSONIC FLIGHT / HYPERSONICS /
MISSILE / NOZZLE / PERFORMANCE / PROPULSION / RAMJET / *RAMJET ENGINE /
RANGE / *SUPERSONIC COMBUSTION RAMJET MISSILE

14. Abstract

This Lecture Series provided an introduction to modern ramjet technology; and applications to missiles were especially emphasized. The survey and characterization of various types of ramjets were followed by the discussion of ramjet components. Three of the lectures given on the second day dealt with the main types of subsonic combustion ramjets. There was one lecture devoted to supersonic combustion ramjets. The experience gained from the research and development of existing systems and components was covered in detail in all the lectures.

The AGARD Lecture Series was sponsored by the AGARD Propulsion and Energetics Panel and implemented by the Consultant and Exchange Programme.

AGARD-LS-136

Ramjet engines
Missile propulsion

AGARD Lecture Series No.136
Advisory Group for Aerospace Research and Development, NATO
RAMJET AND RAMROCKET PROPULSION SYSTEMS FOR MISSILES
Published October 1984
246 pages

This Lecture Series provided an introduction to modern ramjet technology; and applications to missiles were especially emphasized. The survey and characterization of various types of ramjets were followed by the discussion of ramjet components. Three of the lectures given on the second day dealt with the main types of subsonic combustion ramjets. There was one lecture devoted to supersonic combustion ramjets. The experience gained

P.T.O

---

from the research and development of existing systems and components was covered in detail in all the lectures. This AGARD Lecture Series was sponsored by the AGARD Propulsion and Energetics Panel and implemented by the Consultant and Exchange Programme.	from the research and development of existing systems and components was covered in detail in all the lectures. This AGARD Lecture Series was sponsored by the AGARD Propulsion and Energetics Panel and implemented by the Consultant and Exchange Programme.
ISBN 92-835-0360-0	ISBN 92-835-0360-0
from the research and development of existing systems and components was covered in detail in all the lectures. This AGARD Lecture Series was sponsored by the AGARD Propulsion and Energetics Panel and implemented by the Consultant and Exchange Programme.	from the research and development of existing systems and components was covered in detail in all the lectures. This AGARD Lecture Series was sponsored by the AGARD Propulsion and Energetics Panel and implemented by the Consultant and Exchange Programme.
ISBN 92-835-0360-0	ISBN 92-835-0360-0